Gorgon Barrow Island
Net Conservation Benefits Fund
www.gorgon-ncb.org.au

Pilbara Marine Conservation Partnership – Final Report

Volume 2

Gorgon Barrow Island Net Conservation Benefits Program

Final Report

December 2017

Citation

1 Contents

Part III Coral Reef Health

6. Coral community dynamics

6.1 Multi-year coral bleaching episode in NW Australian and associated declines in coral cover.

Authors: Babcock RC, Thomson D, Haywood MDE, Vanderklift M, Pillans R, Rochester W, Miller M, Speed C, Shedrawi G, Field S, Evans R, Stoddart J, Hurley T, Thompson A, Depczynski M.

ABSTRACT

Coral reef development is extensive in the shallow waters off the northwestern Australian coastline from northern Ningaloo to the Dampier Archipelago. Whilst many reefs elsewhere in the Indo-Pacific have been heavily impacted by coral bleaching since the late 1990's, until recently, this region has been relatively unaffected. We used time series of SST and DHW combined with coral cover data from the region collected over a period of up to 15 years from reef systems throughout the region to describe the temporal and spatial variability in bleaching and associated coral mortality. Given the inevitable increase in underlying seawater temperature due to global warming, and the increase in intensity and frequency of extreme climate events, there is a high likelihood that reefs in the west Pilbara and northern Ningaloo regions will experience more frequent coral bleaching and mortality events in the future. It is likely that we are already seeing the effects of this trend, with declines in coral cover throughout the region since 2013. At least one of these sites may show impaired ability to recover, relative to previous observations. In absolute terms declines ranged from 12.5-37% across the study region with relative declines ranging from 38-92%. These observations are consistent with trends in other parts of the world where repeated severe bleaching impacts have led to changes in coral cover and to the ability of reefs to recover from disturbance. Predictions that World Heritage Sites, such as Ningaloo, will experience severe bleaching twice per decade as early as 2041 may appear pessimistic, yet sites within this study region have already experienced this. While the west coast of Ningaloo may be buffered from bleaching to an extent, due to upwelling-favourable summer conditions, there are other parts of the west Pilbara that do not have this advantage, and may be affected even earlier by changes to climate. Urgent consideration of steps that could be taken now is needed to increase the resilience of coral reef ecosystems in the region, which is arguably the most important coral reef province on Australia's west coast.

6.1.1 INTRODUCTION

Global coral bleaching and threats to coral reefs

Reef-building corals face a wide range of threats directly related to human activities, including changes to water quality, overfishing and coastal development (Wilkinson 2004). However, processes related to changing climate, in particular warming sea temperatures, which can lead to bleaching and death of corals due to heat induced breakdown in the relationship between corals and their endosymbiotic zooxanthellae (Glynn et al. 2001, Smith et al. 2005), are recognised increasingly as existential threats to coral reefs (Heron et al. 2017). Bleaching can lead to changes in the composition of coral communities (Perry and Morgan 2017a) and in zooxanthellae (Glynn et al. 2001, Smith et al. 2005), as well as declines in total coral cover, with subsequent reductions in reef calcification rates and structural complexity (Perry and Morgan 2017b). The loss of corals from coral reef ecosystems will fundamentally change the nature of coral reefs, with concomitant changes in the biodiversity and biomass of associated fish (Pratchett et al. 2011, Graham 2014) and invertebrate communities (Przeslawski et al. 2008), and a greater dominance of macroalgae (Graham et al. 2014). Coral reefs, including the world's largest reef, the Great Barrier Reef (GBR), are not immune to these threats, despite receiving a highest level of legal protection and management of any reef (De'ath et al. 2012).

The increasing severity and geographic scale of coral bleaching and mortality, caused by anomalously high seawater temperatures, is a growing threat to coral reefs globally (Oliver et al. 2009, Baker et al. 2008). High temperature anomalies are caused by intensification of variations in the global ocean circulation at interannual and decadal time scales, as well as being exacerbated by underlying warming trends in the world's oceans (Cai et al. 2014, 2015, Han et al. 2013, Doi et al. 2011). Large-scale impacts of temperature anomalies and coral bleaching can be long lasting (Hoegh-Guldberg et al. 2007, Gilmour et al. 2013) and the effects of coral bleaching are felt on a wide range of reef organisms, such as fish, that rely on corals for food and shelter (Graham et al. 2008, Pratchett et al. 2008).

The response of corals to predicted changes in ocean temperature is likely to vary among regions, in part due to regional differences in the background seasonal and year-to-year variation in ocean temperature. First, the biological response of coral to a given temperature anomaly can depend on the temperature variability the coral has experienced in the past (Carilli et al. 2012). Second, because the accumulation of heat stress (measured by degree heating weeks - DHW) increases nonlinearly with temperature, the level, frequency and regularity of accumulated heat stress resulting from a given change in mean ocean temperature is directly affected by the background seasonal and year-to-year temperature variation (Langlais et al. 2017).

Coral bleaching in Australia:

On the east coast of Australia, the (GBR), was most severely affected by coral bleaching in 1998, which was a year in which bleaching impacts were severe globally (Goreau et al. 2000). The GBR has been affected by bleaching eight times, between 1980 and 2005 (Oliver et al. 2009). Though bleaching was most widespread in 1998 and 2002, more recently in 2016 & 2017, the GBR for the first time experienced bleaching two years in a row (Hughes et al. 2016, 2017). In contrast, known previous exposure of coral reefs in Western Australia (WA) has been limited to documentation of severe bleaching in 1998 at oceanic atolls off the Kimberley shelf of north-western WA, principally at Scott and Seringapatam Reefs (Skewes et al. 1999; Gilmour et al. 2013). Less documented bleaching has been observed in the Dampier Archipelago in 1998 (Wilkinson 2000, Gilmour 2004) and in 2005 and 2008 (MScience 2008), and at the Mangrove Islands off the coast of Onslow in 1998 (Wilkinson 2000).

Recent Western Australian marine heatwaves (2011-2016)

The 2010–2011 extreme La Niña conditions in WA resulted in sea surface temperatures as much as 5°C above normal off the west coast of Australia which were the most extreme on record for this area (Feng et al. 2015). Coral bleaching during this marine heat wave (MHW) occurred across 12 degrees of latitude; from the Montebello Islands in the north (19°) to Rottnest Island in the south (31°). Mortality of corals was high in many areas, with the north-eastern (Bundegi) and southern areas of Ningaloo reef (Coral Bay) and the Houtman-Abrolhos Islands (Depczynski et al. 2013, Moore et al. 2012) worst affected. The bleaching and mortality was however patchy; for example, north-western Ningaloo reef was barely affected while areas immediately to its south and east were severely damaged. A similar picture was evident in the Montebello and Barrow Islands region (Moore et al. 2012). Interestingly, the most intense heating was experienced in the central part of the west coast where it led to impacts on a wide range of flora and fauna (Wernberg et al. 2012) while the tropics, including areas affected in the 1998 bleaching event, appeared to be minimally affected (Moore et al. 2012).

Heatwave conditions on the WA coast abated in 2012, but anomalously warm waters were again present in 2013 in north-western Australia (21.75° to 20.3° S), immediately north of the region worst affected by the 2011 MHW. Bleaching and mortality of corals were recorded on reefs across this region of the coast on both nearshore (51–68%, Lafratta et. al. 2017) and offshore reefs (69.3%, Ridgway et al. 2016). The temperature anomaly that caused this MHW was the result of persistent La Niña conditions and the development of the Ningaloo Niño in the eastern Indian Ocean (Feng et al. 2013, 2015), which brings warm surface waters along the west coast of WA (Zhang et al. 2017) combined with regional climatological conditions that produced localised warming on the west Pilbara shelf. In 2016, the return of El Niño conditions resulted in bleaching further to the north in the Kimberley region of WA (Fromont et al. 2017), as well as on offshore atolls in the Timor Sea.

Global warming, through its effects on ocean circulation patterns and global climate variability, is predicted to increase the frequency and intensity of high temperature anomalies on Australia's west coast (Feng et al. 2011, 2015, Doi et al. 2015, Cai et al. 2015). Since WA's MHW of 2011, high temperature anomalies, bleaching and coral mortality have continued to manifest themselves in the region between Ningaloo and the Dampier Archipelago (Ridgway 2016, Lafratta et al. 2017), a scenario which may become increasingly common in the near future.

The intervals between bleaching events and other impacts in WA have generally been sufficient that recovery has occurred between these stressors, leading to the characterization of coral cover on WA coral reefs as being in a state of "dynamic stability" (Speed et al. 2013), in which overall coral cover has appeared to remain stable over the recorded past. In the north-western area of WA, it is important to understand the cumulative effects of factors such as coral bleaching in the context of various developments, such as port developments, oil and gas extraction, and the establishment of marine parks. The GBR and other parts of the world are now seeing consecutive years of bleaching (Hughes et al. 2016, 2017). Here we use historical and recent measures of coral cover throughout north-western Australia, to document the timing and extent of bleaching, mortality and recovery of corals in this region from 1985 to 2017. In particular we examine the fine scale spatio-temporal variability among locations within the Pilbara in relation to no only SST anomalies but also SST variability, and discuss these observations of coral bleaching in the context of regional and global trends.

6.1.2 METHODS

Study area

The Ningaloo and west Pilbara coastal regions of WA lie just north of the Tropic of Capricorn and are characterised by extensive reef development and diverse coral assemblages (Veron and Marsh 1988). Coastal fringing reefs are well developed in the Ningaloo Region. They comprise some of the most extensive continuous fringing reef systems in the world and have recently been inscribed on the World Heritage List based on their outstanding and universal natural values. The continental shelf is narrow adjacent to Northern Ningaloo but broadens markedly to the north in the west Pilbara coast between Bundegi and Dampier. Coral habitat in the relatively shallow (<20 m) waters of this area is provided by over 1000 islands and reefs exposed at low tide, notably the Dampier Archipelago, Montebello and Barrow Islands, and the nearshore islands of the south Pilbara off the coast of Onslow (Figure 6.1.1).
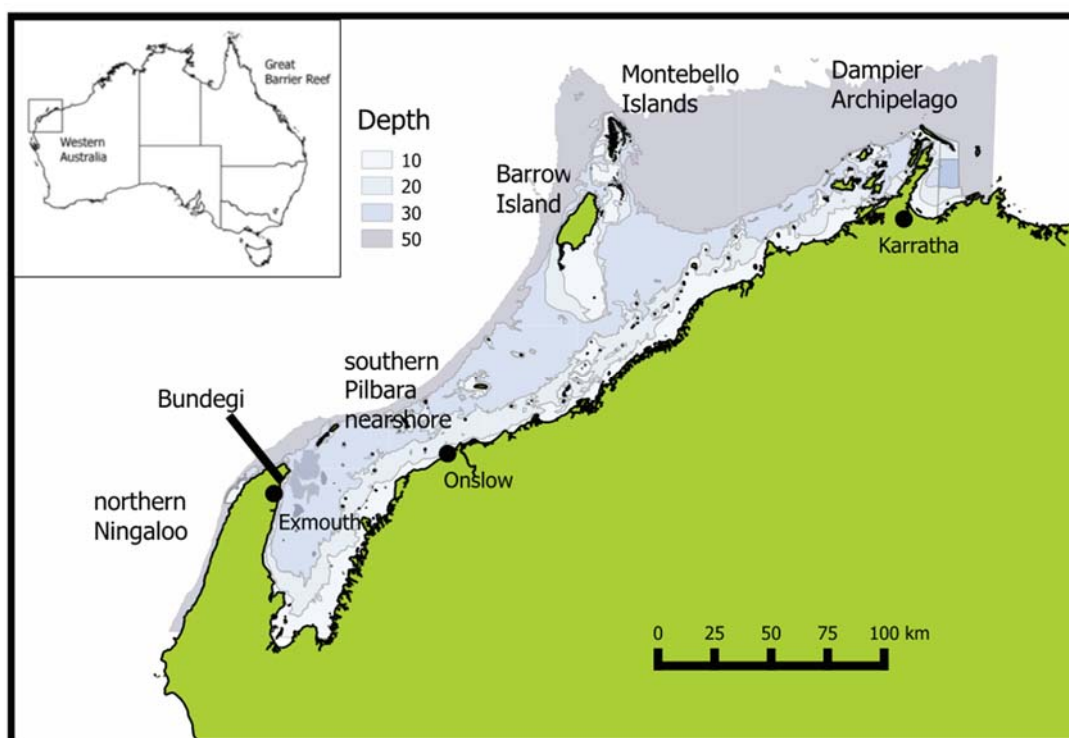
Figure 6.1.1 Western Pilbara and Ningaloo coastal region, Australian mainland in green.

Sea Surface Temperature

Remotely sensed data were used to produce maps and time series graphs of sea surface temperature (SST) and degree heating weeks (DHW). Time series were plotted for 5 locations: northern Ningaloo, Bundegi, south Pilbara nearshore, Montebello and Barrow Islands, and the Dampier Archipelago. The data plotted for each location were averages over a 0.1° square centred on the location. The SST data were from the IMOS GHRSST L3S night-only 1-day, 0.02° dataset (IMOS 2017), which is the dataset used for the ReefTemp system on the GBR (Garde 2014). We calculated DHW using the method of NOAA (NOAA 2017). We calculated the monthly climatology over the 10-year period from 2002 to 2011 (matching that of ReefTemp). From the climatology, we calculated the mean SST of the hottest month (MMM SST). The bleaching threshold at each point is 1°C above MMM SST at that point. DHW for a day was calculated as the sum over the 12-weeks ending on that day of SST minus MMM SST—for days when SST was at or above the bleaching threshold.

DHW is sensitive to missing SST data—affecting not only average DHW values but in our study also comparisons of relative DHW among years. To reduce that problem, we partially imputed missing data with a weighted running average using a window of 11 days. Weight declined linearly from one at zero days, to zero at 6 days. Imputation was performed only when there were at least two data points in the window. This method balanced imputing data with minimising bias from over-extrapolation (e.g. of isolated high SST values). To check for anomalies caused by imputation, we compared the DHW time series graphs with graphs calculated from raw SST data and SST data imputed by loess regression. Significant coral bleaching usually occurs when DHW values reach 4°C-weeks. By the time values reach 8°C-weeks, widespread bleaching is likely and significant mortality is expected (https://coralreefwatch.noaa.gov/satellite/methodology/methodology.php).

To help with interpretation, daily SST anomaly maps were calculated as the difference between the 11-day weighted running average and a daily climatology. The daily climatology was calculated in the same way as a monthly climatology, except that a 31-day window centred on each day was used in place of month.

Coral at different locations in the Pilbara experiences the heating represented by DHW in different contexts of temperature norms and variation. To summarise these contexts, we calculated maps representing summer temperature, seasonal variation of temperature and year-to-year variation of summer temperature. The data period was July 1994 to June 2017 (24 years). For summer temperature, we calculated the long-term 90th percentile of year-round temperature. To reduce bias due to missing values, we weighted observations such that each month (over all years) had the same weight. For seasonal variation, we calculated seasonal range from a daily climatology calculated using a 31-day smoothing window. For year-to-year variation, we calculated the standard deviation of the yearly 90th percentile temperature from July to June. Again, observations were weighted to reduce bias due to missing values; however, the maximum weight was limited to a factor of five to constrain the influence of observations from months with few data points. To examine whether the norms and variation had changed over time, we also calculated them for the first and second halves of the data period (12 years each). To put the Pilbara itself in context, we also calculated these maps for the Kimberley and Great Barrier Reef regions. To help with interpretation, we note that in these regions the 90th percentile SST was similar to MMM SST used for DHW calculation (90% of differences—0.2–0.5°C).

Coral Cover

There were three data sources considered for inclusion in our study: 1) peer-reviewed literature (journal articles), 2) grey literature (reports), and 3) unpublished data that were collected for research purposes or environmental monitoring programs (Table S1). Studies that provided an estimate of hard coral cover from sites off the coast of WA were included in our database. Studies were included in our database, provided they also included other metadata including depth (or depth range), habitat type(s) surveyed, and collection method. Data collected from *in situ* monitoring were used, including still photography, video and *in situ* visual estimates from transects, quadrats, manta-tows, towed video and ROV (c.f. Speed et al. 2013).

We were primarily interested in coral cover of shallow coastal and offshore areas due to availability of data, and increased vulnerability to prominent natural and anthropogenic impacts. We therefore restricted data collection to surveys that were done at depths ≤20 m, with the majority of data collected at average depths of ≤10 m (80% of surveys). This also reduced potentially confounding results of coral cover patterns due to varying depth gradients. Surveys included were also generally restricted to subtidal zones. A complete list of studies and sources from which data were derived is included in Table S6.1.1.

Analysis

Coral cover time series involved change point analysis to determine if and when a significant change in coral cover occurred. This technique uses serial bootstrap sampling to determine when changes in time series data large enough that they cannot reasonably be explained by chance alone have occurred (Sharma et al. 2016). Each bootstrap sample is a random re-ordering of the coral cover which was iterated 1000 times in each analysis. This procedure allowed estimates of variances associated with the changes in coral cover to be calculated. Analysis then identified break points where substantial deviations from the range of expected rates occurred as well as producing confidence intervals around those points where significant changes have occurred (Taylor 2000).

6.1.3 RESULTS
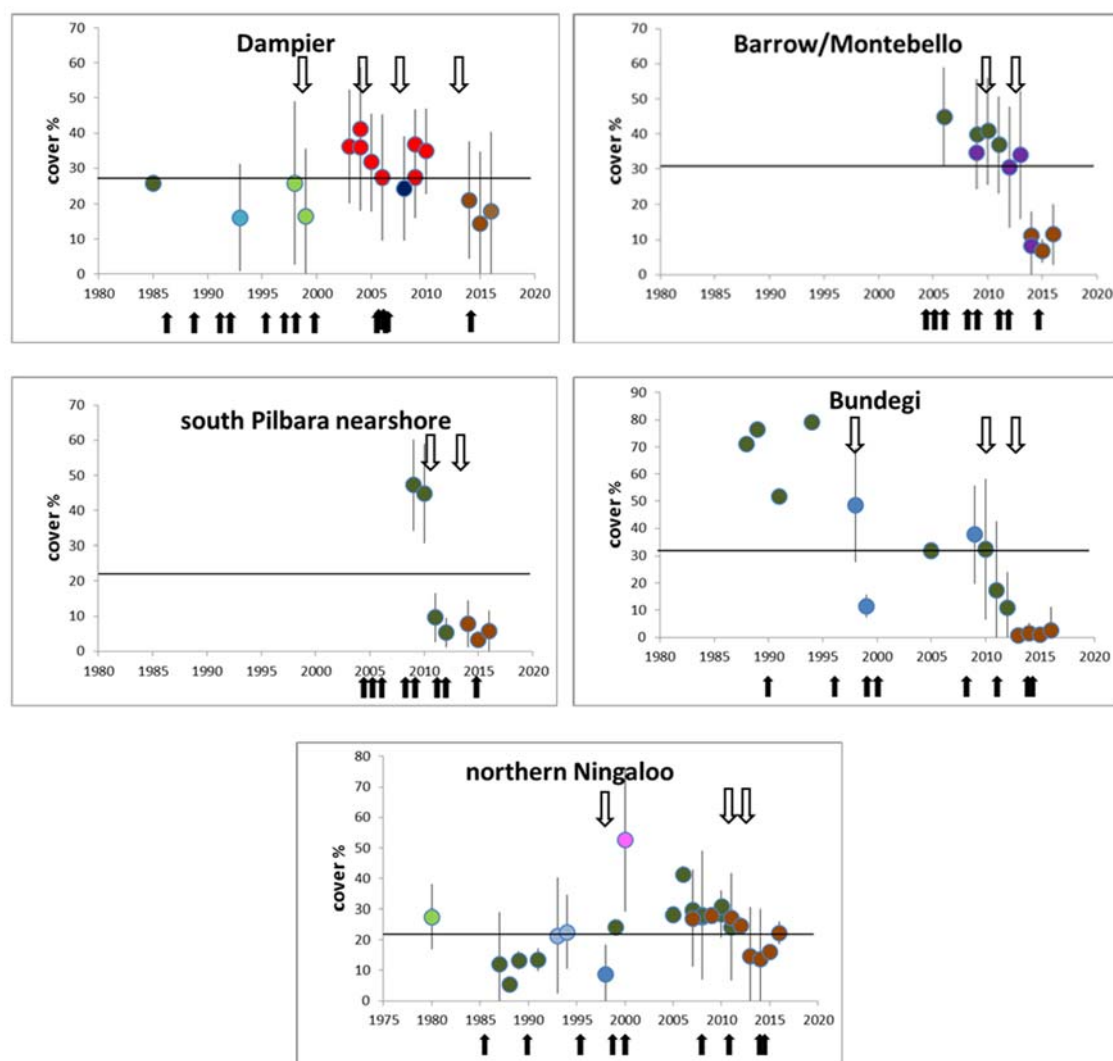
Figure 6.1.2 Coral cover from coastal coral reefs off northwestern Australia. Data are means and standard deviations derived from point-intercept transects. Long-term average coral cover – horizontal line. Brown – present study, Dark Green – DCBA, Light Blue – AIMS, Light Green – WAM, Purple – Chevron, Red – MScience, Dark Blue - Worley Parsons. Black arrows; cyclones passing within 100km of region, white arrows; years of reported bleaching in the region.

Dampier

The long-term average level of coral cover in the Dampier Archipelago is 27.1 ±16.5% (mean ± 1 SD). While the earliest estimate of coral cover comes from a single site, the level of sampling effort during subsequent years has been relatively high, driven by environmental impact monitoring, and covers a range of nearshore and offshore sites (Figure 6.1.2). Since 2003, sampling has been annual with a gap of three years (2011–2013). While coral cover was slightly below the long-term average prior to 2003, the period 2003–2010 was characterised by above average coral cover. There was a dip in cover between 2005 and 2009, corresponding with reports of bleaching and mortality in the region in 2005 and 2008 (MScience 2008) followed by an increase in cover in 2010. Satellite SST indicated elevated temperatures between 2005 and 2007 were typically mild and confined to coastal areas, in whereas in 2008 and 2009 heating levels of about 4 DHW, resulting in the slight mortality evident (Figure 6.1.3, Figure 6.1.4). These variations in coral cover were relatively minor and short term, and did not constitute significant breaks in long-term trends. However, by 2014, a significant decline below the long-term average of coral cover (14%) was evident (Table 6.1.1, Figure 6.1.5), and in 2015 coral cover was at historically low levels. This change could have occurred prior to 2014 as there was no sampling between 2010 and 2014. Coral bleaching was reported anecdotally at high levels in 2013 (https://www.youtube.com/watch?v=HQk3J7p9yWg) but no mortality was reported at that time. Bleaching was also observed at low levels in 2014. Satellite SST indicated that parts of the Dampier Archipelago experienced 6–8 degree heating weeks (DHW) in 2013 and 2014, although in 2014 this was spatially patchy throughout the Dampier Archipelago (Figure 6.1.5, Figure 6.1.4). Levels of coral cover in 2016 showed a slight recovery relative to the previous year. Of our five study locations, Dampier Archipelago had the summer temperature and seasonal range of SST, but the lowest year-to-year variation of summer temperature (Figure 6.1.6).
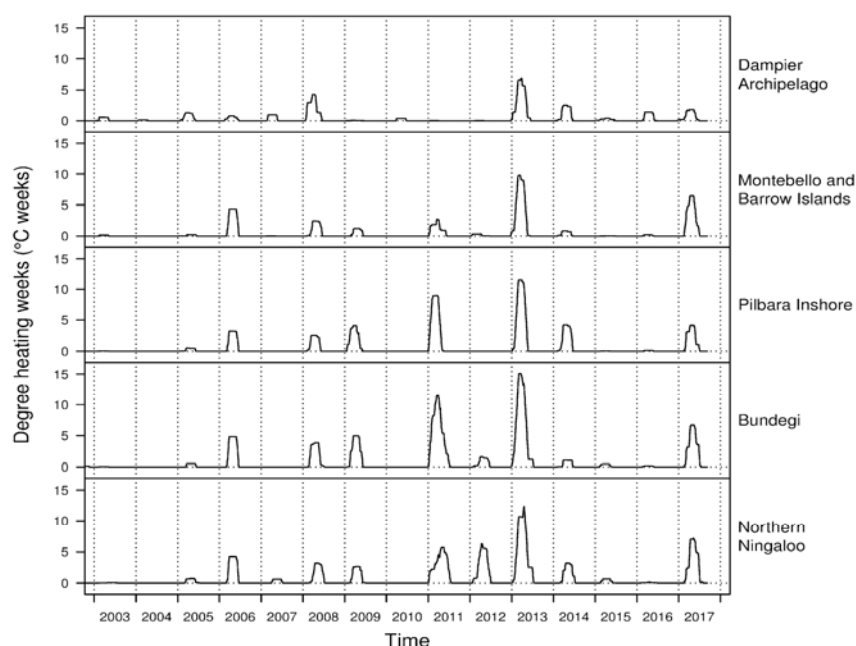
Figure 6.1.3 Time series of DHW in the Pilbara region off Western Australia 2002–2017.

Barrow and Montebello Islands

Records of coral cover at Barrow Island and the Montebello Islands extend back only as far as 2005 but have been continuous since then (Figure 6.1.2). For the initial part of this period, coral cover was at or above the long-term average of 31.3 ±12.9%. Coral cover declined from a high of around 45% in 2005 to just above 32% in early 2013. Since 2013 the level of coral cover has declined significantly
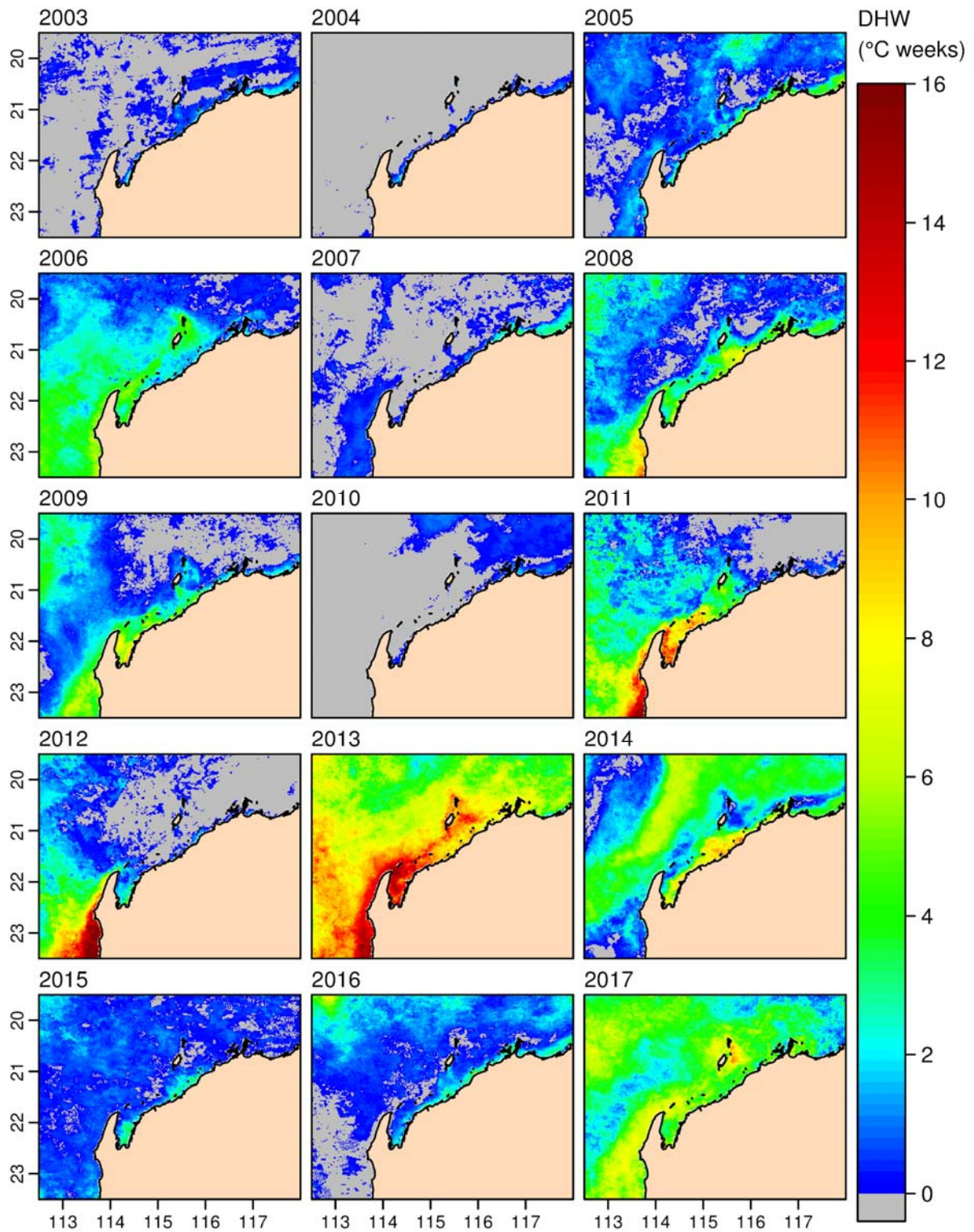
Figure 6.1.4 SST Degree Heating Weeks (DHW) in the Pilbara region off Western Australia 2003–2017. The maps show the maximum DHW from December to May. The year is the year in which the summer ended.

Table 6.1.1 Change-point analysis for significant changes in coral cover. Table shows years in which significant change was detected to occur, with confidence level relating to that change having occurred, and the confidence interval around this timing (95%).

		CONFIDENCE LEVEL		
	CONFIDENCE INTERVAL	(%)	FROM	TO
Northern Ningaloo				
1999	(1994,1999)	100	15.57	30.16
2013	(2000,2013)	100	30.16	16.67
Bundegi				
1998	(1994,1998)	93	69.55	32.41
2011	(2010,2011)	93	32.41	5.66
Montebello & Barrow Islands				
2014	(2014,2014)	97	37.41	9.45
Dampier				
2014	(2004,2014)	99	29.26	17.79
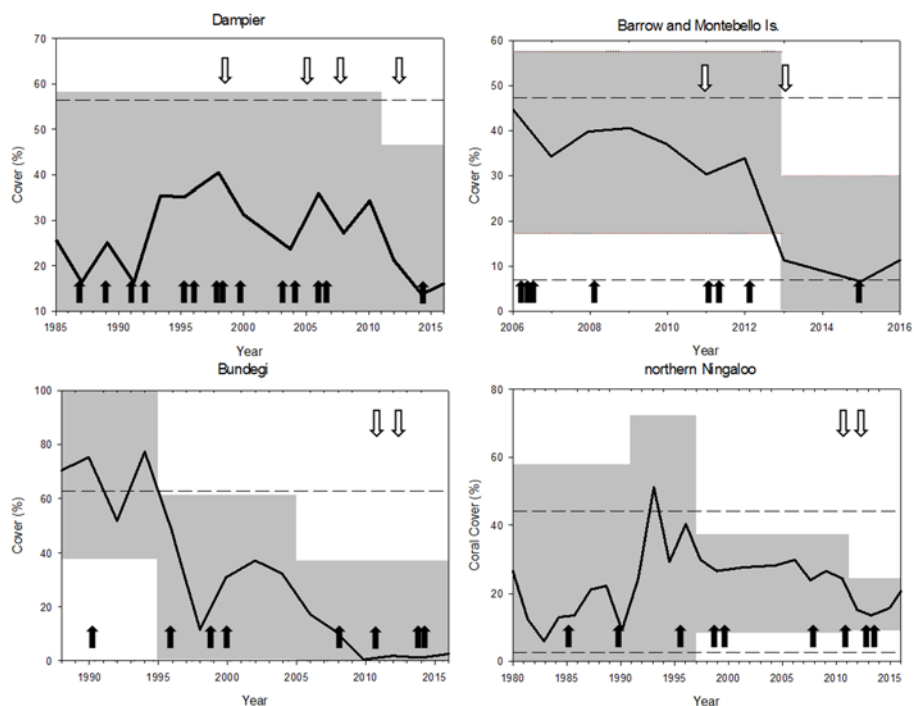
Figure 6.1.5 Coral cover trends and significant break points in coral cover. Control levels; dashed lines, Change point analysis charts. Shaded regions are parts of the data expected to contain all the values for intervals between points when changes occurred. Values on y-axis for shaded regions represent the confidence level for each interval. Black arrows; cyclones passing within 100 km of region, white arrows; years of reported bleaching in the region.

(Table 6.1.1, Figure 6.1.5) to between 8% and 11% and reached a minimum of 6.7% in 2015 (Table 6.1.1, Figure 6.1.5), an overall decline of over 25%. Satellite SST indicated that in 2011 there was only mild warming between Barrow and Montebello islands, with more widespread but still moderate warming of about 4 DHW (Figure 6.1.5, Figure 6.1.3, Figure 6.1.4. Conditions were much warmer in early 2013 however, with more than 8 DHW recorded throughout the waters around Barrow and Montebello islands, and in early 2014 anomalous warming of up to 4 DHW was again recorded in parts of the region (predominantly towards the south of Barrow Island) (Figure 6.1.5). There was a non-significant increase in coral cover to 11.5% in 2016, although this remains well below the long-term average of 31.3 ±12.9%.

South Pilbara Nearshore

Average coral cover on reefs of the south Pilbara Nearshore was 22.9 ±8.9%, over the period 2009–2016. Cover reached levels of 47% in 2009 and remained high in 2010 (Figure 6.1.2), but in 2011 declined precipitously to an average of 9.6% in 2011, a decrease of over 37% in absolute terms. The number of years sampled was insufficient to allow for break-point testing however there was a clear and substantial change across all sampling sites, which were sampled both before and after 2011. Satellite SST indicated warming of approximately 9 DHW over much of the area in early 2011 (Figure 6.1.3, Figure 6.1.4). Higher temperatures occurred in 2013 (over 11 DHW) and further warming occurred in 2014 (about 6 DHW, mainly nearshore). Coral cover continued to decline from 2011 levels and reached a low of 3.4% in 2015. Whilst the initial bleaching event caused a substantial change in the cover of coral, subsequent bleaching episodes in 2013 and 2014 resulted in further mortality of the already depleted coral community equivalent to a relative decline of approximately 65%. In absolute terms, this second reduction in coral cover was not as great as in 2011 because it was so low to start with, but in relative terms this represented a further reduction of around 65%. Coral cover showed a slight increase in 2016 to 5.8%, still well below the long-term average (Figure 6.1.2). The context in which warming occurred in the south Pilbara Nearshore is spatially complex because the location is within gradients of summer temperature, seasonal variation and year-to-year variation (Figure 6.1.6).

Bundegi

The record for coral cover at Bundegi is relatively consistent stretching back to 1988 (Figure 6.1.2). Since that time coral cover has averaged 30.77 ±13.29% (Figure 6.1.2). However coral cover has been highly variable over time, with periods of very high coral cover, such as in the late 1980's when it was greater than 70% at times. This early trend of high coral cover changed significantly after 1998 (Table 6.1.1, Figure 6.1.5) and in 1999 coral cover declined to 11.6% as a result of cyclone Vance. Following that low point, coral recovered rapidly between 1999 and 2005 to the long-term average levels of around 32%, although cover was still significantly lower than previously, and remained at around that level until 2011. Coral cover declined again significantly in 2011 to 17%, with a further decline in 2013 to less than 1% cover. This represents a decline of 31.6% between 2010 and 2013. Exmouth Gulf experienced warming of about 11 DHW in 2011 and 15 DHW in 2013, followed by 6 DHW in coastal areas in 2014 (Figure 6.1.3, Figure 6.1.4). By 2016, cover had remained at extremely low levels (2.5%). The apparent absence of recovery was notable relative to the recovery following 1999. Several cyclones passed near the Bundegi/Ningaloo region between 2011 and 2017, including TC Olwyn which passed almost directly over the site in 2015. Surveys within a week prior and following the passage of TC Olwyn did reported virtually no visible damage either on Bundegi or the northern Ningaloo west coast (R. Babcock, unpublished data). Of our five study locations, Bundegi experienced the highest year-to-year variation in summer temperature (Figure 6.1.6).
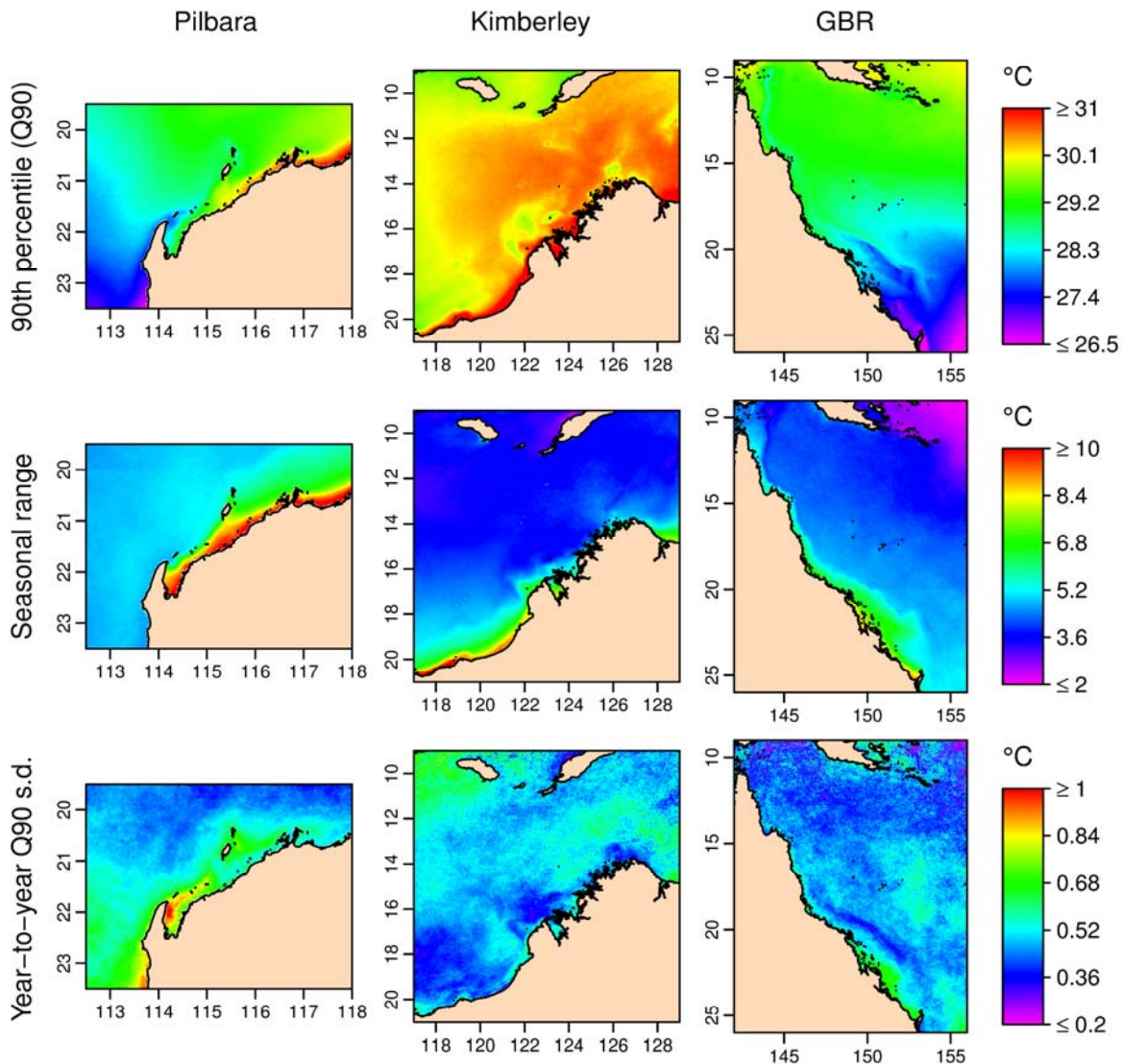
Figure 6.1.6 Temperature norms and variation in the Pilbara, Kimberley and Great Barrier Reef regions for the period 1994–2017. The maps represent typical summer temperature (long-term 90th percentile of year-round SST), seasonal variation (seasonal range of SST) and year-to-year variation of summer temperature (standard deviation of yearly 90th percentile SST).

Northern Ningaloo

Northern Ningaloo coral cover has averaged 21.8 ±9.3% since 1980. At the time first measurements were made in 1980, coral cover was 27% but by 1987 it was lower than the long-term average (Figure 6.1.2) and continued at similar levels. A significant change point in coral cover was evident from 1999 as coral cover increased (Table 6.1.1, Figure 6.1.5) and remained above average levels until 2012, when it averaged 27% (Table 6.1.1, Figure 6.1.5). There was a significant decline of 12.5% and from 2013 coral cover was again below average at 14.5%, though cover in 2016 had increased slightly to levels equivalent to the long-term average of 21.8 ±9.3% (Figure 6.1.2). The SST warming anomaly was about 6 DHW in 2011 and 2012, and then about 12 DHW in 2013, (Figure 6.1.3, Figure 6.1.4). Little or no warming was observed in 2014. Although warming in 2011 was moderate, it was sustained over an extended period (above-threshold SST occurred in 12 weeks over a 15-week period from January to April). Of our five study locations, northern Ningaloo experienced the lowest summer temperature and seasonal variation, but moderately high year-to-year variation of summer temperature (Figure 6.1.6).

Geographical patterns of temperature norms and variation

At a regional level, the context provided by temperature norms and variation in the Pilbara differed from those in the Kimberley and the GBR (Figure 6.1.6). Among the three regions, the Pilbara had a moderate summer temperature, high seasonal range and high year-to-year variation of summer temperature. The high seasonal range was consistent with the general increase in seasonal range towards the south and towards the coast. The Kimberley was characterised by high summer temperature. The GBR tended to be moderate in all three attributes. In summary the Ningaloo-Pilbara region appears to be transitional with a much higher level of variation in terms of these parameters than other much larger regions such as the GBR.

Within the Pilbara, summer temperature increased from south to north and, in the north, towards the coast (Figure 6.1.6). Seasonal range was high in coastal waters from Exmouth Gulf to the north. Year-to-year variation of summer temperature was particularly high in Exmouth Gulf (including Bundegi) and south of North West Cape. This variation was higher in the second half of the period (2006–2017) than in the first half (1994–2005) (Figure 6.1.7). At Bundegi, the change in year-to-year variation (standard deviation of the yearly 90th percentile) (0.29°C) was comparable with the increase in summer temperature (long-term 90th percentile) (0.27°C). The levels of SST variability experienced over the past decade in the southwest Pilbara and Exmouth Gulf are clearly greater than the region has experienced prior to that.
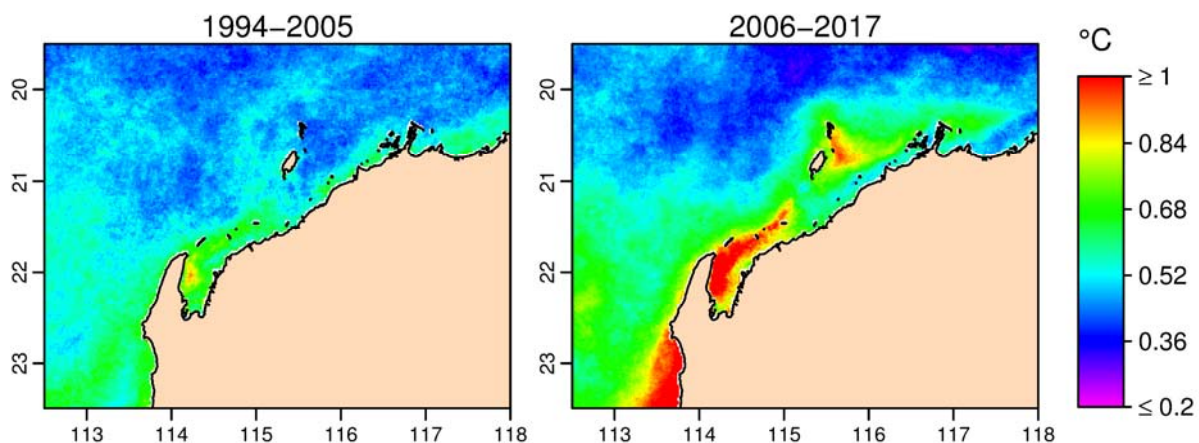
Figure 6.1.7 Year-to-year variation of summer temperature (standard deviation of yearly 90th percentile SST) in the Pilbara in the first and second halves of the period 1994–2017.

6.1.4   DISCUSSION

It is becoming increasingly clear that episodes of coral bleaching cannot be viewed as one-off events, but rather as recurring phenomena (Oliver et al. 2009, Trapon et al. 2011, Guest et al. 2012,). Moreover, these events are re-occurring at increasingly re-occurring after very short intervals, such as on the GBR in 2016 and 2017(Hughes et al. 2017, Hughes and Kerry 2017, Babcock et al. 2017) and as we report here. While the back-to-back bleaching of the GBR caught many by surprise, this should not have been unexpected given observations of the series of coral bleaching and mortality events in northwestern Australia in 2011 and 2013. Coral bleaching accompanied by severe mortality (>80%) was reported in the Exmouth Gulf in the north-east of Ningaloo (Moore et al. 2012, Depczynski et al. 2013), with bleaching and mortality again reported in the nearshore south Pilbara area near Onslow, less than 100 km away in 2013 (Lafratta et al. 2017), and bleaching reported in

both years at Barrow Island (Moore et al. 2012, Ridgway 2016). Coral mortality was relatively minor in 2011 (Moore et al. 2012), however there was widespread mortality around Barrow Island in 2013 (Ridgway 2016). Previously in the region there have also been relatively minor bleachings in close succession in 2005 and 2008 (MScience 2008).

Our observations draw together data on levels of coral cover from the west Pilbara and northern Ningaloo to more completely describe the temporal and spatial variability in the pattern of bleaching related mortality in the region as a result of these repeated temperature anomalies. In particular, they are instructive of the fine spatial scales over which different outcomes can be observed. These fine scale differences in outcomes may be due to spatial variation of both DHW (Figure 4) and the sensitivity of corals to a given level of DHW. These different responses may in part be due to the seasonal and year-to-year variation in temperature that the corals have experienced in the past (Carilli 2012). At locations where it is low, coral will have experienced fewer and/or milder heating events, and potentially be more sensitive to a given level of DHW. At locations where variation is high, two possibilities arise: (1) the variation matches historical patterns, and the coral may be less sensitive to a given level of DHW or (2) the variation has recently increased, and the coral is under stress. We checked for recent changes by comparing temperature norms and variation between the early and late halves of our 24-year analysis period.

The Dampier Archipelago in the north-west Pilbara region experienced little or no thermal anomaly in 2011 during the MHW in WA, but there were signs of anomalous warming in 2013, when the area experienced 6–8 DHW. Though no coral mortality was reported in the region at the time, trends in coral cover showed a step down in coral between 2010 and 2014. This is most likely due to the observed heating. Bleaching and mortality of corals has been reported in Dampier previously in 1998 (Wilkinson 2000, Gilmour 2004), although Gilmour (2004) attributed most of the mortality in his study to factors such as dredging and cyclone activity. Bleaching reported in 2005 and 2008 (MScience 2008), appears not to have resulted in a change in trend for coral cover though there may have been some mortality, as average cover did decline for a period immediately after 2005. The Dampier Archipelago, particularly the central part of the archipelago, presently appears to have some of the highest levels of coral cover in the west Pilbara, despite the history of multiple bleaching events in the rest of the region. This could be related to the lack of multiple severe bleaching episodes in the Dampier with severe bleaching and mortality only evident in 2013.

There was also a drastic decline in coral cover on reefs of the nearshore south Pilbara near Onslow in 2011, an area affected similarly in terms of thermal stress in 2011 and 2013. It is evident from our data that the major bleaching related coral mortality in this area took place in 2011, confirming previous inferences (Lafratta et al. 2017). While there was a larger thermal anomaly and significant bleaching reported in 2013 (Lafratta et al. 2017) this appeared to have little further impact on overall coral cover. This is most likely related to the observation that prior to 2011 reefs in the area were dominated by the genera remaining corals were bleaching resistant taxa Lafratta et al. 2017). Corals in the Onslow area have bleached previously, in 1998 (Wilkinson 2000), and prior history of bleaching does not appear to consistently provide protection from bleaching (Hughes et al. 2017).

Thermal anomalies at the Montebello and Barrow Islands in 2011 were not as great as in nearshore reefs of the south Pilbara, possibly in part due to the cooling effects of several cyclones which passed through the area in early 2011 (Moore et al. 2012). Thus these reefs, which are located only 100 km from the severely affected nearshore south Pilbara reefs, escaped major coral mortality in 2011. Even though bleaching of corals did occur in 2011 (Moore et al. 2012, Ridgway 2016) this did not afford protection from bleaching and mortality (e.g. Guest et al. 2012).of corals at Montebello and Barrow Islands, as there was a substantial reduction in coral cover following thermal anomalies in 2013.

At Bundegi in the northwestern part of the Exmouth Gulf, there was a greater level of heating in 2011 and mortality of corals exceeded 80% (Moore et al. 2012, Depczynski et al. 2013). In 2013, heating was even more extreme, with a peak of 15 DHW, but little bleaching was observed, primarily because so few corals remained to be affected. Coral cover has remained at less than 3% up to the present time, with no indications of recovery. This lack of recovery differs from observations following Tropical Cyclone Vance which devastated the reef at Bundegi in early 1999. This cyclone caused a drop in hard coral cover to around 15%, but Bundegi recovered to levels of over 30% cover by 2005, after just six years. Similar recovery might have been predicted based on the survival of small colonies following bleaching in 2011 (Depczynski et al. 2013), although coral cover declined further in the years following this event suggesting small colonies detected during post bleaching surveys in 2011 may have been impacted during subsequent events. Repeated bleaching impacts may have reduced the ability of the reef to recover rapidly and low absolute levels of cover are also likely to have been a factor as the potential for self-seeding of coral populations (e.g. Gilmour et al. 2013) and recovery from colony fragments (e.g. Depczynski et al. 2013) would have been virtually wiped out. The apparent lack of adaptation of Bundegi corals to heating patterns such as those experienced in recent years is consistent with the observation that these patterns have changed: summer temperature and year-to-year variation of summer temperature were both higher in the last 10 years than they were in the previous 10 years (Figure 7 and Results).

In contrast, less than 20 km away on the other side of Ningaloo on the west coast although bleaching was reported in 2011 in northern Ningaloo, coral mortality was not reported to be significant (Moore et al. 2012). However, we detected a significant break in the trend of coral cover at that time. Although thermal anomalies on the northern Ningaloo west coast in 2011 were moderate, they were sustained over a relatively long period. Anomalies were also observed in 2012, and in 2013 strong heating was present, apparently without any further significant reductions in coral cover. Although the level of reduction in cover was relatively modest, cover remains at historically low levels, below 20%. There appears to be signs of recovery, although further monitoring is required in order to confirm this trend.

Given the likely increase in underlying seawater temperature due to global warming, and the increase in intensity and frequency of extreme climate events (Oliver et al. 2017, Babcock et al. 2017) there is a high likelihood that reefs in the west Pilbara and northern Ningaloo regions will experience more frequent bleaching and mortality events in the future. It is likely that we are already seeing the effects of this trend, with changes in the composition of coral assemblages at northern Ningaloo (Thomson et al. 2017) and declines in coral cover for regions within the Pilbara where historical coral cover data exists, since at least 2013. At least one of these sites shows impaired ability to recover relative to previous observations, due to repeated impacts, or lack of larval supply from other sources in the region. These observations are consistent with trends in other parts of the world where repeated and severe bleaching impacts have led to changes in the composition of coral reef species assemblages (Hughes and Kerry 2017) and to the ability to recover from disturbance (Osborne et al. 2017, Neal et al. 2017).

Predictions that World Heritage Sites, such as Ningaloo, will experience severe bleaching twice per decade as early as 2041 (Heron et al. 2017) may appear pessimistic, but evidence presented here indicates that areas within the west Pilbara region have already been exposed to this level of disturbance. While the west coast of Ningaloo is buffered from bleaching to an extent, due to upwelling favourable summer conditions there (Xu et al. 2015), other parts of the Pilbara are located further from the shelf edge and are less exposed to seasonal longshore summer winds. These areas may be affected even earlier by changes to climate. Urgent consideration of steps that could be taken now is needed to increase the resilience of coral reef ecosystems in the region, which is arguably the most important coral reef province on Australia's west coast.

In developing mitigation strategies, we need to consider that global warming and extreme climate events can trigger fundamental shifts in ecosystems (van der Pol et al. 2017), and the loss of resilience often precedes ecosystem shifts (Scheffer et al. 2001). Therefore, management strategies that maintain ecosystem resilience are important. Further, mitigation strategies need to be flexible and adapt to the information revealed by monitoring and assessment (Schindler and Hilborn 2015). This requires closely integrating management interventions with ecosystem research. Recent climate simulations indicate that seasonal and interannual variability in SST maxima may be an important factor in determining bleaching frequency (Langlais et al. 2017). As areas of high and low seasonal and interannual SST variability appear to exist in the west Pilbara and appear to coincide with patterns of bleaching in the period 2011-2016. It may be useful to investigate these further to better understand how temporal refugia provided by such variability, which appears to be greater than that on Australia's other tropical coasts, may interact with ecosystem properties such as regional connectivity. An understanding of connectivity regimes among coral populations within the region is emerging based on both hydrodynamic modelling (Feng et al. 2016, Boschetti et al. 2017) and genetic studies. Modelling shows that reefs to the north of Barrow Island have relatively low connectivity with those to the south, while recent genetic studies of coral, fish and mangroves (Thomas et al 2017, DiBattista et al in Press, Binks et al in review, Evans et al submitted) show the Pilbara region is well mixed from northern Ningaloo to Dampier. At a larger scale, Southern Ningaloo and Shark Bay are isolated from tropical populations to the north on ecological time-scales This recent understanding of the connectivity of the region suggests that larval connectivity is not the sole driver of declines such as those at Bundegi but has likely been exacerbated by the lack of survivability of new recruits due to repeated disturbance events at intervals too frequent to allow recovery.

6.1.5 ACKNOWLEDGEMENTS

6.1.6 REFERENCES

Babcock RC, Bustamante R, Fulton E, Fulton D, Haywood, MDE, Hobday AJ, Kenyon R, Matear, RJ, Plagányi EE, Richardson AJ, Vanderklift M. Severe and extensive climate change impacts are happening now: Recent dieback of marine habitat forming communities across 40% of the Australian coast. (in review) Global Change Biology

Baker AC, Glynn PW, Riegl B (2008) Climate change and coral reef bleaching: An ecological assessment of long-term impacts, recovery trends and future outlook. Estuar Coast Shelf Sci 80: 435–471.

Boschetti F, Babcock RC, Doropoulos C, Thomson DP, Feng M, Slawinski D, Berry O, Vanderklift MA (2017) Setting priorities for conservation initiatives at the interface between ocean circulation, larval connectivity, and population dynamics . In RC Babcock et al. eds. Pilbara Marine Conservation Partnership – Final Report Vol. 1:249-272. CSIRO, Brisbane.

Bruno JF, Selig ER (2007) Regional Decline of Coral Cover in the Indo-Pacific: Timing, Extent, and

Subregional Comparisons. PLoS ONE 2: e711. doi:10.1371/journal.pone.0000711.

Cai W, Borlace S, Lengaigne M, Van Rensch P, Collins M, Vecchi G, Timmermann A, et al. (2014) Increasing frequency of extreme El Niño events due to greenhouse warming. Nature Climate Change 4: 111-116.

Cai W, Wang G, Santoso A, McPhaden MJ, Wu L, Jin F-F, Timmermann, A, et al. (2015) Increased frequency of extreme La Nina events under greenhouse warming. Nature Climate Change 5: 132-137.

Carilli J, Donner SD, Hartmann AC (2012) Historical Temperature Variability Affects Coral Response to Heat Stress. PLoS ONE 7(3): e34418. https://doi.org/10.1371/journal.pone.0034418.

Depczynski M, Gilmour JP, Ridgway T, Barnes H, Heyward AJ, Holmes TH, et al. (2013) Bleaching, coral mortality and subsequent survivorship on a West Australian fringing reef. Coral Reefs 32: 233-238.

Doi T, Behera SK, Yamagata T (2013) Predictability of the Ningaloo Nino/Nina. Sci. Rep. 3: 2892. DOI:10.1038/srep02892.

Feng M, Colberg F, Slawinski D, Berry O, Babcock R. (2016) Ocean circulation drives heterogeneous recruitments and connectivity among coral populations on the North West Shelf of Australia. J Mar Systems 164:1-12

Han W, Meehl GA, Hu A, Alexander MA, Yamagata T, Yuan D, et al. (2014) Intensification of decadal and multi-decadal sea level variability in the western tropical Pacific during recent decades. Climate Dynamics 43: 1357-1379.

Hoegh-Guldberg O, Mumby PJ, Hooten AJ, Steneck RS, Greenfield P, et al. (2007) Coral reefs under rapid climate change and ocean acidification. Science 318: 1737–1742. doi:10.1126/science.1152509.

Gilmour JP (2004) Size-structures of populations of the mushroom coral *Fungia fungites*: the role of disturbance. Coral Reefs 23(4):493-504.

Gilmour JP, Smith LD, Heyward AJ, Baird AH, Pratchett MS (2013) Disturbance and Recovery of an Isolated Coral Reef System Following Severe Disturbance. Science 340: 69-71. DOI: 10.1126/science.1232310.

Goreau TJ, McClanahan T, Hayes R, Strong AE (2000) Conservation of coral reefs after the 1998 global bleaching event. Conserv Biol 14: 5–15.

Guest JR, Baird AH, Maynard JA, Muttaqin E, Edwards AJ, Campbell SJ, et al. (2012) Contrasting patterns of coral bleaching susceptibility in 2010 suggest an adaptive response to thermal stress. PLoS ONE 7(3): e33353. https://doi.org/10.1371/journal.pone.0033353

Heron SF, Eakin CM, Douvere F, Anderson K, Day JC, Geiger E, Hoegh-Guldberg O, van Hooidonk R, Hughes T, Marshall P, Obura D (2017) Impacts of Climate Change on World Heritage Coral Reefs : A First Global Scientific Assessment. Paris, UNESCO World Heritage Centre. 16pp.

Hughes TP, Kerry JT, Álvarez-Noriega M, Álvarez-Romero JG, Anderson KD, Baird AH, et al. (2017). Global warming and recurrent mass bleaching of corals. Nature 543(7645): 373-377.

Hughes TP, Kerry JT (2017). Back-to-back bleaching has now hit two-thirds of the Great Barrier Reef, The Conversation, published online April 12 2017, retrieved on June 6, 2017 from http://theconversation.com/back-to-back-bleaching-has-now-hit-two-thirds-of-the-great-barrier-reef-76092

Graham NAJ, McClanahan TR, MacNeil MA, Wilson SK, Polunin NVC, Jennings S, Chabanet P, Clark S, Spalding MD, Letourneur Y, Bigot L, Galzin R, Öhman MC, Garpe KC, Edwards AJ, Sheppard CRC (2008) Climate warming, marine protected areas and the ocean-scale integrity of coral reef ecosystems PloS One 3: e3039

Lafratta A, Fromont J, Speare P, Schönberg CHL (2017) Coral bleaching in turbid waters of north-western Australia. Marine and Freshwater Research 68(1): 65-75.

Langlais CE, Lenton A, Heron SF, Evenhuis C, Sen Gupta A, Brown JN, Kuchinke M (2017) Coral bleaching pathways under the control of regional temperature variability. Nature Climate Change. doi:10.1038/nclimate3399.

Moore JAY, Bellchambers LM, Depczynski MR, Evans RD, Evans SN, Field SN, Friedman KJ, Gilmour JP, Holmes TH, Middlebrook R, Radford BT, Ridgway T, Shedrawi G, Taylor H, Thomson DP, Wilson SK (2012) Unprecedented Mass Bleaching and Loss of Coral across 12° of Latitude in Western Australia in 2010–11. PLoS ONE 7(12): e51807. doi:10.1371/journal.pone.0051807

Mscience (2007) Pluto LNG Development-Coral health monitoring: baseline.

MScience (2008) Bleaching Patterns Across The Pilbara In Early 2008 . MScience, Perth, Western Australia. 56pp.

Neal BP, Khen A, Treibitz T, Beijbom O, O'Connor G, Coffroth MA, Knowlton N, Kriegman D, Mitchell BG, Kline DI (2017) Caribbean massive corals not recovering from repeated thermal stress events during 2005–2013. Ecology and evolution 7(5): 1339-53.

Oliver JK, Berkelmans R, Eakin CM (2009) Coral Bleaching in Space and Time. In: van Oppen MJH, Lough JM, eds. Coral Bleaching: Patterns, Process, Causes and Consequences. Berlin: Springer-Verlag. 21–39. http://dx.doi.org/10.1007/978-3-540-69775-6_3.

Oliver ECJ, Donat MG, Burrows MT, Moore PJ, Smale DA, Alexander LV, Benthuysen JA, Feng M, Sen Gupta A, Hobday AJ, Holbrook NJ, Perkins-Kirkpatrick SE, Scannell HA, Straub SC, Wernberg T (in review). Ocean warming brings longer and more frequent marine heatwaves. Nature Communications.

Osborne K, Thompson AA, Cheal AJ, Emslie MJ, Johns KA, Jonker MJ, Logan M, Miller IR, Sweatman H (2017) Delayed coral recovery in a warming ocean. Global Change Biology. 23: 3869–3881.

Pratchett MS, Munday PL, Wilson SK, Graham NAJ, Cinner JE, Bellwood DR, Jones GP, Polunin NVC, McClanahan TR (2008) Effects of climate-induced coral bleaching on coral-reef fishes – ecological and economic consequences. Oceanography and Marine Biology: An Annual Review 46: 251–296.

Scheffer M, Carpenter S, Foley JA, Folke C, Walker B (2001) Catastrophic shifts in ecosystems, Nature 413(6856): 591.

Sharma S, Swayne DA, Obimbo C (2016) Trend analysis and change point techniques: a survey. Energ. Ecol. Environ. 1(3):123–130.

Schindler DE, Hilborn R (2015) Prediction, precaution, and policy under global change. Science, 347(6225): 953-954. doi:10.1126/science.1261824

Skewes TD, Gordon SR, McLeod IR, Taranto TJ, Dennis DM, Jacobs DR, Pitcher CR, Haywood MDE, Smith GP, Poiner IR, Milton D (1999). Survey and stock estimates of the shallow reef (0-15 m deep) and shoal area (15-50 m deep) sedentary marine resources and habitat mapping within the Timor Sea MOU74 Box. Volume 2: Habitat mapping and coral dieback. Client FRRF May 1999

Speed CW, Babcock RC, Bancroft KP, Beckley LE, Bellchambers LM, Depczynski M, Stuart N. Field SN, Friedman KJ, Gilmour JP, Hobbs JPA, Kobryn HT, Moore JAY, Nutt CD, Shedrawi G, Thomson DP, Wilson SK (2013) Dynamic Stability of Coral Reefs on the West Australian Coast. PLoS ONE 8(7): e69863. doi:10.1371/journal.pone.0069863

Taylor WA (2000) Change-point analysis: a powerful new tool for detecting changes. Available from: http: //www.variation. com/cpa/tech/changepoint.html

Thomson DP, Babcock RC, Haywood MDE, Pillans R, Vanderklift MA, Boschetti F. (2017) 10-year declines in *Acropora* and *Turbinaria* corals and a shift toward more generalist life-history traits at northern Ningaloo Reef, Western Australia. In RC Babcock et al. eds. Pilbara Marine Conservation Partnership – Final Report Vol. 2:492-509. CSIRO, Brisbane.

Trapon ML, Pratchett MS, Penin L, others (2011) Comparative effects of different disturbances in coral reef habitats in Moorea, French Polynesia. J Mar Biol 2011: 11 pp. doi: 10.1155/2011/807625.

van de Pol M, Jenouvrier S, Cornelissen JH, Visser ME (2017). Behavioural, ecological and evolutionary responses to extreme climatic events: challenges and directions. Philosophical Transactions of the Royal Society of London Series B 372, 20160134; DOI: 10.1098/rstb.2016.0134.

Wilkinson C, (2000). Status of coral reefs of the world: 2000. Australian Institute of Marine Science, Townsville. 372pp.

Xu J, Lowe RJ, Ivey GN, Jones NL, Brinkman R. (2015) Observations of the shelf circulation dynamics along Ningaloo Reef, Western Australia during the austral spring and summer. Continental Shelf Research 95: 54-73.

6.1.7 SUPPLEMENTARY MATERIAL

Table S6.1.1 Data sources

AUTHOR/S	YEAR	DETAILS
AIMS	2006	Coral reef communities at the Rowley Shoals, north-western Australia: state of knowledge and management implications. Perth, Australian Institute of Marine Science.
Armstrong SJ	2005	The abundance and distribution of Drupella corallivorous gastropods at Ningaloo Reef, Western Australia. Honours Thesis, Southern Cross, University.
Armstrong SJ	2009	Assessing the effectiveness of sanctuary zones in the proposed Dampier Archipelago Marine Park. Perth, Department of Environment and Conservation.
Ayling T, Ayling AL, et al.	1987	Ningaloo Marine Park: Preliminary Fish Density Assessment and Habitat Survey: with Information on Coral Damage Due to Drupella Cornus Grazing: a Report Prepared for the Department of Conservation and Land Management, Western Australia, Department of Conservation and Land Management.
Bancroft KP	2011	Long-term coral community monitoring in the Montebello/Barrow Islands marine protected areas: site descriptions and summary analysis of baseline data collected in December 2006 Marine Science Program Data Report, MSPDR9, June 2011. Department of Environment and Conservation, Perth, Western Australia
Cary JL, Grubba TL, Mahendran M, Radford B	2000	Ningaloo Marine Park Monitoring program: benthic monitoring sites established in 1999 - data report. CALM, Perth
Fitzpatrick B, Penrose H	2002	A preliminary marine ecological survey of Bateman Bay, Ningaloo Reef, Oceanwise & Murdoch University.
Forde JM	1994	Ecology of the muricid gastropod Drupella cornus (Roding, 1798) and its significance as a corallivore on Ningaloo reef, Western Australia. Master of Science thesis, University of Western Australia
Grubba TL, Cary JL	2000	Survey of the monitoring sites established in 1989 after coral mortality in Bills Bay from the coral mass spawning event of March 1989. Marine Conservation Branch, Department of Conservation and Land Management, Perth, Western Australia
Johansson CL, Bellwood DR, Depczynski M	In Press	The importance of live coral for small sized herbivorous reef fishes in physically challenging environments
Johansson CL, Bellwood DR, et al.	2010	Sea urchins, macroalgae and coral reef decline: a functional evaluation of an intact reef system, Ningaloo, Western Australia." Mar Ecol Prog Ser 414: 65-74.
Morrison PF	2004	A general description of the subtidal habitats of the Dampier Archipelago, Western Australia. Records of the Western Australian Museum Supplement No. 66: 51-59.
Mscience	2007	Pluto LNG Development-Coral health monitoring: baseline.
Mscience	2008	Cape Lambert Benthic Habitat Mapping Report: MSA123R1 MScience Pty Ltd, 239 Beaufort St, Perth, WA 6003, Australia. Benthic Marine Habitats at Cape Lambert West, Bezout, Dixon and Delambre Islands. Perth, Report to Maunsell Australia Pty Lty.
Mscience	2009	Wheatstone LNG Development: Baseline coral community description, Report to URS Australia.
Osborne S, Williams MR	1989	*Unpublished data*
Osborne S, Williams MR	1991	*Unpublished data*
Osborne S, Williams MR	1995	Status of Drupella cornus outbreak at Status of Drupella cornus outbreak at Ningaloo Reef. Final report prepared for the Australian Nature Conservation Agency. Department of Conservation and Land Management, Perth, Western Australia.
Rees M, AIMS, Australia. Dept. of the Environment	2003	Surveys of Trochus, Holothuria, Giant Clams, and the Coral Communities at Ashmore Reef, Cartier Reef, and Mermaid Reef, Northwestern Australia, Australian Institute of Marine Science.
Simpson CJ, Cary JL, et al.	1993	Destruction of corals and other reef animals by coral spawn slicks on Ningaloo Reef, Western Australia. Coral Reefs 12(3): 185-191.

Simpson CJ, Field S	1995	*Unpublished data*
Simpson CJ, Grey KA	1989	Survey of Crown-of-Thorns starfish and coral communities in the Dampier Archipelago, Western Australia. Western Australian Environmental Protection Authority, Technical Series 25. Technical Series 25: 1–24.
Stoddart JA, Grey KA, et al.	2004	Rapid high-precision monitoring of coral communities to support reactive management of dredging in Mermaid Sound, Dampier, Western Australia. Corals of the Dampier Harbour: their survival and reproduction during the dredging programs of: 31-48.
Verges A, Vanderklift MA, et al.	2011	Spatial patterns in herbivory on a coral reef are influenced by structural complexity but not by algal traits. PLoS One 6(2): e17115.
Wilson B, Blake S, Ryan D, Hacker J	2001	Reconnaissance of species-rich coral reefs in a muddy, macro-tidal, enclosed embayment, - Talbot Bay, Kimberley, Western Australia. Journal of the Royal Society of Western Australia 94:251-268
Woodside	2008	Scott Reef Status Report 2008
Woodside	2009	Scott Reef Status Report 2009
Woodside	2010	Scott Reef Status Report 2010, Woodside.
Worley-Parsons	2009	*Unpublished data*

6.2 10-year declines in *Acropora* and *Turbinaria* corals and a shift toward more generalist life-history traits at northern Ningaloo Reef, Western Australia

Authors: Thomson DP, Babcock RC, Haywood MDE, Pillans R, Vanderklift MA, Boschetti F.

ABSTRACT

Considerable research on coral reefs has documented declines in the percent cover of hard corals and changes in the abundance of the taxa following disturbance events. Responses of the most dominant hard coral taxa have been studied in detail, but little work has assessed the responses of less dominant hard coral taxa and coral functional groups. We conducted a temporal assessment of coral assemblages at northern Ningaloo Reef in Western Australia over a 10 year period with known disturbance history. The study period encompassed one thermal heating event; sufficiently large in magnitude to be classified as a one in 50 year event. We assessed annual trends in the percent cover of functional and taxonomic groups over the 10 year period and compared the responses of functional groups with that of taxonomic groups. Changes in the functional composition of coral assemblages were detected which were not evident using the taxonomic assessment. Generalist corals increased at an average rate (U) of 0.14 per year, despite there being no increase in the abundance of any of the 31 taxonomic coral groups. In comparison, trends in the most dominant functional group, competitive corals, were similar to the trends observed in the two most abundant taxonomic groups, *Acropora* and *Turbinaria.* Given the ability of the two different approaches to detect different trends, we suggest both approaches should be adopted to better understand the response of taxonomic and functional coral groups to future environmental change.

6.2.1 INTRODUCTION

Coral reefs around the world are threatened by a combination of natural and anthropogenic stressors (Pandolfi et al. 2003). Many studies have described persistent declines in the health of coral reefs caused by pressures such as elevated nutrients (McCook 1999), sedimentation (Fabricius 2005), coral disease (Pollock et al. 2014), elevated water temperatures (McClanahan et al. 2004; Sampayo et al. 2008), physical damage from storms (Harmelin-Vivien 1994; Madin and Connolly 2006) and predation by coral predators such as crown-of-thorns starfish and *Drupella* snails (De'ath et al. 2012).

Percentage cover of corals is the most widely used indicator of coral reef health because it is easily measures and reliably represents declines in the abundance of living hard corals (Osborne et al. 2011)**.** However, monitoring coral cover alone provides little insight into changes in the taxonomic composition of coral assemblages. Strong shifts in the composition of coral assemblages are already occurring in many regions of the world (Persian Gulf—Riegl and Purkis 2015; western Indian Ocean—McClanahan et al. 2007; eastern Indian Ocean—Speed et al. 2013; southern Japan—Hajime et al. 2002; French Polynesia—Pratchett et al. 2011; Great Barrier Reef—Osborne et al. 2011; the Caribbean—Perry et al. 2013. The frequency and intensity of disturbances that negatively impact corals are projected to increase, so further shifts in the composition of coral assemblages are predicted (Stocker et al. 2013).

Relationships between disturbance and shifts in coral community composition are complex because the extent to which coral taxa dominate coral assemblages is often a function of the frequency and intensity of disturbances (Hoey et al. 2016). For example, coral genera that are quite susceptible to bleaching, e.g. *Seriatopora*, *Stylophora* and *Acropora,* can be capable of rapid recovery following bleaching due to their high rates of recruitment and growth (Trapon et al. 2010; Gilmour et al. 2013). If subjected to frequent mild-disturbance, these taxa may dominate the assemblage. However, if disturbances are more severe, it may result in widespread mortality of all but the most physically resistant taxa, which over time, may come to dominate the assemblage (Hoey et al. 2016). Understanding how different coral taxa respond to, and recover from, different types and intensities of disturbance is, therefore, essential to being able to better predict how coral assemblages will respond to environmental change. Functional group classification of coral species has recently been proposed to offer new insights into patterns of function and diversity on coral reefs, and to provide a more mechanistic understanding of how coral assemblages respond to environmental change (Darling et al. 2012; Madin et al. 2016). Functional group classifications have the potential to reveal shifts in coral community structure which might not be evident when monitoring only coral cover. It has also been suggested that functional groups may respond in a more linear fashion to moderate levels of disturbance than species diversity (Cadotte et al. 2011), with evidence from land habitats of species diversity remaining stable while functional diversity decreases in areas that move from being lightly disturbed to severely disturbed (Cadotte et al. 2011). Functional groups may, therefore, allow for the detection of smaller, more subtle shifts in coral assemblages as a result of disturbances, and may be more sensitive indicators of disturbance and change than coral cover alone.

Coral assemblages at Ningaloo Reef have been exposed to numerous recent disturbances including tropical cyclones (Speed et al. 2013), elevated water temperatures (Depczynski et al. 2013), disease (Onton et al. 2011), outbreaks of predatory snails (Armstrong 2007) and discharges from floods on land (Lozano-Montes et al. 2017). Disturbances known to have impacted reefs in the north-western section of Ningaloo Reef during our study period include one extreme thermal heating event in March 2011 (see Moore et al. 2012). Here we compare annual changes in the abundance of taxonomic and functional coral groups over a 10-year period to determine if trends can be detected using a functional groups approach, which may not be evident using a taxonomic approach. We discuss whether these changes are associated with specific disturbance events and the implications

for the future resilience of coral assemblages at northern Ningaloo.

6.2.2 METHODS

Study site

This study was located along the north-western section of Ningaloo Reef between S22°17'00"
E113°49'00" and S21°49'00" E114°03'00" (Figure 6.2.1). The north-western section of Ningaloo Reef
consists of well-developed reef slope, reef flat and lagoon habitats with the reef crest varying in
distance from the mainland from between 200 m and 1.0 km. The water depth within habitats varies
from 1 m to 3.5 m in the lagoon, 0.1 m to 2 m on the reef flat and 3 m to 15 m on the reef slope.
Sites were distributed amongst the three habitats based on prior knowledge of the distribution of
coral assemblages within each habitats. More sites were located in habitats with higher percentage
coral cover (reef flat) and fewer sites were located in habitats with lower percentage coral cover
(inshore; see Table 6.2.1). Annual rainfall in the region is extremely low (<300 mm), but the region is
subject to frequent tropical cyclones (0.5 per year) during which rainfall can exceed 100 mm.
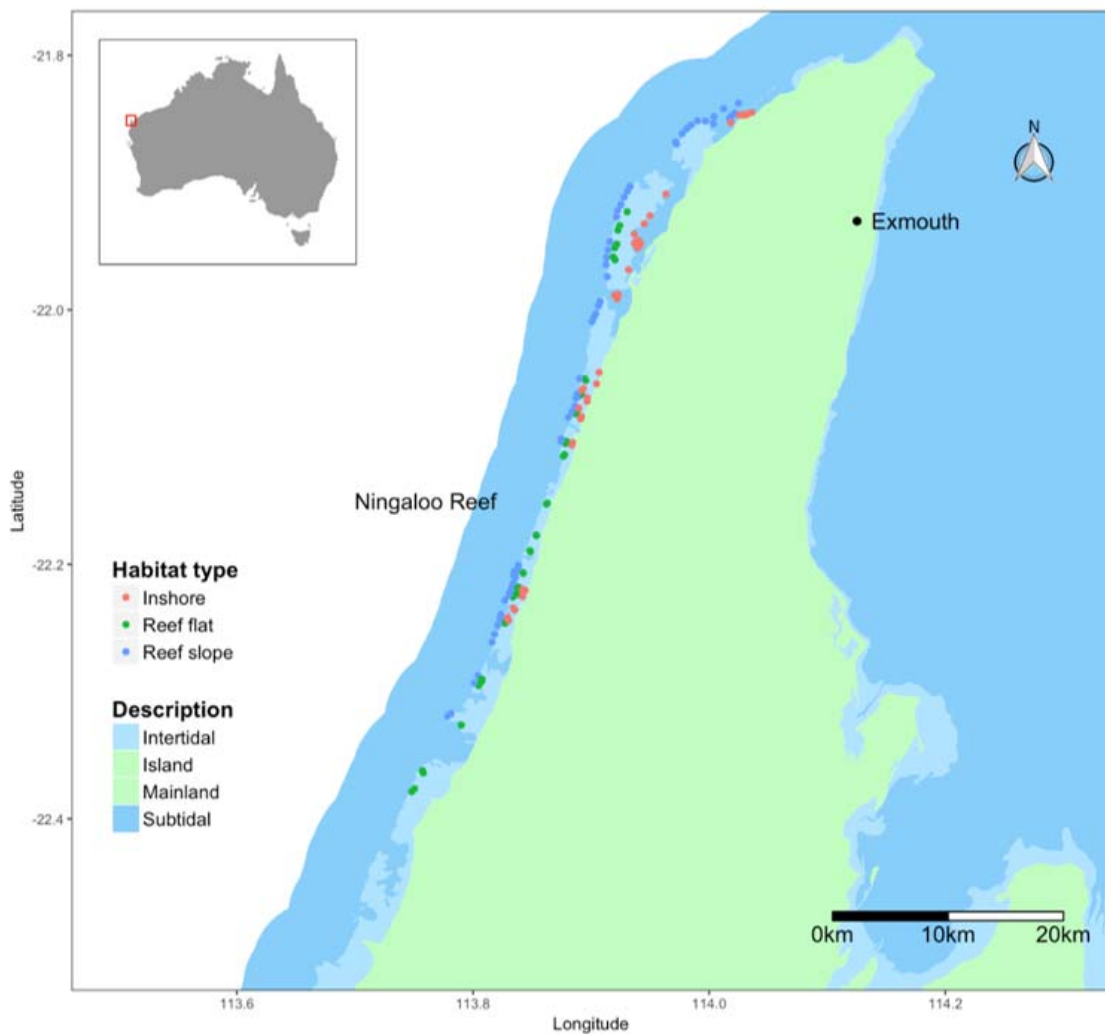
**Figure 6.2.1 Map showing the location of the study sites within reef slope, reef flat and inshore habitats at
Ningaloo Reef, Western Australia.**

Benthic surveys

Coral assemblages were surveyed using photographic line transects of between 25 m and 30 m in length. A total of 818 transects were completed between March 2007 and May 2016 with transects stratified among the three major habitats (reef slope, reef flat and inshore) based on the abundance of coral (measured as percentage cover of living hard coral) within each habitat, i.e. more transects were conducted in habitats featuring higher percentage cover (Table 6.2.1). To quantify percentage cover, photographs were taken at approximately 0.5 m intervals along each transect. To ensure replicates were independent, photographs were randomly selected within each transect (32 photographs) and the genus of any scleractinian (hard) corals was recorded for five (2007 and 2008 data) or six (2011 to 2016 data) fixed points per photograph using the software Transect Measure™ (www.seagis.com.au), i.e. 160 or 180 points per transect.

Table 6.2.1 The number and percentage of transects surveyed within each year for the three major habitats (inshore, reef flat, reef slope). The timing of the marine heatwave in relation to the sampling timing is shown.

YEAR	SURVEY DATES	INSHORE	REEF FLAT	REEF SLOPE	TOTAL
2007	April and May	NA	106/100%	NA	106 / 100%
2008	Feb and Oct	24/26%	50/54%	18/20%	92 / 100%
2009	NA	NA	NA	NA	NA
2010	NA	NA	NA	NA	NA
-----------------------------	*Marine heatwave March 2011*	--------------------			
2011	April	6/10%	54/90%	NA	60 / 100%
2012	NA	NA	NA	NA	NA
2013	May and June	NA	115/79%	29/21%	144 / 100%
2014	March and May	NA	129/100%	NA	129 / 100%
2015	April and Oct	54/30%	99/56%	77/24%	184 / 100%
2016	March and May	17/16%	52/50%	34/33%	103 / 100%
Total		**84 / 10%**	**610 / 74%**	**124 / 18%**	**818 / 100%**

Percent cover of functional groups

Coral genera were assigned to one of four life-history groups based on the classifications described in Darling et al. (2012): competitive, stress-tolerant, weedy and generalist (Table 6.2.2). Life-history traits were then inferred from the life-history classifications. In the two circumstances where genera contained species which were distributed between to two or more functional groups i.e. *Acropora* and *Pocillopora*, the genera were assigned to the functional group of the most abundant species within that genus i.e. *Acropora = Acropora spicifera =* Competitive functional group. **Competitive corals** typically have fast growth rates, reproduce by broadcast spawning and are most abundant at shallow depths. In shallow water, this group can quickly dominate available space. However, this group is also extremely sensitive to physical damage (Madin and Connolly 2006), coral bleaching-induced mortality (McClanahan et al. 2007), predation by crown-of-thorns starfish (De'ath et al. 2012) and *Drupella spp.*, and coral disease. In the Indo-Pacific, this group includes the genera *Montipora, Pocillopora*, *Turbinaria* and some species of *Acropora*. **Stress-tolerant corals** typically

Table 6.2.2 The 31 coral groups recorded during surveys at northern Ningaloo between 2007 and 2016 with their life-history*, typical growth form*, susceptibility to physical damage**, susceptibility to coral bleaching*** and reproductive mode**** provided.

BENTHIC GROUP	LIFE-HISTORY*	GROWTH FORM	PHYSICAL DAMAGE SUSCEPTIBILITY**	CORAL BLEACHING SUSCEPTIBILITY***	REPRODUCTIVE MODE****
Isopora	Competitive	encrusting, branching	low	low	Brooding
Turbinaria	Competitive	sheets	high	low	Broadcast spawning
Heliopora	Competitive	sheets, bushes	high	medium	Broadcast spawning
Acropora	Competitive	sheets, bushes, branching	medium to high	high	Broadcast spawning
Hydnophora	Generalist	branching	high	low to medium	Broadcast spawning
Montipora	Generalist	branching	high	medium to high	Broadcast spawning
Echinopora	Generalist	branching, small bushes	high	low	Broadcast spawning
Merulina	Generalist	encrusting	low to medium	medium	Broadcast spawning
Montipora	Generalist	encrusting, sheets	low	medium to high	Broadcast spawning
Pachyseris	Generalist	sheets	medium	high	Broadcast spawning
Coscinarae	Generalist	encrusting, sheets	low	high	Broadcast spawning
Diploastrea	Stress-tolerant	massive	low	low	Broadcast spawning
Echinophyllia	Stress-tolerant	encrusting, sheets	high	low	Broadcast spawning
Porites	Stress-tolerant	massive	low	low	Broadcast spawning
Coeloseris	Stress-tolerant	massive	medium	low	Broadcast spawning
Cyphastrea	Stress-tolerant	massive	low	low	Brooding
Favia	Stress-tolerant	massive	low	medium	Brooding
Favites	Stress-tolerant	massive	low	low to medium	Broadcast spawning
Galaxea	Stress-tolerant	massive	low	medium	Broadcast spawning

Goniastrea	Stress-tolerant	massive	low	low to medium	Broadcast spawning
Leptoria	Stress-tolerant	massive	medium	medium	Broadcast spawning
Lobophyllia	Stress-tolerant	massive	low to medium	high	Broadcast spawning
Montastrea	Stress-tolerant	massive	low	medium	Broadcast spawning
Platygyra	Stress-tolerant	massive	low	medium	Broadcast spawning
Favia	Stress-tolerant	encrusting	low	low to medium	Broadcast spawning
Pavona	Stress-tolerant	sheets	medium	medium	Broadcast spawning
Fungia	Stress-tolerant	solitary	medium	low	Broadcast spawning
Seriatopora	Weedy	branching	high	high	Brooding and spawning
Stylophora	Weedy	branching	medium	high	Brooding
Leptastrea	Weedy	massive	medium	low	Broadcast spawning
Pocillopora	Weedy	small bushes	medium	medium to high	Brooding

Reference sources
* (Darling et al. 2012)
** (Madin et al. 2016)
*** (Madin et al. 2016)
**** (Baird et al. 2009; Gilmour et al. 2016; Madin et al. 2016)

have slow growth rates, reproduce by broadcast spawning, have high fecundity, form massive-shaped colonies and can attain a large maximum size. These traits are considered advantageous for survival in harsh environments (van Woesik et al. 2012). This group includes *Porites, Favia, Favites, Platygyra* and *Goniastrea* in the Indo-Pacific. **Weedy corals** typically have slow to moderate growth rates, reproduce by brooding larvae, have small colony sizes and are considered to opportunistically colonise recently disturbed habitats more so than other groups (Darling et al. 2012). In the Indo-Pacific, this group includes *Stylophora, Seriatopora, Leptastrea* and most species of *Pocillopora.* **Generalist corals** typically have moderate growth rates and can attain large maximum colony sizes. This group shares many of the traits exhibited by the other three groups and includes *Echinopora, Hydnophora, Montipora* and *Pachyseris* in the Indo-Pacific. Coral genera recorded in our study which had not been assigned to a functional group in Darling et al. (2012), were assigned to one of the four life-history groups based on four of their documented life history traits (Madin et al. 2016) which were considered most important for predicting their response to disturbance: growth form, susceptibility to physical damage, susceptibility to bleaching and reproductive mode (Darling et al. 2012; see Table 6.2.2 for categories).

Changes in abundance of coral genera and functional groups

Broad-scale changes in taxonomic and functional composition of coral assemblages were analysed over the 10-year period (2007–2016) using two techniques. Firstly, we used Multivariate Auto-Regressive State-Space modelling (MARSS package in R; Holmes et al. 2012) to assess the rate and direction of change and statistical significance of these rates of change within coral genera and functional groups. MARSS is well suited to the analysis of ecological time-series data sets as it is designed to accommodate missing observations and observation error variance that cannot be estimated or known *a priori* (Holmes et al. 2012). We used data averaged for each year (when there were more than one survey per year) and *NA* for missing years (years with no data). Because the proportion of sampling within each habitat was similar pre- and post-heatwave (10% inshore, 70% reef flat, 20% reef slope), and we were interested in identifying only linear trends in the change in abundance of taxonomic and functional groups over the 10 years, data were pooled for all habitats. MARSS provides confidence intervals for estimates of *U* (annual rates of change), with an assumption that (the logarithm of) the data is approximated by a linear process with Gaussian errors. To assess the statistical significance of *U* we used a bootstrapping approach (n=1000), which consists of generating an ensemble of surrogate time series and comparing the trend of the observed data against the distribution of trends computed from the surrogate time series (Unsworth et al. 2001). The surrogate time series are generated by shuffling the observations with respect to time; i.e. we keep the set of observations, but we randomly shuffle their time indices. This results in a new time series with the same observations (including observation errors), but random time ordering. We then used the same MARSS approach to calculate *U* for the new time series and repeat this 999 times to assess whether the observed *U* fits within the distribution of *U* from this reshuffling process.

Secondly, to identify differences in the coral assemblages between years, we used E-Primer V7 to conduct an analysis of similarity (ANOSIM and SIMPER) using a Bray-Curtis similarity/dissimilarity index calculated on square-root transformed percent cover data (Anderson et al. 2008). To accommodate for missing year values (Table 6.2.1) and to allow for the detection of change between coral assemblages pre- and post-heatwave (March 2011), data were pooled into four time-steps (07/08, 11/12, 13/14, 15/16; Table 6.2.1). A pairwise analysis was used to quantify the degree of similarity between coral assemblages between the four time-steps.

6.2.3 RESULTS

Trends in taxonomic and functional groups

Trends were identified in the functional group analysis which were not evident in the taxonomic group analysis. Estimates of the annual trend *(U)* for the taxonomic groups indicated an annual decrease of *Acropora* corals (-0.11) and *Turbinaria* corals (-0.09) and no change in any of the other taxonomic groups (Table 6.2.3). In contrast, estimates of annual trend indicated a decrease in competitive corals (-0.12) alongside an annual increase in generalist corals (0.14). The increase in generalist corals was recorded despite there being no trend in taxonomic groups within the generalist group (Table 6.2.3).

Table 6.2.3 Estimated annual change *U* for the 12 most abundant coral groups and the four functional groups, along with probability (p) that *U* exceeds the distribution of values from a reshuffling process (1000x). Competitive coral groups are shown in blue, generalist coral groups are shown in red. Those that are significant at the p = 0.05 level are shown in bold.

	U	p
Taxonomic group		
Acropora	**-0.11**	**0.01**
Turbinaria	**-0.09**	**0.02**
Goniastrea	-0.02	0.19
Favites	-0.02	0.31
Millepora	-0.01	0.44
Montipora	0.01	0.58
Favia	0.04	0.83
Platygyra	0.04	0.84
Echinopora	0.12	0.92
Leptastrea	0.99	0.97
Pocillopora	0.07	0.98
Porites	0.21	0.99
Functional group		
Competitive	**-0.12**	**0.01**
Weedy	0.14	0.24
Generalist	**0.14**	**0.02**
Stress-tolerant	0.08	0.31

The percentage cover of hard coral declined consistently throughout the 10-year survey period from a 29% ± 1.40% (mean ± SE) in 2007 to 13% ± 0.52% in 2016 (Figure 6.2.2). Declines in hard coral cover were largely due to declines in the cover of the dominant hard coral genera *Acropora*, and to a lesser extent, *Turbinaria* (Figure 6.2.2). The cover of *Acropora* declined from a mean of 25% ± 1.31% in 2007 to approximately 10% ± 0.70% in 2016. *Turbinaria* cover declined consistently throughout the survey period at a rate of -0.09% per year (Figure 6.2.3). No change was observed in the cover of the remaining coral groups over the 10-year period (Table 6.2.3).
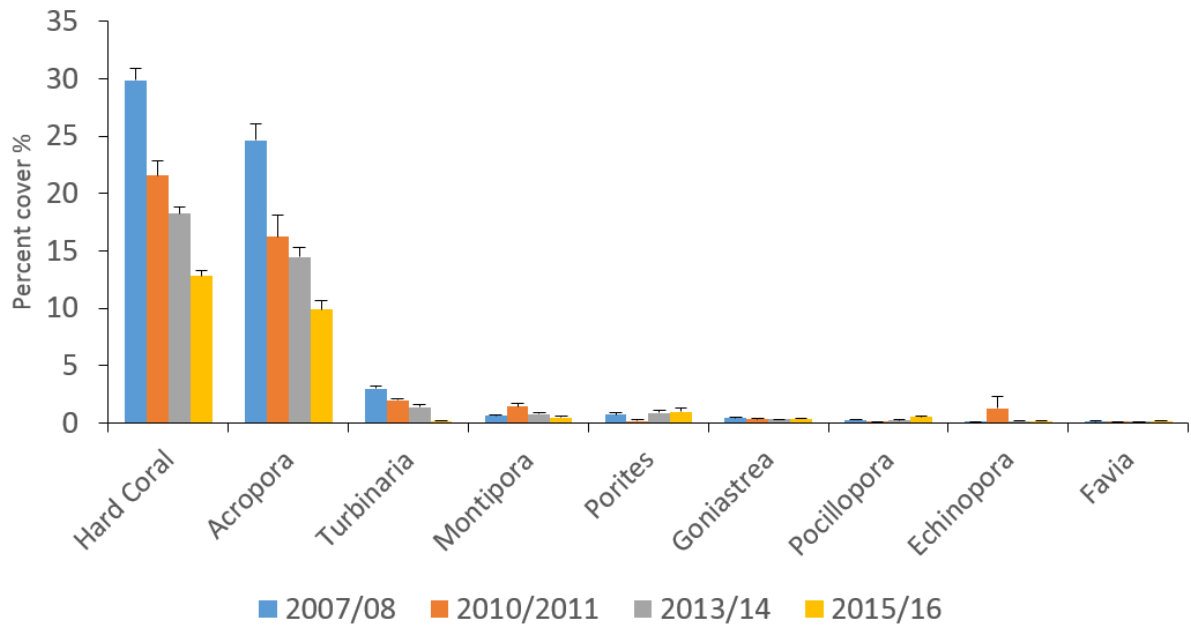
Figure 6.2.2 Mean percent cover (± SE) of hard coral cover and individually for the eight dominant coral genera observed at northern Ningaloo Reef between 2007 and 2016.
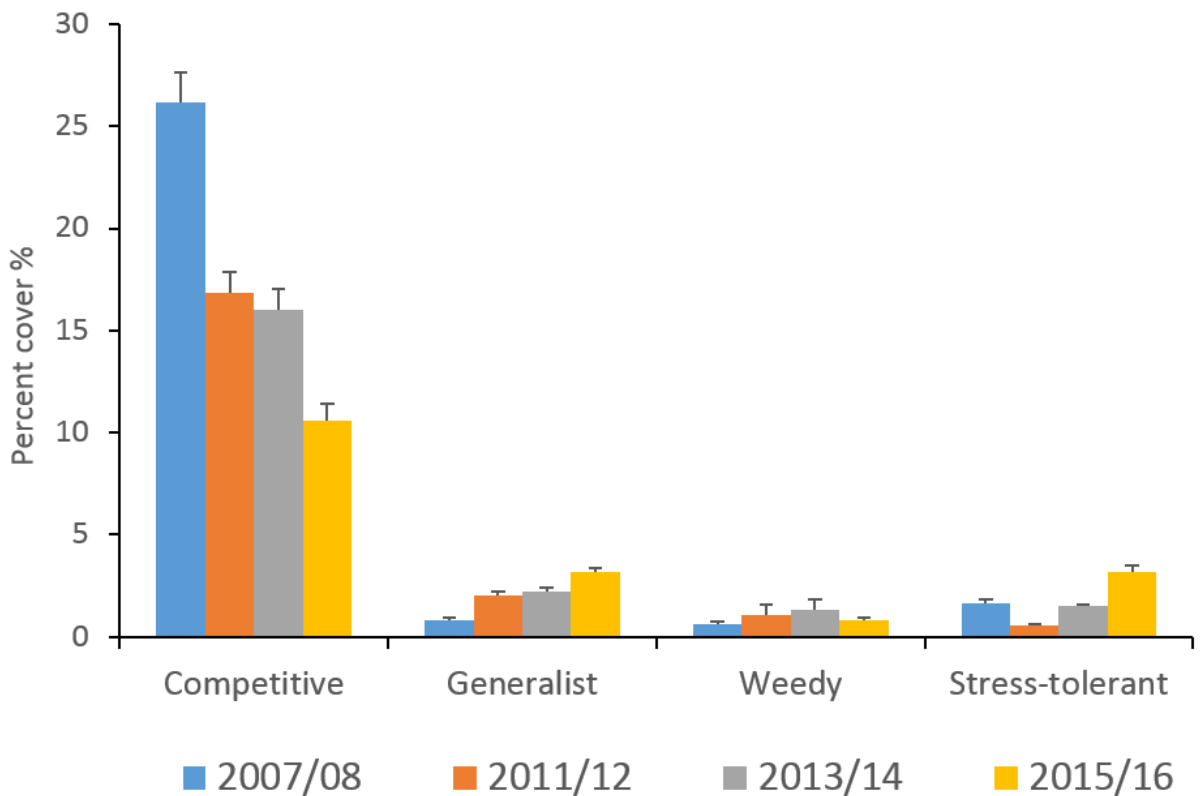
Figure 6.2.3 Mean percent cover (±SE) of the four functional groups at northern Ningaloo Reef between 2007 and 2016.

Strong trends were observed in the cover of different functional groups over the 10-year period. The percentage cover of competitive corals declined from 26% ± 1.46% in 2007 to 10% ± 0.83% in 2016

(Figure 6.2.3). Increases in the cover of generalist and stress-tolerant functional groups were also observed, however, only the increase in generalist corals was significant at the $p < 0.05$ level (Table 6.2.4).

Differences were observed between coral assemblages pre- and post-heatwave (Table 6.2.4). ANOSIM and SIMPER analyses showed coral assemblages in all years (with the exception of 11/12 and 13/14) were statistically different, however, the low R (Rho) value (R<0.2) indicated marginal dissimilarity between some years (Table 6.2.4; Anderson et al. 2008). SIMPER analysis revealed that just four coral groups contributed to 90% of the dissimilarity between years: *Acropora, Montipora Turbinaria* and *Porites* (Supplementary Material Table S6.2.1).

Table 6.2.4 Results of ANOSIM analysis testing for differences in the coral assemblages at northern Ningaloo; pre- and post-disturbance event (March 2011 heatwave) and between all year groups. Groups which are statistically and ecologically dissimilar are shown in bold.

TAXONOMIC GROUPS	P	R (RHO)	PERM. #
Pre/Post heatwave (March 2011)	**<0.001**	**0.313**	**999**
07/08, 11/12	0.408	0.149	999
07/08, 13/14	**0.004**	**0.241**	**999**
07/08, 15/16	0.002	0.130	999
11/12, 13/14	0.408	0.001	999
11/12, 15/16	0.877	0.088	999
13/14, 15/16	**<0.001**	**0.217**	**999**

6.2.4   DISCUSSION

Functional group approaches for investigating temporal variability in coral assemblages have been proposed to offer new insights into patterns of function and diversity on coral reefs, and to provide a more mechanistic understanding of how coral assemblages respond to environmental change. Here, we provide evidence that the long-term decline in coral cover was associated with changes in the taxonomic and functional composition of coral assemblages at northern Ningaloo Reef. In particular, the generally fast-growing, competitive functional group showed the most significant decline over the 10-year study period, which may have decreased the capacity of coral assemblages to recover quickly from future perturbations due to the reduced abundance of the group with the greatest capacity to recover quickly following disturbance.

Overall, hard coral cover at northern Ningaloo Reef declined 11% between 2007 and 2016, and by 2015 had decreased to 13%. The average rate of change in hard coral cover during this study was -2.5% per year and although similar declines in the cover of hard coral have been recorded on the Great Barrier Reef (13.5%; De'ath et al. 2012), in the Caribbean (Gardner et al. 2003), in the Indo-Pacific (Bruno and Selig 2007) and, most recently, in the Eastern Indian Ocean (Speed et al. 2013), the annual rate of change in hard coral cover observed here is greater than that observed in many of these previous studies (maximum rate in other studies totaled <-1.5% per year). This is surprising given that Ningaloo Reef is considered to be largely unaffected by many of the pressures attributed with declines in hard coral cover in other locations, such as large-scale terrestrial run-off, nutrient input, high rates of sedimentation and crown-of-thorns starfish outbreaks (De'ath et al.

2012). One explanation for the higher rate of decline observed at northern Ningaloo Reef may be the disproportionate abundance of *Acropora* corals within coral assemblages. *Acropora* are highly susceptible to coral bleaching, physical damage, predation by corallivores and coral disease (Willis et al. 2004; Bruno et al. 2007; Graham et al. 2011). During this study period, coral assemblages at Ningaloo Reef have been subject to at least one coral bleaching event, several cyclones, a flood event and sustained high density of the corallivorous snail, *Drupella*. Most of these events had no immediate impact on coral assemblages within our study area (except nearby Bundegi Reef), however, aerial surveys conducted during the marine heatwave in 2011 indicated moderate levels of coral bleaching at multiple reef flat locations (Parks and Wildlife, 2011 unpublished data), so the long-term impact of this bleaching event on regenerative processes, such as coral recruitment and growth of *Acropora* corals, cannot be discounted.

Changes in the taxonomic composition of coral assemblages indicate that environmental conditions at northern Ningaloo Reef have become less favourable for two coral groups, *Acropora* and *Turbinaria*. The cover of *Acropora* declined from 24% in 2007 to 10% in 2016, at an average rate of -2% per year, while *Turbinaria* declined from 4% in 2007 to less than 1% in 2016. Similar declines in the cover of *Acropora* corals have been recorded on the Great Barrier Reef (Hughes at al. 2017), in the Red Sea (Cantin et al. 2011) and the Indian Ocean (Sheppard et al. 2003). These declines have been linked with reductions in reef complexity, reef fish abundance, fish diversity and the availability of food for coral feeding fish and invertebrates. A recent study at southern Ningaloo Reef also found that *Acropora* are particularly sensitive to small-scale water circulation patterns, with the most rapid decreases in the cover of *Acropora* occurring at locations with long water residence times (Shedrawi et al. 2017). Interestingly, the long-term declines in *Turbinaria* corals recorded in this study have not been reported elsewhere. *Turbinaria* and *Acropora* possess similar life-history traits in that they are fast growing, reproduce by broadcast spawning and have a high susceptibility to physical damage. However, unlike *Acropora*, *Turbinaria* are highly resistant to elevated water temperatures and the effects of coral bleaching and are often associated with more marginal reef environments. In north-western Australia, *Turbinaria* are also known to display different patterns of reproduction to most broadcast spawning corals (including *Acropora*) (Gilmour et al. 2016), which may influence patterns in the availability of new recruits to northern Ningaloo. These contrasting levels of susceptibility to coral bleaching and differences in reproductive patterns suggest the environmental conditions driving the observed declines in these two coral groups may be quite different.

The rate of decline in *Acropora* was variable over the 10-year period and indicated that specific disturbance events may have contributed disproportionately to the observed declines. Declines in the cover of *Acropora* were greatest pre- and post- heatwave in 2011. Previous studies investigating the impact of the heatwave on coral assemblages at north-western Ningaloo, found little to no short-term effects (Moore et al. 2012). However, this study acknowledged the potential for longer term, chronic impacts such as reduced growth rates and/or fecundity. Although we did not measure coral growth rates or fecundity during our study, corals are known to be particularly sensitive to the chronic effects of increased water temperatures and lowered salinity, and there is evidence of long-term suppression of coral growth rates in eastern Australia as a result of increased ocean temperatures (Cooper et al. 2008; De'ath et al. 2009). The chronic effects of the marine heatwave on coral growth at northern Ningaloo can therefore not be eliminated as possible causes of the observed decline in cover of *Acropora* and *Turbinaria* corals.

Changes in the functional composition of coral assemblages at northern Ningaloo Reef suggest a decreased ability to recover quickly from future disturbances. Over the 10-year period we recorded declines in the abundance of competitive corals at an average annual rate (U) of -0.12 per year, which equated to -1.6% per year. Competitive corals typically have fast growth rates, reproduce by broadcast spawning and have a high potential for rapid recolonisation and recovery following disturbance (e.g. Sheppard et al. 2002; Graham et al. 2011). The 16% decline in the cover of

competitive corals we observed could reasonably be expected to result in a net loss of capacity for rapid recruitment and growth. We do acknowledge, however, that recovery potential is influenced by not just the functional composition of the coral community, but also the level of connectivity between reefs, their physical characteristics, disturbance history, herbivore composition and anthropogenic influences. A recent meta-analysis looking at the recovery of coral assemblages at 48 locations around the world, found reefs in the eastern Pacific were slowest to recover following disturbance, largely due to their geographical isolation, low functional diversity and lack of corals with competitive functional traits (Graham et al. 2011). Although Ningaloo Reef is well connected with reefs to the north by a strong southward flowing current in most years (Feng et al. 2016), large declines in coral cover as a result of coral bleaching in 2011 and 2013 have been recorded to the north of Ningaloo (Speed et al. 2013, LaFratta et al. 2017, Ridgway 2016, Babcock et al. 2017) and thus, the capacity of reefs in this region to supply coral larvae to Ningaloo Reef has been substantially reduced.

Here, we detected changes in the functional composition of coral assemblages, some of which were not evident using a taxonomic based approach. Generalist corals increased at an average rate (U) of 0.14 per year, while there was no increase in any of the taxonomic coral groups. The lack of response in taxonomic groups could be due to a number of reasons, but it is most likely that the changes within taxonomic groups were too small to be detected at the p = 0.05 level. Only when taxonomic groups exhibiting generalist traits were grouped, did the response become detectable at the p = 0.05 level. It is also possible that functional groups may respond more quickly to changes in local environmental conditions than taxonomic groups, in which case it is reasonable to hypothesise that a change in the abundance of generalist corals would be detected prior to that of individual taxonomic groups. There is evidence that this may already be happening on many reefs throughout the Indo-Pacific with generalist, weedy and stress-tolerant corals replacing competitive corals on many reefs (McClanahan et al. 2007; Rachello-Dolmen and Cleary 2007; Alvarez-Filip et al. 2013). There is also evidence of competitive corals recovering quickly to pre-disturbance levels following major disturbances, but the frequency and cumulative impacts of disturbances is likely to affect their recovery and more research is required before we can be confident that functional groups can be used to predict long-term shifts in coral assemblages.

Our study provides evidence of long-term declines in *Acropora* and *Turbinaria* corals, corresponding to a shift away from corals with competitive life history traits in favour of corals with generalist life history traits. Importantly, we show that changes in the composition of coral assemblages can be detected using a functional based approach when changes are not evident using a taxonomic approach. We suggest that both approaches should be adopted to better understand the responses of both taxonomic and functional coral groups to future environmental change. Continued research is required to better comprehend if these changes represent the beginning of a longer-term shift in community composition, or simply the latter stages of a decade-long cycle of stochastic stability.

6.2.5 ACKNOWLEDGEMENTS

6.2.6 REFERENCES

Alvarez-Filip L, Carricart-Ganivet JP, Horta-Puga G, Iglesias-Prieto R (2013) Shifts in coral-assemblage composition do not ensure persistence of reef functionality. Scientific Reports 3: 3486.

Anderson MJ, Gorley RN, Clarke KR (2008) PERMANOVA+ for PRIMER: guide to software and statistical methods. PRIMER-E: Plymouth, UK.

Armstrong S (2007) Ningaloo Marine Park *Drupella* long-term monitoring program: results of the 2006 survey. NIN/NMP-2007/03 Marine Science Program, Department of Environment and Conservation, Perth, Western Australia (unpublished report).

Baird AH, Guest JR, Willis BL (2009) Systematic and biogeographical patterns in the reproductive biology of scleractinian corals. Annual Review of Ecology, Evolution, and Systematics 40: 551 - 571.

Bruno JF and Selig ER (2007) Regional decline of coral cover in the Indo-Pacific: Timing, extent, and subregional comparisons. Plos One 2(8): e711.

Bruno JF, Selig ER, Casey KS, Page CA, Willis BL, Harvell CD, Sweatman H, Melendy AM (2007) Thermal stress and coral cover as drivers of coral disease outbreaks. PLOS Biology 5(6): e124.

Cantin NE, Cohen AL, Karnauskas KB, Tarrant AM, McCorkle DC (2010) Ocean warming slows coral growth in the central Red Sea Science 329: 322–325.

Cooper TF, De'Ath G, Fabricius KE, Lough JM (2008). Declining coral calcification in massive *Porites* in two nearshore regions of the northern Great Barrier Reef. Global Change Biology 14(3): 529-538.

Darling ES, Alvarez-Filip L, Oliver TA, McClanahan TR, Côté IM (2012) Evaluating life-history strategies of reef corals from species traits. Ecology Letters 15(12): 1378-1386.

De'ath G, Fabricius KE, Sweatman H, Puotinen M (2012) The 27–year decline of coral cover on the Great Barrier Reef and its causes. Proceedings of the National Academy of Sciences 109(44): 17995-17999.

De'ath G, Lough JM, Fabricius KE (2009) Declining coral calcification on the Great Barrier Reef. Science 323, 116–119.

Depczynski M, Gilmour JP, Ridgway T, Barnes H, Heyward AJ, Holmes TH, Moore JAY, Redford BT, Thomson DP, Tinkler P, Wilson SK (2013) Bleaching, coral mortality and subsequent survivorship on a West Australian fringing reef. Coral Reefs 32(1): 233-238.

Fabricius KE (2005) Effects of terrestrial runoff on the ecology of corals and coral reefs: review and synthesis. Marine Pollution Bulletin 50(2): 125-146.

Feng M, Colberg F, Slawinski D, Berry O, Babcock R (2016) Ocean circulation drives heterogeneous recruitments and connectivity among coral populations on the North West Shelf of Australia. Journal of Marine Systems. 164:1-12.

Gardner TA, Côté IM, Gill JA, Grant A, Watkinson AR (2003) Long-term region-wide declines in Caribbean corals. Science 301(5635): 958-960.

Gilmour J, Speed CW, Babcock R (2016) Coral reproduction in Western Australia. PeerJ 4: e2010.

Gilmour JP, Smith LD, Heyward AJ, Baird AH, Pratchett MS (2013) Recovery of an isolated coral reef system following severe disturbance. Science 340(6128): 69-71.

Graham NAJ, Nash KL, Kook JT (2011) Coral reef recovery dynamics in a changing world. Coral Reefs 30(2): 283-294.

Hajime K, Saki H, Ide Y, Akimoto F (2002) Recovery of coral populations after the 1998 bleaching on Shiraho Reef, in the southern Ryukyus, NW Pacific. Marine Ecology Progress Series 239: 93-103.

Harmelin-Vivien ML (1994) The effects of storms and cyclones on coral reefs: a review. Journal of Coastal Research: 211-231.

Hoey AS, Howells E, Johansen JL, Hobbs JPA, Messmer V, McCowan DM, Wilson SK, Pratchett MS (2016) Recent advances in understanding the effects of climate change on coral reefs. Diversity 8(2): 12.

Holmes EE, Ward EJ and Wills K (2012) MARSS: Multivariate autoregressive state-space models for analyzing time-series data. R Journal 4: 11-19.

Lafratta, A., Fromont, J., Speare, P., & Schönberg, C. H. L. (2017). Coral bleaching in turbid waters of north-western Australia. Marine and Freshwater Research, 68(1), 65-75.

Lozano-Montes HM, Keesing JK, Grol MG, Haywood MDE, Vanderklift MA, Babcock RC et al. (2017) Limited effects of an extreme flood event on corals at Ningaloo Reef. Estuarine, Coastal and Shelf Science 191: 234-238.

Madin JS and Connolly SR (2006) Ecological consequences of major hydrodynamic disturbances on coral reefs. Nature 444(7118): 477-480.

Madin JS, Hoogenboom MO, Connolly SR, Darling ES, Falster DS, Huang D, Keith SA, Mizerek T, Pandolfi JM, Putnam HM, Baird AH (2016) A trait-based approach to advance coral reef science. Trends in Ecology & Evolution 31(6): 419-428.

McClanahan TR, Ateweberhan M, Muhando CA, Maina J, Mohammed MS (2007) Effects of climate and seawater temperature variation on coral bleaching and mortality. Ecological Monographs 77(4): 503-525.

McClanahan TR, Baird AH, Marshall PA, Toscano MA (2004) Comparing bleaching and mortality responses of hard corals between southern Kenya and the Great Barrier Reef, Australia." Marine Pollution Bulletin 48(3-4): 327-335.

McCook LJ (1999) Macroalgae, nutrients and phase shifts on coral reefs: scientific issues and management consequences for the Great Barrier Reef. Coral Reefs 18(4): 357-367.

Moore JAY, Bellchambers LM , Depczynski MR, Evans RD, Evans SN, Field SN, Friedman KJ, Gilmour JP, Holmes TH, Middlebrook R, Radford BT, Ridgway T, Shedrawi G, Taylor H, Thomson DP, Wilson SK (2012) Unprecedented mass bleaching and loss of coral across 12° of latitude in Western Australia in 2010-11. Plos One 7(12): e51807.

Onton K, Page CA, Wilson SK, Neale S, Armstrong S (2011) Distribution and drivers of coral disease at

Ningaloo Reef, Indian Ocean. Marine Ecology Progress Series 433: 75-84.

Osborne K, Dolman AM, Burgess SC, Johns KA (2011) Disturbance and the dynamics of coral cover on the Great Barrier Reef (1995–2009). Plos One 6(3): e17516.

Pandolfi JM, Bradbury RH, Sala E, Hughes TP, Bjorndal KA, Cooke RG, McArdle D, McClenachan L, Newman MJ, Paredes G, Warner RR, Jackson JB (2003) Global trajectories of the long-term decline of coral reef ecosystems. Science 301(5635): 955-958.

Perry CT, Murphy GN, Kench PS, Smithers SG, Edinger EN, Steneck RS, Mumby PJ (2013) Caribbean-wide decline in carbonate production threatens coral reef growth. 4: 1402.

Pollock FJ, Lamb JB, Field SN, Heron SF, Schaffelke B, Shedrawi G, Bourne DG, Willis BL (2014) Sediment and turbidity associated with offshore dredging increase coral disease prevalence on nearby reefs. Plos One 9(7): e102498.

Pratchett MS, Trapon M, Berumen ML, Chong-Seng K (2011) Recent disturbances augment community shifts in coral assemblages in Moorea, French Polynesia. Coral Reefs 30(1): 183-193.

Rachello-Dolmen PG and Cleary DFR (2007) Relating coral species traits to environmental conditions in the Jakarta Bay/Pulau Seribu reef system, Indonesia. Estuarine, Coastal and Shelf Science 73(3): 816-826.

Ridgway, T., Inostroza, K., Synnot, L., Trapon, M., Twomey, L., & Westera, M. (2016). Temporal patterns of coral cover in the offshore Pilbara, Western Australia. *Marine Biology*, *163*(9), 182.

Riegl B and Purkis S (2015) Coral population dynamics across consecutive mass mortality events. Global Change Biology 21(11): 3995-4005.

Sampayo EM, Ridgway T, Bongaerts P, Hoegh-Guldberg O (2008) Bleaching susceptibility and mortality of corals are determined by fine-scale differences in symbiont type. Proceedings of the National Academy of Sciences of the United States of America 105(30): 10444-10449.

Shedrawi G, Falter JL, Friedman KJ, Lowe RJ, Pratchett MS, Simpson CJ, Speed CW, Wilson SK, Zhang Z (2017) Localised hydrodynamics influence vulnerability of coral assemblages to environmental disturbances. Coral Reefs: 1-12.

Sheppard CRC, Spalding M, Bradshaw C, Wilson S (2002) Erosion vs. recovery of coral reefs after 1998 El Nino: Chagos reefs, Indian Ocean. Ambio 31(1): 40-48.

Sheppard, C.R.C. Predicted recurrences of mass coral mortality in the Indian Ocean (2003) Nature 425: 294–297.

Speed CW, Babcock RC, Bancroft KP, Beckley LE, Bellchambers LM, Depczynski M, Field SN, Friedman KJ, Gilmour JP, Hobbs JPA, Kobryn HT, Moore JAY, Nutt CD, Shedrawi G, Thomson DP, Wilson SK (2013) Dynamic Stability of Coral Reefs on the West Australian Coast. Plos One 8(7): e69863.

Stocker TF, Qin D, Plattner GK, Tignor MMB, Allen SK, Boschung J, Nauels A, Xia Y, Bex V, Midgley PM (2013) Technical Summary. Climate Change 2013: The Physical Science Basis. Contribution

of Working Group I to the Fifth Assessment Report of the Intergovernmental Panel on Climate Change. Stocker TF, Qin D, Plattneret GK et al. Cambridge, United Kingdom and New York, NY, USA, Cambridge University Press: 33–115.

Trapon ML, Pratchett MS, Penin L (2010) Comparative effects of different disturbances in coral reef habitats in Moorea, French Polynesia. Journal of Marine Biology 2011: 807625.

Unsworth CP, Cowper MR, McLaughlin S, Mulgrew B (2001) A new method to detect nonlinearity in a time-series: synthesizing surrogate data using a Kolmogorov–Smirnoff tested, hidden Markov model. Physica D: Nonlinear Phenomena 155: 51–68.

Willis BL, Page CA, Dinsdale EA (2004) Coral disease on the Great Barrier Reef. In: Coral health and disease. Rosenberg E, Loya Y (eds). Springer-Verglag, Heidelberg, pp. 69-104.

Van Woesik R, Irikawa A, Anzai R, Nakamura T (2012) Effects of coral colony morphologies on mass transfer and susceptibility to thermal stress. Coral Reefs: 31(3): 633-639.

6.2.7 SUPPLEMENTARY MATERIAL

Table S6.2.1 Results of the SIMPER analysis testing for differences in the coral communities among group years. Listed are the top 5-6 coral groups which contributed most to the dissimilarity between years.

Groups 2007/08 & 2011/12. Average dissimilarity = 60.19

CORAL GROUP	AV.ABUND	AV.ABUND	AV.DISS	DISS/SD	CONTRIB%	CUM.%
Acropora	4.31	3.50?	24.47	1.09	40.65	40.65
Montipora	0.37	0.81	6.20?	0.87	10.30	50.96
Turbinaria	0.52	0.42	5.09	0.77	8.46	59.42
Porites	0.45	0.14	3.62	0.62	6.02	65.43
Goniastrea	0.33	0.28	3.47	0.66	5.77	71.20

Groups 2007/08 & 2013/14. Average dissimilarity = 62.11

CORAL GROUP	AV.ABUND	AV.ABUND	AV.DISS	DISS/SD	CONTRIB%	CUM.%
Acropora	4.31	3.20	25.76	1.10	41.47	41.47
Turbinaria	0.52	0.63	7.01	0.68	11.28	52.75
Montipora	0.37	0.52	5.06	0.71	8.15	60.90
Porites	0.45	0.35	4.84	0.57	7.79	68.69
Goniastrea	0.33	0.27	3.57	0.59	5.74	74.43

Groups 2011/12 & 2013/14. Average dissimilarity = 59.60

CORAL GROUP	AV.ABUND	AV.ABUND	AV.DISS	DISS/SD	CONTRIB%	CUM.%
Acropora	3.50	3.20	22.74	1.12	38.16	38.16
Montipora	0.81	0.52	6.86	0.99	11.52	49.68
Turbinaria	0.42	0.63	6.53	0.71	10.96	60.63
Goniastrea	0.28	0.27	3.75	0.63	6.30	66.93
Echinopora	0.47	0.10	3.52	0.38	5.91	72.84

Groups 2007/08 & 2015/16. Average dissimilarity = 67.62

CORAL GROUP	AV.ABUND	AV.ABUND	AV.DISS	DISS/SD	CONTRIB%	CUM.%
Acropora	4.31	2.53	26.59	1.15	39.32	39.32
Porites	0.45	0.88	7.32	0.73	10.83	50.15
Turbinaria	0.52	0.12	4.24	0.53	6.27	56.41
Montipora	0.37	0.35	4.01	0.58	5.92	62.34
Goniastrea	0.33	0.33	3.70	0.64	5.48	67.81
Pocillopora	0.23	0.36	3.13	0.68	4.64	72.45

Groups 2011/12 & 2015/16. Average dissimilarity = 67.10

CORAL GROUP	AV.ABUND	AV.ABUND	AV.DISS	DISS/SD	CONTRIB%	CUM.%
Acropora	3.50	2.53	22.97	1.11	34.23	34.23
Porites	0.14	0.88	6.64	0.72	9.90	44.13
Montipora	0.81	0.35	6.38	0.93	9.51	53.63
Goniastrea	0.28	0.33	3.95	0.65	5.88	59.52
Turbinaria	0.42	0.12	3.78	0.64	5.63	65.15
Echinopora	0.47	0.14	3.69	0.40	5.49	70.64

Groups 2013/14 & 2015/16. Average dissimilarity = 68.14

CORAL GROUP	AV.ABUND	AV.ABUND	AV.DISS	DISS/SD	CONTRIB%	CUM.%
Acropora	3.20	2.53	23.30	1.06	34.20	34.20
Porites	0.35	0.88	7.76	0.71	11.39	45.59
Turbinaria	0.63	0.12	6.16	0.57	9.04	54.63
Montipora	0.52	0.35	5.01	0.81	7.35	61.98
Goniastrea	0.27	0.33	4.11	0.59	6.03	68.01
Pocillopora	0.18	0.36	3.19	0.65	4.67	72.69

6.3 Limited effects of an extreme flood event on corals at Ningaloo Reef

Authors: Lozano-Montes HM, Keesing JK, Grol MG, Haywood MDE, Vanderklift MA, Babcock RC, Bancroft K.

ABSTRACT

In late April 2014 Ningaloo Reef was exposed to significant freshwater and sediment outflow following an extreme rainfall event (>200 mm in 48 h). It produced a plume of brown water of 9.63 km^2 that was that present two days after the rainfall event. The extent of the plume decreased by 55.9% within ten days, indicating that it was rapidly dispersed. Benthic surveys were conducted at eleven sites along Ningaloo (three of them within the plume and eight out of the plume) using 25 m line transects to assess the percentage cover of all major benthic encrusting organisms, including hard corals, soft corals, algae, turf and sponges. Results from the May 2014 survey (approximately one month after the flooding) were compared with the March 2014 survey (before the extreme rainfall event). Corals from the genus *Acropora* were the dominant species in the coral assemblages surveyed. Our results indicate that *Acropora* coral cover did not vary significantly between sites inside and outside of the plume. Non-*Acropora* coral cover estimated after the flooding varied significantly among plume and non-plume sites. Patterns of *Acropora* and non-*Acropora* coral covers between plume and non-plume sites were already present before the flood with a trend to be higher in the northern region. The results show that the coral reefs at Ningaloo resisted the impact of a flooding with limited damage.

6.3.1 INTRODUCTION

Extreme events, such as cyclones and heavy rain, can strongly influence the structure and dynamics of coral reefs (Jones and Berkelmans 2014). Disturbances due to extreme events can result in degradation of coral reefs by causing coral mortality (Jones et al., 2011; Butler et al., 2013). Heavy rainfall events can form flood plumes that bring low salinity water, nutrients, suspended sediments and toxicants to coral reefs (Devlin et al. 1998). Flood plumes can cause bleaching (van Woesik et al. 1995; Berkelmans and Oliver 1999; Butler et al. 2013), reduce light availability and increase growth rates of micro- and macroalgae (Madin and Connolly 2006). In general, corals are thought to be negatively affected by chronic sediment deposition rates greater than 10mg cm^{-2} day-^{1} and total suspended solids (SST) above 10 mg.L^{-1} (Rogers 1990), but this is highly dependent on sediment properties, with finer sediments causing greater damage (Weber e al. 2006). Recent experiments with coral species found that full colony mortality for colonies of *Montipora aequituberculata* occurred at 30 mg.L^{-1} SST, and for *Acropora millepora* at 100 mg.L^{-1} TSS after 12 weeks (Flores et al. 2012). However, these experiments used corals taken from offshore reefs, which may be less adapted to high sedimentation environments (Weber et al. 2006). Turbidity alone is not necessary an adequate measure of negative conditions to coral reefs, as particle size, contaminants and organic content of the suspended sediments are crucial factors in determining the extent of damage in corals (Weber et al. 2012).

An extreme rainfall event that occurred on April 27 2014 (207 mm within 48 hours; www.australia.gov.au/bom) caused major flooding on land, and produced flood plumes that were estimated by remote sensing imagery (Landsat 7—29 April 2014) up to 50 km long on the west coast of the North West Cape and 70 km long in Exmouth Gulf (Figure 6.3.1). Western Australia rainfall data were accessed from the Australian Government Bureau of Meteorology website (www.australia.gov.au/bom). The objective of this study, conducted one month after the peak flooding occurred in April 27th 2014 (Government Bureau of Meteorology), was to investigate the potential effects of a flood plume on the cover of reef-building corals of Ningaloo Reef.

6.3.2 METHODS

Site description

Ningaloo Reef lies on the western coast of Australia and it stretches over 290 kilometres from North West Cape (22.23°S, 113.96°E) to Red Bluff (24.18°S, 113.28°E). It is the largest fringing coral reef in Australia. The reef tract runs parallel to the cost line and consists of a barrier reef ~1–6 km offshore (average 2.5km width), backed by a shallow, sedimentary lagoon (mean depth about 2m) with occasional patch and nearshore platform reefs (Taebi et al. 2011). Surface currents are primarily shoreward over the reef flat, alongshore in the lagoon and then offshore out through reef channels (Taebi et al. 2011). This circulation pattern is primarily caused by breaking waves, with tides playing a secondary role and minimal wind driven effects (Taebi et al. 2011). The coral reefs of Ningaloo reef are predominantly in good condition and are exposed to fewer local impacts than most other reefs around the world (Wilkinson et al. 2004).

Study methods

Surveys were conducted by CSIRO and Department of Biodiversity, Conservation and Attractions (DBCA) on the inshore reefs in the Mandu, Mangrove Bay and Tulki regions of the Ningaloo Marine Park (Figure 6.3.1). The percentage cover of corals and other benthos of these three regions have been measured during most years since 2007. Data for the present study was collected in March

2014 (before the extreme rainfall event) and in May 2014 (approximately one month after event).
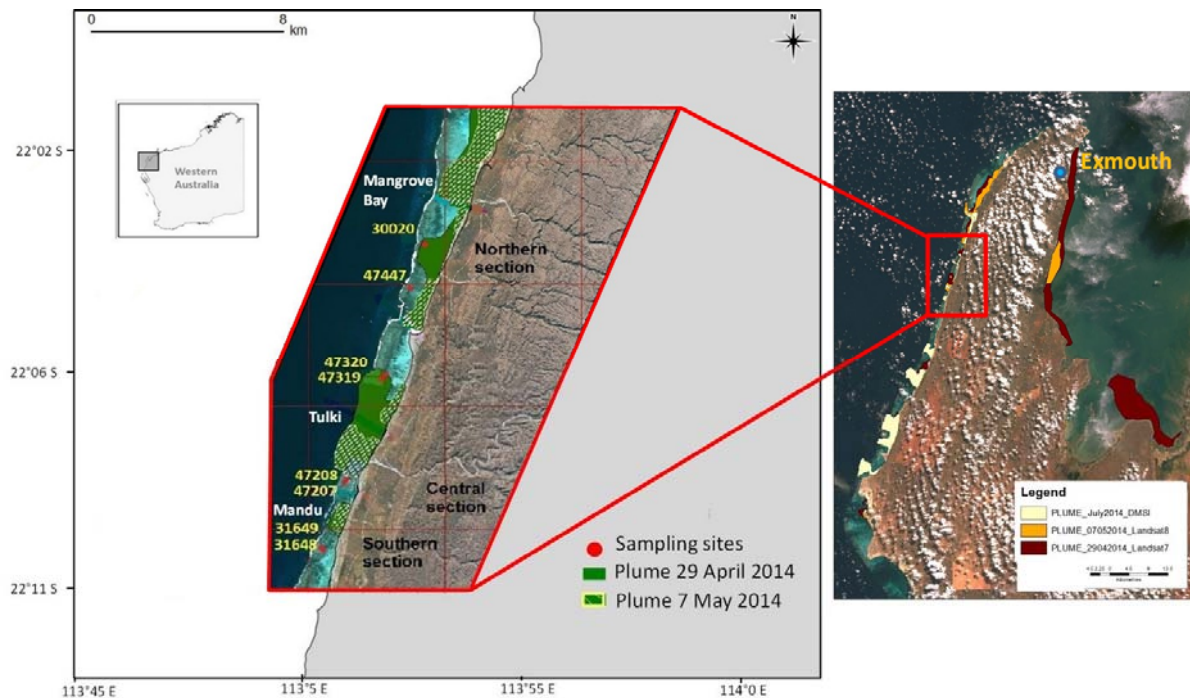
Figure 6.3.1 Spatial extent of the sediment plumes generated two and ten days after the extreme rainfall event occurred on 27 April 2014 across Ningaloo and Exmouth Regions of Western Australia. The red circles represent the eight sampling sites (identified by the 5-digit numbers) surveyed in 2014 before and after flooding. It is important to notice that spatial resolution of the sites sampled is not comparable with that used to Landsat analyses used to estimate the area of the plume. (For interpretation of the references to colour in this figure legend, the reader is referred to the web version of this article.)

The measurements for this study were conducted at 8 sites on the shallow reef flat (<5 m depth) in the 3 main regions (Figure 6.3.1): i.e. Mangrove Bay ("northern sector", sites 30020, 47319, 47320, 47447), Tulki ("central region"; sites 47207, 47208) and Mandu ("southern section"; sites 31648, 31649). At each site, 3 buoys were deployed at random: these buoys marked the beginning of transects. For each transect, a 25-m tape measure was run out in a north, south and west direction. A snorkeler swam slowly and at a continuous speed along each transect while taking digital photos in continuous-shooting mode (Canon Powershot D10 or Nikon AW1 cameras). The camera was held at a consistent distance from the substrate (approximately 50 cm). On average a total of 80-100 images were taken per transect and each image covered approximately 40×40 cm. Images were analysed using Transect Analysis Software (Australian Institute of Marine Science, Townsville; AVTAS) as per English et al. (1997). For each transect, thirty photographs were randomly selected by AVTAS, yielding 90 photographs per site. Six points were analysed per photograph. The benthos underlying each point was classified into one of 8 broad categories: *Acropora* coral, non-*Acropora* coral, soft coral, dead coral, macroalgae, turf algae, other organisms (e.g. sponges) and abiotic (rubble, sand, silt). When a point was situated over hard coral or algae, the genus was identified if possible. We considered macroalgae and turf algae separately and *Acropora* and non-*Acropora* hard corals separately, independent of their growth form. We compared the effects of flooding on the percentage of cover for all species using an ANOVA model, including transect data for all species all sites in the plume and outside of the plume (Figure 6.3.1). We used the computer program R for the analysis.

Flood impact analysis

SEDIMENT PLUME PATTERN

The spatial extents of the plumes that formed following the rainfall event (27 April 2014) were estimated using cloud-free Landsat 7 (29 April 2014) and Landsat 8 (7 May 2014) satellite remote sensing imagery. These images were visually enhanced by adjusting spectral bands to highlight the sediment plumes. The spatial extents of the sediment plumes were determined by manually digitising polygons at a scale of 1:4000. Only image pixels (25m × 25m) that suggested the presence of sediment (associated with brown colour) were included in the analysis. The area of each plume was measured using ESRI ArcMap 10.1. This analysis produced a map of the sediment plumes, which in turn allowed us to identify the location of the sampling sites relative to the plumes. The ability to predict turbidity and the area of sediment plume from satellite reflectance data (Landsat 7, Landsat 8) is complicated by the lack of coincident *in situ* and satellite data. However, for the purpose of this study, we overlapped the sites sampled with the sediment plume acknowledging that the resolution of the monitoring sites is not comparable to the Landsat analyses. Sites 30020, 47319, 47447 (northern sector) were within the plume and sites 31648, 31649, 47207, 47208 and 47230 were outside the direct influence of the flood plume (Figure 6.3.1).

6.3.3   RESULTS AND DISCUSSION

Sediment Plume Cover

The plumes in the study area originated from Tulki Creek in the North Sector, Mandu Creek in the Central Sector and the Blackwood Creek in the Southern Sector (Figure 6.3.1). The total area of plumes within the study area, two days after the flood event (29 April 2014) was 9.63 km^2 comprising 6.71 km^2, 2.3 km^2 and 0.62 km^2 respectively for the North, Central and Southern Sectors. Ten days after the flood event (7 May 2014) the total area of plumes was 4.25 km^2: comprising individual plumes encompassing 1.66 km^2, 2.13 km^2 and 0.46 km^2 respectively (Table 6.3.1). This represented a total reduction of 55.9% in plume extent in 8 days. This is consistent with the current understanding of water circulation in the lagoon areas of Ningaloo Reef where residence time of water in the lagoon is low, because rates of circulation are high due to strong offshore-directed outflows through channels in the reef explained mainly by the effects of wave braking (Taebi et al. 2011).

Table 6.3.1 Area of terrestrial plumes formed two and ten days after the flood event at Ningaloo Reef.

SECTOR	PLUME SOURCE	SAMPLING SITES	SITES WITHIN THE FLOOD PLUME	29 APRIL 2014 PLUME AREA (KM²)	7 MAY 2014 PLUME AREA (KM²)	PLUME LOSS (%)
North	Tulki Creek & Mandu Creek	30020, 47447, 47319, 47320	30020, 47319, 47320	6.71	1.66	-75.2
Central	Mandu Creek	47208, 47209		2.30	2.13	-7.4
South	Bloodwood Creek	31648, 31649		0.62	0.46	-25.8
Total				**9.63**	**4.25**	**-55.9**

Flood impact

CORAL CONDITION

No evidence of recent coral mortality was observed during the May 2014 survey. At some locations, such as Mandu and Tulki, large tree branches (some ~1.5 m long) were present that were not observed before the rainfall event (Figure 6.3.2; author's pers. obs.). However, no physical damage (e.g. broken coral branches or overturned colonies) was observed, except for one site at Tulki, which had some dead Acropora. Some sediment accumulation on the upper surfaces of hard coral colonies was observed at Mandu (Figure 6.3.2). The accumulation rate of these sediments was not quantified, but our observations (photographic transects) did not indicate that were larger amounts of sediment on the reef. At Tulki, two colonies of encrusting Acropora were partially bleached where sediment had settled.
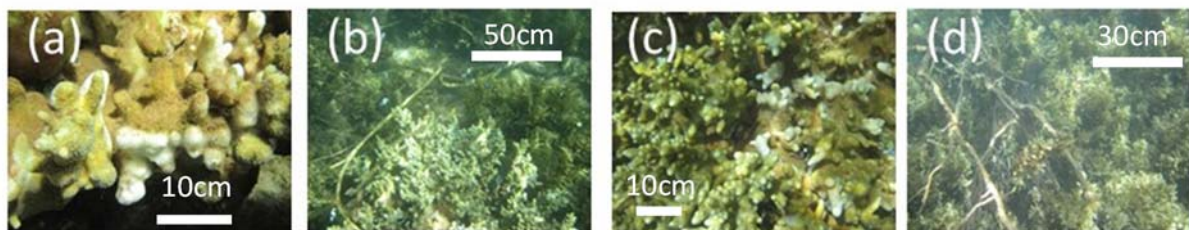
Figure 6.3.2 Terrigenous sediment accumulation and tree branches (~1.5 m) deposited at Mandu (a,b) and Tulki (c,d). No breaking coral branches, overturning   colonies or dislodged coral pieces were found in these locations. Luxuriant brown algae growth was observed at both sites. White bars represent an approximate scale bar.

CORAL COVER

Mean percentage cover of *Acropora* coral before the 2014 flooding ranged between <1% and 21% across the eight stations (Table 6.3.1), with the lowest cover in the northern sector (Mangrove Bay) with 0.8% (Figure 6.3.3). After the flooding, the mean percentage *Acropora* coral cover ranged from 1% to 23% with a similar spatial distribution as observed before the flooding with the lowest cover in the northern sector with 1.1% (Figure 6.3.3). The mean percentage cover of non-*Acropora* coral cover ranged from 0% to 4% in March 2014 (pre-flooding) and 0%—6.9% in May 2014 (after the flood). Corals from the genus *Acropora* were the dominant species in the coral assemblages surveyed. Our results indicate that in May 2014 the percentage cover of *Acropora* coral did not vary significantly between sites inside and outside of the plume (ANOVA, $F_{1,8} = 0.0001$, P=0.99). However, at one site within the plume in the northern sector (47319; Mangrove Bay) percentage cover of *Acropora* declined from 21.4% before the flood to 1.1% after the flood (Figure 6.3.3). Percentage cover of soft coral (ANOVA, $F_{1,8} = 3.7$, P = 0.068) and dead coral (ANOVA, $F_{1,8} = 4.6$, P = 0.058) did not vary between plume and non-plume sites in May of 2014.

Our results show limited impact of the floods on the coral reefs of the section sampled of Ningaloo, with no significant changes in percentage cover of *Acropora*. Although Ningaloo Reef is located very close to the coast (<1 km), the action of the consistent south-westerly swell in the region results in the reef lagoon being regularly flushed (Taebi et al. 2011). The short residence time of water inside the lagoon could provide relief during stressful conditions associated with lower salinity and high suspended sediment during floods. The dynamic water circulation of the lagoon at Ningaloo could prevent sediment accumulation. We suggest that the effects of physical process such as waves, tides and circulation around the Ningaloo Reef could enhance the capacity of this reef system to short term, local-scale floods. Relatively few studies have focused on the physical oceanography of Ningaloo Reef, but recent oceanographic modelling suggests that its mean circulation is dominantly

driven by the effects of breaking waves (Taebi et al. 2011). Future work is needed to develop models that simulate circulation over larger sections of Ningaloo to improve predictions on the transport of material (e.g. sediments, nutrients and contaminants).
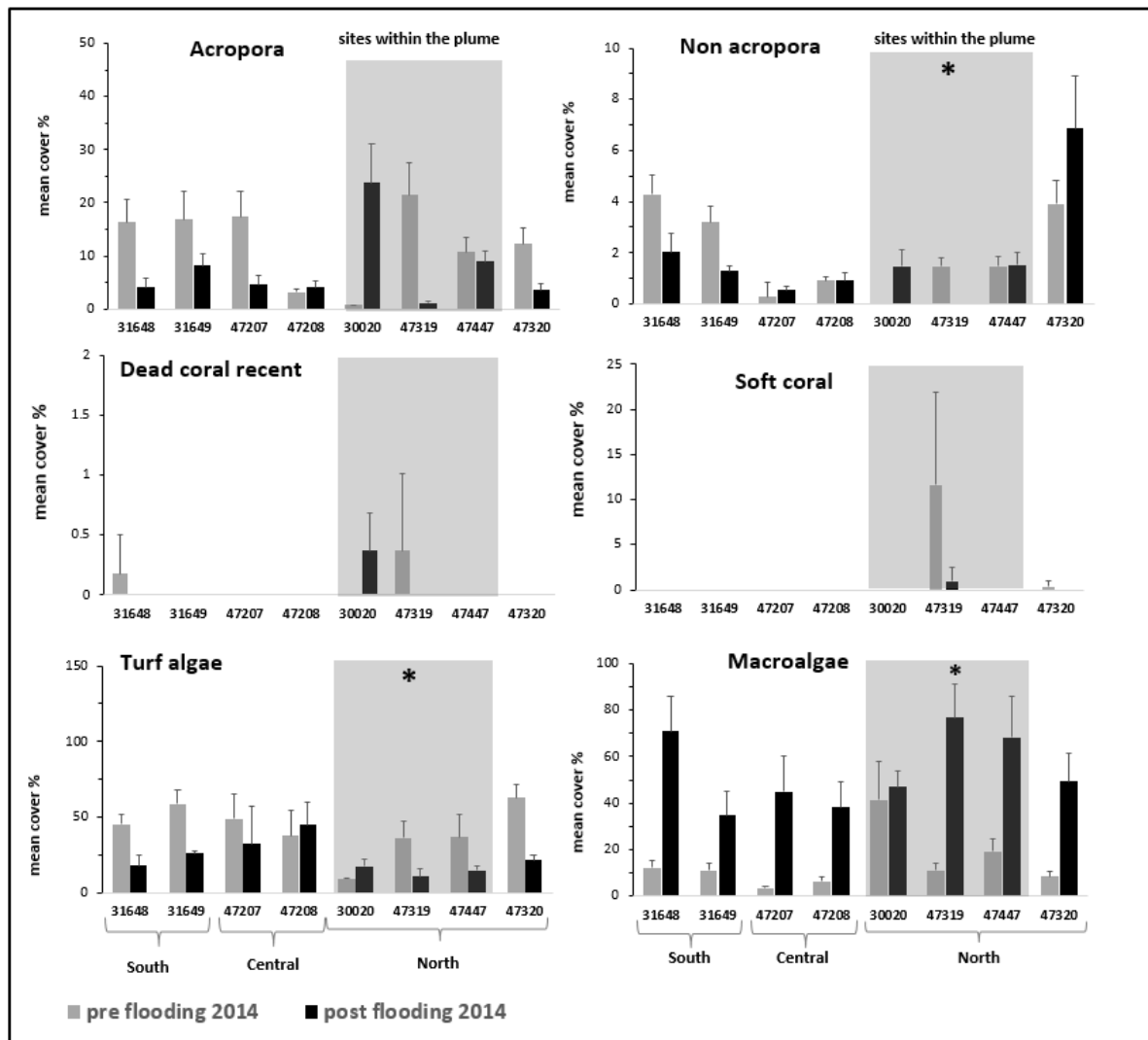
Figure 6.3.3 Changes in the percentage of cover (mean ± 1SE) of algae (macroalgae, turf) and coral cover (*Acropora*, non-*Acropora*, soft coral, dead coral recent) at eight sites sampled in March 2014 (pre flooding) and May 2014 (post flooding). Asterisk (*) over the bars indicate the relative level of p-value<0.05 (nested ANOVA, $F_{1,8}$) to test differences in cover between sites situated inside and outside of the flood plume.

Elsewhere, coral mortality caused by flooding has been documented in the world's major coral reef regions such as Great Barrier Reef, Indian Ocean, Red Sea, and Caribbean (Gardner et al. 2003; Bruno and Selig 2007; Hoegh-Guldberg et al. 2007., Fabricius et al. 2010; Cantin et al. 2010; Hinrichs et al. 2013). Coral reefs can cope with natural disturbances like floods however, water quality remains a key environmental driver impacting their health (Berkelmans et al. 2012). Global warming is expected to increase rainfall variability in northern Australia, resulting in more frequent, intense floods (Lough 2011). Depending on its ability to sustain more frequent disturbance, this could affect the biodiversity and ecological integrity of Ningaloo Reef.

In conclusion, our study, conducted immediately before and after a major flood event, indicated that the fringing reef at Ningaloo did not experience significant changes in abundance of a variety of corals, displaying an ability to withstand a short-period stress associated with flooding.

6.3.4 ACKNOWLEDGEMENTS

6.3.5 REFERENCES

Baird AH and Marshall PA (2002) Mortality, growth and reproduction in Scleractinian corals following bleaching on the Great Barrier Reef. Mar Ecol Prog Ser 237:133–141.

Bruno JF and Selig ER (2007) Regional decline of coral cover in the Indo-Pacific: Timing, extent, and subregional comparisons. PLoS ONE 2:711-716.

Berkelmans R and Oliver JK (1999) Large-scale bleaching of corals on the Great Barrier Reef. Coral Reefs 18:55–60.

Berkelmans R, Jones AM and Schaffelke B (2012) Salinity thresholds of *Acropora* spp. on the Great Barrier Reef. Coral Reefs 31: 1103–1110.

Butler IR, Sommer B, Zann M, Zhao J and Pandolfi JM (2013) The impacts of flooding on the high-latitude, terrigenoclastic influenced coral reefs of Hervey Bay, Queensland, Australia. Coral Reefs 32: 1149–1163.

Cantin NE, Cohen AL, Karnauskas KB, Tarrant AM and McCorkle DC (2010) Ocean warming slows coral growth in the central Red Sea. Science 329:322–325.

Devlin MJ, Taylor JP and Brodie J (1998) Flood plumes, extent, concentration and composition. Reef Research 8:27-36

English S, Wilkinson C and Baker B (1997) Survey manual for tropical marine resources. Australian Institute of Marine Science, Townsville, Australia. 390 pages.

Fabricius KE, Okaji K and De'ath G (2010*)* Three lines of evidence to link of the crown-of-thorns seastar *Acanthaster planci* to the release of larval food limitation. Coral Reefs 29: 593-605.

Flores F, Hoogenboom MO, Smith LD, Abrego D and Negri AP (2012) Chronic exposure of corals to fine sediments: lethal and sub-lethal impacts. PLoS One 7:e37795. Doi:37710.31371/journal.pone.0037795

Gardner TA, Côté IM, Gill JA, Grant A and Watkinson AR (2003) Long-term region-wide declines in Caribbean corals. Science 301:958–960.

Hinrichs S, Pattern NL, Feng M, Strickland D and Waite AM (2013*)* Which environmental factors predict seasonal variation in the coral health of *Acropora digitifera* and *Acropora spicifera* at Ningaloo Reef?. PLos ONE 8: e60830. Doi:10.1371/journal.pone.0060830

Hoegh-Guldberg O, Mumby PJ, Hooten AJ, Steneck RS, Greenfield P, Gomez E, Harvell DR, Sale PF, Edwards AJ, Caldeira K, Knowlton N, Eakin CM, Iglesias-Prieto R, Muthiga N, Bradbury RH, Dubi A and Hatziolos ME (2007) Coral reefs under rapid climate change and ocean acidification. *Science* 318: 1737-1742.

Jones AM and Berkelmans R (2014) Flood Impacts in Keppel Bay, Southern Great Barrier Reef in the Aftermath of Cyclonic Rainfall. PLoS ONE 9(1), e84739. http://doi.org/10.1371/journal.pone.0084739

Jones AM, Berkelmans R and Houston W (2011) Species richness and community structure on a high latitude reef: Implications for conservation and management. Diversity 3:329–355

Lough JM (2011) Great Barrier Reef coral luminescence reveals rainfall variability over north-eastern Australia since the 17th century. Paleoceanography 26:PA2201

Madin JS, Connolly SR (2006) Ecological consequences of major hydrodynamic disturbances on coral reefs. Nature 444:477–480

Olson DM and Dinerstein E (2002) The Global 200: Priority ecoregions for global conservation. Annals of the Missouri Botanic Gardens 89:199–224

Taebi S, Lowe RJ, Pattiaratchi CB, Ivey GN and Symonds G (2011) Nearshore circulation in a tropical fringing reef system. Journal of Geophysical Research: oceans 116 (C2).doi.10.1029/2010JC006439

van Woesik R, De Vantier LM and Glazebrook JS (1995) Effects of Cyclone 'Joy' on nearshore coral communities of the Great Barrier Reef. Mar Ecol Prog Ser 128:261–270

Weber M, Lott C and Fabricius KE (2006) Sedimentation stress in a scleractinian coral exposed terrestrial and marine sediments with contrasting physical, organic and geochemical properties. Journal of Experimental Marine Biology 336:18-32.

Weber M, de Beer D, Lott C, Polerecky L, Kohls K, Abed RMM, Ferdelmen TG and Fabricius KE (2012) Mechanisms of damage to corals exposed to sedimentation. Proceedings of the National Academy of Sciences 109:E1558-E1567.

Wilkinson C (2004) Status of the coral reefs of the world report: 2004.Australian Institute of Marine Science.

6.4 Coral recruitment patterns in the Dampier Archipelago, Western Australia

Authors: Thomson DP, Trapon M, Rule M, Slawinski D, Feng M, Babcock RC.

ABSTRACT

Understanding spatiotemporal variability in coral recruitment is a management priority for coral reefs, with successful management relying on good knowledge of not only the current state of the adult community but also the processes that will impact on the future state of the reef, such as rates of recruitment. In the present study, we investigated spatiotemporal variability in recruitment around the Dampier Archipelago between 2015 and 2017, and identified the best predictors for the patterns of coral recruitment over this period. Dramatic differences in recruitment were observed among years with a 350% increase in the density of recruits detected. These differences are likely due to strong variability in the prevailing oceanographic currents among years combined with recovery from effects of bleaching on coral reproductive output. Despite these large differences in recruitment, the rank order of sites remained similar over the study period suggesting that reef scale recruitment within the Dampier Archipelago is partly deterministic and predictable. The best predictors of recruitment during the three years were the hydrodynamic particle tracking model predictions of recruitment, percent coral cover and reef structural complexity. We observed a positive relationship between recruitment and coral cover at multiple spatial scales with the highest density of recruitment (>10 recruits/tile) occurring on reefs with greater than 25% coral cover and within regions with greater than 30% coral cover. Our results demonstrate that predictive coral recruitment models, when used in combination with simple metrics such as percent hard coral cover, can provide predictions of the relative abundance of coral recruits over large geographical areas to provide essential information for the management of the region.

6.4.1 INTRODUCTION

A key ecological process in the formation and maintenance of coral reefs is the settlement of larvae from the plankton onto the reef substrata. For marine organisms with a dispersive larval phase such as corals, the rate and success of larval settlement is an important process influencing population and community dynamics. For scleractinian corals, recruitment is commonly defined as the period when individuals become established in the local population (Keough and Downes 1982; Harrison and Wallace 1990). Thus, recruitment combines the arrival of larvae, the settlement and metamorphosis of larvae, and any early post-settlement mortality of settlers prior to visible recruitment.

Recruitment is a vital component in the connectivity and resilience of open populations such as corals. For example, coral populations that have consistently high levels of recruitment will likely recover more quickly following a disturbance than populations receiving fewer recruits or less consistent recruitment (Boschetti et al. 2017). Similarly, it seems logical that populations that receive consistently high numbers of recruits from neighbouring reefs will maintain higher levels of coral cover due to ongoing recruitment of larvae from multiple species. The successful conservation and management of coral reefs relies on good knowledge of not only the current state of the adult community but also the processes that will impact on the future state of the reef. These include rates of recruitment, as well as understanding spatiotemporal patterns in coral recruitment, both of which are also important for optimising protected area networks (Burgess et al. 2014)

Coral recruitment varies at multiple spatial scales, including latitudinal gradients (Hughes et al. 2002) and across the continental shelf (Sammarco 1991), among reefs separated by kilometres (Sammarco and Andrews 1989, Fisk and Harriott 1990) and among sites separated by hundreds of metres (Baggett and Bright 1985). This is because the causes of spatial variation in coral recruitment involve complex interactions among biophysical processes including hydrodynamics (Sammarco and Andrews 1987, Eagle et al. 2012), larval supply (Hughes et al. 2000), habitat complexity (Baird and Hughes 2000), light availability (Bak and Engel 1979, Baird et al. 2003), predation (Carlton 2001) and the presence of adult conspecifics (Mundy and Babcock 2000, Vermeij 2005). The complex nature of these interactions has led to the development of numerous numerical models, which aim to predict patterns in recruitment on coral reefs over varying spatial scales (Sammarco and Andrews 1989, Black and Moran 1991, Crabbe and Smith 2003). However, the majority of these models remain untested, which continues to impede our understanding of the factors that are most important for predicting patterns of recruitment (Radford et al. 2014, Kool and Nichol 2015). Subsequently, there is a great need to develop, apply and test recruitment models to improve our ability to predict the rates of processes that impact on the future state of reefs and our capacity to manage them.

A high resolution larval recruitment model was developed for the North West Shelf (NWS) in Western Australia (Feng et al. 2017), which provides a good opportunity to test such a model. Here, Feng et al. (2017) simulated larval dispersal patterns in the broadcast spawning coral *Acropora millepora* during the autumn (March–May) mass spawning between 2004 and 2009 for the NWS (19°S to 22°S). The model provides estimates of coral recruitment over a 1 km × 1 km grid by incorporating wind, tide and large-scale oceanographic currents. The model results highlight the importance of large-scale hydrodynamics on the dispersal of coral larvae and indicate that, on average, only 22% of larvae settle on reefs within 15 km of where they originate (see Feng et al. 2016 for further details). The model results also suggest that the reefs of the Dampier Archipelago, Western Australia, appear to be relatively isolated from other reefs in the west Pilbara; therefore, they may recover more slowly following disturbance.

Here, we take advantage of the larval recruitment model for the Pilbara region to empirically investigate the relative importance of a range of predictors for coral recruitment throughout the

Dampier Archipelago over a three-year period. Owing to its complex hydrodynamics (Kool and Nichol 2015, Feng et al. 2016), globally significant fringing coral reefs (Roberts et al. 2002), high conservation value (DPaW 2013) and potential isolation, the Dampier Archipelago represents a good opportunity to quantify the relative importance of mesoscale processes (model predictions) versus local scale interactions (coral cover and reef structural complexity) on patterns of coral recruitment.

6.4.2 METHODS
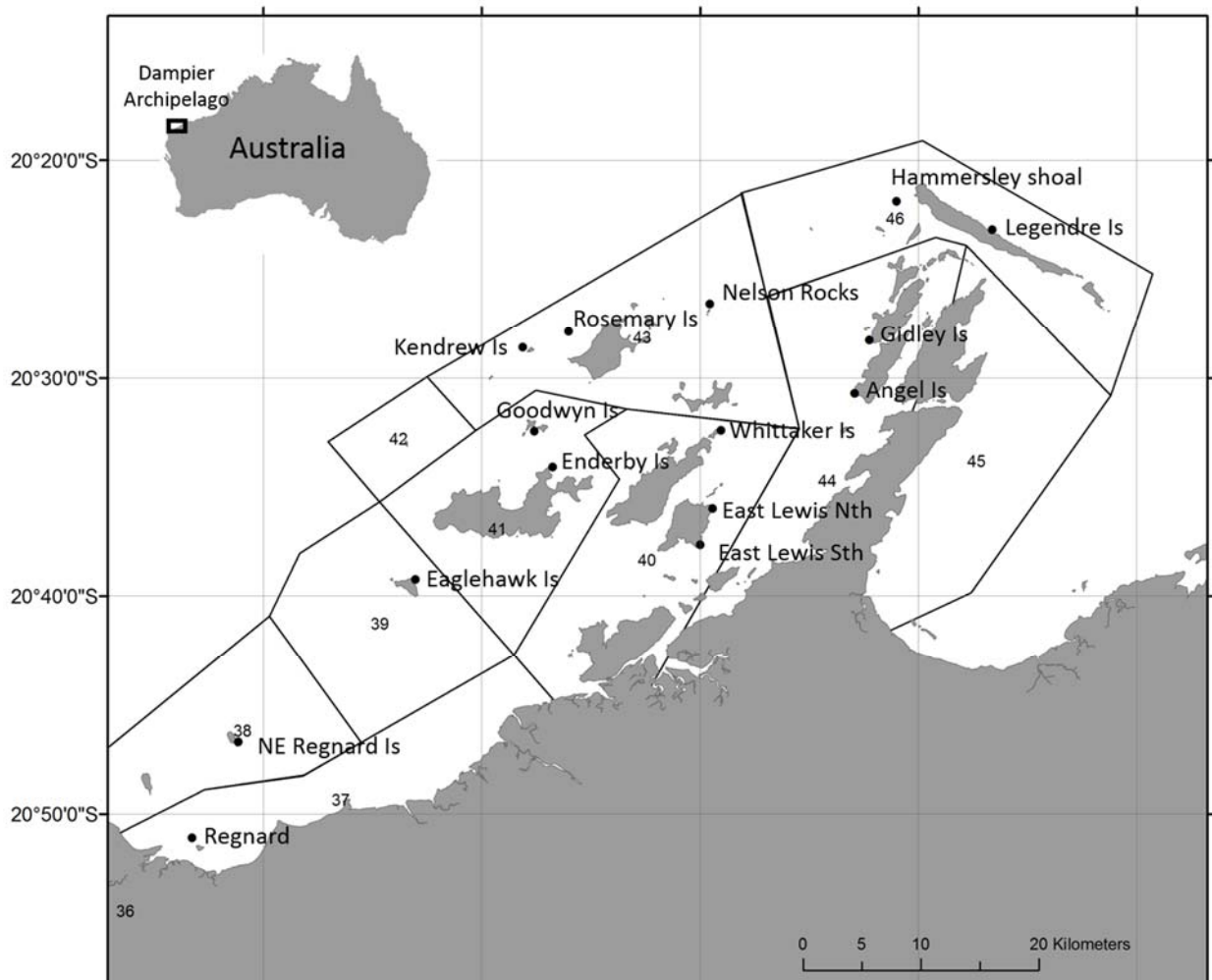
Figure 6.4.1 Map showing the location of the 15 sites within the Dampier Archipelago where coral recruitment tiles were deployed in 2015, 2016 and 2017. The boundaries of the 10 model regions are illustrated within the straight lines.

Site description

The Dampier Archipelago sits within the Pilbara inshore bioregion and is characterised by 12 large islands and 30 small islands or shoals (Semeniuk et al. 1982) (Figure 6.4.1). The region has low annual rainfall (290 mm per year) and sediment input, largely due to the lack of nearby river systems and freshwater run-off (Forde 1985). Suspended sediment loads are variable and are strongly influenced by the prevailing wind and tide conditions. Sediment loads of between 0.7 mg/L^{-1} (offshore locations) and 2.6 mg/L^{-1} (nearshore locations) have been recorded with higher turbidity characteristics of nearshore reefs during ebb tides (Forde 1985). The large tidal range (spring

maximum 5.1 m, mean 1.9 m) and wide continental shelf produce current velocities up to 0.5 ms^{-1} during spring tides (Forde 1985).

The region is influenced by large-scale oceanographic currents such as the southward flowing Holloway and Leeuwin Currents, which transports warm, clear waters to the westernmost islands and shoals (Semeniuk et al. 1982). These islands include Kendrew Island, Rosemary Island, Hammersley Shoal and Legendre Island, where the influx of clear oceanic waters can result in photic depths of greater than 50 m (Forde 1985). In contrast, the nearshore waters surrounding East Lewis Island, Enderby Island, Goodwyn Island, Angel Island and Gidley Island usually have a photic depth of less than 20 m due to higher levels of turbidity (Simpson 1988).

Well-developed coral assemblages occur throughout the Dampier Archipelago with 216 species of hard corals from 57 genera recorded (Veron and Marsh 1988). Coral assemblage composition varies throughout the region with *Acropora* and *Pocillopora* most abundant on offshore island reefs and *Pavona* and *Porites* most abundant on inshore island reefs (Veron and Marsh 1988). Coral recruitment patterns throughout the region are poorly understood; however, a recent review of coral reproductive patterns in Western Australia suggest that between 60% and 70% of coral species occurring within the Dampier Archipelago spawn during the austral autumn (March–April) (Gilmour et al. 2016).

Predictions of coral recruitment

Predicted numbers of coral recruits were obtained for the Dampier Archipelago (1 km × 1 km grid) using a three-dimensional larval dispersal model (see Feng et al. 2016), which was based on the Regional Ocean Modeling System (ROMS hydrodynamic model; Marrchesiello et al. 2003) and incorporated the behavioural characteristics of larvae from the broadcast spawning coral *A. millepora.* The larval dispersal model provides predictions of the total number of coral larvae settling for each grid point (1 km × 1 km grid) between the southern Ningaloo Reef (23°S) and northern Pilbara (19.3°S). Recruitment abundance predictions were obtained for our 15 study sites by averaging the model values for the years 2004 to 2009 from the grid cell closest to the study sites.

Spatial and temporal patterns in recruit abundance

The abundance of recruits was recorded annually between 2015 and 2017 at 15 sites within the Dampier Archipelago (Figure 6.4.1). Sites were distributed throughout the Dampier Archipelago based on the predicted recruitment (high, mid, low; Feng et al. 2014) distance from the mainland (inshore, midshore and offshore) (see Table 6.4.1) and evidence of well-developed coral assemblages (authors' pers. obs.). At each location, 15 unglazed recruitment tiles (11 cm × 11 cm × 1 cm) were deployed on stainless steel mounting plates (Mundy and Babcock 2000) within an area of 10 m × 10 m. To minimise movement and/or dislodgement of the tiles, care was taken to ensure that the tiles were attached to the solid reef matrix free from abrasion by macroalgal laminae Tiles were deployed four weeks prior to the predicted autumn spawning nights and then retrieved eight to ten weeks after the spawning period. On retrieval, organic material was removed from the tiles using chlorine bleach and the tiles were dried and examined under a stereo microscope (Mundy 2000). The abundance of coral recruits on the top, bottom and sides of each tile was recorded.

Spatial and temporal patterns in recruit abundance were examined using the permutational multivariate analysis of variance (PERMANOVA, Anderson 2008). PERMANOVA was carried out in Primer 7 using a Bray Curtis dissimilarity/similarity matrix, once assumptions of homogeneity of variance data were met. Any significant differences were further investigated using pairwise t-tests where the P value was calculated from permutations.

Spatial patterns in coral cover and reef structural complexity

Percent coral cover and reef structural complexity were measured at three spatial scales: 5 m, 200 m and 15 km. Within 5 m of the recruitment tiles, visual estimates of percent coral cover were obtained from high resolution photographic mosaics of the substrate. A GoPro4™ was utilised to capture overlapping images of the substrate, which were then applied to construct a photo mosaic with the structure from motion software Agisoft™. Photo mosaics provided 100% coverage of the coral assemblage over a 10 m × 10 m area and allowed for accurate estimation of the percent coral cover. A paired t-test failed to detect a significant difference between estimates of percent coral cover and measurements of coral cover obtained from 50 randomly distributed points on 8 photo mosaics (t_8, p = 0.314). The percent coral cover within 200 m and 15 km of the recruitment tiles was measured using photographic line transects. Photographs were taken at 0.5 m intervals along 3 × 50 m line transects. To ensure replicates were independent, 40 photographs were randomly selected within each transect and the genus of any scleractinian (hard) corals was recorded for 6 fixed points per photograph using the Transect Measure™ software (www.seagis.com.au). To quantify percent coral cover within 15 km of the recruitment tiles, the percent coral cover from all transects within model regions (Figure 6.4.1) were averaged.

Table 6.4.1 The model prediction recruitment category, predicted recruitment (average), model regions/number of 50 m transects used to calculate coral cover within the region and the site name for the 15 sites where recruitment tiles were deployed around the Dampier Archipelago in 2015, 2016 and 2017.

MODEL PREDICTION CATEGORY	PREDICTED RECRUITMENT PER TILE (MEAN 2004–2009)	MODEL REGION/ NUMBER OF TRANSECTS	REEF NAME
HIGH	869.3	41 / 9	Enderby Is
HIGH	734.5	44 / 15	Gidley Is
MID	603.3	43 / 22	Nelson Rocks
HIGH	552.5	46 / 9	Hamersley Shoal
HIGH	545	40 / 61	East Lewis South
HIGH	496.8	40 / 51	East Lewis North
MID	480.8	39 / 3	Eaglehawk Is
MID	472.2	44 / 15	Angel Is
MID	444	46 / 9	Legendre Is
MID	395.3	40 / 51	Whittaker Is
LOW	341.8	41 / 9	Kendrew Is
LOW	241.3	38 / 3	NE Regnard Is
LOW	229.3	41 / 9	Goodwyn Is
LOW	157.7	41 / 9	Rosemary Is
LOW	137.5	37 / 3	Regnard Is

Predictors of recruitment

To determine the relative importance of mesoscale (oceanographic) and local scale (percent coral cover) influences on coral recruitment, we applied a generalised additive model (Fisher et al. in review). Predictors of recruit abundance were identified from a group of likely predictors including model predictions of total recruitment, percent coral cover within 5 m, 200 m & 15 km of recruitment tiles, and reef structural complexity. For each year (2015, 2016 and 2017), the two best models were identified using Akaike information criterion (AIC) (lowest two values) and the relative importance of each predictor was identified. To determine the best model for all years, we analysed data for the three years individually then repeated the analysis with all years combined and the addition of two more predictors: number of years since bleaching and the southern oscillation index (SOI). Years since bleaching represented the time in years since the site had experienced greater than eight degrees heating weeks (DHW) with data obtained from the DHW time series in Babcock et al. (2017). SOI represented the average monthly SOI value for the six months prior to coral spawning (September to February).

6.4.3   RESULTS

Spatial and temporal patterns in recruit abundance

Recruitment density varied widely among sites (F = 34.2, p < 0.001) from a low of 0.1 recruits per tile at Regnard Island to a high of 72 recruits per tile at Whitaker Island (Figure 6.4.2). The overall mean density for the three years was 9.6 recruits per tile. Sites with consistently high recruitment over the three years included Whittaker Island (40.9 recruits per tile), East Lewis North (33.2 recruits per tile), Hammersley Shoal (8.3 recruits per tile), Rosemary Island (9.2 recruits per tile) and Gidley Island (9.0 recruits per tile). In contrast, reefs that had consistently low recruitment over the three years included Eaglehawk Island (0.6 recruits per tile), Regnard Island (0.5 recruits per tile), NE Regnard Island (0.9 recruits per tile) and Enderby island (2.2 recruits per tile) (Figure 6.4.2).

The rank order of sites (density of recruitment) was similar between years, despite the large variability among sites (Kruskal-Wallis, χ^2 = 3.49, df = 2, p = 0.17) (Figure 6.4.2). Two sites had consistently high recruitment in all years, which were East Lewis North and Whittaker Island, with mean recruitment densities ranging from 9 to 73 recruits per tile. In contrast, four sites had consistently low recruitment: Eaglehawk Island, Regnard Island, NE Regnard Island and Enderby Island, with mean recruitment densities ranging from 0.04 to 6 recruits per tile (Figure 6.4.2).

Recruitment varied significantly among the tile surfaces (F = 38.9, df = 2, p <0.001) with eight times the density of recruits observed on the sides of tiles compared to the top and bottom of tiles (Figure 6.4.3). There was no difference in recruitment density between the top and bottom of tiles (t = 7.3, p = 0.457). Mean recruit density on the sides of tiles was 0.14 recruits per cm^2, compared to 0.02 recruits per cm^2 (range 0–0.07) on the top and 0.01 recruits per cm^2 (range 0–0.05) on the bottom of tiles. Preferential settlement on the sides of tiles was observed at all sites with the exception of Legendre Island, where the greatest density of recruits was observed on the bottom of tiles (Figure 6.4.3).
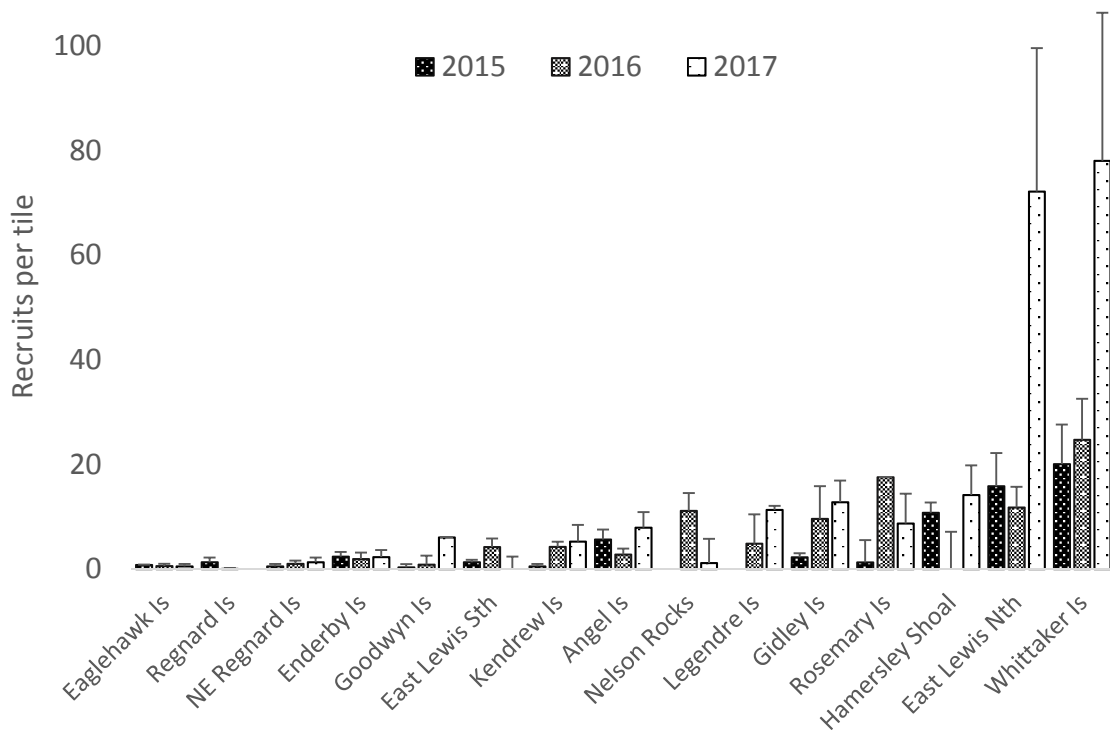
Figure 6.4.2 Mean number of recruits per tile (± 1 SE) recorded in 2015, 2016 and 2017 at the 15 sites throughout the Dampier Archipelago. Sites are ranked in order from lowest to highest mean number of recruits per tile.
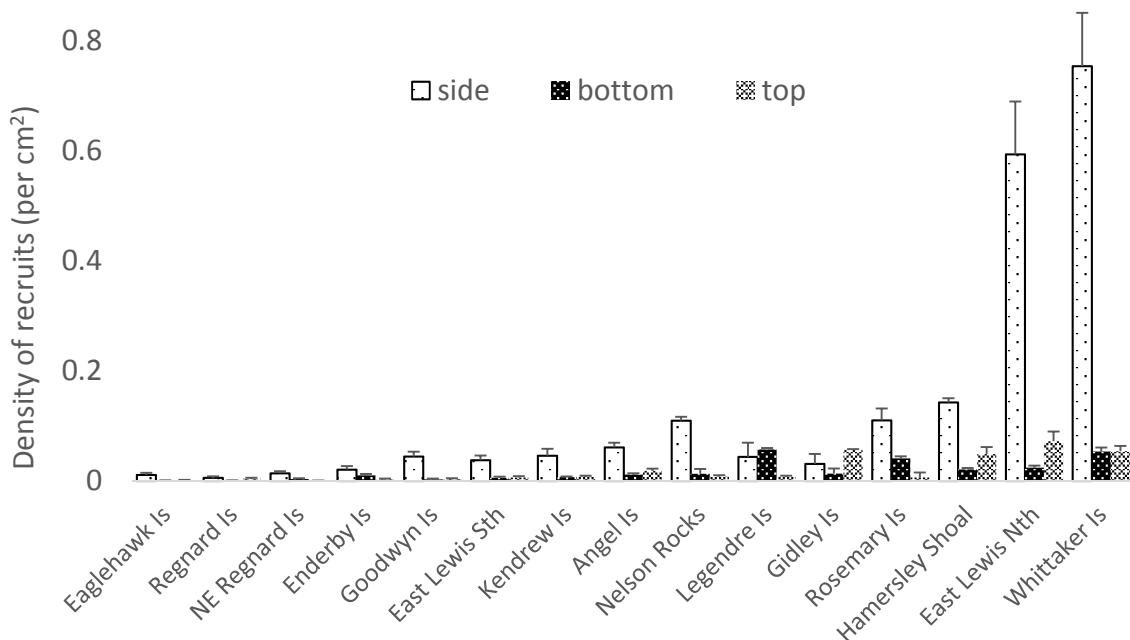
Figure 6.4.3 Mean density of recruits (± SE) observed on the side, bottom and top of recruitment tiles at the 15 sites throughout the Dampier Archipelago over the three years (2015 to 2017).

Recruitment densities varied widely among years (F = 34.2, df = 2, p < 0.001), increasing 350% over the three years from 3.9 recruits per tile in 2015 to 17.6 recruits per tile in 2017 (Figure 6.4.4). The

increase in recruitment between 2015 and 2017 was consistent among most sites, with higher recruitment densities in 2016 than in 2015 recorded for 66% of sites and higher recruitment densities in 2017 than in 2016 recorded for 95% of sites (Figure 6.4.2). Recruitment variability did not differ among years (F = 1.92, df = 2, p = 0.15).
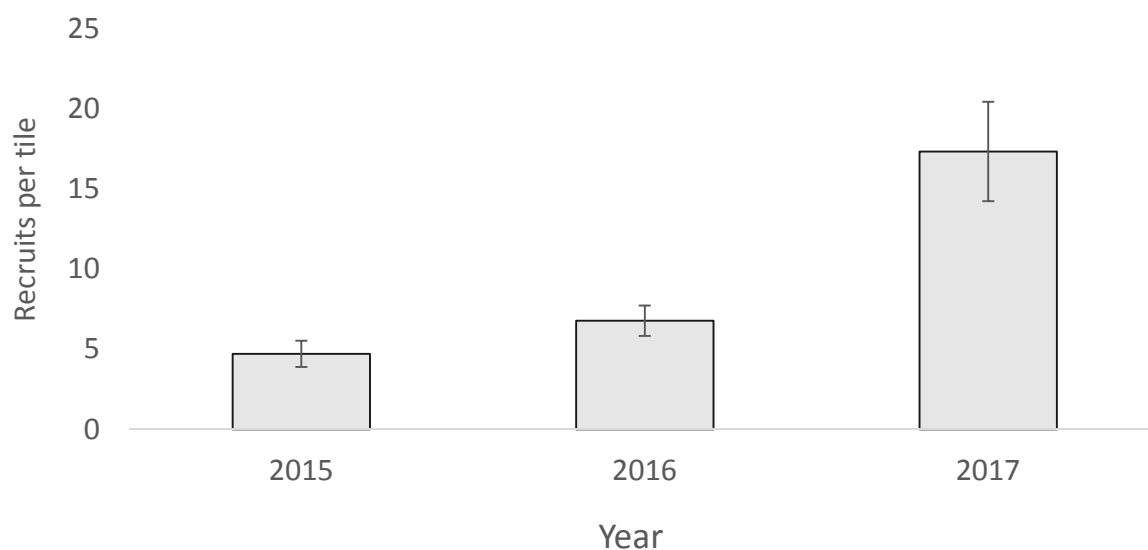
Figure 6.4.4 Mean number of recruits per tile (± SE) observed throughout the Dampier Archipelago in 2015, 2016 and 2017.

Table 6.4.2 Best models for explaining variance in recruit abundance in 2015, 2016, 2017 and all years combined. Explanatory variables considered were model predictions of recruitment, estimated coral cover within 5 m of recruitment tiles, coral cover within 200 m of recruitment tiles, coral cover within 15 km of recruitment tiles, reef structural complexity, years since bleaching and SOI.

YEAR	MODEL	DF	ΔAICC	R²
2015	Prediction + coral cover (200 m)	9	0	0.23
	Prediction + coral cover (5 m)	9	38.23	0.20
2016	Prediction + coral cover (5 m) + reef complexity	9	0	0.19
	Coral cover (15 km) + reef complexity	9	24.64	0.16
2017	Prediction + coral cover (200 m) + reef complexity	9	0	0.22
	Prediction + coral cover (5 m) + reef complexity	9	1.6	0.22
All years	Coral cover (15 km) + reef complexity	25	0	0.19
	Prediction + coral cover (5 m)	25	8.9	0.20

Predictors of recruitment

The best predictors of recruitment over the three years were the predictions from the hydrodynamic model, percent coral cover and reef structural complexity (Table 6.4.2). The best model in each year as selected by AIC included the hydrodynamic model prediction, coral cover at the scale of the reef (200 m) or region (15 km) and, in 2016 and 2017, reef structural complexity (Figure 6.4.5). The best models in each year were similar to the best model for all years, with the exception that the best

model for all years did not include the hydrodynamic model prediction. Models explained between 19% and 23% of the variation in recruitment (Table 6.4.2).

The relationships between coral cover and recruits per tile varied depending on the scale of coral cover observations (Figure 6.4.6). Coral cover at the scale of reef (200 m) and region (15 km) were generally positively correlated with recruitment when coral cover was greater than 30%. In contrast, coral cover in close proximity to the recruitment tiles (2 m) was positively correlated with recruitment until coral cover exceeded 30%, after which the correlation with recruitment was negative.
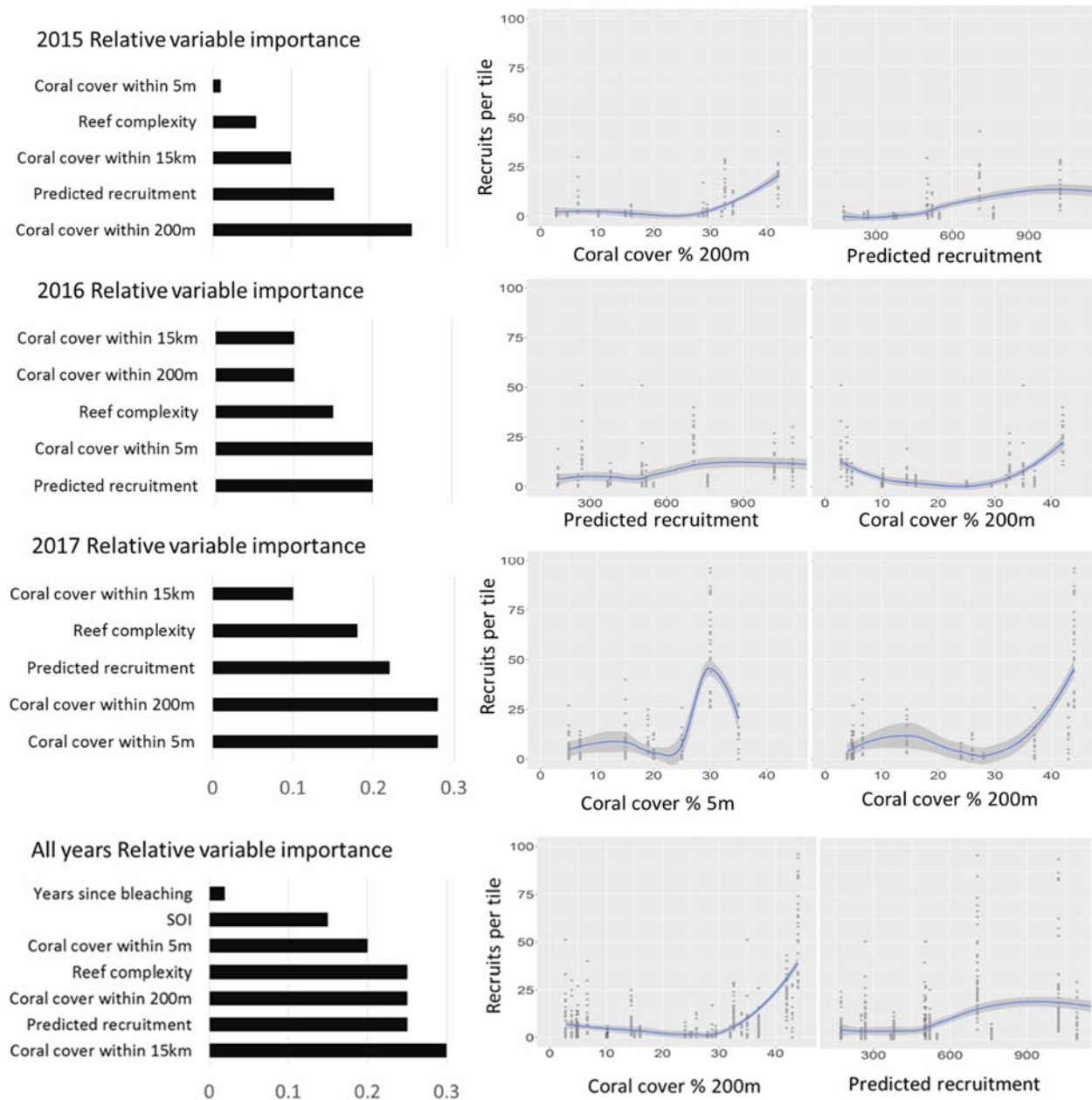
Figure 6.4.5 Ranking of variable importance in explaining variance in the abundance of recruits in 2015, 2016, 2017 and all years combined. Bi-plots show the relationship between the number of recruits per tile and the two most important predictors for the model as identified by AIC (Table 6.4.2). Shaded areas represent 95% confidence intervals.
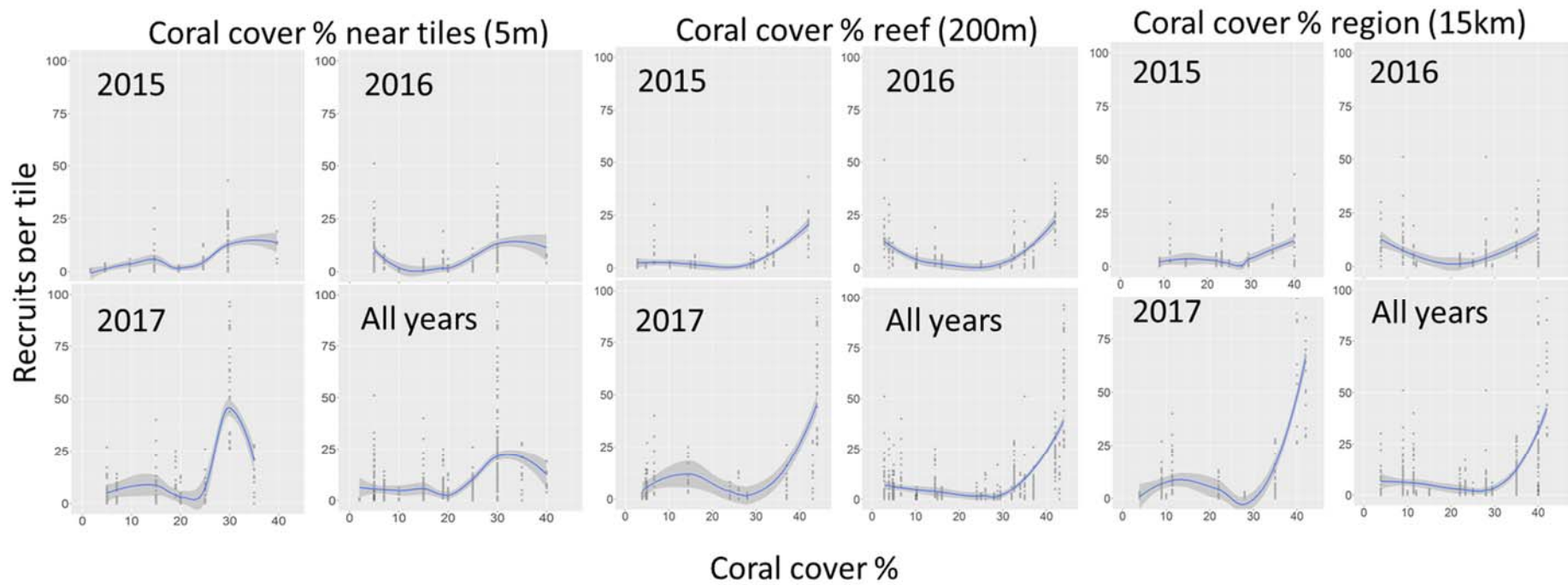
Figure 6.4.6 Bi-plots showing the relationship between the number of recruits per tile and the percent coral cover at three different scales; within 5 m, within 200 m and within 5 km of recruitment tiles. Shaded areas are present 95% confidence intervals.

6.4.4 DISCUSSION

It is widely acknowledged that patterns of larval dispersal are closely aligned with large-scale ocean currents; however, validation of predicted patterns of larval dispersal within nearshore environments is very difficult due to the complex interactions between conditions of wind, tide and geomorphology. Arguably, the most successful attempt to validate a larval dispersal model for corals was conducted over thirty years ago. This study demonstrated that models could successfully predict larval supply and recruitment (Sammarco and Andrews 1989), however, the study had several limitations including the use of settlement substrata suspended in midwater at off-reef locations. As a result, the ability of the model to predict coral recruitment on reefs remains in question. Subsequent attempts to use models to predict larval supply and recruitment on reefs have been largely unsuccessful (Oliver et al. 1992). Here, we show that a predictive coral recruitment model when used in combination with simple metrics, such as percent hard coral cover, can provide predictions of the relative abundance of coral recruits over large geographical areas to provide essential information for the future management of the region.

Dramatic differences in recruitment were observed among years with a 350% increase in the density of recruits observed over the three years studied. There was extensive coral bleaching and mortality recorded in the Pilbara in 2011 and 2013, including mortality in the Dampier Archipelago (Lafratta et al. 2016, Ridgway et al. 2016). Corals were also observed to be bleached in 2014 although no significant mortality was observed in that year (Babcock et al. 2017). However we found the number of years since bleaching to be a poor predictor of recruitment abundance in all years. Coral fecundity was not measured, therefore it is possible that differences in oceanographic conditions among years also caused differences in fecundity and larval survivorship. It is also possible that regional-scale oceanographic conditions prevalent around the time of coral spawning in 2017 (18 March), differed from those that prevailed in 2015 (14 March) and 2016 (2 April). Inter-annual variability in patterns of coral recruitment are well documented (Harrison and Wallace 1990, Harriott and Fisk 1988, Hughes et al. 1999), with the cause of this variability attributed to differences in larval transport and connectivity which can in turn affect patterns of dispersal and early life history survivorship (Harrison and Wallace 1990). Indeed, connectivity models for the Pilbara region have revealed large changes in oceanographic conditions around the same time as the coral spawning period, with the predominant current direction changing from a north-easterly direction to a south-westerly direction in mid-March (Feng et al. 2016). Given that the predicted time of spawning varied by 16 days between 2015 and 2017 (14 March to 2 April) it is likely the predominant current direction differed among years and may have influenced the direction of larval dispersal or early life history survivorship. This might have contributed to the increased recruitment observed over the period of our study.

Despite large differences in recruitment among years, the rank order of sites was similar over the study period and model predictions of recruitment remained one of the best predictors. This suggests that despite variability in large-medium scale oceanography, reef scale recruitment within the Dampier Archipelago is partly deterministic and predictable. Two sites had consistently high recruitment in all years (Whitaker Island and East Lewis North) and four sites had consistently low recruitment in all years. Similar consistency in spatial patterns of coral recruitment have been observed in the central Indian Ocean (Adjeroud et al. 2005), on the Great Barrier Reef (Sammarco and Andrews 1989, Eagle et al. 2012) and in the Caribbean (Sammarco 1985); however, often temporal variation is too high to detect any persistent spatial patterns in recruitment (Fitzhardinge 1985, Hughes et al 2000, Soong et al. 2003). Previous studies have suggested that recruitment patterns are likely to recur at the scale of reefs (Oliver et al. 1992, Sammarco 1994) because currents interact with local topography in a consistent way (Alldredge and Hamner 1980, Wolanski and Hamner 1988). The causes of the observed spatial patterns in our study are difficult to determine; however, our results indicate that recruitment among sites within the Dampier Archipelago may be

partly deterministic and predictable in terms of the rank order of recruitment, even though the magnitude of differences among sites may vary from year to year. If these patterns are shown to be consistent over long periods, then the recovery capabilities of different reef areas can be more confidently incorporated into decision making when designating reef areas for use or conservation.

Similar to many previous studies, we found a higher proportion of recruits on the sides of tiles than on their upper and lower surfaces (Babcock 1988, Fisk and Harriott 1990, Carlton 2001). This trend was consistent across all sites with the exception of one, Legendre Island. Several hypotheses have been proposed to explain the variation of recruitment among tile surfaces, including changes in light intensity and quality (Babcock and Mundy 1996), rates of sedimentation (Smith et al. 2003), availability of suitable substrate (Harriott and Fisk 1987) and spatial competition and grazing by predators (Carlton 2001). The variation in recruitment orientation has also been suggested to be an adaptive behaviour for some species of coral larvae to maximise post settlement survival (Mundy and Babcock 2000). The lack of difference in orientation preferences among sites that have strongly contrasting conditions of water visibility and sedimentation may reflect the fact that tradeoffs between optimizing settlement orientation in relation to light and sedimentation vary inversely (Babcock and Mundy 1996). Similarly, the lack of difference between recruitment on the top and bottom of tiles suggests grazing by predators is unlikely to have produced the patterns we observed. In contrast, our results suggest multiple influences may be driving the differences in recruit densities we observed and future studies should include competitive interactions between coral larvae and other competitors for space on the tile surfaces.

Interestingly, we found a density dependent relationship between recruitment and coral cover at multiple scales. We observed a positive relationship between recruitment and coral cover at the reef (200 m) and regional scales (15 km), with sites with high recruitment (>10 recruits/tile) generally occurring on reefs with greater than 25% coral cover and within regions with greater than 30% coral cover. These findings were consistent with model results, which showed coral cover at the scale of the reef (200 m) and region (15 km) were two of the four best predictors of recruitment in all years. It seems logical that sites located on reefs containing higher coral cover should receive higher levels of recruitment; however, our results are somewhat inconsistent with previous studies, which found a poor correlation between adult abundance and recruitment abundance (Hughes et al. 1999, Edmunds 2000, Eagle et al. 2012) at local spatial scales. Previous studies have suggested that adult assemblages are likely to be the product of 10-year averages in variations in recruitment and, as such, are unlikely to correlate well with short-term observations of recruitment (Hughes 1999, Edmunds 2000) but there may be a positive relationship between coral cover and recruitment at larger regional scales (Hughes et al. 2000). The density dependent relationship we observed here, therefore, may be due to high levels of larval retention within the Dampier Archipelago in most years, a theory supported by larval dispersal models for the region (Kool and Nichol 2015, Feng et al. 2016).

Recruitment densities observed around the Dampier Archipelago are low in comparison to other reefs located at the same latitude; however, they are high in comparison to the central Pilbara and Ningaloo regions immediately to the south. For example, reefs located at the same latitude in the western Indian Ocean (13 recruits per tile, South Africa; Glassom 2006) and western Pacific Ocean (25 recruits per tile, Swain reefs, GBR; Hughes et al. 1999) have higher recruitment densities than the Dampier Archipelago. However, on reefs located immediately to the south at Ningaloo (3 recruits per tile, Ningaloo Reef; Turner et al. 2017) and the central Pilbara (2 recruits per tile; R. Evans pers. comm.) lower recruitment densities were recorded during the same period. Modelling of the resilience of the coral reef network in the west Pilbara suggests that some regions within the Dampier Archipelago are likely to be of high importance to the recovery and/or maintenance of the coral reefs throughout the region (Boschetti et al. 2017). As a result, reefs of the Dampier Archipelago should be given priority for protection to ensure the long term health of coral reef

ecosystems throughout the Pilbara. However, the relationship between connectivity, recruitment and regional resilience is complex, and ongoing comparisons of specific annual predictions and measures of recruitment are required.

6.4.5 ACKNOWLEDGEMENTS

6.4.6 REFERENCES

Adjeroud M, Chancerelle Y, Schrimm M, Perez T, Lecchini, D, Galzin R, Salvat B (2005) Detecting the effects of natural disturbances on coral assemblages in French Polynesia: a decade survey at multiple scales. Aquat. Living Resour. 18: 111–123.

Alldredge AL, Hamner WM (1980) Recurring aggregation of zooplankton by a tidal current. Estuarine, Coastal and Shelf Science 10:31-37

Anderson MJ, Gorley RN, Clarke KR (2008) PERMANOVA+ for PRIMER: guide to software and statistical methods. PRIMER-E Ltd, Plymouth

Babcock RC (1988) Fine-scale spatial and temporal patterns in coral settlement. Proceedings of the 6th International Coral Reef Symposium, Australia, 2:635–639

Babcock RC, Thomson D, Haywood MDE, Vanderklift M, Pillans R, Rochester W, Miller M, Speed C, Shedrawi G, Field S, Evans R, Stoddart J, Hurley T, Thompson A, Decpzynski M (2017) Multi-year coral bleaching episode in NW Australia and associated declines in coral cover. Coral Reefs. In RC Babcock et al. eds. Pilbara Marine Conservation Partnership – Final Report Vol. 2:471–490. CSIRO, Brisbane.

Baggett LS, Bright TJ (1985) Coral recruitment at the East Flower Garden Reef (North eastern Gulf of Mexico). Proceedings of the 5th Coral Reef Symposium, Tahiti 4: 379–384

Baird AH, Babcock, RC, Mundy CP (2003) Habitat selection by larvae influences the depth distribution of six common coral species. Mar. Ecol. Prog. Ser. 252: 289–293

Baird AH, Hughes TP (2000) Competitive dominance by tabular corals: an experimental analysis of recruitment and survival of understorey assemblages. J. Exp. Mar. Biol. Ecol. 251:117-132

Bak RPM, Engel MS (1979) Distribution, abundance and survival of juvenile hermatypic corals (Scleractinia) and the importance of life history strategies in the parent coral community. Mar. Biol. 54: 341–352

Boschetti F, Babcock R, Doropoulos C, Thomson D, Feng M, Slawinski D, Berry O, Vanderklift M, (2017) Setting priorities for conservation initiatives at the interface between ocean

circulation, larval connectivity, and population dynamics. Submitted

Burgess SC, Nickols KJ, Griesemer CD, Barnett LAK, Dedrick AG, Satterthwaite EV, Yamane L, Morgan SG, White JW, Botsford LW (2014) Beyond connectivity: how empirical methods can quantify population persistence to improve marine protected-area design. Ecol. Appl. 24: 257–270

Carlton DB (2001) Depth-related patterns of coral recruitment and cryptic suspension-feeding invertebrates on Guana Island, British Virgin Islands. Bull. Mar. Sci. 68 (3): 525–541

DPaW (2013) http://www.dpaw.wa.gov.au/management/marine/marine-parks-andreserves/69-new-and-proposed-marine-parks-and-reserves

Eagle JV, Baird AH, Jones GP, Kingsford MJ (2012) Recruitment hotspots: consistent spatial patterns in the relative abundance of coral recruits at One Tree Island, Australia. Galaxea 14: 5–22

Edmunds PJ (2000) Patterns in the distribution of juvenile corals and coral reef community structure in St. John, US Virgin Islands. Mar. Ecol. Prog. Ser. 202: 113–124.

Feng M, Colberg Slawinski D, Berry O, Babcock R (2016) Ocean circulation drives heterogeneous recruitments and connectivity among coral populations on the North West Shelf of Australia. J Marine Systems. 164: 1-12

Fisher R, Wilson SK, Sin TM, Lee AC, Langlois TJ (In Review) A simple function for full subsets multiple regression in ecology with R. Methods in Ecology and Evolution

Fisk DA, Harriott VJ (1990) Spatial and temporal variation in coral recruitment on the Great Barrier Reef: implications for dispersal hypotheses. Mar. Biol. 107: 485–490

Fitzhardinge R (1985). Spatial and temporal variability in coral recruitment in Kaneohe Bay (Oahu, Hawaii). Proc. 5th Int. Coral Reef Cong., vol. 4: 373–377

Forde MJ (1985) Technical report on suspended matter in Mermaid Sound, Dampier Archipelago. Department of Conservation and Land Management. Perth, Western Australia. Bulletin 215

Harriott VJ, Fisk DA (1988) Recruitment patterns of scleractinian corals: a study of Three Reefs. Aust. J. Mar. Freshw. Res. 39, 409–416.

Harrison PL, Wallace CC (1990) Reproduction, dispersal and recruitment of scleractinian corals. In: Dubinsky, Z. (Ed.), Ecosystems of the World, vol. 25: 133–207

Hughes TP, Baird AH, Dinsdale EA, Moltschaniwskyj NA, Pratchett MS, Tanner JE, Willis BL (1999) Patterns of recruitment and abundance of corals along the Great Barrier Reef. Nature 397: 59–63

Hughes TP, Baird AH, Dinsdale EA, Moltschaniwskyj NA, Pratchett MS, Tanner JE, Willis BL (2000) Supply-side ecology works both ways: the link between benthic adults, fecundity, and larval recruits. Ecology 81 (8): 2241–2249

Hughes TP, Baird AH, Dinsdale EA, Harriott VJ, Moltschaniwskyj NA, Pratchett MS, Tanner JE, Willis BL (2002) Detecting regional variation using meta-analysis and large-scale sampling: latitudinal patterns in recruitment. Ecology 83 (2): 436–451

Keough MJ, Downes BJ (1982) Recruitment of marine invertebrates: the role of active larval choices and early mortality. Oecologia 54:348–352

Kool JT, Nichol SL (2015) Four-dimensional connectivity modelling with application to Australia's north and northwest marine environments. Environ. Modell. Softw. 65: 67–78

Lafratta A, Fromont J, Speare P, Schönberg CHL (2017) Coral bleaching in turbid waters of north-western Australia. Marine and Freshwater Research 68(1): 65-75.

Marchesiello P, McWilliams JC, Shchepetkin A (2003) Equilibrium structure and dynamics of the California current system. J. Phys. Oceanogr. 33: 753–783.

Mundy CN (2000) An appraisal of methods used in coral recruitment studies. Coral Reefs 19: 124–131.

Mundy C, Babcock R (2000). Are vertical distribution patterns of scleractinian corals maintained by pre- or post-settlement processes? A case study of three contrasting species. Mar. Ecol. Prog. Ser. 198: 109–119

Oliver JK, King BA, Willis BL, Babcock RC, Wolanski E (1992) Dispersal of coral larvae from a lagoonal reef - II. Comparisons between model predictions and observed concentrations. Cont. Shelf Res. 12: 873–889

Radford B, Babcock R, Niel K, Done T (2014) Are cyclones agents for connectivity between reefs? J. Biogeogr. 41: 1367–1378

Ridgway T, Inostroza K, Synnot L, Trapon M, Twomey L, Westera M (2016) Temporal patterns of coral cover in the offshore Pilbara, Western Australia. Marine Biology, *163*(9), 182.

Roberts CM, et al. (2002) Marine biodiversity hotspots and conservation priorities for tropical reefs. Science 295: 1280–1284

Sammarco PW (1985) The Great Barrier Reef vs. the Caribbean: comparisons of grazers, coral recruitment patterns and reef recovery. Proc. 5th Int. Coral Reef Cong., vol. 4: 391–397

Sammarco PW (1991) Geographically specific recruitment and post settlement mortality as influences on coral communities: the cross continental shelf transplant experiment. Limnol. Oceanogr. 36 (3): 496–514

Sammarco PW (1994) Larval dispersal and recruitment processes in Great Barrier Reef corals: analysis and synthesis. In: Sammarco PW, Heron ML (Eds) The Biophysics of Marine Larval Dispersal. American Geophysical Union, Washington D.C.: 35–71

Sammarco PW, Andrews JC (1989) The Helix experiment: differential localized dispersal and recruitment patterns in Great Barrier Reef corals. Limnol. Oceanogr. 34 (5): 896–912

Semeniuk V, Chalmer PN, Le Provost I (1982) The Marine Environments of the Dampier Archipelago, Western Australia. Journal of the Royal Society of Western Australia, Vol. 69, Part 3: 97-114

Simpson CJ, Cary j (1998) Environmental Guidelines and Procedures in Relation to CALM Advise on the Marine Aspects of Aquaculture and Pearling Proposals in Western Australia. Report No.: MPC –01/1998, Marine Conservation Branch, Department of Conservation and Land Management. Perth, Western Australia.

Smith LD, Hughes TP (1999) An experimental assessment of survival, re-attachment and fecundity of coral fragments. J. Exp. Mar. Biol. Ecol. 235: 147–164

Soong K, Chen MH, Chen CL, Dai CF, Fan TY, Li JJ, Fan HM (2003) Spatial and temporal variation of coral recruitment in Taiwan. Coral Reefs 22:224-228

Vermeij MJA (2005) Substrate composition and adult distribution determine recruitment patterns in a Caribbean brooding coral. Mar. Ecol. Prog. Ser. 295: 123–133

Wolanski E, Hamner WM (1988) Topographically controlled fronts in the ocean and their biological influence. Science 241: 177-181

Veron JEN, Marsh LM (1988) Hermatypic corals of Western Australia: records and annotated species list. Western Australian Museum Memoir 29: 1-136

6.5 Density-dependent coral recruitment displays divergent responses during distinct early life-history stages

Authors: Doropoulos C, Evensen NR, Gómez-Lemos LA, Babcock RC.

ABSTRACT

Population growth involves demographic bottlenecks that regulate recruitment success during various early-life history stages. The success of each early-life history stage can vary in response to population density, interacting with intrinsic (e.g. behavioural) and environmental (e.g. competition, predation) factors. Here, we used the common reef-building coral *Acropora millepora* to investigate how density-dependence influences larval survival and settlement in laboratory experiments that isolated intrinsic effects, and post-settlement survival in a field experiment that examined interactions with environmental factors. Larval survival was exceptionally high (>80%) and density-independent from 2.5 to 12 days following spawning. In contrast, there was a weak positive effect of larval density on settlement, driven by gregarious behaviour at the highest density. When larval supply was saturated, settlement was 3-times higher in crevices compared to exposed microhabitats, but a negative relationship between settler density and post-settlement survival in crevices and density-independent survival on exposed surfaces resulted in similar recruit densities just one month following settlement. Moreover, a negative relationship was found between turf algae and settler survival in crevices, whereas gregarious settlement improved settler survival on exposed surfaces. Overall, our findings reveal divergent responses by coral larvae and newly settled recruits to density-dependent regulation, mediated by intrinsic and environmental interactions.

6.5.1 INTRODUCTION

The recruitment of new individuals is a key ecological process for the maintenance and recovery of natural populations. Following major disturbances, new individuals supplied from remnant populations recruit to newly available space, with their subsequent growth and survival driving population recovery (Connell and Keough 1985, Nathan and Muller-Landau 2000, Young et al. 2005, Doropoulos et al. 2015). But recruitment and population growth are not infinite, and there are density-dependent processes that regulate populations (Caley et al. 1996, Courchamp et al. 1999, Hixon and Johnson 2009). Population dynamics are (1) density-dependent when proportional growth is negative above a carrying capacity, (2) inverse density-dependent when proportional growth is positive below a carrying capacity, or (3) density-independent when proportional growth or loss do not respond to density. Inverse density-dependence can also lead to an Allee effect, where a population declines past a lower threshold and leads to extinction (Courchamp et al. 1999). Hence, understanding how propagule density influences recruitment is necessary to quantify the thresholds needed for population recovery.

For many benthic marine invertebrates and fish, recruitment involves a bipartite life-history with pelagic larvae and benthic recruits. Recruitment is thus a complex process, often divided into three major life-history phases involving (1) larval availability and transport, (2) larval settlement ecology, and (3) post-settlement ecology (Pawlik 1992, Pineda et al. 2009, Ritson-Williams et al. 2009). Each life-history phase can be considered a recruitment bottleneck, strongly influenced by bio-physical interactions (Wahle and Steneck 1991, Vermeij and Sandin 2008, Doropoulos et al. 2016). In open, size-structured populations, early post-settlement survival is often considered the most severe bottleneck, given the minute size and high mortality of newly settled individuals (Werner and Gilliam 1984, Rice et al. 1993, Gosselin and Qian 1997, Hunt and Scheibling 1997). Yet, the aggregative behaviour of marine fish and invertebrates as pelagic and settling larvae (Burke 1986, Pawlik 1992, Selkoe et al. 2006) means that density-dependence is a central contributor to demographic bottlenecks at both pre- and post-settlement life-history phases.

Interactions between intrinsic and environmental factors can change the strength and direction of density-dependent effects (Hixon et al. 2002, White 2007). Inverse density-dependent settlement for benthic invertebrates and fish is often driven by high availability of settlement space and refugia, whereas competition and predation often cause direct density-dependent survival (e.g. Vermeij and Sandin 2008, White et al. 2010). This is particularly evident in coral reef fish, where density-dependence has been shown: (1) only in the presence of both resident-ambush and transient-pursuit predators, with survival becoming density-independent when only one type of predator is present (Hixon and Carr 1997); or (2) in the presence of only resident-ambush predators when the availability of refugia is limited and causes strong intraspecific competition (Holbrook and Schmitt 2002). For benthic marine invertebrates that attach themselves to the substratum, two-dimensional space is always ultimately limited. Settlement is often proportional to available space, with space limitation driving density-dependent and gregarious settlement (Gaines and Roughgarden 1985, Raimondi 1990, Vermeij and Sandin 2008). Gregarious settlement increases post-settlement survival in some cases (Raymundo and Maypa 2004, Linden and Rinkevich 2017), mediated by size-escape mechanisms, but not others (Puill-Stephan et al. 2012). At low settlement densities survival is often density-independent (Connell 1985, Gaines and Roughgarden 1985, Raimondi 1990), but at high densities, gregarious settlement can also attract predators and increase post-settlement mortality (Gaines and Roughgarden 1985).

Coral populations are often in a state of recovery, making degraded coral reef ecosystems particularly vulnerable to Allee effects due to habitat and population fragmentation that act on coral recruitment (Knowlton 2001). Bottlenecks to coral recovery can be driven by limited larval supply (Hughes et al. 2000, Hughes and Tanner 2000), environmental factors such as refugia, predation

(direct or indirect), grazing, and competition that interact with settlement and post-settlement stages (Brock 1979, Arnold et al. 2010, Doropoulos et al. 2016), or a combination of both. Surprisingly, only a limited number of studies have investigated the role of density-dependent effects on coral recruitment processes. Patterns reveal that: (1) larval survival is negatively related to density in *Montipora capitata* (Vermeij et al. 2009); (2) larval settlement increases with larval density using mass *in situ* culturing with gametes collected from spawning slicks (Heyward et al. 2002), *Acropora digitifera* (Edwards et al. 2015), and *A. muricata* and *A. tenuis* (Suzuki et al. 2012); larval settlement is (3) positively related to crustose coralline algae but negatively related to turf algae cover with *Siderastrea radians* (Vermeij and Sandin 2008); and, (4) the relationship between coral settlers and recruits is density-dependent so that increasing settlement density does not improve recruit densities in *Acropora* spp. (Suzuki et al. 2012, Edwards et al. 2015). Yet, no study has conducted a systematic evaluation of density-dependent effects at each major early life-history stage for a single species and mechanistic understandings are vague. Hence, we used three complimentary experiments aimed to examine how intrinsic and environmental factors can drive density-dependent responses during coral larval survival, larval settlement, and post-settlement survival in *Acropora millepora*. Experiments examining density-dependent regulation of larval survival and settlement were conducted in a laboratory and excluded any environmental interactions, while the experiment examining post-settlement survival was conducted in a field setting and included interactions with environmental factors.

6.5.2   METHODS

Study location and coral larvae culturing

This study was conducted at Coral Bay Research Station and nearby reefs, Ningaloo Reef, Western Australia, from March until May 2016. Eight gravid colonies of the common branching coral *Acropora millepora* were collected from shallow reefs (~3 m depth) in Coral Bay (23.173984°S, 113.760459°E) and transported to the local jetty for access during spawning. Colonies were isolated in 60 L tubs at sunset and all spawned on the 2nd of April from 21:00-22:00, 10 days after the full moon. The egg-sperm bundles were collected and transported to the research station where they were transferred into two 20 L tubs of filtered seawater. Water agitation broke apart the bundles to promote cross-fertilisation. Fertilisation success was periodically monitored using a dissecting microscope and after three hours >50% of subsampled eggs were fertilised and had undergone division. Eggs were removed from the top of the water column and placed into large outdoor 150 L sumps for rearing with filtered seawater and aeration. Half water changes took place every 6 hours for the first 48 hours, and every 24 hours thereafter. Similarly, aeration was low for the first 48 hours and was increased thereafter. All seawater used for fertilisation and rearing was filtered using a 4-stage canister stack and UV sterilisation (Odyssea CFS-1000). The mean temperature of the seawater during the larval culturing period was 24.9°C (± 0.9 SD, min = 22.5°C, max = 26.8°C).

Experimental overview

Three experiments were conducted to test density-dependent responses of larval survival, larval settlement, and post-settlement survival. The two experiments investigating larval survival and larval settlement were conducted in laboratory conditions that excluded variations in environmental factors, isolating the effects of larval density only. In contrast, the experiment investigating post-settlement survival was conducted using tiles that incorporate microhabitat rugosity and were transplanted onto reefs, incorporating the effects of density interacting with environmental factors (i.e. refugia, competition, and predation).

Experiment 1: Density-dependent larval survival

We began an experiment to examine the effect of larval density on larval survival once the coral larvae had developed into swimming planulae, 60 hours following spawning. Acropora millepora planulae are lecithotrophic (i.e., non-feeding), and non-feeding Acropora planulae have been shown to remain competent in laboratory conditions for at least 6 weeks following spawning (Graham et al. 2013b). Swimming and healthy coral larvae were sampled and placed into sterile 20 ml glass containers (scintillation vials) with filtered seawater (0.2 μm and UV). Previous work has shown that coral larvae are found at maximum densities of ~5 individuals per 20 ml in multispecies spawning slicks (Oliver and Willis 1987), so we chose densities that ranged below and above this maximum. Larvae were stocked at 1, 3, 6, 10, and 20 individuals per 20 ml, with five replicate containers per density. At 60, 85, 107, 130, 154, 210, 263 and 288 hours following spawning, the number of swimming and dead larvae were individually counted and surviving larvae transferred into new filtered seawater. Larvae were recorded as alive if they were observed (by eye) swimming, but if not moving, they were assessed under a dissecting microscope to verify if they were dead or alive. The experiment took place in a laboratory at 26°C.

Larval survival data were analysed using two approaches. Firstly, trends in larval survival at the different densities were investigated using a random-effects Cox proportional hazard model (Coxme) with the "coxme" package (Therneau 2012) in R, with containers treated as a random effect. The model is a time-to-event analysis that allows for the stochastic rate at which an event occurs to vary, but makes a proportional hazards assumption that the relative effect among treatments is consistent over time. Second, because time had no obvious effect on larval survival rates (Coxme, $p = 0.567$), a subsequent analysis investigated the effect of larval-density on proportional larval survival 12 days after spawning using a generalised linear mixed effects model (GLMM) with binomial error structure. Larval survival was the binomial response variable, initial larval density the continuous predictor, and replicate containers incorporated as a random effect.

Experiment 2: Density-dependent larval settlement

A complimentary experiment was then conducted to examine the effect of larval density on larval settlement once the coral larvae were competent to settle, 7 days following spawning. Larvae were stocked at 1, 3, 6, 10, 20 and 50 individuals per 20 ml, with five replicate containers per density. Experimental settlement assays generally followed the procedures of Heyward and Negri (1999), explained below. Swimming and healthy planulae that were searching and testing the substrata for settlement were sampled and placed into sterile 20 ml polystyrene cell culture wells with filtered seawater (0.2 μm and UV). The crustose coralline algae (CCA) Porolithon onkodes was used as a settlement inducer. Porolithon onkodes was collected using chisel and hammer from nearby reefs at a depth of ~1 m, fragmented into equally sized 5 × 5 mm chips, the thalli cleaned with a toothbrush and tweezers under a dissecting microscope, and the dead carbonate underside fraction of the chip was scraped off so that only the very thin surface layer of the CCA remained. Upmost care was taken to standardise the CCA chip size to 5 × 5 mm to remove any potential confounding interaction between larval density and CCA chip size. A single chip was placed in each well with the larvae.

The experiment took place for 24 hours in a lab at 26°C from the time the larvae and CCA were introduced into the wells. Settlement was then scored by directly counting all larvae that had attached and metamorphosed in each well on the CCA chip and container surfaces under a dissecting microscope. The effect of larval density on proportional larval settlement was analysed using a GLMM with binomial error structure, with larval settlement as the response variable, initial larval density the continuous predictor, and replicate containers incorporated as a random effect.

Experiment 3: Density-dependent post-settlement survival

A final experiment then took place to understand effects of gregariousness, initial settler-density, and competition on post-settlement survival. The experiment used a field-based approach, and generally followed procedures described in Doropoulos et al. (2016). Larvae were settled onto 10×10 cm settlement tiles made from a mix of calcium carbonate sand and cement at a ratio of 4:1. The tiles are a custom design that incorporate microhabitat complexity, with 24 crevices (total area = 54.8 cm^{-2} per tile) and 24 exposed surfaces (total area = 34.6 cm^{-2} per tile), previously shown to characterise coral recruitment on the reef benthos (Doropoulos et al. 2016). Tiles were preconditioned for a month at a shallow reef (~3 m depth) in Coral Bay to develop a microbial and encrusting community important to coral settlement (Heyward and Negri 1999). Upon retrieval, tiles were gently cleaned using toothbrushes to remove any turf algae, encrusting fleshy algae, foliose macroalgae, and heterotrophic invertebrates, and were placed with the competent coral larvae in the rearing tub at 6 days after spawning. Corals that settled onto the tiles were scored after 2-3 days using a dissecting microscope. Only individuals that settled on the upward facing exposed and crevice microhabitats were included, with all other individuals scraped off including those on tile undersides and vertical edges (Figure S6.5.1).

Each settler was mapped according to its location on the tile and gregariousness (i.e., whether an individual was settled touching another individual or not). Tiles were then out-planted to five replicate reef-flat sites at 2-3 m depth, each separated by >8 km, with five tile replicates per site. Tiles were attached 2 cm above the reef substrate using base plates following the technique of Mundy (2000). Three extra tiles were mapped and used as a handling control by transporting them to the field sites during deployment, returning them to the laboratory the same day after 14 hours, and rescoring them. Controls showed that transportation of the experimental tiles to the field did not affect settler survival with <3% change in abundances. For the experimental tiles, all settlers were rescored in situ by a single observer (CD) following a 30 day period. The location and gregariousness were recorded over the previously drawn maps, indicating the outcome (mortality/survival) for every coral settler.

To assess the influence of competition on post-settlement survival, photographs of the tiles were taken in situ to quantify the community covering the settlement tiles. A grid of cells that corresponded to every exposed and crevice microhabitat was then overlaid onto the image of each tile and proportional cover of the different substrata within a cell estimated. Thus, the substrata in the immediate area surrounding any coral settler was known. Substrata were categorised as biofilmed tile, crustose coralline algae (CCA), turf algae (Turf), sediment, encrusting fleshy algae (EFA), foliose macroalgae (MA), and heterotrophic invertebrates (ascidians, bryozoans, sponges).

Analysis of the field experiment was conducted in multiple stages to understand the (1) distribution of corals between microhabitats (exposed, crevice) upon settlement and 30-days post-settlement; (2) community composition between microhabitats at 30-days post-settlement; and (3) the effect of microhabitat, settler density, gregariousness (single, aggregated), and competition on the post-settlement survival of newly-settled corals at 30-days post-settlement. Firstly, to investigate the distribution of coral settlers between microhabitats, settler density was standardised to number of individuals cm^{-2} to normalise for the greater space availability in crevices compared to exposed surfaces. The same approach was applied to coral recruits at 30-days post-settlement. Paired t-tests were conducted to statistically test for any differences in the density of settlers or recruits between microhabitats, incorporating the correlation structure between crevice and exposed microhabitats within a tile. Secondly, multivariate community cover of the dominant groups found on the settlement tiles at 30-days post-settlement was then tested among microhabitats using a mixed effects model compared with sites incorporated as a random effect. The multivariate analysis was

conducted on a Bray-Curtis similarity matrix, using 999 permutations to generate P values, on the raw data that was homogeneous without transformation (tested using permDISP).

The final analysis on post-settlement survival then used a step-wise modelling approach. Initial analyses showed significant interactions between microhabitats × gregariousness and microhabitats × density on coral post-settlement survival. Considering that benthic communities were also distinct between the two microhabitats (see Results), two separate analyses were conducted that investigated the effects of gregariousness, settler density, and competition on post-settlement survival within each microhabitat. For each microhabitat, the original GLMM included the survival of every settler as the binomial response variable, gregariousness (single, aggregated) as a categorical predictor, initial settler abundances a continuous predictor, cover of the seven substrata in a cell surrounding the settlers as continuous predictors, and site and tile replicates as random effects with tile replicate nested in site. All continuous variables were centred by their mean to make their effects comparable. Model simplification was then conducted using backwards elimination of predictors, comparing full and reduced models using likelihood ratio test (LRT, χ^2) p values. For exposed microhabitats, the best fit model incorporated settler survival as a function of gregariousness, and the cover of CCA, turf, EFA, and sediment. For crevice microhabitats the best fit model included settler survival as a function of settler density, and the cover of CCA, turf, EFA, sediment, and MA. Both GLMMs had site and tile replicates as random effects with tile replicates nested in site.

All GLMMs were conducted using 'lme4' (Bates et al. 2015), post-hoc tests of categorical interactions used 'multcomp' (Hothorn et al. 2008), and paired t-tests used the 'stats' package in R (R Development Core Team 2017). Fits of binomial GLMMs were estimated using 'blemco' (Korner-Nievergelt et al. 2015), and dispersion was not found to be problematic for analyses of larval settlement and post-settlement survival. However, for larval survival, data were overdispersed so an observation level random factor was added to the model. Multivariate analysis of the tile community was conducted in Primer with the perMANOVA extension (Anderson et al. 2008).
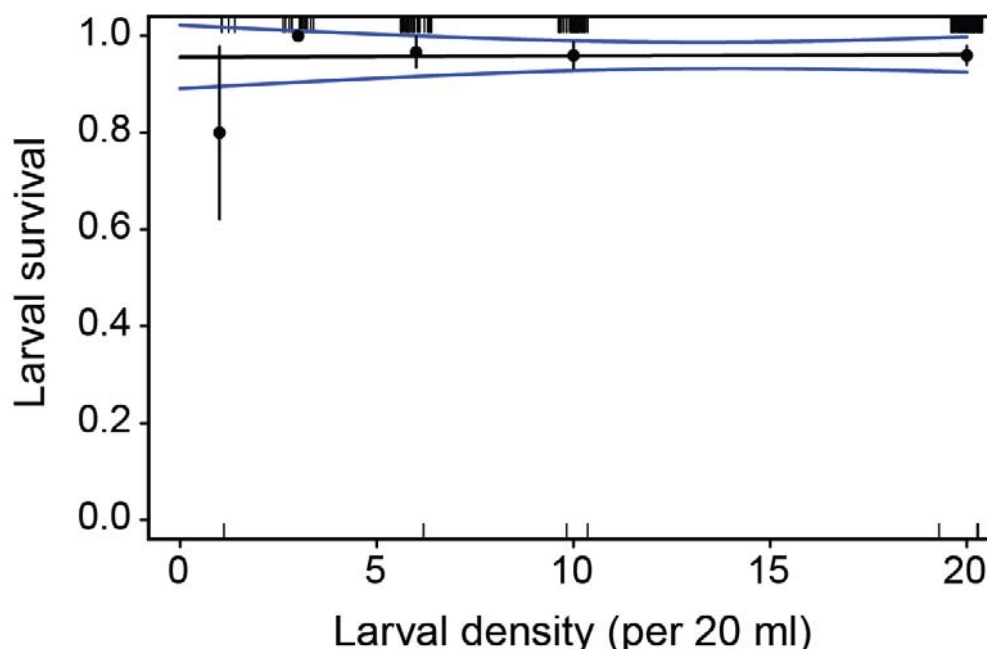
Figure 6.5.1 Relationship between larval density and proportional survival of *Acropora millepora* coral larvae 226 hours following spawning. Experiment began 60 hours following spawning. The black solid line represents the mean model fit, blue lines represent the SEM of the model fit, black circles and vertical bars represent the mean and SEM among tanks, and the small notches (top and bottom x-axes) represent individual data points. There were five replicate tanks per larval density.

6.5.3   RESULTS

Density-dependent larval survival

No relationship was observed between initial larval density and larval survival from 2.5 to 12 days following the spawning of the *Acropora millepora* (Figure 6.5.1, Figure S6.5.2, Table 6.5.1a). Thus, coral larval survival was density-independent and averaged >80% for densities ranging from 3 to 20 larvae per 20 ml.

Density-dependent larval settlement

There was a positive relationship between the initial density of *A. millepora* and the probability of settlement (Figure 6.5.2). Settlement ranged from 40-50% at densities of 1-20 larvae per 20 ml, increasing to >70% at the highest density of 50 larvae per 20 ml. Variability among replicate containers within larval density was high, especially at lower densities (Figure 6.5.2), resulting in a weak overall effect between settlement and density (LRT, *p* = 0.066; Table 6.5.1b).

Table 6.5.1 Summary of generalised (binomial) linear mixed effects models testing density-dependent effects on coral larvae (a) survival and (b) settlement, and (c) post-settlement survival. The direction of effects are indicated, as well as statistical model details and outcomes. + = positive relationship; – = negative relationship; ~ no relationship. LRT = likelihood ratio test. Boldfaced text indicates effects with *p* < 0.1.

RECRUITMENT STAGE	RESPONSE	PREDICTOR	DIRECTION	LRT	*p*
a. Larvae [1]	Survival	Initial density	~	0.016	0.899
b. Settlement [1]	Settlement	**Initial density**	+	**3.367**	**0.066**
c. Post-settlement [2]	Survival	**Micro. [3] × Greg. [4]**		**7.561**	**0.006**
		Micro. [3] × Density		**3.260**	**0.071**
Exposed microhabitat		**Gregariousness**	+	**10.013**	**0.002**
		CCA [5]	+	2.025	0.155
		Turf	-	1.631	0.201
		EFA [6]	-	1.044	0.307
		Sediment	-	2.240	0.134
Crevice microhabitat		**Initial density**	-	**7.328**	**0.007**
		CCA [5]	+	2.316	0.128
		Turf	-	**7.728**	**0.005**
		EFA [6]	~	0.031	0.860
		Sediment	-	1.017	0.313
		Macroalgae	~	0.076	0.782

[1] Five tank replicates per density.

[2] Five site replicates; five tile replicates per site.

[3] Microhabitat = categorical with two levels (exposed, crevice).

[4] Gregariousness = categorical with two levels (single, aggregated).

[5] CCA = crustose coralline algae.

[6] EFA = encrusting fleshy algae.
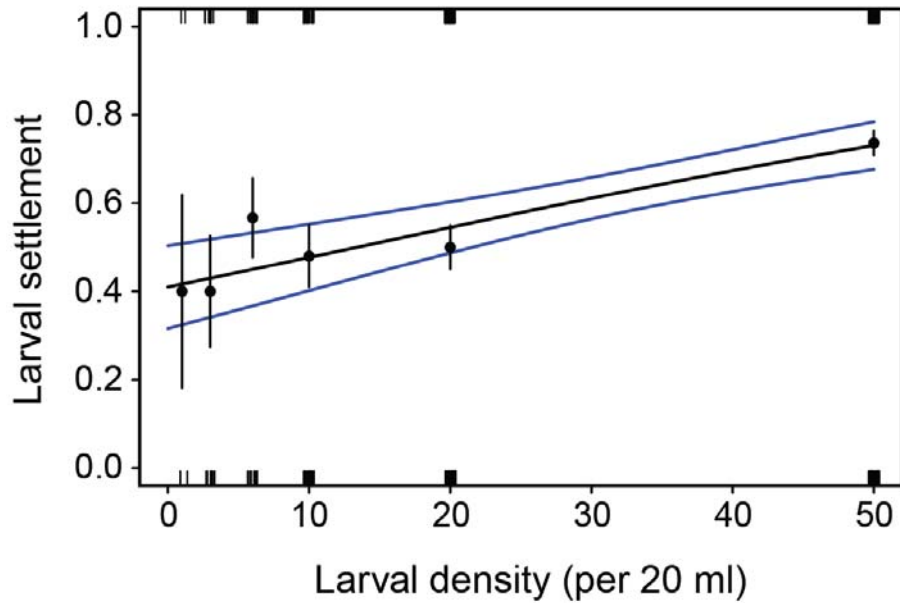
Figure 6.5.2 Relationship between larval density and proportional settlement of *Acropora millepora* after 24 hours in settlement experiments conducted 7 days following spawning. See Figure 6.5.1 legend for description of the symbols in the plots. There were five replicate tanks per larval density.
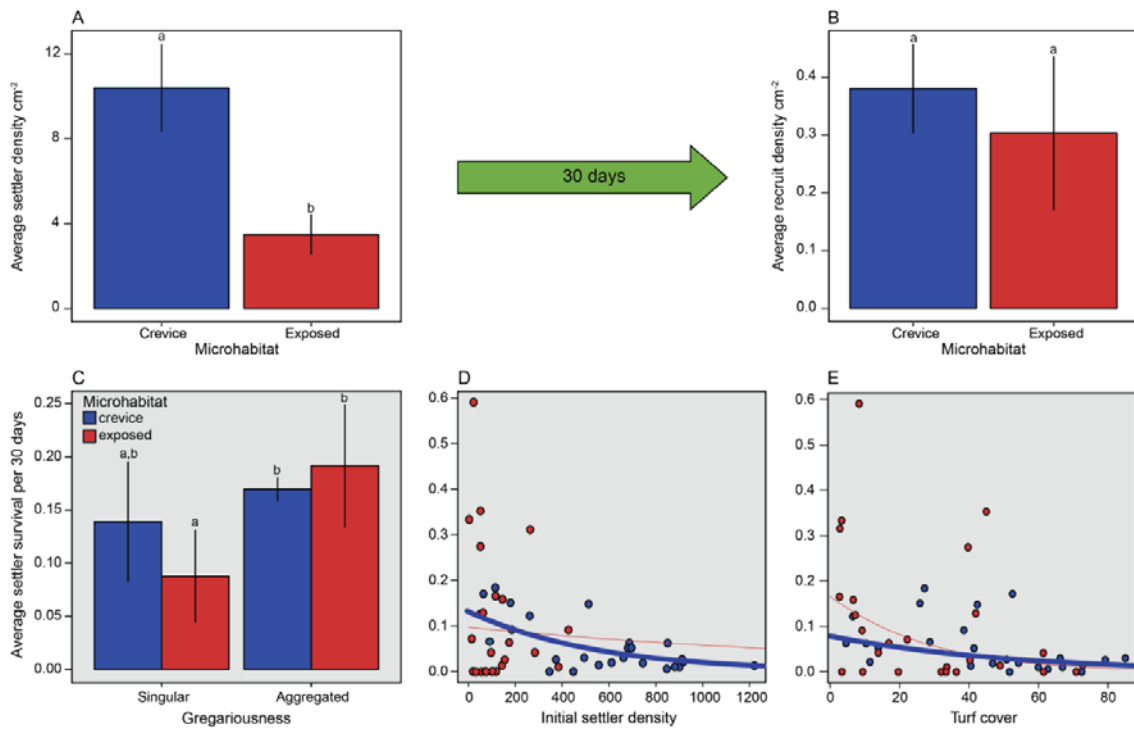
Figure 6.5.3 Average *Acropora millepora* densities (cm^{-2}) among crevice (blue) and exposed (red) microhabitats at (a) settlement and (b) following 30 days in field experiments. Explanatory variables of post-settlement survival are displayed in grey panels and include the effects of (c) gregariousness, (d) initial settler density, and (e) turf cover. Bars with different letters above them in a, b, and c are significantly different, and solid lines in d and e represent the mean prediction of significant (thick and blue) and non-significant (thin and red) model fits. There were five replicate sites with five replicate tiles per microhabitat. Note the different scales for *y*-axes.

Density-dependent post-settlement survival

When competent larvae were provided with complex substrata, a total of 17241 *A. millepora* settlers were mapped from 25 tiles, with a strong preference to settle in crevices compared to exposed microhabitats. There were 3.0-times more settlers in crevices compared to exposed surfaces (paired t-test, $p < 0.001$), with a mean ± SEM of 10.39 ± 1.13 settlers cm^{-2} *versus* 3.48 ± 0.64 settlers cm^{-2}, respectively (Figure 6.5.3a). Subsequently, the proportion of gregarious settlement was higher in crevices than exposed microhabitats (59.7 ± 3.0% *versus* 48.1 ± 4.7%). However, just 30-days following settlement, average recruit density was the same in both microhabitats (paired t-test, $p = 0.47$), averaging 0.38 ± 0.06 recruits cm^{-2} in crevices and 0.30 ± 0.10 recruits cm^{-2} on exposed surfaces (Figure 6.5.3b).

The community found on the settlement tiles 30-days following deployment also differed between exposed and crevice microhabitats (PERMANOVA, $p = 0.024$; Figure 6.5.4a). On exposed surfaces, crustose coralline algae (CCA) was dominant (48% cover) over turf algae (27%) followed by encrusting fleshy algae cover (11%; Figure 6.5.4b). A contrasting pattern was found in crevices, with turf algae dominating (43% cover) over CCA cover (26%), followed by sediment (16%) and EFA cover (7%; Figure 6.5.4b).
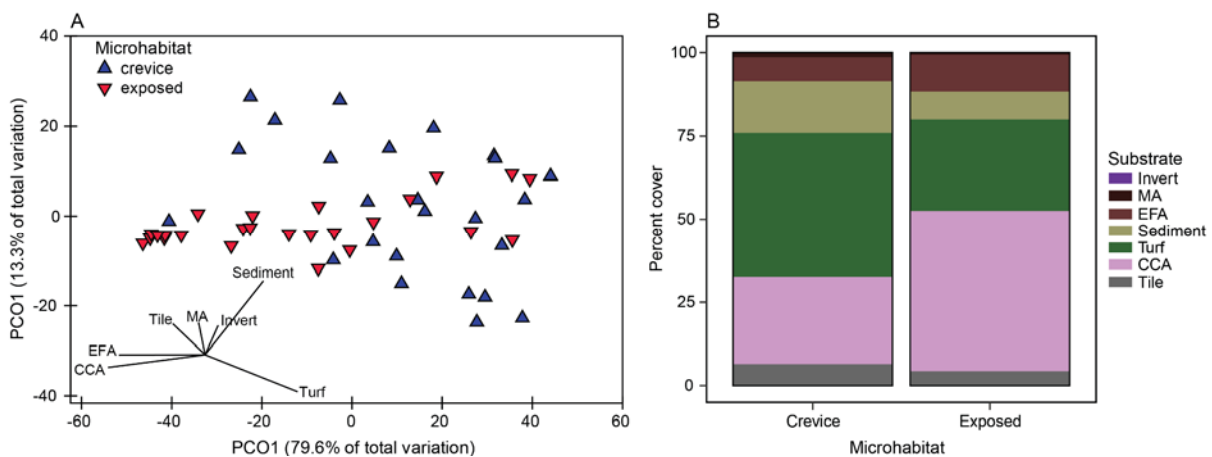
Figure 6.5.4 (a) Principal coordinate analysis and Pearson correlation vector of the substrata found in crevices (upward facing blue triangles) and exposed (downward facing red triangles) microhabitats on the settlement tiles 30 days following deployment. (b) Relative percent cover of each substrate found in crevice and exposed microhabitats on the settlement tiles 30 days.

Contrasting responses to intrinsic and environmental factors drove differential coral settler mortality between the microhabitats. Firstly, gregarious settlement behaviour increased survival by >2-times on exposed surfaces but did not improve post-settlement survival in crevices (Figure 6.5.3, Table 6.5.1c). On exposed surfaces, survival of singular settlers averaged only 9% after 30 days compared to 19% for aggregated settlers. Second, a non-linear negative relationship was observed between settler density and proportional survival of settlers found in crevices (Figure 6.5.3d, Table 6.5.1c). Survival averaged 13-10% for the lowest densities <200 settlers per tile, decreased to 6% and 4% for densities of 400 and 600 settlers, and was lowest at 3 to 1% for densities ranging from 800 to 1200 settlers per tile. In contrast, there was no relationship between settler density and survival on exposed microhabitats, with highly variable survival occurring at densities <200 settlers per tile (Figure 6.5.3d). Finally, of all the potential competitors, only increasing turf algae had a significant negative effect on post-settlement coral survival and this only occurred in crevice microhabitats (Figure 6.5.3e, Table 6.5.1c).

6.5.4 DISCUSSION

While it has previously been shown that density-dependence has varying effects during coral recruitment that depends on the life-history phase and taxonomic identity (Heyward et al. 2002, Vermeij and Sandin 2008, Vermeij et al. 2009, Suzuki et al. 2012, Edwards et al. 2015), no previous work had conducted a systematic study to mechanistically understand how density-dependence influences recruitment success during each major early life-history stage in a single species. Our series of experiments demonstrates the complexities of density-dependent effects on coral recruitment, from the survival and behaviour of swimming and settling larvae isolated in laboratory settings, to ecological interactions that drive early post-settlement survival up to one-month following settlement. Larval survival in the experimental arena free of competitors, predators, or microbes, was extremely high and density-independent from 2.5 days until 12 days following spawning. Using the same experimental arena, larval settlement displayed a weak positive response to increasing larval density due to the gregarious settlement behaviour of marine invertebrates. When offered settlement substrata with microhabitat rugosity, larval settlement was 3-times higher in crevice microhabitats that offer refugia from predators compared to exposed surfaces. However, settler survival was density-dependent in those crevice microhabitats but density-independent on exposed surfaces. Ultimately, the contrasting density-dependent and –independent survival of settlers led to similar densities of coral recruits in both microhabitats just one month following settlement, supporting the findings of Suzuki et al. (2012) and Edwards et al. (2015) that very high densities of settled larvae do not improve coral recruitment.

Propagule supply is the key first step to population recovery, and for coral reefs the supply of coral larvae is critical for habitat recovery following disturbances. Due to their minute size, direct estimates of the actual supply of coral larvae and larval survival remain a mystery on reefs (Jones et al. 2009). Hence, density-dependent thresholds for ecologically relevant abundances of coral larvae that can contribute to recruitment on reefs are unknown, but laboratory experiments can partly provide the information necessary for application to predictive modelling (e.g. Connolly and Baird 2010, Feng et al. 2016). Apart from the current study where we found extremely high and density-independent survival of *Acropora* larvae (>80%) from 2.5 days until 12 days following spawning, only one previous study has addressed the relationship between coral larval density and survival and found strong density-dependent survival of *Montipora* larvae from 2 days to 7.5 days following spawning (Vermeij et al. 2009). However, those experiments by Vermeij et al. (Vermeij et al. 2009) had densities of around 250 to 11250 larvae L^{-1}, well above the maximum of 230 larvae L^{-1} found in spawning slicks (Oliver and Willis 1987) and the maximum of 1000 larvae L^{-1} used in our study. Notably, similarly high rates of survival to our study were found with *Montipora* larvae at densities <1250 larvae L^{-1} (Vermeij et al. 2009). Other studies using *Acropora* spp. at densities of 1000-1500 larvae L^{-1} have found survival ranges from <50% (Connolly and Baird 2010) and 15-90% (Graham et al. 2013a) in the first 12 days following spawning, showing that larval survival is highly variable even in controlled laboratory conditions. Future experiments that incorporate refugia and predators with varying densities of coral larvae in laboratory settings are needed to more thoroughly examine whether the density-independent response observed in this study remains when environmental interactors are present. In addition, density-dependent responses may occur in the earliest stages following spawning when positively buoyant developing embryos are distributed predominantly on the water surface in the highest densities in spawning slicks.

Upon arrival of larvae to a patch of reef, the transition from the plankton to the benthos is the next key step in recruitment. Experiments that supersaturate larval densities *in situ* have found that settlement is enhanced compared to controls (Heyward et al. 2002, Suzuki et al. 2012, Edwards et al. 2015). Our laboratory study supports these previous field experiments, showing that increasing larval density increases settlement rate, but here we also show that the relationship is not proportional and there appears a minimum threshold beyond which settlement is maximised. To illustrate,

settlement rates were 50% at 20 larvae per 20 ml (and no different to the lower larval densities), but 75% at 50 larvae per 20 ml, resulting in a non-linear increase in the abundance of settlers at the highest density. Suzuki et al. (2012) also found no difference in settlement between low (25 larvae L^{-1}) and medium (120 larvae L^{-1}) larval densities, but significantly higher settlement at the highest larval density (600 larvae L^{-1}), although the difference between the number of settlers was relatively proportional (Suzuki et al. 2012). The positive relationship between larval density and settlement probability was statistically weak in our settlement assays (Table 1b), due to the high among tank variability associated with settlement at the lower larval densities (especially 1 and 3 larvae per 20 ml). High settlement variability at lower larval densities is expected considering that invertebrate settlement is facilitated by positive chemical cues derived from conspecifics (Burke 1986), and aggregative settlement of *Acropora millepora* has previously been shown in experimental studies (Puill-Stephan et al. 2012). It is also interesting that the variability of settlement rate declined at higher densities because more consistent or less variable recruitment is an important attribute when considering the resilience of a community or population following disturbance (Jones et al. 2009). At the settlement stage of recruitment, non-linear increases in settler abundances resulting from increasing larval densities supports the notion that larval densities need to surpass minimal thresholds to achieve settlement success and avoid potential Allee effects to population recovery (Courchamp et al. 1999, Knowlton 2001).

Microhabitat suitability for coral settlement is driven by known physical and chemical cues in marine invertebrates, and similar to previous work with coral larvae (Whalan et al. 2015, Doropoulos et al. 2016, Doropoulos et al. 2017), *Acropora millepora* larvae preferentially settled within crevices rather than exposed surfaces when provided with complex substrata in this study. However, in contrast to previous work (Nozawa 2008, 2012, Edmunds et al. 2014, Doropoulos et al. 2016, Doropoulos et al. 2017), the refugia provided by crevices did not enhance post-settlement survival compared to exposed surfaces, averaging only 3.7% survival in crevices compared to 8.6% on exposed surfaces for the 30-day post-settlement period. In crevices, there was an overwhelming non-linear negative relationship with increasing settler density, which was not apparent on exposed surfaces where post-settlement survival was density-independent. Moreover, non-linear negative competitive interactions were also found with turf algae in crevices, exemplifying the influence of negative competitive effects found in cryptic microhabitats between turf algae and coral recruits (Arnold et al. 2010, Doropoulos et al. 2017). No competitive effects were found to influence settler survival on exposed surfaces, but gregarious settlement doubled post-settlement survival compared to individual settlement. While we did not directly quantify predation in our field experiment, we infer the relationship between size-escape mechanisms and indirect predation by herbivorous fish drove the positive response. On exposed surfaces, turf abundance was reduced and CCA abundance was increased, most likely a result of herbivorous fish grazing (Arnold et al. 2010, Brandl and Bellwood 2016, Doropoulos et al. 2016, Doropoulos et al. 2017). Subsequently, the action of herbivorous fish grazing may have indirectly targeted individual coral settlers because indirect predation by herbivorous fish occurs on the smallest coral recruits, which are quickly avoided as their size increases (Brock 1979, Christiansen et al. 2009, Doropoulos et al. 2012, Doropoulos et al. 2016). The alternative hypothesis that aggregative settlement increases post-settlement mortality by attracting predators, as seen at high-densities of barnacle (Gaines and Roughgarden 1985) and coral (Jayewardene et al. 2009, Gibbs and Hay 2015, Gallagher and Doropoulos 2017) recruits, is not supported by the results found in this study.

Collectively, our study shows that both excessively high and low densities of larvae and settlers are likely to contribute little to population recovery. Within the context of coral reef degradation (e.g. Knowlton 2001), low larval supply causing recruitment limitation from bottlenecks at settlement appear the first risk to coral recovery. On the other hand, excessively high larval supply that results in supersaturated settlement densities will not contribute to the recruitment of individuals that survive early post-settlement bottlenecks, and thus promote population recovery, because of density-

dependent regulation (Holm 1990, Suzuki et al. 2012, Edwards et al. 2015). Thus, while successful coral recruitment and population recovery are likely to be optimal with consistent supplies of larvae to disturbed patches of reef without space limitation, the density threshold that enhances recruitment success remains elusive and requires further investigation. Importantly, regulators of early recruitment success can act at very local (e.g. microhabitat) to regional (e.g. meta-population larval connectivity) scales, interacting with multiple stressors, so the use of generic rules to model recovery dynamics of coral populations needs to be applied conservatively within a context-specific approach.

6.5.5 ACKNOWLEDGEMENTS

6.5.6 REFERENCES

Anderson MJ, Gorley RN and Clarke KR (2008) PERMANOVA+ for PRIMER: guide to software and statistical methods. PRIMER-E, Plymouth, UK.

Arnold SN, Steneck RS and Mumby PJ (2010) Running the gauntlet: inhibitory effects of algal turfs on the processes of coral recruitment. Marine Ecology Progress Series 414:91-105.

Bates D, Maechler M, Bolker B and Walker S (2015) Fitting Linear Mixed-Effects Models Using lme4. Journal of Statistical Software 67:1-48.

Brandl SJ and Bellwood DR (2016) Microtopographic refuges shape consumer-producer dynamics by mediating consumer functional diversity. Oecologia 182:203-217.

Brock RE (1979) Experimental study on the effects of grazing by parrotfishes and role of refuges in benthic community structure. Marine Biology 51:381-388.

Burke RD (1986) Pheromones and the gregarious settlement of marine invertebrate larvae. Bulletin of Marine Science 39:323-331.

Caley MJ, Carr MH, Hixon MA, Hughes TP, Jones GP and Menge BA (1996) Recruitment and the local dynamics of open marine populations. Annual Review of Ecology and Systematics 27:477-500.

Christiansen NA, Ward S, Harii S and Tibbetts IR (2009) Grazing by a small fish affects the early stages of a post-settlement stony coral. Coral Reefs 28:47-51.

Connell JH (1985) The consequences of variation in intial settlement vs postsettlement mortality in rocky intertidal communities. Journal of Experimental Marine Biology and Ecology 93:11-45.

Connell JH and Keough MJ (1985) Disturbance and patch dynamics of subtidal marine animals on hard substrata. Pages 125-152 in S. T. A. Pickett and P. S. White, editors. The Ecology of Natural Disturbance and Patch Dynamics. Academic Press, Orlando.

Connolly SR and Baird AH (2010) Estimating dispersal potential for marine larvae: dynamic models applied to scleractinian corals. Ecology 91:3572-3583.

Courchamp F, Clutton-Brock T and Grenfell B (1999) Inverse density dependence and the Allee effect. Trends in Ecology & Evolution 14:405-410.

Doropoulos C, Roff G, Bozec Y-M, Zupan M, Werminghausen J and Mumby PJ (2016) Characterizing the ecological trade-offs throughout the early ontogeny of coral recruitment. Ecological Monographs 86:20-44.

Doropoulos C, Roff G, Visser M-S and Mumby PJ (2017) Sensitivity of coral recruitment to subtle shifts in early community succession. Ecology 98:304-314.

Doropoulos C., Ward S, Marshell A, Diaz-Pulido G and Mumby PJ (2012). Interactions among chronic and acute impacts on coral recruits: the importance of size-escape thresholds. Ecology 93:2131-2138.

Doropoulos C., Ward S, Roff G, González-Rivero M and Mumby PJ (2015) Linking demographic processes of juvenile corals to benthic recovery trajectories in two common reef habitats. PloS One 10:e0128535.

Edmunds PJ, Nozawa Y and Villanueva RD (2014) Refuges modulate coral recruitment in the Caribbean and the Pacific. Journal of Experimental Marine Biology and Ecology 454:78-84.

Edwards AJ, Guest JR, Heyward AJ, Villanueva RD, Baria MV, Bollozos IS and Golbuu Y (2015) Direct seeding of mass-cultured coral larvae is not an effective option for reef rehabilitation. Marine Ecology Progress Series 525:105-116.

Feng M, Colberg F, Slawinski D, Berry O and Babcock R (2016) Ocean circulation drives heterogeneous recruitments and connectivity among coral populations on the North West Shelf of Australia. Journal of Marine Systems 164:1-12.

Gaines S and Roughgarden J (1985) Larval settlement rate: a leading determinant of structure in an ecological community of the marine intertidal zone. Proceedings of the National Academy of Sciences of the United States of America 82:3707-3711.

Gallagher C and Doropoulos C (2017) Spatial refugia mediate juvenile coral survival during coral–predator interactions. Coral Reefs 36:51-61.

Gibbs DA and Hay ME (2015) Spatial patterns of coral survivorship: impacts of adult proximity versus other drivers of localized mortality. PeerJ 3:e1440.

Gosselin LA and Qian PY (1997) Juvenile mortality in benthic marine invertebrates. Marine Ecology Progress Series 146:265-282.

Graham EM, Baird AH, Connolly SR, Sewell MA and Willis BL (2013a) Rapid declines in metabolism explain extended coral larval longevity. Coral Reefs 32:539-549.

Graham EM, Baird AH, Willis BL and Connolly SR (2013b) Effects of delayed settlement on post-settlement growth and survival of scleractinian coral larvae. Oecologia 173:431-438.

Heyward AJ and Negri AP (1999) Natural inducers for coral larval metamorphosis. Coral Reefs 18:273-279.

Heyward AJ, Smith LD, Rees M and Field SN (2002) Enhancement of coral recruitment by in situ mass culture of coral larvae. Marine Ecology Progress Series 230:113-118.

Hixon MA and Carr MH (1997) Synergistic predation, density dependence, and population regulation in marine fish. Science 277:946-949.

Hixon MA and Johnson DW (2009) Density Dependence and Independence. Encyclopedia of life sciences (eLS).

Hixon MA, Pacala SW and Sandin SA (2002) Population regulation: historical context and contemporary challenges of open vs. closed systems. Ecology 83:1490-1508.

Holbrook SJ and Schmitt RJ (2002) Competition for shelter space causes density-dependent predation mortality in damselfishes. Ecology 83:2855-2868.

Holm ER (1990) Effects of density-dependent mortality on the relationship between recruitment and larval settlement. Marine Ecology Progress Series 60:141-146.

Hothorn T, Bretz F and Westfall P (2008) Simultaneous inference in general parametric models. Biometrical journal 50:346-363.

Hughes TP, Baird AH, Dinsdale EA, Moltschaniwskyj NA, Pratchett MS, Tanner JE and Willis BL (2000) Supply-side ecology works both ways: the link between benthic adults, fecundity, and larval recruits. Ecology 81:2241-2249.

Hughes TP and Tanner JE (2000) Recruitment failure, life histories, and long-term decline of Caribbean corals. Ecology 81:2250-2263.

Hunt HL and Scheibling RE (1997) Role of early post-settlement mortality in recruitment of benthic marine invertebrates. Marine Ecology Progress Series 155:269-301.

Jayewardene D, Donahue MJ and Birkeland C (2009) Effects of frequent fish predation on corals in Hawaii. Coral Reefs 28:499-506.

Jones G, Almany G, Russ G, Sale P, Steneck R, van Oppen M and Willis B (2009) Larval retention and connectivity among populations of corals and reef fishes: history, advances and challenges. Coral Reefs 28:307-325.

Knowlton N (2001) The future of coral reefs. Proceedings of the National Academy of Sciences of the United States of America 98:5419-5425.

Korner-Nievergelt F, Roth T, Felten S, Guelat J, Almasi B and P. Korner-Nievergelt (2015) Bayesian Data Analysis in Ecology using Linear Models with R, BUGS and Stan. Elsevier.

Linden B and Rinkevich B (2017) Elaborating an eco-engineering approach for stock enhanced sexually derived coral colonies. Journal of Experimental Marine Biology and Ecology 486:314-321.

Mundy CN (2000) An appraisal of methods used in coral recruitment studies. Coral Reefs 19:124-131.

Nathan R and Muller-Landau HC (2000) Spatial patterns of seed dispersal, their determinants and consequences for recruitment. Trends in Ecology & Evolution 15:278-285.

Nozawa Y (2008) Micro-crevice structure enhances coral spat survivorship. Journal of Experimental Marine Biology and Ecology 367:127-130.

Nozawa Y (2012) Effective size of refugia for coral spat survival. Journal of Experimental Marine Biology and Ecology 413:145-149.

Oliver JK and Willis BL (1987) Coral-spawn slicks in the Great Barrier Reef - preliminary observations. Marine Biology 94:521-529.

Pawlik JR (1992) Chemical ecology of the settlement of benthic marine-invertebrates. Oceanography and Marine Biology 30:273-335.

Pineda J, Reyns NB and Starczak VR (2009) Complexity and simplification in understanding recruitment in benthic populations. Population Ecology 51:17-32.

Puill-Stephan E, van Oppen MJH, Pichavant-Rafini K and Willis BL (2012) High potential for formation and persistence of chimeras following aggregated larval settlement in the broadcast spawning coral, Acropora millepora. Proceedings of the Royal Society B: Biological Sciences 279:699-708.

R Development Core Team (2017) R: A language and environment for statistical computing. R Foundation for Statistical Computing, Vienna, Austria.

Raimondi PT (1990) Patterns, mechanisms, consequences of variability in settlement and recruitment of an intertidal barnacle. Ecological Monographs 60:283-309.

Raymundo LJ and Maypa AP (2004) Getting bigger faster: mediation of size-specific mortality via fusion in juvenile coral transplants. Ecological Applications 14:281-295.

Rice JA, Miller TJ, Rose KA, Crowder LB, Marschall EA, Trebitz AS and DeAngelis DL (1993) Growth rate variation and larval survival: inferences from an individual-based size-dependent predation model. Canadian Journal of Fisheries and Aquatic Sciences 50:133-142.

Ritson-Williams R, Arnold SN, Fogarty ND, Steneck RS, Vermeij MJ and Paul VJ (2009) New perspectives on ecological mechanisms affecting coral recruitment on reefs. Smithsonian Contributions to the Marine Sciences 38:437-457.

Selkoe KA, Gaines SD, Caselle JE and Warner RR (2006) Current shifts and kin aggregation explain genetic patchiness in fish recruits. Ecology 87:3082-3094.

Suzuki G, Arakaki S, Suzuki K, Iehisa Y and Tayashibara H (2012) What is the optimal density of larval seeding in Acropora corals? Fisheries science 78:801-808.

Therneau TM (2012) coxme: Mixed effects Cox models. R package version.

Vermeij MJA and Sandin SA (2008) Density-dependent settlement and mortality structure the earliest life phases of a coral population. Ecology 89:1994-2004.

Vermeij MJA, Smith JE, Smith CM, Thurber RV and Sandin SA (2009) Survival and settlement success of coral planulae: independent and synergistic effects of macroalgae and microbes. Oecologia 159:325-336.

Wahle R and Steneck R (1991) Recruitment habitats and nursery grounds of the American lobster Homarus americanus: a demographic bottleneck? Marine Ecology-Progress Series 69:231.

Werner EE and Gilliam JF (1984) The ontogenetic niche and species interactions in size-structured populations. Annual Review of Ecology and Systematics 15:393-425.

Whalan S, Wahab MAA, Sprungala S, Poole AJ and de Nys R (2015) Larval Settlement: The Role of Surface Topography for Sessile Coral Reef Invertebrates. PloS One 10:e0117675.

White JW (2007) Spatially correlated recruitment of a marine predator and its prey shapes the large-scale pattern of density-dependent prey mortality. Ecology Letters 10:1054-1065.

White JW, Samhouri JF, Stier AC, Wormald CL, Hamilton SL and Sandin SA (2010) Synthesizing mechanisms of density dependence in reef fishes: behavior, habitat configuration, and observational scale. Ecology 91:1949-1961.

Young TP, Petersen DA and Clary JJ (2005) The ecology of restoration: historical links, emerging issues and unexplored realms. Ecology Letters 8:662-673.

6.5.7 SUPPLEMENTARY MATERIAL
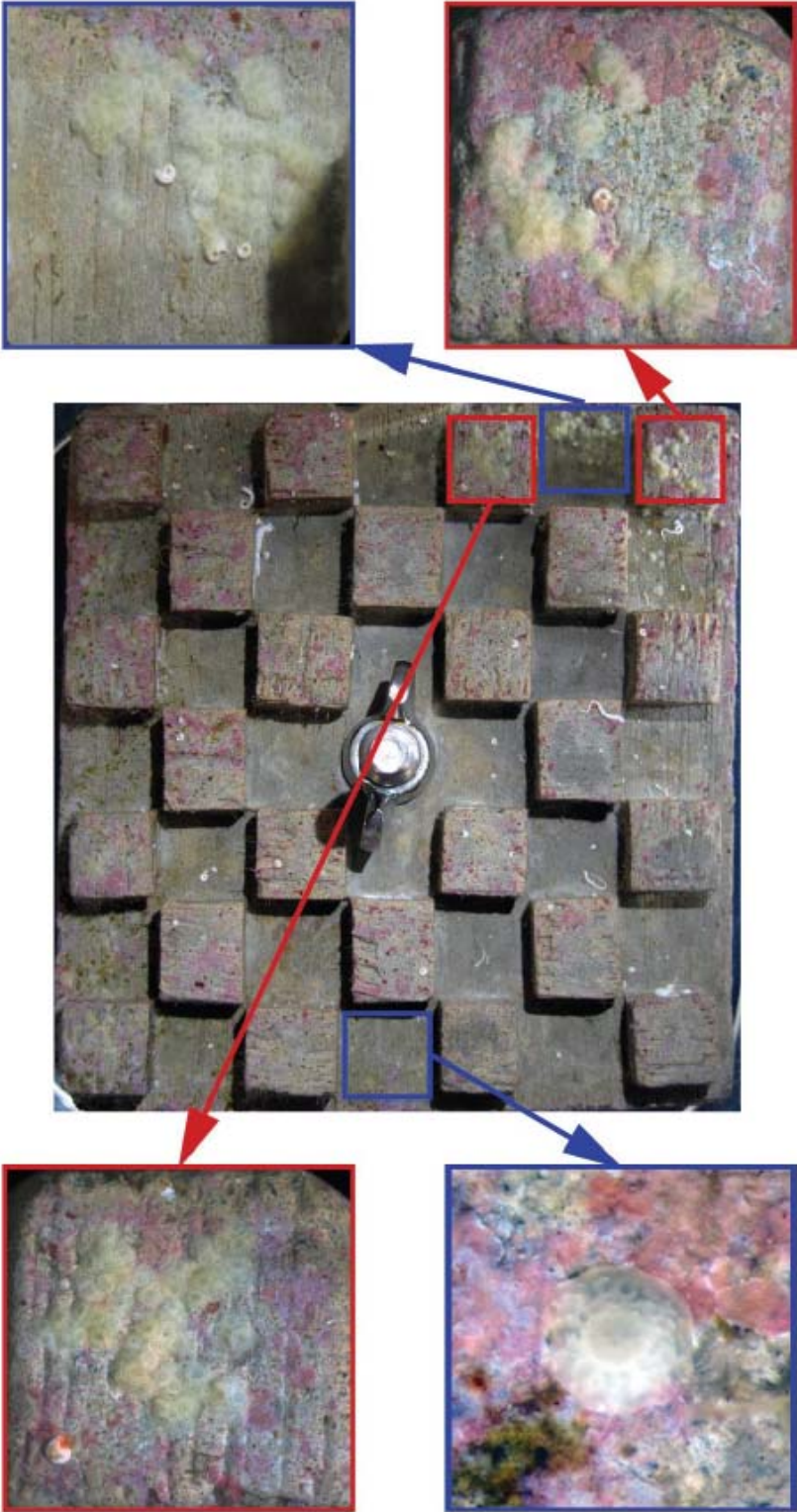
Figure S6.5.1 An example custom made settlement tile with newly settled *Acropora millepora* recruits that are singular or aggregated on exposed (red borders) and crevice (blue borders) microhabitats.
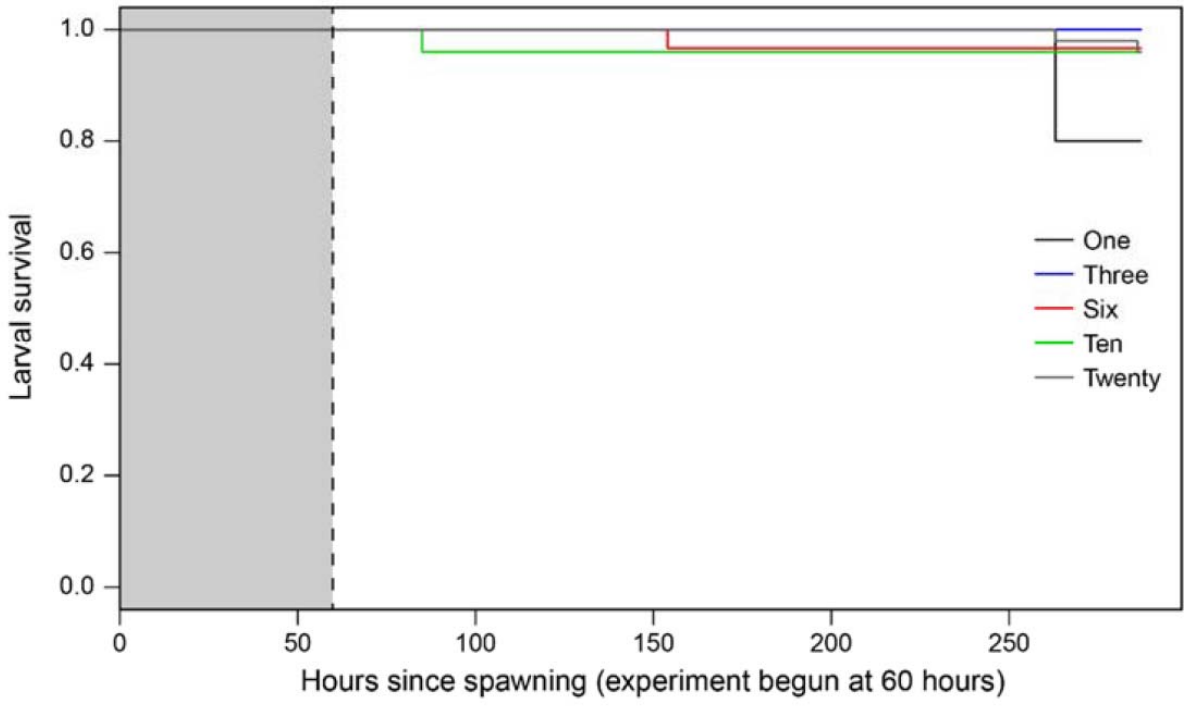
Figure S6.5.2 Proportional survival of *Acropora millepora* larvae from 60 to 288 hours following spawning as a function of larval density.

6.6 Exploring variable patterns of density-dependent larval settlement among corals with distinct and shared functional traits

Authors: Doropoulos C, Gómez-Lemos LA, Babcock RC.

ABSTRACT

Coral settlement is a key process for the recovery and maintenance of coral reefs, yet interspecific variations in density-dependent settlement are unknown. Settlement of the submassive *Goniastrea retiformis* and corymbose *Acropora digitifera* and *A. millepora* were quantified at densities ranging from 1 to 50 larvae per 20 mL from 110 to 216 h following spawning. Settlement patterns were distinct for each species. *Goniastrea* settlement was rapid and increased linearly with time; whereas both *Acropora* spp. hardly settled until crustose coralline algae was provided. Both *Goniastrea* and *A. digitifera* showed positive density-dependent settlement, but the relationship was exponential for *Goniastrea* but linear for *A. digitifera.* Settlement was highest but density independent in *A. millepora.* Our results suggest that larval density can have significant effects on settler replenishment and highlight variability in density-dependent settlement among corals with distinct functional traits as well as those with similar functional forms.

6.6.1 INTRODUCTION

The settlement of marine invertebrates from the plankton to the benthos is a key step in recruitment and population recovery (Connell and Keough 1985). Following gamete release and development, larvae respond to biophysical cues for induction of settlement once competent. These cues are often associated with particular algae (Morse et al. 1996), light (Mason et al. 2011), and microhabitat structure (Doropoulos et al. 2016). Larvae also respond to chemical cues released by conspecific metamorphosis and adult tissue, so that recruits form aggregations near adult habitats that can improve the likelihood of recruitment success (Pawlik 1992). Determining the density-dependent relationships of larval settlement is therefore key to understanding recovery bottlenecks resulting from Allee effects (Courchamp et al. 1999).

Tropical reefs are populated by diverse corals that are often grouped according to functional traits related to growth rates and form, reproductive mode, and resistance to stress (Darling et al. 2012). Reproductive output is known to vary more among different morphologies than among species with similar morphologies (Álvarez-Noriega et al. 2016), and larval survival and competency can vary significantly both within and among morphologies (Wilson and Harrison 1998; Connolly and Baird 2010), as can larval settlement preferences for crustose coralline algae (Ritson-Williams et al. 2016). Yet few studies have investigated density-dependent relationships between coral larvae and settlement; those that have, all studied corymbose and branching *Acropora* and found positive responses of settlement with increasing larval density (Suzuki et al. 2012; Edwards et al. 2015; Doropoulos et al. 2017). Hence, in this study, we explore density-dependent relationships of larval settlement using corals with similar (*Acropora* spp.) and distinct (*Goniastrea* sp.) functional traits. Corymbose *Acropora* are fast growing and have high reproductive output but are sensitive to stress, whereas submassive *Goniastrea* are slow growing, have low reproductive output, but are highly resistant to stress (Darling et al. 2012; Álvarez-Noriega et al. 2016).

6.6.2 METHODS

Study area

This study was conducted at Coral Bay Research Station, Western Australia. Gravid coral colonies were collected using hammer and chisel from shallow reef flats at a depth of 2–3 m, transported to the local jetty, and isolated in 60-L tubs at sunset. Four *Goniastrea retiformis* colonies spawned at 2105–2140 hrs on 20 March 2017, and nine colonies of *Acropora millepora* spawned at 2120–2230 hrs, followed by eight colonies of *A. digitifera* at 2200–2300 hrs on 21 March 2017. Egg–sperm bundles were collected and mixed within each species, transported to the research station, and transferred into 20-L buckets of filtered seawater. Water was agitated to break up the egg–sperm bundles and promote cross-fertilisation. After 3 h, >50% of eggs had fertilised and were undergoing cell division. Eggs were rinsed with filtered seawater to remove excess sperm and transferred to 60-L (*Goniastrea*) or 200-L (*Acropora* spp.) tubs of filtered seawater for larval rearing. Half water changes took place after 6 h and every 12 h thereafter, and light aeration began after 20 h. Seawater temperature used during fertilisation and larval rearing was an average of 25.1 °C and seawater was filtered through a sponge canister stack with UV sterilisation (Odyssea CFS-1000).

Experimental approach

At 68 h after spawning, larvae were fully developed and actively swimming. To investigate the effects of larval density on survival and settlement among the three coral species, larvae were placed in 20-mL glass scintillation vials of filtered seawater (0.2 μm and UV-treated) at densities of 1, 5, 10, 20, 35

and 50 individuals. Previous work has shown that coral larvae are found at maximum densities of five individuals per 20 mL in spawning slicks (Oliver and Willis 1987), so we chose densities below and above this maximum. Following initiation of the experiments at 68 h, the number of larvae that were alive, dead, or settled were counted at 110, 134, 188, and 216 h after spawning for *Goniastrea*, and 89, 117, 168 and 191 h after spawning for *A. digitifera* and *A. millepora*. Settled larvae represent those that had changed from free swimming or transitorily attached pear-shaped forms, to those firmly attached and metamorphosed (Heyward and Negri 1999). Larvae were recorded as alive if they were observed swimming (by eye), but if not moving were assessed under a dissecting microscope to verify whether they were dead or alive. Each time the larvae were counted, they were transferred into new vials with fresh filtered seawater. Dead or settled individuals were not transferred. After the penultimate sampling point, a 5 × 5 mm chip of the crustose coralline algae (CCA) *Porolithon onkodes* was added to each vial to act as a settlement inducer. CCA were collected from reefs where the coral colonies were collected, fragmented into small chips, cleaned with toothbrush and tweezers, and the carbonate underside scraped off to leave only a thin layer of thallus. There were six replicate vials for every coral species for each larval density combination, and replicates were fully randomised on a laboratory bench. The temperature of the laboratory was set to 25 °C to match the daily mean local water temperature (25.1 °C).

Data analyses

Trends in larval survival at the different densities were investigated using a random-effect Cox proportional hazard model for each species, with replicate vials incorporated as a random effect. The model is a time-to-event analysis that allows for the stochastic rate at which an event occurs to vary, but makes a proportional hazards assumption that the relative effect among treatments is consistent over time.

Three analyses were conducted for each coral species to investigate how time, the addition of CCA and larval density influenced proportional larval settlement using generalised linear mixed-effects models with binomial error. The first analysis investigated settlement as a function of time (continuous) with replicate vials incorporated as a random factor. However, because replicates were resampled, temporal autocorrelation was then accounted for in the second analysis that investigated coral settlement as a function of the interaction of CCA addition (categorical) and larval density (continuous), with time and replicate vials incorporated as random effects. For significant interaction terms, pairwise comparisons were conducted after the addition of CCA among different larval densities that were treated as fixed. The final analysis then investigated total settlement throughout the entire experiment as a function of larval density with replicate vials incorporated as a random factor.

Statistical significance for all models was based on comparisons between full and reduced models using likelihood ratio test (χ^2) P values. Analyses were conducted using the coxme (Therneau 2012) and lme4 (Bates et al. 2015) packages in R (R Development Core Team 2017).

6.6.3   RESULTS AND DISCUSSION

Larval survival was high among all coral species (>87%) and there were no differences among densities of *G. retiformis* (P = 0.890), *A. digitifera* (P = 0.155) and *A. millepora* (P = 0.842). Larval mortality of *Goniastrea* was 7% after 188 h and 13% after 216 h. After 191 h mortality of *A. digitifera* was 9% and of *A. millepora* was 4%.
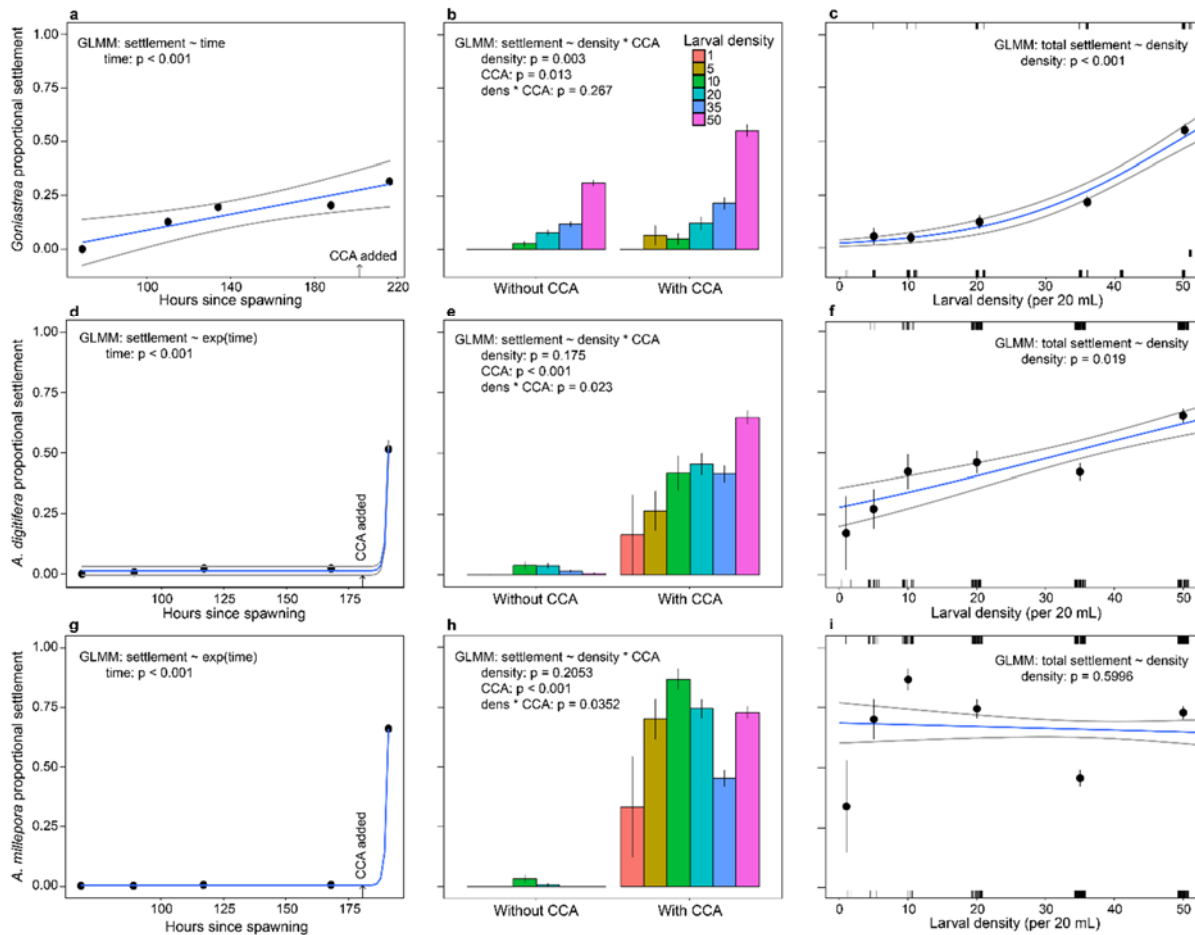
Figure 6.6.1 Effects of time since spawning, addition of crustose coralline algae, and coral larval density on the proportional settlement of *Goniastrea retiformis* (a–c), *Acropora digitifera* (d–f) and *A. millepora* (g–i). Black dots and coloured bars represent means, errors are standard errors, n = 6, and binomial data points are represented by small notches on top and bottom x-axes (c, f, i). Text within each panel describes the statistical model and outputs for each analysis.

Distinct patterns of settlement were among species (Figure 6.6.1), especially between submassive *G. retiformis* (Figure 6.6.1a–c) and corymbose *A. digitifera* (Figure 6.6.1d–f) and *A. millepora* (Figure 6.6.1g–i). Larvae of *Goniastrea* began to settle prior to the addition of any settlement inducer, from 110 h until the final sampling point at 216 h, with proportional settlement linear over time (Figure 6.6.1a). Submassive faviids, including *Goniastrea*, are known to settle shortly after fertilisation, some reaching peak competency as early as 60–66 h after fertilisation (Miller and Mundy 2003; Nozawa and Harrison 2005). In contrast, virtually no *Acropora* spp. settled (<2%) prior to the addition of CCA. Following CCA addition at 168 h, proportional settlement was rapid at 191 h; the temporal response curves for both species were best explained by exponential models (Figure 6.6.1d, g). *Acropora* spp. have a known sensitivity to CCA as settlement inducers, and settlement often peaks at 7–8 d following spawning (Morse et al. 1996; Heyward and Negri 1999). At the end of the experimental period, *A. millepora* had the highest overall settlement of 66%, followed by *A. digitifera* at 52% and *Goniastrea* at 32%.

The effects of larval density before and after the addition of CCA varied among coral species. Settlement of *Goniastrea* was significantly higher after CCA was added, and positive density-dependent settlement was observed prior to and after CCA addition, with no interaction detected (Figure 6.6.1b). In contrast, *A. digitifera* showed positive density-dependent settlement only following the addition of CCA, with minimal settlement and no relationship with density observed

beforehand (density × CCA, p = 0.02; Figure 6.6.1e). There was also a weak interaction between larval density and CCA for settlement of *A. millepora* (p = 0.04), although the nature of the interaction differed (Figure 6.6.1h). There was no consistent relationship between larval density and settlement either prior to or following the addition of CCA. Following the addition of CCA, settlement was >70% for densities of 5, 10, 20 and 50 larvae, significantly lower for the density of 35 larvae with 45 ± 3% (SE) settlement, and lower for the density of 1 larvae with 33 ± 21% settlement but this was only significantly different compared to densities of 10, 20, and 50 larvae (Figure 6.6.1h).

Three distinct relationships were observed between total settlement and larval density (Figure 6.6.1c, f, i). *Goniastrea* and *A. digitifera* both showed positive relationships between proportional settlement and increasing larval density, yet the relationship of the positive responses differed. Proportional settlement in *Goniastrea* was exponential, with no settlement at the lowest larval density, <22% settlement for densities of 5–35 larvae per 20 mL, doubling to 55% settlement at 50 larvae per 20 mL (Figure 6.6.1c). Proportional settlement in *A. digitifera* increased linearly with increasing density, at 17% settlement for 1 larvae to 65% settlement for 50 larvae per 20 mL (Figure 6.6.1f). Surprisingly, settlement of *A. millepora* was density independent (Figure 6.6.1i). This result contrasts the positive density-dependent settlement patterns quantified for *A. millepora* the previous year that used almost identical protocol (Doropoulos et al. 2017), highlighting the often variable nature of larval settlement (Hughes et al. 1999).

The patterns of settlement observed in this study have two main implications for recruitment. First, there is an obvious temporal distinction and sensitivity to inducers between the submassive *Goniastrea* and corymbose *Acropora*. The shorter time to begin settlement and lack of inducer required for *Goniastrea* suggests that at least a proportion of these corals may settle closer to their natal habitat than *Acropora*. Studies on relationships between coral egg size, larval survival and competency over time among multiple acroporids and faviids have found that the smaller eggs of *G. retiformis* have rapid competency resulting in the highest self-retention and lowest dispersal potential, whereas *A. millepora* and *A. valida* have the lowest self-retention and highest dispersal potential (Connolly and Baird 2010; Figueiredo et al. 2013). Second, *Goniastrea* displayed an exponential settlement response to increasing larval density, as well as lower rates of settlement at peak density than either *Acropora* species. The low rates of settlement combined with high density thresholds suggest lower recruitment potential for stress-tolerant submassive corals that may limit recruitment following spawning. This low rate of settlement may contribute to their lower abundance than highly competitive acroporids in many Indo-Pacific reef habitats (e.g. Done 1982).

While further investigations on density-dependent settlement responses among corals from diverse functional groups are needed, this study is the first attempt at systematic exploration. Combined with the relatively slow growth rates of submassive coral recruits and juveniles (e.g. Doropoulos et al. 2015), these outcomes suggest that recovery from disturbances are likely to take longer for taxa such as *Goniastrea* that show (1) limited dispersal relative to long-distance dispersers such as *Acropora* and (2) higher larval density thresholds to facilitate settlement.

6.6.4 ACKNOWLEDGEMENTS

6.6.5 REFERENCES

Álvarez-Noriega M, Baird AH, Dornelas M, Madin JS, Cumbo VR, Connolly SR (2016) Fecundity and the demographic strategies of coral morphologies. Ecology 97:3485-3493

Bates D, Maechler M, Bolker B, Walker S (2015) Fitting Linear Mixed-Effects Models Using lme4. Journal of Statistical Software 67:1-48

Burke RD (1986) Pheromones and the gregarious settlement of marine invertebrate larvae. Bull Mar Sci 39:323-331

Connell JH, Keough MJ (1985) Disturbance and patch dynamics of subtidal marine animals on hard substrata. In: Pickett STA, White PS (eds) The ecology of natural disturbance and patch dynamics. Academic Press, Orlando, pp 125–152

Connolly SR, Baird AH (2010) Estimating dispersal potential for marine larvae: dynamic models applied to scleractinian corals. Ecology 91:3572-3583

Courchamp F, Clutton-Brock T, Grenfell B (1999) Inverse density dependence and the Allee effect. Trends Ecol Evol 14:405-410

Darling ES, Alvarez-Filip L, Oliver TA, McClanahan TR, Cote IM (2012) Evaluating life-history strategies of reef corals from species traits. Ecol Lett 15:1378-1386

Done TJ (1982) Patterns in the distribution of coral communities across the central Great Barrier Reef. Coral Reefs 1:95-107

Doropoulos C, Evensen NR, Gómez-Lemos LA, Babcock RC (2017) Density-dependent coral recruitment displays divergent responses during distinct early life-history stages. Royal Society Open Science 4:170082

Doropoulos C, Ward S, Roff G, González-Rivero M, Mumby PJ (2015) Linking demographic processes of juvenile corals to benthic recovery trajectories in two common reef habitats. PLoS One 10:e0128535

Doropoulos C, Roff G, Bozec Y-M, Zupan M, Werminghausen J, Mumby PJ (2016) Characterizing the ecological trade-offs throughout the early ontogeny of coral recruitment. Ecol Monogr 86:20-44

Edwards AJ, Guest JR, Heyward AJ, Villanueva RD, Baria MV, Bollozos IS, Golbuu Y (2015) Direct seeding of mass-cultured coral larvae is not an effective option for reef rehabilitation. Mar Ecol Prog Ser 525:105-116

Figueiredo J, Baird AH, Connolly SR (2013) Synthesizing larval competence dynamics and reef-scale retention reveals a high potential for self-recruitment in corals. Ecology 94:650–659

Heyward AJ, Negri AP (1999) Natural inducers for coral larval metamorphosis. Coral Reefs 18:273-279

Hughes TP, Baird AH, Dinsdale EA, Moltschaniwskyj NA, Pratchett MS, Tanner JE, Willis BL (1999) Patterns of recruitment and abundance of corals along the Great Barrier Reef. Nature 397:59-63

Mason B, Beard M, Miller M (2011) Coral larvae settle at a higher frequency on red surfaces. Coral Reefs:1-10

Miller K, Mundy C (2003) Rapid settlement in broadcast spawning corals: implications for larval dispersal. Coral Reefs 22:99-106

Morse ANC, Iwao K, Baba M, Shimoike K, Hayashibara T, Omori M (1996) An ancient chemosensory mechanism brings new life to coral reefs. Biol Bull 191:149-154

Nozawa Y, Harrison PL (2005) Temporal settlement patterns of larvae of the broadcast spawning reef coral *Favites chinensis* and the broadcast spawning and brooding reef coral *Goniastrea aspera* from Okinawa, Japan. Coral Reefs 24:274-282

Oliver JK, Willis BL (1987) Coral-spawn slicks in the Great Barrier Reef - preliminary observations. Mar Biol 94:521-529

Pawlik JR (1992) Chemical ecology of the settlement of benthic marine-invertebrates. Oceanography and Marine Biology 30:273-335

R Development Core Team (2017) R: A language and environment for statistical computing. R Foundation for Statistical Computing, Vienna, Austria

Ritson-Williams R, Arnold SN, Paul VJ (2016) Patterns of larval settlement preferences and post-settlement survival for seven Caribbean corals. Mar Ecol Prog Ser 548:127-138

Suzuki G, Arakaki S, Suzuki K, Iehisa Y, Hayashibara T (2012) What is the optimal density of larval seeding in *Acropora* corals? Fisheries science 78:801-808

Therneau TM (2012) coxme: Mixed effects Cox models R package version

Wilson J, Harrison P (1998) Settlement-competency periods of larvae of three species of scleractinian corals. Mar Biol 131:339-345

6.7 Declining abundance of coral reef fish in a world-heritage listed marine park

Authors: Vanderklift MA, Babcock RC, Boschetti F, Haywood MDE, Pillans RD, Richards SA, Thomson DP.

ABSTRACT

Ningaloo Marine Park (NMP) is a multiple use marine park located on the west coast of Australia. It includes one of the world's longest continuous tracts of fringing coral reef, and was first declared in 1984. In late 2006 the park was rezoned to include 34% no take coverage, mostly over the shallow waters of the reef itself. We surveyed coral reef fishes inhabiting shallow reef flat habitat in Mandu Sanctuary Zone (SZ) and adjacent Recreation Zones (RZ) in the NMP between 2007 and 2016. We surveyed fish in most years during that period, and also quantified the relative percentage cover of major benthic habitat categories (living hard coral, algae, non-living substrate) in 2007 and again in each year from 2013. There was greater density and biomass in the SZ than the RZ in most years— but not all—for Lethriniae, Labridae, Scaridae and Acanthuridae. There was a decrease in the density and biomass of fish in some targeted (Lethrinidae) and non-targeted families (Labridae and Chaetodontidae), but no evidence for a decrease in the density of fish from the families Scaridae, Acanthuridae and Siganidae. The estimated range of decline in abundance of emperors (Lethrinidae) ranged from 7–21% for counts, and 10–22% for biomass (95% CI). The highest rates of decline in biomass of emperors occurred in the SZ (range 2–37%), but analyses indicated that there was an overall downward trend common to SZ and RZ. The most abundant species of lethrinid inhabiting the reef flat, *Lethrinus atkinsoni* also declined significantly in both abundance and biomass during this time (estimated decline of 8-20% per year for counts, 11–21% per year for biomass). The biomass of wrasses (Labridae) declined by an estimated 8–21% per year. This was mirrored by patterns in the large-bodied wrasse *Coris aygula*, which declined by 7-2% per year for counts, and 8–24% per year for biomass. The abundance of butterflyfishes (Chaetodontidae) declined by 0–19% per year for counts, and 4–18% per year for biomass. The most abundant species of butterflyfish, *Chaetodon plebeius*, declined in abundance by 3–22% per year, and by 9–19% per year in biomass. There was some evidence in a decline in counts, but not biomass, of the rabbitfish *Siganus nebulosus* (0–50% per year), but no strong evidence of overall trends for the family Siganidae.

There was a concomitant decline in the percentage cover of living coral (6% per year), which is a plausible cause of the declines in some taxa, especially butterflyfish.

The results of this study highlight two areas of concern for management of the NMP. The first is evidence of declining trends in abundance—measured as counts of individuals and biomass—inside the Mandu SZ, and in adjacent areas. Finfish are a Key Performance Indicator (KPI) in the park's management plan, and the performance measure for this KPI stipulates no loss of abundance in sanctuary zones as a result of human activities. Although the design of NMP follows 'best practice' recommendations to include a high representation of 'no-take' sanctuary zones, overall abundances of key taxa are declining. Some of these declines might be caused by influences that are outside the direct control of park managers (declines in coral cover) others might be due to fishing. For example, declines in the abundance of lethrinids, which are not correlated with living coral, are more likely to

be affected by fishing, which is a pressure that can be managed at the scale of the marine park. In order to achieve the goals outlined in NMP's management plan, additional steps are likely needed to adequately conserve some species.

6.7.1 INTRODUCTION

Protected areas are a common tool used by managers to protect and conserve species and their habitats, both on land and in the sea. Management plans for protected areas frequently set goals that imply (or explicitly state) maintenance or restoration of abundances of species (or groups of species) deemed especially worthy of protection (or conversely to reduce abundances of species deemed unworthy). In the sea this protection is most commonly implemented as marine parks. One type of marine park is the 'no-take area', marine parks where fishing is excluded, are commonly promoted as a solution to protecting species from fishing—on average, such "no-take" protected areas tend to host greater abundances and biomasses of fish than fished areas (see reviews by Rowley 1994, Mosquera et al. 2000).

To assess whether protected areas are meeting objectives requires information, it cannot be assumed that desired outcomes will automatically occur. Monitoring trends in abundance is important if park objectives include protection or restoration of species. In theory (although rarely in practice: e.g. Barnes et al. 2016), information on trends is embedded in an "adaptive approach" in which management actions are implemented to reverse undesirable trends. Understanding which taxa are declining allows managers to focus investment on actions that arrest or reverse declines. In the context of protected areas the options include ensuring that their location and dimensions are well-matched to the ecology and life history of the species. However reliably detecting trends in abundance presents a number of challenges for ecologists. Accurately estimating abundance is one of the most fundamental areas of inquiry in ecology. A challenge perhaps even greater than that of accurately estimating abundance (especially of mobile or cryptic fauna) is the ability to accurately quantify the direction and rates of changes in abundance through time. Yet, such information is central to evaluating the performance of parks—as well as decisions about which species to protect, and how to protect them. For example, the IUCN Red List (iucnredlist.org) classifies species according to their level of extinction risk on the basis of estimates of abundance and trends in abundance (Holmes et al. 2014).

Abundance can be quantified in different ways, including the number of individuals, counts of individuals per unit area (density), and biomass (this latter metric is frequently used to estimate the abundance of fish). Each of these can yield different estimates of trend, because they can be influenced by demographic characteristic such as size- and age-structure.

The amount of area and types of habitat requiring protection in order to meet protection or restoration goals will vary for different species and habitats, but a range of general guidelines have been proposed. A figure of 10% representation of no-take area for each major habitat type is recommended as a global standard (CBD 2006) however other targets have been called for, up to 20–30% by some (20% CRTF in Fernandes et al. 2009, 20–30% Bohnsack et al. 2003).

Here, we evaluate trends in the abundance (measured as counts of individuals, and biomass) of fish in fished and protected areas of the multiple use Ningaloo Marine Park (NMP), located within the Ningaloo Coast World Heritage Area, in north-western Australia. In late 2006 NMP was rezoned to include 34% 'no-take' zones—a proportion that is considered global best practice. Several previous studies have indicated that sanctuary zones (SZ) within the park have higher levels of abundance and/or biomass than do other zones which allow recreational fishing (Westera 2003, Fitzpatrick et al. 2015) but these studies have used disparate techniques (visual census and baited video) and have been carried out at different locations, hampering the ability to detect long term trends. We surveyed fish assemblages of shallow reefs in the northern section of Ningaloo Marine Park at Mandu in the majority of years from 2007–2016, and we sought to determine whether estimates of abundance showed evidence of trends either (increasing or decreasing) during that period, and if so to quantify what the trend was and if it varied between management zones designed to control

fishing.

6.7.2 METHODS

Study area and survey design

Our study was conducted on shallow reef flats within and adjacent to the Mandu Sanctuary Zone (SZ: 1,185 ha) within the Ningaloo Marine Park (NMP: 22°S, 113°E), which was established in 1989. The coral reefs in NMP are mainly fringing reef located 0.2–2 km from the shore. The climate is arid and there is little runoff from land. The reef flat is ~150 m wide, generally submerged even at low tide, and typically dominated by the plate coral *Acropora spicifera* growing on limestone bedrock (Collins et al. 2003).

We surveyed eight sites in the SZ, and eight sites in the adjoining Recreation Zone (RZ). Sites were selected at random from a 200 m × 200 m grid. Surveys were first conducted in 2007 (18 years after the NMP was established), and again in 2009, 2010, and each year from 2012–2016. In most years a single survey was conducted, but in 2015 and 2016 we conducted two surveys per year. Using a GIS, a 200-m grid was overlaid across the study area, from which potential sites were selected by generating a single random point within each 200-m grid cell using the Sample 3.03 extension for ArcView 3.3. Sites from among the randomly-generated points were then selected to ensure balanced distribution of sites within and to the north and south of the SZ.

Commercial fishing is not permitted in the NMP. Recreational angling is permitted in RZs and is the main type of fishing within the reef flat habitat in NMP; spear fishing is not permitted anywhere in the Mandu region, including RZs. Although human population density along the coast is low, fishing can be intense; for example, a survey in 1998–99 recorded >85,000 fisher days in the Ningaloo Marine Park during 12 months (Sumner et al. 2002, Williamson et al. 2006).

Survey methods

Fish were surveyed by visual census along three 25 × 5 m transects at each site. All fish species were included except small (<3 cm) or cryptic species that are poorly surveyed using non-destructive visual methods. The species identity, number and size (estimated to nearest 5 cm) of all fish were recorded. Surveys were not always carried out in the same month each year.

The entire 25 m transect was photographed at approximately 0.5 m intervals using a digital camera held at a distance of approximately 0.5 m above the substrate facing directly downwards. Thirty-two photographs per transect were randomly selected, and the benthos located immediately beneath five (2007 and 2008) or six (2009 to 2016) points per photograph was recorded (yielding 160 or 180 observations per transect). Analysis was conducted using the software Transect Measure™ (www.seagis.com.au). Variation in the three dimensional complexity of the substratum (rugosity) along each transect was quantified by the absolute horizontal distance covered by 10 m of light chain which was moulded to the contours of the substratum.

Statistical analyses

To test for the presence of correlations between counts or biomasses of fish and the measurements of habitat (percentage cover of living coral, algae and non-living substrate, and rugosity) we used multiple linear regressions in the R statistical software package.

The fish families included in analyses were chosen so that they were likely to be reliably and consistently surveyed by the method, were the highest ranked in terms of their contribution to overall biomass, and must have been recorded on more than 25% of transects (avoid analytical problems associated extreme numbers of zeros). The species included were those that comprised highest biomass contribution for each family.

EFFECT SIZE

Patterns in counts and biomasses the selected families were investigated using log response ratios: *LRR = ln(SZ) – ln(RZ)*, where *SZ* is the mean observation in the Sanctuary Zone, and *RZ* is the mean observation in the adjacent Recreation Zone. Separate analyses were conducted for each taxon in each survey, and 95% confidence intervals around the estimates were calculated.

MARSS

The annual rate of change *U* in counts and biomasses of selected abundant and frequently encountered families and species using Multivariate Auto-Regressive State-Space modelling (MARSS: Holmes et al. 2012). Data were log transformed prior to analysis. We used means calculated from all transects surveyed in each year (when there were multiple surveys within a year). For years in which surveys were not conducted we allocated a missing data value. MARSS provides confidence intervals for estimates of *U*, with an assumption that the (logarithm of) the data is suitably approximated by a linear process with Gaussian errors. We did not define a model structure *a priori*. If 95% confidence intervals of *U* did not overlap zero, we inferred support for a statistically-significant change in abundance at $P<0.05$. We assessed support for the competing hypotheses that (a) SZ and RZ have different trends and (b) SZ and RZ share a common trend by comparing AIC_c of models. We used $AIC_c>2$ to indicate that models received different support, considered the model with the lowest AIC as the most parsimonious—or "best" model.

Fish counts and sizes were converted to biomass (kg), using the formula $B = a \times L^b$, where B is biomass, L is total length estimated by divers, and a and b are constants taken from the average values for the relevant family from among species for which relevant conversions using total length were present in FishBase (www.fishbase.org).

6.7.3 RESULTS

The biomass and counts of butterflyfishes (Chaetodontidae) were linearly correlated with the percentage cover of living coral (r^2=0.25. p<0.001 for counts, r^2=0.29. p<0.001 for biomass) and rugosity (r^2=0.25. p<0.001 for counts, r2=0.30. p<0.001 for biomass). No correlations were observed for any other taxa for any other measurement of habitat.

Effect Size

Counts of Lethrinidae (emperors), Scaridae (parrotfish), and Acanthuridae (surgeonfish) tended to be higher in the SZ, but robust evidence of a strong effect (i.e. 95% CI not overlapping zero) was only present for Scaridae (2007 and 2014) and Lethrinidae (2012) (Figure 6.7.1). This pattern tended to be more pronounced for biomass, with robust evidence for higher biomass in the SZ for Lethrinidae (2007, 2012), Scaridae (2007, 2010, 2012, 2016), Labridae (wrasses: 2013) and Acanthuridae (2009, 2013) (Figure 6.7.2). For each family, both counts and biomass tended to fluctuate from year to year during the study (Figure 6.7.3, Figure 6.7.4).
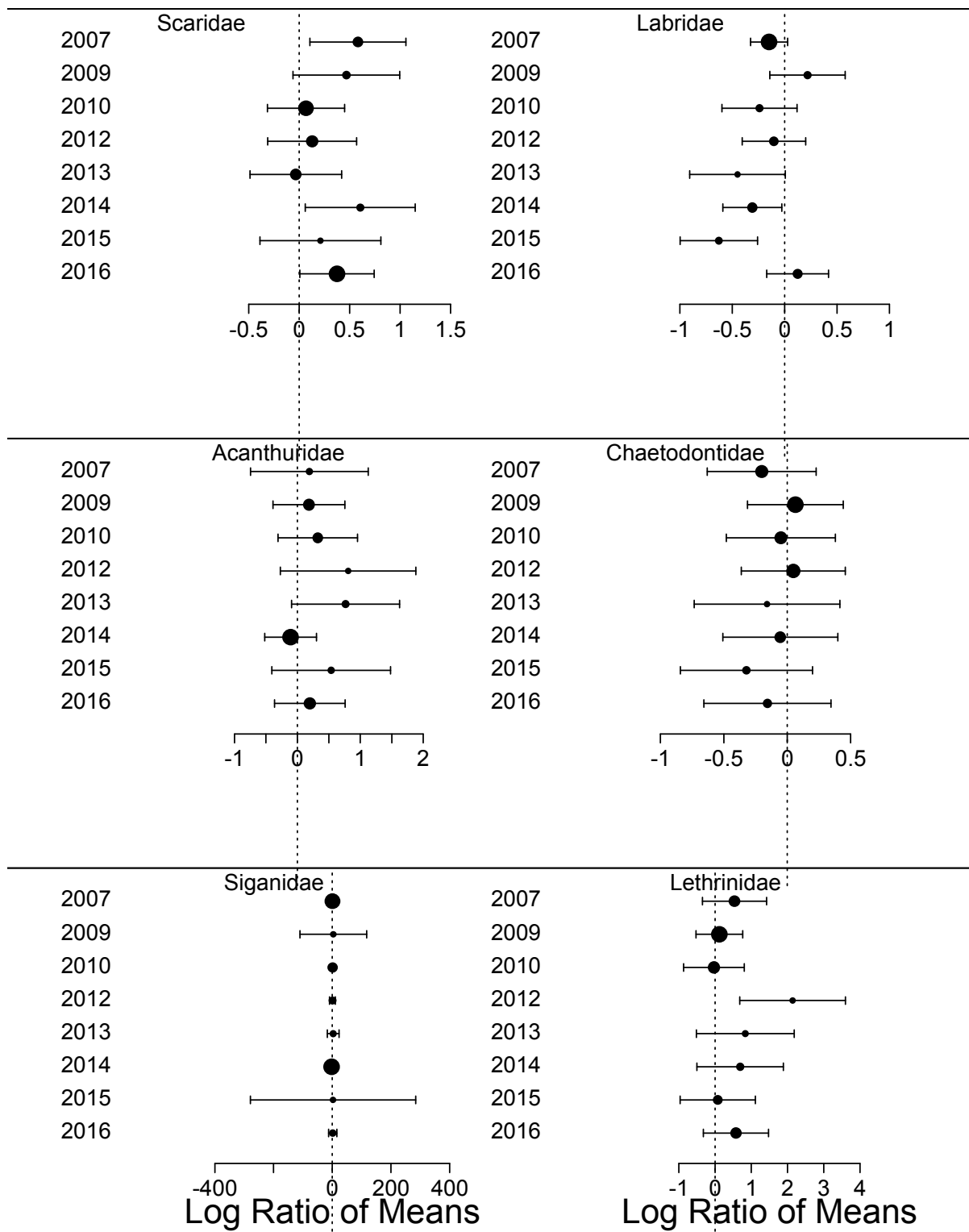
Figure 6.7.1 Log response ratios (± 95%CI) of six families of fishes calculated from counts. The sizes of symbols are proportional to the precision of the estimates. Dotted line runs through zero (which would reflect observations from SZ and RZ would be identical).
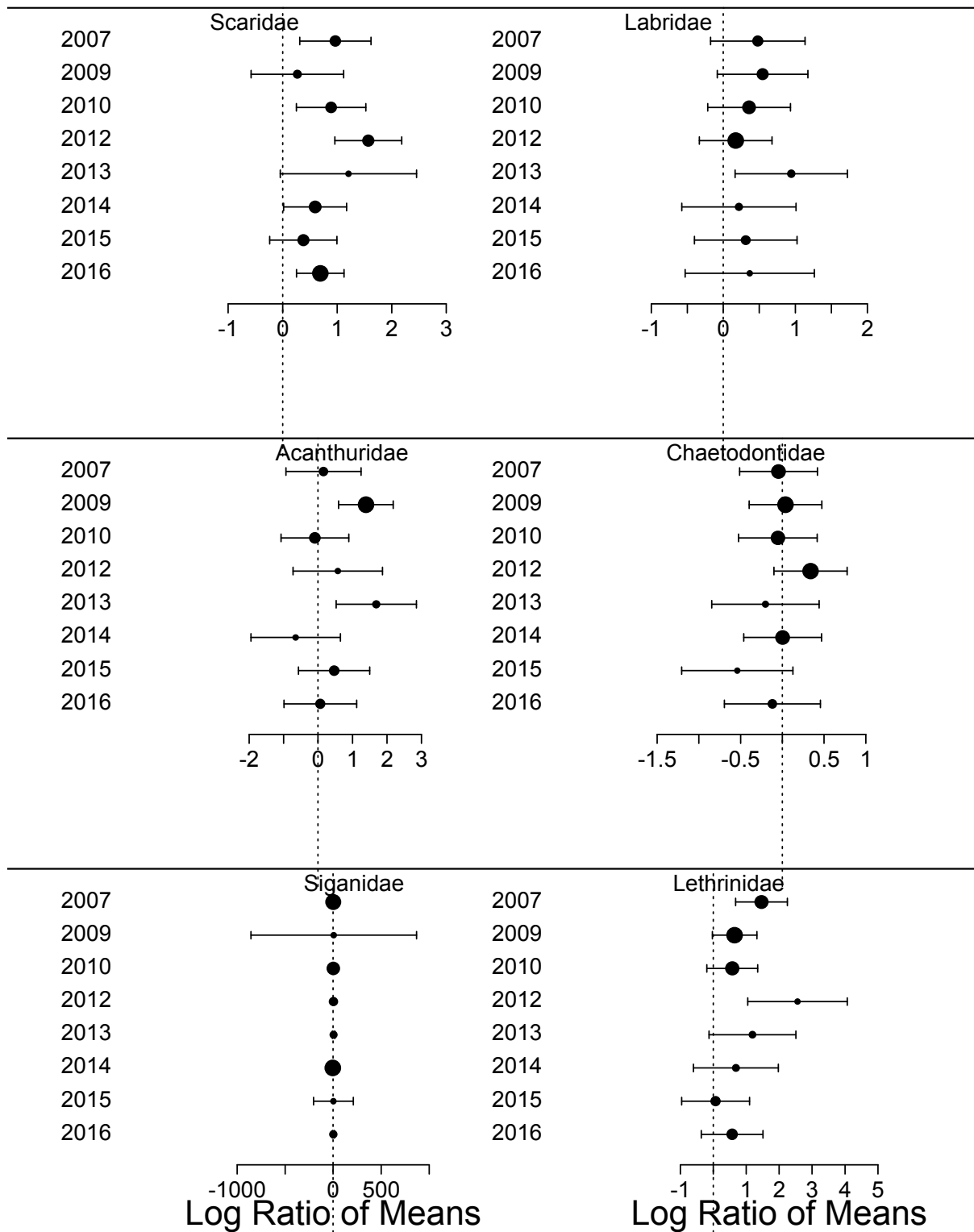
Figure 6.7.2 Log response ratios (± 95%CI) of six families of fishes calculated from biomass. The sizes of symbols are proportional to the precision of the estimates. Dotted line runs through zero (which would reflect observations from SZ and RZ would be identical).
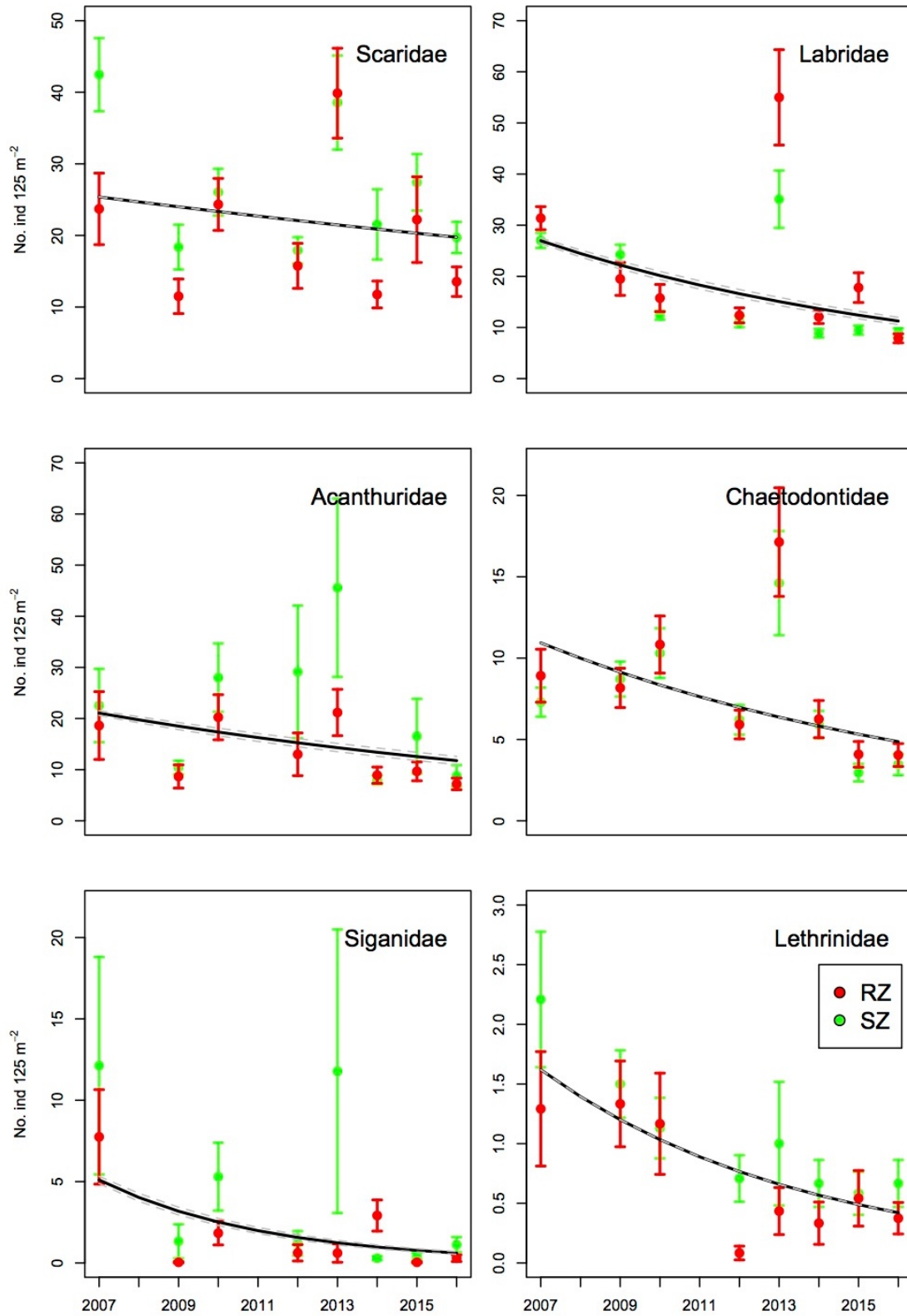
Figure 6.7.3 Mean counts (±SE) of six families of fishes for SZ (green symbols) and RZ (red symbols) and estimated trend from MARSS model (black line).
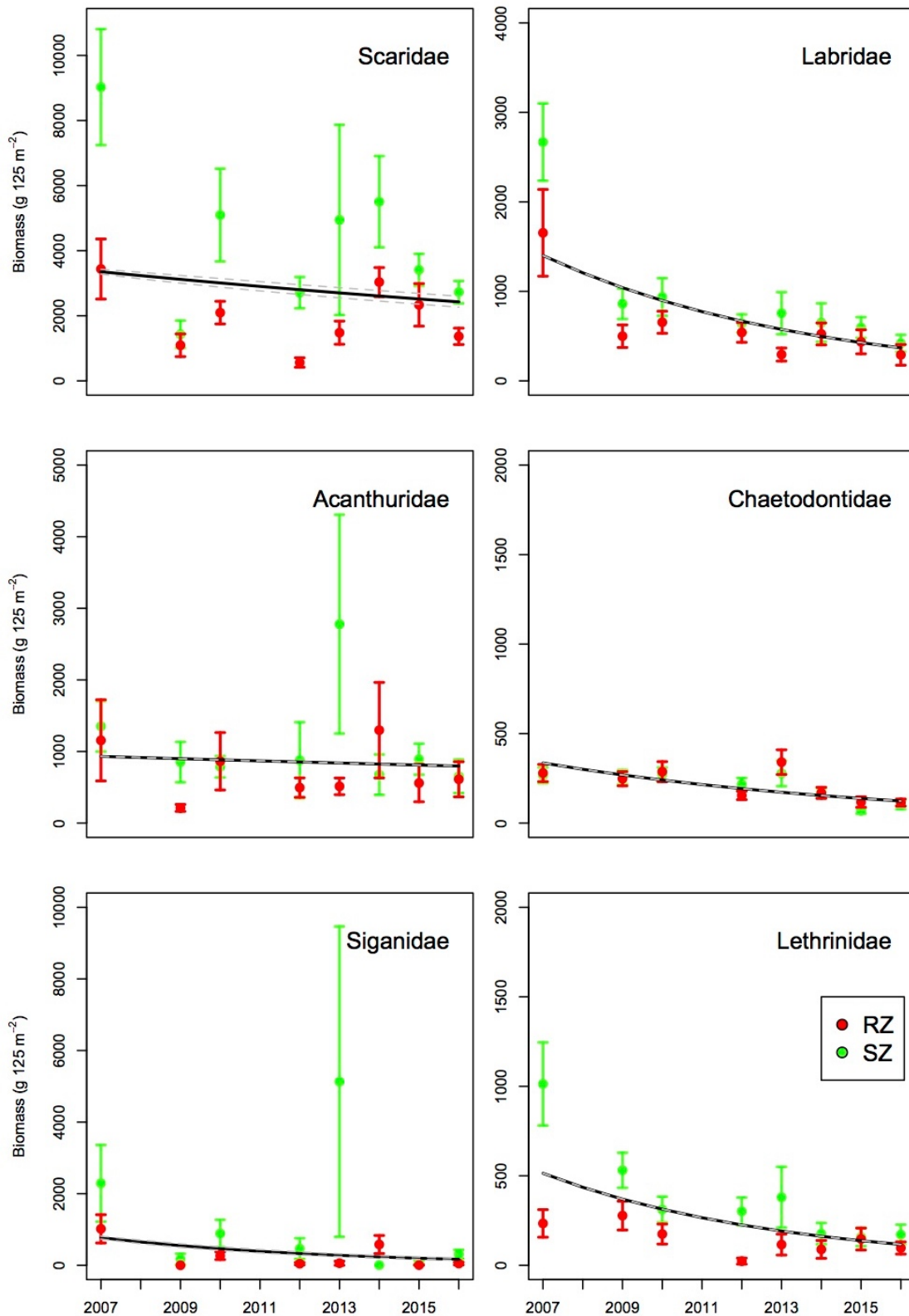
Figure 6.7.4 Mean biomasses (±SE) of six families of fishes for SZ (green symbols) and RZ (red symbols) and estimated trend from MARSS model (black line).

Similar patterns were observed for the main species analysed (Figure 6.7.5, Figure 6.7.6). Analyses based on counts yielded variable results, while analyses based on biomass yielded higher biomasses in SZ for *Chlorurus sordidus* (2007, 2010, 2012, 2014, 2016), *Acanthurus triostegus* (2013, 2015) and

Lethrinus atkinsoni (2007, 2009, 2012). Results for *Siganus nebulosus* were variable, with surveys in some years yielding higher biomass in SZ and other years yielding higher biomass in RZ.
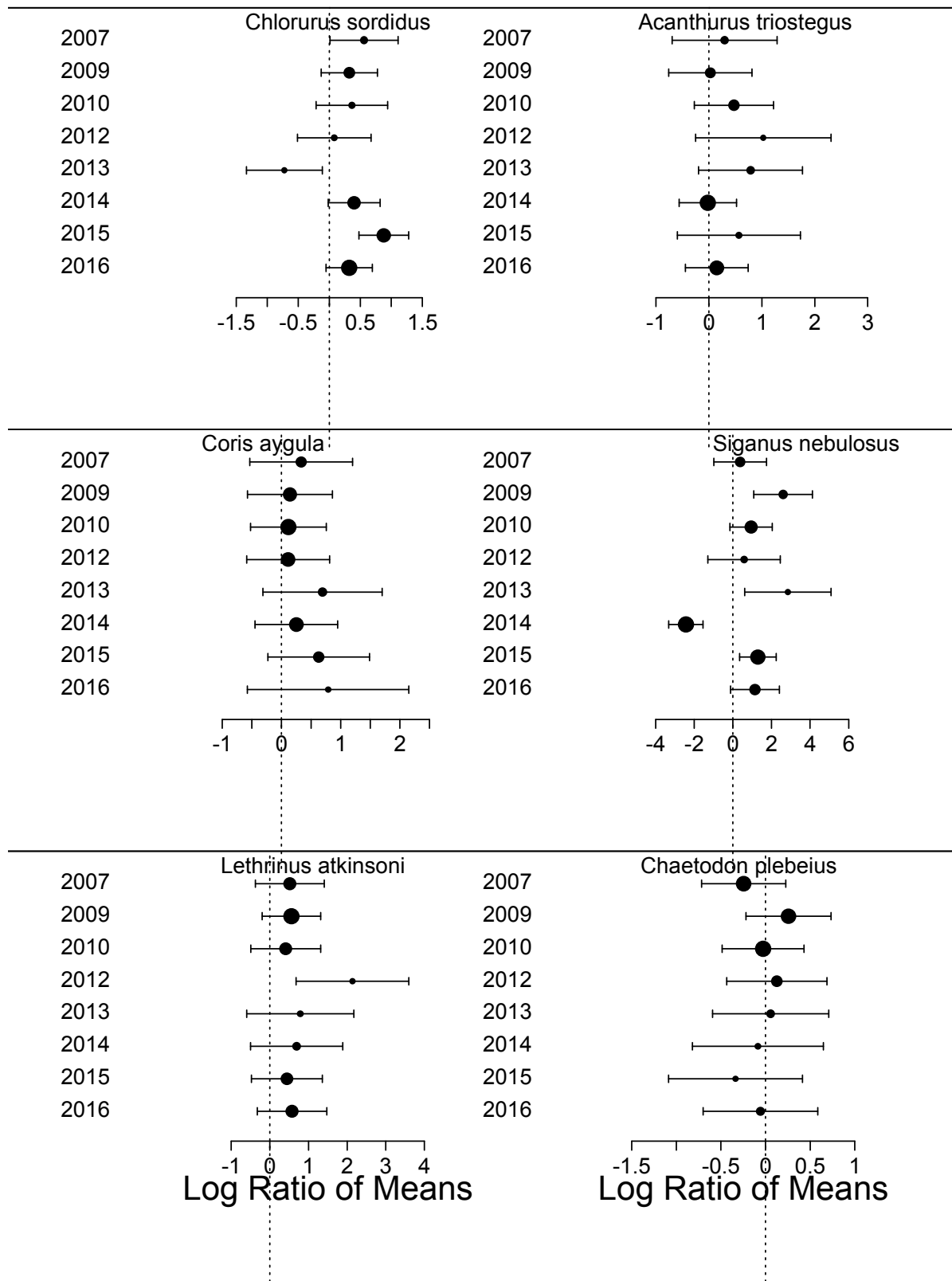
Figure 6.7.5 Log response ratios (± 95%CI) of six species of fishes calculated from counts. The sizes of symbols are proportional to the precision of the estimates. Dotted line runs through zero (which would reflect observations from SZ and RZ would be identical).
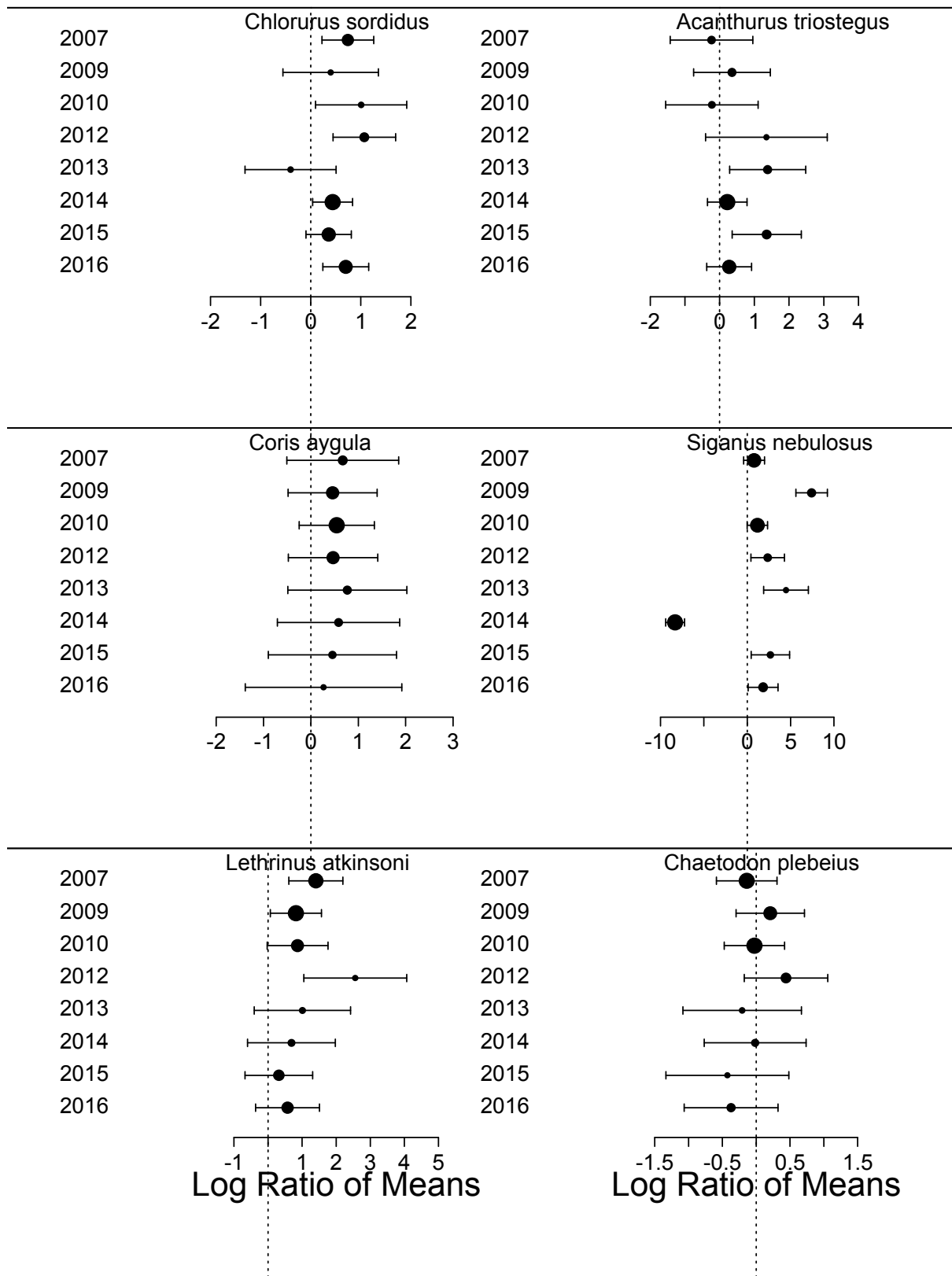
Figure 6.7.6 Log response ratios (± 95%CI) of six species of fishes calculated from biomass. The sizes of symbols are proportional to the precision of the estimates. Dotted line runs through zero (which would reflect observations from SZ and RZ would be identical).

Table 6.7.1 AIC$_c$ of models with equal or different trends U for SZ and RZ, for counts and biomass of each of the families (a) and species (b) analysed. ΔAIC$_c$ indicates the difference in AIC$_c$ between the two models.

	AIC$_c$ *U* EQUAL (SZ=RZ)	AIC$_c$ *U* DIFFERENT (SZ≠RZ)	ΔAIC$_c$
Counts			
(a)			
Scaridae	33.6	41.8	8.2
Labridae	37.1	45.7	8.6
Acanthuridae	37.1	45.7	8.6
Chaetodontidae	17.9	25.7	7.8
Siganidae	78.9	87.2	8.3
Lethrinidae	54.4	62.6	8.2
(b)			
Chlorurus sordidus	38.6	46.9	8.3
Acanthurus triostegus	45.2	53.7	8.5
Coris aygula	36.0	42.4	6.4
Siganus nebulosus	112.5	119.9	7.4
Lethrinus atkinsoni	50.3	58.8	8.5
Chaetodon plebeius	28.1	35.7	7.6
Mass			
(a)			
Scaridae	48.2	56.7	8.5
Labridae	27.0	35.4	8.4
Acanthuridae	49.6	58.0	8.4
Chaetodontidae	25.8	33.8	8.0
Siganidae	92.1	100.3	8.2
Lethrinidae	53.1	61.6	8.5
(b)			
Chlorurus sordidus	48.1	56.1	8.0
Acanthurus triostegus	54.2	61.4	7.2
Coris aygula	21.7	29.9	8.2
Siganus nebulosus	121.8	129.2	7.4
Lethrinus atkinsoni	49.3	57.2	7.9
Chaetodon plebeius	25.9	32.1	6.2

Table 6.7.2 Estimated annual trend U, and upper and lower 95% confidence intervals generated by MARSS using annual mean counts for (a) each family and (b) each species. Bold font indicates estimates with 95% confidence intervals overlapping zero, and so a robust evidence of a declining trend.

	POOLED			SZ			RZ		
	U	LOWER CI	UPPER CI	*U*	LOWER CI	UPPER CI	*U*	LOWER CI	UPPER CI
(a)									
Scaridae	-0.028	-0.110	0.054	-0.039	-0.108	0.031	-0.022	-0.122	0.078
Labridae	-0.097	-0.221	0.019	**-0.098**	**-0.191**	**-0.005**	-0.098	-0.22	0.023
Acanthuridae	-0.065	-0.190	0.065	-0.078	-0.211	0.055	-0.092	-0.186	0.003
Chaetodontidae	-0.090	-0.195	0.004	**-0.097**	**-0.191**	**-0.003**	-0.089	-0.183	0.004
Siganidae	-0.236	-0.499	0.040	**-0.249**	**-0.484**	**-0.014**	-0.156	-0.488	0.175
Lethrinidae	**-0.150**	**-0.214**	**-0.073**	**-0.105**	**-0.151**	**-0.060**	-0.156	-0.337	0.025
(b)									
Chlorurus sordidus	-0.008	-0.086	0.067	-0.012	-0.068	0.043	0.011	-0.089	0.111
Acanthurus triostegus	-0.070	-0.216	0.071	-0.093	-0.257	0.070	-0.085	-0.185	0.014
Coris aygula	**-0.140**	**-0.222**	**-0.072**	**-0.129**	**-0.227**	**-0.031**	**-0.178**	**-0.243**	**-0.113**
Siganus nebulosus	**-0.260**	**-0.509**	**-0.003**	-0.277	-0.563	0.010	0.269	-0.810	1.347
Lethrinus atkinsoni	**-0.141**	**-0.202**	**-0.076**	**-0.096**	**-0.142**	**-0.050**	-0.117	-0.279	0.045
Chaetodon plebeius	**-0.123**	**-0.217**	**-0.028**	**-0.129**	**-0.227**	**-0.032**	**-0.112**	**-0.199**	**-0.025**

Table 6.7.3 Estimated annual trend U, and upper and lower 95% confidence intervals generated by MARSS using annual mean biomass for (a) each family and (b) each species. Bold font indicates estimates with 95% confidence intervals overlapping zero, and so a robust evidence of a declining trend.

	POOLED			SZ			RZ		
	U	LOWER CI	UPPER CI	*U*	LOWER CI	UPPER CI	*U*	LOWER CI	UPPER CI
(a)									
Scaridae	-0.036	-0.166	0.085	-0.064	-0.199	0.071	-0.059	-0.168	0.05
Labridae	**-0.148**	**-0.215**	**-0.085**	**-0.154**	**-0.219**	**-0.088**	**-0.164**	**-0.225**	**-0.104**
Acanthuridae	-0.017	-0.107	0.077	-0.047	-0.158	0.064	-0.018	-0.133	0.097
Chaetodontidae	**-0.111**	**-0.179**	**-0.042**	**-0.128**	**-0.195**	**-0.06**	**-0.110**	**-0.182**	**-0.038**
Siganidae	-0.171	-0.471	0.129	-0.266	-0.625	0.093	-0.097	-0.584	0.39
Lethrinidae	**-0.164**	**-0.221**	**-0.105**	**-0.197**	**-0.369**	**-0.025**	-0.120	-0.288	0.047
(b)									
Chlorurus sordidus	-0.014	-0.142	0.128	-0.046	-0.189	0.097	-0.011	-0.116	0.095
Acanthurus triostegus	-0.133	-0.281	0.021	-0.127	-0.289	0.036	**-0.201**	**-0.327**	**-0.075**
Coris aygula	**-0.156**	**-0.244**	**-0.078**	**-0.178**	**-0.246**	**-0.11**	**-0.167**	**-0.237**	**-0.096**
Siganus nebulosus	-0.179	-0.493	0.135	-0.267	-0.64	0.105	0.474	-0.967	1.915
Lethrinus atkinsoni	**-0.159**	**-0.210**	**-0.108**	**-0.134**	**-0.192**	**-0.077**	-0.078	-0.225	0.068
Chaetodon plebeius	**-0.141**	**-0.185**	**-0.093**	**-0.159**	**-0.292**	**-0.026**	**-0.125**	**-0.182**	**-0.069**

MARSS

For each of the families and species, and for both counts and biomass, models with equal *U* were more parsimonious than those with different *U* for SZ and RZ (Table 6.7.1). There were significantly decreasing trends (i.e. 95% CI not overlapping zero) in abundance (i.e. counts of individuals) from 2007 to 2016 for Lethrinidae (emperors; 95% CI 7–21% per year), but not for other families, although trends for Chaetdontidae (butterflyfish) only just overlapped zero (0–19%, Table 6.7.2—models for SZ and RZ shown for comparison). Among the species analysed, counts of the wrasse *Coris aygula,* the rabbitfish *Siganus nebulosus*, the emperor *Lethrinus atkinsoni* and the butterflyfish *Chaetodon plebius* all declined during the course of the survey period (Table 6.7.2). For biomass, which is a product of fish abundance and fish size, there were declining trends for wrasses (Labridae), butterflyfish (Chaetodontidae), and emperors (Lethrinidae), (Table 6.7.3, Figure 6.7.4). Similarly, there were decreasing trends in biomass of *Coris aygula*, *Lethrinus atkinsoni* and *Chaetodon plebeius* (Table 6.7.3). No families or species showed an increasing trend in either counts or biomass.

There was an overall decreasing trend in percentage cover of hard coral (a decline of 6% per year), but no statistically significant overall trends in the percentage cover of algae, abiotic substrate, or rugosity (Table 6.7.4).

Table 6.7.4 Estimated annual trend U, with upper and lower 95% confidence intervals generated by MARSS using percentage cover of three habitat types, and rugosity. Bold font indicates estimates with 95% confidence intervals overlapping zero, and so a robust evidence of a declining trend.

	U	LOWER CI	UPPER CI
Hard coral (%)	**-0.060**	**-0.077**	**-0.042**
Algae (%)	0.022	-0.036	0.075
Abiotic (%)	-0.009	-0.201	0.175
Rugosity	0.023	0.002	0.046

6.7.4 DISCUSSION

Overall, ten years of observations in and around the Mandu Sanctuary zone revealed that there were typically higher counts and biomasses of some taxa in the Sanctaury Zone than the adjacent Recreation Zone, but the abundance of several taxa declined substantially during the survey. Emperors (Lethrinidae, counts and biomass) and wrasses (Labridae, biomass only) tended to be more abundant in the SZ, but abundance declined. In contrast, abundances of parrotfish (Scaridae, counts and biomass) and surgeonfish (Acanthuridae, biomass only) tended to be higher in the SZ but did not decline significantly during the study. The abundance of butterflyfish was roughly similar in the SZ and RZ, but declined significantly during the survey.

The global consensus on the effectiveness of marine reserves is that they are generally successful in achieving conservation outcomes (Halpern et al. 2002, Lubchenko et al. 2003, Claudet et al. 2008) with higher density and biomass of fished species inside protected areas than outside them. Meta-analyses suggest effect sizes (ratio fish inside vs outside protected areas) of between 2 and 3 times can be expected on average, with much larger effects possible (Claudet et al. 2008, Lester et al. 2009), mainly due to increases of targeted species in protected areas. Although these can take some time to develop (McClanahan 2007, Babcock et al. 2010) in other cases they can be quite rapid (Denny et al. 2004).

In contrast to expectations raised by these studies, we found either no significant change or

significant declines in counts or biomass, or both, for several taxa. While abundance of several taxa was always greater in the SZ than in the RZ, their declining abundance suggests that the SZ might have limited effectiveness. Our results also indicate that effect size alone should be used with caution in terms of evaluating marine reserve success (Babcock et al. 2010)—effect size did not tend to decline during the survey because abundances declined at similar rates in both the SZ and RZ.

The presence and magnitude of a positive effect of reserve on fish abundance is likely to depend on a range of factors, which might include regulations that prohibit fishing (i.e. "no-take"), size of reserve, age, effectiveness of enforcement of (or compliance with) regulations and degree of isolation. Sanctuary Zones at Ningaloo are "no-take", and at the time our study commenced had been established for over 20 years, and there is a high level of compliance with zoning (Smallwood et al. 2012) so at least three of the key ingredients for success are present at Mandu (i.e. regulations that prohibit fishing, age and effective compliance regulations); however the size of the Mandu SZ is only 13.49 km^2 and the reef habitat is not isolated. One of the unique aspects of the fringing reef at Ningaloo is that it is one of the world's longest continuous stretches of coastal fringing reef and the reef within Mandu SZ is contiguous with the reef in adjacent zones. In this respect one of Ningaloo's greatest claims to fame may be one of the greatest weaknesses in terms of attempts to use marine park zoning in order to protect species targeted by fishing.

The management plan for the Ningaloo Marine Park contains an explicit performance measure of no loss of abundance of fish inside SZs as a result of human activities (CALM 2005). Our results show that there has been a decline in abundance of several families inside (and adjacent to) Mandu SZ. There are several potential reasons for the decline, and different taxa are likely to be declining due to different pressures.

There are several possible causes for the declining abundance, and it seems plausible—even likely—that the causes are different for different taxa. We can speculate about the possible causes by drawing on knowledge of the biology and ecology of the taxa. The declining abundance of lethrinids and labrids is plausibly due to fishing. Fishing effort at Ningaloo is high—although the human population in the region is small it is the focus of a vigorous recreational fishery (Sumner et al. 2002, Smallwood et al. 2011). Although abundances for several taxa were higher in SZs (e.g. Lethrinidae, Labridae), there was a general decline in both the SZ and RZ. This declining trend in these taxa could be explained by a general increase in fishing pressure (Smallwood et al. 2011) and the fact that Mandu is a small reserve nested in a larger contiguous area of fringing reef. The movement ranges of some taxa—such as lethrinids (Pillans et al. 2014, Babcock et al. 2017)—may result many individuals moving outside the SZ, which could in turn cause enough mortality to produce a decline. Although *Lethrinus atkinsoni* (the most abundant emperor on the reef flat) does not feature strongly in catch statistics, it is frequently caught by campers on the coast, who do not tend to be included in boat ramp surveys, and is also used as bait for larger fish (Babcock, personal observations). Even relatively low rates of fishing might tend to decrease abundance if recruitment and growth rates are low or individual fish move widely.

There is evidence that this trend may have existed for some time as estimates of Lethinid density and biomass at Mandu in 2007 were somewhat lower than those made in 2000 (Westera et al. 2003). The largest lethrinid at Ningaloo, *L. nebulosus* was only observed on our transects twice since 2010 (it was recorded during each survey from 2007 to 2010); while it would have been desirable here to analyse trends in abundance of this species, the very low numbers of individuals observed precluded such analyses. However, our observations are consistent with modelling of the recreational fishery for *L. nebulosus* immediately following rezoning in 2007 indicated that the population of *L. nebulosus* on Ningaloo was at around half of unfished biomass and that, given status quo management, the population of *L. nebulosus* would likely continue to decline (Thébaud et al. 2014). Declines in the abundance of the large wrasse *Coris aygula* are also plausibly caused by

fishing—it is not specifically targeted by anglers but it is a large bodied carnivorous fish and is likely to be captured and retained opportunistically, particularly if more highly sought-after species become uncommon.

Fishing is implausible as an explanation for the observed decrease in abundance of butterflyfishes (Chaetodontidae). Instead, a more plausible explanation is a change in habitat—particularly the living corals that are a food source for several of the species that inhabit the reef flat at Mandu. The abundance of butterflyfishes is strongly correlated with the percentage cover of living hard coral. Our results are consistent with a decline in the percentage cover of living coral that were likely the result of mortality during the coral bleaching episodes experienced on the western Australian coast in 2011 and 2013 (Moore et al. 2012; also see Thomson et al. MS, Babcock et al. MS). The potential decline in cover of living hard coral is not likely to be a cause of declines in abundance of wrasses or emperors, for which significant correlation with any of the measures of habitat were present.

Considerations for management

The results of this study highlight two areas of concern for management of the Ningaloo Marine Park. First, is evidence of declining trends in abundance—measured as counts of individuals and biomass—inside the Mandu SZ, and in adjacent RZ. Finfish are a Key Performance Indicator in the park's management plan, and have a performance measure that stipulates no loss of abundance in sanctuary zones as a result of human activities. Although the causes of the declines remain inconclusive, it seems likely that some of the declines are due, at least in part, to human activity— the direct influence of fishing is a plausible explanation for several families and species. We note that the declines occurred inside the SZ, where all forms of fishing are prohibited, as well as outside the SZ, where recreational angling is prohibited. This might be explained by the fact that that many individuals move regularly in and out of SZs (Pillans et al. 2014, Babcock et al. 2017).

A second consideration is the apparent decline in the abundance of living hard coral. This is consistent with the results of other studies in the region, which have shown that the abundance of hard corals has declined over the past decade (Thomson et al. 2017, Bessey et al. 2017, Babcock et al. 2017). It is possible that the declines in abundance of butterflyfishes and wrasses are due in part to the declining abundance of living hard coral. Coral reef communities are also a KPI in the Ningaloo Marine Park management plan, with performance measures that stipulate constant or increasing trends in coral biomass.

To achieve the KPIs for finfish, it seems likely that some changes to park and/or fisheries management. For taxa for which declining abundances are possibly—or likely—caused by fishing, several changes are possible, including changing the design of SZs so that they are larger and encompass contiguous areas of reef, and stricter limits on the number of fish that can be taken (Thébaud et al. 2014).

Given the declines observed at Mandu, continued long-term survey effort is needed to monitor whether declines continue, and how the reef ecosystem responds to management intervention.

6.7.5   ACKNOWLEDGEMENTS

6.7.6 REFERENCES

Agardy T, Bridgewater P, Crosby MP, Day J, Dayton PK, Kenchington R, Laffoley D, McConney P, Murray PA, Parks JE, Peau L (2003) Dangerous targets? Unresolved issues and ideological clashes around marine protected areas. Aquatic Conservation: Marine and Freshwater Ecosystems 13(4):353-67.

Babcock RC, Pillans RD, Rochester WA (2017) Environmental and individual effects on the behaviour and spawning movements of Lethrinus nebulosus on a coral reef. Marine and Freshwater Research 68:1422-1437.

Barnes M, Craigie ID, Hockings M (2016) Towards understanding of drivers of wildlife population trends in terrestrial protected areas. Pages 134- *in* L. N. Joppa, J. N. Baillie, and J. G. Robinson, editors. Protected Areas: Are They Safeguarding Biodiversity? John Wiley & Sons, Oxford.

Bohnsack JA, Causey B, Crosby MP, Griffis RB, Hixon MA, Hourigan TF, Koltes KH, Maragos JE, Simons A, Tilmant JT (2002) A rationale for minimum 20-30% no-take protection. In: Proceedings of the Ninth International Coral Reef Symposium, Bali, 23-27 October 2000, Vol. 2, pp. 615-619.

CALM (2005) Management plan for the Ningaloo marine park And muiron islands Marine management area 2005 – 2015 Management Plan Number 52. WA Dept of Conservation and Land Management, Perth Western Australia. 115 pp.

CBD (2006) Decisions Adopted by the Conference of the Parties to the Convention on Biological Diversity at its Eighth Meeting (Decision VIII/15, Annex IV). Convention on Biological Diversity, Curitiba, Brazil.

Claudet J, Osenberg CW, Benedetti-Cecchi L, Domenici P, Garcı´a-Charton JA, et al (2008) Marine reserves: Size and age do matter. Ecology Letters 11:481-489

Collins LB, Zhu ZR, Wyrwoll K-H, Eisenhauer A (2003) Late Quaternary structure and development of the northern Ningaloo Reef, Australia. Sedimentary Geology 159:81-94.

Denny CM, Willis TJ, Babcock RC (2004) Rapid recolonisation of snapper *Pagrus auratus*: Sparidae within an offshore island marine reserve after implementation of no-take status. Mar Ecol Prog Ser 272:183-190

Edgar GJ, Stuart-Smith RD, Willis TJ, Kininmonth S, Baker SC, Banks S, Barrett NS, Becerro MA, Bernard AT, Berkhout J, Buxton CD (2014) Global conservation outcomes depend on marine protected areas with five key features. Nature 506(7487):216-20.

Fernandes L, Day J, Kerrigan B, Breen D, De'ath G, Mapstone B, Coles R, Done T, Marsh H, Poiner I, Ward T (2009). A process to design a network of marine no-take areas: Lessons from the Great Barrier Reef. Ocean & Coastal Management, 52(8), pp.439-447.

Fitzpatrick BM, Harvey ES, Langlois TJ, Babcock R, Twiggs E 2015 Effects of fishing on fish assemblages at the reefscape scale. Marine Ecol Progr. Ser. 524: 241–253, doi: 10.3354/meps11077

Holmes EE, Ward EJ, Scheuerell MD (2014) Analysis of multivariate time-series using the MARSS package. NOAA Fisheries, Northwest Fisheries Science Center, Seattle.

Holmes EE, Ward EJ, Wills K (2012) MARSS: Multivariate Autoregressive State-space Models for Analyzing Time-series Data. R Journal 4:11-19.

Lubchenco J, Palumbi SR, Gaines SD, Andelman S eds (2003) The science of marine reserves. Ecol Appl 13 S1-S228

Ojala M, Garriga GC (2010) Permutation tests for studying classifier performance. Journal of Machine Learning Research 11:1833-1863.

McClanahan TR (2000) Recovery of a coral reef keystone predator, Balistapus undulatus, in East African marine parks. Biol Conserv 94: 191-198

McClanahan TR, Graham NAJ, Calnan JM, MacNeil MA (2007) Toward pristine biomass: Reef fish recovery in coral reef marine protected areas in Kenya. *Ecol Appl* 17:1055-1067

Moore JA, Bellchambers LM, Depczynski MR, Evans RD, Evans SN, Field SN, ... & Radford BT (2012) Unprecedented mass bleaching and loss of coral across 12 of latitude in Western Australia in 2010–11. PLoS One, 7(12), e51807.

Pillans RD, Bearham D, Boomer A, Downie R, Patterson TA, Thomson DP, Babcock RC (2014) Multi Year Observations Reveal Variability in Residence of a Tropical Demersal Fish, Lethrinus nebulosus: Implications for Spatial Management. PLoS ONE 9.

R Development Team (2016) RStan: the R interface to Stan. R package version 2.14.1.

Smallwood CB, Beckley LE, Moore SA, Kobryn HT (2011) Assessing patterns of recreational use in large marine parks: A case study from Ningaloo Marine Park, Australia. Ocean & Coastal Management 54(4):330-40.

Smallwood CB, Beckley LE (2012) Spatial distribution and zoning compliance of recreational fishing in Ningaloo Marine Park, north-western Australia. Fisheries Research 125:40-50.

Sumner NR, Williamson PC, Malseed BE (2002) A 12-month survey of recreational fishing in the Gascoyne bioregion of Western Australia during 1998-99. Department of Fisheries, Western Australia.

Thébaud O, Ellis N, Little LR, Doyen L, Marriott RJ (2014) Viability trade-offs in the evaluation of strategies to manage recreational fishing in a marine park. Ecological Indicators 46:59-69.

Unsworth CP, Cowper MR, McLaughlin S, Mulgrew B (2001) A new method to detect nonlinearity in a time-series: synthesizing surrogate data using a Kolmogorov–Smirnoff tested, hidden Markov model. Physica D: Nonlinear Phenomena 155:51–68.

Williamson PC, Sumner NR, Malseed BE (2006) A 12-month survey of recreational fishing in the Pilbara region of Western Australia during 1999-2000. Department of Fisheries, Western Australia.

6.8 A model Ningaloo coral reef system to test cause-effect pathways

Authors: Boschetti F, Prunera K, Vanderklift M, Babcock RC, Thomson DP.

ABSTRACT

We developed a simple model to test questions about potential causes of patterns we observe in nature at Ningaloo, and to explore the plausible outcomes of changes in dome of the key ecological groups (i.e. corals, macroalgae and fish).

Time series analyses of field observations in companion studies have highlighted statistically significant decreases in the biomass of a number of coral (Thomson et al. 2017) and fish (Vanderklift et al. 2007) taxa in and around the Mandu Sanctuary Zone in the Ningaloo Marine Park. Those analyses have been carried out *independently* for different taxa. Here we carry out a *joint* analysis of these same time series via a numerical model which accounts for the interaction between taxa. The purpose of this analysis is to explore possible causal explanations of the observed biomass declines. One hypothesis currently under consideration suggests that declines may be due to forcing external to the dynamics of the ecosystem and that this forcing may be the result of increased fish mortality, for example due either fishing or climate-driven coral mortality.

To test this hypothesis, we first fitted the model to observed mean biomass densities and we studied the model dynamics under this parameterisation. We obtained two significant results: first, the model provides an accurate fit when observations from the sanctuary zone and the recreational zone are processed separately, but not when they are processed jointly. Two different parameter sets are needed to model the two zones, which suggests that they may function as two different systems. Second, the time scale of their response to external perturbations is approximately 5-10 years, after which the system returns to stable state. This suggests that trends with a longer time scale, as the ones observed over the 2007-2016 interval, may indeed result from external forcing rather than internal dynamics.

Next, we fitted the model to a surrogate time series in which real observations have been shuffled in time, in order to remove trends in the data without affecting the error distribution. The model displays a reasonable fit, but high standard deviation in the data forces us to be cautious about drawing firm conclusions from this analysis. Finally, we fix the model parametrisation from the de-trended surrogate time series and test whether the actual observed time series can be fitted when the system is driven by external forcing which imposes additional mortality on both fish and coral. These results are less clear, suggesting acceptable model fit for some groups in one of the zones but not for others. Like the surrogate time series, the high observation error forces us to be cautious in interpreting these results.

Two important messages arise from this work. First, it is possible to turn questions of management relevance (eg. '*Is the observed biomass loss in Ningaloo reefs due to internal processes or external forcing?*') into modelling questions and to test alternative hypotheses against observations. Second, the main hurdle in providing reliable answers to questions of management relevance lies in observation error, which highlights the importance of accurate time series spanning long time intervals.

6.8.1 INTRODUCTION

In the last few years significant research effort has focused on studying coral reef systems with the tools of system dynamics (Mumby 2009; Mumby et al. 2013). A motivation for this approach is the empirical observation that some coral reefs appear to transition fairly quickly from coral-dominated to algae-dominated systems, with significant impact on local biodiversity. System dynamics aims to study how systems evolve in time as a result of internal processes and external forcing (Meadows 2008). It mostly focuses on studying what configurations a system may display as a result of feedback loops, time delays, flows, stock accumulation and the interplay of dynamics at different spatial and temporal scales. As such, it is naturally suited to address questions related to the state, dynamics and resilience of coral reef ecosystems.

Because humans, experts included, are generally poor at predicting the dynamics of even fairly simple systems (Sterman 2008), modelling is integral to system dynamics. Modelling approaches to studying coral reef ecosystems range from fairly simple spatially (Mumby 2006) and non-spatially explicit models (Holmes and Johnstone 2010; van de Leemput et al. 2016) to large size fully spatial ecological models (Gurney et al. 2013).

Here we present a model of intermediate complexity which describes the interaction between 6 functional groups: corals (C), macroalgae (M), filamentous turf algae (T), browsing fish (B), grazing (also known as scraping) fish (G) and piscivorous fish (P). The system undergoes internal dynamics as well as external forcing in terms of additional mortality on each group. Starting from standard ecological relations, the model equations and parameterisation are modified to reflect both the observations and the expert knowledge acquired by studying the coral reef ecosystems in the Ningaloo Marine Park, in Western Australia.

The purpose of this analysis is threefold. First, we use observations of *mean* biomass density of corals (C), browsing fish (B), grazing fish (G) and piscivorous fish (P) *inside* and *outside* the Mandu Sanctuary Zone (SZ) in the Ningaloo Marine Park to determine a model parameterisation compatible with observations. Second, given this parametrisation, we study the model behaviour in terms of its internal dynamics and response to external pressure. Third, we use a *time series* of density measurements of C, B, G and P carried out between 2007 and 2016. *Separate* analyses have highlighted statistically significant decreases in biomass of some coral (Thomson et al. 2017) and fish (Vanderklift et al. 2007) taxa in and around the Mandu SZ. Here, we test whether similar trends emerge from the *joint* analysis of these functional groups.Here we aim to elucidate the spatial and temporal distributions of the dominant drivers of productivity in the Indian Ocean off Australia´s northwest (Figure 6.8.1) using statistical analyses of satellite derived chlorophyll-*a* measurements and temperature records. We show that there are zones of coherent variation present, and their boundaries likely reflect the influences of different physical oceanographic drivers of production. Identification and understanding of these zones will assist in future management of regional ecosystem resources.

6.8.2 METHODS

Outline of the approach

Here we present a brief outline of the overall approach used in this study. More details are provided in the following sections and in the Supplementary Material.

First, we designed the ecological model (we term this *Recife* from hereon) to represent the

conceptual understanding (mental model from hereon) of the functioning of the Ningaloo coral reef system. This mental model was developed via the interaction between modellers and marine ecologists who have worked extensively in the area. Ranges of the model parameters were determined from local observations and local knowledge wherever possible, and from the literature when local information was not available. Model development and parameterisation are described in the section titled "Model and development parameterisation".

Second, we addressed model parameter estimation. Rather than carrying this out manually, that is by a modeller-guided trial-and-error process, we opted for an automated approach via numerical optimisation. This is described in the section titled "The study area and benthic surveys".

Third, we estimated a parameter set which allows the model to reach a stable state which fits observations of mean density of C, B, G and P. This showed that the model can fit the observations and that the parameter estimation works efficiently. This also provided a model parametrisation compatible with observations which can be used to study the system dynamics under realistic conditions.

Next, we proceed to fit the model to the observed time series. Following the results in (Vanderklift et al. 2007; Thomson et al. 2017) a two-stage approach was used.

- First, a surrogate time series was generated by shuffling the observations with respect to time. This results in new time series with the actual observations, but random time ordering. This can be interpreted as a time series from which possible trends have been removed without affecting the mean process and observation error. We applied the parameter estimation algorithm to see whether the model could fit this time series without external forcing.
- Second, the same approach was used to fit the model to the original (not time-shuffled) time series, to see whether the observed trends could result from external forcing.

The study area and benthic surveys

Our study was conducted on shallow reef flats within and adjacent to the Mandu Sanctuary Zone (SZ: 1,185 ha) within the Ningaloo Marine Park (NMP: 22°S, 113°E). The coral reefs in this area are mainly fringing reef located 0.2-2 km from the shore. The reef flat is ~150 m wide, generally submerged even at low tide, and typically dominated by the plate coral *Acropora spicifera* growing on limestone bedrock ((Collins et al. 2003)). Field surveys of fish and coral on the reef flat were first conducted in 2007 (18 years after the NMP was established), and were conducted regularly through to 2016.

Model development and parameterisation

Here we briefly describe the main features of the *Recife* model while detailed information needed to reproduce both model and results is provided in Appendix 1.

The model components and their interactions are graphically summarised in Figure 6.8.1. The initial model structure and equations were loosely based on the Corset model (Fung et al. 2011; Melbourne-Thomas et al. 2011) which have been modified to reflect the experts' mental model of the local processes we aim to study. The main modifications include:

1) In most ecological models of this kind, C, M and T are represented as percentage of surface cover. This is convenient since it simplifies the implementation of the competition for space. However, in this work we opted to represent all groups as biomass for two reasons. First,

this simplifies the feeding (grazing and browsing) relations. Second, we do not need to assume the model domain to be strictly 2D (or at least of constant area), which can be significant for both coral and macroalgae growth. As a result, empirical conversion between observed area cover and biomass of C, M and T is addressed in the model parametrisation rather than in the model dynamics.

2) Interaction between C, M and T is implemented in functional form as perturbations to the groups' carrying capacity and growth terms (see the first terms in Equations 1-3 in Appendix 1). These functional forms aim to approximate qualitative empirical observations from the literature or expert knowledge.

3) Similarly, we imposed density dependence on the fish groups via a carrying capacity term (see Predators' growth in Appendix 1) where a groups' carrying capacity depends on the (dynamically changing) food availability (see Predation/Grazing in Appendix 1). In particular, carrying capacity is computed as the ratio between food availability and the group's minimum food requirement which determines the average number rations available for growth and survival.

4) As afforded by the previous point, we assume that fish natural mortality is accounted for by either predation or density dependence and that the additional mortality terms (last terms in equations 4-6 in Appendix 1) represent external pressure.
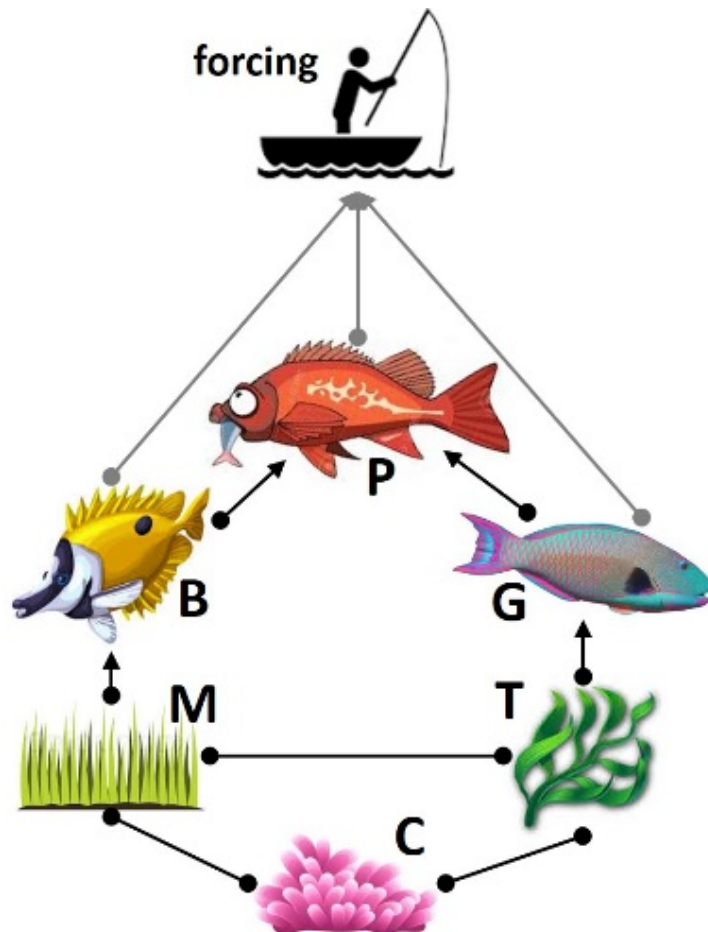
Figure 6.8.1 Graphic representation of the Recife model, showing the six functional groups, their interaction and the external forcing, represented by fishing mortality on the three fish groups.

Definitions and ranges for the model parameters are provided in Appendix 2 where parameter ranges are colour coded to represent their provenance (literature vs expert assessment vs other models).

Parameter estimation

Computer driven parameter estimation comes under different names in different fields of research (numerical inversion, optimisation, regression, Bayesian inference, among others). In recent years Bayesian inference has gained popularity in ecological applications (Dowd and Meyer 2003; Wilkinson 2011; Parslow et al. 2013). Its main strength lies in treating uncertainty on both observations and model parameters via the formal machinery of Bayesian statistics. Its main weakness is the heavy computation effort leading to possibly slow convergence. We tested this approach by using the 'smfsb' R package (Wilkinson 2011). Convergence was indeed very slow. We then tested the hybrid Genetic Algorithm (GA) described in (Boschetti 2008), which proved more computationally efficient. To avoid possible confusion, the term 'genetic' in the GA refers to how the computation is carried out and has no relation to the biological processes we study. For the purpose of this work, the GA can be treated as a black box.

Genetic Algorithms were originally explored in the field of Artificial Intelligence and Complex System Science and further developed with little interaction with the field of Bayesian inference. This led to little overlap in their literature and terminology despite the fact that they can be used for fairly similar purposes. The key to understand their similarity is to recognise that any parameter estimation approach consists of: i) a component which searches among different parameter configurations and ii) one which assesses how well the model fits the observations. The core of our approach lies in using the search component from the Genetic Algorithm, while allowing the model fit to be assessed within a Bayesian framework. In particular, two kinds of model estimations are carried out:

1) the first, which below we term 'exact', aims to fit the model to the observations without accounting for observation error. More specifically the Genetic Algorithms aim to minimise $cost = \sum \left(\frac{observations - simulations}{observations} \right)^2$, which is a fairly common cost function in numerical optimisation

2) the second approach, which below we term 'probabilistic', aims to fit the model to the observations accounting for observation error. The Genetic Algorithms aim to maximise $p = dnorm(simulations|observations, SD)$ where *dnorm* is the probability density for the normal distribution of the model output (*simulations*) given the *observations* and SD is the observations standard deviation.

6.8.3 RESULTS

Stable state analysis

First, we aim to model a system at stable state, for which the biomass density for C, B, G and P equates the mean biomass density as observed in 2007. Here we aim to fit this mean biomass density 'exactly', that is without accounting for observation error. The purpose of this exercise will become clear below.

Figure 6.8.2 shows the model fit when the Sanctuary Zone (SZ) and Recreation Zone (RZ) are analysed separately, that is the parameter estimation routine is used to reconstruct two separate parameter sets for SZ and RZ *independently*. Here as in all remaining figures dark dots refer to observation and solid line to model output. Both stable states are reconstructed to very high precision, which implies that i) the parameter estimation approach works efficiently and ii) the *Recife* model can reproduce these observations.
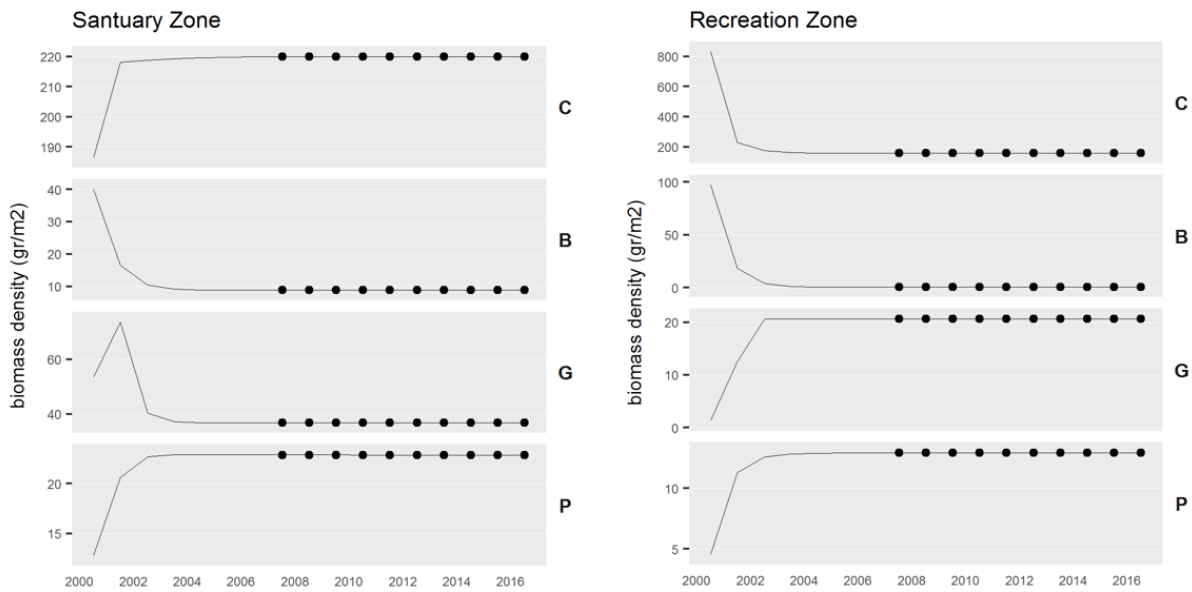
Figure 6.8.2. Stable state analysis. Independent parameter estimation for 'SZ' and 'RZ'. Observations are represented by dark dots and model output by continuous lines. Each panel refers to a single functional group.

Figure 6.8.3 shows the result of the same analysis when SZ and RZ are jointly analysed. In this case the parameter estimation searches for a single model parameter set which can reproduce both stable states simultaneously. A good fit is obtained for all fish groups but not so for coral (top panel). Notice that no external forcing is imposed on the model. This indicates that the SZ and RZ systems seem to differ somehow and that this difference results in different coral biomass density.
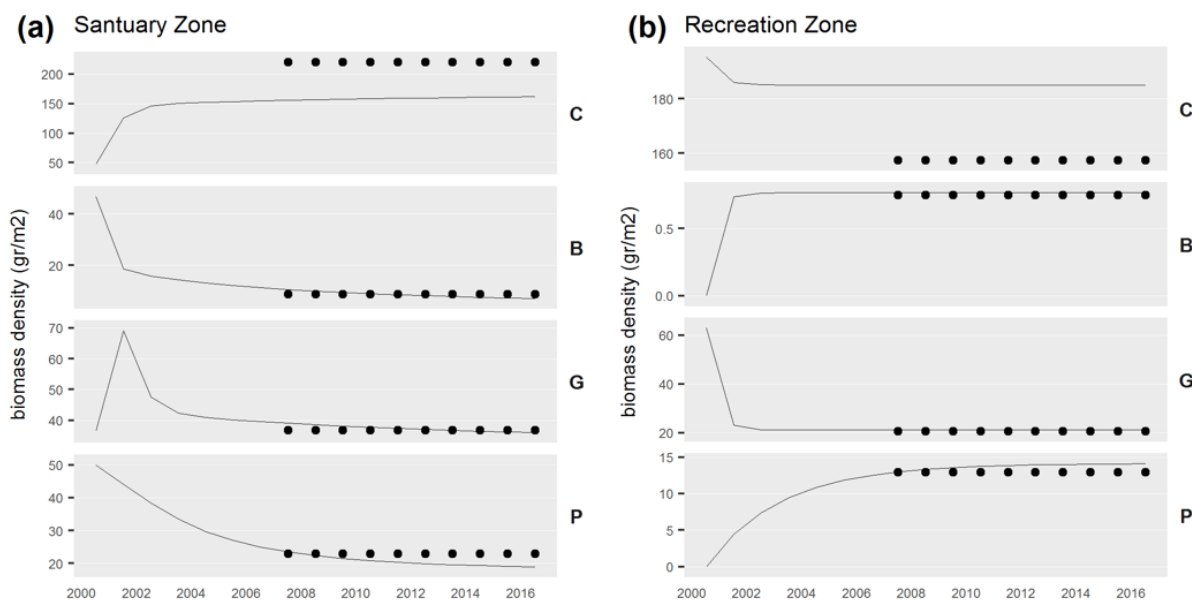
Figure 6.8.3. Stable state analysis. Joint parameter estimation for both 'SZ' and 'RZ'.

Analysis of model dynamics

Figure 6.8.2 shows the output of a model parameterisation leading to a stable state which matches the observations in 2007. This does not necessarily imply that this parameter set is 'correct' in the sense of realistically describing the actual system. First we have reasons to believe that the system in

2007 was not in a stable state (Vanderklift et al. 2007; Thomson et al. 2017) and second, other parameter sets may describe the observations equally well. However, it provides a parameter set which reproduces values of biomass densities compatible with observations. Here we use this parameter set to study the model dynamics under reasonably realistic configuration.

Figure 6.8.4 shows a simulation in which the stable state is disturbed by a perturbation which halves the coral biomass. M and T benefit by reduced competition and increase in biomass allowing for the fish groups to also increase. This system appears to be significantly perturbed for ~5 years and returns to the original state within 10 years, with the exception of P which takes a little longer. A similar response is achieved by perturbing the other groups (results not shown).
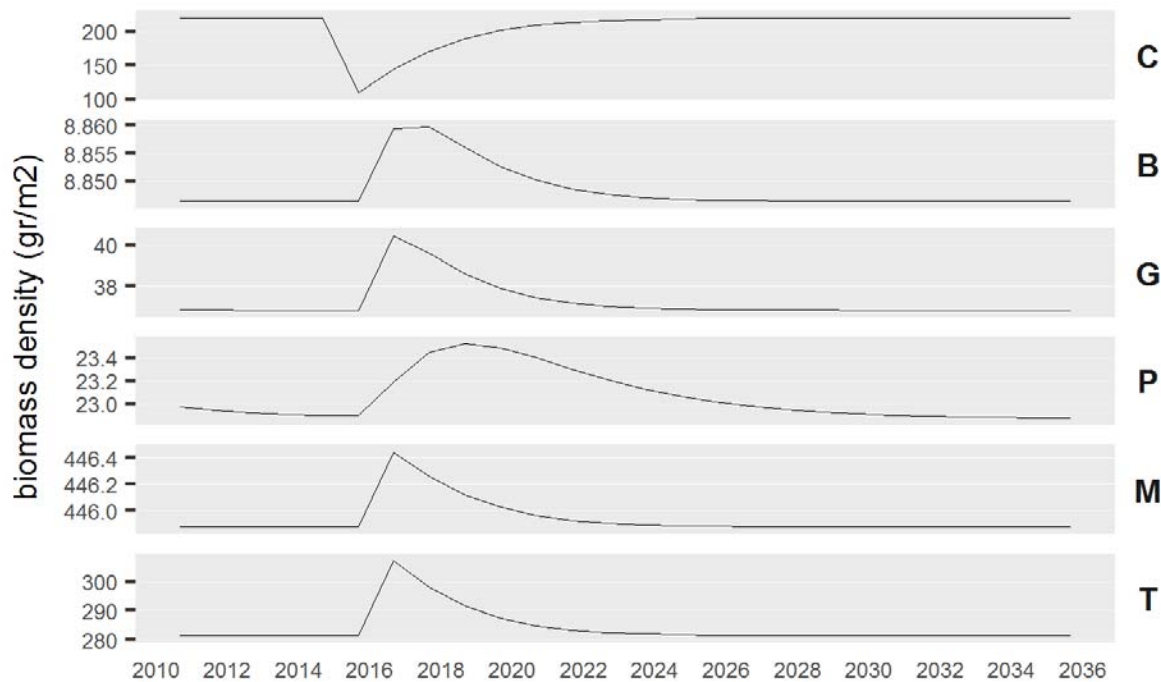
Figure 6.8.4 System response to a perturbation which halves coral biomass.

Figure 6.8.4 shows the system response, and thus sensitivity, to external perturbation to a group's biomass. Figure 6.8.5 shows the local sensitivity analysis to perturbation (by -20%, -10%, 10% and 20%) of each individual parameter in the parameter set. Only one parameter at a time is perturbed. This is one of the most basic sensitivity analyses possible and it is just a first pass. On the left we see changes in the amount of biomass at the end of the simulation against the baseline simulation. On the right, we see the cumulative variation per each parameter. The rows on the left and ranked per increasing sensitivity. In Figure 6.8.5 it is clear that for this parameter set, the system is mostly sensitive to alpha_MT, which controls the competition between M and T; M carrying capacity; alpha_MC which controls the competition between M and C. This highlights the important role M plays in the system.

Figure 6.8.6 shows ternary plots of Coral vs Macroalgae vs Fish (where fish is the sum of B, G and P). A ternary plot shows the relative contribution of three components when these components sum to 1. The dot size maps the overall system biomass. It is interesting to notice that all model runs align along three main lines suggesting that the overall model behaviour may lie in a subset of low dimension. For example, the longer line from vertex F shows a high variability in fish biomass while the ratio between C and M remains family constant. Similarly, the line from vertex C shows a high variability in coral biomass while the ratio between F and M slightly increases.
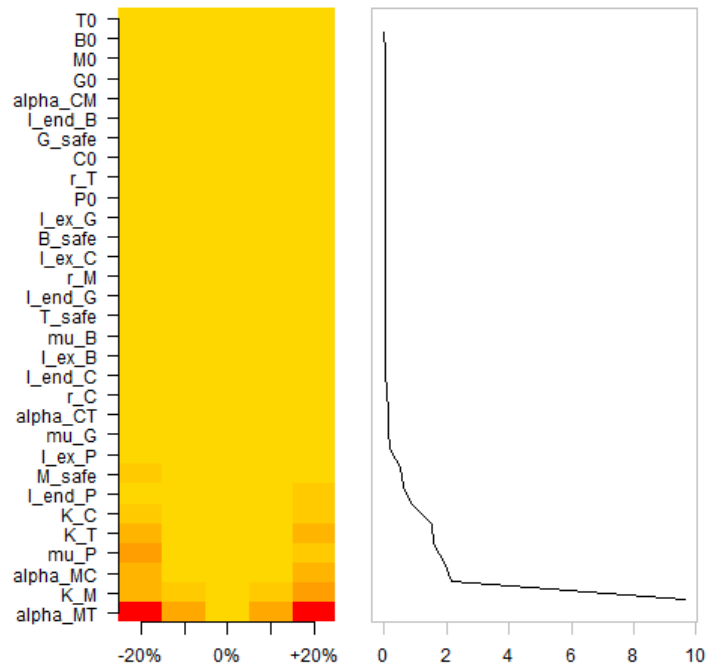
Figure 6.8.5 Local sensitivity analysis around the parameter set used to reproduce Figure 6.8.2.
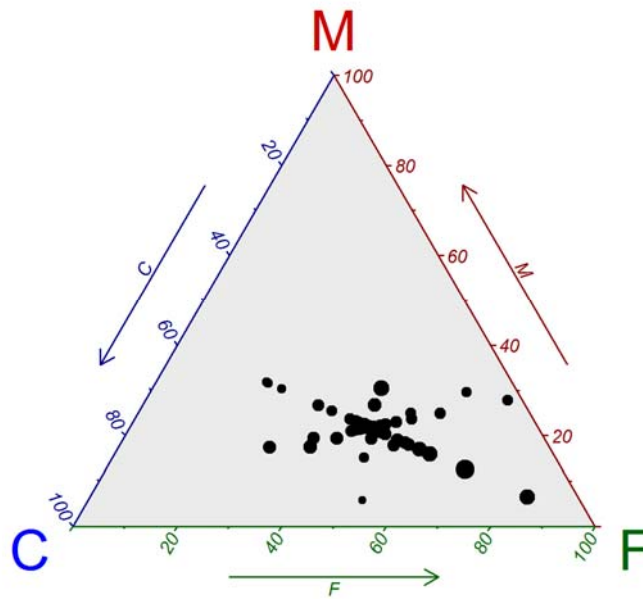
Figure 6.8.6 Ternary plot of the relative biomass of C, M and fish for different parameter sets.

Analysis of surrogate time series

Here we fit the model to the surrogate time series generated by shuffling the observations with respect to time, effectively de-trending the observations. As in the previous section, we aim to recover the model parameters under the assumption of no external forcing on the system. Here however we employ the 'probabilistic' parameter estimation, by accounting for observation uncertainty in terms of standard deviations.

The result is shown in Figure 6.8.7. For both SZ and RZ, after an initial 5-6 year transient dynamics, the parameter estimation fits the observations in a manner which is visually acceptable. Nevertheless, the model posterior probability given the observation is <u>very</u> low (~1e-40). This is due to the standard deviation in the observation being very high.
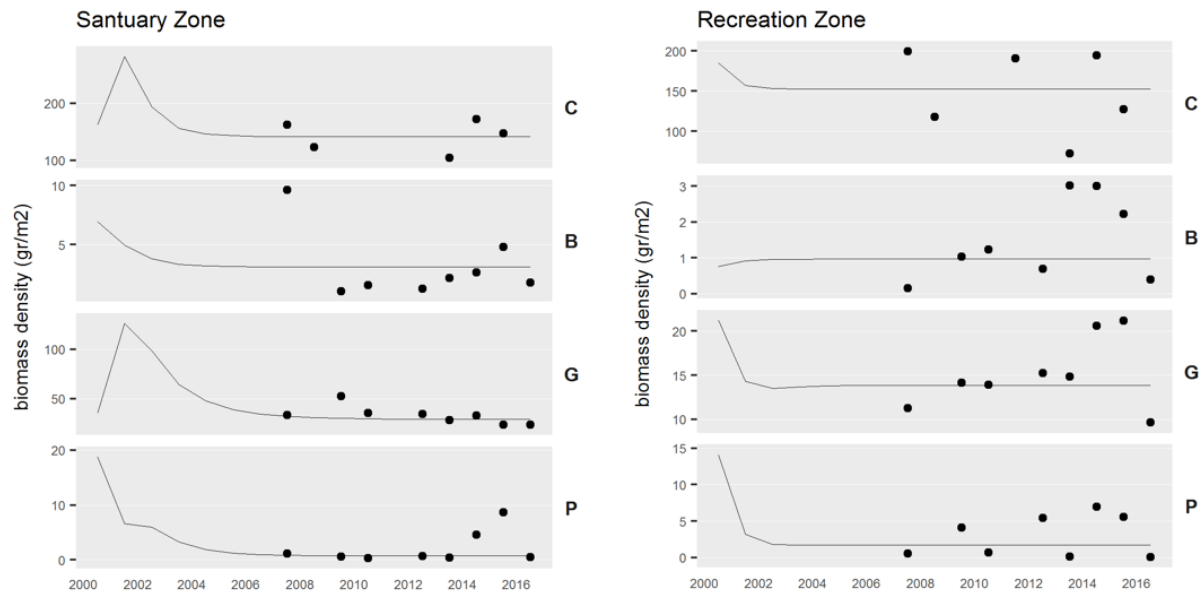
Figure 6.8.7 Analysis of de-trended surrogate time series. Independent parameter estimation for 'SZ' and 'RZ'. Observations are represented by dark dots and model output by continuous lines. Each panel refer to a single functional group.
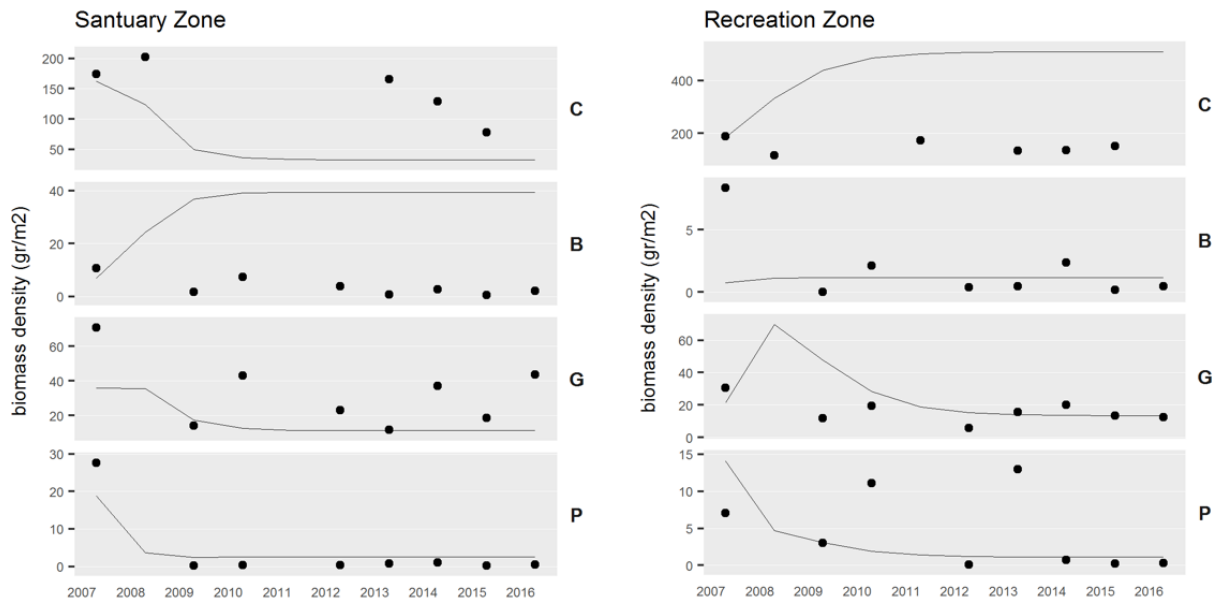
Figure 6.8.8 Analysis of observed time series. Independent parameter estimation for 'SZ' and 'RZ'. Observations are represented by dark dots and model output by continuous lines. Each panel refer to a single functional group.

Analysis of time series of biomass observations

Finally, here we fit the model to the observed biomass time series. As in the previous section, we employ the 'probabilistic' parameter estimation, by accounting for observation uncertainty in terms

of standard deviations. However, here we assume that the observed biomass trend results from increased mortality due to some external pressure. This is one of the hypotheses currently under consideration to explain the declining biomass trends in the region.

The results are shown in Figure 6.8.8. For SZ, G and P fit the observations reasonably well. C shows a decreasing trend but poor fit to observations while B displays an increasing biomass trend which does not match the observations. For RZ, G, P and P shows a reasonable fit while C displays an increasing biomass trend which also does not seem to be justified by the observations.

6.8.4 DISCUSSION

Simple ecological models can generate important insights into the processes that determine the structure and function of ecosystems. They have been particularly useful for understanding the somewhat complex dynamics of coral reef ecosystems (e.g. Mumby 2009, Melbourne-Thomas et al 2011). Our approach built on some of the methods and insights of previous authors, modified to use biomass as the model's only currency, and applied to observations generated from ten years of research at Ningaloo reef.

Our model generated an accurate fit when observations from the SZ and the RZ were modelled separately, but not when they were modelled jointly — two different sets of parameters were needed to accurately reflect the observations we have for Ningaloo (Vanderklift et al 2017, Thomson et al 2017). This result implies that the two management zones function somewhat differently, and that patterns are caused by processes that operate differently between the zones. Given that the interactions between components of the model were the same, this further implies that these processes are from parts of the system not modelled. Since the two zones reflect management units whose primary difference is the regulation of fishing — SZs are "no-take" areas with no fishing, while recreational angling (but not commercial fishing or recreational spearfishing) is allowed in the RZ adjacent to Mandu — fishing effort is an obvious candidate. Further research could investigate this further by introducing fishing as an additional mortality term in the model.

Another key result of the model is that the duration of the response of abundances of (model) fish and coral taxa to perturbations is approximately 5-10 years, after which they return to a stable state. This further implies that trends that persist for longer than 10 years might be caused by external forcing influences. The results of our long-term studies of fish and coral (Vanderklift et al 2017) have revealed a long-term decline over 10 years for several fish taxa. Observations have also revealed a decline in the abundance of corals, which appears to be caused primarily by one (or perhaps several) marine heatwaves — the reduction in abundance has persisted for at least six years so far. The duration of the observed declines are therefore incongruent with the 5-10 year duration of model responses. One possibility for this is that the observed declines are caused by external influences not accounted for in the model.

Although the model yielded a reasonable fit, high standard deviation in the data forces us to be cautious about drawing firm conclusions, highlighting that a substantial hurdle in providing reliable answers to questions of management relevance lies in observation error, which emphasises the importance of accurate time series spanning long time intervals.

Overall, our model has revealed important insights into the plausible mechanisms underlying change at Ningaloo. The model system provides a test bed for investigation of potential ecological responses to change.

6.8.5 ACKNOWLEDGEMENTS

6.8.6 REFERENCES

Boschetti F (2008) A local linear embedding module for evolutionary computation optimization. Journal of Heuristics 14, 95-116.

Collins LB, Zhu ZR, Wyrwoll K-H, Eisenhauer A (2003) Late Quaternary structure and development of the northern Ningaloo Reef, Australia. Sedimentary Geology 159, 81-94.

Dowd M, Meyer R (2003) A Bayesian approach to the ecosystem inverse problem. Ecological Modelling 168, 39-55.

FultonCJ, Depczynski M, Holmes TH, Noble MM, Radford B, Wernberg T, Wilson SK (2014) Sea temperature shapes seasonal fluctuations in seaweed biomass within the Ningaloo coral reef ecosystem. Limnology and Oceanography 59, 156–166.

Fung T, Seymour RM, Johnson CR (2011) Alternative stable states and phase shifts in coral reefs under anthropogenic stress. Ecology 92, 967–982.

Gurney GG, Melbourne-Thomas J, Geronimo RC, Aliño PM, Johnson CR (2013) Modelling Coral Reef Futures to Inform Management: Can Reducing Local-Scale Stressors Conserve Reefs under Climate Change? PLoS ONE 8, e80137.

Holmes G, Johnstone RW (2010) Modelling coral reef ecosystems with limited observational data. Ecological Modelling 221, 1173-1183.

Meadows DH (2008) Thinking in systems: A primer. Chelsea green publishing.

Melbourne-Thomas J, Johnson CR, Fung T, Seymour RM, Chérubin LM, Arias-González JE, Fulton EA (2011) Regional-scale scenario modeling for coral reefs: a decision support tool to inform management of a complex system. Ecological Applications 21, 1380–1398.

Mumby PJ (2006) The impact of exploiting grazers (Scaridae) on the dynamics of Caribbean coral reefs. Ecological Applications 16, 747–769.

Mumby PJ (2009) Phase shifts and the stability of macroalgal communities on Caribbean coral reefs. Coral Reefs 28, 761-773.

Mumby PJ, Steneck RS, Hastings A (2013) Evidence for and against the existence of alternate attractors on coral reefs. Oikos 122, 481–491.

Parslow J, Cressie N, Campbell EP, Jones E, Murray L (2013) Bayesian learning and predictability in a stochastic nonlinear dynamical model. Ecological Applications 23, 679-698.

Sterman JD (2008) Risk Communication on Climate: Mental Models and Mass Balance. Science 322, 532-533.

Thomson D, Babcock RC, Haywood M, Pillans RD, Vanderklift MA, Boschetti F (2017) Evidence of long term declines in Acropora and Turbinaria corals and a shift toward more generalist life-history traits at northern Ningaloo Reef, Western Australia. In Preparation

van de Leemput IA, Hughes TP, van Nes EH, Scheffer M (2016) Multiple feedbacks and the prevalence of alternate stable states on coral reefs. Coral Reefs 35, 857-865.

Vanderklift MA, Babcock RC, Boschetti F, Haywood MDE, Pillans RD, Richards S, Thomson D (2007) Declining abundance of coral reef fish in a world-heritage listed marine park. In Preparation

Wilkinson DJ (2011) 'Stochastic modelling for systems biology.' (CRC press:

6.8.7 APPENDICES

Appendix 1. Model description

$$C = \left(\frac{\left(l_C^{ex} + l_C^{en} C \right) \left(\left(e^{M_{slope}(M - M_{Centre})} + 1 \right)^{-1} \left(e^{T_{slope}(T - T_{Centre})} + 1 \right)^{-1} \right)}{C} + r_C \left(1 - \frac{C}{K_C f(\alpha_{T \to C} T) f(\alpha_{M \to C} M)} \right) \right) C - d_C C$$ **Coral recruitment on turf and macroalgae +growth and competition with T and M for recruitment** ⎵ **competition with T and M for growth and space** ⎵	Eq 1
$$T' = r_T \left(1 - \frac{T}{K_T f(\alpha_{C \to T} C) f(\alpha_{M \to T} M)} \right) T - Grazing^{T \to G} - d_T T$$	Eq 2
$$M' = \left(r_M f(\alpha_{C \to M} C) f(\alpha_{T \to M} T) \right) \left(1 - \frac{M}{K_M} \right) M - Grazing^{M \to B} - d_M M$$ **competition with T and C for growth** ⎵	Eq 3
$$B' = \delta_B \left(l_B^{ex} + l_B^{en} B \right) + \mu_B Grazing^{M \to B} - Eat^{B \to P} - d_B B$$	Eq 4
$$G' = \delta_G \left(l_G^{ex} + l_G^{en} G \right) + \mu_G Grazing^{T \to G} - Eat^{G \to P} - d_G G$$	Eq 5
$$P' = P + \delta_P \left(l_P^{ex} + l_P^{en} P \right) + \mu_P Eat^{B \to P} + \mu_P Eat^{G \to P} - d_P P$$	Eq 6

Availabilities	Predation/Grazing	Predators' growth
$T^{avail} = T \dfrac{T}{T^{safe} + T}$	$Grazing^{T \to G} = \min(T^{avail}, GG_{max}^{meal})$	$Growth^G = (1 - \dfrac{GG_{min}^{meal}}{T^{avail}})$
$M^{avail} = M \dfrac{M}{M^{safe} + M}$	$Grazing^{M \to B} = \min(M^{avail}, BB_{max}^{meal})$	$Growth^B = (1 - \dfrac{BB_{min}^{meal}}{M^{avail}})$
$B^{avail} = B \dfrac{B}{B^{safe} + B}$	$Eat^P = \min(B^{avail} + G^{avail}, PP_{max}^{meal})$	$Growth^P = (1 - \dfrac{PP_{min}^{meal}}{B^{avail} + G^{avail}})$
$G^{avail} = G \dfrac{G}{G^{safe} + G}$	$Eat^{B \to P} = Eat^P \dfrac{B^{avail}}{B^{avail} + G^{avail}}$	
	$Eat^{G \to P} = Eat^P \dfrac{G^{avail}}{B^{avail} + G^{avail}}$	

Appendix 2. Model parameters

Parameter	Definition
Parameters related to the Lotka Volterra Model	
r_i	The intrinsic growth rate of the population i.
K_i	The carrying capacity of the reef for the population i.
$\alpha_{j \to i}$	The competition coefficient of the population j over the population i. It measures the fractional reduction in the per capita growth rate of the population i produced by a small increase in the density of the population j (Holt, 1985).
Parameters related to the recruitment of new individuals	
l_i^{ex}	The rate of exogenous recruitment for the population i.
l_i^{end}	The rate of endogenous recruitment for the population i.
Parameters related to predation	
g_{ji}	The maximum predation rate of the population j on the population i.
μ_i	The proportion of consumed biomass which is used for somatic growth for the population i.
i_{ji}	A parameter that measures the inaccessibility of the population i to predation by the population j.
Other parameters related to mortality	
d_i	The residual mortality for the population i which is not due to anything explicitly modelled.

Parameter	Derived value(s)	Reference
r_C	[1.07 − 1.33] yr^{-1}	Expert assessment
r_M	[1.2 − 4.6] yr^{-1}	(Fulton et al. 2014)
r_T	[1333 − 2000] yr^{-1}	Expert assessment
K_C	[600 − 1000] g.m^{-2}	Expert assessment
K_M	[2000 − 3000] g.m^{-2}	Expert assessment
K_T	[100-150] g.m^{-2}	Expert assessment
$\alpha_{C \to M}$	[0.2 − 0.3]	(Mumby 2006)
$\alpha_{C \to T}$	[0.3 − 0.7]	Expert assessment
$\alpha_{M \to C}$	[0.25 − 0.75]	Expert assessment
$\alpha_{M \to T}$	[0.3 − 0.7]	Expert assessment
$\alpha_{T \to C}$	0	(Mumby 2006)
$\alpha_{T \to M}$	0	Expert assessment
l_C^{ex}	[0 − 1×10^{-5}] g.m^{-2}.yr^{-1}	Corset Model
l_B^{ex}	[1.30 − 8.54] g.m^{-2}.yr^{-1}	Corset model
l_G^{ex}	[1.30 − 8.54] g.m^{-2}.yr^{-1}	Corset model
l_P^{ex}	[0.14 − 5.07] g.m^{-2}.yr^{-1}	Corset model
l_U^{ex}		
l_C^{en}	[0.0009 − 0.41] yr^{-1}	Corset model
l_B^{en}	[0 − 0.3] yr^{-1}	Corset model
l_G^{en}	[0 − 0.3] yr^{-1}	Corset model
l_P^{en}	[0 − 0.1] yr^{-1}	Corset model
g_{BM}	[0.01 g_{GT} − g_{GT}] yr^{-1}	Corset model
g_{GT}	[5 − 15] yr^{-1}	Corset model
g_{PB}	[0 − 1] yr^{-1}	Ningaloo EwE model
g_{PG}	[0 − 3] yr^{-1}	Ningaloo EwE model
μ_B	[0.040 − 0.11]	Ningaloo EwE model
μ_G	[0.085 - 0.125]	Ningaloo EwE model
μ_P	[0.19 - 0.30]	Ningaloo EwE model
d_B	0-1	Expert assessment

d_C	0-1	Expert assessment
d_G	0-1	Expert assessment
d_M	0-1	Expert assessment
d_P	0	Expert assessment
d_T	0	Expert assessment

Data source	
	Expert assessment based on local knowledge
	Data approximated from the Ningaloo EwE model
	Data from Corset Model
	Data from the literature

7. Corals past and future

7.1 Differential response of corals to regional mass-warming events as evident from skeletal Sr/Ca and Mg/Ca ratios

Authors: Clarke H, D'Olivo JP, Flater J, Zinke J, Lowe R, McCulloch M.

ABSTRACT

During the summer of 2010/11, a regional marine heat wave resulted in coral bleaching of variable severity along much of the western coastline of Australia. At Ningaloo Reef, a 300km long fringing reef system and World Heritage site, highly contrasting coral bleaching was observed between two morphologically distinct nearshore reef communities located on either side of the Ningaloo Peninsula: Tantabiddi (~20% bleaching) and Bundegi (~90% bleaching). For this study, we collected coral cores (Porites sp.) from Tantabiddi and Bundegi reef sites to assess the response of the Sr/Ca temperature proxy and Mg/Ca ratios to the variable levels of thermal stress imposed at these two sites during the 2010/11 warming event. We found that there was an anomalous increase in Sr/Ca and decrease in Mg/Ca ratios in the Bundegi record that was coincident with the timing of severe coral bleaching at the site, while no significant changes were observed in the Tantabiddi record. We show that the change in the relationship of Sr/Ca and Mg/Ca ratios with temperature at Bundegi during the 2010/11 event reflects changes in related coral 'vital' processes during periods of environmental stress. These changes were found to be consistent with a reduction in active transport of Ca^{2+} to the site of calcification leading to a reduction in calcification rates and reduced Rayleigh fractionation of incorporated trace elements.

7.1.1 INTRODUCTION

Coral reefs are undergoing rapid decline worldwide (Hoegh-Guldberg 1999; Hughes et al. 2003; Pandolfi et al. 2003). This decline has been attributed largely to an increase in the frequency and severity of widespread coral bleaching events as a result of the increased occurrence of acute, regional ocean warming events (Veron et al. 2009; Hoegh-Guldberg 1999; Feng et al. 2013). These large-scale marine heat waves are often driven by regionally specific and transient climate phenomena superimposed on longer-term trends in global warming. For example, the El Niño Southern Oscillation (ENSO) has been shown to drive periodic (around 3-7yr) warm sea surface temperature (SST) anomalies of up to several degrees across the Indo-Pacific, Caribbean, and Red Sea (Rasmussen and Carpenter 1982; Wilkinson et al. 1999), which, in turn, have caused mass coral bleaching events across the globe. In Australia, the most noteworthy coral bleaching events occurred during the summers of 1998 and 2002 (Hoegh-Guldberg 1999; Bruno et al. 2001; Veron et al. 2009; Oliver et al. 2009) as well as 2011 (Moore et al. 2012) and most recently during the summer of 2016 (e.g. Hoegh-Guldberg and Ridgway 2016; Normile 2016)

However, at smaller scales (100s m's to several km's), spatial patterns of coral bleaching resulting from regional warming events can vary considerably within individual reef ecosystems (e.g. Berkelmans et al. 2004; Moore et al. 2012). Corals have shown the ability to acclimatise to a wide range of local temperature regimes (Brown 1997; Guest et al. 2012; Schoepf et al. 2015). As such, coral bleaching thresholds can vary considerably for specific coral taxa between different reef environments (Jokiel and Coles 1990; Fitt et al. 2001; Howells et al. 2012). In addition, differences in reef environment can also affect the magnitude of reef-scale SST anomalies and hence, coral bleaching responses during regional ocean-warming events (e.g. Depczynski et al. 2013; Falter et al. 2014). For instance, small-scale differences in the circulation and residence times of reef waters combined with variations in local atmospheric heating can drive strong spatial variations in SST anomalies across reef systems (e.g. Davis et al. 2011; Zhang et al. 2013; Li and Reidenbach 2014), which can also cause similar variations in coral bleaching responses (Berkelmans et al. 2004; McClanahan et al. 2007; Pineda et al. 2013).

Coral bleaching thresholds are typically calculated as one degree above the highest long-term (~7 year) average monthly SST (often referred to as the Maximum of the Monthly Mean (MMM) SST climatology) for any given reef environment (Liu et al. 2003; Liu et al. 2006; Skirving et al. 2006). However, resolving small-scale variations in SST climatologies as well as variations in the magnitude of SST anomalies during regional warming episodes can sometimes be difficult using conventional SST products (i.e. satellite records and instrumental SST loggers) due to their spatial and temporal limitations. For example, although satellite temperature products have become invaluable for monitoring the development of ocean-basin and regional-scale SST anomalies (e.g. Feng et al. 2013; Liu et al. 2003), they often cannot resolve small-scale SST variability within reef systems due to their limited spatial resolution (typically >5 km). Similarly, instrumental temperature loggers require both the foresight and logistic support to provide the necessary spatial and temporal coverage in *in situ* data, which can be particularly problematic when working in remote areas. Where such limitations are encountered, paleoclimate proxy records from coral cores offer an alternate method to assess fine scale differences in SST climatologies between reef environments (e.g. Alibert et al. 1997; Marshall and McCulloch 2002; Fallon et al. 2003) as well as local variations in stress and bleaching responses of reef habitats following anomalous ocean warming episodes (Thompson and Woesik 2009; D'Olivo et al. 2013; Cantin and Lough 2014).

To date, the geochemical analysis of environmental proxies (e.g. Sr/Ca, Mg/Ca, U/Ca, $\delta^{18}O$) from coral cores is a commonly used approach for generating long term, high-resolution (bi-weekly to annual) records of tropical seawater temperatures and other environmental parameters for the period prior to when instrumental and remotely sensed data became available (i.e. before the

1980's) (Gagan et al. 2000; Eakin et al. 2009). As such, coral geochemical proxy records have become an invaluable tool for assessing long-term ocean warming trends; providing unequivocal evidence of global climate change related to the burning of fossil fuels since the onset of the industrial revolution (around mid-1700's; Gagan et al. 2000; Grottoli and Eakin 2007). Furthermore, the distinct annual density banding pattern observed in massive Porites sp. skeletons permits the measurement of skeletal growth parameters from coral cores (i.e. extension and calcification (Lough and Barnes 1997; Lough 2008; D'Olivo et al. 2013)). This, in turn provides a quantitative method by which to directly assess the impacts of acute warming events (Cantin and Lough 2014; Hetzinger et al. 2016) as well as the longer-term impacts of gradual changes in reef environmental conditions on coral growth (Cantin et al. 2010; Cooper et al. 2012; D'Olivo et al. 2013).

While the incorporation of trace elements (Sr, Mg, U etc.) in the aragonite crystals ($CaCO_3$) of coral skeletons have been shown to be related to a variety of environmental parameters such as ambient seawater temperatures (Beck et al. 1992; Fallon et al. 2003; Felis and Pätzold 2003), they are also subject to varying levels of physiologic control. This is because corals precipitate their skeleton from a calcifying fluid which is partially isolated from the ambient seawater and then physiochemically modified (Al-Horani 2003, Sinclair 2005; Trotter et al. 2011; McCulloch et al. 2012); thereby potentially influencing how trace elements are incorporated in the coral skeleton (i.e. via so-called 'vital effects' (Sinclair 2005; Gaetani and Cohen 2006; Allison and Finch 2007)). Although the exact mechanisms responsible for observed coral 'vital effects' are not yet fully understood, their influence on skeletal trace element-calcium ratios (Te/Ca) is clear. For example, Sr/Ca ratios in coral skeletons are systematically lower (~10%) than that of inorganic aragonite precipitated from an infinite reservoir of seawater (Kinsman and Holland 1969; Cohen and Gaetani 2010). Similarly, the observed relationship between Mg/Ca and temperature for coral skeletons is the opposite of that expected for experimentally precipitated abiotic aragonite (Cohen and Gaetani 2010).

Current knowledge about the role of coral 'vital effects' have been largely limited to inferences based on comparisons between the geochemical composition of aragonite in coral skeletons collected in situ and laboratory inorganic experiments abiotically precipitating aragonite under known physicochemical conditions (e.g. Sinclair 2005; Cohen and Gaetani 2010). Consequently, the significance of 'vital effects' on long-term geochemical proxy records is poorly understood. For example, the slope and intercept of regressions of Sr/Ca and Mg/Ca-versus temperature can vary significantly between different corals of the same species (Corrège 2006), which may either reflect physiological differences between coral colonies or differences in their local habitat. Geochemical anomalies observed in monthly- to seasonal-resolution coral core records that correspond with the timing of past coral bleaching events (e.g. Marshall and McCulloch 2002; Hetzinger et al. 2016) allude to the importance of vital effects to modulate the climate signal preserved in proxy records; however, they have yet to be studied in detail. Thus, the transient effects of environmental perturbations such as ocean warming events on coral core geochemical records are potentially useful for understanding the mechanisms responsible for coral 'vital effects' and the impact of elevated thermal stress on coral physiological and calcification processes.

In this study, we report records of Sr/Ca and Mg/Ca at monthly resolution from coral cores collected from Tantabiddi and Bundegi reef sites at Ningaloo Reef, each located ~20 km apart in the northwest region of Western Australia. Despite their relatively close proximity, these reef sites experienced highly contrasting severities of coral bleaching (around 20% of colonies at Tantabiddi versus 90% at Bundegi (Moore et al. 2012; Depczynski et al. 2013)) during an unprecedented regional ocean-warming event, associated with strong La Nina conditions during the austral summer of 2010/11 (Feng et al. 2013). We compare the response of the Sr/Ca and Mg/Ca proxies, and coral growth rates during the summer of 2010/11 at the two sites. We assess the veracity with which geochemical records can act as short-term recorders of extreme temperatures and the response of coral Te/Ca temperature calibrations to assess thermal stress of coral colonies. We then discuss the potential

role of the coral Ca^{2+}ATPase enzyme and kinetic processes to explain the anomalous Sr/Ca and Mg/Ca ratios observed during the thermal stress event of 2010/11.

7.1.2 METHODS

Study Sites

Tantabiddi reef is located on the offshore side of the Ningaloo Peninsula (Figure 7.1.1) and forms part of the nearshore lagoon complex of the larger Ningaloo fringing reef system (Wyrwoll et al. 1993). Significant swells (heights >1 m) impact the outer reef edge at Ningaloo for much of the year (Collins et al. 2003), which drives wave-driven circulation patterns that lead to rapid water exchange and ventilation of the inner lagoon at Tantabiddi with waters from offshore (Taebi et al. 2011).

Conversely, Bundegi Reef is situated on the protected north-eastern coastline of the Ningaloo Peninsula within the Exmouth Gulf (Figure 7.1.1); a shallow (mean depth 12 m), inverse estuarine embayment (Brunskill et al. 2001). Bundegi Reef is protected from offshore wave energy and as such, circulation at the reef is predominantly driven by tides (Massel et al. 1997). However, locally generated wind-waves within the Exmouth Gulf probably also influence nearshore circulation at Bundegi to a lesser degree, although this has yet to be quantified at the site.
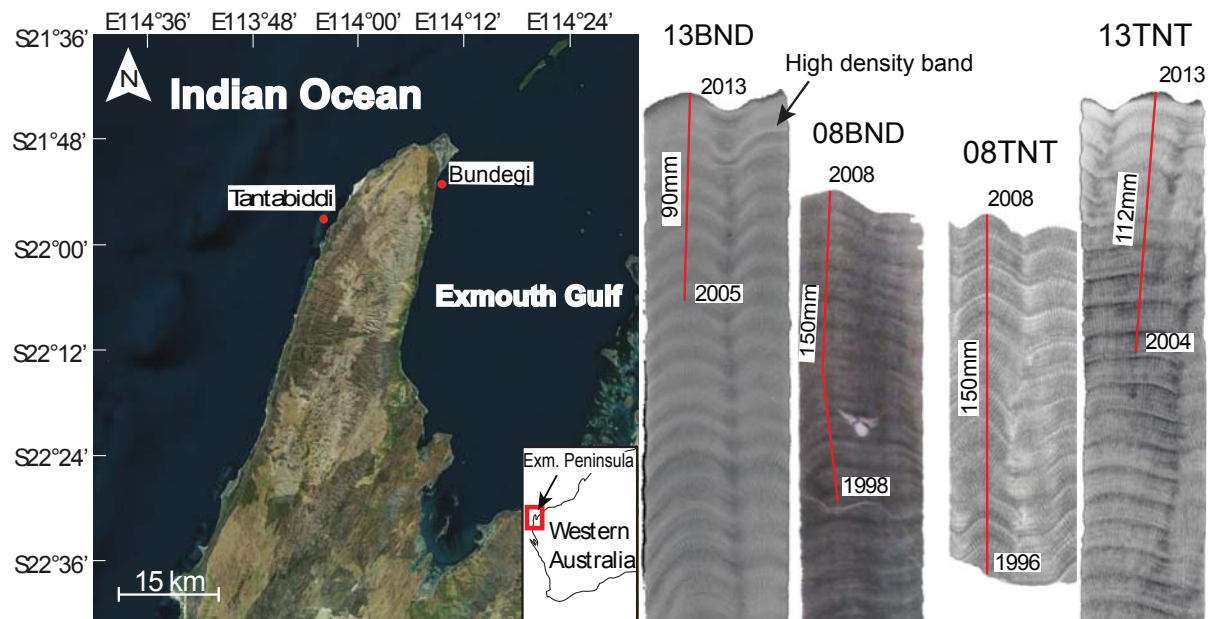
Figure 7.1.1 Location of Tantabiddi and Bundegi coral sites in the northern region of Ningaloo Reef (left) and core slab X-rays (right). Coral cores were collected from massive *Porites* sp. colonies from the two sites in 2008 (08BND and 08TNT) and again in 2013 (13BND and 13TNT). The red lines indicate sampling transects for Sr/Ca and Mg/Ca analysis and approximate start and end dates for the core records (years) are provided alongside.

Coral sample collection and preparation

During August of 2008, the Australian Institute of Marine Science (AIMS) recovered coral cores from massive Porites sp. corals located in shallow waters (within 200-300 m of their respective shorelines) at Tantabiddi (5 m, 21° 54' 35'' S, 113° 58' 12'' E) and Bundegi (3.5 m, 21° 52' 11'' S, 114° 09' 23'' E)

reef sites at Ningaloo (Figure 7.1.1). The University of Western Australia recovered additional coral cores from the same coral colonies in August 2013 several years after the 2010/11 bleaching event. All coral cores were sliced along to their main growth axes into rectangular slabs approximately 6 mm thick and soaked in a sodium hypochlorite solution to remove residual organic matter. The slabs were then rinsed repeatedly with de-ionised water in an ultrasonic bath and dried at 45 °C in an oven for 24 hours.

Annual density band couplets (evident as alternating light and dark coloured bands from x-ray images of coral slices) (Figure 7.1.1) were used to make preliminary determinations of core chronology and growth axis orientation (see Lough and Cooper 2011). Coral slices were sampled continuously along major growth axes using a Zenbot ® Precision Mill equipped with a ~3 mm diameter drill bit. Sample powders were collected at millimetre increments (~monthly resolution) along major growth axis (sampling tracts shown in Figure 7.1.1). A temporal overlap (2-4 years) between the new (2013) and old (2008) samples was ensured to check the agreement between trace element ratios measured between the pairs of cores from the two sites. One hundred and fifty samples were collected from each of the Tantabiddi and Bundegi cores collected in 2008 (hereafter referred to as 08TNT and 08BND cores) covering growth periods of 1996-2008 and 1998-2008, respectively. For the coral cores collected in 2013 (hereafter referred to as 13TNT and 13BND), one hundred and twelve samples were collected from the 13TNT core, covering the 2004-2013 period and seventy five were collected from the 13BND core, which covered the 2006-2013 period.

Sample powders were weighed to 5 ± 0.25 mg for cores obtained in 2008 and to 10 ± 0.25 mg for cores obtained in 2013. Samples were then dissolved in nitric acid and diluted through two stages to produce 100 ppm and 10 ppm Ca^{2+} solutions for trace element analysis (Holcomb et al. 2015). Sr/Ca and Mg/Ca was analysed from the 10 ppm Ca^{2+} solutions using a Thermo Fisher Scientific (Bremen, Germany) X Series II quadrupole inductively coupled plasma mass spectrometer using the standard Xt interface and plasma screen fitted at the University of Western Australia AGFIOR laboratory. Long-term reproducibility (RSD, 2 sigma) was derived from the repeated analyses of a gravimetrically prepared standard and yielded up to 0.3% for Sr/Ca and Mg/Ca for the analysis of the cores collected in 2008 (n = 300) and up to 0.2% and 0.3% for the Sr/Ca and Mg/Ca analysis of the cores collected in 2013 (n = 187).

Tantabiddi and Bundegi *in situ* and remote SST data

Approximately 18 months of in-continuous *in situ* temperature data was collected from the Tantabiddi coral site between January 2012 and April 2014. The *in situ* temperature data was used to validate a separate, remotely-sensed (OISST) sea surface temperature (SST) record for the calibration of the Tantabiddi Sr/Ca and Mg/Ca core records. The average of two, long-term (1996-2013), monthly resolution OISST (50 km^2) records (within coordinates: 113.5° E, 21.5° S and 113.5° E, 22.5 °S) was taken to give the closest SST record to the Tantabiddi site (OISST v2, http://apdrc.soest.hawaii.edu/las/v6/dataset) which showed good agreement with the *in situ* data within the range of 'normal' temperatures (~22-30 °C) for the reef site (SST = 1.078×$T_{in\ situ}$ – 2.0, R^2 = 0.93).

For the Bundegi site, we collected approximately two years (January 2012 to March 2014) of near continuous *in situ* temperature data. This in situ data was combined with a prior 12 month record of *in situ* temperature previously reported in Depczynski et al. (2012) to generate a three year, continuous, record of monthly average *in situ* (nearshore) SST for the period Feb 2011 to March 2014. To extend the temperature record for Bundegi further back in time, the *in situ* data was used to adjust a longer-term OISST record (1998-2013), which provided complete temporal overlap with the two core records. We took the average of two OISST datasets generated for the coordinates: 114.5° E and 21.5° S and 114.5° E and 22.5° S, which gave the closest possible, long-term SST record

for the Bundegi coral site (i.e. at 114.5° E, 22° S). For the period of overlap between the Bundegi *in situ* and OISST records, maximum annual SSTs were in good agreement (average of 29.3 °C during February for OISST versus 29.4 °C during February for *in situ* record); however, strong differences were observed between the records during winter months where the *in situ* temperature record showed an average annual SST minimum of 21 °C occurring during July compared to 23.2 °C during August for the OISST record. We thus adjusted the OISST record by subtracting the average monthly difference in SST between the OISST and *in situ* records from the long-term OISST record to generate a pseudo-nearshore temperature record for Bundegi reef for the period from 1998-2013 (hereafter referred to as the nearshore SST record).

Sr/Ca and Mg/Ca age model determination

Age models for the Tantabiddi and Bundegi Sr/Ca and Mg/Ca datasets were determined by aligning the seasonal minima and maxima in the Sr/Ca records with maxima and minima in the respective SST records for the two sites using Analyseries software (Paillard et al. 1996). To further refine the seasonality of the coral core age models, additional 'anchor points' were added between matching sections of the Sr/Ca and temperature records (Alibert and McCulloch 1997) until the strongest correlation coefficients were obtained. Trace-element data from the top ~1 cm of both the 13TNT and 13BND core records (June 2012 to April 2013) were omitted from the final datasets to exclude the possibility of contamination from the presence of organic material (e.g. Alibert and McCulloch 1997; Marshall and McCulloch 2002). Lastly, the Sr/Ca and Mg/Ca datasets were interpolated to monthly resolution, using Analyseries, to produce two continuous monthly Sr/Ca records for each of the 08TNT and 08BND core records that covered the periods April 1996 to July 2008 (08TNT) and April 1998 to October 2008 (08BND) and two Sr/Ca and Mg/Ca records for the 13TNT and 13BND records that covered the periods March 2004 to May 2012 (13TNT) and October 2005 to May 2012 (13BND).

Calibration of the Sr/Ca temperature proxy and Mg/Ca relationships

Bulk Sr/Ca and Mg/Ca-SST correlations were calculated for each of the Sr/Ca and Mg/Ca datasets from Tantabiddi and Bundegi. For the 13BND record, anomalous Sr/Ca and Mg/Ca data observed from November 2010 to April 2011 were excluded from the calculation of the bulk 13BND Sr/Ca-SST and Mg/Ca-SST correlations. The linear regression equations of the bulk correlations were used to separately calibrate each of the Sr/Ca and Mg/Ca records with temperature from Tantabiddi and Bundegi to produce two long-term Sr/Ca-SST reconstructions and one long-term Mg/Ca-SST reconstruction for each site. Monthly temperature residuals (Sr/Ca-SST minus instrumental SST and Mg/Ca-SST minus instrumental SST) were calculated for each of these long-term temperature reconstructions to highlight periods where changes in the Sr/Ca-SST and Mg/Ca-SST relationships occurred.

To analyse the effects of thermal stress on the Sr/Ca and Mg/Ca temperature proxies, for the 2013 core records from Tantabiddi and Bundegi, we calculated short-term (6 months) Sr/Ca and Mg/Ca-SST correlations that corresponded with the timing of the 2010/11 Ningaloo Niño event and severe coral bleaching at Bundegi (i.e. from November 2010 to April 2011). For the 13BND record, we also calculated additional short-term Sr/Ca and Mg/Ca-SST correlation for the 12 months following the suspected bleaching of the coral (i.e. from May 2011 to May 2012), to see if and how the function of the two proxies changed once temperatures at the coral site returned below bleaching thresholds.

Linear extension rates

Annual rates of linear extension were calculated from the monthly-interpolated Sr/Ca records by measuring the distance between Sr/Ca maxima (i.e. temperature minima) in each record. For the

period of overlap for the 08BND and 13BND core records (July 2006 to June 2007 and July 2007 to June 2008), the 13BND record showed reduced (slower) linear extension rates compared to the 08BND record (i.e. -2.27 and -3.42 mm yr-1, respectively), presumably reflecting the effects of sampling different growth axes. We therefore proportionally adjusted all linear extension rates measured in the13BND record by a factor of 1.29 to account for the observed differences in average linear extension rates during the overlap period. It was not necessary to make any such adjustment for the two Tantabiddi core records.

7.1.3 RESULTS

Skeletal trace element abundances at Tantabiddi

The 08TNT and 13TNT Sr/Ca records were generally in good agreement with the offshore SST record (r^2 = 0.94 and 0.87, respectively; Figure 7.1.2a, Table 7.1.1). Both the slope and y-intercept terms of the linear regressions for the 08TNT and 13TNT bulk Sr/Ca-SST data indicated the two bulk calibrations were not statistically different from one another (p > 0.05, Figure 7.1.2a, Table 7.1.1). Root mean squared errors (RMSE) for the individual monthly Sr/Ca-SST estimates for the two records were 0.5 °C and 0.8 °C for the 08TNT and 13TNT records respectively. Both Sr/Ca records showed strong inter-annual and inter-decadal variability in the magnitude of their respective seasonal maxima and minima (equivalent to ~3 °C) over the 1996-2013 period; results consistent with the seasonal warming and cooling trends displayed in the instrumental SST record (Figure 7.1.3a). For the 13TNT Sr/Ca record, Sr/Ca-SST estimates from the bulk calibration showed a cool bias of -0.5 °C on average compared to the offshore SST record for the period from April-2004 to June-2008 (-0.53 ± 0.49 °C, average ±1 S.E. p < 0.01, n = 51, Figure 7.1.3b). This was followed by a warm bias in Sr/Ca-SST estimates from the bulk calibration of +0.6 °C on average from July 2008 to May 2012 (0.58 ± 0.51, average ±1 S.E. p < 0.01, n = 47). For the bulk 13TNT Mg/Ca-SST calibration, temperature estimates were largely consistent across the entire record and showed good general agreement with OISST record (RMSE = 0.7 °C, R^2 = 0.87; Figure 7.1.2b, Figure 7.1.3a). During the summer of 2010/11 (when mass coral bleaching occurred at Bundegi), no anomalous Sr/Ca or Mg/Ca values were observed in the 13TNT record (see red markers, Figure 7.1.2a, b). From November 2010 to April 2011, Sr/Ca and Mg/Ca temperatures derived from the bulk calibrations were within 1°C of the remote SST record (see red markers, Figure 7.1.3a), suggesting no short-term changes to the temperature relationship of either proxy occurred.

For the subdivided 13TNT record, a significant decline in the slope of the Sr/Ca-SST regression was observed for the period from July 2008 to May 2012 compared to the period from April 2004 to June 2008 (i.e. -0.12, p < 0.05, Figure 7.1.2a, Table 7.1.1). The change in the coral Sr/Ca-SST sensitivity recorded between these two periods corresponded with a change in the direction of the coral growth axis evident around the year 2008 in the core x-ray (Figure 7.1.1). Conversely, no significant changes in Mg/Ca-SST relationships were observed between these same periods in the 13TNT Mg/Ca record (p>0.05) (Figure 7.1.2b, Table 7.1.1). For the short-term Sr/Ca-SST and Mg/Ca-SST linear regressions calculated for the period in the 13TNT record from November 2010 to April 2011, no significant changes were observed compared to the bulk calibrations (p>0.05) (Figure 7.1.2a, b, Table 7.1.1). Similarly, no change in the linear regression of the Sr/Ca vs Mg/Ca correlation was observed across this period compared to the bulk 13TNT Sr/Ca vs Mg/Ca correlation (p>0.05) (Figure 7.1.4)
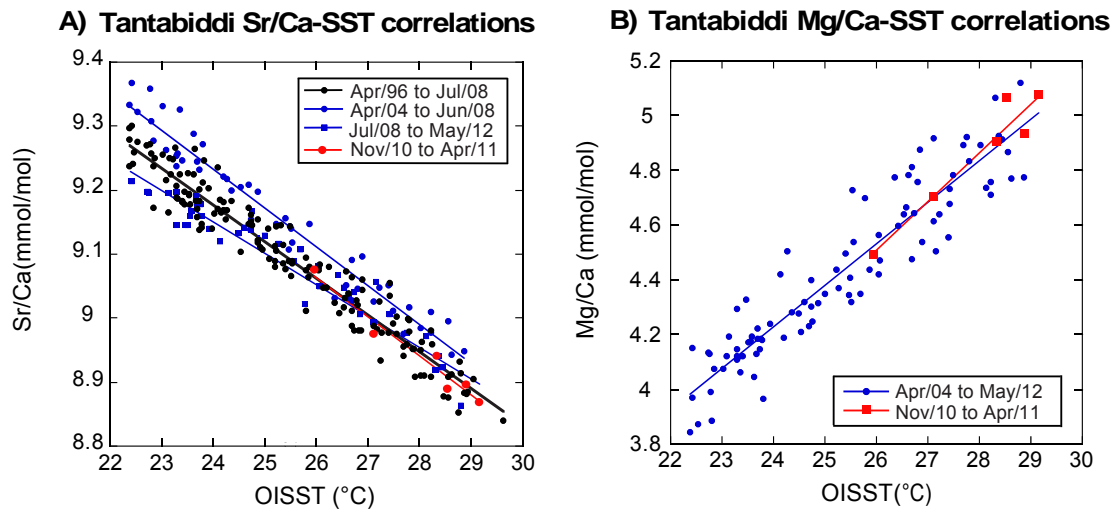
Figure 7.1.2 A) Sr/Ca-SST correlations for the two Tantabiddi (08TNT and 13TNT) coral core records; and **B)** Mg/Ca-SST correlations calculated for the 13TNT coral core record (linear regression equation coefficients are shown in Table 7.1.1). For the subdivided 13TNT Sr/Ca and Mg/Ca records, no significant change in the linear regressions of the Sr/Ca-SST and Mg/Ca-SST correlations was observed from November 2010 to April 2011 as indicated by the red circles (A) and the red squares (B); thus, suggesting thermal stress did not have a significant impact on coral 'vital effects' during the 2010/11 warming event

Table 7.1.1 Slope (m) and y-intercept (b) terms for the Sr/Ca-SST and Mg/Ca-SST linear regressions equations calculated for the two Tantabiddi core records (08TNT and 13TNT). The bulk Sr/Ca-SST and Mg/ Ca-SST linear regression equations were used to calibrate the coral temperature records shown in Figure 7.1.3a and included all Sr/Ca and Mg/Ca data up to May 2012. For the subdivided 13TNT record, the periods listed above correspond to the linear regressions shown in Figure 7.1.2 (except coefficients for Mg/Ca-SST equations indicated by * which are not shown in Figure 7.1.2b).

		BULK TNT CALIBRATIONS							
PERIOD		**SR/CA**				**MG/CA**			
	n	**m**	**b**	**r^2**	**p**	**m**	**b**	**r^2**	**p**
08TNT Apr/1996 to Jul/2008	148	-0.057 (±0.002)	10.552 (±0.061)	0.94	<0.001				
13TNT Apr/2004 to May/2012	98	-0.056 (±0.004)	10.549 (±0.104)	0.87	<0.001	0.152 (±0.011)	0.587 (±0.288)	0.88	<0.001
Subdivided 13TNT core record calibrations									
Apr/2004 to Jun/2008	51	-0.061 (±0.004)	10.692 (±0.099)	0.95	<0.001	*0.150 (±0.016)	*0.591 (±0.399)	0.88	<0.001
July/2008 to May/2012	47	-0.049 (±0.004)	10.332 (±0.098)	0.94	<0.001	*0.150 (±0.016)	*0.670 (±0.401)	0.90	<0.001
Nov/2010 to Apr/2011	6	-0.061 (±0.019)	10.642 (±0.520)	0.95	<0.001	0.178 (±0.071)	-0.116 (±1.988)	0.92	<0.01
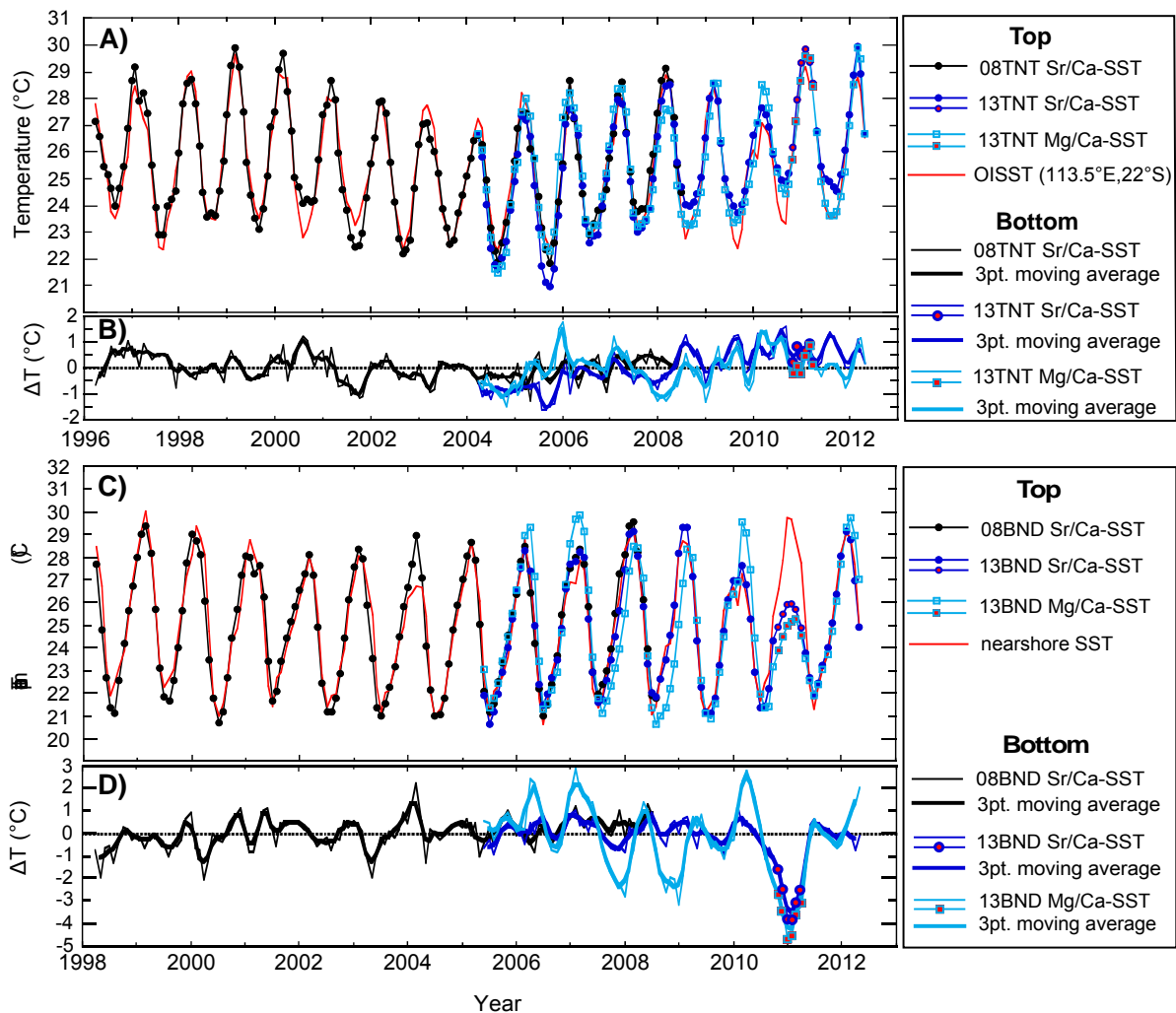
Figure 7.1.3 A, C) Sr/Ca-SST records (black circles – 08TNT and 08BND records, blue circles – 13TNT and 13BND records) and Mg/Ca-SST records (light blue squares – 13TNT and 13BND records) for the Tantabiddi (A) and Bundegi (C) coral core records. **B, D)** Monthly temperature residuals (i.e. Sr/Ca-SST and Mg/Ca-SST minus instrumental SST) for Tantabiddi (B) and Bundegi (D) Sr/Ca-SST and Mg/Ca-SST records. The Sr/Ca-SST and Mg/Ca-SST records were calibrated using the respective linear regression equations of the bulk correlations obtained for each of the core records from the two sites (see Figure 7.1.2, Figure 7.1.5, Table 7.1.1, Table 7.1.2). For the 13TNT and 13BND records, Sr/Ca-SST's and Mg/Ca-SST's recorded during the 2010/11 marine heat wave are indicated by marker points with red fill. For the 13BND record, the anomalous increase and decrease in Sr/Ca and Mg/Ca ratios recorded during the summer of 2010/11 (see red markers, Figure 7.1.5a, b) lead to Sr/Ca-SSTs and Mg/Ca-SSTs underestimating the instrumental temperature record by up to ~5 °C (D) during this period. Where no such changes in Sr/Ca and Mg/Ca ratios were observed in the Tantabiddi record, this was consistent with reports of increased coral bleaching (and hence thermal stress) at Bundegi (~90% bleaching) compared to Tantabiddi (~20% bleaching) (Moore et al. 2012).

Skeletal trace element abundances at Bundegi

Unlike the Tantabiddi records, the 13BND bulk Sr/Ca-SST calibration showed a significant reduction in Sr/Ca-SST sensitivity compared to the 08BND bulk calibration (-0.052 ± 0.003 vs. -0.058 ± 0.003 mmol/°C, p ≤ 0.05, Figure 7.1.5a, Table 7.1.2). Errors (RMSE) were 0.7°C for all Sr/Ca-SST predictions made from the 08BND time series (n = 125) and 1.0°C for the 13BND time series (n = 84); or just ~6% and ~13% of the total variance in the nearshore SST record. Compared to the Tantabiddi records, the 08BND and 13BND records on average showed increased seasonal variability of Sr/Ca maxima and minima (Figure 7.1.2a, Figure 7.1.5a). This contributed to Sr/Ca-SST minima that were ~1.5°C cooler

and maxima that were ~0.5°C warmer than the Tantabiddi records on average (Figure 7.1.3a, c). However, the Bundegi records also showed reduced inter-annual variability of Sr/Ca-SST maxima and minima (~ 2°C vs. ~3°C for Tantabiddi records) over the 1998-2013 period (Figure 7.1.3a, c).
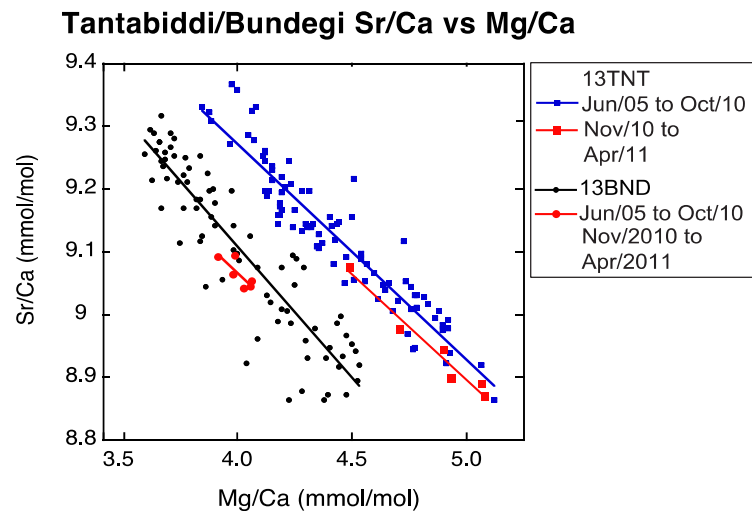
Figure 7.1.4 Sr/Ca versus Mg/Ca for the 13TNT (blue) and 13BND (black) core records. The red markers indicate values recorded during the 2010/11 marine heatwave at Ningaloo.
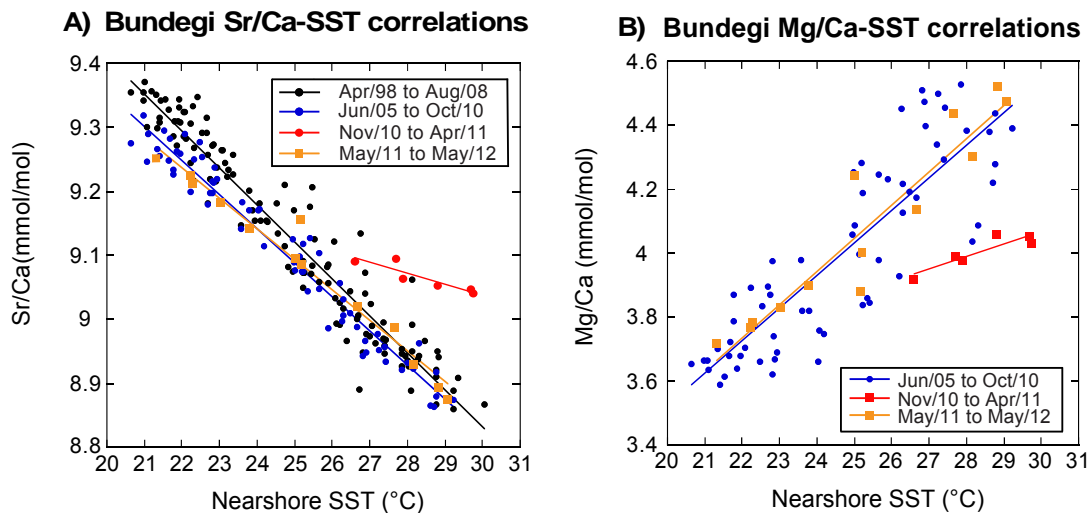
Figure 7.1.5 A) Sr/Ca-SST correlations for the two Bundegi coral core records (08BND and 13BND); and B) Mg/Ca-SST correlations calculated for the 13BND coral core record. For the subdivided 13BND Sr/Ca and Mg/Ca records, corresponding with the timing of the 2010/11 marine heat wave at Ningaloo, a strong (~70%) decline in the slope of the Sr/Ca-SST and Mg/Ca-SST regressions was observed (see red markers, Table 7.1.2) suggesting thermal stress strongly affected coral 'vital' processes, leading to changes in the incorporation of Sr and Mg in coral skeleton deposited during this period. For Sr/Ca-SST and Mg/Ca-SST regressions calculated for the 12 months following this warming event (see orange markers), both linear regressions returned to their pre-thermal stress configurations, suggesting that conditions within the calcifying fluid returned to 'normal' shortly after SSTs at the site returned below bleaching thresholds.

During the 2010/11 warming event from November 2010 to April 2011, an anomalous increase in Sr/Ca ratios (up to +2.5%) and decrease in Mg/Ca ratios (up to -10.8%) was observed in the 13BND record (see red markers, Figure 7.1.5a, b). This in turn, resulted in predicted Sr/Ca-SSTs and Mg/Ca-

SSTs from the bulk calibrations underestimating observed SSTs by up to 3.5 °C and 4.5 °C respectively during this period (see red markers, Figure 7.1.3c, d). These Sr/Ca and Mg/Ca anomalies were observed to correspond with significant short-term declines (~70%, $p < 0.05$) in the slopes of both the Sr/Ca-SST and Mg/Ca-SST regressions calculated from November 2010 to April 2011, compared to their pre-thermal stress values (i.e. from June 2005 to October 2010, Figure 7.1.5a, b, Table 7.1.2). Interestingly, no significant change in the relationship of Sr/Ca versus Mg/Ca was observed during or just after the severe warming event ($p > 0.05$, n = 6, Figure 7.1.4). Following the 2010/11 event, no significant differences in the slopes of either Sr/Ca-SST or Mg/Ca-SST linear regressions were observed between the post-thermal stress period (May 2011 to May 2012) and the pre-thermal stress period (June 2005 to October 2010, $p > 0.05$, Figure 7.1.5a, b, Table 7.1.2).

Table 7.1.2 Slope (m) and y-intercept (b) terms for the Sr/Ca-SST and Mg/Ca-SST linear regressions equations calculated for the two Bundegi core records (08BND and 13BND). The bulk Sr/Ca-SST and Mg/ Ca-SST linear regression equations were used to calibrate the coral SST records shown in Figure 7.1.3c and included all Sr/Ca and Mg/Ca data up to May 2012 except anomalous values recorded during the 2010/11 Ningaloo marine heat wave from November 2010 to April 2011. For the subdivided 13BND record, the periods listed above correspond to the linear regressions shown in Figure 7.1.5.

| | BULK BND CALIBRATIONS | | | | | | | | |
| PERIOD | | SR/CA | | | | | MG/CA | | |
	n	m	b	r^2	p	m	b	r^2	p
08BND Apr/1998 to Aug/2008	125	-0.058 (±0.003)	10.572 (±0.07)	0.93	<0.001				
13BND Jun/2005 to May/2012	78	-0.052 (±0.003)	10.4 (±0.063)	0.96	<0.001	0.102 (±0.013)	1.473 (±0.32)	0.77	<0.001
Subdivided 13BND core record calibrations									
Jun/2005 to Oct/2010	65	-0.054 (±0.003)	10.425 (±0.07)	0.96	<0.001	0.102 (±0.015)	1.485 (±0.373)	0.74	<0.001
Nov/2010 to Apr/2011	6	-0.017 (±0.011)	9.544 (±0.313)	0.82	<0.05	0.039 (±0.026)	2.908 (±0.738)	0.81	<0.05
May/2011 to May/2012	13	-0.048 (±0.006)	10.291 (±0.153)	0.97	<0.001	0.104 (±0.024)	1.452 (±0.608)	0.89	<0.001

Linear extension rates

The Tantabiddi records (08TNT and 13TNT) showed a mean linear extension rate of 11.1±1.6 mm yr^{-1} (±1 std. dev.) for the 1996-2013 period (Figure 7.1.6) with no abrupt changes in extension rate observed in either record. The Bundegi records (08BND and 13BND) showed a mean linear extension rate of 12.3 ± 2.4 mm yr^{-1} for the 1998-2013 period (after adjusting for differences in the growth rate of separate primary growth axes, see Methods and Figure 7.1.1) and 13.2 ± 1.4 mm yr^{-1} for the 12 years prior to the summer of 2010/11 (i.e. from1998 to mid-2010). However, there was a significant decrease in the rate of linear extension (7.5 mm yr^{-1}) observed in the 13BND record over the 12-month period following the warming event of 2010/11. This abrupt decline in the linear extension rate was accompanied by a thin, high-density band, typically indicative of environmental stress (Lough and Cooper, 2011) that was evident in the x-ray image of the core (Figure 7.1.1). For the two years following the 2010/11 thermal stress event, annual rates of linear extension in the Bundegi

coral averaged just 9.0 ± 0.9 mm yr^{-1} between July 2011-and June 2013; i.e. the coral was growing at a significantly slower rate (~30%) than before the warming event (Welch's T-test, $p < 0.05$).
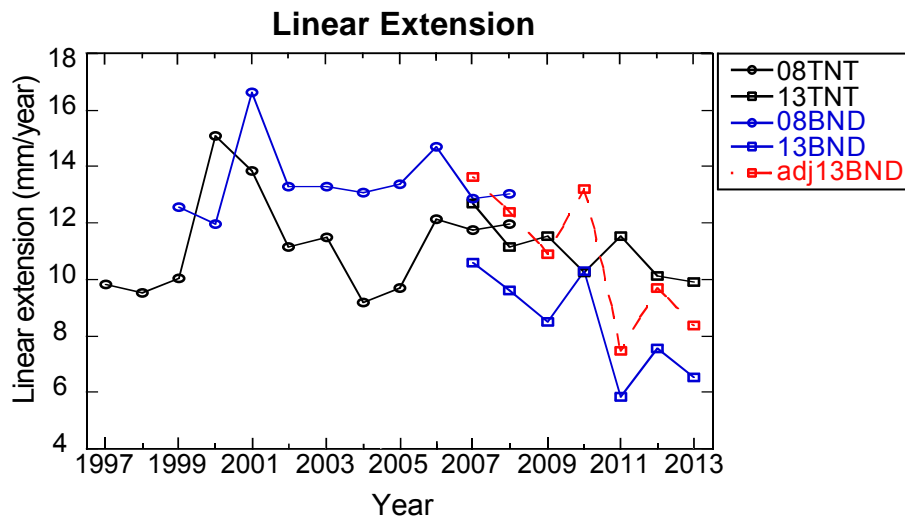
Figure 7.1.6 Linear extension calculated for the 08TNT (black circles), 08BND (blue circles), 13TNT (black squares) and 13BND Sr/Ca data (blue squares). Linear extension was measured for the 12 months from July to June of each year (i.e. centred on January) by measuring the distance between Sr/Ca maxima's (SST minima's) for each of the core records. For the overlapping section of the 08BND and 13BND cores, the later 13BND showed reduced extension rates (by a factor of 1.3 on average). Thus, to enable comparisons of extension rates between the two Bundegi cores, we generated an adjusted 13BND linear extension record (red squares) by multiplying all the 13BND extension values by a factor of 1.3.

7.1.4 DISCUSSION

Absence of thermal stress signatures at Tantabiddi

In comparison to the Bundegi core records, the Tantabiddi records showed no significant short-term variability in either Sr/Ca-SST or Mg/Ca-SST regressions or abrupt declines in annual linear extension corresponding with the timing of the 2010/11 warming event at Ningaloo Reef. This suggests that thermal stress during the summer of 2010/11 was much lower (or not present) at Tantabiddi relative to Bundegi; results consistent with in situ observations of bleaching made throughout the Ningaloo Peninsula following this regional warming episode (Moore et al. 2012). During the peak of the 2010/11 heat wave in January 2011, maximum weekly averaged temperatures reached 31.8 °C (*in situ*) at Bundegi (Depczynski et al. 2013), or 3.6 °C degrees above the highest 7-year average monthly maximum for the reef site (28.2 °C from 2003-2010). Thus it was not surprising that ~90% of the coral bleached (Depczynski et al. 2013). In comparison, maximum weekly average temperatures for January 2011 at Tantabiddi reached 28.9 °C, which was only 1.0 °C above the highest 7-year average monthly maximum for the reef site (27.9 °C); thus explaining why only moderate coral bleaching (~20%) was observed at the site (Moore et al. 2012). As such, where the peak temperature anomaly at Tantabiddi only just reached the coral bleaching threshold for the site (i.e. 28.9 °C) (Fitt et at. 2001), this was probably insufficient to result in significant stress of the sampled Porites sp. colony. We suspect that coral bleaching at Tantabiddi was probably largely confined to the more thermally sensitive branching coral species (e.g. Acropora sp. (Guest et al. 2012)). These sensitive coral species are also more abundant in the shallower and more shoreward reef habitats (Collins et al. 2003; Cassata and Collins 2008) that are more susceptible to reef scale temperature anomalies (Falter et

al. 2014) than the deeper channel at Tantabiddi where the sampled Porites corals were located.

Although no signs of thermal stress were observed in the Tantabiddi 13TNT core record, we did observe a significant shift in the Sr/Ca-SST regression where there was a prominent change in the direction of the coral growth axis along the sampling transect (around the year 2008, Figure 7.1.1). If these differences in Sr/Ca-SST regressions were unaccounted for, this could produce a bias in temperature reconstructions of up to ~2 °C for predicted temperature minima and ~0.5 °C for predicted temperature maxima. Thus, these results are consistent with the findings of Alibert and McCulloch (1997) and Delong et al. (2013) in showing how off-axis sampling of coral slices can lead to significant deviations in derived Sr/Ca-SST calibrations.

Impact of thermal stress on trace element chemistry at Bundegi

The anomalous increase in Sr/Ca ratios and decrease in Mg/Ca ratios recorded from November 2010 to June 2011 in the 13BND record was consistent with the timing of the regional marine heat wave along the western coastline of Australia during the summer of 2010/11 (Feng et al. 2013) as well as the onset of severe coral bleaching observed at Bundegi reef (Depczynski et al. 2013). These anomalous trace element ratios were further accompanied by a strong decline in the linear extension rate (Figure 7.1.6) and an apparent high-density stress band in the 13BND record; both of which provide additional compelling evidence for acute thermal stress impacting the reef site and, in particular, the sampled coral colony during the summer of 2010/11.

The anomalous increase in Sr/Ca ratios during the 2010/11 thermal stress event for the Bundegi colony is consistent with previous research that has suggested that the ability of Porites sp. to pump calcium from the ambient seawater into the calcifying fluid via the Ca^{2+} ATPase transport enzyme can become impaired during periods of thermal stress (Marshall and McCulloch 2002; Sinclair 2005). Although still an unresolved issue, if its assumed that the Ca^{2+} ATPase enzyme is specific for Ca^{2+} (e.g. Tanaka et al. 2015), then inhibition of the enzyme would result in reduced concentrations of Ca^{2+} in the calcifying fluid relative to other ions transported to the calcifying fluid via passive seawater pathways (e.g. Sr^{2+} and Mg^{2+}) (Sinclair 2005). As Sr^{2+} directly substitutes for Ca^{2+} in coralline aragonite (Speer 1983), reduced concentrations of Ca^{2+} in the calcifying fluid would therefore lead to increases in skeletal Sr/Ca ratios (Sinclair 2005); thus, potentially explaining the anomalously high Sr/Ca ratios observed in the Bundegi core record during the 2010/11 warming event.

Although a disruption of the Ca^{2+} ATPase enzyme could occur via direct temperature effects; that is the enzyme is forced to operate at sub-optimal temperatures that result in a reduced ability to transport calcium across the calicoblastic layer (Cossins and Bowler 1987; Marshall and Clode 2004; Al-Horani 2005); it is also possible that a reduction in calcium pumping could occur due to reduction in the supply of the energy needed to drive the molecular pump (e.g. Fang et al. 1991). Given that symbiotic algae provide the principle source of energy supporting calcification by the coral host (Muscatine 1990), some reduction in the supply of metabolic energy (in the form of ATP) to the coral host during periods of thermal stress could be expected (Fang et al. 1991; Jones et al. 1998). This, in turn could lead to a reduction in the activity of the Ca^{2+} ATPase enzyme during periods of thermal stress that is similar to what has been shown to occur during night-time calcification when active Ca^{2+} transport is reduced compared to during the day (Al-Horani et al. 2003). Interestingly, we observed that the decline in slope of the Sr/Ca-SST calibration for the Bundegi coral during the 2010/11 thermal stress event (~70%) was similar to the differences in slopes observed between day and night-time skeletal deposits (~80%) for Porites lutea (Cohen et al. 2001). Thus, the reduction in the slope of the Sr/Ca-SST regression could suggest that the chemical conditions of the calcifying fluid of the Bundegi coral during the 2010/11 warming event were more similar to that of night-time and thus ambient seawater conditions due to a reduction in the activity of the Ca^{2+} ATPase enzyme. This idea is further supported by the decline in linear extension and hence calcification (Lough and

Barnes 2000) observed in the Bundegi record corresponding with the timing of the 2010/11 event. The removal of two H^+ ions in exchange for the addition of Ca^{2+} by the Ca^{2+} ATPase enzyme plays a crucial role in the elevation of pH and aragonite saturation state of the calcifying fluid (Tambuttè et al. 2011; McCulloch et al. 2012), which in turn, permits the rapid deposition of coral skeleton (Gattuso et al. 1998; Al-Horani et al. 2003; Tambuttè et al. 2011). Therefore both the decline in slope of the Sr/Ca-SST regression and the decrease in calcification observed during the 2010/11 event provide strong evidence for reduced activity of the Ca^{2+} ATPase enzyme due to thermal stress of the sampled Porites colony.

In contrast to the Sr/Ca data, the decrease in Mg/Ca ratios observed in the 13BND record during the 2010/11 heatwave could appear to contradict the idea that a reduction in active Ca^{2+} transport to the calcifying fluid occurs when corals are exposed to high levels of thermal stress. However, given the strong decrease in calcification observed in the Bundegi record during the 2010/11 event, a decrease in the precipitation efficiency (i.e. the mass fraction of aragonite precipitated from a given batch of calcifying fluid) of the coral during this time could be expected (Gaetani and Cohen 2006). As such, the opposite response of Sr/Ca and Mg/Ca ratios observed during this period probably reflects the differential effect of decreased Rayleigh fractionation on the incorporation of Sr and Mg into the growing aragonite skeleton (Cohen and Gaetani 2010). Strong differences between the aragonite-seawater exchange coefficients (K_D) for Sr/Ca ($K_D^{Sr/Ca}$ = ~1.2) and Mg/Ca ($K_D^{Mg/Ca}$ = ~0.001) (Cohen and Gaetani 2010) indicate that precipitating skeletal aragonite will have lower Mg/Ca ratios and higher Sr/Ca ratios relative to the calcifying fluid (Rimstidt et al. 1998). Thus, as calcification progresses (assuming a semi-enclosed calcification environment), the calcifying fluid would become progressively enriched in Mg and depleted in Sr, leading to increasing Mg/Ca ratios and decreasing Sr/Ca ratios in the precipitating coral skeleton (Cohen and Gaetani 2010). A reduction in the precipitation efficiency of the coral would therefore act to lower skeletal Mg/Ca ratios and increase Sr/Ca ratios and could explain the opposite behaviour observed for these two trace element ratios from November 2010 to April 2011 in the 13BND record. This idea is supported by the observed differences in magnitude between the Sr/Ca and Mg/Ca anomalies in the 13BND record during the 2010/11 event (i.e. +2.5% versus -10% respectively). Where the magnitude of the Mg/Ca anomaly was five times larger than the Sr/Ca anomaly, this was observed to be consistent with previous research showing modelled precipitation efficiency related changes being ~ 6 times larger for Mg/Ca ratios than for Sr/Ca ratios in Diploria corals (Gaetani and Cohen 2006). Furthermore, the combined effect of a decrease in active Ca^{2+} transport to the calcifying fluid and a decrease in Rayleigh Fractionation could also explain why the slope of the Sr/Ca-SST calibration observed during the 2010/11 event decreased below that of experimentally precipitated abiogenic aragonite precipitated from seawater (-0.038±0.004 mmol mol^{-1} $°C^{-1}$ (Gaetani and Cohen 2006)).

In addition to changes in precipitation efficiency, we also note that the incorporation of Mg into the coral skeleton can be further complicated by other mechanisms. For example, Mg is probably trapped (incorporated) in lattice defects (Amiel et al. 1973; Cross and Cross 1983; Watanabe et al. 2001, Montagna et al. 2014) and slower calcification rates lead to reduced rates of defect occurrence in coral skeleton, which can thereby also lower skeletal Mg/Ca ratios (Sinclair 2005; Gaetani and Cohen, 2006). Furthermore, the concentration of Mg is heterogeneous in coral skeleton with enrichments observed in the centres of calcification (COC) relative to the adjacent fibres (Meibom et al. 2006; Holcomb et al. 2009). Diurnal variations in the aragonite saturation state of the cf are thought to control the formation of these two distinct skeletal components; with COCs deposited during the day (high aragonite saturation states) and fibres deposited during the night (lower saturation states) (Holcomb et al. 2009). Therefore, a decrease in the number of COCs per mass of aragonite could also have contributed to the observed decrease in Mg/Ca ratios in the Bundegi record during the summer of 2010/11 as suggested by the strong decline in calcification rates observed during this time.

Modelling of trace element thermal stress induced changes

To constrain the relative effects of changes in precipitation efficiency and active Ca^{2+} transport to the calcifying fluid on skeletal Mg/Ca and Sr/Ca ratios, a closed system, Rayleigh-type equation can be applied (Albarede and Bottinga 1972; Gagnon et al. 2007; Cohen and Gaetani 2010; Sinclair 2015; Stewart et al. 2016). Using the equation from Sinclair (2015) (see below), the observed and predicted Sr/Ca and Mg/Ca ratios for January 2011 in the 13BND record were modelled considering the effects of variations in the concentration of Ca^{2+} in the calcifying fluid or changes in P (Figure 7.1.7).
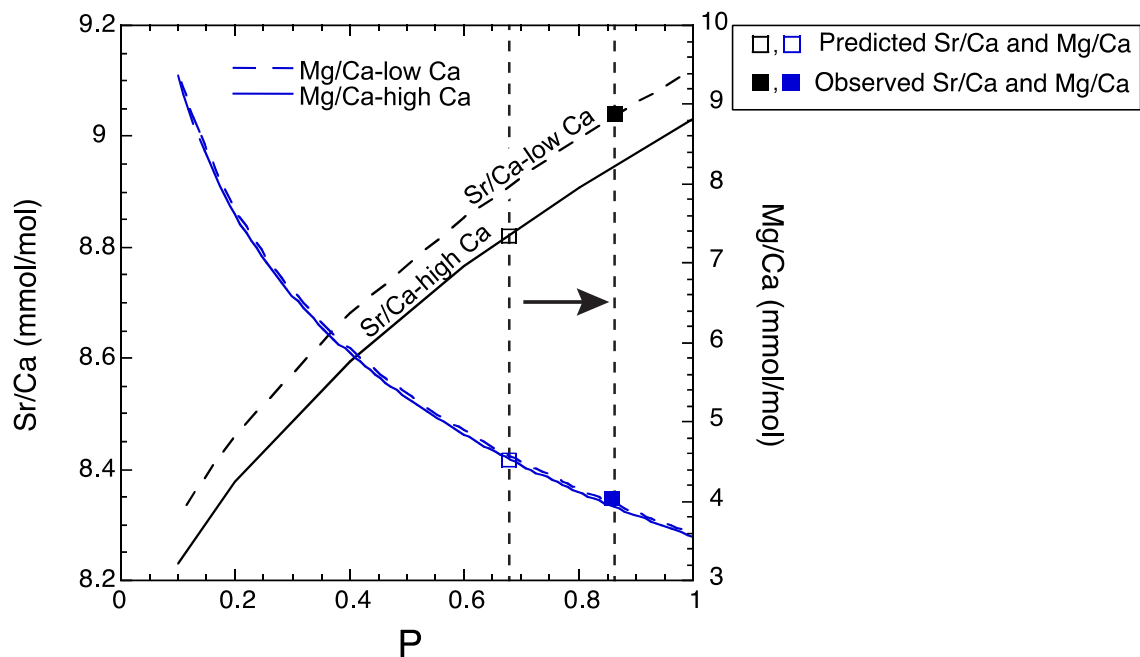
Figure 7.1.7 Modelled response of Sr/Ca and Mg/Ca ratios to variations in *P* (i.e. 0 to 1) and the concentration of Ca^{2+} in the calcifying fluid (i.e. 10.53 for "low Ca" versus 10.63 for "high-Ca"). Calculations were based on the Rayleigh fractionation definitions from Sinclair (2015) using a $K_{DSr} = e^{(-1.86+600/T)}$ from Gaetani and Cohen (2006) and $K_{DMg} = e^{(-12.9+1729/T)}$). It was assumed that the active transport to CF is specific only to Ca. The predicted and observed Sr/Ca and Mg/Ca ratios for January 2011 for the 13BND coral record are shown with the square markers (no fill = predicted, black/blue fill = observed). The predicted Sr/Ca and Mg/Ca ratios were determined from the long-term, pre thermal stress calibrations (i.e. June-05 to Oct-2010 calibrations, Figure 7.1.5a, b, Table 7.1.2) for a temperature of 29.8 °C.

Eqn 1:

$$\left(\frac{Me}{Ca}\right)_{coral} = \left(\frac{Me}{Ca}\right)_{i} \frac{\left(1 - P^{K_D \frac{Me}{Ca}}\right)}{(1 - P)}$$

where Me/Ca_{coral} is the metal/calcium ratio (Sr/Ca or Mg/Ca) in the coral skeleton, Me/Ca_i is the initial metal/calcium in the calcifying fluid before precipitation begins, and P is the proportion of Ca remaining in a batch of cf after precipitation has ended (P). The changes in Ca_i can be considered to reflect changes in the activity of Ca^{2+} ATPase enzyme: its ability to pump the concentration of Ca^{2+} within the calcifying fluid above the seawater end member of ~10.28 mmol (no up-regulation) (Millero 1979) while changes in P reflect changes in precipitation efficiency. The model confirms that the opposite response of Sr/Ca and Mg/Ca ratios observed in the Bundegi record for the summer of 2010/11 could be explained by a decrease in precipitation efficiency of the coral (increase in P).

However, the model suggests an increase in P alone could not account for the observed magnitude of both the Sr/Ca (+2.5%) and Mg/Ca (-10%) anomalies and, in order to obtain a single P value for both Sr/Ca and Mg/Ca, some decrease in Ca_i, is also required. For example, the stress response observed in the BND coral Sr/Ca and Mg/Ca data during the summer of 2011 was able to be realistically matched (i.e. with a single P obtained for each of the pairs of the predicted and observed Sr/Ca and Mg/Ca ratios) by assuming an increase in P (reduction in precipitation efficiency) from 0.68 to 0.87 and a small reduction in Ca^{2+} from 10.63 to 10.53 (~1% decline). Regarding the latter, given previous estimates of coral Ca^{2+} up-regulation of ~0.5 mmol kg^{-1} above seawater values (Al-Horani et al. 2003; McCulloch et al. 2012), this small decline in Ca_i could be considered to represent an ~20% decline in active Ca^{2+} transport to the calcifying fluid although actual changes could vary substantially depending on slight variations in sensitive input parameters (e.g. $K_D^{Mg/Ca}$). We emphasize that this model does not accommodate active Ca^{2+} transport that occurs during calcification (i.e. closed system assumption); thus, the effect of reduced Ca^{2+} transport on skeletal Sr/Ca and Mg/Ca ratios could in reality be more complicated. Nonetheless, our data provides strong evidence for changes in Ca^{2+} ATPase and precipitation efficiency to account for the observed Sr/Ca and Mg/Ca anomalies observed in the Bundegi record during the summer of 2010/11. As such, because no significant change in the slope of the Sr/Ca vs Mg/Ca linear regression was observed for the Bundegi coral during the 2010/11 event (Figure 7.1.4), this provides strong evidence suggesting changes in coral precipitation efficiency are related, either directly or indirectly to changes in the activity of the Ca^{2+} ATPase enzyme.

Recovery of Bundegi coral following thermal stress

Following the summer of 2010/11 in the Bundegi (13BND) record, the re-establishment of the original bulk Sr/Ca and Mg/Ca-SST relationships from May 2011 to May 2012 (see orange markers, Figure 7.1.5a, b) could be indicative of the return to 'normal' calcification conditions for Bundegi coral. Previous research has shown that in some cases, it is possible for corals to recover from thermal stress and bleaching within a few months following acute warming events (e.g. Brown 1997); however, substantially longer recovery times, of up to several years, have also been reported for Porites sp. corals following major bleaching events on the Great Barrier Reef (D'Olivo et al. 2013; Cantin and Lough 2014). In this case, because linear extension rates for the Bundegi coral were observed to remain anomalously low for at least 2 years following the 2010/11 thermal stress event (Figure 7.1.6), it is unlikely that the coral had experienced a complete recovery within such a short time frame. Nonetheless, the different recovery times between trace elements (months) and growth rates (years) suggest that, while the basic physiology governing the chemistry of the calcifying fluid appeared to have returned to normal, the absolute rate at which the coral could precipitate its skeleton had clearly not.

Conclusions

Our results show that coral core geochemical records can provide a distinct signature of past environmental stress events making them useful for understanding the variable impacts of acute ocean warming episodes within individual reef systems. The presence of Sr/Ca and Mg/Ca anomalies in the Bundegi core record during the 2010/11 marine heat wave at Ningaloo, and the absence of any such anomalies in the Tantabiddi record, was consistent with the respective instrumental temperature records and contrasting reports of coral bleaching from the two reef sites (~20% bleaching at Tantabiddi vs. ~90% at Bundegi) (Moore et al. 2012). The anomalous increase in Sr/Ca ratios and decrease in Mg/Ca ratios observed during the summer of 2010/11 in the Bundegi coral core record indicated that thermal stress can strongly influence the 'vital' effects governing the incorporation of trace elements in the skeletons of Porites sp. corals resulting in significant short-term changes in coral Sr/Ca and Mg/Ca ratios and; thus, biased predictions of in situ temperature. We show that the increase in skeletal Sr/Ca ratios in *Porites* sp. could partially be explained by a

reduction in active (Ca^{2+} ATPase) Ca^{2+} transport to the calcifying fluid during thermal stress events (Marshall and McCulloch 2002). However, the strong decline in skeletal Mg/Ca ratios recorded during this same period can only be explained by secondary growth effects (i.e. a decline in the precipitation efficiency and/or defect entrapment of Mg), that could have directly or indirectly resulted from a decline in active Ca^{2+} transport to the calcifying fluid.

Although short-term deviations in coral Sr/Ca-SST and Mg/Ca-SST relationships due to changing vital effects are a source of error for paleo-climate temperature reconstructions, they provide clear evidence of the significance of 'vital' effects to modulate the climate signal preserved in coral core records. However, given that the geochemical signature of a stress event could appear as a reduction in the seasonal amplitude of Sr/Ca and Mg/Ca minima and maxima, distinguishing a past stress event from a cold year could prove difficult solely based on the information from these geochemical proxies. We therefore suggest future research investigate combining Sr/Ca and Mg/Ca analyses with additional trace element or isotopic proxies whose abundance may be unaffected by changes in calcification processes during thermal stress events (e.g. Li/Mg (Montagna et al. 2014)). This could potentially allow for historic stress events to be identified in coral core records without the need for overlapping temperature data.

7.1.5 ACKNOWLEDGEMENTS

7.1.6 REFERENCES

Al-Horani F, Al-Moghrabi S and De Beer D (2003) The mechanism of calcification and its relation to photosynthesis and respiration in the scleractinian coral Galaxea fascicularis. Marine Biology 142(3):419-426.

Al-Horani FA (2005) Effects of changing seawater temperature on photosynthesis and calcification in the scleractinian coral Galaxea fascicularis, measured with O 2, Ca 2+ and pH microsensors. Scientia Marina 69(3):347-354.

Albarede F and Bottinga Y (1972) Kinetic disequilibrium in trace element partitioning between phenocrysts and host lava. Geochimica et Cosmochimica Acta 36(2):141-156.

Alibert C and McCulloch MT (1997) Strontium/calcium ratios in modern Porites corals from the Great Barrier Reef as a proxy for sea surface temperature: calibration of the thermometer and monitoring of ENSO Paleoceanography 12(3):345-363.

Allison N and Finch AA (2007) High temporal resolution Mg/Ca and Ba/Ca records in modern Porites lobata corals. Geochemistry Geophysics, Geosystems, 8(5).

Amiel AJ, Friedman GM and Miller DS (1973) Distribution and nature of incorporation of trace elements in modern aragonitic corals. Sedimentology 20(1):47-64.

Beck JWE, dwards RL, Ito E, Taylor FW, Recy J, Rougerie F, Joannot P and Henin C (1992) Sea-surface temperature from coral skeletal strontium/calcium ratios Science 257(5070):644-647.

Berkelmans R, De'ath G, Kininmonth S and Skirving WJ (2004) A comparison of the 1998 and 2002 coral bleaching events on the Great Barrier Reef: spatial correlation patterns and predictions. Coral reefs 23(1):74-83.

Brown BE (1997) Adaptations of Reef Corals to Physical Environmental Stress In: JHS Blaxter and AJ Southward (Editors) Advances in Marine Biology. Academic Press pp 221-299.

Bruno J, Siddon C, Witman J, Colin P and Toscano M (2001) El Nino related coral bleaching in Palau western Caroline Islands Coral Reefs 20(2):127-136.

Brunskill G, Orpin A, Zagorskis I, Woolfe K and Ellison J (2001) Geochemistry and particle size of surface sediments of Exmouth Gulf Northwest Shelf Australia. Continental Shelf Research 21(2):157-201.

Cantin NE, Cohen AL, Karnauskas KB, Tarrant AM and McCorkle DC (2010) Ocean warming slows coral growth in the central Red Sea. Science 329(5989):322-325.

Cantin NE and Lough JM (2014) Surviving coral bleaching events: Porites growth anomalies on the Great Barrier Reef. PloS one 9(2):e88720.

Cassata L and Collins LB (2008) Coral reef communities habitats and substrates in and near sanctuary zones of Ningaloo Marine Park. Journal of Coastal Research: 139-151.

Cohen A and Gaetani GA (2010) Ion partitioning and the geochemistry of coral skeletons: solving the mystery of the vital effect. EMU Notes in Mineralogy 11:377-397.

Cohen AL, Layne GD, Hart SR and Lobel PS (2001) Kinetic control of skeletal Sr/Ca in a symbiotic coral: Implications for the paleotemperature proxy. Paleoceanography 16(1):20-26.

Collins LB, Zhu ZR, Wyrwoll K-H and Eisenhauer A (2003) Late Quaternary structure and development of the northern Ningaloo Reef Australia. Sedimentary Geology 159(1):81-94.

Cooper TF, O'Leary RA and Lough JM (2012) Growth of Western Australian corals in the Anthropocene. Science 335(6068):593-596.

Corrège T (2006) Sea surface temperature and salinity reconstruction from coral geochemical tracers Palaeogeography Palaeoclimatology Palaeoecology 232(2):408-428

Cossins A R and Bowler K (1987) Temperature biology of animals Chapman and Hall London.

Cross TS and Cross BW (1983) U Sr and Mg in Holocene and Pleistocene corals A. palmata and M. annularis. Journal of Sedimentary Research 53(2).

D'Olivo J, McCulloch M and Judd K (2013) Long-term records of coral calcification across the central Great Barrier Reef: assessing the impacts of river runoff and climate change. Coral Reefs 32(4):999-1012.

Davis K, Lentz S, Pineda J, Farrar J, Starczak V and Churchill J (2011) Observations of the thermal environment on Red Sea platform reefs: a heat budget analysis. Coral Reefs 30(1):25-36.

DeLong KL, Quinn TM, Taylor FW, Shen C-C and Lin K (2013) Improving coral-base paleoclimate reconstructions by replicating 350years of coral Sr/Ca variations. Palaeogeography Palaeoclimatology Palaeoecology 373:6-24.

Depczynski M, Gilmour ,J Ridgway T, Barnes H, Heyward A, Holmes T, Moore J, Radford B, Thomson D and Tinkler P (2013) Bleaching coral mortality and subsequent survivorship on a West Australian fringing reef. Coral Reefs 32(1):233-238.

Eakin C, Lough J and Heron S (2009) Climate variability and change: monitoring data and evidence for increased coral bleaching stress Coral bleaching. Springer pp. 41-67.

Fallon SJ, McCulloch MT and Alibert C (2003) Examining water temperature proxies in Porites corals from the Great Barrier Reef: a cross-shelf comparison. Coral Reefs 22(4):389-404.

Falter JL, Zhang Z, Lowe RJ, McGregor F, Keesing J and McCulloch MT (2014) Assessing the drivers of spatial variation in thermal forcing across a nearshore reef system and implications for coral bleaching. Limnology and Oceanography 59(4):1241-1255.

Fang L-S, Chen Y-W and Chen C-S (1991) Feasibility of using ATP as an index for environmental stress on hermatypic coral. Mar. Ecol. Prog. Ser 70:257-262.

Felis T and Pätzold J (2003) Climate records from corals Marine Science Frontiers for Europe. Springer pp. 11-27

Feng M, McPhaden MJ, Xie S-P and Hafner J (2013) La Niña forces unprecedented Leeuwin Current warming in 2011 Sci Rep 3.

Fitt WK, Brown BE, Warner ME and Dunne RP (2001) Coral bleaching: interpretation of thermal tolerance limits and thermal thresholds in tropical corals. Coral Reefs 20(1):51-65.

Gaetani GA and Cohen AL (2006) Element partitioning during precipitation of aragonite from seawater: a framework for understanding paleoproxies. Geochimica et Cosmochimica Acta 70(18):4617-4634.

Gagan M, Ayliffe L, Beck J, Cole J, Druffel E, Dunbar R and Schrag D (2000) New views of tropical paleoclimates from corals. Quaternary Science Reviews 19(1):45-64.

Gagnon AC, Adkins JF, Fernandez DP and Robinson LF (2007) Sr/Ca and Mg/Ca vital effects correlated with skeletal architecture in a scleractinian deep-sea coral and the role of Rayleigh fractionation. Earth and Planetary Science Letters 261(1):280-295.

Gattuso J-P, Frankignoulle M, Bourge I, Romaine S and Buddemeier R (1998) Effect of calcium carbonate saturation of seawater on coral calcification. Global and Planetary Change 18(1):37-46.

Grottoli AG and Eakin CM (2007) A review of modern coral δ 18 O and Δ 14 C proxy records. Earth-Science Reviews 81(1):67-91.

Guest JR, Baird AH, Maynard JA, Muttaqin E, Edwards AJ, Campbell SJ, Yewdall K, Affendi YA and Chou LM (2012) Contrasting patterns of coral bleaching susceptibility in 2010 suggest an adaptive response to thermal stress. PLoS One 7(3):e33353.

Hetzinger S, Pfeiffer M, Dullo W-C, Zinke J and Garbe-Schönberg D (2016) A change in coral extension rates and stable isotopes after El Niño-induced coral bleaching and regional stress events Scientific Reports 6.

Hoegh-Guldberg O (1999) Climate change coral bleaching and the future of the world's coral reefs. Marine and freshwater research 50(8):839-866.

Hoegh-Guldberg O and Ridgway T (2016) Coral bleaching hits Great Barrier Reef as global temperatures soar. Green Left Weekly (1090):10.

Holcomb M, Cohen AL, Gabitov RI and Hutter JL (2009) Compositional and morphological features of aragonite precipitated experimentally from seawater and biogenically by corals. Geochimica et Cosmochimica Acta 73(14):4166-4179.

Holcomb M, DeCarlo TM, Schoepf V, Dissard D, Tanaka K and McCulloch M (2015) Cleaning and pre-treatment procedures for biogenic and synthetic calcium carbonate powders for determination of elemental and boron isotopic compositions. Chemical Geology 398:11-21.

Howells EJ, Beltran VH, Larsen NW, Bay LK, Willis BL and van Oppen MJH (2012) Coral thermal tolerance shaped by local adaptation of photosymbionts. Nature Clim. Change 2(2):116-120.

Hughes TP, Baird AH, Bellwood DR, Card M, Connolly SR, Folke C, Grosberg R, Hoegh-Guldberg O, Jackson JBC, Kleypas J, Lough JM, Marshall P, Nyström M, Palumbi SR, Pandolfi JM, Rosen B and Roughgarden J (2003) Climate Change Human Impacts and the Resilience of Coral Reefs. Science 301(5635):929-933.

Jokiel P and Coles S (1990) Response of Hawaiian and other Indo-Pacific reef corals to elevated temperature. Coral reefs 8(4):155-162.

Jones R, Hoegh-Guldberg O, Larkum A and Schreiber U (1998) Temperature-induced bleaching of corals begins with impairment of the CO2 fixation mechanism in zooxanthellae. Plant Cell & Environment 21(12):1219-1230.

Kinsman DJ and Holland H (1969) The co-precipitation of cations with CaCO3—IV The co-precipitation of Sr2+ with aragonite between 16° and 96° C. Geochimica et Cosmochimica Acta 33(1):1-17.

Li A and Reidenbach MA (2014) Forecasting decadal changes in sea surface temperatures and coral bleaching within a Caribbean coral reef. Coral Reefs 33(3):847-861.

Liu G, Strong AE and Skirving W (2003) Remote sensing of sea surface temperatures during 2002 Barrier Reef coral bleaching. Eos Transactions American Geophysical Union 84(15):137-141.

Liu G, Strong AE, Skirving W and Arzayus LF (2006) Overview of NOAA coral reef watch program's near-real time satellite global coral bleaching monitoring activities Proceedings of the 10th International Coral Reef Symposium. June.

Lough J and Barnes D (1997) Several centuries of variation in skeletal extension density and calcification in massive Porites colonies from the Great Barrier Reef: A proxy for seawater temperature and a background of variability against which to identify unnatural change. Journal of Experimental Marine Biology and Ecology 211(1):29-67.

Lough JM (2008) Coral calcification from skeletal records revisited. Marine Ecology Progress Series 373:257-264.

Lough J and Barnes D (2000) Environmental controls on the growth of the massive coral Porites Journal of Experimental Marine Biology and Ecology 245(2):225-243.

Lough JM and Cooper TF (2011) New insights from coral growth band studies in an era of rapid environmental change. Earth-Science Reviews 108(3):170-184.

Marshall A and Clode P (2004) Calcification rate and the effect of temperature in a zooxanthellate and an azooxanthellate scleractinian reef coral. Coral reefs 23(2):218-224.

Marshall JF and McCulloch MT (2002) An assessment of the Sr/Ca ratio in shallow water hermatypic corals as a proxy for sea surface temperature. Geochimica et Cosmochimica Acta 66(18):3263-3280.

Massel S, Brickman R, Mason L and Bode L (1997) Water circulation and waves in Exmouth Gulf Proceedings of the Australian Physical Oceanography Conference. Macquarie University Sydney pp 48.

McClanahan TR, Ateweberhan M, Muhando CA, Maina J and Mohammed MS (2007) Effects of climate and seawater temperature variation on coral bleaching and mortality. Ecological Monographs 77(4):503-525.

McCulloch M, Falter J, Trotter J and Montagna P (2012) Coral resilience to ocean acidification and global warming through pH up-regulation. Nature Climate Change 2(8):623-627.

Meibom A, Yurimoto H, Cuif JP Domart-Coulon I, Houlbreque F, Constantz B, Dauphin Y, Tambutté E, Tambutté S and Allemand D (2006) Vital effects in coral skeletal composition display strict three-dimensional control. Geophysical Research Letters 33(11).

Millero FJ (1979) The thermodynamics of the carbonate system in seawater. Geochimica et Cosmochimica Acta 43(10):1651-1661.

Montagna P, McCulloch M, Douville E, Correa ML, Trotter J, Rodolfo-Metalpa R, Dissard D, Ferrier-Pages C, Frank N and Freiwald A (2014) Li/Mg systematics in scleractinian corals: Calibration of the thermometer. Geochimica et Cosmochimica Acta 132:288-310.

Moore JA, Bellchambers LM, Depczynski MR, Evans RD, Evans SN, Field SN, Friedman KJ, Gilmour JP, Holmes TH and Middlebrook R (2012) Unprecedented mass bleaching and loss of coral across 12 of latitude in Western Australia in 2010–11.

Muscatine L (1990) The role of symbiotic algae in carbon and energy flux in reef corals Ecosystems of the world 25:75-87

Normile D (2016) El Niño's warmth devastating reefs worldwide. Science 352(6281):15-16.

Oliver J, Berkelmans R and Eakin C (2009) Coral bleaching in space and time Coral bleaching. Springer pp. 21-39.

Paillard D, Labeyrie L and Yiou P (1996) Macintosh program performs time-series analysis. Eos Transactions American Geophysical Union 77(39):379-379.

Pandolfi JM, Bradbury RH, Sala E, Hughes TP, Bjorndal KA, Cooke RG, McArdle D, McClenachan L, Newman MJH, Paredes G, Warner RR and Jackson JBC (2003) Global Trajectories of the Long-Term Decline of Coral Reef Ecosystems. Science 301(5635):955-958.

Pineda J, Starczak VR, Tarrant AM, Blythe JN, Davis KA, Farrar JT, Berumen ML and da Silva JC (2013) Two spatial scales in a bleaching event: Corals from the mildest and the most extreme thermal environments escape mortality.

Rasmusson EM and Carpenter TH (1982) Variations in tropical sea surface temperature and surface wind fields associated with the Southern Oscillation/El Niño. Monthly Weather Review 110(5):354-384.

Rimstidt JD, Balog A and Webb J (1998) Distribution of trace elements between carbonate minerals and aqueous solutions. Geochimica et Cosmochimica Acta 62(11):1851-1863.

Schoepf V Stat M Falter JL and McCulloch MT 2015 Limits to the thermal tolerance of corals adapted to a highly fluctuating naturally extreme temperature environment. Scientific reports 5.

Sinclair DJ (2005) Correlated trace element "vital effects" in tropical corals: a new geochemical tool for probing biomineralization. Geochimica et cosmochimica acta 69(13):3265-3284.

Sinclair DJ (2015) RBME coral temperature reconstruction: An evaluation modifications and recommendations. Geochimica et Cosmochimica Acta 154:66-80.

Skirving W, Liu G, Strong AE, Liu C, Sapper J and Arzayus F (2006) Extreme events and perturbations of coastal ecosystems Remote sensing of aquatic coastal ecosystem processes. Springer pp. 11-25.

Speer A (1983) The kinetics of calcium carbonate dissolution and precipitation Carbonates: Mineralogy and Chemistry 11:145-190.

Stewart JA, Anagnostou E and Foster GL (2016) An improved boron isotope pH proxy calibration for the deep-sea coral Desmophyllum dianthus through sub-sampling of fibrous aragonite. Chemical Geology.

Taebi S, Lowe R, Pattiaratchi C, Ivey G and Symonds G (2011) Modelling nearshore circulation in a fringing reef system: Ningaloo Reef Australia. J Coast Res 2(SI 64):1200-1203.

Tambutté S, Holcomb M, Ferrier-Pagès C, Reynaud S, Tambutté É, Zoccola D and Allemand D (2011) Coral biomineralization: from the gene to the environment. Journal of Experimental Marine Biology and Ecology 408(1):58-78.

Tanaka K, Holcomb M, Takahashi A, Kurihara H, Asami R, Shinjo R, Sowa K, Rankenburg K, Watanabe T and McCulloch M (2015) Response of Acropora digitifera to ocean acidification:

constraints from δ11B Sr Mg and Ba compositions of aragonitic skeletons cultured under variable seawater pH. Coral Reefs 34(4):1139-1149.

Thompson D and Van Woesik R (2009) Corals escape bleaching in regions that recently and historically experienced frequent thermal stress. Proceedings of the Royal Society of London B: Biological Sciences 276(1669):2893-2901.

Trotter J, Montagna P, McCulloch M, Silenzi S, Reynaud S, Mortimer G, Martin S, Ferrier-Pagès C, Gattuso J-P and Rodolfo-Metalpa R (2011) Quantifying the pH 'vital effect' in the temperate zooxanthellate coral Cladocora caespitosa: Validation of the boron seawater pH proxy. Earth and Planetary Science Letters 303(3):163-173.

Veron J, Hoegh-Guldberg O, Lenton T, Lough J, Obura D, Pearce-Kelly P, Sheppard C, Spalding M, Stafford-Smith M and Rogers A (2009) The coral reef crisis: The critical importance of< 350ppm CO 2. Marine Pollution Bulletin 58(10):1428-1436.

Watanabe T, Minagawa M, Oba T and Winter A (2001) Pretreatment of coral aragonite for Mg and Sr analysis: Implications for coral thermometers. Geochemical journal 35(4):265-269.

Wilkinson CR (1999) Global and local threats to coral reef functioning and existence: review and predictions. Marine and Freshwater Research 50(8):867-878.

Wyrwoll K, Kendrick G and Long J (1993) The geomorphology and Late Cenozoic geomorphological evolution of the Cape Range-Exmouth Gulf region. Records of the Western Australian Museum Supplement 45:1-23.

Zhang Z, Falter J, Lowe R, Ivey G and McCulloch M (2013) Atmospheric forcing intensifies the effects of regional ocean warming on reef-scale temperature anomalies during a coral bleaching event. Journal of Geophysical Research: Oceans 118(9):4600-4616.

7.2 Coral core geochemical records from Onslow: long and short term Sr/Ca, Li/Mg and Ba/Ca records provide an environmental context to assess the impacts of recent widespread coral bleaching events in the region

Authors: Clarke H, D'Olivo JP, McCulloch M.

ABSTRACT

Long term, annual resolution (75–150 yr) together with shorter-term monthly resolution (20 yr length), coral core records of Sr/Ca, Li/Mg and Ba/Ca were generated from two nearshore (Ward and Herald islands), a mid-shelf (Airlie Island) and an offshore site (Montebello Islands) in the southern Pilbara region of Western Australia. We aimed to assess long-term environmental changes in the region and, in particular, whether changes in sedimentation and turbidity regimes influenced the sensitivity of corals to thermal stress during the recent widespread coral bleaching events of 2010/11 and 2012/13. The long-term Sr/Ca and Li/Mg records provided evidence for increases in background temperatures of ~0.6°C at Airlie Island, but a larger ~3°C increase at the more offshore Montebello Islands. The annual Ba/Ca record for Airlie Island extended back to the mid 1870's and showed the highest values occurred from the early 1960's to early 1990's. This relatively recent increase is consistent with major changes in land use (e.g. mining and increased pastoralism) that impacted the Ashburton River catchment during this period.

The impact of recent acute ocean warming events during the summers of 2010/11 and 2012/13 was assessed from the shorter term, high resolution Sr/Ca and Li/Mg records. The records indicated strong declines in calcification rate occurred at all the sites during both these events and strong increases in Sr/Ca and Li/Mg ratios were also observed in the nearshore records, suggesting coral bleaching impacts were unprecedented, although spatially variable across the region. The high-resolution Ba/Ca records provided no evidence to suggest the nearshore corals were significantly impacted by nearby dredging operations conducted from 2013–2015. We caution however, that in this instance, the Ba/Ca proxy appeared to not be effective for resolving sediment re-suspension events. Nonetheless, consistent with previous research, our data suggest that continued background ocean warming is primarily responsible for the widespread reductions in live coral cover that have been observed across the southern Pilbara region over the last 5 years.

7.2.1 INTRODUCTION

It is well known that the continued and expected ongoing effects of man-made changes to the earth's climate will have a deleterious effect on the composition and growth of coral reef communities; particularly key reef calcifiers such as coral (e.g. Hoegh-Guldberg et al. 2007; Castillo et al. 2012). Reef building corals are hosts to dinoflagellate symbionts, commonly referred to as zooxanthellae (Pearse and Muscatine 1971), which contribute to the energy budget of the coral through photosynthesis (Muscatine and Porter 1977). However, the mutualistic symbiosis between corals and their symbionts is particularly sensitive to a variety of external environmental parameters, notably, temperature (Glynn 1996; Brown 1997). If the environmental thresholds within which corals survive are exceeded, this symbiosis can break down, leading to the ejection of zooxanthellae and bleaching of the coral host (Fitt et al. 2001; Brown 1997). Significant increases in background global ocean temperatures over the last century (~0.75°C)(IPCC, 2007), have resulted in an increase in the frequency and severity of widespread regional marine heat waves in recent decades (Hughes et al. 2017; Hoegh-Guldberg 1999; Bruno et al. 2001). In turn, this has been matched by a near proportional increase in the frequency and severity of widespread coral bleaching events (Hoegh-Guldberg and Ridgway 2016; Hughes et al. 2003; Hoegh-Guldberg 1999) and as such, globally, coral reefs are in a state of rapid decline (e.g. Hughes et al. 2017; Pandolfi et al. 2003). For example, the cumulative footprint of recurrent widespread coral bleaching events on the Great Barrier Reef (GBR) now covers almost the entire of the marine park and the proportion of live coral cover is currently estimated to be around 50–70% compared to levels of the early 1990s (Hughes et al. 2017; De'ath et al. 2012). However, temperature increases are not the sole factor responsible for all of the recent observed declines in live coral cover. Given the sensitivity of corals to their ambient environment (Brown 1997), a variety of other natural (light, heterotrophic status, etc.; Anthony et al. 2007; Grottoli et al. 2006) and anthropogenic factors can both directly cause stress to corals or, more indirectly, influence their susceptibility to thermal stress and bleaching (Dunne 2010; Carilli et al. 2009; Berkelmans 2002; Fitt et al. 2001)

Corals have shown the ability to acclimatize to their local reef habitats (Schoepf et al. 2015; Brown 1997). As such, thermal tolerances are not fixed for specific species and can vary considerably where strong differences in reef environment exist (e.g. Howells et al. 2012; Carilli et al. 2009; Fabricius et al. 2013). For example, the effects of increased sedimentation and turbidity, a common environmental impact of dredge spoil dispersment, has been highlighted as a significant local reef stressor with deleterious effects coral growth (Erftemeijer et al. 2012). Increased sedimentation and turbidity can reduce the tolerance of corals to thermal stress, thereby exacerbating coral bleaching impacts during anomalous warming events (Carilli et al. 2010; Carilli et al. 2009). Increased sedimentation and nutrient concentrations have also been observed to increase coral recovery times following bleaching (Carilli et al. 2009; Wooldridge 2009; Fabricius et al. 2013) and reduce the resilience of corals to subsequent thermal stress events (Carilli et al. 2009).

Although satellite records have become an invaluable tool for monitoring the development of basin-regional scale sea surface temperature (SST) anomalies (e.g. Feng et al. 2013; McClanahan et al. 2007), they cannot accommodate for the combined effects of elevated temperatures with other reef stressors. Furthermore, satellite records often lack the resolution to resolve fine-scale differences in SST anomalies between nearby reef sites during anomalous warming events, which can vary significantly due to a number of physical and climate-related factors (Lowe and Falter 2015). As such, the use of satellite records alone is typically not sufficient to understand fine scale differences in reef environments and resolve small-scale differences in coral bleaching impacts following regional ocean warming events. However, many of these limitations can be overcome when satellite SST data is used in conjunction with other analyses. In particular, the analysis of coral core geochemical records provides a historical context to assess current changes in reef environments, as well as a unique insight into how corals respond and recover from episodic thermal stress events.

The analysis of coral core geochemical and calcification records offers an alternate method to assess differences in reef environments and the relative impacts of thermal stress event within reef ecosystems following widespread marine heat waves. Since the early 1990's, coral core geochemical records from massive *Porites* sp. corals have primarily been used to assess both long-term and seasonal changes in ocean temperatures (Zinke et al. 2014; Grottoli and Eakin 2007; McCulloch et al. 1994; Beck et al. 1992) .The incorporation of trace elements in coral skeleton (e.g. Sr, Li, Mg, B) has shown to be related to a variety of external parameters, thereby making it possible to generate paleo-climate records from coral cores at temporal resolutions (bi-weekly to decadal) proportional to down-core sampling intervals (i.e. mm's to cm's). However, recent developments in the understanding of coral 'vital effects', which also exert a significant control on the incorporation of trace elements, has brought to question the reliability of these records to accurately reflects seasonal changes in reef environments. In particular, because corals do not calcify in chemical equilibrium with their ambient seawater (McCulloch et al. 2012; Al-Horani et al. 2003), the degree to which corals up-regulate their calcifying fluid environment, as well as the various physio-chemical processes involved in the bio-mineralisation of new skeleton (e.g. Rayleigh Fractionation, bio-smoothing), also influence the ratio of many commonly analysed trace elements in coral skeleton (e.g. Sr/Ca, Mg/Ca) (Gagan et al. 2012; Cohen and Gaetani 2010; Sinclair et al. 2005; Al-Horani et al. 2003; Cohen et al.2001). Although the magnitude of seasonal cycles of trace-element to calcium (Te/Ca) ratios are usually strongly correlated with ambient temperatures (Corrège 2006; Fallon et al. 2003; Sinclair et al.1998), observed variations in the linear relationships used to calibrate such Te/Ca paleo-temperature records both within and between different coral species indicate the significant influence of 'vital' effects on derived Te/Ca-SST calibrations (e.g. Corrège et al., 2006; de Villiers, 2004). Where some part of these variations may be explained by the accuracy and precision of overlapping satellite or *in situ* temperature data and/or slight changes in seawater Te/Ca values (e.g. Shen et al. 1996), strong anomalies observed during periods of thermal stress in high-resolution Te/Ca records (Clarke et al. 2017; Marshal and McCulloch 2002) provide a clear example of the significance of "vital effects' to modulate the paleo-temperature signal preserved along the growth axes of massive coral skeletons (can lead to Te/Ca-SSTs underestimating actual SSTs by up to 4℃) (Clarke et al. 2017). Although the influence of vital effects can add considerable uncertainty to the estimation of paleo-temperatures from coral cores (e.g. de Villiers 2004), where temporal changes in vital effects can be observed in core records, this can provide a signature of past environmental disturbances (Clarke et al. 2017). In particular, where abrupt changes in Te/Ca-SST calibrations are observed in coral records, this can provide information about how corals are impacted and recover from episodic thermal stress events. When calcification data is also available, such analyses allow for an assessment of the incidence and severity of thermal stress events and their direct impact on calcification rates of the coral host. This is crucial for predicting how reefs will respond to expected increases in the frequency and severity of widespread coral bleaching events into the future.

Coral Ba/Ca ratios are a well-established proxy for suspended sediment outputs from rivers and upwelling of deep ocean waters along continental margins (Prouty et al. 2010; Alibert et al. 2003; McCulloch et al. 2003; Tudhope et al. 1996; Lea et al. 1989). Unlike most other Te/Ca ratios, Ba/Ca ratios of shallow coastal waters are highly variable (Walther et al. 2013; Lea and Boyle 1990) and primarily controlled by the sediment output from river systems into coastal environments (Sinclair 2005). As such, the incorporation of barium in coral skeleton is predominantly controlled by ambient seawater concentrations (Prouty et al. 2010) and the influence of 'vital effects' could be expected to be minimal. However, following its initial desorption from fluvial sediments once they mix with more saline/estuarine waters, complex bio-geochemical cycling of barium has been shown to occur (Coffey et al. 1997; Dehairs et al. 1980). Therefore, whether sediment re-suspension events also correspond with Ba/Ca enrichments in core records is probably dependent upon a variety of local environmental factors that either promote the retention or removal of barium in marine sediments (Saha et al. 2016; Coffey et al. 1997).

For this study, coral cores were collected from 4 reef sites in the Onslow region of Western Australia in 2015 to assess the impacts of two recent widespread coral bleaching events during the summers of 2010/11 and 2012/13. High-resolution (~monthly) coral Sr/Ca, Li/Mg, Ba/Ca and linear extension records were generated from two nearshore sites (Ward and Herald islands) and sites located further offshore (Airlie and the Montebello islands) in an attempt to resolve variations in the spatial impacts of these recent thermal stress between the different reef environments. The nearshore coral sites were located within 5–10 km of where substantial dredging operations took place between April 2013 and February 2015. As such, in addition to the resolving differences in sediment outputs from the Ashburton River, this allowed us to test the effectiveness of Ba/Ca ratios to resolve recent dredging disturbances in the region. Lastly, two long-term (75–150 yr) records of Sr/Ca, Li/Mg and Ba/Ca were also generated from the offshore coral records to provide a context of historical environmental variability for the region and to constrain the likely environmental drivers responsible for recent widespread declines in reef health.

7.2.2 METHODS

Coral core collection and sampling

The University of Western Australia (UWA) collected coral cores (*Porites* sp.) from the Montebello Islands in June 2014. Additional coral cores were collected from study sites to the south (~100 kms): Airlie Is., Herald Is. and Ward Reef in January 2015 as part of a joint fieldwork expedition in Onslow with The Department of Biodiversity, Conservation and Attractions (DBCA) (Figure 7.2.1). Once back at UWA, the collected cores were sliced along their long-axes and left to soak overnight in a 1:1 NaOCL solution to remove superficial (non-skeletal bound) organic contaminants. Following this, the slices were rinsed repeatedly in an ultrasonic bath and then dried in an oven. For each core, the slices with the most prominent and consistent growth apexes were x-rayed and selected for trace element analysis
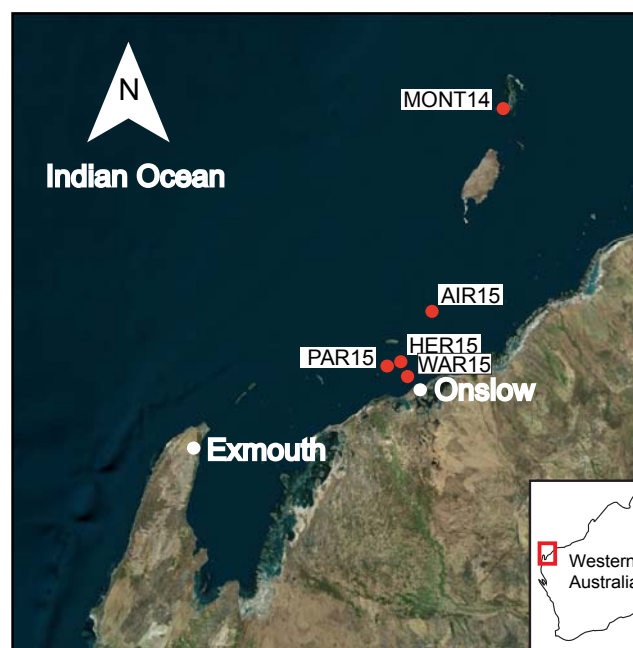
Figure 7.2.1 Location of reef sites where coral cores were collected during January 2015 and April 2014 (red circles). Abbreviations as follows: PAR15 (Paroo), WAR15 (Ward Is.), HER15 (Herald Is.), AIR15 (Airlie Is.) and MONT14 (Montebello Is.).
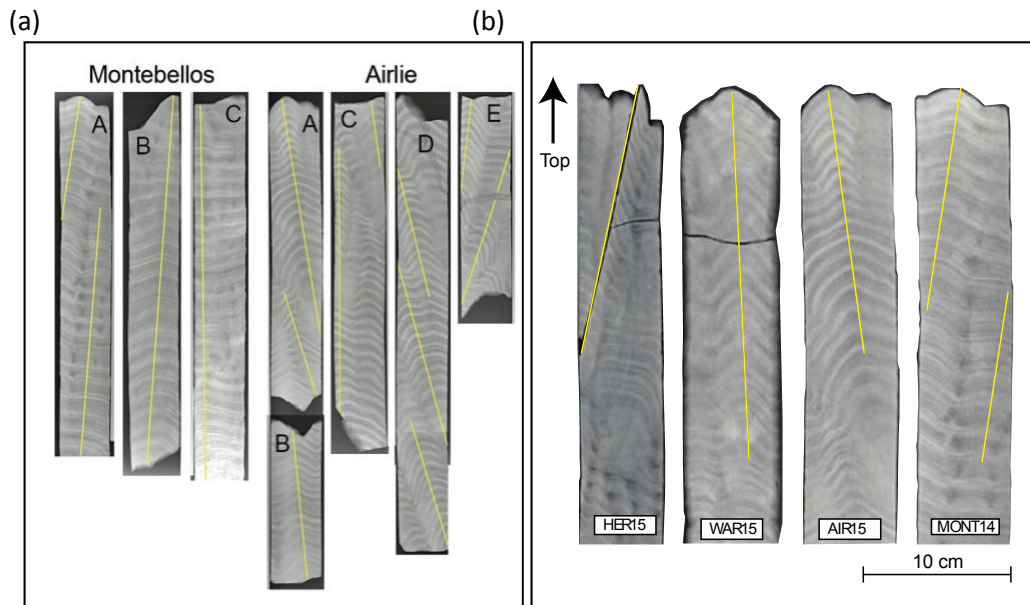
Figure 7.2.2 (a) X-rays of the coral core slices for the long-term annual Sr/Ca and Li/Mg records. The coral slices were sampled continuously at ~1-1.6cm increments along major growth axes (see yellow lines). (b) X-rays of the coral core slices that were selected for high-resolution (~monthly) analysis of Sr/Ca and Li/Mg ratios. Sample powders were collected at 1 mm (HER15, WAR15, AIR15) and 2mm (MONT14) increments along major growth axes (yellow lines).

Annual and high-resolution (~monthly) sampling was undertaken on two, long cores (~1.5–2 m) collected from Airlie Island and the Montebello Islands (Figure 7.2.2). Additional high-resolution sampling was then done on the two additional cores collected from Herald Island and Ward Reef (Figure 7.2.2b). For the annual samples, sample powders were collected along growth apexes at intervals determined by calculating average extension rates over each section of the core record. These sampling intervals ranged from 14.9 to 16.4 mm for the Montebello core and between 9.1–10.3 mm for the Airlie record. For the high-resolution records, the Airlie, Herald and Ward core slices were sampled along maximum growth axes at fixed 1 mm increments. The Montebello core showed markedly higher average annual extension rates and was sampled at 2 mm increments (Figure 7.2.2b). In total, 140 annual samples were collected from the Airlie core and 75 annual samples were collected from the Montebello core. For the high-resolution records, 190 samples were collected from the Airlie core, 90 samples from the Montebello core, 180 samples from the Herald core and 240 samples from the Ward core. Lastly, following the initial analyses of the high resolution records, sample powders collected from the top ~2 cm of the Airlie coral slice were bleached (in addition to the initial bleaching of the coral slabs) and re-analysed to test if anomalous Ba/Ca enrichment observed in this section of the record might have been due to organic contamination from the coral tissue later.

ICP-MS analysis for Sr/Ca, Li/Mg and Ba/Ca

All geochemical analyses were performed at the Advanced Geochemical Facility for Indian Ocean Research (AGFIOR) located at UWA. Sample powders were weighed to 10 ± 0.2 mg and dissolved in a nitric acid solution. This solution was then diluted through two stages to produce a 100 ppm [Ca^{2+}] solution for Li/Mg analyses and a 10 ppm [Ca^{2+}] solution for Sr/Ca and Ba/Ca analyses (see Holcomb et al. 2015). All trace element analyses were performed using a Thermo Fisher Scientific (Bremen, Germany) X Series II quadrupole inductively coupled plasma mass spectrometer (ICP-MS) using the standard Xt interface and plasma screen fitted at the University of Western Australia AGFIOR laboratory. For the high resolution sampling (excl. MONT14), long-term reproducibility (RSD) was

derived from the repeated analyses of a gravimetrically prepared standard and yielded up to 0.4% for Sr/Ca (n=74), 1.3% for Li/Mg (n=74) and 1.1% for Ba/Ca (n=74). Lastly, following the initial high resolution analyses, the remaining sample powders collected from the top ~2 cm of the Airlie coral slice were bleached (in addition to the initial bleaching of the coral slabs) and re-analysed to test if anomalous Ba/Ca enrichment observed in this section of the record might have been due to organic contamination from the coral tissue later.

Te/Ca age model determination

ANNUAL RECORDS

Age models for the annual Te/Ca records from Airlie and Montebello islands were determined by sampling each core section (i.e. A-C for Montebello's and A-E for Airlie, Figure 7.2.2a) at fixed intervals, equal to the average annual extension rate for each section. Average annual extension rates were calculated from the core x-rays by counting the total number of years (i.e. pairs of light and dark coloured bands) in each core section and dividing this by the total length of each section. It is important to note that this 'fixed interval' approach to annual sampling is considerably easier than trying to specifically sample the full length of calcification for each year, which can be very difficult given the ambiguities in interpretation of the density banding patterns of core x-rays. However, this approach can introduce warm and cool biases in individual measurements when sampling intervals drift across years due to slight changes in extension rates within each section.

HIGH RESOLUTION RECORDS AND LINEAR EXTENSION

Age models for each of the high-resolution datasets (which included distance from the top of the core) were determined using *Analyseries* software (see Paillard et al. 1996) by aligning the seasonal Sr/Ca maxima and minima in each of the records with minima and maxima in high-resolution (0.02° × 0.02°), remotely sensed SST records obtained for each core site: IMOS – SRS Satellite - L3S – 1 month composite- day/night composite, available at: https://portal.aodn.org.au/search. The accuracy of these remotely sensed SST record were verified with approximately three years of overlapping, monthly averaged *in situ* SST data collected from each coral site between June 2011 and March 2016. For all the core sites, the *in situ* SST data showed excellent agreement with the satellite records (±0.3°C, $R^2 > 0.97$) indicating they were suitable for determination of the age model and the calibration of the Sr/Ca-SST and Li/Mg-SST proxies for each record. Lastly, Te/Ca datasets for each site were interpolated to monthly resolution to produce final, high-resolution Te/Ca records and corresponding records of linear extension for each core site. Annual extension measurements were calculated from the interpolated Sr/Ca records for the period from July to June of each year. By calculating extension rates between winter-time Sr/Ca maxima (SST minima), this effectively confined the effects of thermal stress events to single measurements. To accommodate for difference in mean extension rates between the different cores, annual extension rates were standardised for each record to compare differences in the calcification responses between the reef sites to the recent widespread thermal stress events.

Calibration of the Sr/Ca-SST and Li/Mg-SST proxies

The high resolution, remotely sensed SST records (described above) were used to calculate 'bulk' Sr/Ca-SST and Li/Mg-SST linear regressions for each of the core records. These 'bulk' regressions included all the Sr/Ca and Li/Mg data for each of the core records, however, omitted anomalous Sr/Ca and Li/Mg data recorded during the summers of 2010/11 and 2013, if the slopes of the linear regressions calculated across these short term periods: ~October 2010 to June 2011 and January 2013 to June 2013, were significantly different from the longer-term linear regressions. In addition, for the Ward Island record, the linear regression from January 1997 to May 2000 was observed to be

significantly different from the longer-term regression and thus this period was also omitted from the calculation of the respective bulk Sr/Ca-SST and Li/Mg-SST calibrations. Similarly, for the Herald Island record, anomalous Sr/Ca and Li/Mg ratios were observed from the beginning of the record, from around 1996 to 2000 and were also excluded for the calculation of the bulk calibration.

The annual Sr/Ca and Li/Mg records from Airlie and the Montebello islands were calibrated using the respective 'bulk' Sr/Ca-SST and Li/Mg-SST calibrations from the high-resolution records. Sr/Ca and Li/Mg anomalies were calculated for both records based on mean values recorded across the 1961-1990 period (in accordance with the international standard for the calculation of climate averages) (Jones et al. 1999; Jones and Hulme 1996). Long-term warming trends in both records were compared against a single long-term offshore SST anomaly record: Extended Reconstructed Sea Surface Temperature (ERSST v5) record, for the co-ordinates: 21°S, 115°E (http://apdrc.soest.hawaii.edu/las/v6/constrain?var=960) and also based on mean values from 1961–1990, to assess for differences in long-term warming trends between the two reef environments.

7.2.3   RESULTS

Annual Sr/Ca, Li/Mg and Ba/Ca records

The annual core record from Airlie Island showed an overall decrease in Sr/Ca ratios (-0.048 mmol/mol, R^2= 0.07, p < 0.01) for the 139 years from 1875 to 2014 which equated to an increase in temperature of 0.9°C (Figure 7.2.3a). In contrast, the Li/Mg record showed no significant long-term change in values across this same period (Li/Mg = -0.001 mmol/mol, R^2 < 0.01, p > 0.05, Figure 7.2.3b). The trend in Sr/Ca-SSTs was very similar to the 0.8°C increase recorded by the ERSST record from 1875-2014 (R^2 = 0.22, p < 0.01). Both the Sr/Ca and Li/Mg anomaly records showed inter-annual variability (equivalent to ~4°C) that was about twice that than inter-annual variability recorded in the offshore ERSST record (~2°C). However, the Sr/Ca and Li/Mg records were only weakly correlated with one another (R^2 = 0.21, p <0.05), even when long-term trends were removed (de-trended)(R^2 = 0.23, p < 0.05). For the Ba/Ca record, values for the top two years (2012 to 2014) were omitted from the analysis due to anomalous enrichment from the coral tissue layer (Alibert and Kinsley 2008). The Ba/Ca record showed moderate variability over the 1875–2012 (mean=3.3 ± 1.1, n=138, 2σ), with the highest values recorded between 1955 and 1990 (mean=4.1 ± 0.8, n=35). For the recent period, from 1991 to 2012, mean Ba/Ca values (3.1 ± 0.3, n= 22) were the same as their pre ~1950s values (3.1 ± 0.3, n=80) suggesting minimal anthropogenic influences on sediment transport to the outer reefs for the recent period.

For the annual Montebello core record, strong decreases in mean Sr/Ca (-0.19, R^2=0.5, p<0.01) and Li/Mg ratios (-0.2, R^2=0.5, p<0.01) were observed across the 75 years from 1939–2014 (Figure 7.2.4b). These decrease in Sr/Ca and Li/Mg values equated to increases in mean temperatures of 3.6°C and 3.2°C respectively, from the bulk high-resolution Sr/Ca-SST and Li/Mg-SST calibrations (Figure 7.2.5g, Figure 7.2.6g) and greatly exceeded the magnitude of warming recorded by the offshore ERSST record across the same period (+0.7°C, R^2=0.21, P<0.01, see red lines in Figure 7.2.4). The de-trended Sr/Ca and Li/Mg records showed similar inter-annual and decadal SST variability at the coral site (~3°C). However, unlike the Airlie record, the Montebello Sr/Ca and Li/Mg records were strongly correlated with one another (R^2=0.84, p<0.01), although a slightly weaker correlation was observed when both records were de-trended (R^2=0.69, p<0.01). The Montebello Ba/Ca record showed strong variability over the 1939–2012 period (top two years omitted) (mean = 5.3 ± 3.3, 2σ, n = 76). Similar to the Airlie record, the Ba/Ca record showed the lowest values before ~1950 (mean

= 3.3 ± 1.3, n = 11) and the highest values during the late 1950's (Ba/Ca values up to 10.9), 1980's and 90's (Ba/Ca up to ~7). Unlike the Airlie record, baseline Ba/Ca values appeared to have increased gradually over the duration of the core record with values reaching a plateau around the year 2000 and remaining steady up until 2012 (mean from 2000 to 2012 of 5.8 ± 1.8, n=15).
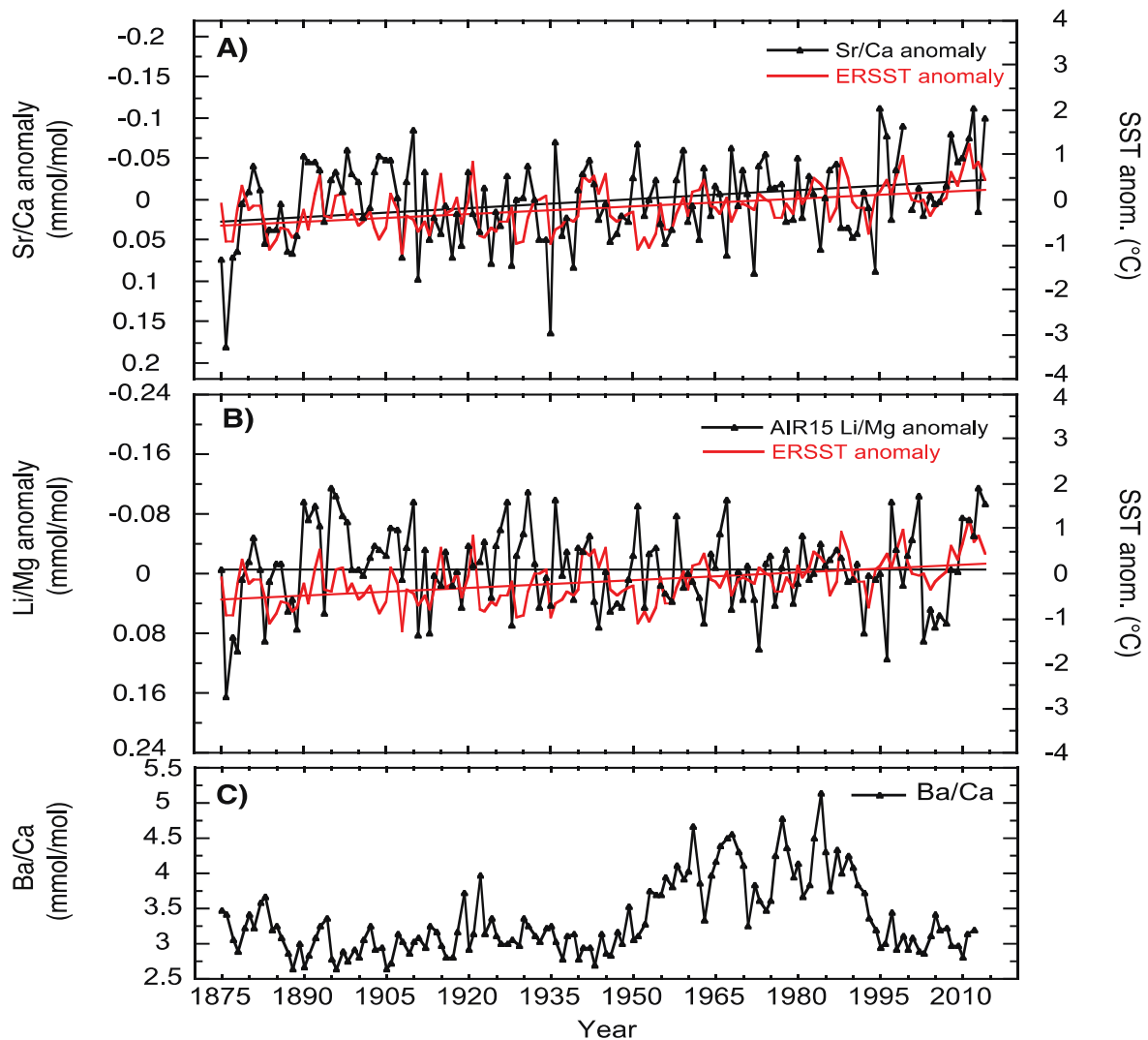
Figure 7.2.3 Long-term Sr/Ca (A) and Li/Mg (B) anomalies, and the Ba/Ca (C) record, determined from the Airlie Island annual coral record. The SST anomaly (y2) axes in plots A and B were calibrated using the linear regression relationships for the bulk Sr/Ca-SST and Li/Mg-SST relationships shown in Figure 7.2.5 and 6 and thus also show Sr/Ca and LI/Mg anomalies in temperature terms. The Sr/Ca record showed a long term warming trend (0.6° 100yr^{-1}, R^2 = 0.07, p < 0.01, see black line) that was highly consistent with the instrumental temperature record (i.e. 0.6° 100yr^{-1}, R^2 = 0.22, p < 0.01, see red line) whereas the Li/Mg record showed no significant long-term trend in values for the same period. For the annual Ba/Ca record, values between ~1950 and 1990 were ~1.5 times higher than those after 1990, which could reflect major land uses changes in the region after the 1950s that resulted in increased terrestrial sediment transport to outer reefs.
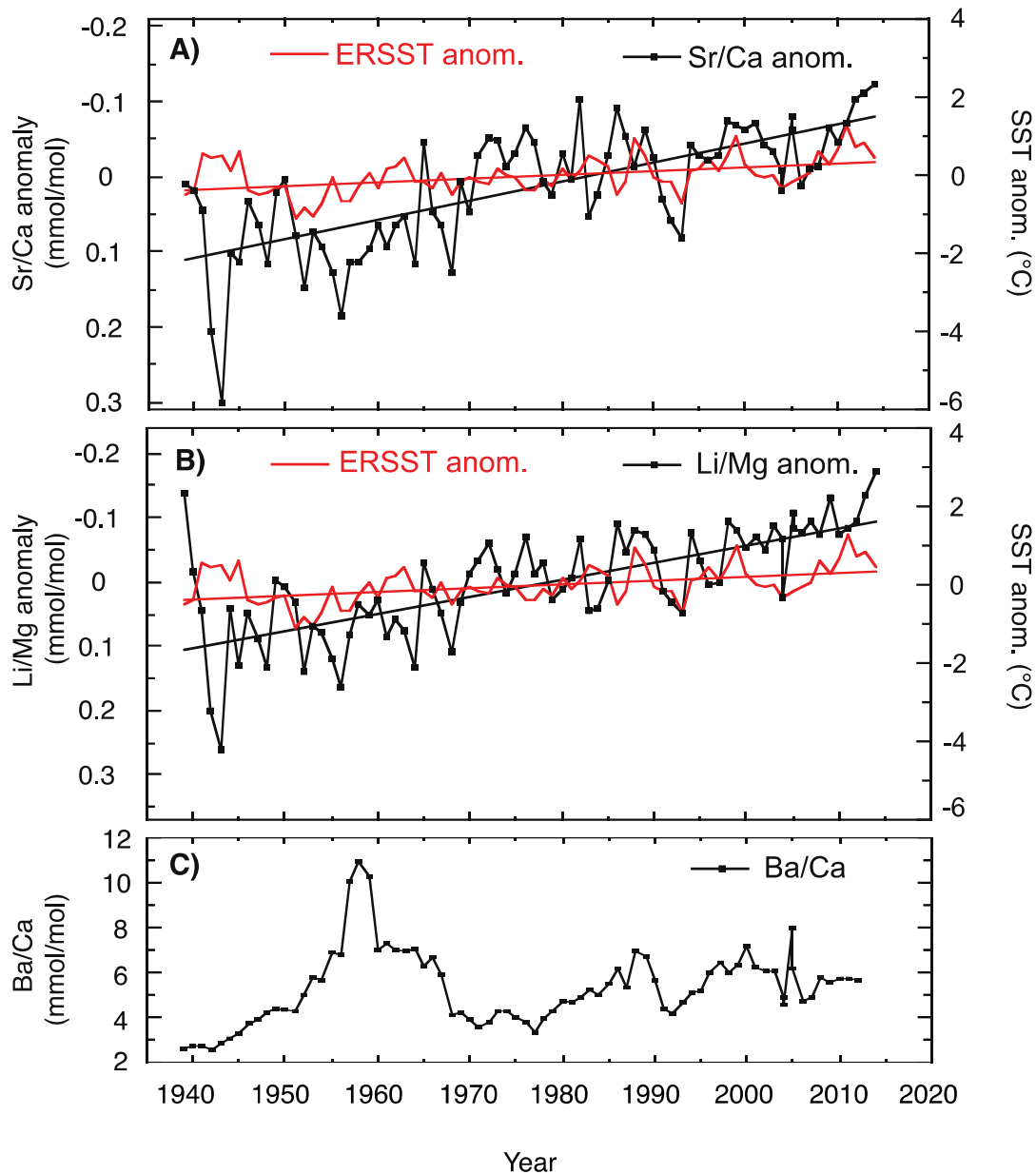
Figure 7.2.4 Long-term Sr/Ca (A) and Li/Mg (B) anomalies, and the Ba/Ca (C) record, determined from the Montebello Island annual coral record. The SST anomaly (y2) axes in plots A and B were calibrated using the linear regression relationships for the bulk Sr/Ca-SST and Li/Mg-SST relationships shown in Figure 7.2.5 and Figure 7.2.6 and thus, also show Sr/Ca and LI/Mg anomalies in temperature terms. The Sr/Ca and Li/Mg records showed similar strong warming trends (3.6°C, R^2= 0.5, $p < 0.01$ and 3.2°C, R^2 = 0.5, $p < 0.01$, respectively) that were much stronger than that recorded by the offshore ERSST record (0.7°C). The Ba/Ca record showed higher mean Ba/Ca values than the Airlie record which could be indicative of increased mixing of deeper waters at the Montebello coral site.
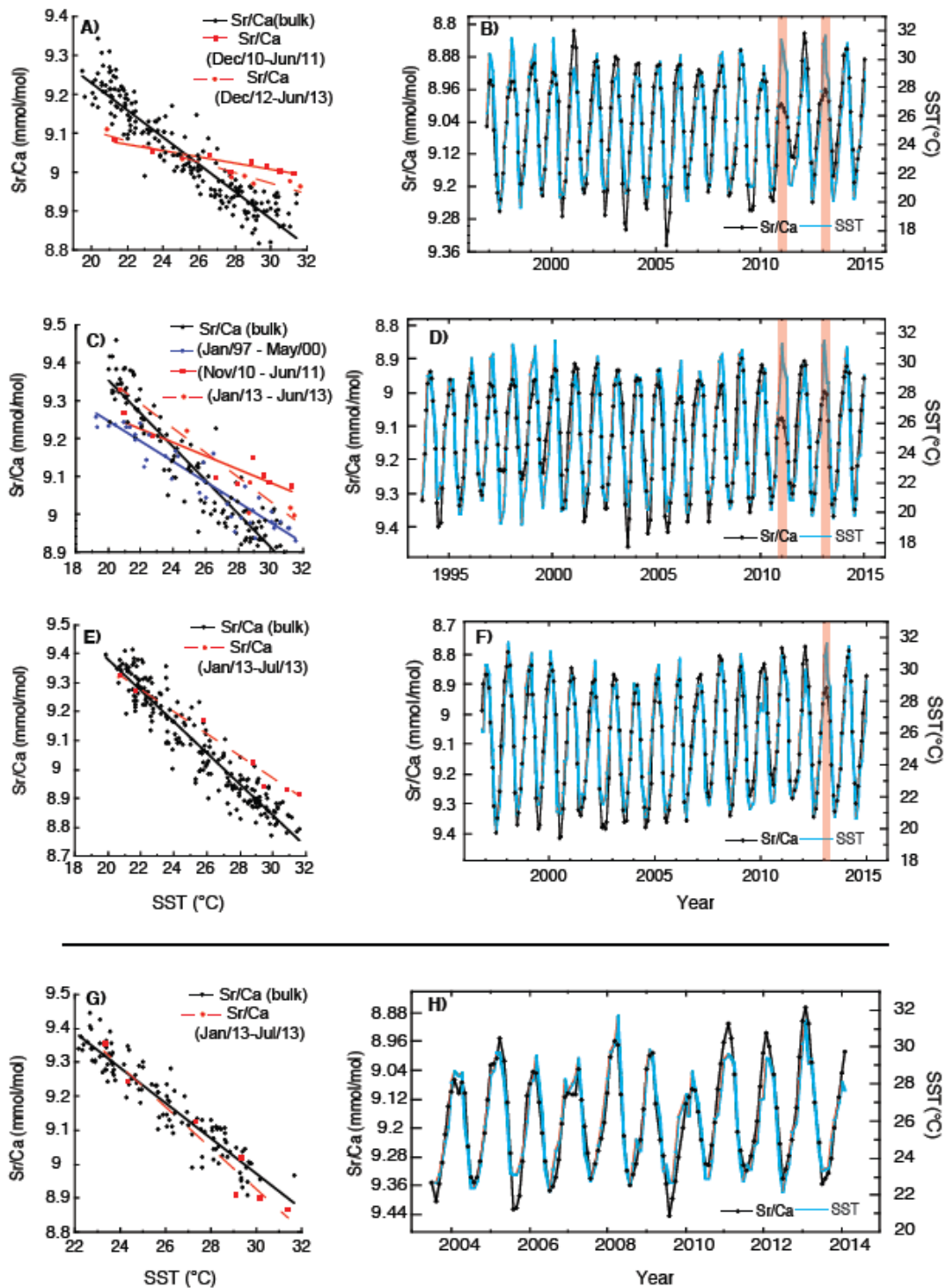
Figure 7.2.5 High-resolution Sr/Ca records for the Herald Island (A-B), Ward Island (C-D), Airlie Island (E-F) and Montebello Island (G-H) coral core records. The linear regressions of the bulk Sr/Ca-SST correlations (see black lines, A, C, D, E) were used to calibrate the y and y2 axes for the line plots (B, D, F, H) to show Sr/Ca-SSTs for each of the core records. The vertical shaded rectangles (red) show episodes of suspected coral bleaching at the Herald, Ward and Airlie coral sites as indicated by significant short term changes in the slope of the linear regressions for the short term Sr/Ca-SST calibrations calculated for the summers for 2010/11 and 2012/13. For the Ward Island record, an anomalous decrease in the seasonality (amplitude) of the Sr/Ca record was observed across a ~3 year period from January 1997 to May 2000 (D), which also corresponded with a significant decline in the slope of the Sr/Ca-SST regression for this period (see blue line, C).
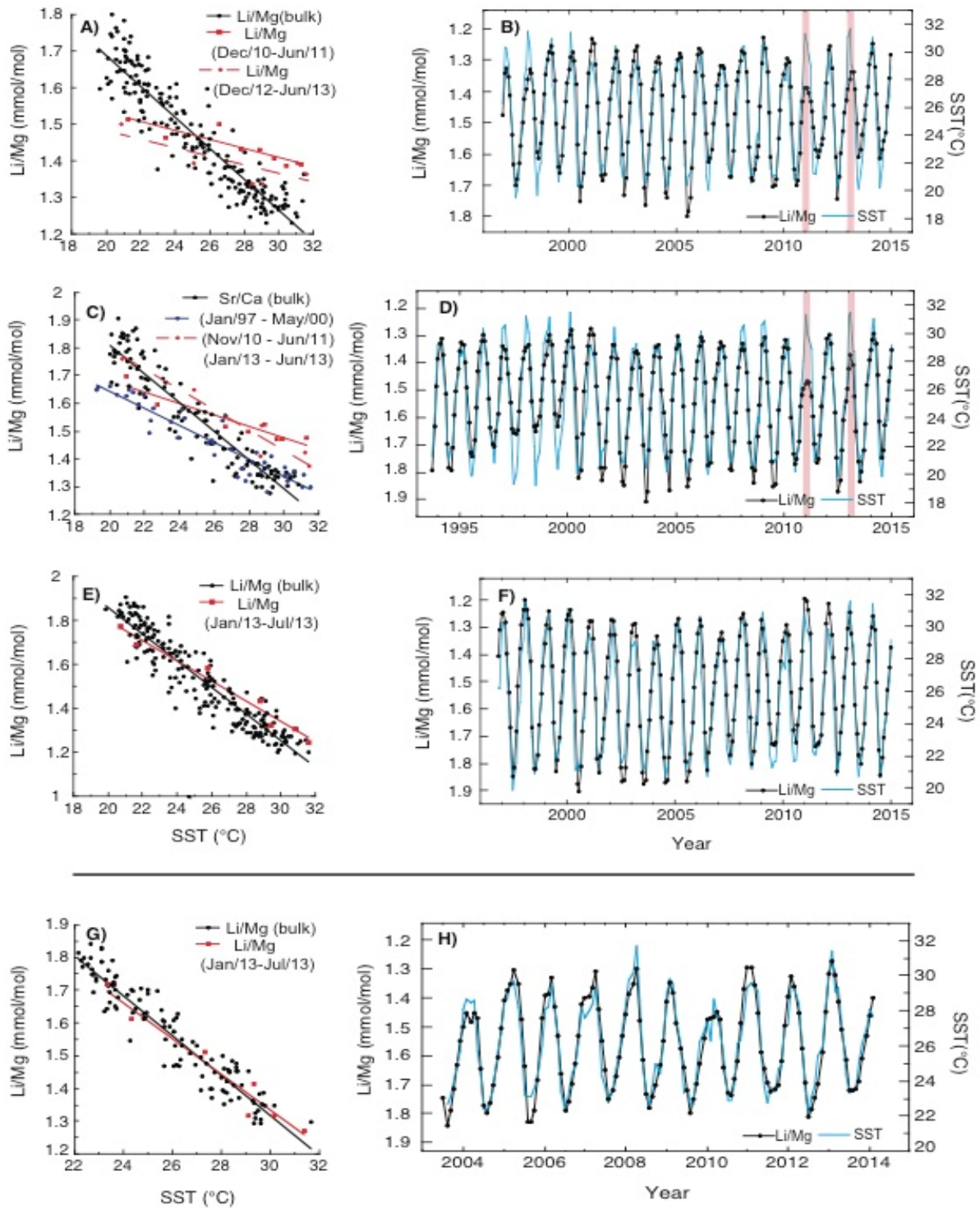
Figure 7.2.6 High-resolution Li/Mg records for the Herald Island (A-B), Ward Island (C-D), Airlie Island (E-F) and Montebello Island (G-H) coral core records. The linear regressions of the bulk Li/Mg-SST correlations (see black lines, A, C, E, G) were used to calibrate the y and y2 axes for the line plots (B, D, F, H) to show LI/Mg-SSTs for each of the core records. The vertical shaded bands (red) highlight periods where significant short-term (~6 months) shift in the slope of the Li/Mg-SST regressions occurred during the summers of 2010/11 and 2012/13, suggesting thermal stress significantly impacted the coral host during these anomalously warm periods. For the Ward Island record, an anomalous decrease in the seasonality (amplitude) of the Li/Mg record was observed across a ~3 year period from January 1997 to May 2000 (D), which also corresponded with a significant decline in the slope of the Li/Mg-SST regression for this period (see blue line, C).

High resolution Sr/Ca and Li/Mg

Table 7.2.1 Linear regression coefficients for the Sr/Ca-SST and Li/Mg-SST correlations calculated for different periods in each of the 4 high-resolution records. The bulk calibrations, which were used to estimate temperatures from each of the Sr/Ca and Li/Mg records, are shown in bold. The regressions with an asterix (*) indicate they were not significantly different from the bulk calibrations.

Period	n	SST = m × (Sr/Ca) + c				SST = m × (Li/Mg) +b			
		m (±95%)	c (±95%)	r^2	p	m (±95%)	c (±95%)	r^2	p
Ward Island									
Bulk Jun/00 - Oct/10	**125**	**-0.044 (±0.003)**	**10.24 (±0.08)**	**0.88**	**<0.01**	**-0.052 (±0.004)**	**2.841 (±0.088)**	**0.88**	**<0.01**
Nov/10 - June/11	8	-0.017 (±0.009)	9.605 (±0.236)	0.8	<0.01	-0.020 (±0.007)	2.086 (±0.202)	0.89	<0.01
*Jan/13 – Jun/13	6	-0.032 (±0.012)	9.994 (±0.328)	0.93	<0.01	-0.036 (±0.014)	2.514 (±0.395)	0.93	<0.01
Jan/97 - May/00	41	-0.027 (±0.003)	9.774 (±0.081)	0.88	<0.01	-0.031 (±0.004)	2.265 (±0.092)	0.89	<0.01
Oct/93 – Jan/15 (Entire record)	256	-0.038 (±0.002)	10.096 (±0.055)	0.83	<0.01	-0.045 (±0.003)	2.668 (±0.066)	0.83	<0.01
Herald Island									
Bulk Dec/96 - Oct/10, July/11 - Oct/12, Jun/13 - Jan/15	**203**	**-0.035 (±0.002)**	**9.933 (±0.048)**	**0.87**	**<0.01**	**-0.042 (±0.002)**	**2.532 (±0.061)**	**0.86**	**<0.01**
Oct/10 – Jun/11	9	-0.008 (±0.003)	9.250 (±0.088)	0.86	<0.01	-0.012 (±0.006)	1.774 (±0.176)	0.78	<0.01
Dec/12 – June/13	7	-0.014 (±0.004)	9.381 (±0.120)	0.93	<0.01	-0.012 (±0.012)	1.721 (±0.327)	0.57	<0.05
*Dec/96 – Jan/15 (Entire record)	218	-0.033 (±0.002)	9.875 (±0.051)	0.83	<0.01	-0.039 (±0.003)	2.463 (±0.064)	0.82	<0.01
Airlie Island									
Bulk Nov/96-Dec/12, Aug/13 – Jan/15	**212**	**-0.054 (±0.003)**	**10.458 (±0.066)**	**0.89**	**<0.01**	**-0.060 (±0.003)**	**3.056 (±0.078)**	**0.88**	**<0.01**
*Oct/10 – Jun/11	9	-0.047 (±0.013)	10.255 (±0.348)	0.93	<0.01	-0.052 (±0.019)	2.808 (±0.538)	0.88	<0.01
Jan/13 – Jul/13	7	-0.039 (±0.003)	10.133 (±0.066)	0.98	<0.01	-0.046 (±0.009)	2.724 (±0.253)	0.97	<0.01
*Nov/96 – Jan/15 (Entire record)	219	-0.053 (±0.003)	10.431 (±0.066)	0.89	<0.01	-0.059 (±0.003)	3.034 (±0.076)	0.88	<0.01
Montebello Islands									
Bulk Jul/03 – Dec/12, Aug/13 – Feb/14	**121**	**-0.052 (±0.004)**	**10.537 (±0.094)**	**0.88**	**<0.01**	**-0.061 (±0.004)**	**3.148 (±0.097)**	**0.9**	**<0.01**
*Oct/10 – Jun/11	9	-0.055 (±0.019)	10.563 (±0.528)	0.89	<0.01	-0.055 (±0.024)	2.957 (±0.672)	0.84	<0.01
*Jan/13 – Jul/13	7	-0.061 (±0.017)	10.751 (±0.471)	0.95	<0.01	-0.054 (±0.014)	2.967 (±0.405)	0.95	<0.01
*Jul/03 – Feb/14 (Entire record)	128	-0.053 (±0.003)	10.562 (±0.090)	0.89	<0.01	-0.060 (±0.003)	3.136 (±0.091)	0.91	<0.01

The high-resolution (~monthly), coral-core Sr/Ca and Li/Mg records from Herald Is., Ward Is, Airlie Is., and Montebello Is. are shown, alongside their respective SST correlations, in Figure 7.2.5 and Figure 7.2.6. Table 7.2.1 provides a summary of the all the linear regression coefficients for the Sr/Ca-SST and Li/Mg-SST correlations calculated across different periods in each of the records,

including those shown in Figure 7.2.5 and Figure 7.2.6. The linear regressions of the 'bulk' Sr/Ca-SST and Li/Mg-SST correlations for each core record (see black lines, Figure 7.2.5 and Figure 7.2.6; a, c, e, g) showed good agreement with the high-resolution (IMOS) SST records compiled for each core site (R^2 = 0.87-0.89 for Sr/Ca and 0.86–0.9 for Li/Mg, Table 7.2.1). Excluding anomalous values recorded during the summers of 2010/11 and 2012/13 in the core records, the standard deviation of the monthly temperature residuals for each record (i.e. RMSE), showed temperature estimates derived from the bulk Sr/Ca-SST and Li/Mg-SST calibrations for each of the core records were mostly within (±1S.D): 1.3°C of the SST record for the Herald and Ward Island Sr/Ca-SST and Li/Mg-SST records, 1.1°C and 1.2°C of the SST record for the Airlie Is. Sr/Ca-SST and Li/Mg-SST records and 0.9°C and 0.8°C of the SST record for the Montebello Is. Sr/Ca-SST and Li-Mg-SST records.

For the Airlie and Montebello core records, no significant short-term changes in Sr/Ca-SST and Li/Mg-SST correlations were observed outside of periods of previously reported coral bleaching from the Onslow region (i.e. summers of 2010/11, 2012/13). However, for the Herald and Ward records, various short-term (from ~6 months to 3 years) decreases in the seasonality (amplitude) of Sr/Ca and Li/Mg maxima and minima were observed during the late 1990's. These anomalous short-term changes in Sr/Ca and Li/Mg ratios corresponded with significant declines in the slope (up to ~50%) for Sr/Ca-SST and Li/Mg-SST regressions for both core records. This, in-turn, led to Sr/Ca-SST's and Li/Mg-SST's underestimating the instrumental SST record by up to ~3°C during this period when the bulk calibrations were applied. Although these anomalous periods were excluded from the calculation of the 'bulk' Sr/Ca-SST and Li/Mg-SST calibration for Herald and Ward records, they gave rise to markedly weaker total Sr/Ca-SST and Li/Mg-SST calibrations (R^2=0.82-0.83, see "entire record" coefficients, Table 7.2.1) compared to the Airlie and Montebello records (R^2=0.88-0.91).

CORAL BLEACHING EVENTS (2010/11 AND 2012/13)

For the summer of 2010/11, the two nearshore sites (Herald Is. and Ward Is.) showed anomalous, short term increases in Sr/Ca and Li/Mg ratios, which led to SST estimates from the bulk calibrations underestimating the SST record for the two sites by up to ~5°C for Sr/Ca (Figure 7.2.5b, d) and ~4.5°C for the Li/Mg records between October 2010 to June 2011 (Figure 7.2.6b, d). These increases in Sr/Ca and Li/Mg ratios corresponded with strong decreases (60–80%) in the slopes of the linear regressions of the Sr/Ca-SST (Figure 7.2.5a, c) and Li/Mg-SST correlations (Figure 7.2.6a, c) calculated from between October 2010 to June 2011 (Table 7.2.1). The SST records for the two sites showed the summer of 2010/11 was amongst the warmest on record (+1.2°C and +1°C above the average calculated from 1996–2015) with average SSTs of 29.9°C and 29.7°C recorded for the three months from Dec to Feb for the two sites respectively. In contrast, the SST records from Airlie Is. and Montebello Is. showed slightly cooler average SSTs (29.6°C and 28.9°C respectively) and weaker SST anomalies (+0.8°C–0.9°C) during the summer of 2010/11 and no significant, short-term declines in the slope of Sr/Ca-SST and Li/Mg-SST correlations were observed during this period in either record.

For the summer of 2012/13, similar increases in Sr/Ca and Li/Mg ratios were observed in the Herald and Ward island records and also in the Airlie Island Sr/Ca record, for the period from December/January 2012/13 to June 2013 in each of the records. The SST records showed average SSTs were warmer at all four coral sites during the summer of 2012/13 than during the summer of 2010/11: ranging from 30°C at Ward and the Montebello's (SST anomalies of +1.2°C and 1.9°C respectively) to 30.2°C at Herald and Airlie islands (SST anomalies of +1.5°C at both). Despite this, temperature residuals between the Sr/Ca-SST, Li/Mg-SST and the SST records for the two sites between January and June 2013 were weaker than those recorded during the summer of 2010/11 (i.e. up to 3.8°C for Sr/Ca-SSTs and 3.2°C for Li/Mg-SSTs for both records). Similarly, the declines in the slope of Sr/Ca-SST and Li/Mg-SST regressions observed in both records across this period were also weaker than those observed during the summer of 2010/11 (i.e. 60–70% for Herald and ~30% for Ward). In particular, the decline in slope of the Sr/Ca-SST and Li/Mg-SST observed between

January and June 2013 for the Ward. record was not significantly different (p>0.05) from the bulk calibration. However, when the period used to calculate the short-term regression for the Ward record for the summer of 2012/13 was shortened to include only the warmest months (i.e. Jan-April), significantly different Sr/Ca-SST and Li/Mg-SST linear regressions could be obtained. For the Airlie record, Sr/Ca-SST residuals with the SST record for the coral site were up to 2.7°C from January to June 2013, which corresponded with a ~30% decline in the slope of the linear regression of the short term Sr/Ca-SST correlation calculated for this same period. Interestingly, the linear regression of the Li/Mg-SST correlation across this same period was also significantly different from the bulk correlation. However, the Li/Mg–SST temperature residuals recorded across this period were markedly weaker (up to 1.1°C) and not outside the normal range of precision for Li/Mg-SST estimates across the entire record.

High resolution coral Ba/Ca records
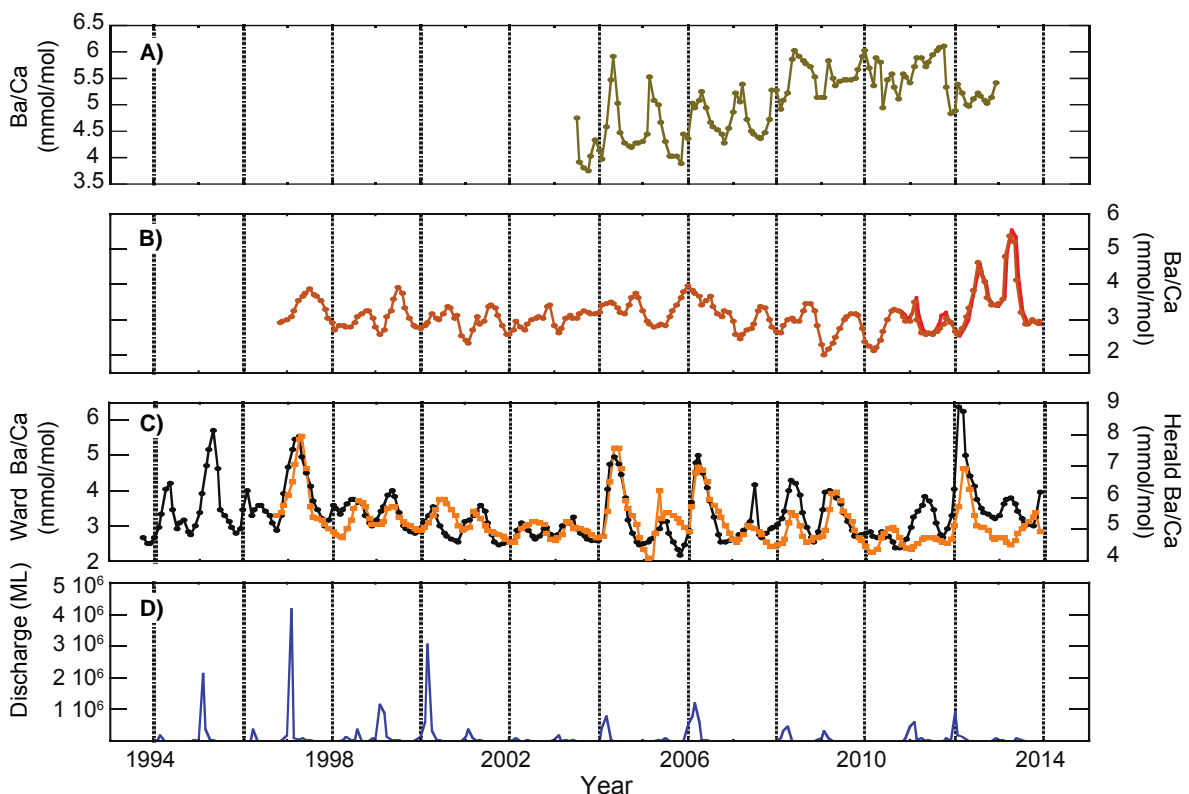
Figure 7.2.7 Seasonal Ba/Ca records from the Montebello (A), Airlie Island (B), Ward and Herald (C, black and orange lines respectively) coral core records and; a river discharge for the Ashburton River, Onslow (D) which was based on ~monthly water sampling at Nanutarra Bridge. Repeat analyses of sample powders collected from the top ~2 cm of the Airlie core after additional bleaching in NaOCL are shown with the solid red line (B).

Figure 7.2.7 shows the high-resolution Ba/Ca records for each of the core sites (A-C) and monthly discharge recorded from Nanutarra Bridge (D): one of the major tributaries which feeds into the Ashburton River, located ~200 km inland from Onslow (Nanutarra Department of Water and Environmental Regulation, http://kumina.water.wa.gov.au/waterinformation/wir/reports/publish/706003/g02.htm). The top 12 months of each Ba/Ca record showed highly anomalous Ba/Ca enrichments due to tissue layer contamination of the samples and were omitted from each of the records. The Herald and Ward Island records (Figure 7.2.7c, see orange and black lines respectively) showed the strongest seasonal and inter-annual variability in Ba/Ca ratios and higher absolute Ba/Ca ratios compared to the core

records from the sites further offshore: Airlie Is (Figure 7.2.7b) and Montebello Is. (Figure 7.2.7a). The timing of acute Ba/Ca spikes (enrichments) in the Herald, Ward and Airlie records was observed to be largely consistent with the discharge record from the Ashburton River. Many of the larger Ba/Ca peaks were observed to correspond with periods where river discharge was the highest (i.e. discharge greater than ~1.5×10^6 ML). However, Ba/Ca peaks of similar magnitude were also observed to occur where significant river discharge occurred following a period of prolonged dry weather (e.g. the peaks during the summer of 2004). A very strong agreement was observed between the Herald and Ward Ba/Ca records, which showed near identical seasonal and inter-annual variability (R^2=0.5, p<0.01, n=207). No significant correlations were observed between the Airlie and Ward, or the Airlie and Herald Ba/Ca records. However, when a phase adjustment of (-3 to -4 months) was applied to the Airlie record, most of the Ba/Ca peaks were observed to align with those in the Herald and Ward records and significant correlations were observed: Airlie vs Ward, R^2=0.2, p<0.01, Airlie vs Herald, R^2=0.17, p<0.01. The Montebello record showed the smallest range of Ba/Ca ratios (i.e. from 4–6, Figure 7.2.7a) and smoother Ba/Ca enrichments compared to the cores collected from sites closer to shore. Unlike the other records, the record from the Montebello's showed a significant trend of increasing values over the 2004–2013 period. A weak correlation was observed between the Airlie and Montebello record (R^2=0.12, p<0.01), which did not increase if phase adjustments were applied to either record. Lastly, the re-sampling of the anomalous top section of the Airlie record (i.e. from 2011 to 2014, see red line, Figure 7.2.7b), where the original sample powders were individually bleached in a 1:1 NaOCl solution and reanalysed for Ba/Ca, showed no difference in Ba/Ca values from the original results (Ba/Ca$_{bleached}$ = Ba/Ca$_{original}$, R^2=0.98, p<0.01).

Linear Extension

Average extension rates (±2σ) calculated from the entire length of each high-resolution core record were: 10.3 ± 3.4 mm.yr^{-1} (Ward Is.), 8.7 ± 2.2 mm.yr^{-1} (Herald Is.), 9 ± 3 mm.yr^{-1} (Airlie is.) and 15.7 ± 3.5 mm.yr^{-1} for the Montebello Is. record. The standardised annual extension data for each core record are shown in Figure 7.2.8. Of the longer extension records (i.e. excluding the Montebello record), only the Airlie record recorded a significant long-term trend in extension rates: (-0.2 mm.yr^{-1} over 1998–2014 period, R^2=0.47, p<0.01). All the records showed strong inter-annual variability (up to ±2σ) although only the Ward and Herald, and Herald and Montebello records were significantly correlated with one another (R^2=0.29, p<0.05 and R^2=0.45, p<0.05 respectively). However, from the year 2010 onwards, the Ward, Herald and Montebello records were all significantly correlated with one another (R^2= 0.55-0.95, p<0.05) and all the records (including Airlie) showed negative calcification anomalies corresponding with the thermal stress events of 2010/11 and 2012/13. For the year 2011 (i.e. extension calculated from July 2010–June 2011 for each record) The Ward, Herald and Montebello. records all showed strong decreases in extension rates from the previous 12 months: decrease of -7.2 mm (to 6.5 mm.yr^{-1}) for Ward, -3.4 mm (7.3 mm.yr^{-1}) for Herald and -2 mm (13.3 mm.yr^{-1}) for the Montebello record; whereas the Airlie record showed a slight increase from the previous 12 months (+2 mm), however still recorded extension rates that were below average (8.8 mm.yr^{-1}). For the following 12 months, from July 2011 to June 2012, extension rates increased from the previous 12 months in all records and were close to mean values: Ward (9.8 mm.yr^{-1}), Herald (10 mm.yr^{-1}), Montebello (15.5 mm.yr^{-1}) and Airlie (9.9 mm.yr^{-1}). Lastly, for the year 2013, for the 12 months from July 2012 to June 2013, strong declines in extension rate were again observed and below average extension rates were recorded at all sites: Herald (8.6 mm.yr^{-1}), Ward (7.1 mm.yr^{-1}), Airlie (6.5 mm.yr^{-1}) and Montebello (13.2 mm.yr^{-1}).
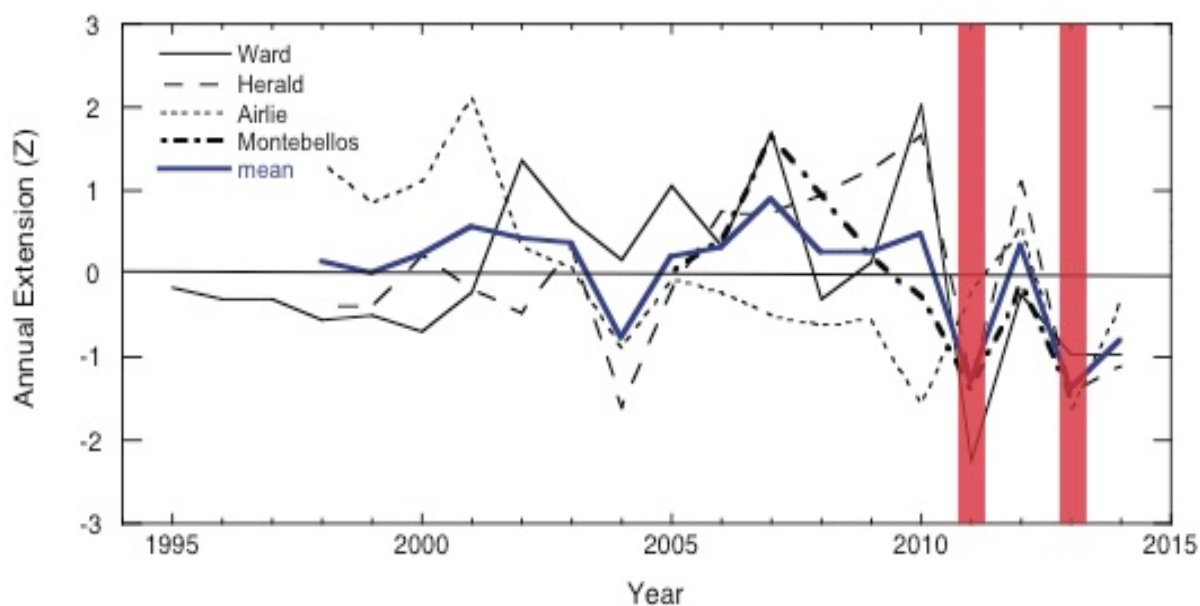
Figure 7.2.8 Standardised annual extension rates for each of the coral core records. Extension rates were calculated from July to June to constrain the effects of thermal stress events to individual measurements. All the records showed strong declines in extension rates corresponding with the timing of thermal stress events during the summers of 2010/11 and 2012/13 (vertical red bands), which, for Herald, Ward and Airlie (2012/13 only) were also accompanied by anomalous increases in Sr/Ca and Li/Mg ratios in the high resolution records.

7.2.4 DISCUSSION

Thermal stress impacts on coral reefs in the Onslow region

Unlike on the east coast of Australia, which has shown recurrent widespread coral bleaching events since the late 1990's (Hughes et al. 2017; Berkelmans et al. 2004; Berkelmans et al. 1999), the first documented incidence of widespread coral bleaching from the central region of WA only occurred during the summer of 2010/11 (Feng et al. 2013; Moore et al. 2012). Since then, another major widespread coral bleaching event during the summer of 2012/13 (up to ~60% of all corals bleached) (Lafratta et al. 2016) resulted in further degradation of the shallow reef environments around Onslow with widespread reductions in coral cover and changes in reef community structures reported (Lafratta et al. 2016). Shortly following this latter event, dredging for the Wheatstone Project commenced in April 2013. This was Australia's largest single capital dredging project to date, and involved the excavation and relocation of some ~30 Mm^3 of substrate to facilitate new shipping tanker LNG exports from Onslow Harbor. Dredging impacts in the region were closely monitored throughout the program (Abdul Wahab et al. 2017) with *in situ* water quality sensors deployed across a range of near and offshore reef sites, including at Ward Reef, Herald Island and Airlie Island, where coral cores from this study were collected.

High resolution coral Sr/Ca and Li/Mg records

For this study, the presence of Sr/Ca, Li/Mg and calcification anomalies in the Ward and Herald Island core records, that coincided with the timing of the 2010/11 and 2012/13 thermal stress events, provided further strong evidence for recent widespread coral bleaching events in the region. The Ward and Herald Island reef sites recorded both the highest monthly maximum SSTs (31.3°C

versus 30.8 versus 29.6 °C at Airlie and the Montebello's) and the highest SST anomalies for the three months from Dec–Jan 2010/11 (+1°C and +1.2°C), thus it's not surprising that they showed the strongest Sr/Ca and Li/Mg anomalies and hence, evidence of thermal stress during the summer of 2010/11 compared to the cores collected from sites further offshore (i.e. from Airlie and the Montebello's). For the summer of 2012/13, SST anomalies were higher at all the sites (i.e. ranging from +1.2°C to +1.9°C), and, in addition to the Ward and Herald records, the Airlie record also showed a Sr/Ca and weaker Li/Mg anomaly, suggesting the impacts of this later event extended further offshore and were more widespread in the region. For the summer of 2012/13, the absence of Sr/Ca and Li/Mg anomalies in the Montebello record was unexpected given the site experienced the highest SST anomaly (+1.9°C) and a similar maximum monthly SST to the nearshore sites (31.4°C versus 31.5°C–31.6°C at the other sites). However, all the coral records were observed to experience anomalous declines in extension rates during both the 2010/11 and 2012/13 events (Figure 7.2.8), suggesting optimal calcification temperatures were exceeded throughout the region during both these anomalous warming events (Lough et al. 2011; Fitt et al. 2001; Jokiel and Coles, 1977). These results demonstrate that high-resolution analyses of coral core records can be used to reconstruct past coral bleaching and thermal stress events. In particular, these analyses can also be used to determine the incidence and impacts of past anomalous warming events in regions that have not been closely monitored, allowing for a better understanding of spatial variations in impacts and the regions most at risk of thermal stress during periods of anomalous warming.

The presence of calcification anomalies that were not accompanied by anomalous increases in Sr/Ca and Li/Mg ratios in the Airlie and Montebello records provides new insights into the mechanisms responsible for the formation of Te/Ca anomalies during periods of thermal stress. Previous research has suggested anomalous increases and decreases in Sr/Ca and Mg/Ca ratios observed in core records during periods of thermal stress are the result of a decrease in active Ca^{2+} pumping by the coral host (Marshall and McCulloch 2002; Sinclair 2005; Clarke et al. 2017), leading to decreases in the precipitation efficiency and Rayleigh Fractionation of trace elements into coral aragonite (Sinclair 2005; Clarke et al. 2017). In particular, reduced Rayleigh Fractionation of trace elements is thought to explain why increases in compatible trace element (e.g. Sr) to calcium ratios, and decreases in incompatible trace element (e.g. Mg) to calcium ratios are observed during periods of thermal stress (Clarke et al. 2017). However, the presence of Li/Mg anomalies in the Onslow records was (is) not consistent with these (this) previously suggested mechanisms. Both Li and Mg are highly incompatible in coral skeleton, with partition coefficients <<1 (Montagna et al. 2014; Hathorne et al. 2013) and, as such, should both respond similarly (be similarly affected by) to changes in Rayleigh Fractionation. Therefore, changes in calcification parameters should have a minimal effect on Li/Mg ratios, leaving temperature as the dominant factor controlling the ratio of the two trace elements in coral skeleton (Montagna et al. 2014). Where the magnitude of Sr/Ca and Li/Mg anomalies were observed to be similar in the Ward and Herald records during the summers of 2010/11 and 2012/13, this was inconsistent with expected Rayleigh Fractionation effects on both ratios. Therefore, an alternate mechanism is required to explain the formation of Li/Mg anomalies and perhaps also other Te/Ca anomalies (i.e. Sr/Ca and Mg/Ca) observed in coral records during periods of thermal stress.

One such alternate explanation for the formation of Te/Ca anomalies during periods of thermal stress (Li/Mg, Sr/Ca and Mg/Ca) is they result from increased bio-smoothing of seasonal Te/Ca signals due to reductions in calcification rate. Bio-smoothing has shown to be an important process influencing the seasonality of high-resolution coral records as continuous infilling of new coral skeleton over the entire thickness of the tissue layer results in the attenuation of the amplitude of Te/Ca signals (Gagan et al. 2012). The effect of bio smoothing has shown to be somewhat proportional to extension rates, with greater smoothing effects observed for slower growing corals than faster growing corals (Gagan et al. 2012). Therefore, this could potentially explain both the increased incidence of Sr/Ca and Li/Mg anomalies in the slower growing nearshore corals and also the increased magnitude of these anomalies during the 2010/11 for the Ward record and 2012/13

for the Herald record, which coincided with the timing of the lowest extension rates observed in each of the two records respectively. For the offshore records, variations in the extent of bio-smoothing could also explain why Sr/Ca and Li/Mg anomalies were only observed for the later thermal stress event in the Airlie record, when extension rates were the lowest on record (i.e. 6.5 mm.yr^{-1} versus 8.8 mm.yr^{-1} during 2013) and no anomalies were observed in the Montebello core record, despite temperatures during the summer of 2012/13 averaging almost 2 degrees above normal.

In addition, the anomalous decrease in the seasonality of Sr/Ca and Li/Mg ratios observed in the Ward record from around the year 1997 to 2000 also lends to support the idea that bio-smoothing is a significant process influencing skeletal Te/Ca ratios. Although this period in the Ward record only corresponded with weak negative extension anomalies, the amplitude of seasonal Sr/Ca and Li/Mg cycles was observed to return to normal around the time extension rate anomalies returned to positive values (around the year 2001). Further evidence for increased bio-smoothing of the Ward record for this period was provided by the application of a 12-month moving average through Sr/Ca and Li/Mg values across this anomalous period. The averaged Sr/Ca and Li/Mg values were observed to be consistent with the inter-annual warming trend displayed in the SST record; showing decreases in mean values (increased Sr/Ca-SST and Li/Mg-SSTs) up to the year 2000. As such, the retention of the inter-annual SST signal in the Ward record through this period could be expected to be consistent with the effects of increased attenuation of seasonal Sr/Ca and Li/Mg variability due to increased bio-smoothing. Lastly, a similar, although less pronounced effect was also observed in the Herald record around the same time (i.e. 1997–1998). This could suggest that both these nearshore sites were also impacted by thermal stress during this period of increased decadal SSTs. However, the duration of these anomalies in both records (up to 3 years) was inconsistent with the more acute thermal stress signals observed during 2010/11 and 2012/13 and as such, we can only speculate as to whether these periods of anomalous Sr/Ca and Li/Mg variability might have been related to earlier thermal stress events not previously reported from the western Australian coastline.

Annual Sr/Ca and Li/Mg records

The long-term Sr/Ca and Li/mg records from Airlie and the Montebello islands provided mixed evidence for increases in background temperatures in the region over the last 50–150 years (Figure 7.2.3 and Figure 7.2.4). Rates of background ocean warming estimated from the two long-core records were highly variable (0 to 0.9°C warming since 1875 at Airlie versus 3.2 to 3.6°C warming at the Montebello's) since 1940. Although the overall trend at the two sites appears to be one of increasing background SSTs, the discrepancies between rates of warming estimated between the sites cannot be ignored. In particular, given the close proximity of the two reef environments (~100 km) and their similar distances from the margin of the northwest shelf (70–100 km), it would seem unlikely that the two habitats would have experienced markedly different rates of background ocean warming. As such, we suspect the Airlie Sr/Ca record provides the most realistic estimation of long-term changes in SSTs for the region, due to its closer agreement with the long term ERSST record (stats) as well as other long-term coral Sr/Ca and δ^{18}O records previously generated from the Houtman Abrolhos islands to the south (see Zinke et al. 2014; Kuhnert et al. 1999).

The suspected overestimation of warming trends in the Montebello annual Sr/Ca an Li/Mg records further lend to support the ideas of Gagan et al. (2012) who suggested the suitability of seasonal Sr/Ca-SST and, by inference, Li/Mg-SST calibrations for the calibration of longer-term annual records bears some dependence on calcification parameters. In particular, Gagan et al. (2012) showed that calibrations obtained from seasonal records can lead to the overestimation of long-term changes in SSTs because seasonal signals in coral records are attenuated by tissue layer bio-smoothing (as previously discussed) prior to Sr/Ca-SST regression analysis. The seasonal Sr/Ca-SST sensitivity determined from the Montebello record (~0.05 mmol/mol°C) was observed to be unusually low

compared to other *Porites* sp. corals with similar fast extension rates (~18 mm.yr^{-1})(Gagan et al. 2012). However, applying the more sensitive Sr/Ca-SST calibration of 0.08 mmol/mol°C, which is at the higher end of all those previously reported (Corrège et al. 2006), still results in an estimated SST increase of 2.3°C at the coral site over the past 75 years which still exceeds the magnitude of global warming recorded over this same period in most long term instrumental records (Casey and Cornillon 2001; Jones et al. 1999). Nonetheless, regardless of what SST calibration is used, the strong differences in the trends of the absolute Sr/Ca and Li/Mg ratios in the two records warrants the need for further research into these two reef environments. In particular, additional coral cores should be obtained and analysed from the Montebello's to check if anomalous warming trends are replicated.

Coral Ba/Ca records

The seasonal Ba/Ca records from Herald, Ward and Airlie islands showed variations consistent with their relative distances from the mouth of the Ashburton River. The timing of Ba/Ca peaks in the Herald and Ward records were observed to be very similar and largely corresponded with periods of discharge from the Ashburton River. However, there was not a strong relationship between the intensity of Ba/Ca spikes and river discharge as strong Ba/Ca anomalies were also observed in the records following extended periods of dry weather (e.g. Autumn-2004). This was consistent with past studies from the GBR (e.g. McCulloch et al. 2003), indicating that along with high rainfall events, periods of drought also strongly contribute to the erosion of topsoils in the Onslow catchment area and hence suspended sediment concentrations of the Ashburton River. For the Airlie record, a significant correlation with the nearshore Ba/Ca records could only be obtained when a time adjustment of ~3 months was applied to the record. This suggests a considerable lag for the time it takes sediments to reach the outer reef sites from the river mouth, which could be indicative of complex circulation dynamics within the region.

In comparison, the Montebello Ba/Ca record showed little to no similarities with the records from the sites, including the discharge record from the Ashburton River. The higher average Ba/Ca values observed in the Montebello record compared to the Airlie record suggest that strong oceanographic differences exist between the two outer reef sites. In particular, consistent with its position further offshore, the Ba/Ca record from the Montebello's could reflect an increase in the influx and mixing of deeper waters at the coral site (e.g. Tudhope et al. 1996; Lea and Boyle 1990). Strong upwelling has previously been reported along the north-west shelf and has shown to be an important factor contributing to the complex circulation dynamics observed across the region (Feng et al. 2016; Lowe et al. 2012). For outer reef sites such as the Montebello's, the influence of local tidal variability on reef circulation is probably less than at the more nearshore sites. This in turn probably increases the influence of more regional, offshore circulation patterns at the Montebello's, in particular, on the offshore side of the Island group, where the sampled coral was located. The apparent reduction in seasonal atmospheric-ocean heat exchange observed in the Montebello SST record, which showed a smaller range of seasonal SST variability than the Airlie record (i.e. 4.6°C versus 6.9°C on average for the two sites respectively), could also be consistent with greater mixing of offshore waters at the coral site. Reduced atmospheric heating of surface waters at the Montebello's during summer months could also account for the absence of significant thermal stress indicators in the Sr/Ca and Li/Mg records during the summers of 2010/11 and 2012/13 and reports of widespread coral bleaching from the site to date (e.g. Falter et al. 2014). However, given the Montebello's are still ~70 km inshore from the north-west shelf margin, we cannot exclude that differences in terrestrial sediment inputs at the two sites are responsible for the observed differences between the Montebello and Airlie Ba/Ca records.

Lastly, the annual Ba/Ca records from Airlie and the Montebello Islands showed strong increases in Ba/Ca values for several decades after ~1950 compared to the present day. The increases observed around 1950 in both records may well be related to major land use changes in the Onslow

catchment during the mid part of the 20th century. Similar studies from the GBR have shown increases in coral core Ba/Ca values from around the time of first European settlement (~1870s) that were attributed to increased topsoil erosion in the catchment due widespread land clearing and overstocking of farm lands (McCulloch et al. 2003). Although the intensity of land uses in the Onslow catchment could be expected to be well below that of the catchments on Australia's tropical north-east coast, the arid climate and erratic rainfall patterns of the Onslow region probably make the region highly susceptible to increased topsoil erosion from anthropogenic interference in the landscape. Livestock were first introduced in the Onslow catchment in the late 1880s (Shire of Ashburton, 2017). Strong increases in population growth and the establishment of offshore trade markets increased the intensity of livestock farming within the region throughout the early to mid part of the 20th century (Australian Government, 2017). In particular, a market driven transition from sheep to mainly cattle pastures in the region around the mid 20th century could also have contributed to increased erosion of the catchment (Australian Government, 2017). Furthermore, the 1950's coincided with the timing of increased development of the Onslow and Pilbara region more generally as the extent of the vast mineral wealth of the region became more understood. The stockpiling of mineral ores and increased shipping out of the port of Onslow are also likely factors that could also explain the increase in Ba/Ca values observed in the coral records during this time. However, we can only speculate as to the anthropogenic factors responsible for increased Ba/Ca values in the annual coral records due to a lack of long-term records for the region.

Sediment and turbidity impacts since 2010/11

During the summer of 2010/11, no anomalous Ba/Ca enrichments were observed in either the Ward or Herald records. This suggests that turbidity and sedimentation at the coral sites during the summer of 2010/11 probably contributed little to the stress response observed in coral records during this anomalous warm period. Similarly, for the summer of 2013, Ba/Ca ratios were observed to be slightly higher in both nearshore records however were still relatively low when compared to much of the earlier period of the two records. As such, the Ba/Ca records provided little to no evidence for sediment disturbances contributing to the observed decline in reef health in the region since 2010/11.

Coinciding with period of recent dredging activities around Onslow (April 2013–January 2015), no obvious Ba/Ca anomalies were observed in the nearshore records from Ward and Herald islands. This was somewhat unexpected as these sites were classified as amongst the most affected by increases in in turbidity and sedimentation during the dredging operation (Abdul Wahab et al. 2017). *In situ* monitoring at the two sites showed turbidity levels roughly doubled and light levels halved over the period of dredging (compared to mean values observed from 2011–2013). However, despite the increases in turbidity at both sites, no clear Ba/Ca enrichment associated with the dredging was observed in either record, particularly when compared to the large peaks observed during the autumn of 2012 in both records. On the contrary, the Airlie record showed strong increases in Ba/Ca ratios that slightly preceded the onset of dredging activities (i.e. from July 2012–February 2013), however, appeared to be unrelated to discharge from the Ashburton River. This increase in Ba/Ca values was replicated when the sample powders from the first analysis were individually bleached and re-analyzed. This suggests the Ba/Ca enrichment was due to increased Ba skeletal incorporation and not organic contamination from the coral tissue layer. It's possible that the timing of this Ba/Ca enrichment in the Airlie record could be slightly distorted due to progressive infilling and bio smoothing (as discussed earlier). However, the presence of a dredging related Ba/Ca anomaly in the Airlie record was still inconsistent with the *in situ* water quality monitoring from the site, which showed increases in turbidity were substantially less than at Herald and Ward islands (increases of up 40%). As such we cannot conclude the cause of this Ba/Ca anomaly observed in the Airlie record although, for this study Ba/Ca ratios appeared to not be an effective proxy for the re-suspension of marine sediments, contrary to other research findings (e.g. Esselmont et al. 2004).

Lastly, because the linear extension rates in all the cores were at around their lowest levels at the time that dredging commenced in April 2013, we cannot exclude that dredging might have adversely impacted some of the sampled corals. In particular, it's possible that the evidence for thermal stress observed in the Ward, Herald and Airlie cores during the summer of 2012/13 masked the effects of any dredging related impacts on the corals later in the year. However, the similarities between the trends in extension rates observed in all the records (including the Montebello record) after ~2010/2011, suggests that thermal stress was key driver of the observed calcification and geochemical anomalies, as the Montebello site was probably too far away to have been affected by the dredging. The absence of any clear, dredging related impacts in the coral cores was consistent with recent research, which suggested dredging had no marked effects on hard coral populations at Ward, Herald and Airlie islands (Abdul Wahab et al. 2017).

Conclusion

In summary, our detailed coral core analysis from reef sites around Onslow suggests that ocean warming is the primary factor responsible for recent widespread declines in coral reef health observed in the region. The rapid succession of two, unprecedented widespread bleaching events in the region suggests that corals have not been able to adapt to gradual increases in temperature and will probably begin to bleach more frequently in the future as they function increasingly closer to their bleaching thresholds during summer months. Although the coral cores from the nearshore sites showed the strongest evidence of thermal stress during the summers of 2010/11 and 2012/13, there was no direct evidence to suggest levels of thermals stress were exacerbated by increased turbidity at either of the two coral sites. The Ba/Ca records indicated the nearshore reef environments around Onslow are naturally exposed to high levels of sedimentation and turbidity during runoff events. This natural exposure probably increased their resilience to deleterious impacts from recent dredging operations, which also could not be clearly resolved in any of the records. However, for this study, Ba/Ca ratios did not appear to resolve sediment re-suspension events and it's therefor possible that high-suspended sediment concentrations, in addition to other anthropogenic stressors (high levels of nutrients etc.) could have exacerbated stress responses, giving rise to the observed gradient in bleaching responses between the nearshore and offshore sites. More research is required into new geochemical proxies and sampling methods to allow for better assessments of how anthropogenic activities might be influencing coral bleaching responses during periodic ocean warming events. As these events are expected to become increasingly frequent and severe into the future, de-coupling the relative effects of different stressors is paramount for the best management and protection of reef ecosystems along the north-west Australian coastline.

7.2.5 ACKNOWLEDGEMENTS

7.2.6   REFERENCES

Abdul Wahab MA, Fromont J, Gomez O, Fisher R, Jones R (2017) Comparisons of benthic filter feeder communities before and after a large-scale capital dredging program. Marine Pollution Bulletin 122:176-193

Al-Horani F, Al-Moghrabi S, De Beer D (2003) The mechanism of calcification and its relation to photosynthesis and respiration in the scleractinian coral Galaxea fascicularis. Marine Biology 142:419-426

Alibert C, Kinsley L (2008) A 170-year Sr/Ca and Ba/Ca coral record from the western Pacific warm pool: 1. What can we learn from an unusual coral record? Journal of Geophysical Research: Oceans 113

Alibert C, Kinsley L, Fallon SJ, McCulloch MT, Berkelmans R, McAllister F (2003) Source of trace element variability in Great Barrier Reef corals affected by the Burdekin flood plumes. Geochimica et cosmochimica acta 67:231-246

Anthony K, Connolly SR, Hoegh-Guldberg O (2007) Bleaching, energetics, and coral mortality risk: Effects of temperature, light, and sediment regime. Limnology and oceanography 52:716-726

Beck JW, Edwards RL, Ito E, Taylor FW, Recy J, Rougerie F, Joannot P, Henin C (1992) Sea-surface temperature from coral skeletal strontium/calcium ratios. Science 257:644-647

Berkelmans R (2002) Time-integrated thermal bleaching thresholds of reefs and their variation on the Great Barrier Reef. Marine ecology progress series 229:73-82

Berkelmans R, De'ath G, Kininmonth S, Skirving WJ (2004) A comparison of the 1998 and 2002 coral bleaching events on the Great Barrier Reef: spatial correlation, patterns, and predictions. Coral reefs 23:74-83

Berkelmans R, Oliver J (1999) Large-scale bleaching of corals on the Great Barrier Reef. Coral reefs 18:55-60

Brown B (1997) Coral bleaching: causes and consequences. Coral reefs 16:S129-S138

Bruno J, Siddon C, Witman J, Colin P, Toscano M (2001) El Nino related coral bleaching in Palau, western Caroline Islands. Coral Reefs 20:127-136

Carilli JE, Norris RD, Black B, Walsh SM, McFIELD M (2010) Century-scale records of coral growth rates indicate that local stressors reduce coral thermal tolerance threshold. Global Change Biology 16:1247-1257

Carilli JE, Norris RD, Black BA, Walsh SM, McField M (2009) Local Stressors Reduce Coral Resilience to Bleaching. PLoS ONE 4:e6324

Casey KS, Cornillon P (2001) Global and regional sea surface temperature trends. Journal of Climate 14:3801-3818

Castillo KD, Ries JB, Weiss JM, Lima FP (2012) Decline of forereef corals in response to recent warming linked to history of thermal exposure. Nature Climate Change 2:756

Clarke H, D'Olivo JP, Falter J, Zinke J, Lowe R, McCulloch M (2017) Differential response of corals to regional mass-warming events as evident from skeletal Sr/Ca and Mg/Ca ratios. Geochemistry, Geophysics, Geosystems

Coffey M, Dehairs F, Collette O, Luther G, Church T, Jickells T (1997) The Behaviour of Dissolved Barium in Estuaries. Estuarine, Coastal and Shelf Science 45:113-121

Cohen A, Gaetani GA (2010) Ion partitioning and the geochemistry of coral skeletons: solving the mystery of the vital effect. EMU Notes in Mineralogy 11:377-397

Cohen AL, Layne GD, Hart SR, Lobel PS (2001) Kinetic control of skeletal Sr/Ca in a symbiotic coral: Implications for the paleotemperature proxy. Paleoceanography 16:20-26

Corrège T (2006) Sea surface temperature and salinity reconstruction from coral geochemical tracers. Palaeogeography, Palaeoclimatology, Palaeoecology 232:408-428

de Villiers S, Shen GT, Nelson BK (1994) The SrCa-temperature relationship in coralline aragonite: Influence of variability in (SrCa) seawater and skeletal growth parameters. Geochimica et Cosmochimica Acta 58:197-208

De'ath G, Fabricius KE, Sweatman H, Puotinen M (2012) The 27–year decline of coral cover on the Great Barrier Reef and its causes. Proceedings of the National Academy of Sciences 109:17995-17999

Dehairs F, Chesselet R, Jedwab J (1980) Discrete suspended particles of barite and the barium cycle in the open ocean. Earth and Planetary Science Letters 49:528-550

Depczynski M, Gilmour J, Ridgway T, Barnes H, Heyward A, Holmes T, Moore J, Radford B, Thomson D, Tinkler P (2013) Bleaching, coral mortality and subsequent survivorship on a West Australian fringing reef. Coral Reefs 32:233-238

Dunne R (2010) Synergy or antagonism—interactions between stressors on coral reefs. Coral reefs 29:145-152

Erftemeijer PL, Riegl B, Hoeksema BW, Todd PA (2012) Environmental impacts of dredging and other sediment disturbances on corals: a review. Marine Pollution Bulletin 64:1737-1765

Esslemont G, Russell R, Maher W (2004) Coral record of harbour dredging: Townsville, Australia. Journal of Marine Systems 52:51-64

Fabricius KE, Cséke S, Humphrey C, De'ath G (2013) Does trophic status enhance or reduce the thermal tolerance of scleractinian corals? A review, experiment and conceptual framework. PloS one 8:e54399

Fallon SJ, McCulloch MT, Alibert C (2003) Examining water temperature proxies in Porites corals from the Great Barrier Reef: a cross-shelf comparison. Coral Reefs 22:389-404

Falter JL, Zhang Z, Lowe RJ, McGregor F, Keesing J, McCulloch MT (2014) Assessing the drivers of spatial variation in thermal forcing across a nearshore reef system and implications for coral bleaching. Limnology and Oceanography 59:1241-1255

Feng M, Colberg F, Slawinski D, Berry O, Babcock R (2016) Ocean circulation drives heterogeneous recruitments and connectivity among coral populations on the North West Shelf of

Australia. Journal of Marine Systems 164:1-12

Feng M, McPhaden MJ, Xie S-P, Hafner J (2013) La Niña forces unprecedented Leeuwin Current warming in 2011. Sci Rep 3

Fitt WK, Brown BE, Warner ME, Dunne RP (2001) Coral bleaching: interpretation of thermal tolerance limits and thermal thresholds in tropical corals. Coral Reefs 20:51-65

Gagan MK, Dunbar GB, Suzuki A (2012) The effect of skeletal mass accumulation in Porites on coral Sr/Ca and δ18O paleothermometry. Paleoceanography 27

Glynn PW (1996) Coral reef bleaching: facts, hypotheses and implications. Global Change Biology 2:495-509

Grottoli AG, Eakin CM (2007) A review of modern coral δ 18 O and Δ 14 C proxy records. Earth-Science Reviews 81:67-91

Grottoli AG, Rodrigues LJ, Palardy JE (2006) Heterotrophic plasticity and resilience in bleached corals. Nature 440:1186-1189

Hathorne EC, Felis T, Suzuki A, Kawahata H, Cabioch G (2013) Lithium in the aragonite skeletons of massive Porites corals: A new tool to reconstruct tropical sea surface temperatures. Paleoceanography 28:143-152

Hoegh-Guldberg O (1999) Climate change, coral bleaching and the future of the world's coral reefs. Marine and freshwater research 50:839-866

Hoegh-Guldberg O, Mumby P, Hooten A, Steneck R, Greenfield P, Gomez E, Harvell C, Sale P, Edwards A, Caldeira K (2007) Coral reefs under rapid climate change and ocean acidification. science 318:1737-1742

Hoegh-Guldberg O, Ridgway T (2016) Coral bleaching hits great barrier reef as global temperatures soar. Green Left Weekly:10

Howells EJ, Beltran VH, Larsen NW, Bay LK, Willis BL, van Oppen MJH (2012) Coral thermal tolerance shaped by local adaptation of photosymbionts. Nature Clim Change 2:116-120

Hughes TP, Kerry JT, Álvarez-Noriega M, Álvarez-Romero JG, Anderson KD, Baird AH, Babcock RC, Beger M, Bellwood DR, Berkelmans R (2017) Global warming and recurrent mass bleaching of corals. Nature 543:373-377

Jokiel P, Coles S (1977) Effects of temperature on the mortality and growth of Hawaiian reef corals. Marine Biology 43:201-208

Jones P, Hulme M (1996) Calculating regional climatic time series for temperature and precipitation: methods and illustrations. International journal of climatology 16:361-377

Jones PD, New M, Parker DE, Martin S, Rigor IG (1999) Surface air temperature and its changes over the past 150 years. Reviews of Geophysics 37:173-199

Kuhnert H, Pätzold J, Hatcher B, Wyrwoll K-H, Eisenhauer A, Collins L, Zhu Z, Wefer G (1999) A 200-year coral stable oxygen isotope record from a high-latitude reef off Western Australia. Coral Reefs 18:1-12

Lafratta A, Fromont J, Speare P, Schönberg C (2017) Coral bleaching in turbid waters of north-western Australia. Marine and Freshwater Research 68:65-75

Lea DW, Boyle EA (1990) Foraminiferal reconstruction of barium distributions in water masses of the glacial oceans. Paleoceanography 5:719-742

Lea DW, Shen GT, Boyle EA (1989) Coralline barium records temporal variability in equatorial Pacific upwelling. Nature 340:373-376

Lough JM, Cooper TF (2011) New insights from coral growth band studies in an era of rapid environmental change. Earth-Science Reviews 108:170-184

Lowe RJ, Falter JL (2015) Oceanic forcing of coral reefs. Annual review of marine science 7:43-66

Lowe RJ, Ivey GN, Brinkman RM, Jones NL (2012) Seasonal circulation and temperature variability near the North West Cape of Australia. Journal of Geophysical Research: Oceans (1978–2012) 117

Marshall JF, McCulloch MT (2002) An assessment of the Sr/Ca ratio in shallow water hermatypic corals as a proxy for sea surface temperature. Geochimica et Cosmochimica Acta 66:3263-3280

McClanahan TR, Ateweberhan M, Muhando CA, Maina J, Mohammed MS (2007) Effects of climate and seawater temperature variation on coral bleaching and mortality. Ecological Monographs 77:503-525

McCulloch M, Fallon S, Wyndham T, Hendy E, Lough J, Barnes D (2003) Coral record of increased sediment flux to the inner Great Barrier Reef since European settlement. Nature 421:727-730

McCulloch M, Falter J, Trotter J, Montagna P (2012) Coral resilience to ocean acidification and global warming through pH up-regulation. Nature Climate Change 2:623-627

McCulloch MT, Gagan MK, Mortimer GE, Chivas AR, Isdale PJ (1994) A high-resolution Sr/Ca and δ 18 O coral record from the Great Barrier Reef, Australia, and the 1982–1983 El Niño. Geochimica et Cosmochimica Acta 58:2747-2754

Montagna P, McCulloch M, Douville E, Correa ML, Trotter J, Rodolfo-Metalpa R, Dissard D, Ferrier-Pages C, Frank N, Freiwald A (2014) Li/Mg systematics in scleractinian corals: Calibration of the thermometer. Geochimica et Cosmochimica Acta 132:288-310

Moore JA, Bellchambers LM, Depczynski MR, Evans RD, Evans SN, Field SN, Friedman KJ, Gilmour JP, Holmes TH, Middlebrook R (2012) Unprecedented mass bleaching and loss of coral across 12 of latitude in Western Australia in 2010–11.

Muscatine L, Porter JW (1977) Reef corals: mutualistic symbioses adapted to nutrient-poor environments. Bioscience 27:454-460

Paillard D, Labeyrie L, Yiou P (1996) Macintosh program performs time-series analysis. Eos, Transactions American Geophysical Union 77:379-379

Pandolfi JM, Bradbury RH, Sala E, Hughes TP, Bjorndal KA, Cooke RG, McArdle D, McClenachan L, Newman MJH, Paredes G, Warner RR, Jackson JBC (2003) Global Trajectories of the Long-

Term Decline of Coral Reef Ecosystems. Science 301:955-958

Pearse VB, Muscatine L (1971) Role of symbiotic algae (zooxanthellae) in coral calcification. The Biological Bulletin 141:350-363

Prouty NG, Field ME, Stock JD, Jupiter SD, McCulloch M (2010) Coral Ba/Ca records of sediment input to the fringing reef of the southshore of Moloka'i, Hawai'i over the last several decades. Marine pollution bulletin 60:1822-1835

Report IPoCCWgIttFA, Adger WN, Kajfež-Bogataj L, Parry ML, Canziani O, Palutikof J (2007) Climate change 2007: impacts, adaptation and vulnerability, Vol. Cambridge University Press Cambridge

Saha N, Webb GE, Zhao J-X (2016) Coral skeletal geochemistry as a monitor of inshore water quality. Science of The Total Environment 566:652-684

Shen C-C, Lee T, Chen C-Y, Wang C-H, Dai C-F, Li L-A (1996) The calibration of D [Sr/Ca] versus sea surface temperature relationship for Porites corals. Geochimica et Cosmochimica Acta 60:3849-3858

Sinclair DJ (2005a) Correlated trace element "vital effects" in tropical corals: a new geochemical tool for probing biomineralization. Geochimica et cosmochimica acta 69:3265-3284

Sinclair DJ (2005b) Non-river flood barium signals in the skeletons of corals from coastal Queensland, Australia. Earth and Planetary Science Letters 237:354-369

Sinclair DJ, Kinsley LP, McCulloch MT (1998) High resolution analysis of trace elements in corals by laser ablation ICP-MS. Geochimica et cosmochimica acta 62:1889-1901

Speed CW, Babcock RC, Bancroft KP, Beckley LE, Bellchambers LM, Depczynski M, Field SN, Friedman KJ, Gilmour JP, Hobbs J-PA (2013) Dynamic stability of coral reefs on the west Australian coast. PloS one 8

Tudhope AW, Lea DW, Shimmield GB, Chilcott CP, Head S (1996) Monsoon climate and Arabian Sea coastal upwelling recorded in massive corals from southern Oman. Palaios:347-361

Walther BD, Kingsford MJ, McCulloch MT (2013) Environmental records from Great Barrier Reef corals: inshore versus offshore drivers. PloS one 8:e77091

Zinke J, Rountrey A, Feng M, Xie SP, Dissard D, Rankenburg K, Lough JM, McCulloch MT (2014) Corals record long-term Leeuwin current variability including Ningaloo Niño/Niña since 1795. Nat Commun 5:3607

8.   Herbivory and predation

8.1 Temporal and spatial patterns in growth and grazing of canopy-forming *Sargassum* in the Pilbara

Authors: van Hees DH, Olsen YS, Vanderklift M, Babcock RC, Kendrick GA.

ABSTRACT

Macroalgae are an important component of shallow reef environments. Their overall extent and standing crop depend largely on the balance between growth and grazing. Grazing activity can vary temporally and among regions as well as across local environmental gradients and can be a key factor in regulating macroalgal assemblages. Patterns in grazing activity can be affected by the abundance and composition of the herbivore assemblage, but also by the palatability of the algae, including their chemical composition (e.g. phenolic compounds and nitrogen content). We assessed grazing and growth rates of canopy-forming *Sargassum* species in two contrasting seasons in the tropical Dampier Archipelago, Western Australia. First, we measured growth and grazing of *Sargassum* and examined how the balance between these processes varied across the Archipelago. Second, to evaluate the importance of chemical composition of the algae on grazing rates, we measured phenolic content and % nitrogen of *Sargassum marginatum* from inshore-and offshore sites. We also cross-transplanted fronds of *S. marginatum* between inshore and offshore areas to examine whether the palatability of macroalgae depended on their origin. Finally, we looked at the effects of fish abundance and standing crop of algae on potential grazing rates.

We found no simple in-offshore patterns in grazing rates on *S. marginatum,* but there was an interaction between in-offshore location, season and the standing crop of algae. Consumption was around three times higher in April at offshore sites with low biomass than any other time/location. These sites had relatively high numbers of herbivorous fish, but the overall pattern in herbivore abundance was not a good predictor of grazing rates. While there were seasonal patterns in phenolic composition and %nitrogen of algae, we observed no differences between inshore and offshore sites that could explain the patterns in grazing. The cross-shelf transplant experiment also suggested that the origin of the algal fronds (inshore versus offshore) did not impact rates of consumption by herbivores. There was high variability in growth rates among fronds of three species of *Sargassum* measured, resulting in no significant spatial or temporal trends and no measurable difference among species.

For the majority of sites, top-down control by grazers could be significant and able to balance growth in both seasons. There will, however, be sites and times with non-existent grazing when biomass can accumulate and bottom-up forces, such as nutrient availability and light, control net growth of *Sargassum*. In contrast, in April when we observed localised heavy grazing offshore, consumption greatly exceeded our estimated rates of growth. This indicates that there are times and locations when top-down control may overwhelm growth rates of *Sargassum*. The Dampier

Archipelago likely experiences seasonal shifts in the conditions that regulate both bottom-up and top-down controls, but these drivers are currently poorly understood in the area.

8.1.1 INTRODUCTION

Herbivore consumption of macroalgae can be a driving factor in the overall community structure of marine environments (Steneck and Dethier 1994; Bennett et al. 2015; Saunders et al. 2015). Many factors influence grazing pressures, including macroalgal assemblage composition, benthic structural complexity (Vergés et al. 2011) and herbivore abundance (Gaines and Lubchenco 1982). Overall grazing pressures are capable of structuring the diversity and distribution of macroalgae (Hay 1997; McCook 1997). Grazing activity on macroalgae varies geographically (Bennett and Bellwood 2011) as well as across macroalgal (Sammarco 1983) taxa but may also be structured within one genera or species (McCarty and Sotka 2013). This variation may result from abiotic factors and overall structure of the herbivore community but may also be driven by morphological or chemical structures of macroalgae (Lewis 1985; Hoey 2010).

Allelopathy, the production of secondary metabolite compounds that can affect growth and survival of other organisms, is one mechanism by which organisms interact (Gross 2003). Allelopathic chemicals found in macroalgae can function as herbivore deterrents (Geiselman and McConnell 1981; Erickson et al. 2006; Lyons et al. 2007; Rasher and Hay 2014), fouling deterrents (Cho et al. 2001) and growth inhibitors of neighboring organisms (Jompa and McCook 2003; Kim et al. 2004; Renjun et al. 2012) and can influence from the individual to the scale of the ecosystem. Some macroalgal allelopathic compounds are species-specific (Paul and Van Alstyne 1988; Van Alstyne et al. 2006; Enge et al. 2012) while others, such as phenolics, are distributed widely throughout algal taxa (Capon et al. 1983; Steinberg 1989). The impacts of phenolic compounds on grazing activity depend both on the concentration within the macroalgae (Van Alstyne and Paul 1990), as well as the susceptibility of herbivores to them (Steinberg 1988).

In this study, we examined temporal and spatial patterns in growth and consumption of canopy-forming *Sargassum* in the tropical Dampier Archipelago, Western Australia. We sampled inshore and offshore sites that were likely to differ in several key abiotic factors. Sampling took place in spring (October) and fall (April) to enable comparison between contrasting seasons. First, we measured growth and grazing rates of *Sargassum* and examined how the balance between these processes varied across the Archipelago and with season. The study focused mainly on *Sargassum marginatum*, which was the dominant species across the study region, but two other species (*S. linearifolium* and *S. polyphyllum*) were opportunistically sampled when available. Second, to evaluate the importance of chemical composition of the algae on grazing rates, we measures phenolic content and % nitrogen of *S. marginatum* from inshore-and offshore sites. We also cross-transplanted fronds of *S. marginatum* between inshore and offshore areas to examine whether the palatability of macroalgae depended on their origin. Finally, we looked at the importance of fish abundance and standing crop of algae on grazing rates.

8.1.2 METHODS

Study Site

The Dampier Archipelago is located on the northern Pilbara coast, Western Australia. It covers an area of 400 km^2 and is comprised of 42 small islands surrounded by shallow reefs and water depths are generally < 35 m. The benthic habitats in the archipelago include lush macroalgal meadows, shallow seagrass meadows and coral reefs. The climate is tropical with hot summers and mild winters. Sampling was conducted in October 2015 (spring) and April 2016 (fall) at three inshore sites (East Lewis, East and West Intercourse Islands near the Port of Dampier) and three offshore sites

(Goodwyn, Kendrew and Rosemary Islands). An additional two sites were sampled in April (at Rosemary Island) (Figure 8.1.1). Depths at the study sites were 4-5 m and the substrate was a mixture of sand and limestone. The macroalgal assemblage was dominated by *Sargassum* (primarily *Sargassum marginatum*), which was distributed throughout the archipelago. The standing crop of *Sargassum* varied among sites, with two of the offshore and two of the inshore sites having lush meadows in both seasons and the remaining sites being almost completely devoid of *Sargassum*.
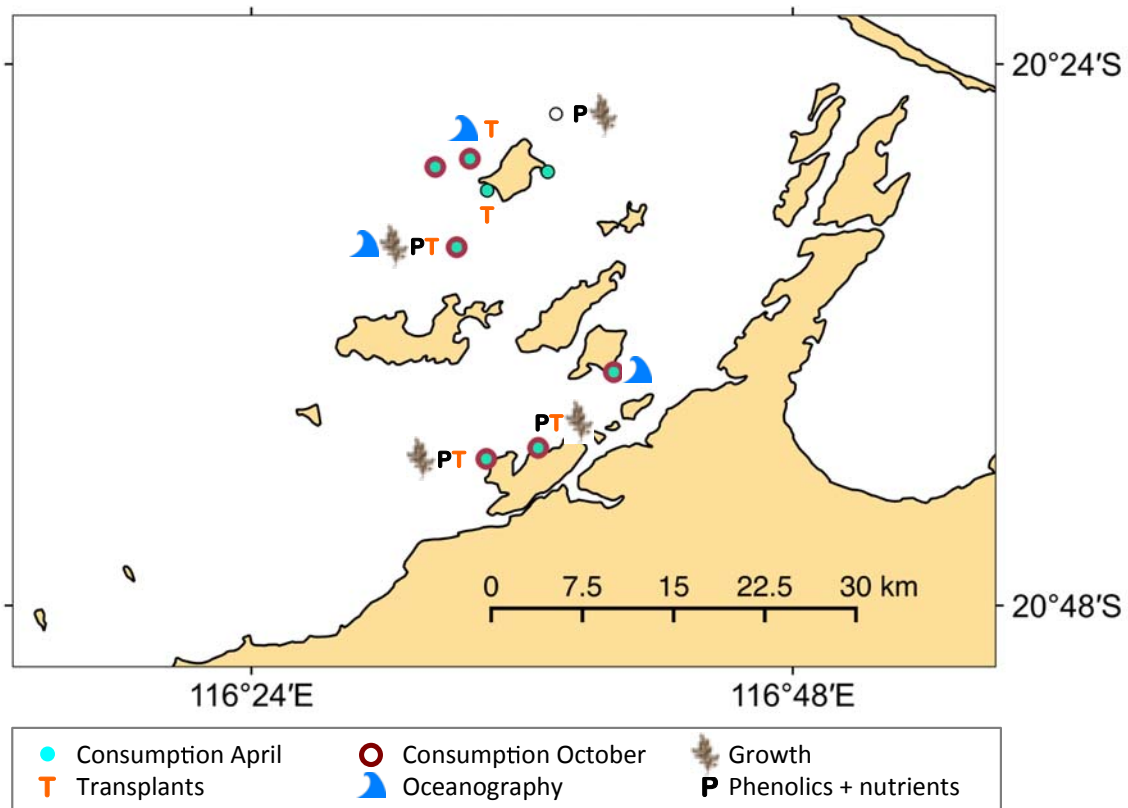
Figure 8.1.1 Map of sample locations in the Dampier Archipelago showing the locations of the different measurements. "Transplants" indicate the sites where cross-transplants between inshore and offshore were carried out. "Oceanography" shows the locations where temperature and significant wave heights were measured.

Wave heights and temperature

Water temperature and significant wave heights were measured at one inshore and two offshore sites (Figure 8.1.1) by deploying one RBR Virtuoso pressure sensor and a HOBO temperature logger that recorded from October to April at each site.

Growth measurements

Growth rates of *Sargassum sp.* (*S. marginatum, S. linearifolium* and *S. polyphyllum*) were measured *in situ* by scuba divers. Inshore fronds were too short to measure in the spring, so measurements of all three species were made offshore. In the fall, growth measurements were made at two inshore sites and one offshore site, but no *S. linearifolium* was found at any of the sites and only *S. marginatum* was present offshore. Five to twenty algal fronds per available species were tagged and measured from the holdfast to the tip of the longest branch. After 4-8 days the fronds were re-measured and growth calculated in cm day^{-1}. Fronds that showed clear signs of grazing or senescence were excluded from the analysis.

Grazing Assays

Changes in algal biomass due to grazing were measured by tethering *Sargassum* at inshore and offshore sites (Figure 8.1.1). Fronds of *Sargassum* were collected by hand no more than 12 h prior to each grazing assay. Algae were kept in aerated seawater until use in tethering experiments. Ten fronds (10-20 g each) per site were cleaned of epiphytes and spun in a salad spinner to remove excess water prior to weighing to the nearest 0.2 g. Each algal piece was attached to a piece of plastic mesh using wooden clothes pegs (Figure 8.1.2). We deployed cage controls consisting of algal fronds enclosed in plastic cages made of plastic mesh to account for autogenic losses during the assays. Tethers were deployed in three different ways:

Figure 8.1.2 Tethering apparatus consisting of a frond of *Sargassum* attached to a piece of plastic mesh with a cable tie.

INSHORE-TO-INSHORE AND OFFSHORE-TO-OFFSHORE TETHERS

To measure consumption rates of algae, *Sargassum marginatum* fronds collected offshore were deployed at the three offshore sites and fronds collected inshore deployed at the three inshore sites in both spring and fall. Algae tethered to open mesh (n = 10) and caged control tethers (n = 10) were deployed haphazardly to the substrate over a 5 m^2 area and secured to the substratum with tent pegs. Tethers were collected after 24 h, spun in a salad spinner and reweighed. We calculated the change in biomass per day as the initial weight minus the final weight. To estimate consumption rates by herbivores, we adjusted the weight change of uncaged tethers by subtracting the average weight change of the caged controls. In a small number of cases this resulted in a slightly negative consumption rate. This was most likely due to a measuring error or an autogenic loss in the caged control, as these samples generally displayed no change in biomass of the open tether. These tethers were therefore considered not grazed and the value was adjusted to "0" to reflect this. All analyses were made using the percent change in biomass to account for differences in the initial weight of the tethered algae and a potential preference of consumers for algae of a particular size.

SPECIES COMPARISON TETHERS

To assess consumption rates of different *Sargassum* species, we deployed tethers of two dominant morphologically different *Sargassum* species simultaneously. We chose *Sargassum linearifolium*, which has elongated leaves that are more delicate than the shorter, rounded leaves of *S. marginatum*. Tethers of both species were deployed in the spring of 2015 at the three inshore and three offshore sites as in experiment (i). We deployed open mesh tethers of *S. linearifolium* and *S. marginatum* (n = 10 per species) and caged controls (n = 10 per species) at each site. Deployments and measurements were carried out as above.

TRANSPLANTED TETHERS

To assess if the palatability of the algae differed between offshore and inshore communities we carried out a cross transplant experiment in the fall of 2016. We measured consumption rates of algae that had been reciprocally transplanted from one inshore and one offshore 'parent' site. Algae transplanted from in-to-offshore or off-to-inshore are here forth referred to as "transplanted" and algae transplanted within inshore or within offshore are referred to as "local". Transplanted tethers (n = 10 per site), local tethers (n = 10 per site) and transplanted tethers in cage controls (n = 10 per site) were deployed at each site simultaneously and left for 24 hours before processing as outlined above.

Chemical Composition

Sargassum marginatum tissue samples (n = 10 per site) from each of the four source sites used for grazing tethers (see Figure 8.1.1) were cleaned of all epiphytes and frozen at -20 °C within two hours of collection. Frozen samples were transferred to the University of Western Australia and stored at -80 °C until further processing.

PHENOLIC CONCENTRATIONS

A subsample of tissue was used to measure phenolic concentrations of the algae. Tissue samples were lyophilized and ground into a fine powder using a mixer-mill. Total soluble phenolic compound concentrations of tissues were measured using a micro Folin-Ciocalteu method (Van Alstyne 1995), a variation on the Folin-Ciocalteu method that was optimized for a microplate reader. Approximately 10 mg of ground *Sargassum* tissue was placed in a microcentrifuge tube with 1.0 mL 80% methanol. Each tube was vortexed, stored in darkness overnight and then centrifuged at 5000 rpm for 2 min. We diluted 50 μL of this extract with 950 μL of Type 1 Reagent-Grade water. We then took three replicate 100 μL aliquots from each diluted extract and plated them on 96-well Grainer clear microplates. To each well, 40 μL of Folin-Ciocalteu reagent was added using a FLUO-Star Omega microplate reader. The plate was agitated for 30 s before incubating for five minutes at 50 °C. Extracts were made alkaline by the addition of 100 μL of 2 N sodium carbonate and incubated for 30 min before reading absorbance in a FLUOStar spectrophotometer at 765 nm. Phloroglucinol dihydrate standards (n = 3 per standard) (Sigma) were included in each plate to create a standard curve. Concentrations were calculated as % per dry weight of tissue.

LEAF NUTRIENT CONTENT

A subsample of ground tissue (1.1-1.2 mg) from each frond (n = 4 per site) was also analyzed for N content by dry weight (expressed as %N). Dried tissue was packed into tin caps and analyzed in a continuous flow system with a Delta V Plus spectrometer and a Thermo Flush.

Herbivore Census

Herbivorous fish abundance and biomass were assessed three inshore and three offshore sites by visual census on scuba. A diver swam three transects (25x5 m or 50x4 m) from a central point at each site and identified and counted all fish within the transect area. Fish abundance and biomass (kg) at each site was calculated per hectare (Vanderklift et al. 2009a).

Statistical Analyses

Data were analysed in R (R Core Team 2016) using the 'lme' function with the 'nlme' package (Pinheiro et al. 2014). Mixed models were used as the experimental designs included nesting (a

random effect of Site was nested within Location) and some of the designs were unbalanced due to missing measurements. Where the residual plots indicated heteroscedasticity (non-constant variance), the variance structure of the data was modelled using the 'weights' option in the 'lme' function. The best variance structure was then determined by comparing AICs and standardised residual plots (Zuur et al. 2009). In cases where residual plots needed further improvement, log, square-root and inverse sine transformations of the data were considered. Once the best variance structure and transformations had been determined, each model was simplified by step-wise dropping terms from the model until a minimum AIC was achieved. Terms in the final models were evaluated by marginal t-tests and p-values using the model 'summary' function.

8.1.3 RESULTS

Wave height and temperature
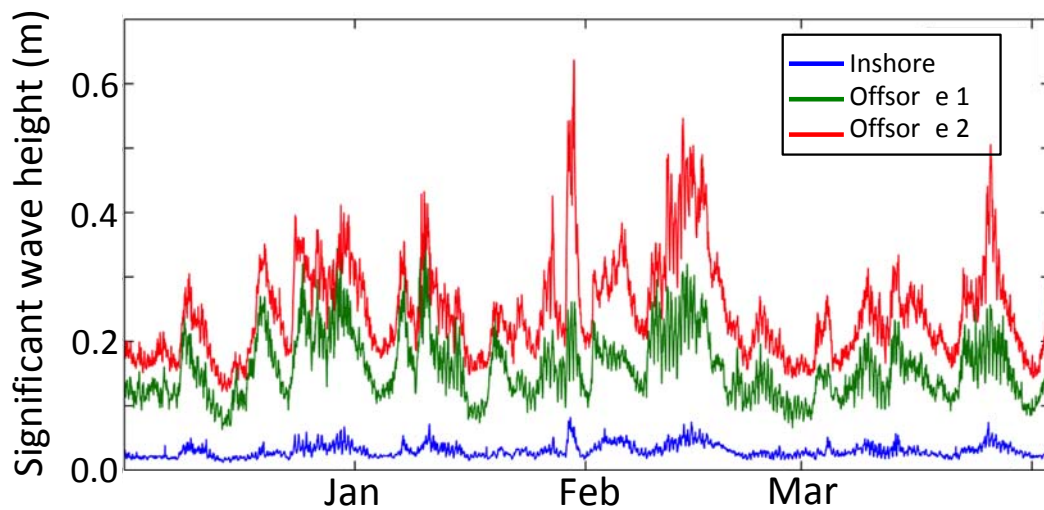
Figure 8.1.3 Wave weights inshore and offshore in the Dampier Archipelago between December 2015 and April 2016.
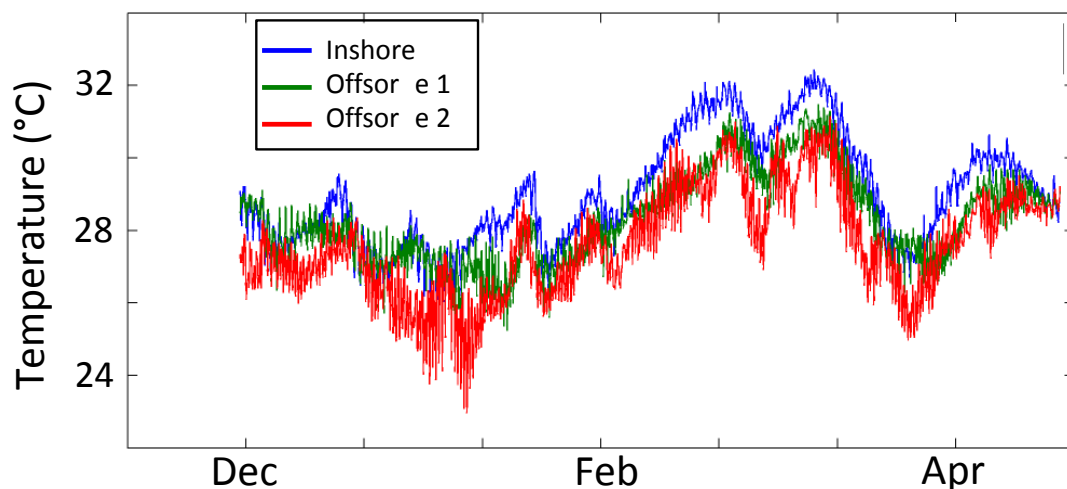
Figure 8.1.4 Continuous benthic temperature record inshore and offshore in the Dampier Archipelago between December 2015 and April 2016.

Significant wave heights in the inshore region of the Dampier Archipelago were <0.1 m for the duration of the sampling period (Figure 8.1.3). In contrast, wave heights in the offshore region reached up to 0.6 m and always exceeded 0.1 m (Figure 8.1.3).

Temperatures also differed between inshore and offshore areas of the Dampier Archipelago. Inshore temperatures were typically 0.5-2 °C higher compared to offshore (Figure 8.1.4).

Growth rates

Growth rates of *Sargassum* were compared both among species (offshore October only), between inshore and offshore sites (April only) and between seasons (offshore only), but due to low replication and large variability among fronds, none of the factors tested were significant (Table S8.1.1). Offshore growth rates of *Sargassum linearifolium* (0.24 cm day^{-1} ± 0.09) and *Sargassum marginatum* (0.3 cm day^{-1} ± 0.11) in October (Figure 8.1.5) were similar. Growth rates of *S. marginatum* were an order of magnitude higher at inshore sites (0.6cm day^{-1} ± 0.15) than offshore sites (0.06cm day^{-1} ± 0.04) in April (Figure 8.1.5). Algal cover was very low at inshore sites in October and growth could not be measured. Growth rates of *S. polyphyllum* were negligible both in April and October. Growth of *S. linearifolium* was not measured in April, as it was not present at any of the study sites.

Since growth of *S. marginatum* did not differ significantly between locations or seasons we could estimate the average growth rate for this species across all sites. The mean growth rate per frond was 0.45 cm day^{-1} ± 0.08, which converted to approximately 0.26 ± 0.04 g day^{-1} frond^{-1} (conversion: weight = 0.57*length, data not shown).
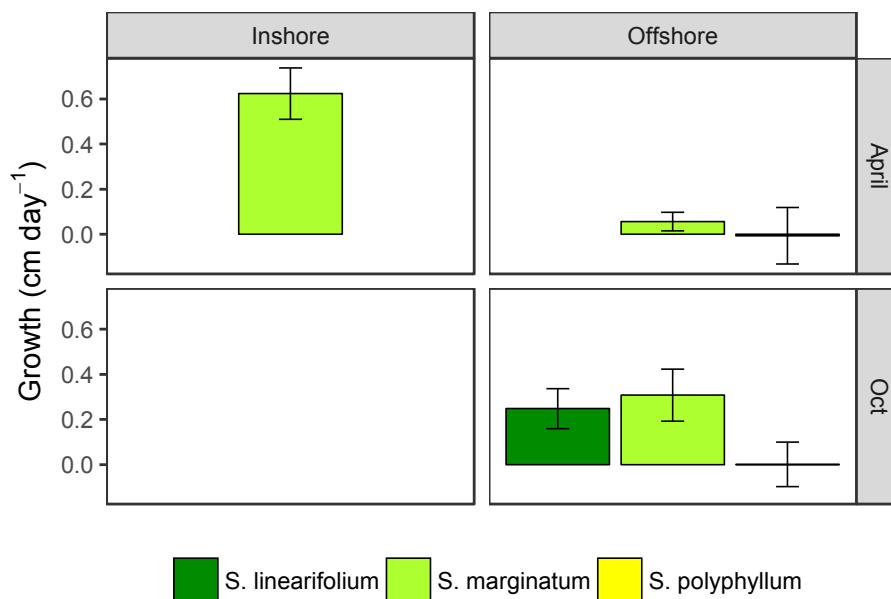
Figure 8.1.5 Growth (mean ± se) of three canopy-forming *Sargassum* species at inshore and offshore sites during the spring of 2015 (October) and fall of 2016 (April).

Seasonal and spatial patterns in chemical composition

Phenolic concentrations were significantly different between seasons but not between inshore and offshore sites (Figure 8.1.6a, Table S8.1.2). Nitrogen content (% dry mass) of *S.* marginatum also displayed a seasonal pattern and was 1.5 times higher in the fall than in the spring (Figure 8.1.6b, Table S8.1.2). No difference was detected in nitrogen content between in- and offshore locations.

There was no relationship between the % nitrogen and the phenolic content (Figure 8.1.7). The fronds of *S. marginatum* used in the cross-transplant experiment in April also did not show differences in nitrogen content or phenolic content between the inshore and offshore 'parent' population (Figure 8.1.8, Table S8.1.3).
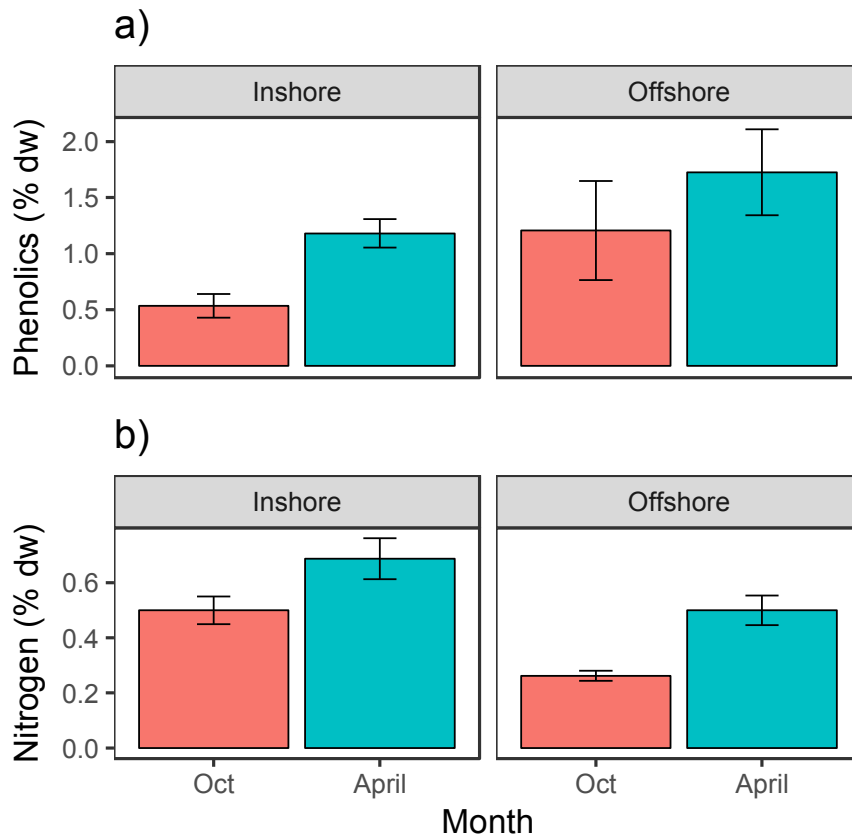
Figure 8.1.6 Phenolic and nitrogen content (mean ± se as % dry weight) of *Sargassum marginatum* tissue collected at inshore and offshore sites in the Dampier Archipelago during October 2015 and April 2016.
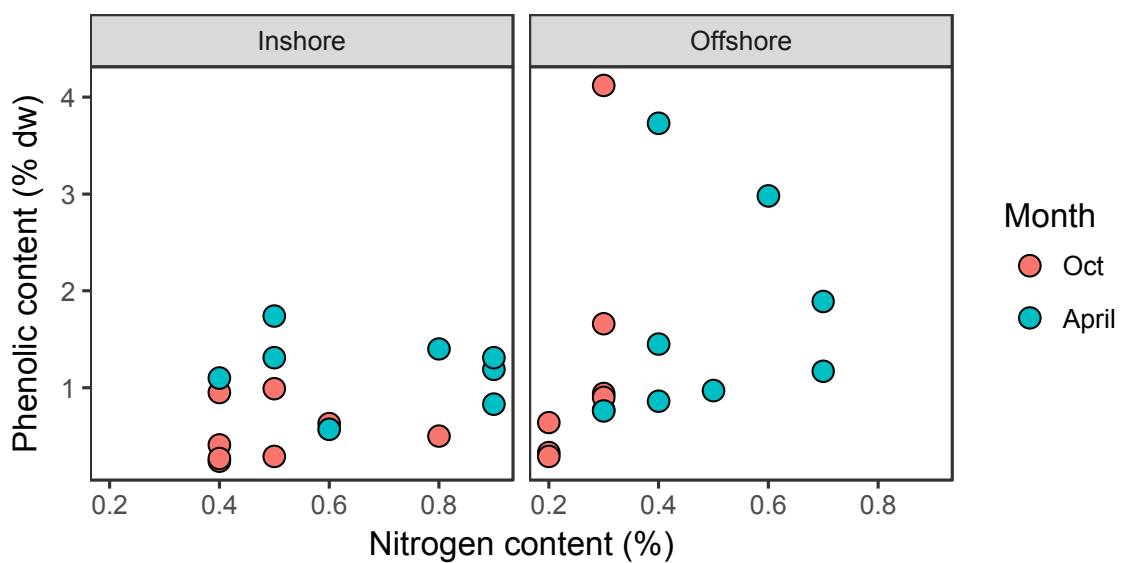
Figure 8.1.7 Phenolic versus nitrogen content of *Sargassum marginatum* from the Dampier Archipelago collected at inshore and offshore sites in October 2015 and April 2016.
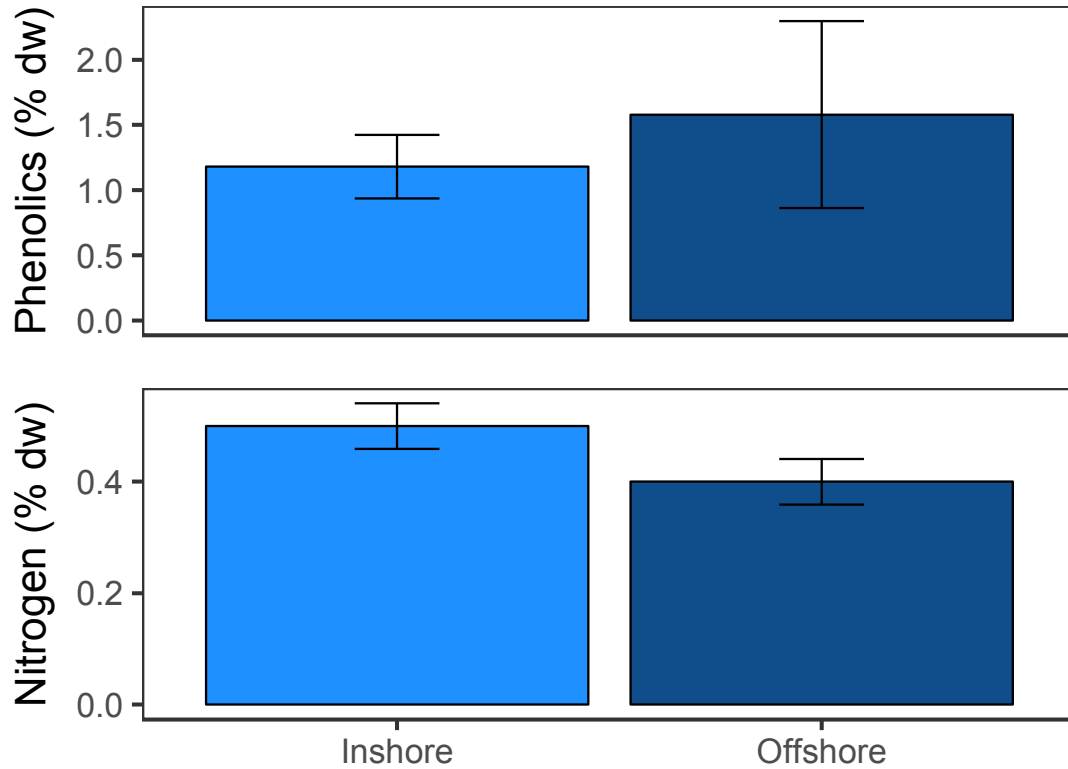
Figure 8.1.8 Phenolic and nitrogen content (mean ± se) in *Sargassum marginatum* fronds from the inshore and offshore "parent populations" for the transplant experiment carried out in April.

Consumption

There was a significant effect of season on consumption rate of *S. marginatum* tethers with a higher overall rate in April (Figure 8.1.9, Table S8.1.4). Mean grazing rates appeared higher in October compared to in April for inshore sites, but the statistical model did not support this, probably due to large variability among fronds. There was, however, a significant interaction between season, site biomass (low or high standing crop of algae) and in-offshore location (Figure 8.1.9, Table S8.1.4): The highest rate of consumption, by far, took place in offshore sites with low standing crop in April where an average of 65.6 ± 4.25% (by weight) was consumed per day (Figure 8.1.9). In comparison, consumption at all other sites in April was between 0.0 ± 1.66% and 7.37 ± 1.5% (Figure 8.1.9). In October the average consumption was 10.8 ± 7.97% to 20.9 ± 7.91% (Figure 8.1.9).

We calculated the mean consumption rates in g per day per frond for each site and season to give us ranges of consumption rates for different combinations of season, in-offshore location and standing crop of algae. All inshore sites across both seasons had similar consumption rates of 0.3 - 1.1 g day^{-1} frond^{-1}. Offshore sites with high biomass across both seasons and offshore sites with low standing crop of algae in October had consumption rates of 0.0 - 1.2 g day^{-1} frond^{-1}. In contrast, in April, offshore sites with low standing crop had much higher rates of consumption of 2.6 - 11.5 g day^{-1} frond^{-1}.

A comparison of grazing rates on *S. linearifolium* and *S. marginatum* in October yielded no significant differences based on species, location or standing crop of algae (site biomass) (Figure 8.1.10, Table S8.1.5). The average grazing rates for both species across all sites was 23 ± 1.8%.
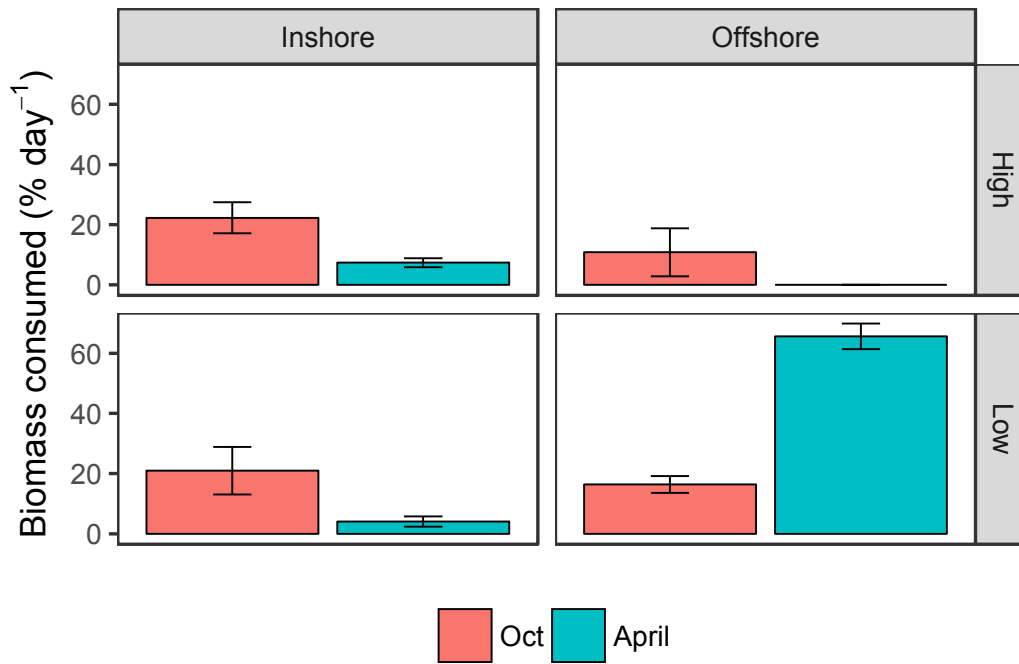
Figure 8.1.9 Seasonal and cross shelf variation in grazing (mean ± se) on *Sargassum marginatum* at Dampier Archipelago. Tethered fronds were deployed at the location (inshore or offshore) where they had been collected. Rates are shown from inshore (left) and offshore (right) sites with high (top) and low (bottom) standing crop of macroalgae
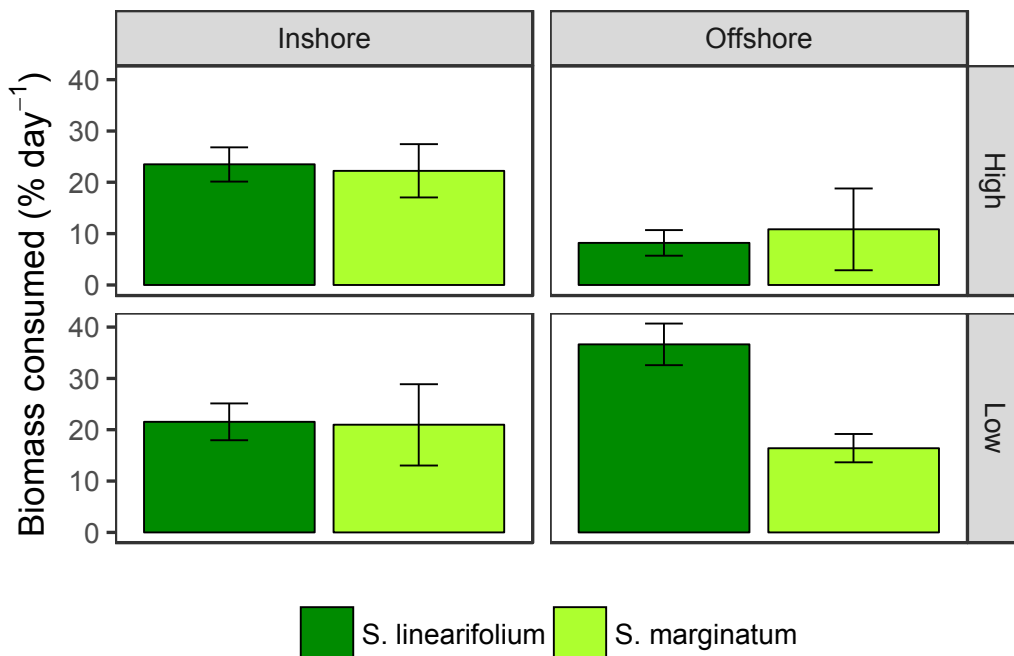
Figure 8.1.10 Grazing rates (mean ± se) on *Sargassum marginatum* and *S. linearifolium* at Dampier Archipelago in October 2015*. Tethered fronds were deployed simultaneously in the location (inshore or offshore) where they had been collected. Rates are shown for inshore (left) and offshore (right) sites with high (top) and low (bottom) standing crop of macroalgae.

Results of the cross-transplant experiment carried out in April 2016 indicated that grazers did not show a preference based on 'parent' population (inshore versus offshore) of the tethers. Due to logistic reasons, the design of the experiment was not orthogonal and the results were evaluated in two separate models: There was no difference in grazing rates on locally sourced and transplanted *S. marginatum* in a mixed model of data from the offshore sites (Figure 8.1.11, p = 0.054, Table S8.1.6a) or in a mixed model of data from the sites with high standing crop (p = 0.249, Table S8.1.6b). No tethers were placed at inshore sites with low biomass preventing us from evaluating the effect of standing crop on consumption inshore. Offshore, however, the standing crop of algae had a large effect on grazing rates of both types of tethers with much higher rates of grazing in areas of low algal biomass (Figure 8.1.11, p = 0.015**, Table S8.1.6b).
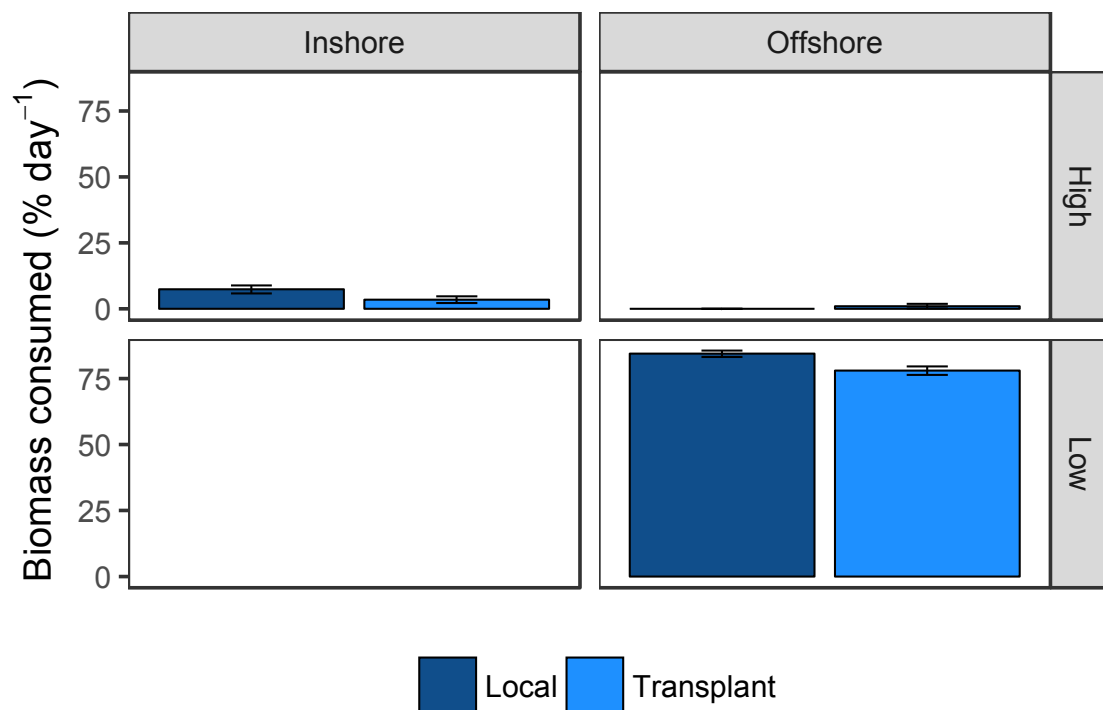
Figure 8.1.11 Grazing rates (mean ± se) of 'local' and 'transplanted' fronds of *Sargassum marginatum* in April 2016. The tethered fronds were either deployed in the same location they had been collected (local, dark blue) or transplanted from inshore to offshore/ offshore to inshore (light blue). Rates are shown for uncaged inshore (left) and offshore (right) sites with high (top) and low (bottom) standing crop of macroalgae. No algal transplants were made inshore in sites of low biomass.

The abundance of herbivorous fish was highly variable among transects and sites. The mean numbers of herbivores were highest offshore at sites with low biomass in October (6440 ± 2731 individuals ha^{-1}) and April (1973 ± 693 individuals ha^{-1}) compared to all inshore sites (360 ± 183 to 813 ± 247 individuals ha^{-1}) and offshore sites of high algal standing crop (80 ± 46 to 813 ± 527 individuals ha^{-1}) (Figure 8.1.12a). Despite the large differences in the means, there was no significant effect of any of the factors tested (season, location, standing crop of algae, Table S8.1.7a). We observed the same pattern for biomass of herbivorous fish (Figure 8.1.12b) with highest means at offshore sites with low biomass in October (1186 ± 433 kg ha^{-1}) and April (560 ± 150 kg ha^{-1}) compared to all inshore sites (4.5 ± 2.3 to 177 ± 88 kg ha^{-1}) and offshore sites of high algal biomass (31 ± 21 to 48 ± 36 kg ha^{-1}), but again, the main effects were not significant (Table S8.1.7b). The majority of the grazers belonged to the genera *Acanthurus*, *Scarus* and *Siganus* (Figure 8.1.13).

a)

b)
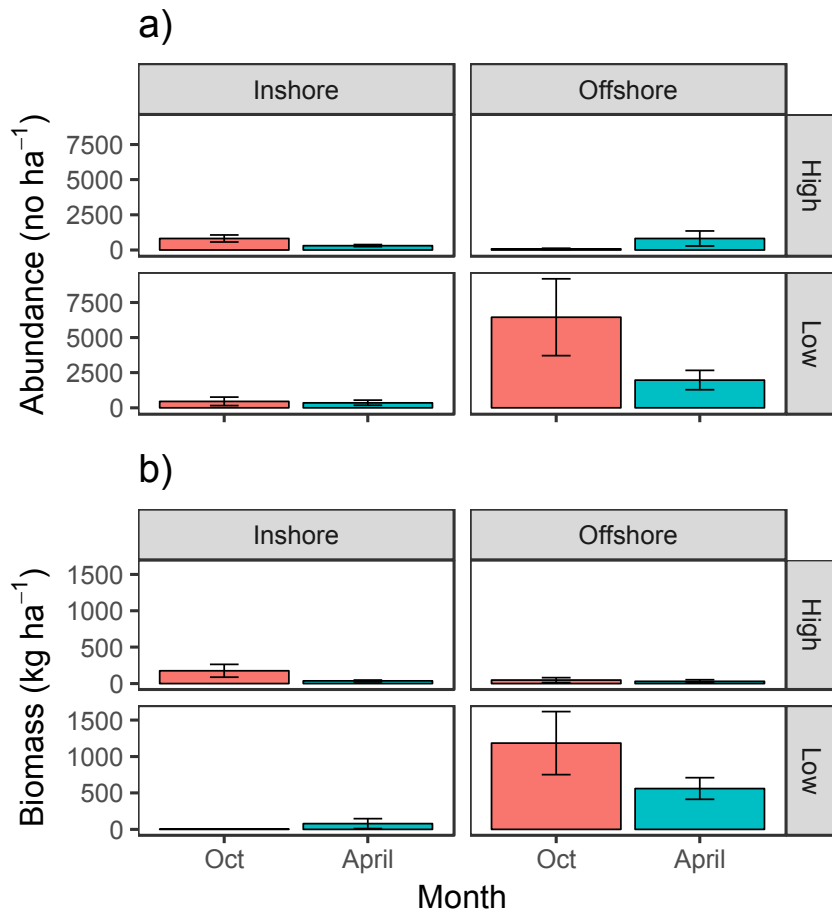
Figure 8.1.12 Cross-shelf a) abundance (no ha^{-1}) and b) biomass (kg ha^{-1}) of herbivorous fish from the Dampier Archipelago at sites with High or Low macroalgal biomass where grazing tethers were deployed. Data shown are means ± se based on observed herbivorous fish from diver-swum transects.
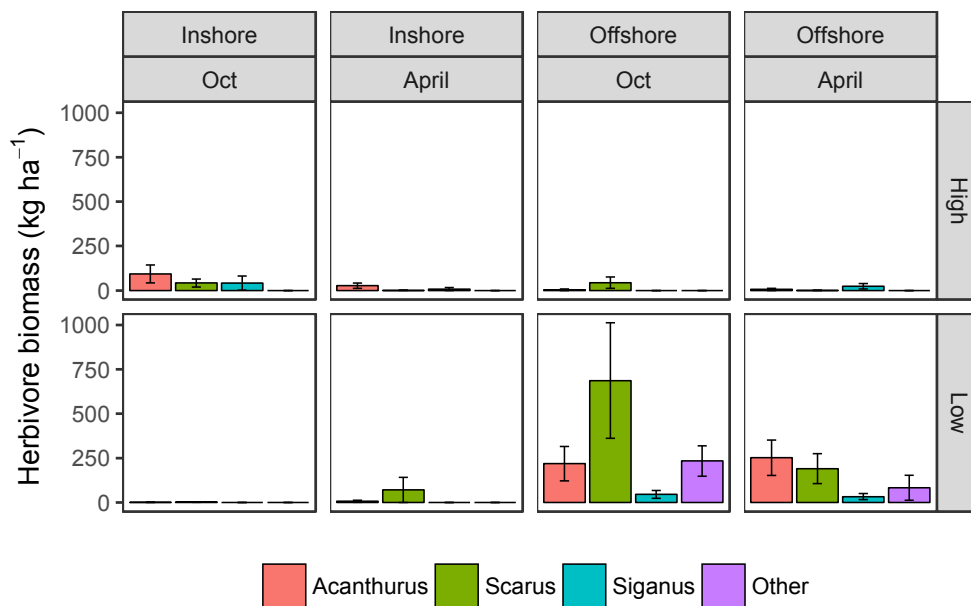
Figure 8.1.13 Cross-shelf biomass (kg ha^{-1}) of major herbivorous fish genera in the Dampier Archipelago at sites with High and Low macroalgal biomass where grazing tethers were deployed. Data shown are means ± se based on average observations from diver-swum transects.

8.1.4 DISCUSSION

Benthic habitats tend to be affected by large spatial and temporal variation in top-down and bottom-up controls. In this study, we examined grazing and growth of canopy-forming *Sargassum* across contrasting seasons and in- and offshore sites in a tropical archipelago. We found few differences in our measurements based on season or location alone. Instead, complex interactions between several factors appear responsible for localized and temporally intense grazing that is potentially preventing large canopies of *Sargassum* from forming at some sites.

Grazing rates were significantly higher in April than October, but this was due to very high rates of consumption at offshore sites with low standing crop of algae. At these sites > 60% of the algal tether biomass was consumed per day in the first experiment and >75% of the tethers in the cross transplant experiment compared to <8% at all other sites in April and an average consumption of 11-21% in October. We would expect consumption to be higher in areas where algal food supply is limited, but this effect was not consistent. The effect of standing algal crop on consumption rate was only evident offshore and only in April suggesting seasonal differences in grazing rates at those locations.

Spatial patterns in macroalgal chemical production and subsequent grazing effects vary across multiple spatial scales, from meters to kilometres (Paul and Van Alstyne 1988; Steinberg 1989; Pavia and Åberg 1996) and between hemispheres (Van Altena and Steinberg 1992). The Dampier Archipelago is characterised by cross-shelf differences in water clarity, temperature and exposure, which may all affect the chemical composition of macroalgae. Despite this gradient, no spatial patterns in macroalgal chemistry were evident. We did, however, find a clear seasonal pattern where phenolic content and % nitrogen were significantly lower in October. It is not clear whether this difference would render the algal fronds more or less palatable since the higher nutritional value associated with an increase in % nitrogen may compensate for the negative effect of phenolics (Van Alstyne et al. 2001; Svensson et al. 2007). The seasonal pattern in phenolic content found here has been observed previously in more temperate habitat-forming seaweeds (Parys et al. 2009). Increased phenolic concentrations late in the growing season may protect from the chronic abiotic stress of prolonged UV exposure (Pavia et al. 1997). It is possible that the temporal patterns in the phenolic content and % N of *S. marginatum* are not directly linked to changes in abiotic conditions, but may follow patterns in growth and reproductive status of the algae.

Grazing activity did not seem to be linked to patterns in phenolic compounds. While phenolic compounds have been suggested to act as herbivory deterrents, their overall role in tropical regions like the Dampier Archipelago remains unclear (Lewis 1985; Steinberg et al. 1991; Steinberg and Van Altena 1992). Our findings support the growing body of research that suggests phenolic compounds of tropical macroalgae have primary functions other than herbivory deterrence, particularly in Australasia (Steinberg 1992, van Hees 2017).

Macroalgal morphology is important to grazer preference and may create differences in grazing rates between macroalgal species (Littler and Littler 1980). *Sargassum marginatum* fronds are typically rounder and tougher than the elongated thin fronds of *S. linearifolium* (Dixon et al. 2012). In the Dampier Archipelago, there was no difference in grazing rate between these two species. This agrees with previous studies that found similar grazing rates on different life stage morphologies (Van Alstyne et al. 2001) and among different *Sargassum* species (Steinberg and Paul 1990). Differences in the morphologies of closely related species do not appear distinct enough to affect overall grazing activity.

Interestingly, the observed patterns in grazing rates were not mirrored by changes in the abundance or biomass of herbivorous fishes. Herbivorous fishes, even a single species, have the potential to

control macroalgal distribution (Hoey and Bellwood 2010; Taylor and Schiel 2010; Bennett and Bellwood 2011). The overall spatial and temporal variability of herbivores is likely to mask clear patterns in their distribution. Wave activity has been hypothesized to reduce herbivory (Vanderklift et al. 2009b), but with higher grazing rates at offshore locations, wave activity in the Dampier Archipelago does not appear to hinder herbivory. It is possible that grazing rates are controlled by other external factors, such as the overall structural complexity of the habitat (Vergés et al. 2011) although this would not explain the seasonal patterns we observed.

Growth did not show any significant spatial or temporal trends and rates were similar for the three species sampled. The *Sargassum* fronds inshore were too small to measure in October and, based on this, we can infer that growth rates inshore did not increase until later in the summer while plants offshore began to grow more slowly as the summer progressed. Senescence is a natural part of the annual *Sargassum* life cycle that occurs later in the growing season after reproduction and following the reduction of growth rates.

The balance between growth and consumption of macroalgae largely determines their proliferation. We estimated that the mean growth rate of *Sargassum marginatum* across locations and seasons was 0.26 g day^{-1} frond^{-1}. While this is a fairly rough estimate, it gives us an indication of how these two processes are balanced across inshore and offshore areas of the Dampier Archipelago in the two contrasting seasons studied here. For the majority of sites, the measured grazing rates were 0 - 1.2 g day^{-1} frond^{-1} suggesting that top-down control by grazers could be significant and able to balance growth in both seasons. There will, however, be sites and times when grazing is non-existent and net growth of *Sargassum* would be controlled by bottom-up forces, such as nutrient availability and light. We found a notable exception in April when the fronds tethered at offshore sites with low standing crop were heavily grazed with rates of 2.6 - 11.5 g day^{-1} frond^{-1}. These rates greatly exceed our estimated rates of growth, indicating that there are times and locations when top-down control may overwhelm growth rates of *Sargassum*. This is one likely mechanism that maintains bare areas in the Archipelago.

The shallow reefs in the Dampier Archipelago are characterised by high spatial and temporal variability in both abiotic and biotic parameters. This variability will, in turn, create spatial and temporal patterns in biotic interactions. We could not explain patterns in grazing across the Dampier Archipelago in terms of simple responses to in-offshore location, herbivore abundance, food quality (chemical composition of the algae) or food availability to herbivores (standing crop of algae at each site). There appeared to be significant interactions between these terms and the interactions varied with season. The Archipelago likely experiences seasonal shifts in the conditions that regulate both bottom-up and top-down controls, but these drivers are currently poorly understood in the area.

8.1.5 ACKNOWLEDGEMENTS

8.1.6 REFERENCES

Bennett S, Bellwood DR (2011) Latitudinal variation in macroalgal consumption by fishes on the Great Barrier Reef. Mar Ecol Prog Ser 426:241–252.

Bennett S, Wernberg T, Harvey ES, Santana-Garcon J, Saunders BJ (2015) Tropical herbivores provide resilience to a climate-mediated phase shift on temperate reefs. Ecol Lett 18:714–723.

Capon RJ, Ghisalberti EL, Jefferies PR (1983) Metabolites of the green algae, Caulerpa species. Phytochemistry 22:1465–1467.

Cho JY, Kwon E, Choi J, Hong S, Shin H (2001) Antifouling activity of seaweed extracts on the green alga *Enteromorpha prolifera* and the mussel *Mytilus edulis*. J Appl Phycol 13:117–125.

Dixon RRM, Huisman JM, Buchanan J, Gurgel CFD, Spencer P (2012) A morphological and molecular study of austral Sargassum (fucales, phaeophyceae) supports the recognition of phyllotricha at genus level, with further additions to the genus sargassopsis. J Phycol 48:1119–1129.

Enge S, Nylund GM, Harder T, Pavia H (2012) An exotic chemical weapon explains low herbivore damage in an invasive alga. Ecology 93:2736–2745.

Erickson AA, Paul VJ, Van Alstyne KL, Kwiatkowski LM (2006) Palatability of macroalgae that use different types of chemical defenses. J Chem Ecol 32:1883–1895.

Gaines SD, Lubchenco J (1982) A unified approach to marine plant-herbivore interactions. II. Biogeography. Annu Rev Ecol Syst 13:111–138.

Geiselman JA, McConnell OJ (1981) Polyphenols in brown algae Fucus vesiculosus and Ascophyllum nodosum: Chemical defenses against the marine herbivorous snail,Littorina littorea. J Chem Ecol 7:1115–1133.

Gross EM (2003) Allelopathy of Aquatic Autotrophs. CRC Crit Rev Plant Sci 22:313–339.

Hay ME (1997) The ecology and evolution of seaweed-herbivore interactions on coral reefs. Coral Reefs 16:S67–S76.

Hoey AS (2010) Size matters : macroalgal height influences the feeding response of coral reef herbivores. Mar Ecol Prog Ser 411:299–302.

Hoey AS, Bellwood DR (2010) Cross-shelf variation in browsing intensity on the Great Barrier Reef. Coral Reefs 29:499–508.

Jompa J, McCook LJ (2003) Coral – algal competition : macroalgae with different properties have different effects on corals. Mar Ecol Prog Ser 258:87–95.

Kim MJ, Choi JS, Kang SE, Cho JY, Jin HJ, Chun BS, Hong YK (2004) Multiple allelopathic activity of the crustose coralline alga Lithophyllum yessoense against settlement and germination of seaweed spores. J Appl Phycol 16:175–179.

Lewis SM (1985) Herbivory on coral reefs : algal susceptibility to herbivorous fishes. Oceologia 65:370–375.

Littler MM, Littler DS (1980) The evolution of thallus from and survival strategies in benthic marine macroalgae: field and laboratory tests of a functional form model. Am Nat 116:25–42.

Lyons DA, Van Alstyne KL, Scheibling RE (2007) Anti-grazing activity and seasonal variation of dimethylsulfoniopropionate- associated compounds in the invasive alga Codium fragile ssp. tomentosoides. Mar Biol 153:179–188.

McCarty AT, Sotka EE (2013) Geographic variation in feeding preference of a generalist herbivore: The importance of seaweed chemical defenses. Oecologia 172:1071–1083.

McCook LJ (1997) Effects of herbivory on zonation of Sargassum spp. within fringing reefs of the central Great Barrier Reef. Mar Biol 129:713–722.

Parys S, Kehraus S, Pete R, Küpper FC, Glombitza K-W, König GM (2009) Seasonal variation of polyphenolics in *Ascophyllum nodosum* (Phaeophyceae). Eur J Phycol 44:331–338. Paul VJ, Van Alstyne KL (1988) Chemical defense and chemical variation in some tropical Pacific species of Halimeda. Coral Reefs 6:263–269.

Pavia H, ÅBerg P (1996) Spatial variation in polyphenolic content of *Ascophyllum nodosum* (Fucales, Phaeophyta). Hydrobiologia 326–327:199–203.

Pavia H, Cervin G, Lindgren A, Åberg P (1997) Effects of UV-B radiation and simulated herbivory on phlorotannins in the brown alga *Ascophylum nodosum*. Mar Ecol Prog Ser 157:139–146.

Pinheiro J, Bates D, DebRoy S, Sarkar D and R Core Team (2017) nlme: Linear and Nonlinear Mixed Effects Models. R package version 3.1-131. https://CRAN.R-project.org/package=nlme

R Core Team (2016) R: A language and environment for statistical computing. R Foundation for Statistical Computing, Vienna, Austria. https://www.R-project.org/

Rasher DB, Hay ME (2014) Competition induces allelopathy but suppresses growth and anti-herbivore defence in a chemically rich seaweed. Proc Biol Sci 281:20132615.

Renjun W, You W, Xuexi T (2012) Identification of the toxic compounds produced by Sargassum thunbergii to red tide microalgae. Chinese J Oceanol Limnol 30:778–785.

Sammarco PW (1983) Effects of fish grazing and damselfish territoriality on coral reef algae. I. Algal community structure. Mar Ecol 13:1–14.

Saunders BJ, Kendrick GA, Harvey ES (2015) Temperate territorial damsel fish act like tropical damsel fish , but have no measurable effect on algae within their feeding areas. J Exp Mar Bio Ecol 472:107–118.

Skrzypek G (2013) Normalization procedures and reference material selection in stable HCNOS isotope analyses: An overview. Anal Bioanal Chem 405:2815–2823.

Steinberg PD (1989) Biogeographical variation in brown algal polyphenolics and other secondary metabolites: comparison between temperate Australasia and North America. Oceologia 78:373–382.

Steinberg PD, Paul VJ (1990) Fish feeding and chemical defenses of tropical brown algae in Western Australia. Mar Ecol Prog Ser 58:253–259.

Steinberg PD, Van Altena I (1992) Tolerance of marine invertebrate herbivores to brown algal phlorotannins in temperate Australasia. Ecol Monogr 62:189–222.

Steinberg PD, Edyvane K, De Nys R, Birdsey R, Van Altena IA (1991) Lack of avoidance of phenolic-rich brown algae by tropical herbivorous fishes. Mar Biol 109:335–343.

Steneck RS, Dethier MN (1994) A Functional Group Approach to the Structure of Algal-Dominated Communities. Oikos 69:476.

Svensson CJ, Pavia H, Toth GB (2007) Do plant density, nutrient availability, and herbivore grazing interact to affect phlorotannin plasticity in the brown seaweed Ascophyllum nodosum. Mar Biol 151:2177–2181.

Taylor DI, Schiel DR (2010) Algal populations controlled by fish herbivory across a wave exposure gradient on southern temperate shores. Ecology 91:201–211. Van Alstyne KL (1995) Comparison of three methods for quantifying brown algal polyphenolic compounds. J Chem Ecol 21:45–58.

Van Alstyne KL, Whitman SL, Ehlig JM (2001) Differences in herbivore preferences, phlorotannin production, and nutritional quality between juvenile and adult tissues from marine brown algae. Mar Biol 139:201–210. doi: 10.1007/s002270000507

Van Alstyne KL, Nelson A V, Vyvyan JR, Cancilla DA (2006) Dopamine functions as an antiherbivore defense in the temperate green alga Ulvaria obscura. Oceologia 148:304–311.

Van Altena IA, Steinberg PD (1992) Are differences in the responses between North American and Australasian marine herbivores to phlorotannins due to differences in phlorotannin structure? Biochem Syst Ecol 20:493–499.

Vanderklift M, Babcock R, Bearham D, Clapin G, Limbourn A, Murphy N, Parker F, Phillips J (2009a) Ecosystem impacts of human usage and the effectiveness of zoning for biodiversity conservation Trophic effects experiments interim final report. Report to WA Dept of Conservation and Western Australian Marine Science Institution.

Vanderklift MA, Lavery PS, Waddington KI (2009b) Intensity of herbivory on kelp by fish and sea urchins differs between inshore and offshore reefs. Mar Ecol Prog Ser 376:203–211.

Vergés A, Vanderklift MA, Doropoulos C, Hyndes GA (2011) Spatial patterns in herbivory on a coral reef are influenced by structural complexity but not by algal traits. PLoS One.

Zuur, A., Ieno, E.N., Walker, N., Saveliev, A.A., Smith, G.M., 2009. Mixed EffectsModels and Extensions in Ecology. R. Springer Science & Business Media.

8.1.7 SUPPLEMENTARY MATERIAL

Table S8.1.1 The models to describe patterns in macroalgal growth. The first model (G1) tested differences in growth of *Sargassum marginatum* by season for offshore sites only. The second model (G2) compared growth of *S. marginatum*, *S. linearifolium* and *S. polyphyllum* at offshore sites in October. The results of ANOVAs for these two models are shown. The third model (G3) was a mixed model that compared growth of *S. marginatum* at inshore and offshore sites in April. For this model, the fixed terms retained in the best model (lowest AIC) are shown along with their estimated coefficient values (Value, standard errors for these values (SE), degrees of freedom (DF), t-values and p-values).

	DF	SUM SQ	MEAN SQ	F-VALUE	P
G1: *S. marginatum* growth by season (offshore sites) **Model: lm(growth ~ season)**					
Season	1	95.38	95.38	3.25	0.07
Residuals	23	54.21	54.21	1.85	0.18
G2: Growth of *S. marginatum*, *S. linearifolium* and *S. polyphyllum* offshore in October **Model: lm(growth ~ species * site)**					
Species	2	29.32	29.32	1.00	0.32
Residuals	46	130.84	130.84	4.46	0.04*
	VALUE	SE	DF	T-VALUE	P
G3: S. marginatum growth by location (in-offshore) in April **Model: lme(growth ~ location, random = ~1|location:site)**					
Location	-0.5578	0.3782	1	-1.475	0.379

Table S8.1.2 The models to describe patterns in (a) phenolic and (b) nitrogen content in *Sargassum marginatum*. The fixed terms retained in the best models (based on lowest AIC) are shown along with their estimated coefficient values (Value, standard errors for these values (SE), degrees of freedom (DF), t-values and p-values.

	VALUE	SE	DF	T-VALUE	P
a) *S. marginatum* phenolic content (% dw)					
Model: lme(phenolics ~ season*location, random = ~1|location:site, weights = varIdent(form = ~1|location))					
Season	0.646	0.165	26	3.924	<0.001***
Location	0.671	0.430	2	1.559	0.259
Season:Location	-0.126	0.609	26	-0.207	0.837
b) *S. marginatum* nitrogen content (% dw)					
Model: lme(nitrogen ~ season*location, random = ~1|location:site, weights = varPower())					
Season	0.188	0.085	26	2.212	0.036*
Location	-0.238	0.101	2	-2.352	0.143
Season:Location	0.500	0.098	26	0.509	0.615

Table S8.1.3 The results of one-way ANOVAs to describe differences in (a) phenolic and (b) nitrogen content in the *Sargassum marginatum* used in the cross transplant experiment.

	DF	Sum Sq	Mean Sq	F-value	p
a) *S. marginatum* phenolic content (% dw) Model: lm(phenolics ~ location)					
Location	1	0.320	0.320	0.279	0.617
Residuals	6	6.894	1.149		
b) *S. marginatum* nitrogen content (% dw) Model: lm(nitrogen ~ location)					
Location	1	0.020	0.020	3.000	0.134
Residuals	6	0.040	0.007		

Table S8.1.4 The models to describe spatial and temporal patterns in consumption of *Sargassum marginatum*. The best model (based on lowest AIC) was of the formula: lme(arcsine(percent consumed) ~ season * algal biomass * location, random = ~1|location:site, weights = varIdent(form = ~1|season)). The fixed terms retained in the model are shown along with their estimated coefficient values (Value, standard errors for these values (SE), degrees of freedom (DF), t-values and p-values.

	VALUE	SE	DF	T-VALUE	P
Season	-0.184	0.085	125	-2.156	0.033*
Algal biomass	-0.022	0.317	4	-0.070	0.947
Location	-0.173	0.317	4	-0.547	0.614
Season:Algal biomass	-0.063	0.146	125	-0.435	0.664
Season:Location	-0.063	0.146	125	-0.429	0.669
Algal biomass:Location	0.264	0.433	4	0.609	0.575
Season:Algal biomass:Location	0.768	0.206	125	3.729	<0.001***

Table S8.1.5 The model describing spatial and temporal patterns in two species of *Sargassum, S. marginatum* and *S. linearifolium* in October 2015. The best model (based on lowest AIC) was of the formula: lme(arcsine(percent consumed) ~ species * algal biomass * location, random = ~1|location:site, weights = varIdent(form = ~1|species)). The fixed terms retained in the model are shown along with their estimated coefficient values (Value, standard errors for these values (SE), degrees of freedom (DF), t-values and p-values.

	VALUE	SE	DF	T-VALUE	P
Species	-0.050	0.086	118	-0.585	0.600
Algal biomass	-0.008	0.122	2	-0.069	0.951
Location	-0.226	0.122	2	-1.852	0.205
Species:Algal biomass	-0.012	0.146	118	-0.082	0.935
Species:Location	0.055	0.146	118	0.375	0.708
Algal biomass:Location	0.406	0.170	2	2.388	0.140
Species:Algal biomass:Location	-0.244	0.204	118	-1.200	0.233

Table S8.1.6 Mixed models describing patterns in grazing on transplanted and local tethers in the cross-transplant experiment (a) for sites with high biomass and (b) offshore sites. The fixed terms retained in the model are shown along with their estimated coefficient values (Value, standard errors for these values (SE), degrees of freedom (DF), t-values and p-values.

	VALUE	SE	DF	T-VALUE	P
a) Local and transplanted tethers at sites with high algal biomass Model: lme(arcsine(percent consumed) ~ transplant, random = ~1|location:site)					
Transplant	-0.071	0.036	55	-1.971	0.0538
b) Local and transplanted tethers at offshore sites Model: lme(arcsine(percent consumed) ~ transplant * algal biomass, random = ~1|location:site, weights = varIdent(form = ~1|transplant))					
Transplant	0.043	0.037	54	1.165	0.249
Algal biomass	1.171	0.027	54	43.561	0.015*
Transplant:Algal biomass	-0.126	0.045	1	-2.787	0.0073**

Table S8.1.7 The model describing spatial and temporal patterns in the (a) number and (b) biomass of herbivorous fish. The fixed terms retained in the best models (based on lowest AIC) are shown along with their estimated coefficient values (Value, standard errors for these values (SE), degrees of freedom (DF), t-values and p-values.

	VALUE	SE	DF	T-VALUE	P
a) Number of herbivorous fish ha⁻¹					
Model: lme(log(number of fish) ~ season * algal biomass * location, random = ~1|location:site, weights = varPower())					
Season	-0.369	0.535	25	-0.690	0.496
Algal biomass	-0.909	0.625	2	-1.455	0.283
Location	-1.379	0.625	2	-2.206	0.158
Season:Algal biomass	0.969	0.898	25	1.079	0.291
Season:Location	1.018	0.898	25	1.134	0.268
Algal biomass:Location	3.066	0.884	2	3.470	0.074
Season:Algal biomass:Location	-2.143	1.260	25	-1.700	0.102
b) Biomass of herbivorous fish kg ha⁻¹					
Model: lme(sqrt(biomass of fish) ~ season * algal biomass * location, random = ~1|location:site, weights = varPower())					
Season	-3.994	2.935	25	-1.361	0.186
Algal biomass	-7.698	5.420	2	-1.420	0.291
Location	-4.153	5.836	2	-0.712	0.551
Season:Algal biomass	8.982	4.244	25	2.116	0.045*
Season:Location	3.089	4.333	25	0.713	0.483
Algal biomass:Location	32.712	9.815	2	3.333	0.079
Season:Algal biomass:Location	-16.585	9.546	25	-1.737	0.095

8.2 The impacts of crown-of-thorns starfish on north-western Australian coral reefs

Authors: Haywood MDE, Thomson DP, Babcock RC, Pillans RD, Keesing JK, Vanderklift MA, Miller M, Rochester WA, Donovan A, Evans R, Shedrawi G, Field S.

ABSTRACT

High densities of the corallivorous crown-of-thorns starfish (COTS; *Acanthaster planci*) have occurred throughout the Indo-Pacific often resulting in widespread coral loss. Whilst they have previously been recorded at Barrow and the Montebello Islands, in the Pilbara offshore bioregion of north-western Australia, their densities were relatively low. Outbreak densities of COTS have been described as the level at which the rate of coral consumption by the starfish is equal to or greater than rate at which the coral grows. In 2014, we recorded densities as high as 320 ± 58 COTS ha^{-1} in the region which is considered an outbreak sized population in the literature. Although the causes of outbreaks of COTS remains unknown, it is thought that either nutrient enrichment resulting in enhanced COTS larval success or reduced predation of the post settlement stages may be responsible. However, whilst there is little terrestrial runoff and agriculture in this region, both temperature and chlorophyll-α levels appear to be sufficient to allow a high degree of COTS larval success in most years. The area is remote from large population centres and is not fished heavily, and so it is unlikely that COTS predators have been reduced markedly. The region was subjected to anomalously high water temperatures during the summers of 2010–11 and particularly 2012–13 which resulted in the mortality of almost 70% of live coral. We hypothesise that the observed high densities of COTS are the result of the starfish aggregating in response to a depleted food resource rather than an outbreak. Given that the coral cover has been reduced so substantially, the high densities of COTS still represent a significant threat to the recovery of the coral communities of the region.

8.2.1   INTRODUCTION

Global threats to coral cover

The extent and condition of coral reefs are declining worldwide; the original area of coral reefs has decreased by 19% and a further 15% are in danger of dying within the next 10–20 years (Wilkinson 2008). The average annual decrease in coral in the Indo-Pacific has been estimated to be 2% between 1997 and 2003, and the current cover of coral in the region is at least 20% below the original baseline (Bruno and Selig 2008). In 2012, coral cover on the Great Barrier Reef (GBR) was been estimated to be 50% less than baseline (De'ath et al. 2012) and following recent severe and extensive bleaching events in 2016 and 2017 is now likely to be even less than this (Hughes et al. 2017). Major causes of coral mortality include several climate mediated influences, such as increasing seawater temperatures, ocean acidification and increased frequency of intense cyclones (Chin et al. 2011; Sobel et al. 2016). Other more direct anthropogenic influences include increased pollution and turbidity, and sedimentation resulting from terrestrial runoff and dredging for port development (Bartley et al. 2014; Burke et al. 2012).

Coral reefs in the Pilbara Offshore bioregion

The coral communities of the Montebello and Barrow Islands and Tryall Rocks (hereafter termed MBI), 60 km off Australia's north-west coast, have been well documented with four published studies giving information on their distribution, diversity and condition (Bancroft 2011; Marsh 2000a; Richards and Rosser 2012; Speed et al. 2013). In 2011, coral cover in the region was recorded as the second highest in Western Australia (40.07 ± 0.82 %, mean ± 1 SE; Speed et al. 2013). As recently as 2007, these communities were characterised as being relatively undisturbed (DEC 2007) and they are a significant centre of coral diversity both in terms of species richness and because they represent a unique group of species that are not found either at the oceanic shoals offshore or the coastal communities inshore of the region (Richards and Rosser 2012).

Widespread coral bleaching occurred throughout the Indian Ocean and much of the Pacific in 1998 (Wilkinson 2008), but coral reefs on the continental shelf of Western Australia were not as exposed to the temperature anomalies that resulted in extensive bleaching on reefs elsewhere (Babcock et al. 2017; Moore et al. 2012). However, during the summer of 2010–11 the most severe marine heat wave recorded along the Western Australian coast occurred (Feng et al. 2013; Pearce et al. 2011; Wernberg et al. 2012), resulting in widespread coral bleaching along 1,200 km of the coastline, spanning 12 degrees of latitude (Depczynski et al.2013; Moore et al. 2012). Whilst coral bleaching was widespread at the MBI, overall, mortality was low following this event (Moore et al. 2012; Speed et al. 2013). However, during the summer of 2012–13 north-western Australia again experienced anomalously high water temperatures resulting in significant (~70 %) mortality of corals on reefs around Barrow Island (Babcock et al. 2017; Ridgway et al. 2016).

Crown-of-thorns starfish

Crown-of-thorns starfish (COTS; *Acanthaster planci*) have been responsible for causing extensive damage to coral reefs throughout the Indo-Pacific, Red Sea and Indonesia-Australia Archipelago (Pratchett et al. 2014). The majority of outbreaks have occurred in the Pacific (Pratchett et al. 2014). On the GBR, COTS have been estimated to be responsible for 42% of the overall loss of coral cover between 1985 and 2012 (De'ath et al. 2012). In contrast, COTS are not thought to have been as destructive on the west coast of Australia (Wilson and Stoddart 1987; Wilson 1972; Wilson and Marsh 1975a). In Western Australia, COTS have been recorded in low numbers to the south of the MBI at Ningaloo Reef, the Murion Islands (pers. obs.), reefs near Onslow (Simpson 1989), the Dampier Archipelago (Benzie and Stoddart 1992; Wilson and Stoddart 1987; Wilson 1972; Wilson

and Marsh 1975a), the Montebello Islands (Marsh 2000b) and north to the Rowley Shoals, Seringapatam and Scott Reefs (Marsh 1986; D. Bearham, pers. comm.). Although historically recorded in low numbers in the offshore Pilbara bioregion on reefs adjacent to Barrow Island (Wilson 1972), COTS were first recorded in high densities (up to 340 ha^{-1}) on reefs in the inshore Pilbara bioregion (Kendrew Island, Dampier Archipelago) in 1971 (Wilson 1972). These aggregations were only ever recorded during October each year and they had dispersed several months later, leading the authors to speculate that the high densities represented a temporary aggregation of animals that came together in response to seasonal variations in either temperature or storm wave exposure (Wilson and Marsh 1975a, 1975b; Wilson et al. 1974). On the GBR, COTS are known to move into deeper water with the onset of the cyclone season (November to April; R. Babcock, pers. comm.), however, subsequent surveys in the Pilbara did not support this theory as Johnson et al. (1987) recorded aggregations during April 1987. Later surveys conducted by Simpson (1989) showed densities of COTS were inversely proportional to coral cover and were significantly higher in the western half of the archipelago. Densities were as high as 170 ha^{-1} where coral cover was lowest (2–30%) and were not present in the east where coral cover was approximately 70%.

During a survey of fish and corals of the Pilbara region conducted in May 2014, high densities (20–100 ha^{-1}) of COTS feeding on massive *Porites* spp. corals and other corals on the south-eastern side of the Montebello Islands were observed (CSIRO, unpublished data). In the context of managing increasing global threats to coral reefs, one potential local action is to attempt to control other threatening processes, such as COTS outbreaks. In response to these observations, we conducted two surveys of the MBI during October 2014 and 2015 to determine: 1) the spatial distribution of COTS, 2) the density of COTS on coral reefs, 3) the coral species COTS were feeding on and 4) potential drivers of the high densities of COTS using sea surface temperature and chloroyphyll-α data.

8.2.2   METHODS

Study area

The Barrow and Montebello Island groups lie 56 and 80 km, respectively, off the Western Australian coast, approximately 1,250 km to the north of Perth; Tryall Rocks are 14 km to the north-west of the Montebello Islands (Figure 8.2.1). The islands of the MBI lie on a long bank of Miocene limestone with Pleistocene carbonate reef deposits (Veron and Marsh 1988). Coral communities around Barrow Island are limited to a small reef on the western side, and the southern and part of the eastern sides of the island (Veron 1988). The Montebello Islands are a group of low-lying, highly dissected limestone islands with a barrier reef on their western margin (Veron 1988). Two hundred and forty-five species of scleractinian coral from 51 genera have been recorded from the MBI, although only eight species dominate the coral community numerically and 38 species are listed as vulnerable by the IUCN (Richards and Rosser 2012).

Sea surface temperatures range from 23 to 31°C (https://www.ghrsst.org). Rainfall in the region is very low (mean = 306 mm; Australian Bureau of Meteorology*)* and highly seasonal mainly being associated with summer tropical low pressure systems that frequently develop into cyclones.

Survey methods

Coral communities in the region are sparsely distributed and are interspersed by large areas of sand, rubble, unvegetated platform or macroalgal beds and much of the region is not defined by a clear reef edge. To help refine our search for COTS, we used satellite imagery and habitat maps (DBCA

unpublished data) to locate areas having live coral. Manta tow surveys were conducted using protocols established for the GBR (Miller et al. 2009). The surveys were conducted by divers using a 5 m Naiad inflatable boat. Every 3–400 m the boat stopped and a snorkel diver determined whether the substrate comprised live hard coral. If live hard coral was present, manta towing commenced with individual tows being 2 min at ~3 knots. Manta towing continued until coral was no longer observed. The GPS track of the vessel (which approximated the path of the manta diver) was recorded and the start and end time of each tow was recorded to extract the portions of the GPS track that described the manta tow path. The tow paths were extracted from the GPS track and loaded into a GIS, projected to WGS 84 UTM zone 49 south and the length of each path was measured.
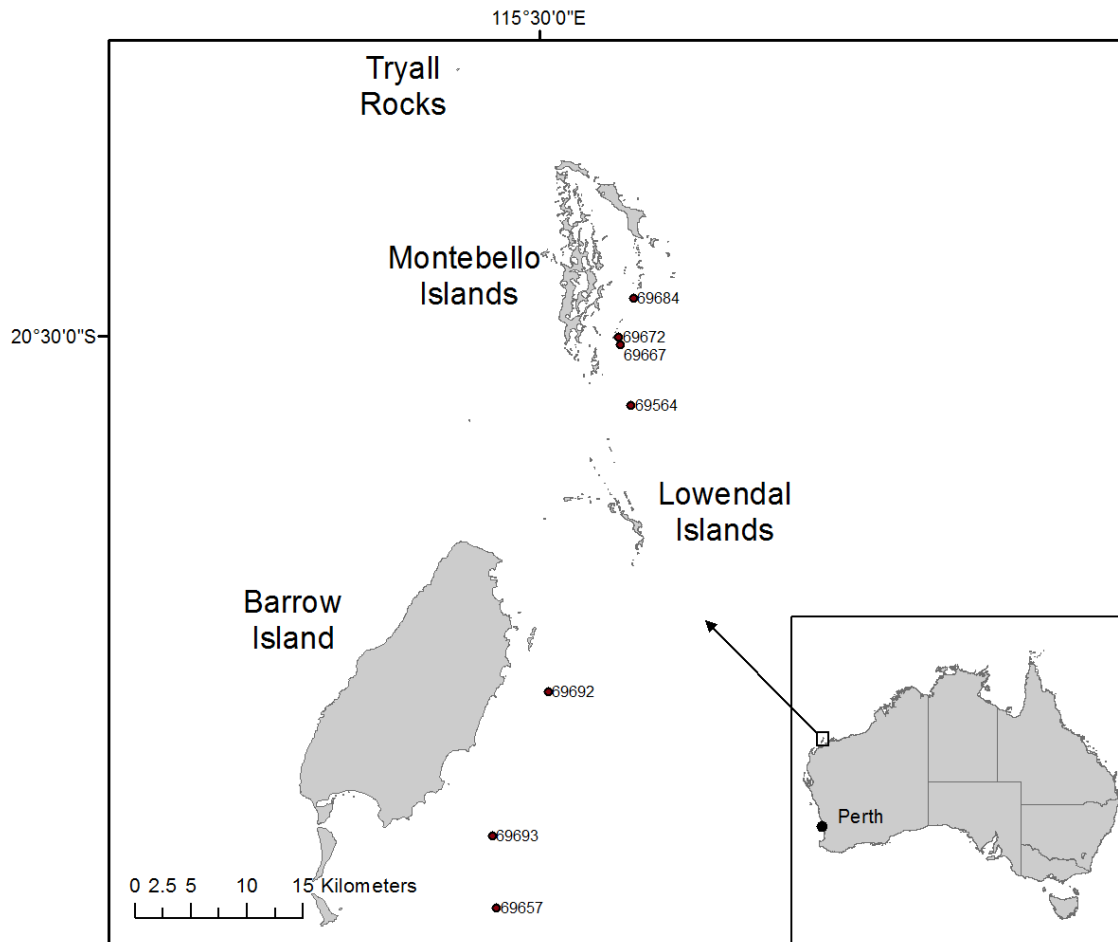
Figure 8.2.1. Map of the study area showing the sites where COTS were present and quantified using 50 × 2 m transects on SCUBA.

At the end of each 2 min tow, the diver recorded the following onto a datasheet fixed to the manta board: average depth, visibility, visual estimates of the percentage cover of sand, rubble, boulders, bommies, consolidated rubble, pavement, live hard coral, dead standing hard coral, soft coral and macroalgae, and counts of sub-adult (≤25 cm diameter), adult (>25 cm diameter) COTS, as well as feeding scars. After a series of ~10 × 2 min manta tows, the diver rotated with another member of the team (Miller et al. 2009).

If the number of COTS observed during a 2 min manta tow ≥3, the vessel was anchored and two SCUBA divers conducted between 4–6 transects (50 × 2 m), recording the number and size of COTS, number of feeding scars, COTS behaviour, any damage to COTS and the coral genera being fed upon.

Manta tows and SCUBA transects were conducted during the initial survey in October 2014. A second survey was done during October 2015, during which the SCUBA transects were repeated at four of the sites surveyed in 2014 and one additional site (Figure 8.2.1; Table 8.2.1).

Manta tow counts of COTS typically underestimate the numbers of COTS seen when compared with intensive SCUBA searches by 65 to 90% (Fernandes et al., 1990). In order to compare the manta tow counts with the densities we observed on the intensive SCUBA transects, we used the calibration model of Moran and De'ath (1992):

$$\sqrt[3]{SC} = 0.8071 + 1.2008 \times \sqrt[3]{MC}$$

where *SC*= the density of COTS estimated from SCUBA transects and *MC*=the count of COTS recorded during a 2 min manta tow.

SCUBA transects were conducted at six sites during 2014. The following year most of the sites were resurveyed, although we were not able to return to two of the sites (69692 and 69657) due to bad weather and added an additional site (69672).

Table 8.2.1 Sites and years when SCUBA transects were conducted in addition to manta tows for COTS in the Montebello and Barrow Islands.

	YEAR	
SITE	2014	2015
69684	Y	Y
69667	Y	Y
69564	Y	Y
69692	Y	N
69693	Y	Y
69657	Y	N

After the counts were completed, 40 digital photographs of the substrate along the first 25 m of each transect were taken. The photographs were taken at a height of ~75 cm above the substrate so that an area of 0.4 × 0.7 m of seabed was recorded by each photograph. For each transect, 32 photographs were randomly selected for analysis (English et al. 1997). Six fixed points were analysed per photograph, giving 192 points per transect. Analysis was conducted using TransectMeasure (SEAGIS) software as per Page et al. (2001). The benthic category underlying each fixed point was recorded and hard corals were identified to genus level classifications based on relevant identification texts (Veron 2000). Data were then tabulated to provide mean percentage cover ± 1 standard error (SE) estimates and plotted using the R package ggplot2 (Wickham 2009).

DBCA habitat and COTS survey methodology

Prior to the present study, the Western Australian Department of Biodiversity, Conservation and Attractions (DBCA, the then Department of Parks and Wildlife) collected information on benthic habitat and invertebrate densities at 23 sites in the waters surrounding the MBI. Data provided by DBCA was used to provide historic context to five of the sites we surveyed for COTS during the present study (all except 69672 and 69684; Figure 8.2.1). The DBCA habitat data were collected in a

similar manner to data collected during the COTS survey above. At each site, 3×50 m transects were established and marked with permanent markers. Divers collected 50 digital images from each transect at a height of 1 m above the substrate, representing 0.93 m^2 of seabed. The photographs were analysed using the point-count method described above, except that all 50 photographs from each transect were analysed and six points were overlaid on each photograph. COTS were counted along the same 50 m transects within a 2 m belt.

Coastal productivity

In an effort to explain the high densities of COTS, we examined some aspects of coastal oceanography that are thought to influence COTS survival–temperature and chlorophyll-α levels. COTS spawning generally only occurs once the water temperature exceeds 27°C (Johnson and Babcock 1994; Lamare et al. 2013). Furthermore, one of the main hypotheses advanced for explaining COTS outbreaks is that food is normally limiting during the larval phase, and peaks in phytoplankton can enhance larval survival leading to very high densities of adult COTS (Birkeland 1982; Brodie et al. 2005; Brodie 1992; Fabricius et al. 2010; Houk and Raubani 2010).

Chlorophyll-α and Sea Surface Temperature (SST) data were sourced from the Environmental Research Division Data Access Program (ERDDAP; http://coastwatch.pfeg.noaa.gov/erddap) server at the NOAA/SWFSC Environmental Research Division in Santa Cruz, California. Both datasets were downloaded and summarised using the R package xtractomatic (Mendelssohn 2017). The chlorophyll-α dataset comprised the chlorophyll-α monthly composite derived from data collected from the MODIS-Aqua satellite (https://oceancolor.gsfc.nasa.gov/data/aqua/). The sea surface temperature data consisted of the monthly composite Group for High Resolution Sea Surface Temperature (GHRSST) which is derived from a number of different satellites (https://podaac.jpl.nasa.gov/dataset/MUR-JPL-L4-GLOB-v4.1).

8.2.3   RESULTS

Manta tow surveys

A total of 335 manta tows (equating to 67 km) were conducted throughout the Montebello Islands and Tryall Rocks, and along the eastern and south-western margins of Barrow Island. Manta tow lengths ranged from 91 to 257 m and averaged 139 ± 2 m (± 1 SE). Unfavourable weather prevented surveying amongst the Lowendal Islands and on the western side of Barrow Island.

COTS were very patchy in their distribution; they were only observed on 25 of the 335 manta tows and were found predominantly on the eastern sides of the MBI (Figure 8.2.2). The highest counts were observed along the south-eastern side of the Montebello Islands where 7 COTS were recorded during a single 2 min tow. No COTS were observed at Tryall Rocks (Figure 8.2.2a). Mean counts of COTS per tow were 2.5 ± 0.6 at the Montebello Islands and 1.5 ± 0.2 at Barrow Island.

The percentage cover of live hard coral estimated by the manta tow divers was generally low being 5.2 ± 0.4 and 10.6 ± 2.4% at the Montebello and Barrow Islands respectively (Figure 8.2.2b). The highest hard coral cover observed on manta tow was 40%; this was found to the south-east of the Montebello Islands, close to site 69564 and on the south Barrow shoals to the south of site 69657 (Figure 8.2.1; Figure 8.2.2).
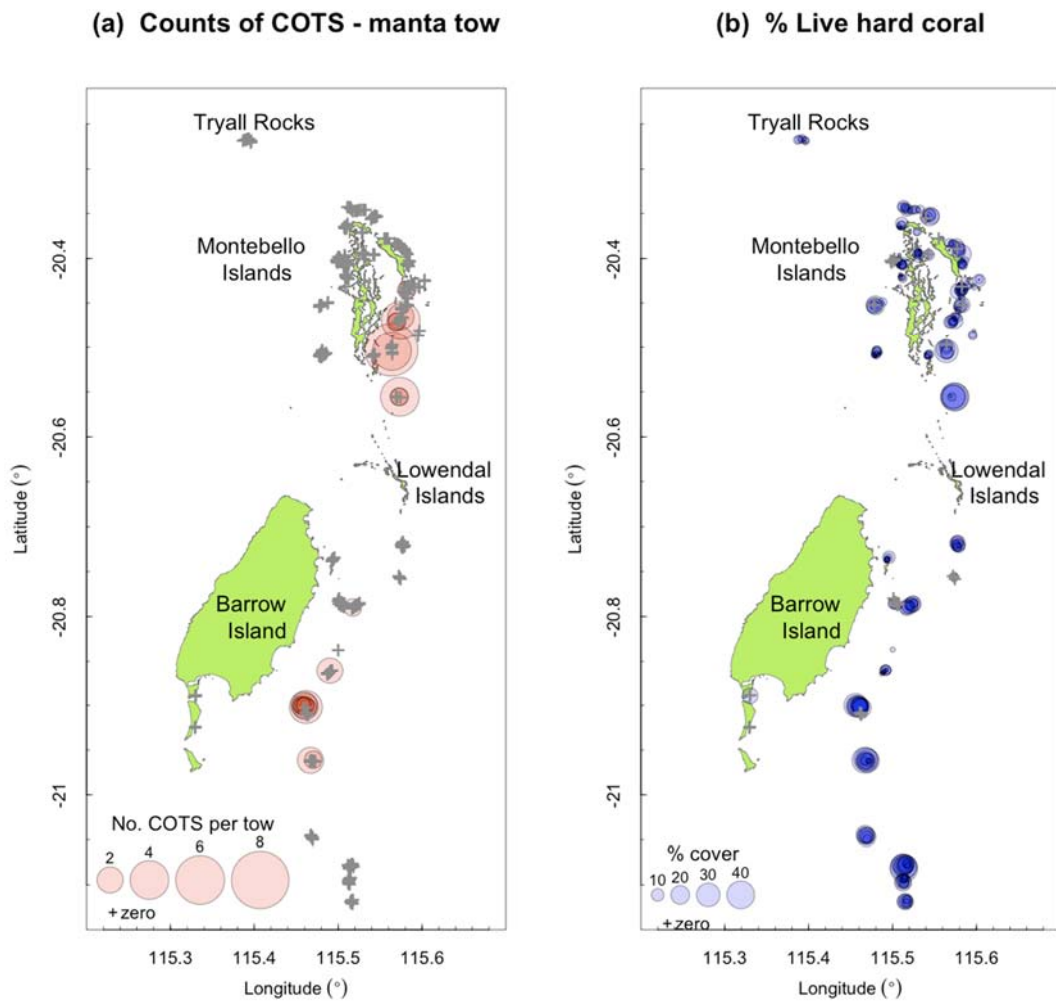
Figure 8.2.2 Bubble plots showing (a) the number of COTS observed per 2-minute manta tow and (b) estimated percentage cover (visual estimates from manta divers) of live hard coral observed during each manta tow.

SCUBA surveys

CORAL COVER

Coral cover in the region declined significantly following the marine heat wave and the resulting bleaching event in the summer of 2012–13 (Ridgway et al. 2016). Prior to the bleaching event in 2013, live hard coral cover ranged from 34.5 ± 18.4 to $38.6 \pm 8.1\%$ at Barrow Island and 36.8 ± 10.7 to $39.8 \pm 11.8\%$ at the Montebello Islands. Following the bleaching event (2013 – 2015) live coral cover ranged from 4.7 ± 6.4 to $23.3 \pm 20.9\%$ at Barrow Island and 6.8 ± 7.4 to $14.9 \pm 12.5\%$ at the Montebello Islands (Figure 8.2.3).

In addition to markedly reducing the total coral cover, the bleaching event also caused differential mortality rates amongst coral taxa. Prior to 2013, acroporids were prominent at two of the survey sites (69692 and 69693; Barrow Island) averaging 57% and 9% prior to the bleaching, and 0.4 and
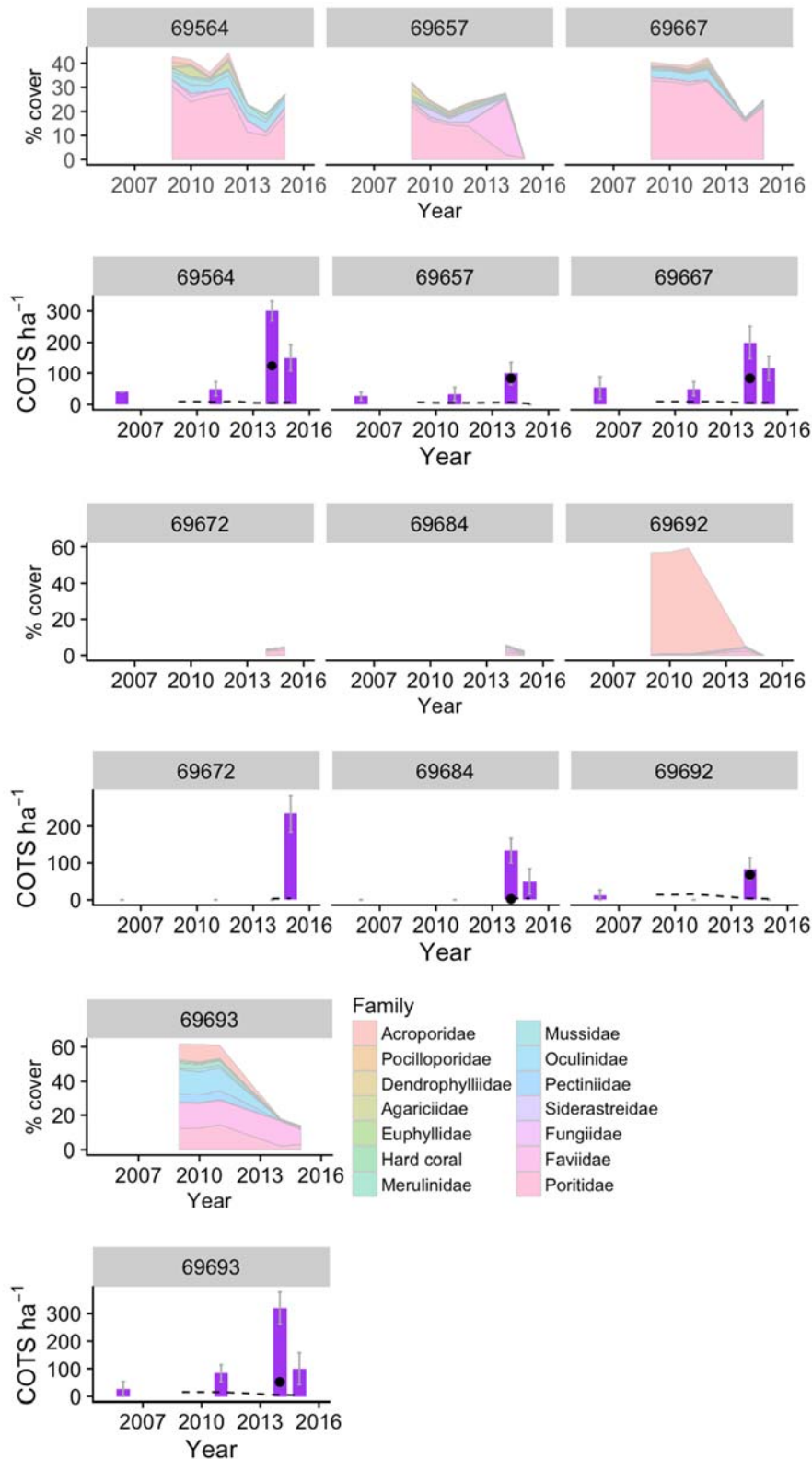
Figure 8.2.3 Mean percentage cover of the major coral families at each of the sites surveyed for COTS (stacked area plots) and mean density of COTS (±1 SE; barplots) at the MBI during 2006, 2011, 2014 and 2015. The points overlaid on the barplots indicate the SCUBA transect estimated density of COTS, predicted from the manta tows conducted during October 2014, using the calibration model developed by Moran and De'ath (1992). The dashed horizontal line represents the outbreak threshold density for COTS as based on the percentage cover of coral at each site during each survey (Babcock et al. 2014). 'Hard coral' = unidentified hard coral.

0.1% respectively, following the bleaching (Figure 8.2.3). Virtually all families present at 69693 prior to the bleaching, apart from Poritidae and Faviidae, were not recorded there post bleaching. In contrast, two of the poritid dominated sites (69654 and 69667; Montebello Islands) recorded a total loss of coral cover by ~50%, however the community composition was not affected as severely. Since the bleaching event, two hard coral families (Dendrophylliidae and Euphyllidae) have not been recorded, reducing the number of recorded coral families from 13 down to 11 (Figure 8.2.3).

COTS DENSITY

The mean density of COTS observed at the sites surveyed on SCUBA during 2006 ranged from 0 to 53 $\pm$ 22 COTS ha^{-1}, 0 to 83 $\pm$ 31 COTS ha^{-1} in 2011, 83 $\pm$ 31 to 320 $\pm$ 58 COTS ha^{-1} in 2014 and 50 $\pm$ 34 to 150 $\pm$ 43 COTS ha^{-1} during 2015. For four of the seven sites, transect based densities were substantially higher (at least double; mean = 120 COTS ha^{-1}) than those estimated by the manta tow counts after the counts had been calibrated using the model of Moran and De'ath (1992) (Figure 8.2.3). Transect estimates of COTS density may have been greater than those for manta tows because transects were either focused on areas of high coral cover (DBCA transects in 2006, 2011) which would attract and concentrate any starfish in the area, or were deployed in areas where high densities of COTS were noted by manta tow observers. However, regardless of whether estimates were based on transects or manta tows, estimated densities were above outbreak level at all but one site (69684; Figure 8.2.3). Of the 103 individual COTS recorded on the 50 $\times$ 2 m SCUBA transects over the two years, only one individual was observed to show any signs of predation (arm damage).
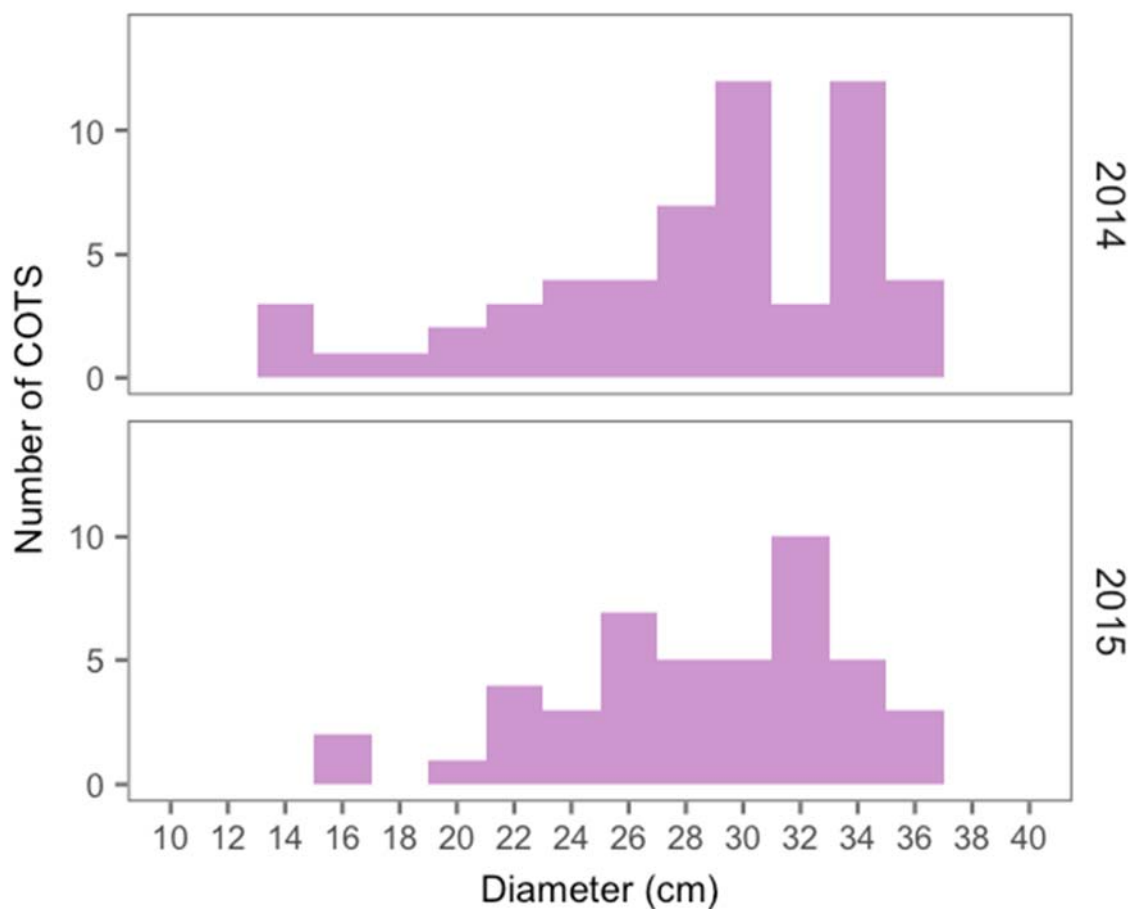
Figure 8.2.4 Length frequency (diameter) histograms of COTS observed on 50 $\times$ 2 m SCUBA transects during 2014 and 2015.

The size of COTS recorded on the SCUBA transects ranged from 14 to 36 cm in diameter. The modal size was 34 cm in 2014 and 32 cm in 2015 (Figure 8.2.4). Based on a collation of size-at-age studies by Pratchett et al. (2014) this would make the majority of these starfish between four to five years of age, although potentially, they could be older as COTS are known to undergo shrinkage at sizes >35 cm (Lucas 1984). A smaller proportion of the population was between three to four years old (~25 cm diameter). The occurrence of several small (14–15 cm; one to two years old) COTS indicated that recruitment was continuing, rather than the population being composed of a single cohort (Figure 8.2.4).

Coastal Productivity

During the period 2003 to 2016, the average chlorophyll-α concentration in surface waters around the MBI generally exceeded the level below which COTS larval success is impeded (0.5 µ chl-α L^{-1}) (Pratchett et al. In review; Wolfe et al. 2017) (Figure 8.2.5). In addition to this, during the probable COTS spawning season (December to February; Pratchett et al. 2014), sea surface temperature was generally greater than the commonly accepted lower temperature threshold for COTS spawning (Johnson and Babcock 1994; Lamare et al. 2013) during the period 2003 to 2016 (Figure 8.2.5). Therefore, conditions would have been suitable for COTS larval survival during the summer of most years since 2003.
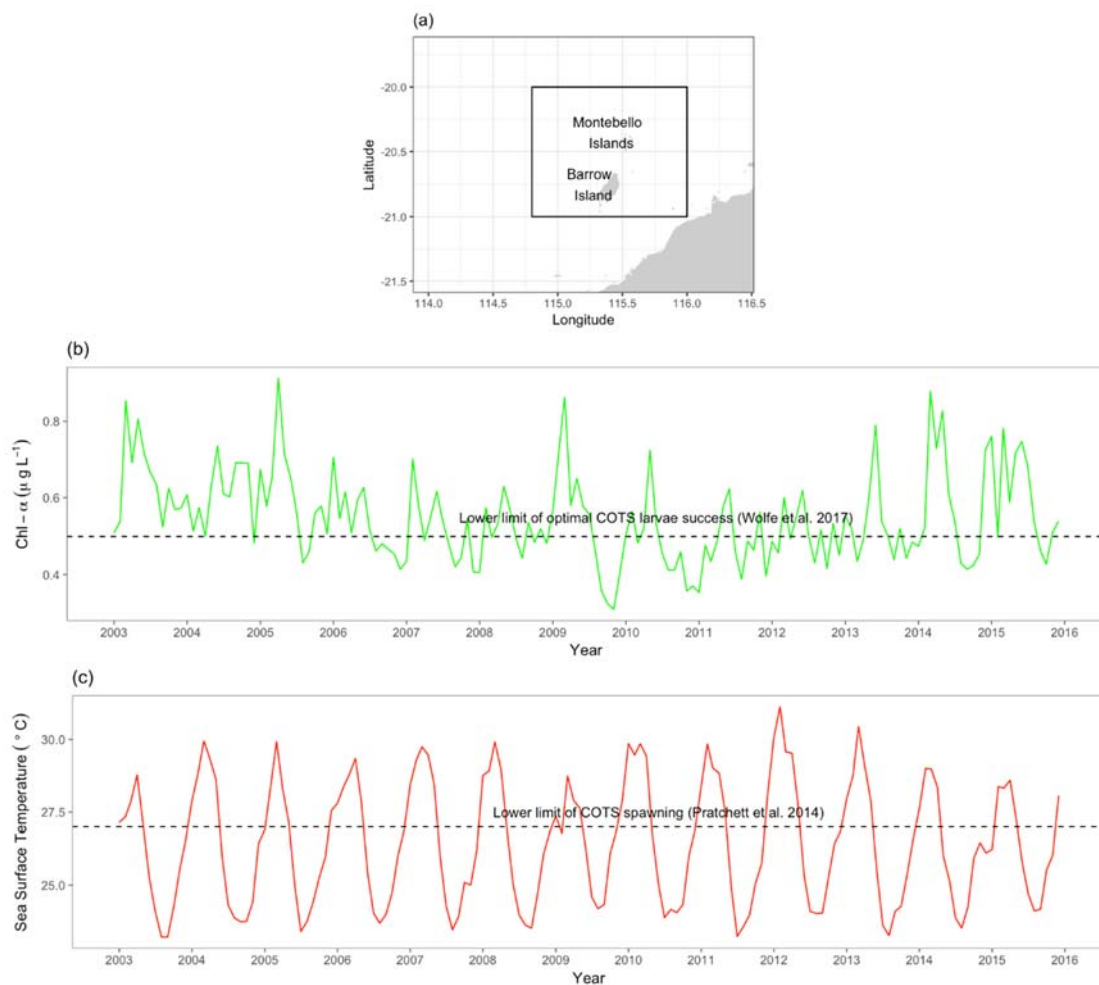
Figure 8.2.5 Average monthly (b) chlorophyll-α and (c) SST from the waters surrounding Barrow and the Montebello Islands (bounding box shown in (a)). The chlorophyll-α dataset was derived from data collected from the MODIS-Aqua satellite (https://oceancolor.gsfc.nasa.gov/data/aqua/). The SST data was from the monthly composite Group for High Resolution Sea Surface Temperature (GHRSST).

Based on the estimated age of the majority of COTS recorded during our 2014 and 2015 surveys (four to five years old), they would have been spawned between 2009 and 2011 (Figure 8.2.5).

8.2.4 DISCUSSION

Crown-of-thorns starfish density

During our SCUBA surveys, we recorded COTS densities between 50–320 ha^{-1}. Two previous studies recorded similarly high densities of COTS on islands of the Dampier Archipelago, ~100 km north-east of Barrow and the Montebello Islands (Simpson and Grey 1989; Wilson et al. 1974). In the early 1970's, Wilson (1974) found COTS at densities averaging 240 ha^{-1} at Kendrew Island whilst Simpson (1989) also recorded densities between 0–170 ha^{-1} (mean = 52 ha^{-1}). Rather surprisingly, Simpson (1989) described these densities as "within the density range for 'normal populations' of *A. planci* on reefs worldwide." There have been numerous definitions of outbreak densities of COTS in the literature (Pratchett et al. 2014), however, it is generally agreed that the outbreak density is that at which the numbers of starfish that markedly exceed the carrying capacity of the habitat (Moore 2013), i.e. the density of starfish at which the consumption rate of coral is greater than the growth rate of the coral. COTS densities on the GBR described as exceeding outbreak levels, range from 7.8–71.4 ha^{-1} (Moran and De'ath 1992; Pratchett 2010). Moran and De'ath (1992) determined the outbreak threshold density as 15 COTS ha^{-1}. However, the outbreak threshold is dependent upon coral cover, and Keesing and Lucas (1992) estimated that a coral cover of >20% was necessary to sustain 10–15 COTS ha^{-1}. At high levels of cover, coral communities can withstand higher densities of COTS, and conversely at lower coral cover it takes fewer COTS to outstrip coral growth. Recent modelling work has determined that for fast growing coral (e.g. Acroporidae, Pocilloporidae) cover in the range 20–50%, the outbreak threshold range is from 5–12 COTS ha^{-1} (Babcock et al. 2014). Given that following the 2013 bleaching, coral cover at our sites was <13% at the Montebello Islands and <24% at Barrow Island, the densities of COTS observed at all sites were significantly greater than the cover-adjusted outbreak threshold density of approximately 5 ha^{-1}. These very high densities of COTS are likely to mean the recovery of the hard coral community of the region will be severely compromised.

It is worth noting that at five of these sites, the DBCA recorded densities of COTS that exceeded outbreak levels in both 2006 and 2011. This was prior to the bleaching event and at that time coral cover was relatively high (>40%) and COTS did not appear to be resulting in declining coral cover, despite their high densities. High densities of COTS have been recorded as not negatively impacting total coral cover at both Molokai Island, Hawaii (Branham et al. 1971) and Panama (Glynn 1973, 1974). However, in both cases, the COTS were feeding selectively on a relatively high cover of fast growing species—*Montipora verrucosa* in Hawaii and *Pocillopora damicornis* in Panama.

Size and age

The size distribution of COTS recorded in this study was very similar to that recorded for the COTS populations at Kendrew Island, 100 km to the east of our study area in the early 1970's (Wilson et al. 1974). In contrast, Simpson and Grey (1989) identified two clear size classes having modes of 16 and 28 cm when they surveyed a number of sites along the western margin of the Dampier Archipelago during October 1985. Pratchett et al. (2014) combined a number of size-at-age studies (laboratory and field based) from COTS in the western Pacific and determined that age could be estimated from size in COTS. Assuming that COTS from the Pilbara grow at a similar rate and no shrinkage occurred, the majority of the COTS population at the MBI were between 4–5 years old (i.e. spawned in either early 2009 or 2010), with a smaller cohort of about of 3–4 years of age. However, recent work has

shown that COTS growth may be inhibited by a lack of their preferred prey (*Acropora* spp.; Caballes et al. 2016) and so given the lack of *Acropora* spp. at the MBI, it is possible that they were older than this.

Regardless of the exact age of the COTS, populations have been present at medium to high densities, and most likely at densities technically defined as outbreak level, since 2006. The presence of multiple size classes in our survey, as well as the sustained presence of COTS on MBI reefs indicates that this COTS outbreak is multigenerational, rather than due to a single influx of larvae, and that a chronic outbreak condition may exist.

Feeding

The 2013 bleaching event reduced hard coral cover in the region from ~ 50% to ~ 10% and also altered the coral community composition. In particular, the cover of the preferred prey of COTS, namely, Acroporidae and Pocilloporidae (Keesing 1993; Pratchett 2007) was reduced to almost zero. Despite this, in a companion paper Keesing (In review) found that the COTS showed a strong preference for Acroporidae and Pocilloporidae, although they also consumed a larger amount of less attractive corals such as Poritidae, Faviidae and Merulinidae. Previous studies have demonstrated that different corals provide variable nutritional value to COTS and can impact their growth rates (Yamaguchi 1974) and larval quality (Caballes et al. 2016), and so the reduction in preferred prey may have reduced starfish growth rates and potentially impacted COTS larval survival following the bleaching event.

The strong selection for particular corals (Acroporidae and Pocilloporidae) may also impact the recovery of the coral community, particularly in conditions of chronic COTS outbreaks, as has occurred in Okinawa, Japan (Keesing 1993). Whilst Pocilloporidae was not a particularly large component of the coral community at the survey sites prior to the bleaching, at two sites, Acroporidae was significant, comprising between 9–57% of the total coral cover before 2013 and only 0.1–0.4% since then.

Outbreak or aggregation?

Two mechanisms are often used to explain periodic changes in COTS distribution and abundance when they occur in densities destructive to coral communities; outbreaks or local aggregations. Outbreaks are perhaps best known on the GBR in Australia (Pearson and Endean 1969), Guam (Chesher 1969) and in the Ryukyu Islands in Japan (Yamaguchi 1986), and occur following large recruitment events, which give rise to a dramatic population increase on affected reefs resulting in extensive coral mortality. Two principal mechanisms have been advanced to explain why such high densities of COTS can occur, enhanced larval survival and a reduction in predator numbers. However, no strong evidence exists to support either of these mechanisms as being important drivers of high COTS densities in north-western Australia.

ENHANCED LARVAL SURVIVAL HYPOTHESIS

Several studies centred around the GBR have suggested that outbreaks of COTS are the result of enhanced survival facilitated by peaks in phytoplankton during the COTS larval phase (Birkeland 1982; Brodie et al. 2005; Brodie 1992; Fabricius et al. 2010; Houk and Raubani 2010). Nutrient enrichment, either as a result of upwelling or terrestrial runoff in areas with high levels of agriculture, is generally a driver for peaks in phytoplankton productivity and biomass in coastal reef waters (Brodie et al. 2005; Brodie 1992).

The time series of the mean chlorophyll-α concentration in surface waters between 2003 and 2016

indicated that chlorophyll-α levels have almost always been above the critical threshold for larval development for COTS larval survival (0.5 µg L⁻¹) (Wolfe et al. 2017). During the summers of 1972 and 1973, Wilson and Marsh (1975b) noted COTS spawning between October to February, similar to COTS in other parts of the southern hemisphere (Birkeland and Lucas 1990; Ciarapica and Passeri 1993; Lucas 1973; Pratchett et al. 2014). In the MBI during the period 2003 to 2016, the water temperature reached the lower limit for COTS spawning (27°C; Pratchett et al. 2014) in December during most years, and so spawning might be expected any time after this. Consequently, the present year classes of COTS in the region were likely spawned in either 2009/10 or 2010/11. Chlorophyll-α levels are usually higher than average in early to late summer which is the period immediately following spawning, so it is likely that conditions are suitable for larval survival and recruitment in most years. Considering chlorophyll-α and temperature are favourable for enhanced larval survival at this time every year, clearly there are additional factors which influenced the abundance of COTS and lead to the high densities observed in 2014 and 2015. It is possible that the successive increases in COTS densities at the MBI from 2006 represents gradual growth within a self-seeding population.

PREDATOR REGULATION HYPOTHESIS

Another mechanism postulated as accounting for COTS outbreaks is the predator removal hypothesis (Endean 1969). The basis of this hypothesis is that on pristine reefs, COTS populations are regulated and kept at low densities by predation on the juveniles and/or adults. Overfishing may reduce the abundance of COTS predators to such a degree that their populations begin to build up and are able to reach outbreak levels as a result of significantly enhanced density-dependent reproductive output and fertilization success (Babcock and Mundy 1992). Apart from the giant triton (*Charonia tritonis*; Pearson and Endean 1969) which was commercially harvested until the 1960's and the maori wrasse (*Chelinus undulatus*; Ormond and Campbell 1974) which was fished recreationally and commercially until it was protected in Western Australia in 1998, the other potential predators of COTS such as the blue-finned triggerfish (*Balistoides viridescens*) and the stars and striped toadfish (*Arothron hisipidus*; Ormond and Campbell 1974) have not been targeted (Brodie et al. 2005). None of these potential predators are common in Western Australian waters and fishing pressure in the MBI region is low, so it seems unlikely that a reduction in predation has resulted in a dramatic increase in COTS.

Despite this, Simpson (1989) recorded significant evidence of COTS predation, with arm damage to 47% of all COTS recorded from the Dampier Archipelago, whereas we only observed a single COTS with arm damage. However, during our study the majority of the COTS observed were adults, whereas most of the COTS with arm damage observed by Simpson (1989) were juveniles which are known to be more vulnerable to predation than adults (Keesing and Halford 1992; Ormond et al. 1990; Sweatman 1995).

AGGREGATION RATHER THAN OUTBREAK

Whilst the high densities of COTS we observed at the MBI were having a significant effect on what coral remained following the bleaching event, there are a number of factors that indicate that the high densities observed in 2014 and 2015 represent an aggregation of the local population rather than an extrinsically driven intensification of the outbreak. The DBCA surveys indicated that COTS were in relatively high densities at the MBI as early as 2006, increased somewhat in 2011, but densities increased markedly following the bleaching and abrupt decline in coral cover in 2013. We postulate that the decline in coral cover resulted in a food shortage for COTS in the region, forcing them to aggregate around the few isolated areas where coral cover remained reasonably high. Whilst the overall population of COTS in the MBI may not have increased substantially, the increased densities aggregating on the few remaining areas of surviving coral is likely to further impact these

coral communities, hampering their ability to recover from the bleaching. Such mechanisms have been reported previously and indeed constitute a third class of theories explaining COTS outbreaks (Dana et al. 1972; Vine 1973). As discussed above, larval food conditions almost always appear to be non-limiting and it is difficult to postulate that there has been a recent dramatic reduction in the numbers of COTS predators in the region.

Implications for management

Considering the historically low levels of coral cover in the MBI (Babcock et al. 2017), and their co-occurrence with historically high and seemingly chronic levels of COTS outbreaks, ongoing and regular (annual) monitoring of reefs should be a high priority for management. These should adopt accepted methods, such as manta tow, for broad scale surveys, supplemented by finer scale diver surveys to obtain data on COTS population structure and coral cover. More frequent surveys would be required in order to begin to assess any dynamic aspects of the COTS population, such as movement and aggregation at remaining sites with coral cover. Active interventions to protect coral reefs both now and in the future are increasingly being advocated as we try to minimise the impacts resulting from the increasing domination of our planet by humans (Anthony et al. 2017). The fact that the COTS are currently aggregated in relatively small areas, presents the possibility that culling programs such as those on the GBR and at Okinawa, Japan (Buck et al. 2016; Nakamura et al. 2016; Pratchett et al. In review) might be effective in preserving the remaining coral in the MBI. Such a program would require a shift from traditional approaches to protection of natural systems but will require ongoing support from conventional monitoring programs in order to direct and evaluate any interventions.

8.2.5   ACKNOWLEDGEMENTS

8.2.6   REFERENCES

Anthony K, Bay LK, Costanza R, Firn J, Gunn J, Harrison P, Heyward A, Lundgren P, Mead D, Moore T (2017) New interventions are needed to save coral reefs. Nat Ecol Evol 1(10): 1420-1422.

Babcock R, Plaganyi E, Morello EB, Rochester W (2014) An integrated overview of the causes of crown-of-thorns starfish (COTS) outbreaks, and scenarios for assessing the efficacy of different combinations of management and mitigation measures. CSIRO Brisbane

Babcock RC, Thomson D, Haywood MDE, Vanderklift M, Pillans R, Rochester W, Miller M, Speed C, Shedrawi G, Field S, Evans R, Stoddart J, Hurley T, Thompson A, Decpzynski M (2017) Multi-year coral bleaching episode in NW Australia and associated declines in coral cover. Coral Reefs. In RC Babcock et al. eds. Pilbara Marine Conservation Partnership – Final Report Vol. 2:471–490. CSIRO, Brisbane.

Babcock RC, Mundy CN (1992) Reproductive biology, spawning and field fertilization rates of *Acanthaster planci.* Mar Freshwat Res 43(3): 525-533.

Bancroft KP (2011) Department of Environment and Conservation, Perth, Western Australia

Bartley R, Bainbridge ZT, Lewis SE, Kroon FJ, Wilkinson SN, Brodie JE, Silburn DM (2014) Relating sediment impacts on coral reefs to watershed sources, processes and management: A review. Sci Total Environ 468-469: 1138-1153.

Benzie JAH, Stoddart JA (1992) Genetic structure of crown-of-thorns starfish (*Acanthaster planci*) in Australia. Mar Biol 112(4): 631-639.

Birkeland C (1982) Terrestrial runoff as a cause of outbreaks of *Acanthaster planci* (Echinodermata: Asteroidea). Mar Biol 69(2): 175-185.

Birkeland C, Lucas J (1990) *Acanthaster planci*: Major management problem of coral reefs. CRC press, Boca Raton.

Branham JM, Reed SA, Bailey JH, Caperon J (1971) Coral-Eating Sea Stars *Acanthaster planci* in Hawaii. Science 172(3988): 1155-7.

Brodie J, Fabricius K, De'ath G, Okaji K (2005) Are increased nutrient inputs responsible for more outbreaks of crown-of-thorns starfish? An appraisal of the evidence. Mar Poll Bull 51(1-4): 266-278.

Brodie JE (1992) Enhancement of larval and juvenile survival and recruitment in *Acanthaster planci* from the effects of terrestrial runoff: a review. Mar Freshwat Res 43(3): 539-553.

Bruno JF, Selig ER (2008) Regional Decline of Coral Cover in the Indo-Pacific: Timing, Extent, and Subregional Comparisons. PLOS One 8: e711.

Buck A, Gardiner N, Boström-Einarsson L (2016) Citric Acid Injections: An Accessible and Efficient Method for Controlling Outbreaks of the Crown-of-Thorns Starfish *Acanthaster* cf. *solaris.* Diversity 8(4): 28.

Burke LM, Reytar K, Spalding M, Perry A (2012) Reefs at risk revisited in the Coral Triangle. World Resources Institute.

Caballes CF, Pratchett MS, Kerr AM, Rivera-Posada JA (2016) The Role of Maternal Nutrition on Oocyte Size and Quality, with Respect to Early Larval Development in The Coral-Eating Starfish, *Acanthaster planci*. PLOS One 11(6): e0158007.

Chesher RH (1969) Destruction of Pacific Corals by the Sea Star *Acanthaster planci*. Science 165(3890): 280-3.

Chin A, Lison de Loma T, Reytar K, Planes S, Gerhardt K, Clua E, Burke L, Wilkinson C (2011) Status of the coral reefs of the Pacific and outlook: 2011. Global Coral Reef Monitoring Network

Ciarapica G, Passeri L (1993) An overview of the Maldiavian coral reefs in Felidu and northern Male´ atoll (Indian Ocean): Platform drowning by ecological crises. Facies 28: 33-66.

Dana TF, Newman WA, Fager EW (1972) *Acanthaster* aggregations: interpreted as primarily responses to natural phenomena.

De'ath G, Fabricius KE, Sweatman H, Puotinen M (2012) The 27-year decline of coral cover on the Great Barrier Reef and its causes. PNAS 109(44): 17995-17999.

DEC (2007) Management plan for the Montebello/Barrow islands marine conservation reserves 2007-2017. Management Plan No. 55. Department of Environment and Conservation, Perth.

Depczynski M, Gilmour JP, Ridgway T, Barnes H, Heyward AJ, Holmes TH, Moore JAY, Radford BT, Thomson DP, Tinkler P, Wilson SK (2013) Bleaching, coral mortality and subsequent survivorship on a West Australian fringing reef. Coral Reefs 32(1): 233-238.

Endean R (1969) Report on investigations made into aspects of the current *Acanthaster planci* (crown-of-thorns) infestation of certain reefs of the Great Barrier Reef. Department of Primary Industries, Brisbane.

English S, Wilkinson C, Baker V (1997) Survey manual for tropical marine resources. Australian Institute of Marine Science, Townsville, 390.

Fabricius KE, Okaji K, De'ath G (2010) Three lines of evidence to link outbreaks of the crown-of-thorns seastar *Acanthaster planci* to the release of larval food limitation. Coral Reefs 29(3): 593 - 605.

Feng M, McPhaden MJ, Xie S-P, Hafner J (2013) La Niña forces unprecedented Leeuwin Current warming in 2011. Sci Rep 3.

Fernandes L, Marsh H, Moran PJ, Sinclair D (1990) Bias in manta tow surveys of *Acanthaster planci.* Coral Reefs 9(3): 155-160.

Glynn PW (1973) *Acanthaster*: effect on coral reef growth in panama. Science 180(4085): 504-6.

Glynn PW (1974) The impact of *Acanthaster* on corals and coral reefs in the eastern Pacific. Environ Conserv 1(4): 295-304.

Houk P, Raubani J (2010) *Acanthaster planci* outbreaks in Vanuatu coincide with ocean productivity, furthering trends throughout the Pacific Ocean. J Oceanogr 66(3): 435-438.

Hughes TP, Kerry JT, Álvarez-Noriega M, Álvarez-Romero JG, Anderson KD, Baird AH, Babcock RC, Beger M, Bellwood DR, Berkelmans R, Bridge TC, Butler IR, Byrne M, Cantin NE, . . . Wilson SK (2017) Global warming and recurrent mass bleaching of corals. Nature 543(7645): 373-377.

Johnson D, Stoddart JJ (1987) Report on surveys of the distribution, abundance and impact of *Acanthaster planci* on reefs within the Dampier Archipelago (Western Australia), April 1987Australian Institute of Marine Science (AIMS), Townsville, Qld.

Johnson LG, Babcock RC (1994) Temperature and the larval ecology of the crown-of-thorns starfish, *Acanthaster planci.* Biol Bull 187(3): 304-308.

Keesing JK, Thomson DP, Haywood MDE, Babcock RC (In review) Two time losers: Selective feeding by crown-of-thorns starfish on corals most affected by successive coral bleaching episodes on western Australian coral reefs. Mar Biol.

Keesing JK (1993) Influence of persistent sub-infestation density *Acanthaster planci* (L.) and high

density *Echinometra mathaei* (de Blainville) populations on coral reef community structure in Okinawa, Japan. In: Proceedings of the 7th International Coral Reef Symposium, Guam, Micronesia, 22-27 June 1992 2: 769-779.

Keesing JK, Halford AR (1992) Importance of postsettlement processes for the population dynamics of *Acanthaster planci* (L.). Mar Freshwat Res 43(3): 635-651.

Keesing JK, Lucas JS (1992) Field measurement of feeding and movement rates of the crown-of-thorns starfish *Acanthaster planci* (L.). J Exp Mar Biol Ecol 156(1): 89-104.

Lamare M, Pecorino D, Hardy N, Liddy M, Byrne M, Uthicke S (2013) The thermal tolerance of crown-of-thorns (*Acanthaster planci*) embryos and bipinnaria larvae: implications for spatial and temporal variation in adult populations. Coral Reefs 33(1): 207-219.

Lucas JS (1973) Reproductive and larval biology of *Acanthaster planci* in Great Barrier Reef waters. Micronesica-Series 9: 197-203.

Lucas JS (1984) Growth, maturation and effects of diet in *Acanthaster planci* (L.) (Asteroidea) and hybrids reared in the laboratory. J Exp Mar Biol Ecol 79(2): 129-147.

Marsh LM (1986) Echinoderms. In: P. F. Berry (Ed.), Records of the Western Australian Museum). Supplement No 25. 106. *Vol. 106.* Faunal surveys of the Rowley Shoals, Scott Reef and Seringapatam Reef, north-western Australia. Western Australian Museum, Perth, Australia, 63-74

Marsh LM (2000a) Scleractinian corals of the Montebello Islands. In: Survey of the Marine Fauna of the Montebello Islands, Western Australia and Christmas Island, Indian Ocean. Records of the Western Australian Museum Supplement 59: 15-19.

Marsh LM (2000b) Echinoderms of the Montebello Islands. In: Survey of the Marine Fauna of the Montebello Islands, Western Australia and Christmas Island, Indian Ocean. Records of the Western Australian Museum Supplement 59: 21-27.

Mendelssohn R (2017) Xtractomatic: accessing environmental data from ERD's ERDDAP server. R package version 3.3.2. https://cran.r-project.org/web/packages/xtractomatic/index.html

Miller IR, Jonker M, Coleman G (2009) Crown-of-thorns starfish and coral surveys using the manta tow and SCUBA search techniques (Vol. 8, pp. 1-65). Australian Institute of Marine Science, Townsville, Australia. Long-term monitoring of the Great Barrier Reef standard operational procedure. Number 9, Edition 3.

Moore JA, Bellchambers LM, Depczynski MR, Evans RD, Evans SN, Field SN, Friedman KJ, Gilmour JP, Holmes TH, Middlebrook R, Radford BT, Ridgway T, Shedrawi G, Taylor H, . . . Wilson SK (2012) Unprecedented mass bleaching and loss of coral across 12° of latitude in Western Australia in 2010-11. PLOS One 7(12): e51807.

Moore R (2013) Persistent and transient populations of the crown-of-thorns starfish, *Acanthaster planci.* In: R. Bradbury (Ed.), *Acanthaster* and the coral reef: A theoretical perspective: Proceedings of a workshop held at the Australian Institute of Marine Science, Townsville, Aug. 6-7, 1988. Springer Science and Business Media, Berlin, 236-277.

Moran PJ, De'ath G (1992) Estimates of the abundance of the crown-of-thorns starfish *Acanthaster planci* in outbreaking and non-outbreaking populations on reefs within the Great Barrier

Reef. Mar Biol 113(3): 509-515.

Nakamura M, Higa Y, Kumagai N, Okaji K (2016) Using Long-Term Removal Data to Manage a Crown-of-Thorns Starfish Population. Diversity 8(4): 24.

Ormond R, Bradbury R, Bainbridge S, Fabricius K, Keesing J, De Vantier L, Medlay P, Steven A (1990) Test of a model of regulation of crown-of-thorns starfish by fish predators. In: R. Bradbury (Ed.), *Acanthaster* and the coral reef: A theoretical perspective: Proceedings of a workshop held at the Australian Institute of Marine Science, Townsville, Aug. 6-7, 1988. Springer Science and Business Media, Berlin, 189-207.

Ormond RFG, Campbell AC (1974) Formation and breakdown of *Acanthaster planci* aggregations in the Red Sea. In: Proc 2nd Int Coral Reef Symp. Great Barrier Reef Committee, Brisbane, 595-619.

Page C, Colemen G, Ninio R, Osborne K (2001) Surveys of benthic reef communities using underwater video. Long-term Monitoring of the Great Barrier Reef Standard Operating Procedure Number 7. Australian Institute of Marine Science, Townsville.

Pearce A, Lenanton R, Jackson G, Moore J, Feng M, Gaughn D (2011) The "marine heat wave" off Western Australia during the summer of 2010/11. Fisheries Research Division, Western Australian Fisheries and Marine Research Laboratories, North Beach, Western Australia.

Pearson RG, Endean R (1969) A preliminary study of the coral predator A*canthaster planci* (L)(Asteroidea) on the Great Barrier Reef. Department of Harbours and Marine.

Pratchett MC, Cablles CF, Rivera-Posada JA, Sweatman HPA (2014) Limits to understanding and managing outbreaks of crown-of-thorns starfish (*Acanthaster* spp.). Oceanogr Mar Biol 52: 133-200.

Pratchett MS (2007) Feeding Preferences of *Acanthaster pla*n*ci* (Echinodermata: Asteroidea) under Controlled Conditions of Food Availability. Pac Sci 61(1): 113-120.

Pratchett MS (2010) Changes in coral assemblages during an outbreak of *Acanthaster planci* at Lizard Island, northern Great Barrier Reef (1995–1999). Coral Reefs 29(3): 717-725.

Pratchett MS, Caballes CF, Wilmes JC, Matthews S, Mellin C, Sweatman HP, Nadler LE, Brodie J, Thompson CA, Hoey J, Bos AR, Byrne M, Messmer V, Valero-Fortunato S, . . . Uthicke S (In Review) 30 Years of research on crown-of-thorns starfish (1986-2016): Scientific advances and emerging opportunities. Diversity.

Richards ZT, Rosser NL (2012) Abundance, distribution and new records of scleractinian corals at Barrow Island and southern Montebello Islands, Pilbara (offshore) bioregion. Journal of the Royal Society of Western Australia 95: 155-165.

Ridgway T, Inostroza K, Synnot L, Trapon M, Twomey L, Westera M (2016) Temporal patterns of coral cover in the offshore Pilbara, Western Australia. Mar Biol 163(9): 182.

Simpson CJ (1989) Mass spawnings of scleractinian corals in the Dampier Archipelago and the implications for management of coral reefs in Western Australia. Bulletin 244. Department of Conservation and Environment, Perth, Western Australia.

Simpson CJ, Grey KA (1989) Survey of crown-of-thorns starfish and coral communities in the Dampier

Archipelago, Western Australia. Technical Series No. 5. Environmental Protection Authority, Perth, Western Australia.

Sobel AH, Camargo SJ, Hall TM, Lee C-Y, Tippett MK, Wing AA (2016) Human influence on tropical cyclone intensity. Science 353(6296): 242-246.

Speed CW, Álvarez I, Babcock RC, Bancroft KP, Beckley LE, Bellchambers LM, Depczynski M, Field SN, Friedman KJ, Gilmour JP, Hobbs J-PA, Kobryn HT, Moore JAY, Nutt CD, . . . Wilson SK (2013) Dynamic Stability of Coral Reefs on the West Australian Coast. PLOS One 8(7): e69863.

Sweatman HPA (1995) A field study of fish predation on juvenile crown-of-thorns starfish. Coral Reefs 14(1): 47-53.

Veron JEN (2000) Corals of the world. Australian Institute of Marine Science, Townsville, Australia.

Veron JEN, Marsh LM (1988) Hermatypic corals of Western Australia: records and annotated species list. Records of the Western Australian Museum, Suplement No. 29. Western Australian Museum, Perth, Australia

Vine PJ (1973) Crown of thorns (*Acanthaster planci*) plagues: the natural causes theory. Atoll Res Bull 166: 1-10.

Wernberg T, Smale DA, Tuya F, Thomsen MS, Langlois TJ, de Bettignies T, Bennett S, Rousseaux CS (2012) An extreme climatic event alters marine ecosystem structure in a global biodiversity hotspot. Nat Clim Change 3(1): 78-82.

Wickham H (2009) Ggplot2: Elegant graphics for data analysis. Springer-Verlag New York. R package version 2.2.1. https://cran.r-project.org/web/packages/ggplot2/index.html

Wilkinson C (2008) Status of coral reefs of the world:2008. Global Coral Reef Monitoring Network and Reef and Rainforest Research Centre, Townsville, Australia.

Wilson B, Stoddart J (1987) A thorny problem. Crown of thorns starfish in W.A. Lanscope 3(1): 35-39.

Wilson BR (1972) Western Australian coral reefs, with preliminary notes on a study at Kendrew Island, Dampier Archipelago. Crown of thorns starfish seminar, 25 August 1972, University of Queensland.

Wilson BR, Marsh LM (1975a) *Acanthaster* studies on a Western Australian coral reef. In: Proceedings of the second International Symposium on Coral Reefs. 621-630

Wilson BR, Marsh LM (1975b) Seasonal behaviour of a normal population of *Acanthaster* in Western Australia. In: Proceedings of the crown-of-thorns seminar. Brisbane, 6 September. 167-169

Wilson BR, Marsh LM, Hutchins B (1974) Puffer fish predator of crown of thorns in Australia. Search 5(11): 601-602.

Wolfe K, Graba-Landry A, Dworjanyn SA, Byrne M (2017) Superstars: Assessing nutrient thresholds for enhanced larval success of *Acanthaster planci*, a review of the evidence. Mar Poll Bull 116(1-2): 307-314.

Yamaguchi M (1974) Growth of juvenile *Acanthaster planci* (L.) in the laboratory. Pac Sci 28(2): 123-138.

Yamaguchi M (1986) *Acanthaster planci* infestations of reefs and coral assemblages in Japan: a retrospective analysis of control efforts. Coral Reefs 5(1): 23-30.

8.3 Two time losers: Selective feeding by crown-of-thorns starfish on corals most affected by successive coral bleaching episodes on Western Australian coral reefs.

Authors: Keesing JK, Thomson DP, Haywood MDE, Babcock RC.

ABSTRACT

Successive, extensive bleaching events have reduced coral cover and altered species assemblages significantly in the Montebello Islands in north-western Australia. In particular branching *Acropora* populations were dramatically reduced while massive coral forms such as *Porites* and Faviid corals were less impacted and now dominate coral assemblages. Subsequent to this perturbation, there have been changes in the abundance and/or distribution of the coral eating crown of thorns starfish, *Acanthaster planci* to densities of up to 190 ha^{-1} that have had a further impact on coral communities selectively targeting the coral taxa most susceptible to bleaching, often referred to as climate change "losers". The feeding preferences of *A. planci* under post-bleaching conditions were studied to determine their likely impact on coral communities and their recovery. We found that even when *Acropora* and *Pocillopora* were extremely rare, *A. planci* demonstrated a preference for these genera although they consumed non-preferred taxa such as Poritid, Faviid and Merulinid corals in greater numbers. The consumption of non-preferred genera and families of corals was influenced by their local (between–site) abundance. The study demonstrates that where *A. planci* populations greatly exceed outbreak threshold densities of 10–15 ha^{-1} they are likely to retard recovery of coral communities from bleaching events.

8.3.1 INTRODUCTION

Predation of corals by the crown-of thorns starfish, *Acanthaster planci* remains a major management issue on coral reefs, more than 40 years since outbreaks were first reported (Chesher 1969) and this phenomenon has been the topic of extensive research in the decades that have followed (Moran 1986; Birkeland and Lucas 1990; Fabricius 2013). More recently, in the face of evidence that destructive outbreaks may be at least partly have been caused by anthropogenic impacts (e.g. nutrient enrichment; Brodie et al. 2005; Fabricius et al. 2010), active management intervention through attempting control programs has been recently instigated on Australia's Great Barrier Reef (Pratchett et al. 2015) and has been practiced in Japan for many years (Yamaguchi 1986; Nakamura et al. 2014).

Although not as well known, *A. planci* populations and their occasional population fluctuations have been reported in north-western Australia since the 1970s (Wilson 1972; Wilson and Marsh 1974; 1975; Wilson and Stoddart 1987; Johnson and Stoddart 1988; Marsh 2000a). With the exception of small industrialised areas of the coastline, the area does not have the severity or the same suite of anthropogenic impacts as on the Great Barrier Reef or elsewhere in the Indo Pacific, however the coral reefs in the region are subject to frequent perturbation from cyclones and more recently from successive, very extensive bleaching events (Moore et al. 2012; Depczynski et al. 2013). Coral cover at the Montebellos and Barrow Island has been greatly depleted. At Barrow Island coral cover averaged 35%–46% from 2008 to 2012 and then decreased to 11 % in 2013 following bleaching (Ridgway et al. 2016). We have also observed a coincident dramatic reduction in coral cover at the Montebellos. Moreover, bleaching mortality has been selective with extensive mortality of Acroporid corals in particular (Ridgway et al 2016). 140km to the south-west on Ningaloo reef coral bleaching in the 2010/11 summer reduced coral cover by 79–92 % (Depczynski et al. 2013). Reports of increases in population size and/or distribution of *A. planci* on reefs subject to extensive mortality from coral bleaching (190 ha^{-1}, Pickrell 2015) have raised concerns that recovery of coral populations may be affected by starfish feeding activity.

Numerous studies have shown beyond doubt that Acroporid and Pocilloporid corals are the preferred prey of *A. planci* in the Indo-Pacific (Pearson and Endean 1969; Brauer et al. 1970; Collins 1975; Ormond et al. 1976; Keesing 1993; De'ath and Moran 1998a; Pratchett 2007) and that when available these taxa will be eaten in preference to other common taxa such as Poritid and Faviid family corals. This raises the question of how selective feeding might influence recovery of coral reefs from bleaching. Depczynski et al. (2013) found that in some areas, coral bleaching at Ningaloo killed almost all Acroporid coral colonies > 10 cm in diameter, with smaller colonies less susceptible to bleaching and potentially provide a base for recovery. But even when Acroporids have been greatly reduced in abundance relative to other taxa by selective feeding of *A. planci*, remaining Acroporids are still the preferred prey of these sea stars (Keesing 1993; De'ath and Moran 1998a) and even very small *Acropora* recruits are eaten in preference to other taxa (Keesing 1993).

The appearance of *A. planci* on the *Acropora* denuded reefs of the Montebellos and Barrow Island in densities an order of magnitude in excess of thresholds (10–15 ha^{-1}) which cause significant coral mortality on the Great Barrier Reef (Keesing and Lucas 1992; Moran and Death 1992) presented the opportunity to examine the feeding preferences of *A. planci* under these changed circumstances and to consider the potential impact of *A. planci* feeding on the recovery of coral reefs from bleaching.

8.3.2 METHODS

Study site

This study was conducted in October 2014 and January 2015 at seven sites within the Barrow and Montebello Island groups (20.7°S, 115.4°E), located 60 km north-west of the Australian mainland and 180 km north east of the World Heritage Listed Ningaloo Reef (Figure 8.3.1). The region consists of over 600 low islands (<6m above sea-level) with extremely low average annual rainfall (mean = 306 mm) (Australian Bureau of Meteorology; http://www.bom.gov.au/jsp/ncc/climate_averages/rainfall/index.jsp?period=an&area=wa#maps). The nearest river systems, the Robe and the Ashburton Rivers, are located over 60km away and as a result turbidity around the islands is largely the result of re-suspension of bottom sediments by strong tidal flows (>4 knots) and wave action. Cyclones are common in the region (average 0.6 per year; Australian Bureau of Meteorologyhttp://www.bom.gov.au/climate/maps/averages/tropical-cyclones/) and have previously resulted in large declines in coral cover within *Acropora* dominated coral assemblages on the western side of the islands (Marsh 2000b). On the eastern sides of the islands, macroalgae dominates many of the channel and patch reefs (*Sargassum* spp., *Turbinaria* spp. *Padina* spp.), however, diverse assemblages of invertebrates have been described with 170 species of echinoderms (Marsh 2000a) and 204 species of hard corals (Richards and Rosser 2012) known to occur. Of the 204 hard coral species described from reefs in the region, 39 are listed as vulnerable by the International Union for the Conservation of Nature (Richards and Rosser 2012).
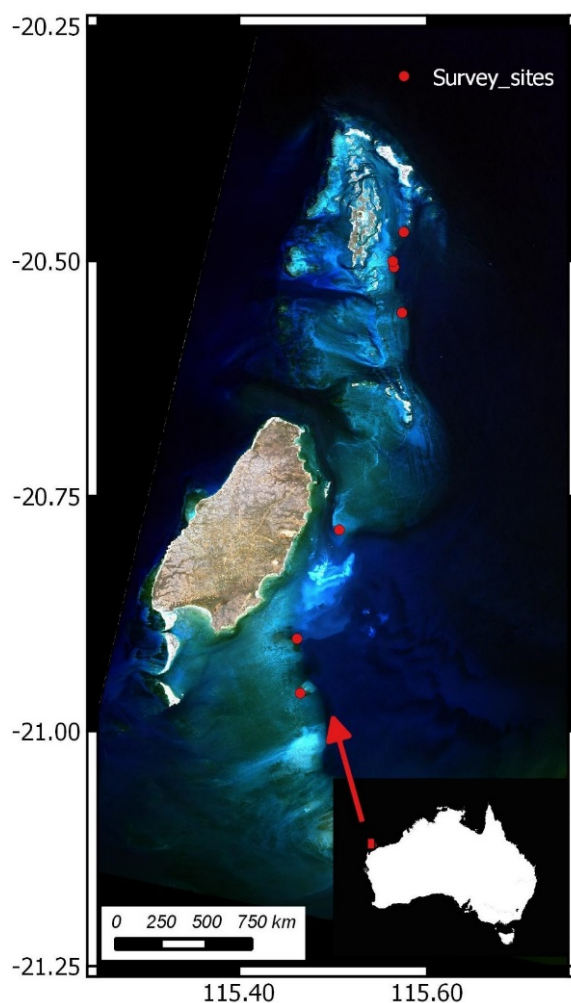
Figure 8.3.1 Location of survey sites at Barrow Island and Montebello Islands in north-western Australia.

Crown of Thorns starfish densities and feeding behaviour

Due to the large areas of rubble and macroalgae dominating reef platforms surrounding the Barrow/Montebello Islands groups an extensive search for suitable reef habitat and crown-of-thorns starfish (COTS) using manta tows (Moran and De'ath 1999) was completed in October 2014. When divers observed high densities of starfish during the manta tows (>3 starfish per 2 minute tow; approximately 10 per hectare) SCUBA surveys were conducted in the immediate area, using 50 m × 2 m transects. Five sites were surveyed in Oct 2014 and two sites surveyed in Jan 2015 (Figure 8.3.1). To determine the density, size, condition and feeding preference of starfish, divers recorded the number, maximum diameter (cm) condition (visible injuries) and behaviour (feeding, moving and stationary) of all starfish observed on the 50 m × 2 m transects. If starfish were observed feeding i.e. starfish stationary with stomach tissues extended, the genus, growth form (massive, sub-massive, branching, tabulate, foliose, encrusting), size (cm) and condition (feeding scar or no feeding scar) of the coral being preyed upon, as well as the nearest four coral colonies, were recorded. Between 3 and 6 randomly placed 50 × 2 m transects were surveyed at each site with a minimum distance between transects of 10 m (horizontal distance) at each site. To prevent starfish being overlooked, especially smaller *A. planci* which maybe cryptic during the day (Keesing 1995), divers progressed along each transect at a constant speed of 2 m per minute (approximately 15 min per transect) searching for starfish within the coral matrix. Transects were located at a constant depth (6–8 m) and conducted by two divers proficient in the identification corals to genus level (MH and DT). Although the allocation of genera among the Faviidae, Mussidae, Merulinidae, and Pectiniidae families of corals recently has been subject to revision based on molecular studies (Arrigoni et al. 2012), we followed convention consistent with past and recent taxonomic studies of corals in the region (e.g. Veron 1986; Veron and Marsh 1988; Marsh 2000b; Richards and Rosser 2012) as this permitted the comparison of the results of our study with those of earlier studies of *A. planci* feeding preferences, the majority of which were published last century.

Benthic composition

The abundances of coral genera over a larger area (approximately 150m × 150m; 22,500m^2) were documented using 25 m photographic line transects (Jonker et al. 2008). Six replicate transects were conducted at each of the six sites, with photos captured at 0.5m intervals along the first 25m of each of the 50 m × 2 m transect used to survey for COTS. To avoid non-independence among samples, 40 photographs were randomly selected (per transect) for analysis with the genus of any scleractinian (hard) corals, alcyonarian (soft) corals, or macroalgae (>5mm in height) recorded for six fixed points per photograph using the software Transect Measure™ (i.e. 6 points per image, 240 points per transect) (Page et al. 2001). A minimum distance of 10 m (horizontal distance) separated each transect.

Statistical analysis

Feeding preferences of *A. planci* were determined by comparing predation of different taxa of corals with their relative abundance of other corals in the immediate vicinity of feeding starfish. Chesson's electivity index α (Chesson 1978) was used to make this evaluation. *α* for each prey or potential prey species is calculated from the equation; $\alpha_i = (r_i / p_i) / \Sigma (r_i / p_i)$, where r_i is the proportion of type *i* items in the diet, p_i is the proportion of type *i* items available, and $\Sigma (r_i / p_i)$ is the sum of all n values of (r_i / p_i), where n is the total number of available prey items. α_{crit} is equal to 1/n, Where α_i exceeds α_{crit}, prey item *i* is preferred, where α_i is less than α_{crit}, prey item *i* is non-preferred. The rank of α_i / α_{crit} denotes the order of preference among all available potential prey types.

Comparisons of the incidence of starfish feeding on different size classes of corals were made by chi-square analysis, testing goodness of fit against the null hypothesis that predation was non-selective,

using Yates correction (Zar 1984) for single degree of freedoms tests. The influence of prey availability on prey selection was determined by regression analysis comparing the availability of the nine taxonomic categories of corals which made up over 90% of all coral cover (see Figure 8.3.2) at each of the seven sites with the incidence of predation on those nine taxa by *A. planci* at each site.
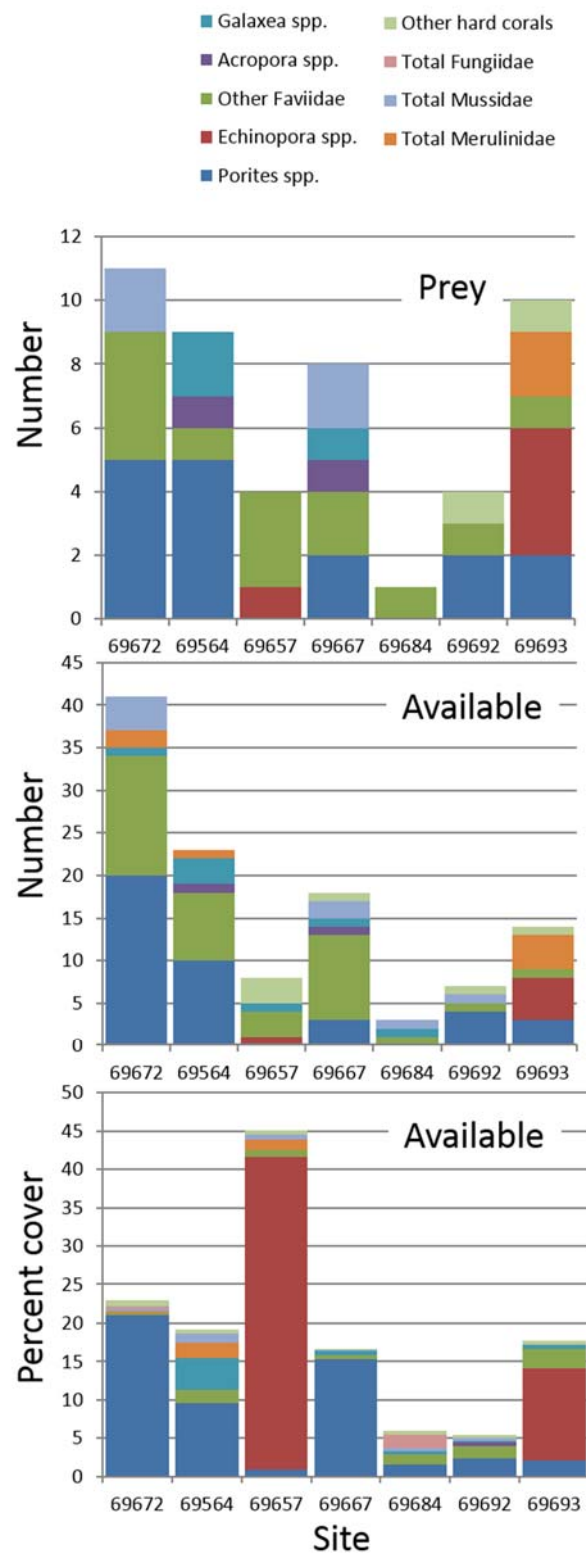
Figure 8.3.2 Number of eaten and available hard corals in immediate vicinity of feeding *Acanthaster planci* at each site (top 2 panels) and coral cover in 100 m² transects at each site (bottom panel).

8.3.3 RESULTS

Feeding rates

Observations were made on 65 *Acanthaster planci* at the seven sites. Of these 48 (74%) were feeding, 13 (20%) were moving and four were stationary. 62% of all feeding observations were on *Porites* and Faviidae corals.

Feeding preferences

From the 48 *A. planci* observed feeding, a total of 53 coral prey items were identified, all but one to genus level. Nearest neighbour observations recorded a total of other 68 colonies with which to compare in order to evaluate feeding preferences.

Table 8.3.1 Eaten and available corals by genus. The critical value of Chesson's electivity index (α) was 0.044. Genera with values exceeding this were preyed upon preferentially by *Acanthaster planci*.

CORAL GENUS	PREY COUNT	PREY PERCENT	AVAILABLE COUNT	AVAILABLE PERCENT	RATIO (%P / %A)	CHESSON'S A	A / A CRIT
Acropora	2	3.8	2	1.7	2.3	0.103	2.4
Oulophyliia	1	1.9	1	0.8	2.3	0.103	2.4
Echinophyllia	2	3.8	2	1.7	2.3	0.103	2.4
Pocillopora	1	1.9	1	0.8	2.3	0.103	2.4
Oxypora	3	5.7	3	2.5	2.3	0.103	2.4
Echinopora	4	7.5	6	5.0	1.5	0.069	1.6
Lobophyllia	6	11.3	9	7.4	1.5	0.069	1.6
Turbinaria	1	1.9	2	1.7	1.1	0.052	1.2
Favia	2	3.8	4	3.3	1.1	0.052	1.2
Merulina	2	3.8	4	3.3	1.1	0.052	1.2
Galaxea	3	5.7	7	5.8	1.0	0.044	1.0
Porites	16	30.2	41	33.9	0.9	0.040	0.9
Favites	5	9.4	13	10.7	0.9	0.040	0.9
Cyphastrea	2	3.8	6	5.0	0.8	0.034	0.8
Goniastrea	3	5.7	10	8.3	0.7	0.031	0.7
Montipora	0	0	1	0.8	0	0	0
Lobophytum	0	0	2	1.7	0	0	0
Barabittoia	0	0	1	0.8	0	0	0
Leptoria	0	0	1	0.8	0	0	0
Platygyra	0	0	2	1.7	0	0	0
Fungia	0	0	1	0.8	0	0	0
Hydnophora	0	0	1	0.8	0	0	0
Pectinidae sp.	0	0	1	0.8	0	0	0
Total	**53**		**121**				

At the generic level, 100% of the available colonies of *Acropora* (2 colonies) and *Pocillopora* (1), *Echinophyllia* (2), *Oulophyllia* (1) and *Oxypora* (3) were eaten by *A. planci* (Table 8.3.1). Of the three most abundant genera; *Porites* (41), *Favites* (13) and *Goniastrea* (10), *A. planci* preyed upon 39.0%, 38.5% and 30% of available colonies respectively. Genera most actively preferred by *A. planci* on the

basis on Chesson's electivity index (α) were *Acropora, Pocillopora, Echinophyllia, Oulophyllia* and *Oxypora*, all with values of α 2.4 times the critical value of α (0.04). *Echinopora* and *Lobophyllia* were also preferred genera (1.6 times critical value of α). Non-preferred genera (α significantly less than 1), where at least one colony of those available was eaten, were *Porites* (0.9 times critical value of α), *Favites* (0.9), *Cyphastrea* (0.8) and *Goniastrea* (0.7). There were 8 genera not eaten at all (α = 0) but these only had 1 or 2 available colonies as near neighbours to eaten colonies (Table 8.3.1).

At the family level, Pocilloporid (2.1 times critical value of α), Pectinid (1.7), Acroporid (1.4) and Mussid (1.4) corals were actively preferred, while Merulinid (0.8), Poritid (0.7) and Faviid (0.7) were non-preferred (Table 8.3.2).

Table 8.3.2 Eaten and available corals by family. The critical value of Chesson's electivity index (α) was 0.091. Families with values exceeding this were preyed upon preferentially by *Acanthaster planci*.

CORAL GENUS	PREY COUNT	PREY PERCENT	AVAILABLE COUNT	AVAILABLE PERCENT	RATIO (%P / %A)	CHESSON'S A	A / A CRIT
Pocilloporidae	1	1.9	1	0.8	2.3	0.190	2.1
Pectinidae	5	9.4	6	5.0	1.9	0.158	1.7
Acroporidae	2	3.8	3	2.5	1.5	0.126	1.4
Mussidae	6	11.3	9	7.4	1.5	0.126	1.4
Dendrophyllidae	1	1.9	2	1.7	1.1	0.095	1.0
Euphyllidae	3	5.7	7	5.8	1.0	0.081	0.9
Merulinidae	2	3.8	5	4.1	0.9	0.076	0.8
Poritidae	16	30.2	41	33.9	0.9	0.074	0.8
Faviidae	17	32.1	44	36.4	0.9	0.073	0.8
Alcyoniidae	0	0	2	1.7	0	0	0
Fungiidae	0	0	1	0.8	0	0	0
Agaricidae	0	0	0	0	0		
Total	**53**		**121**				

Coral cover present in the 100 m² transects at each of the seven study sites (Figure 8.3.2) was correlated with both the availability of potential prey taxa in the immediate vicinity of the feeding *A. planci* (Pearson's r=0.365, n=56, p=0.006) as well as the actual prey taxa (Pearson's r=0.324, n=56, p=0.0.015). A further indication that prey availability at each site had a significant influence of prey selected, is that there was a very high correlation between prey taxa eaten and the availability of potential prey taxa in the immediate vicinity of the feeding *A. planci* (Pearson's r=0.838, n=56, p<0.0001).

Colony size (Figure 8.3.3) was not found to influence prey selection among Faviid family (p=0.319, χ^2 = 0.992, df=1) or *Porites* genus (p=0.610, χ^2 = 0.260, df=1) corals. These were the only taxa with sufficient colonies to compare among size classes.
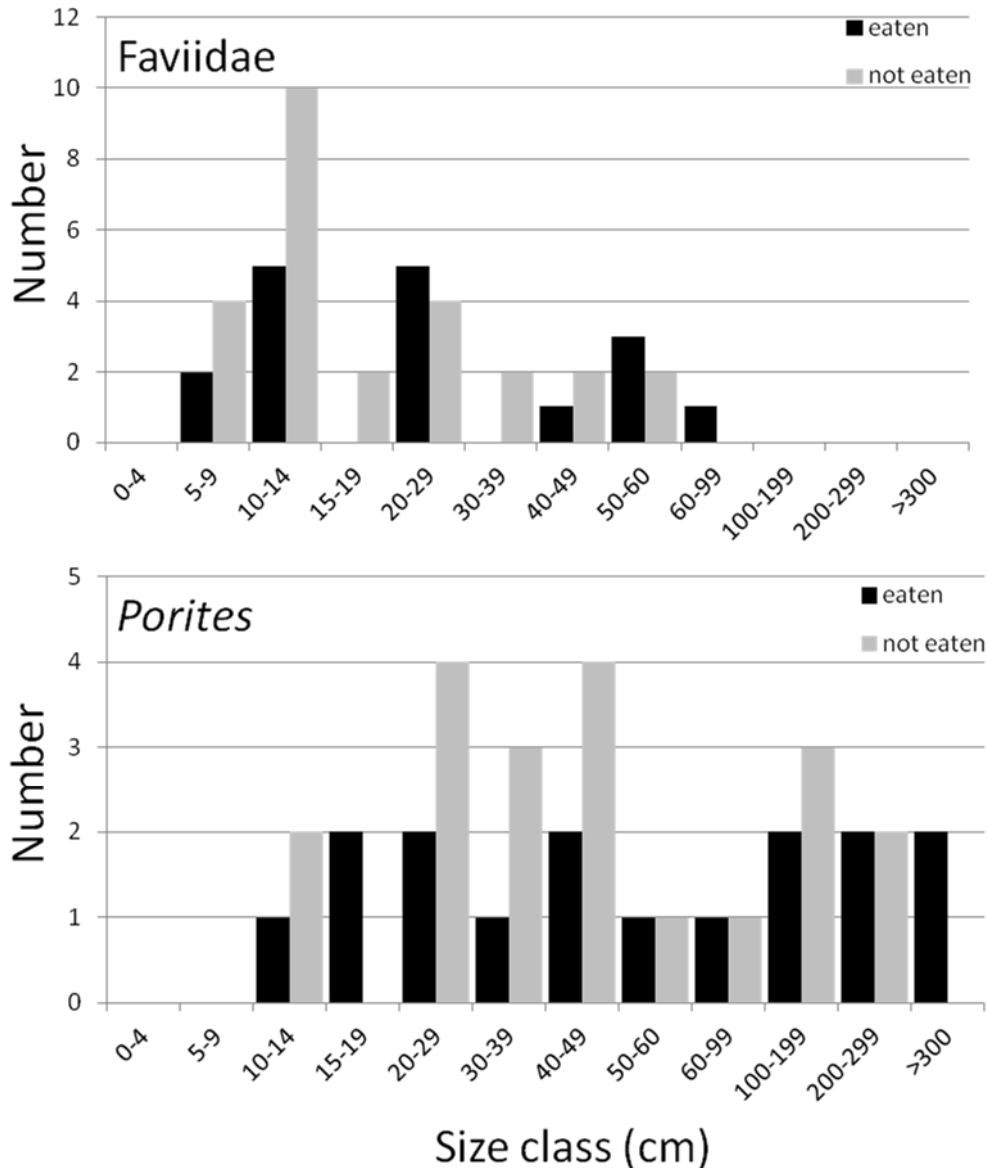
Figure 8.3.3 Number of eaten and available Faviidae family and *Porites* genus corals in each size class in the immediate vicinity of feeding *Acanthaster planci* (all seven sites combined).

8.3.4 DISCUSSION

Ninety-four percent of all starfish observed were feeding or moving indicating a very high level of feeding activity. This is high relative to a study of a large number of *A. planci* populations on the Great Barrier Reef (45%, De'ath and Moran 1998b) but feeding and movement rates there are dependant on numerous factors, principally starfish size, time of day and season and feeding rates can vary from 20–80% (Keesing and Lucas 1992; Keesing 1995). Surprisingly live coral cover has been found to have little influence on feeding rates (measured as incidence of feeding activity) relative to other factors (Keesing 1995), although Keesing and Lucas (1992) showed *A. planci* were less mobile in areas of high coral cover presumably because food is abundant and little searching for preferred prey is required. However, in context of the present study locating preferred prey, which is rare, requires great mobility.

Acroporid, Pocilloporid, Pectinid and Mussid corals were preyed upon by *A. planci* in preference to others. These findings, especially the preference for Acroporid and Pocilloporid corals, are consistent with earlier studies throughout the Indo-Pacific (Pearson and Endean 1969; Brauer et al. 1970; Branham et al. 1971; Ormond et al. 1976; Keesing 1993; De'ath and Moran 1998a). We found that Acroporids were eaten at 2.3 times their availability despite their rarity. Keesing (1992) found under similar circumstances in Japan where preferred species were rare (0.6 % and 0.2 % of available coral cover were Acroporids and Pocilloporids respectively), that *A. planci* consumed Acroporids at a rate 2.6 times their availability and Pocilloporids at 6.6 times their availability. On the Great Barrier Reef, De'ath and Moran (1998b) found that the strength of preference was affected by coral availability with *A. planci* selecting Acroporids at 13.5 times their occurrence when the availability of Acroporids was >90% but that where Acroporids made up ≤30% of available corals that selectivity by *A. planci* dropped to 5 times their abundance. Nevertheless, it is clear that the strong preference for Acroporid corals in particular is strongly ingrained in *A. planci* regardless of the coral's rarity.

However despite this, we found 62% of all feeding observations were on *Porites* and Faviidae corals demonstrating an ability to feed on these taxa. Predation on these taxa by *A. planci* at comparable rates has previously been shown to occur where the availability of preferred species is low and non-preferred species was high. For example, in Japan, Keesing (1993) found that where preferred taxa were rare and *Porites* (27%), *Millepora* (30%) and Alcyoniid soft corals (30%) made up the majority of available coral cover, that 25% of *A. planci* feeding observations were on *Porites*. On the other hand on Great Barrier Reef where scleractinian coral abundance was comparatively high, De'ath and Moran (1998a) found that just 3.6% of *A. planci* feeding records (when the 10 most common prey genera were considered) were on *Porites* despite it making up about 25% of available colonies. In pairwise comparisons of field observations they found *A. planci* were more than 11 times more likely to select *Acropora* over *Porites* again demonstrating the strong comparative preference for *Acropora*.

Our study and that of Keesing (1993) in Japan found that along with Acroporids, that Pocilloporids were strongly selected by *A. planci*. De'ath and Moran (1998a) found this was not the case on the Great Barrier Reef where *Pocillopora* and *Seriatopora* were slightly avoided or slight favoured relative to the abundance. These Pocilloporid genera, along with *Stylophora*, are strongly defended by commensal shrimps and crabs which repel *A. planci* (Glynn 1980; Pratchett 2001). This may have been the reason they were not favoured in the study by De'ath and Moran (1998a) while in the study of Keesing (1993), the *Pocillopora* colonies were very small (70% were 4 cm or less in diameter) and thus unable to be defended by large crabs or shrimps. Beyond demonstrating the high level of selectivity by *A. planci* for favoured coral genera which were rare, our study also showed that local availability of corals did strongly influence which taxa were preyed upon. This is unlikely to be the case when *Acropora* is abundant, as would have been the case prior to bleaching.

The ability of coral communities to recover from disturbance is largely dependent on the successful recruitment of new propagules and/or regrowth of remnant surviving corals (Pearson 1981; van Woesik et al. 2011), the latter being very important where coral mortality is extensive and widespread and/or in areas remote to sources of larval resupply (Gilmour et al. 2013). Selective feeding by *A. planci* on remnant and newly recruited *Acropora* could influence the rate at which reefs recover from the significant bleaching mortality. The same suite of vulnerable coral taxa expected to "lose out" (Loya et al. 2001; van Woesik 2011; Fabricius et al. 2011) as a result of more frequent bleaching events and ocean acidification as a result of climate change, most specifically *Acropora* and *Pocillopora* species, are also highly preferred by *A. planci*, even when alternative prey (such as the climate change "winners"; massive growth form *Porites* and Faviid corals) are much more abundant. At Ningaloo, just south of our study area, Depczynski et al. (2013) found that *Acropora* colonies <10 cm in diameter were less susceptible to bleaching. While this phenomena may help recovery, our study, and that of Keesing (1993) showed that strong feeding preferences for

Acropora by *A. planci* mean that even the smallest Acropora colonies will be eaten in preference to other taxa of corals. Thus the combination of recent increases in abundance of *A.planci* and very severe coral bleaching related mortality at the Montebellos and Barrow Islands might retard potential recovery of these reefs from small remnant surviving *Acropora* colonies, making this genera of corals "two time losers" on coral reefs in the 21st century.

8.3.5 ACKNOWLEDGEMENTS

8.3.6 REFERENCES

Arrigoni R, Stefani F, Pichon M, Galli P, Benzoni F (2012) Molecular phylogeny of the robust clade (Faviidae, Mussidae, Merulinidae, and Pectiniidae): An Indian Ocean perspective. Mol Phylogenet Evol 65:183–193.

Barham EG, Gowdy RW, Wolfson FH (1973) *Acanthaster* (Echinodermata, Asteroidea) in the Gulf of California. US Nat Mar Fish Serv Fish Bull 71:927–942.

Birkeland C and Lucas JS (1990) *Acanthaster planci* Major management problem of coral reefs. CRC Press: Boca Raton. 257 pp.

Branham JM, Reed SA, Bailey JH and Caperon J (1971) Coral eating sea stars *Acanthaster planci* in Hawaii. Science (Wash DC) 172:1155–1157.

Brauer RW, Jordan MR and Barnes DJ (1970) Triggering of the stomach aversion reflex of *Acanthaster planci* by coral extracts. Nature (Lond) 228:344–346.

Brodie J, Fabricius K, De'ath G, Okaji K (2005) Are increased nutrient inputs responsible for more outbreaks of crown-of-thorns starfish? An appraisal of the evidence. Marine Pollution Bulletin 51:266–278.

Chesher RH (1969) Destruction of Pacific corals by sea star *Acanthaster planci*. Science (Wash DC) 165:280–283.

Chesson J (1978) Measuring Preference in Selective Predation. Ecology 59:211–215.

Collins AR (1975) Biochemical investigation of two responses involved in the feeding behaviour of Acanthaster planci (L.). III. Food preferences. J Exp Mar Biol Ecol 17(1):87–94.

De'ath and Moran (1998a) Factors affecting the behaviour of crown-of-thorns starfish (*Acanthaster planci* L.) on the Great Barrier Reef: 2: Feeding preferences. J Exp Mar Biol Ecol 220(1):107–26.

De'ath and Moran (1998b) Factors affecting the behaviour of crown-of-thorns starfish (*Acanthaster planci* L.) on the Great Barrier Reef: 1: Patterns of activity. J Exp Mar Biol Ecol 220(1):83–106.

Depczynski M, Gilmour JP, Ridgway T, Barnes H, Heyward AJ, Holmes TH, Moore JAY, Radford BT, Thomson DP, Tinkler P & Wilson SK (2013) Bleaching, coral mortality and subsequent survivorship on a West Australian fringing reef. Coral Reefs 32(1):233–238.

Fabricius KE, Okaji K, De'ath G (2010) Three lines of evidence to link outbreaks of the crown-of-thorns seastar *Acanthaster planci* to the release of larval food limitation. Coral Reefs 29:593–605.

Fabricius KE, Langdon C, Uthicke S, Humphrey C, Noonan S, De'ath G, Okazaki R, Muehllehner N, Glas MS, Lough JM (2011) Losers and winners in coral reefs acclimatized to elevated carbon dioxide concentrations. Nature Climate Change 1:165–169.

Fabricius KE (2013) Acanthaster planci. In Starfish: Biology and Ecology of the Asteroidea, Lawrence, JM (ed). Baltimore, Maryland: John Hopkins University Press, 132–141.

Gilmour JP, Smith LD, Heyward AJ, Baird AH, Pratchett MS (2013) Recovery of an isolated coral reef system following severe disturbance. Science 340(6128):69–71.

Glynn PW (1980) Defence by symbiotic crustacea of host corals elicited by chemical cues from predator. Oecologia 47:287–290.

Johnson DB, Stoddart JA (1988). Report on surveys of the distribution, abundance and impact of *Acanthaster planci* on reefs within the Dampier Archipelago (Western Australia), April 1987. Australian Institute of Marine Science (AIMS), Townsville.

Jonker MM, Johns KK, Osborne KK (2008) Surveys of benthic reef communities using underwater digital photography and counts of juvenile corals. Long-term Monitoring of the Great Barrier Reef. Standard Operational Procedure Number 10/2008 Australian Institute of Marine Science (AIMS), Townsville.

Keesing JK (1993) Influence of persistent sub-infestation density *Acanthaster planci* (L.) and high density Echinometra mathaei (de Blainville) populations on coral reef community structure in Okinawa, Japan. Proc 7th Int Coral Reef Symp 2:769–779.

Keesing JK (1995) Temporal patterns in the feeding and emergence behaviour of the crown-of-thorns starfish *Acanthaster planci*. Mar Behav Physiol 25:209–232.

Keesing JK, JS Lucas (1992) Field measurement of feeding and movement rates in the crown-of-thorns starfish, *Acanthaster planci* (L.). J Exp Mar Biol Ecol 156:89–104.

Loya Y, Sakai K, Yamazato K, Nakano Y, Sambali H, van Woesik R. (2001) Coral bleaching: the winners and the losers. Ecol Lett 4:122–131.

Marsh LM (2000a) Echinoderms of the Montebello Islands. Rec West Aust Mus Suppl 59:21–27.

Marsh LM (2000b) Scleractinian corals of the Montebello Islands. Rec West Aust Mus Suppl 59:15–19.

Moore JA, Bellchambers L M, Depczynski M R, Evans R D, Evans SN, Field S N, Friedman KJ, Gilmour JP, Holmes T H, Middlebrook R, Radford BT, Ridgway T, Shedrawi G, Taylor H, Thomson D P,

Wilson SK (2012) Unprecedented mass bleaching and loss of coral across 12° of latitude in Western Australia in 2010–11. PLoS One 7(12):e51807.

Moran PJ (1986) The *Acanthaster* phenomenon. Oceanogr Mar Biol Ann Rev 24: 379–480.

Moran PJ, De'ath G (1992) Estimates of the abundance of the crown-of-thorns starfish (*Acanthaster planci* L.) in outbreaking and non-outbreaking populations on reefs with the Great Barrier Reef. Mar. Biol. 113:509–515.

Nakamura M, Okaji K, Higa Y, Yamakawa E, Mitarai S. et al. (2014) Spatial and temporal population dynamics of the crown-of-thorns starfish, *Acanthaster planci*, over a 24-year period along the central west coast of Okinawa Island, Japan. Mar Biol 161:2521–2530.

Ormond RFG, Hanscomb NJ and Beach DH (1976) Food selection in the crown of thorns starfish, *Acanthaster planci* (L.). Mar Behav Physiol 4:93–105.

Page C, Coleman G, Ninio R, Osborne K (2001) Surveys of benthic reef communities using underwater video. Long-term Monitoring of the Great Barrier Reef Standard Operating Procedure. Number 7. Australian Institute of Marine Science, Townsville.

Pearson RG and Endean R (1969) A preliminary study of the coral predator *Acanthaster planci* (L.) (Asteroidea) on the Great Barrier Reef. Qld Dept of Harbour and Marine, Fisheries Notes 3(1):27–55.

Pearson RG (1981) Recovery and recolonization of coral reefs. Mar Ecol Prog Ser 4(1):105–22.

Pickrell J (2015) New threat to Western Australian reefs. Aust Geogr May–June 2015:37.

Pratchett MS (2001) Influence of coral symbionts on feeding preferences of crown-of-thorns starfish *Acanthaster planci* in the western Pacific. Mar Ecol Prog Ser 214:111–119.

Pratchett MS (2007) Feeding Preferences of *Acanthaster planci* (Echinodermata: Asteroidea) under controlled conditions of food availability. Pacific Sci 61(1):113–20.

Pratchett MS, Caballes CF, Rivera-Posada JA, Sweatman HP (2015) Limits to understanding and managing outbreaks of crown-of-thorns starfish (*Acanthaster* spp.). Oceanogr Mar Biol Ann Rev 52:133–200.

Richards Z, Rosser N (2012) Abundance, distribution and new records of scleractinian corals at Barrow Island and Southern Montebello Islands, Pilbara (offshore) bioregion. J Roy Soc West Aust 95:155–65.

Ridgway T, Inostroza K, Synnot L, Trapon M, Twomey L, Westera M (2016) Temporal patterns of coral cover in the offshore Pilbara, Western Australia. Mar Biol 163:182.

van Woesik R, Sakai K, Ganase A, Loya Y (2011) Revisiting the winners and the losers a decade after coral bleaching. Mar Ecol Prog Ser 434:67–76.

Veron JEN (1986) Corals of Australia and the Indo-Pacific. Angus and Robertson: Sydney. 644 pp.

Veron JEN, Marsh LM (1988) Hermatypic corals of Western Australia: records and annotated species list. Rec West Aust Mus Suppl 29:1–136. Western Australian Museum, Perth.

Wilson BR, Stoddart J (1987) A thorny problem: crown of thorns starfish in Western Australia. Landscope 3:35–39.

Wilson BR (1972) Western Australian coral reefs, with preliminary notes on a study at Kendrew Island, Dampier Archipelago. Paper presented at Crown of Thorns Starfish Seminar. University of Queensland, Brisbane. 47–58 pp.

Wilson BR, Marsh LM (1974) Wilson BR, Marsh LM. *Acanthaster* studies on a Western Australian coral reef. Proc 2nd Int Coral Reef Symp 1:621–630.

Wilson BR, Marsh LM (1975) Seasonal behaviour of a 'normal' population of *Acanthaster* in Western Australia. Crown of Thorns Starfish Seminar Proc Brisb 6 September 1974. Aust Govt Publ Serv, Canberra. 167–179 pp.

Yamaguchi M (1986) *Acanthaster planci* infestations of reefs and coral assemblages in Japan: a retrospective analysis of control efforts. Coral Reefs 5:23–30.

Zar JH (1984) Biostatistical analysis, 2nd Edition. Prentice Hall, USA.

8.4 Outbreak thresholds of the coral predator *Drupella* in relation to *in situ Acropora* growth rates on an Indian Ocean fringing reef

Authors: Bessey C, Babcock RC, Thomson D, Haywood MDE.

ABSTRACT

The tipping point between net coral growth and net coral consumption due to predation is defined as the outbreak threshold; the predatory density above which there is a net loss of coral. To investigate the outbreak threshold density of the coral predator *Drupella cornus,* we conducted an *in situ* feeding study in the Ningaloo Marine Park, Western Australia. Over two ten-day periods, we tagged and photographed feeding scars on colonies of the tabulate coral *Acropora spicifera* which harboured *Drupella* feeding aggregations. The quantity and size of feeding *Drupella* present on each colony was determined on day 10. To determine *Acropora* growth rates we tagged and photographed 24 colonies of *Acropora spicifera* at time zero, and re-photographed these tagged coral colonies more than a year later. We calculated a mean consumption rate for *Drupella* of 1.16 ± 1.1 cm^2 of coral tissue.individual^{-1}.day^{-1}. Mean extension rate for actively growing *Acropora spicifera* was 7.9 ± 3.7cm.yr^{-1}, although mean colony extension rates ranged from nearly zero (0.05) to a maximum of 13 cm.yr^{-1}. These data have been used to develop a relationship between coral cover and carrying capacity of *Drupella* for reef flat habitats at Ningaloo. This suggests that the outbreak density of *Drupella* at the average level of coral cover for back reef sites at Mandu in Ningaloo ($17.6 \pm 13.7\%$) is approximately 0.79 individuals m^{-2}. The maximum coral cover observed at Ningaloo was 67.8% and at this level the outbreak density is estimated to be approximately 3 individuals m^{-2}. Understanding the threshold number of *Drupella* that can be sustained based on coral coverage and growth is essential information for monitoring and required to help managers predict possible outbreak abundances.

8.4.1 INTRODUCTION

Outbreaks of the coral predator *Drupella,* a genus of marine gastropod that feeds almost exclusively on living tissue (Robertson 1970; Turner 1994), have been associated with high coral mortality (Moyer et al. 1982; Fujioka and Yamazato 1983; Ayling and Ayling 1987; Turner 1994; Antonius and Reigl 1997; Shafir and Gur 2008; Cumming 2009a). In Japan, coral degradation was associated with large aggregations of *Drupella*, where densities of *Drupella* spp. (mainly *D. fragum*) reached 5.12 individuals.m^{-2} (Moyer et al. 1982; Fujioka and Yamazato 1983). On an artificial limestone quay in the Red Sea, increasing *D. cornus* abundances were monitored following coral mortality, with reports of more than 200 individuals per 30cm diameter branching coral colony with an ultimate mortality rate of 100% (Shafir and Gur 2008). This correlation between declining coral cover and increasing frequency of *D. cornus* was also independently observed in the Gulf of Aqaba (Antonius and Riegl 1997), where average densities of up to 12.24 individuals.m^{-2} were reported (Al-Moghrabi 1997). On the Ningaloo Reef, in Western Australia, *D. cornus* densities of up to 19.4 m^{-2} have been associated with a 75% reduction in coral cover (Ayling and Ayling 1987; Turner 1994). Since corals build the basic reef structure and provide habitat for a myriad of organisms, consisting of economically important, iconic, and endangered species, understanding the threshold number of *Drupella* that can be sustained based on coral coverage and growth is essential information required to help managers monitor and predict possible outbreak abundances.

Drupella are generalist corallivores that occur throughout the shallow waters of the Indo-Pacific. Although *Drupella* can forage on a range of coral morphologies and species using a specialized radula for scraping (branching, tabulate, massive and encrusting; *Acropora*, *Turbinaria*, *Pavona*, *Pocillopora*, *Porites*, *Astreopora*, *Millepora*, *Montipora*, *Stylophora*, and *Seriatopora*; Fujioka and Yamazato 1983; Boucher 1986; Ayling 2000; Shafir and Gur 2008), they display a strong preference for the acroporids (mainly *Acropora* and *Montipora*; Boucher 1986; Cumming 1992, Turner 1994, Schoepf et al 2010, Moerland et al 2016). They tend to create discrete feeding scars and feed at the interface between live and dead corallites during both day and night (although predominately at night), and show an attraction to stressed or damaged coral (Forde 1992; Turner 1994; Morton et al 2002). Field experiments report *D. cornus* moving more than 2 m overnight to aggregate on damaged coral, potentially detecting prey species through species-specific chemical substances released from prey organisms (Kohn 1961; Turner 1994; Kita et al. 2005). Aquarium experiments estimate *Drupella* (*D. cornus* and *D. rugosa* combined) feeding rates at 1.8 cm^2 of coral.individual^{-1}day^{-1}, where the average sized *Drupella* was 28-35 mm (Cumming 2009b) and coral tissue was measured as total surface area by the paper wrapping method. A 28 mm long *D. cornus* at Ningaloo Reef is estimated to be between 2.5 to 3.5 years old and reproductively mature (Black and Johnson 1994). Yet, little is known about *in situ Drupella* feeding rates which are an essential component in calculating the threshold number of *Drupella* that can be sustained based on coral coverage. In addition, laboratory measures of coral consumption which are based on measurements of vertical surfaces on branching corals are difficult to relate to field monitoring data of coral cover.

Obtaining estimates of coral growth for the preferred prey of *Drupella* in the area of interest is another essential component in calculating the threshold number of *Drupella* that can be sustained by the coral community. The growth rates of acroporids, the preferred prey of *Drupella*, can vary depending on growth form, species, and local environment, as well as the method used to quantify their growth (Pratchett et al. 2015, Drury et al. 2017). Obtaining a measure of growth requires direct quantification of colony linear dimensions, area, volume, or weight, taken at various time increments to calculate a time-averaged rate of growth (Pratchett et al. 2015). Linear extension, measured as a change in colony radius over a year, is a common metric of coral growth. There are relatively few studies of coral growth rates in Western Australia, but inter-site comparisons of *Acropora spicifera* annual linear extension were reported as 12.4 ± 1.4 cm for Ningaloo sites compared to 10.5 ± 1.2 at Bundegi (Stimson 1996). The closely related species, *Acropora hyacinthus*,

in the Dampier Archipelago, reported annual growth in radius ranging from 7.3 cm to 14.6 cm (Simpson 1988). Ideally this growth should be expressed as projected surface area, such as is measured by photographic monitoring of percent coral cover (e.g. Speed et al. 2013), rather than more accurate but logistically impractical methods possible only in controlled laboratory observations and not in large scale monitoring programs.

We conducted our study in the Ningaloo Marine Park, Western Australia, because it is not only the largest fringing reef in the world, but it is also the site of previously reported *Drupella* outbreaks that have been associated with substantial declines in coral cover (Turner 1994). The purpose of our study was to i) determine *in situ Drupella* feeding rates on colonies of *Acropora spicifera*, ii) measure *in situ* growth rates for *Acropora spicifera*, the dominant coral on Ningaloo reef flats, and iii) develop estimates of the maximum sustainable density of *Drupella* for maintenance of net coral growth, thereby quantifying a *Drupella* outbreak threshold density for Ningaloo reefs.

8.4.2 METHODS
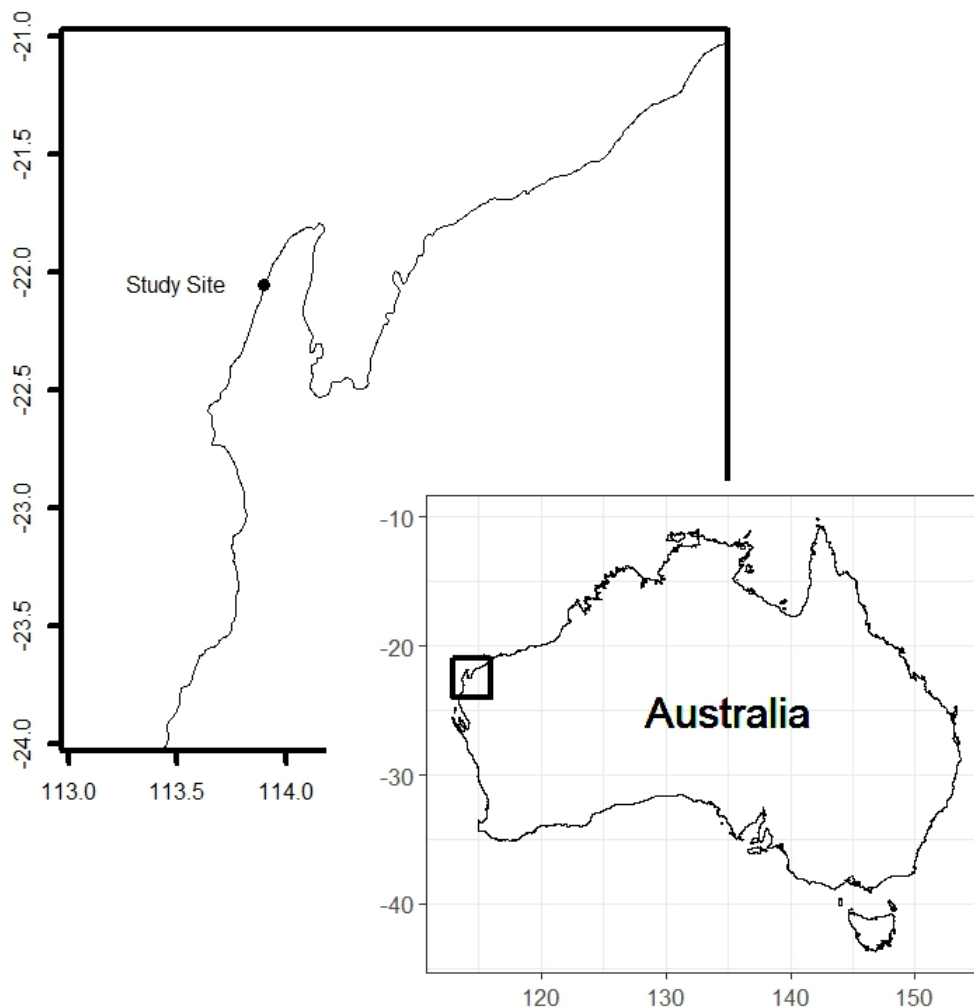
Figure 8.4.1 Location of the study within the Ningaloo Marine Park, north-west of Western Australia.

We conducted *in situ Drupella* feeding and *Acropora* growth experiments on the back reef near the reef flat margin at Mandu (22°03'14.11"S; 113°53'47.80''E) in the Ningaloo Marine Park, located

along the north-west coast of Western Australia (Figure 8.4.1). These habitats are dominated by *Acropora* spp, in particular the tabular *A. spicifera*. Over two 10 day periods (25th October to 4th November 2014, and 8th to 18th March, 2016), we tagged, photographed (day 1) and re-photographed (day 10) coral colonies of *A. spicifera* (tabulate growth morphology) which showed visible signs of *Drupella* feeding, and the presence of multiple *Drupella* (>1) on or under the coral colony. The quantity and size class (5 mm increments from 20 mm to 45 mm) of the *Drupella* present on each colony was determined on day 10 to avoid disturbing the foraging and feeding behavior of the gastropods during the observation period. A total of 29 colonies were successfully surveyed for our *Drupella* feeding experiments; 15 during 2014 and 14 during 2016. To determine *Acropora* growth rates (tabulate growth morphology), a total of 24 initially healthy coral colonies were tagged and photographed (11 colonies in 2014 and 13 colonies in 2016). These colonies were re-photographed more than a year later (490 and 372 days later for the 2014 and 2016 tagged colonies, respectively). All corals were tagged with an 8cm × 3cm uniquely numbered metal tag, which allowed for identification and provided a scale bar. In instances where the tag had become highly overgrown, as was the case for the growth experiments, the tag was scraped to reveal its unique number, and an additional scale bar was included in the photographs (30 cm ruler wrapped with black electrical tape at two 10 cm intervals; 0-10 cm and 20-30 cm).
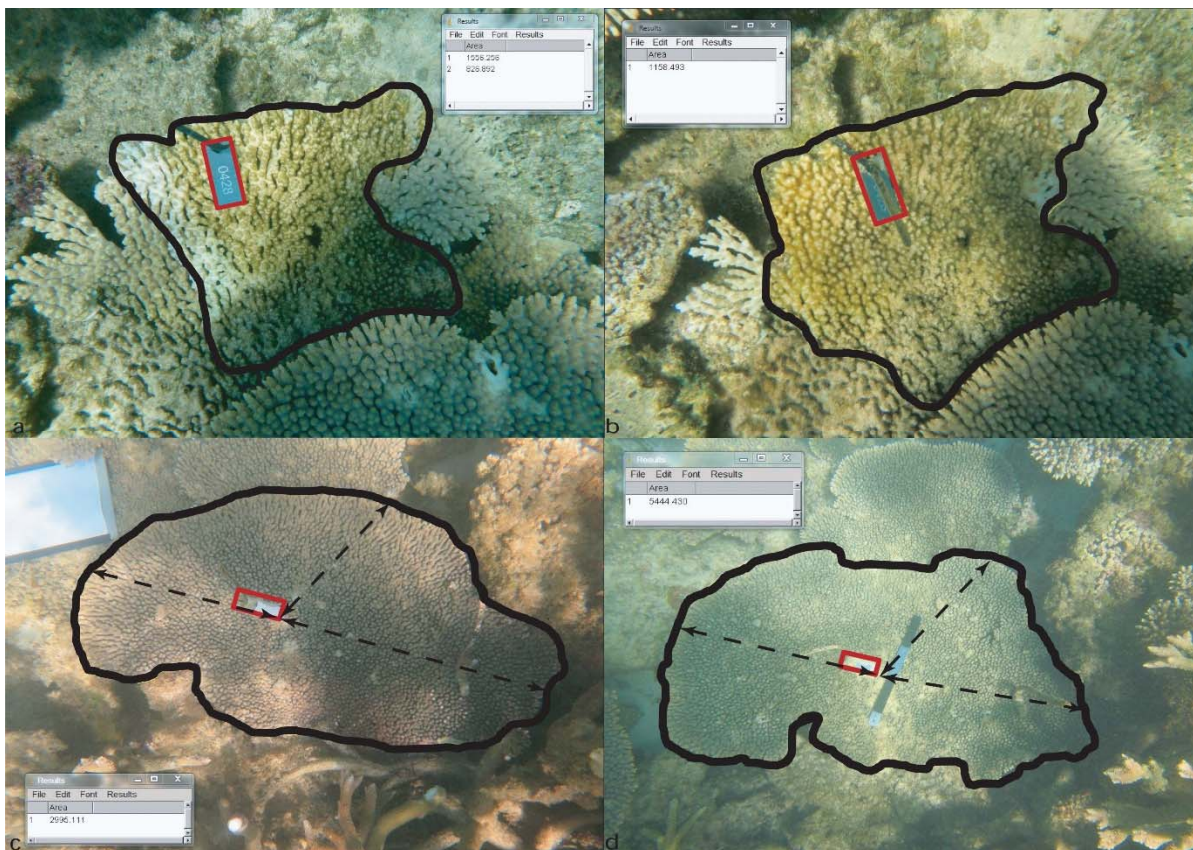
Figure 8.4.2 Determination of dead tissue area (cm^2) on day 1 (a) and day 10 (b) for coral colony #428 observed with multiple *Drupella* (3 × 25 mm, 10 × 30 mm, 5 × 35 mm) under the colony (feeding studies), and the area of live tissue for coral colony #427 on day 1 (c) and day 372 (d) for growth studies. Thick black lines denote the area of tissue measured, with ImageJ results inlaid. An 8 cm × 3 cm unique identification tag (thick red line) was used to standardize area by pixels in each photograph. Dashed lines denote measurements of radial growth used to obtain linear extension rate.

Photographs were analysed using open-source ImageJ software (Schneider et al. 2012) to determine i) initial surface area of live tissue for each tagged coral colony, ii) surface area of dead coral tissue on day one and day 10 for *Drupella* feeding experiments (Figure 8.4.2a,b; solid lines), iii) linear

extension rate of *A. spicifera* colonies (Figure 8.4.2c,d; dashed lines), and iv) final surface area of live coral tissue after one year for *Acropora* growth observations (Figure 8.4.2d; solid line). The known dimensions of the metal tag (or ruler) acted as a scale bar and was used to standardize area by pixels in each photograph. A freehand polygon was then drawn around the area of interest and a measurement of surface area (cm²) was obtained. We determined *Drupella* consumption rates using the following equation:

i) $total\ area\ consumed\ (cm^2\ day^{-1}) = \frac{(area\ t2 - area\ t1)}{10\ days}$

ii) $Drupella\ Consumption\ Rate\ _i\ (cm^2 individual^{-1}day^{-1}) = \frac{total\ area\ consumed}{\sum Drupella}$

where *i*=each coral colony surveyed

We determined *Acropora* linear extension rates for each colony by averaging three measurements of radial growth (Figure 8.4.2; dashed lines). In order to estimate annual growth in colony area for corals at different densities and levels of overall coral cover, we assumed a community dominated by *A. spicifera* composed of different sized circular colonies (5, 10, 20 100 and 200 cm diameter) at increasing densities (0.1 to 3 m²). Total areas were calculated and an annual radial growth increment applied to each colony before re-calculating total area to derive a total annual increase in live coral area (t_2-t_1) for communities at different levels of total coral cover. The number of colonies in each size class was varied randomly and the mean growth and 95% confidence intervals estimated using Monte Carlo simulation (n=1000).

8.4.3 RESULTS
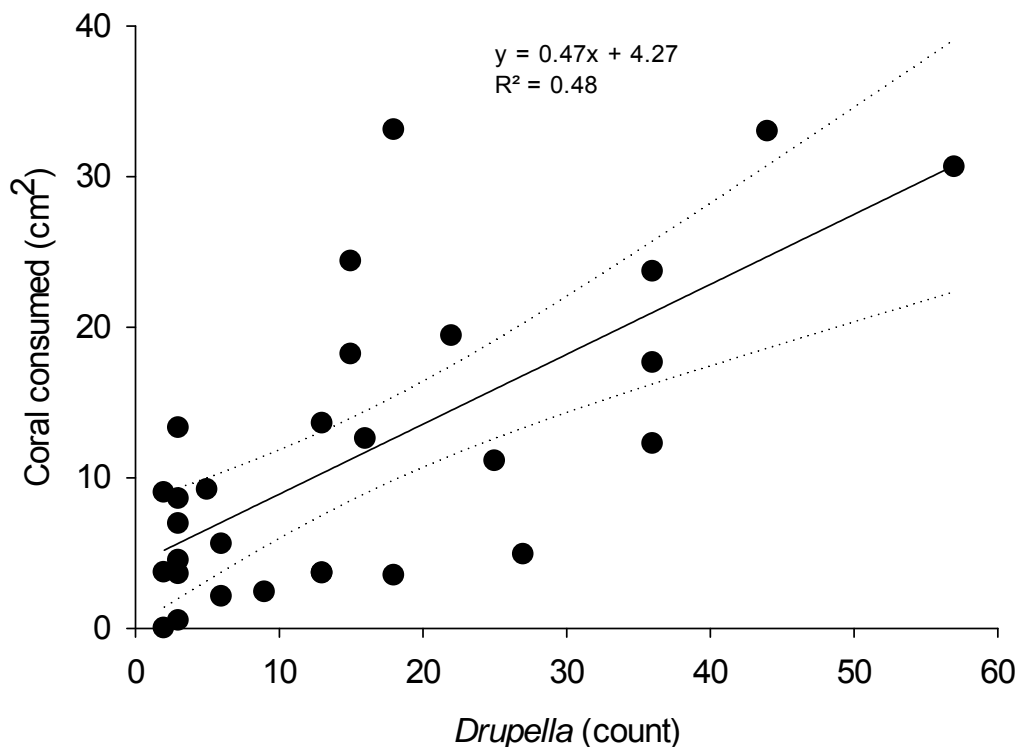
Figure 8.4.3 *Drupella* consumption rates. Total area of *Acropora spicifera* colonies consumed by *Drupella* feeding aggregations of varying sizes, with regression (solid line) and 95% confidence intervals (dashed lines).

Drupella feeding experiments monitored a total of 29 *Acropora spicifera* colonies which contained 454 individual *Drupella* with a mean length of 34mm. There was a significant linear relationship between the number of *Drupella* in a feeding aggregation and the two dimensional area of coral consumed (R^2 = 0.478, p ≤ 0.001; Figure 8.4.3). The maximum, mean, and minimum number of *Drupella* on the coral colonies were 57, 14 and two. We calculated a mean *Drupella* consumption rate of 1.16 ± 1.1 cm^2 of coral tissue day^{-1}.

Growth experiments monitored a total of 24 tabulate *Acropora spicifera* colonies, of which 13 showed positive growth and were used to determine growth rates (mean colony size 2783 ± 1168 cm^2). The remaining colonies were dead (n=6), dying/shrinking (n=4), or appeared healthy but showed no measurable growth (n=1). In particular, during re-photographing in 2017, there was evidence of two tagged colonies having brown band disease with an additional four colonies in close proximity having severe atramentous necrosis. In addition, some colonies had been overturned, but none appeared to have active *Drupella* feeding aggregations. We calculated a mean *Acropora spicifera* extension rate of 7.9 ± 3.7 $cm.yr^{-1}$. Maximum extension rate observed in one colony was 12.6 $cm.yr^{-1}$ and on this colony one measurement recorded an extension rate of 20 $cm.yr^{-1}$. Total tissue area of the tagged corals declined over the monitoring periods, due to the complete mortality and shrinkage of some colonies.
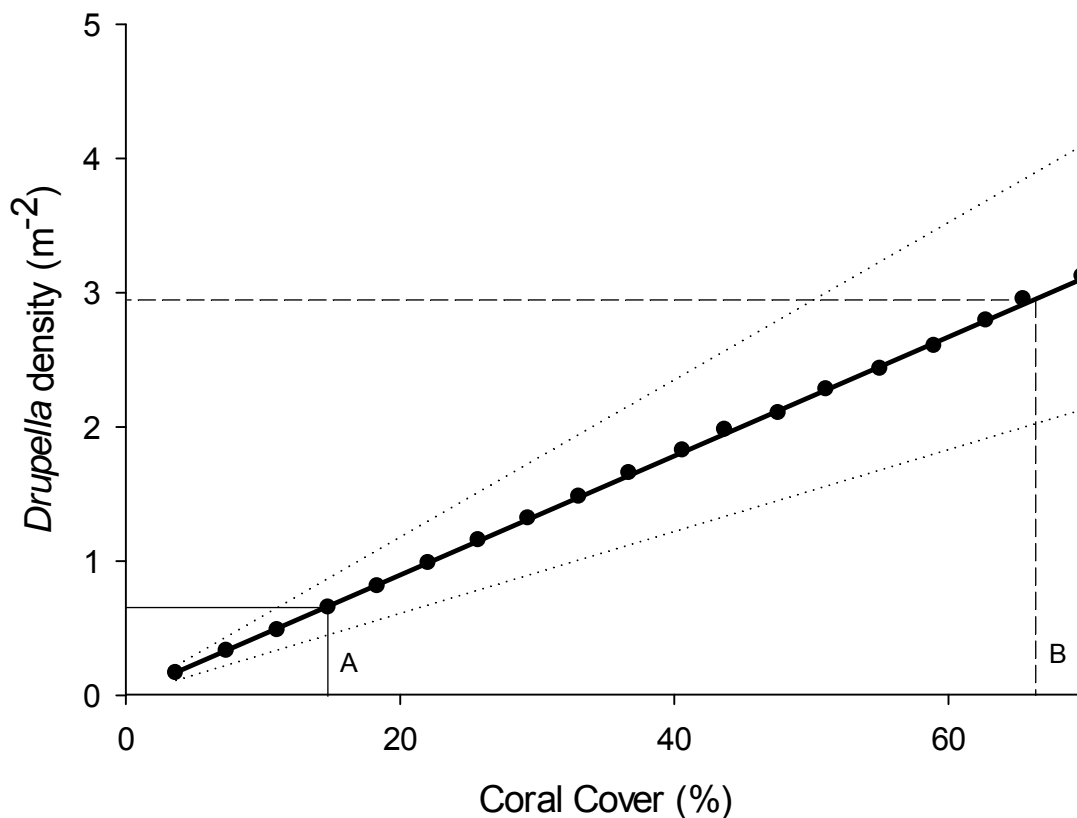
Figure 8.4.4 Outbreak threshold density of *Drupella cornus*. Number of *Drupella* sustained as a function of net live coral tissue growth for coral assemblages across a range of coral cover values. Estimates are based on modelled *Acropora spicifera* growth rates (mean and 95% CI), and mean individual consumption rates. Outbreak threshold at average coral (A) and maximum (B) cover on Ningaloo Back Reefs.

Estimates of total growth in coral cover (tissue area), based on colony extension rates, showed that as total cover increased so did the ability of the coral populations to add tissue, with an annual increment of approximately 23% of initial tissue area. As a result, the number of *Drupella* that could be supported increased, as did the number that would be required in order to consume coral faster

than it could re-grow. The tipping point between net coral growth and net loss of corals is defined as the outbreak threshold; the density of *Drupella* above which there is a net coral loss. Average coral cover at our study site (on back reef habitats at Ningaloo) between 2007 and 2016 averaged 17.6 ± 13.7% (see Supplementary Materials; Table S8.4.1), and at this density as few as 0.79 *Drupella* m^{-2} would represent an outbreak density (Figure 8.4.4), while at the highest observed levels of cover (67%) the outbreak threshold would be approximately 3 m^{-2}.

8.4.4 DISCUSSION

The densities of *Drupella* reported following outbreaks in Israel, Japan, and Australia range from 5.1 m^{-2} to over 19.4 m^{-2}, yet all outbreaks have been associated with substantial or total coral mortality (Moyer et al. 1982; Fujioka and Yamazato 1983; Ayling and Ayling 1987; Turner 1994; Antonius and Reigl 1997; Shafir and Gur 2008; Cumming 2009a). At Ningaloo, average densities in 2008 in back reef habitats averaged 1.4 ± 1.68 m^{-2} (Armstrong 2009) but measures of coral cover were not reported. Understanding the threshold number of the coral predator *Drupella* that can be sustained requires information on coral growth and coverage, as well as the density of *Drupella,* as both are essential information required to predict possible outbreak abundances. Here, we show that *Drupella* abundances greater than 0.8 m^{-2} could consume their preferred prey species faster than these corals grow, thereby resulting in erosion of tabulate coral cover at densities typical of Ningaloo (Figure 8.4.4). Importantly, if abundances of *Drupella* greater than this threshold are sustained over sufficiently large temporal and spatial scales, a net loss to coral cover could ensue. While previous reports of *Drupella* density on Ningaloo are above the current threshold density, coral cover on northern and central reefs at Ningaloo had reported to be increasing over recent decades (Speed 2012). Current densities of *Drupella* on back reefs in Ningaloo at Mandu are 0.34 ± 0.68 m^{-2}, but are reported as high as 0.60 ± 0.40 m^{-2} in 2008 (see Supplementary Material; Table S8.4.1). On the Great Barrier Reef, Australia, *Drupella* abundance (for all species combined; *D. cornus*, *D. fragum* and *D. rugosa*) typically ranges from 0 to 2 m^{-2}, and no known outbreaks have been recorded (Cumming 2009a).

We determined a mean *in situ Drupella* consumption rate of 1.16 ± 1.1cm^2 of *Acropora* coral tissue individual^{-1}.day^{-1}. A 1987 preliminary *in situ* study conducted on the Ningaloo reef reported *Drupella* feeding rates of 2.5cm^2 individual^{-1}.day^{-1}, where they surveyed plates of *Acropora* over a seven day period using similar photographic methods (Ayling 2000). Aquarium studies report a similar mean *Drupella* consumption rate of 1.81 cm^2 individual^{-1}.day^{-1}, ranging from 0 to 3.92, where the average length was between 28-35mm (Cumming 2009b). Interestingly, in the laboratory, *D. cornus* grazing rates showed a positive correlation with seawater temperature, ranging from 0.27 ± 0.11 cm^2 individual^{-1}.day^{-1} at 18°C to 1.31 ± 0.19 at 30°C, but showed no significant difference in grazing rate in relation to body size (Al-Horai et al. 2011). Consumption rates similar to those reported for *Drupella* have also been reported for another corallivorous gastropod, *Coralliophilia abbreviata* (Lamarck); a mean *Acropora* tissue consumption rate of 1.9cm^2 individual^{-1}.day^{-1}, but with a maximum rate of 6.5cm^2 individual^{-1} .day^{-1}in the Caribbean (Bruckner et al. 1997), and an estimated long-term feeding rate of 1.07cm^2 snail^{-1}.day^{-1} for an average 29mm snail (range: 0.44 to 3.28) in Florida (Baums et al. 2003).

There are a number of important caveats to the outbreak threshold estimates we present here. While we have measured feeding in over 400 *Drupella*, over two separate time periods, actual rates of feeding may be higher or lower than those that we have measured. Published estimates (Ayling 2000, Cumming 2009b) of *Drupella* feeding rates were based on different coral prey species and used quite disparate methods (habitat photos vs paper wrapping) and are probably not directly

comparable but, if taken at face value, would result in a threshold density around half the level of those estimated here. It is also important to note that coral communities consist of an array of coral morphologies and species, all of which can result in consumption rates that are different to those of a preferred prey species such as members of the family Acroporidae (Al Horani et al. 2011).

We determined a mean *in situ Acropora spicifera* extension rate of 7.9 ± 3.4 cm^2 yr^{-1}, with a maximum of up to 20 cm yr^{-1}. Our growth rates are nevertheless smaller than those previously observed for *Acropora spicifera* within the Ningaloo Marine Park (annual linear extension of 12.36 ± 1.41 cm at the south central region of the park and 10.52 ± 1.17 cm at Bundegi; Stimson 1996). Indeed, the maximum average rate observed in our current study coincides with the mean growth rate reported for Bundegi. Interestingly, the growth rates reported in our study are more similar to those reported for *Acropora hyacinthus* in the Dampier Archipelago (annual linear extension of 7.3 to 14.6cm; Simpson 1988), as well as on the great Barrier Reef (annual linear extension of 0 to 12.5cm; Pratchett et al. 2015). High spatial and temporal variability in coral growth rates is well documented and can be attributed to interspecific growth variation as well as light, water quality (e.g. turbidity), temperature, and aragonite saturation state (Prachett et al. 2015). However, since tabular *Acropora* species are among the fastest growing of all corals our estimates of carrying capacity and outbreak densities are likely to be somewhat conservative.

Multiple factors, such as competition, predation, disease, mechanical stability and disturbances, can all simultaneously limit colony growth (Madin and Connolly 2006; Madin et al. 2014; Pratchett et al. 2015; Drury et al. 2017, Shaver et al. 2017). Although we used idealized coral assemblages which did not suffer mortality and damage to estimate outbreak thresholds, we found evidence that both disease and disturbance limited the growth of tagged coral colonies in the current study. Consequently, the estimates of threshold densities are likely to be lower than our idealized estimates. However, coral cover on the back reef habitats adjacent to our study site have declined, but not significantly, from 2007 to 2015 (22.7 ± 14% to 14.3 ± 13%) but were slightly higher in 2015 (21.5 ± 14%; see Supplementary Material). During this time the average density of *Drupella* has never exceeded levels that would constitute an outbreak as we have calculated it here (see Supplementary Material). Thus the mean *in situ Drupella* consumption rate determined by our study is consistent with existing data, which do not support a predation driven decline in overall cover, but have providing further evidence to increase our understanding of the effects of these corallivores on coral communities. The observed variability in coral cover is consistent with previously reported dynamic stability of coral communities in northern Ningaloo (Speed et al. 2013). Importantly, our estimates are based on standard photographic techniques used to assess community coral cover in broad-scale surveys and can therefore be used more directly in assessing outbreak thresholds than can data derived from laboratory studies.

Outbreak populations of *Drupella* have been provisionally defined as "any population of elevated density that causes extensive mortality of corals and persists for months or years over large areas of reef" (Cumming 2009a). Our study estimates that the threshold density of outbreak populations is substantially lower than the conclusions made by Cumming (2009a) that non-outbreak *Drupella* densities range from 0 to 2m^{-2}. Cumming (2009a) observed that the majority (69%) of studies reported *Drupella* densities as less than 3 m^{-2}, and that reports of densities > 3 m^{-2} where from outbreak populations at locations in Ningaloo, Aqaba and Japan. Our current study has been based on a series of highly conservative estimates of feeding rate, and coral growth rates. Consequently, there is a possibility that our outbreak threshold estimates are upper estimates and higher than may actually be the case.

Understanding the threshold number of *Drupella* that can be sustained based on coral coverage and growth is essential information required to help managers monitor and predict possible outbreak abundances. Such thresholds have been developed for other coral predators, notably the crown of

thorns starfish (Keesing and Lucas 1992, Moran and De'ath 1992, Babcock et al. 2014), and are becoming a core part of current coral reef management strategies, for example on the Great Barrier Reef. In order to implement any *Drupella* action plan managers need to be able to distinguish between non-problematic *Drupella* abundances, and those that could lead to possible outbreaks situations. Our study, in combination with the previously existing literature, suggests *Drupella* abundances that could lead to a reduction in the preferred prey species of coral, and should be closely monitored as part of effective monitoring systems to enable managers to evaluate reef health.

8.4.5   ACKNOWLEDGEMENTS

8.4.6   REFERENCES

Al-Horani FA, Hamdi M, Al-Rousan SA (2011) Prey selection and feeding rates of *Drupella cornus* (Gastropoda: Muricidae) on corals from the Jordanian Coast of the Gulf of Aqaba, Red Sea. Jordan Journal of Biological Sciences 4:191-198

Al-Moghrabi SM (1997) Bathymetric distribution of *Drupella cornus* and *Coralliophila neritoidea* in the Gulf of Aqaba (Jordan). Proceedings of the 8th International Coral Reef Symposium, 2:1345-1350

Antonius A, Riegl B (1997) A possible link between coral diseases and a corallivorous snail (*Drupella cornus*) outbreak in the Red Sea. Atoll Research Bulletin 447:1-9

Armstrong SJ (2009) Ningaloo Marine Park Drupella long-term monitoring program: data collected during the 2008 survey. Marine Science Program Data Report Series: MSPDR5. Department of Environment and Conservation, Western Australia.

Ayling AM, Ayling AL (1987) Ningaloo Marine Park: preliminary fish density assessment and habitat survey, with information on coral damage due to *Drupella* grazing. Report to the Department of Conservation and Land Management, Western Australia.

Ayling AM (2000) The effects of *Drupella* spp. grazing on coral reefs in Australia. Sea Research, http://www.searesearch.com.au/reports/drupella/drupella.html

Babcock RC, Haywood MDE, Vanderklift M, Clapin G, Kleczkowski M, Dennis D, Skewes T, Milton D, Murphy N, Pillans R, Limbourn A (2008) Ecosystem impacts of human usage and the effectiveness of zoning for biodiversity conservation: broad-scale fish census Final analysis and recommendations 2008. Western Australian Marine Science Institution, Perth. 99 pp.

Babcock RC, Plagányi ÉE, Morello EB, Rochester W. (2014). What are the important thresholds and

relationships to inform the management of COTS? Final Report, 30 June 2014. CSIRO, Australia.

Baums IB, Miller MW, Szmant AM (2003) Ecology of a corallivorous gastropod, *Coralliophila abbreviata*, on two scleractinian hosts. II. Feeding, respiration and growth. Marine Ecology 142:1093-1101

Boucher L (1986) Coral predation by muricid gastropods of the genus *Drupella* at Enewetak, Marshall Islands. Bulletin of Marine Science 38:9-11

Bruckner RJ, Bruckner AW, Williams EH Jr (1997) Life history strategies of *Coralliophila abbreviata* Lamarck (Gastropoda:Coralliophilidae) on the southeast coast of Puerto Rico. Proc 8th Int Coral Reef Sym 1:627–632

Cumming RL (1999) Predation on reef-building corals: multiscale variation in the density of three corallivorous gastropods, *Drupella* spp. Coral Reefs 18:147-157

Cumming RL (2009a) Population outbreaks and large aggregations of *Drupella* on the Great Barrier Reef. Great Barrier Reef Marine Park Authority, Research Publication 96, Townsville, Australia

Cumming RL (2009b) Case study: impact of *Drupella* spp. on reef-building corals of the Great Barrier Reef. Great Barrier Reef Marine Park Authority, Research Publication 97, Townsville, Australia

Drury C, Manzello D, Lirman D (2017) Genotype and local environment dynamically influence growth, disturbance response and survivorship in the threatened coral, *Acropora cervicornis*. PLoS ONE 12:e0174000

Forde MJ (1992) Populations, behaviour and effects of *Drupella cornus* on the Ningaloo Reef, Western Australia. Department of Conservation and Land Management (CALM), CALM Occasional Paper 3/92, Western Australia

Fujioka Y, Yamazato K (1983) Host selection of some Okinawan coral associated gastropods belonging to the genera *Drupella*, *Coralliophila* and *Quoyula*. Galaxea 2:59-73

Keesing JK, Lucas JS (1992) Field measurement of feeding and movement rates of the crown-of-thorns starfish *Acanthaster planci* (L.). Journal of Experimental Marine Biology and Ecology 156:89-104

Kita M, Kitamura M, Tomoyuki K, Teruya T, Matsumoto H, Nakano Y, Uemura D (2005) Feeding attractants for the muricid gastropod *Drupella cornus*, a coral predator. Tetrahedron Letters 46:8583-8585

Kohn AJ (1961) Chemoreception in gastropod molluscs. American Zoologist 1:291-308

Madin JS, Baird AH, Dornelas M, Connolly SR (2014) Mechanical vulnerability explains size dependent mortality of reef corals. Ecology Letters 17:1008–1015

Madin JS, Connolly SR (2006) Ecological consequences of major hydrodynamic disturbances on coral reefs. Nature 444:477–480

Moerland, MS, Scott CM, Hoeksema BW (2016) Prey selection of corallivorous muricids at Koh Tao

(Gulf of Thailand) four years after a major coral bleaching event. Contributions to Zoology 85:291-309

Moran PJ, De'ath G (1992) Estimates of the abundance of the crown-of-thorns starfish *Acanthaster planci* in outbreaking and non-outbreaking populations on reefs within the Great Barrier Reef. Marine Biology 113:509-515

Morton B, Blackmore G, Kwok CT (2002) Corallivory and prey choice by *Drupella rugosa* (Gastropoda: Muricidae) on Honk Kong. Journal of Molluscan Studies 68:217-223

Moyer JT, Emerson WK, Ross M (1982) Massive destruction of scleractinian corals by the muricid gastropod, *Drupella*, in Japan and the Philippines. The Nautilus 96:69–82

Pratchett MS, Anderson KD, Hoogenboom MO, Widman E, Baird AH, Pandolfi JM, Edmunds PJ, Lough JM (2015) Spatial, temporal and taxonomic variation in coral growth – implications for the structure and function of coral reef ecosystems. Oceanography and Marine Biology: An Annual Review 53:215-295.

R Development Core Team (2011) R: A language and environment for statistical computing. www.R-project.org/ (accessed 1 January 2017)

Robertson R (1970) Review of the predators and parasites of stony corals, with special reference to symbiotic prosobranch gastropods. Pacific Science 24:43-54

Schneider CA, Rasband WS, Eliceiri KW (2012) NIH Image to ImageJ: 25 years of image analysis. Nature Methods 102:671

Schoepf V, Herler J, Zuschin M (2010) Microhabitat use and prey selection of the coral-feeding snail *Drupella cornus* in the northern Red Sea. Hydrobiologia 641:45-57

Shafir S, Gur O (2008) A *Drupella cornus* outbreak in the northern Gulf of Eilat and changes in coral prey. Coral Reefs 27:379

Shaver EC, Shantz AA, McMinds R, Burkepile DE, Thurber RLV, Silliman BR (2017) Effects of predation and nutrient enrichment on the success and microbiome of a foundational coral. Ecology 98:830-839

Simpson C (1988) Ecology of Scleractinian corals in the Dampier Archipelago, Western Australia. Technical Report No.23, Environmental Protection Authority, Western Australia.

Speed CW, Babcock RC, Bancroft KP, Beckley LE, Bellchambers LM, Depczynski M, Field SN, Friedman KJ, Gilmour JP, Hobbs JPA, Kobryn HT, Moore JAY, Nutt CD, Shedrawi G, Thomson DP, Wilson SK (2013) Dynamic stability of coral reefs on the West Australian coast. PLoS ONE 8(7): e69863. doi:10.1371/journal.pone.0069863

Stimson J (1996) Wave-like outward growth of some table- and plate-forming corals, and a hypothetical mechanism. Bulletin of Marine Science 58:301-313

Turner SJ (1994) The biology and population outbreaks of the corallivorous gastropod *Drupella* on Indo-Pacific reefs. Oceanography and Marine Biology Annual Review 32:461-530

8.4.7 SUPPLEMENTARY MATERIAL

Methods

The benthic and invertebrate community throughout Ningaloo was surveyed annually most years since 2007, and consists of back reef sites at Mandu Reef; the location of the current study. Benthic surveys consisted of one 25 m long photographic transect line (English et al. 1997) at each site, where a digital camera (Canon Powershot G16) was used to take a photograph every 50 cm, at a height of 0.7 m above the substrate (area of photograph is ~ 0.5 × 0.7 cm). To avoid non-independence among samples, 30 randomly selected photographs from each transect were processed using the TransectMeasure (http://www.seagis.com.au) software package. On each photograph, six fixed points were overlaid and the benthic category (rock, rubble, sand, silt, hard coral, algae) underlying each fixed point was recorded (Jonker et al. 2008). Algae and hard coral were further identified to genus level (and coral growth morphology) using relevant identification texts. Hard coral cover percentage was calculated for all back reef sites at Mandu.

Invertebrate surveys were conducted along a 5 × 1 m section of the benthic survey transects. The area was searched for all invertebrates (>5 mm) and the species identity and number were recorded, including that of *Drupella*. This method was slightly altered in 2013 onwards to consist of 1 × 1 m quadrats at 5 m intervals along each transect.

Here, we present both the percent cover of hard coral and the density of Drupella from surveys conducted at all Mandu sites since 2007 in Table S8.4.1.

Table S8.4.1 Coral cover and *Drupella* density measured on Mandu Reef back reef sites 2007 – 2016.

YEAR	HARD CORAL COVER % (MEAN ± SD)	*Drupella* DENSITY (MEAN M^{-2} ± SD)
2007	22.7 ± 14.3	0.14 ± 0.29
2008	19.2 ± 13.5	0.60 ± 0.40
2009		0.46 ± 0.31
2010		0.23 ± 0.55
2011	18.1 ± 14.4	
2013	18.8 ± 13.1	
2014	16.0 ± 12.8	
2015	14.3 ± 13.2	
2016	21.5 ± 14.3	0.34 ± 0.68
GRAND TOTAL	**17.6 ± 13.7**	**0.35 ± 0.45**

References

English S, Wilkinson C, Baker V (1997) Survey manual for tropical marine resources. Australian Institute of Marine Science, Townsville

Jonker MM, Johns KK, Osborne KK (2008) Surveys of benthic reef communities using underwater digital photography and counts of juvenile corals. Long-term Monitoring of the Great Barrier Reef. Standard Operational Procedure Number 10/2008. Australian Institute of Marine Science (AIMS)

9.   Macrophyte interactions

9.1 Drivers of species richness and abundance of marine macrophytes on shallow tropical reefs of North-Western Australia

Authors: Olsen YS, Mattio L, Perez AZ, Babcock RC, Thompson D, Haywood MDE, Keesing J, Kendrick GA.

ABSTRACT

Marine macrophytes are important components of tropical reefs that are influenced by environmental conditions and biotic interactions. We examined biomass and species richness of macrophytes on shallow reefs in the Pilbara coastal region Western Australia – a diverse region influenced by periodic disturbances from cyclones – and identified correlations with environmental and biotic drivers. Macrophyte richness and biomass were assessed at 75 shallow reef sites in November 2013 and May 2014. The influence of 28 predictor variables including seascape descriptors, physico-chemical variables and herbivore abundances were evaluated using distance based linear models (DistLM) and redundancy analyses (dbRDA). We identified 187 species. Rhodophyta accounted for about 60% of the species while Phaeophyceae made up 67% of the biomass. Chlorophyta and seagrasses were minor components (8% and <1% of biomass respectively). Seabed rugosity, hard coral cover, sediment uniformity and sea surface temperature explained 64% of the variation in total macrophyte biomass. Biomass increased with rugosity for all taxonomic groups, except for Chlorophyta. Species richness and biomass were generally negatively correlated to hard coral cover. Biomass and species richness of Chlorophyta and Phaeophyceae were negatively correlated to herbivore abundance, but grazing did not appear to be an important control of total macrophyte biomass in the Pilbara. Our results underline the spatial heterogeneity and complexity of Pilbara macrophyte communities and point to significant differences in distribution among taxa. Seabed rugosity, hard coral cover, sea surface temperature and salinity were the main factors correlated to overall macrophyte biomass, species richness and community composition with additional factors emerging as important depending on the taxonomic level examined. This study provides baseline data on the structure of macrophyte communities in the Pilbara against which to detect future ecological change.

9.1.1 INTRODUCTION

Macrophytes (macroalgae and seagrass) are important components of tropical reef ecosystems. They contribute to the productivity of the reef, are a major source of food, and provide habitats for invertebrates and fish (Wilson et al. 2010; Evans et al. 2014). They can also have a critical part in reef degradation when the balance between fast-growing macroalgae and relatively slow-growing reef-building corals is shifted (McCook 1999; Hughes et al. 2007).

Environmental conditions influence patterns of composition and abundance in benthic macrophytes. Sea surface temperature and nutrients were identified as important predictors of macroalgal richness on a global scale, particularly at high latitudes, whereas biotic interactions were more important in the tropics (Keith et al. 2014). Other processes, including periodic disturbances, oceanography, nutrient availability and biotic interactions (grazing, competition and facilitation) also drive the structure of macrophyte assemblages across smaller spatial scales, e.g. on the Great Barrier Reef where macroalgal assemblages vary with latitude, across the shelf and within reefs (Wismer et al. 2009). The drivers that control macrophyte assemblages are fundamental to the overall functioning and condition of tropical reefs. Herbivory is key in controlling algal abundance and preventing phase shifts from coral-dominated to macroalgae dominated reefs (e.g. Lirman 2001; Bellwood et al. 2006; Hughes et al. 2007), but a range of other mechanisms may shape coral-macrophyte community structure and create spatial and temporal gradients. These include seasonality (Fulton et al. 2014), latitudinal and cross-shelf position (Wismer et al. 2009), grazing pressure (Hughes et al. 2007; Mumby et al. 2006), nutrient availability (McCook 1999), anthropogenic stress (Ainsworth and Mumby, 2015), and surge/water movement during cyclones or hurricanes (Mumby et al. 2005).

The Pilbara coastline stretches 330 km between Exmouth and Dampier in Western Australia and includes numerous fringing reefs, reef platforms and shoals that are considerably less studied than those in the Great Barrier Reef or the adjacent Ningaloo Reef, which extends to the south. The climate is tropical and characterised by a dry (June-November) and a wet season (December-May) with ~250-300 mm annual rainfall along the coast (CSIRO 2015). Runoff from land is sporadic – 3 to 5 events per year – leading to low nutrient inputs (CSIRO 2015). The coastal habitats are subject to periodic disturbances by extreme surges from seasonal cyclones (2 to 4 per 10 years, Bureau of Meteorology) and intense tropical lows. The area's hinterland is known for its petroleum, natural gas and iron ore deposits and the main human pressures are associated with the exploitation and development of natural resources and associated activities, e.g. ports and dredging. Recreational and commercial fishing as well as tourism occur but at moderate to low levels.

Macrophyte taxonomy has been described for parts of the Pilbara coast (Walker and Prince 1987; Huisman and Borowitzka 2003; Huisman 2004; Huisman et al. 2009) and currently includes 14 species of seagrass, 110 Chlorophyta, 61 Phaeophyceae and around 300 Rhodophyta (Huisman 2015; Huisman pers. com.). The importance of macroalgal beds as nursery habitats at Ningaloo Reef has been highlighted (Wilson et al. 2010; Evans et al. 2014), but we know little of their overall status and function in this regard in the Pilbara region, which differs markedly in its geophysical setting. Due to the remoteness, it has been difficult to carry out a comprehensive assessment of the Pilbara benthos. There is still a lack of quantitative data on the distribution and abundance of macrophytes and the mechanisms that shape macrophyte communities are not well understood.

Here, we characterised communities on shallow reefs along the Pilbara coast by sampling in two contrasting seasons. Specifically, we aimed to: i) benchmark the macrophyte benthos on shallow reefs; and ii) test how environmental and biotic drivers shape macrophyte communities by examining correlations between the macroalgal assemblages across different taxonomic levels with a range of environmental, biotic and geographic variables.

9.1.2 METHODS

Study region and site selection

The study focused on a region spanning ~ 330 km along the coast and as far as 100 km offshore. Sites were chosen to represent a range of reef types, environmental conditions and inshore to offshore reefs in depths 3 - 9 m. We sampled 75 sites at the beginning of the wet season (November 2013; 34 sites) and of the dry season (May 2014; 41 sites) (Figure 9.1.1). To assess spatial patterns the area sampled was split into five roughly equally sized sectors; four along the main coastline and one encompassing Barrow Island and the Montebellos, which are located further offshore (Figure 9.1.1).
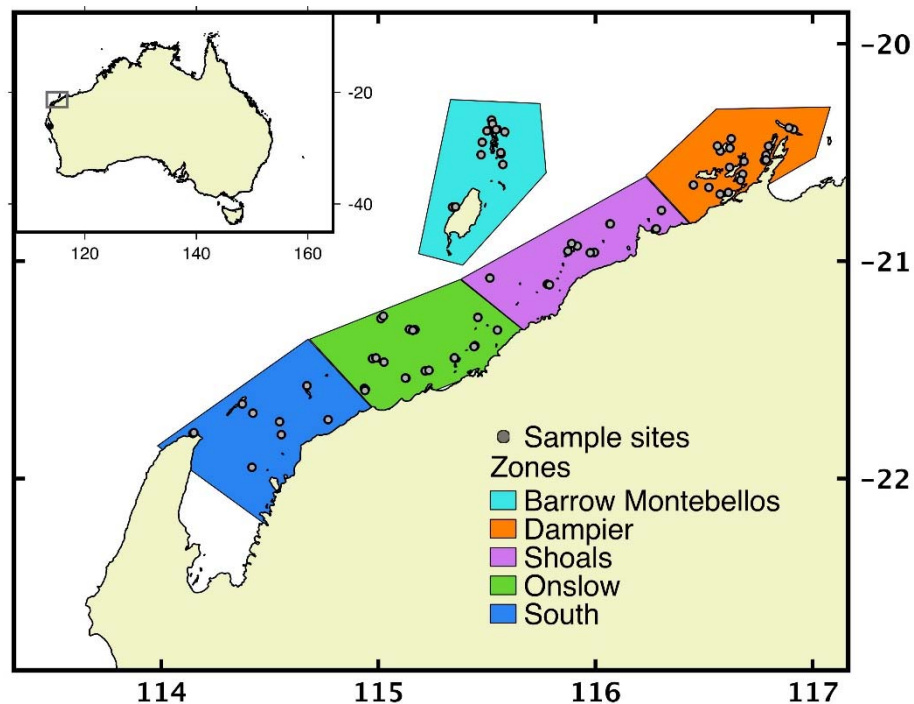
Figure 9.1.1 Map of the study region showing locations of the zones and sites sampled

Macrophyte sampling

At each site, all macrophytes were collected from 6 randomly placed 0.25 m × 0.25 m quadrats using SCUBA. Samples from each quadrat were frozen in plastic bags and before sorting into the lowest taxonomic level possible. For each taxa, total wet weight and dry weight (after drying for 48h at 60˚C) were recorded. The number of species at each location (α-diversity) was recorded. The mean α-diversity, large area species richness (γ) and turnover species richness (β = (γ/ α)-1) were calculated for each sector. In addition the Shannon's diversity index (H') was calculated for each sample and sector in PRIMER 6 (Clarke and Gorley 2006).

Predictor variables

We collated data for geographic, temporal, seascape, biotic, herbivory, and physico-chemical variables Table 9.1.1). *In situ* observations of depth, underwater visibility, rugosity, herbivore abundance (fish and invertebrates) and substrate type (sand, rubble, boulders, consolidated rubble, bommies or pavement) were made at the same time as the macrophyte sampling. We also

Table 9.1.1 List of predictor variables, description and source of data. Variables in italics were highly correlated to other variables (>0.8) and were not included in the analyses.

VARIABLE	DESCRIPTION	DATA SOURCE
Latitude	Latitude	This study
Longitude	Longitude	This study
LonghShPos	Longshore position measured as distance from Learmonth airport in km. Measured in QGIS.	This study
Season	Date of sampling: November 2013 or May 2014	This study
DistShore	Distance to the nearest shore in km. Measured in QGIS.	This study
OffShPos	Distance to the main coast in degrees. Measured in QGIS.	This study
Depth	Depth at sample site.	This study
UVis	Underwater visibility estimated by diver.	This study
Rugosity	Rugosity estimated with 10-m chain.	This study
Abiotic	Photoquadrat estimate of % abiotic benthic cover along 25-m transect.	This study
Hard Coral	Photoquadrat estimate of % (live) hard coral cover along 25-m transect.	This study
Soft Coral	Photoquadrat estimate of % soft coral cover along 25-m transect.	This study
Sponge	Photoquadrat estimate of % sponge cover along 25-m transect.	This study
RovingHerb	Number of roving herbivores observed during visual counts along 100 m transect	This study
InvertHerb	Number of invertebrate herbivores counted in 25 m^2 including *Diadema setosum* and *Echinometra mathaei.*	This study
Sand	Benthic cover of sand estimated by diver along 100-m transect.	This study
Rubble	Benthic cover of rubble estimated by diver along 100-m transect.	This study
Boulders	Benthic cover of boulders estimated by diver along 100-m transect.	This study
ConRubble	Benthic cover of consolidated rubble estimated by diver along 100-m transect.	This study
Bommies	Benthic cover of bommies estimated by diver along 100-m transect.	This study
Pavement	Benthic cover of pavement estimated by diver along 100-m transect.	This study
%Gravel	Sediment gravel content (%)	This study
%Sand	Sediment sand content (%)	This study
%Silt/Clay	Sediment silt and clay content (%)	This study
SedUniform	Sediment uniformity coefficient (Cu)	This study
GrainSize	Average grain size of sediment	This study
Sed%OM	Sediment % organic matter	This study
Chla	Chlorophyll mean for month of sampling (Nov 2013 or May 2014), 4 km resolution.	MODIS
ChlaAnnual	Chlorophyll annual mean for 2013, 4 km resolution.	MODIS
DiffAtten	Diffuse attenuation coefficient at 490 nm, KD2 algorithm. Mean for month of sampling (Nov 2013 or May 2014), 4km resolution.	MODIS
DiffAttenAnnual	Diffuse attenuation coefficient at 490 nm, KD2 algorithm. Annual mean for 2013, 4 km resolution.	MODIS
MeanSSS	Mean Salinity at 5 m depth, average 2000-2008	CARS Coast8
MeanSST	Mean Sea Surface Temperature	Aus BOM
MinSST	Minimum Sea Surface Temperature	Aus BOM
MaxSST	Maximum Sea Surface Temperature	Aus BOM
SST_Inst	Mean Sea Surface Temperature during the month of sampling (Nov 2013 or May 2014)	Aus BOM

photographed quadrats along one 25-m transect at each site and used the images to estimate the cover of biota. Surface sediment was collected for grain size analysis (Table 9.1.1).

A further three variables were determined from spatial measurements in a Geographical Information System (QGIS) including distance from the sample site to the main coastline and to the nearest shore and long-shore position (defined as distance from Learmonth airport located just South of the sample region at S 22°.14'3.10''; E 114°.5'13.09''). In addition, we obtained data on chlorophyll and diffuse attenuation at 4 km resolution from the Aqua MODIS satellite (http://oceancolor.gsfc.nasa.gov) as monthly means for November 2013 and May 2014 and as annual means for the year 2013. Sea surface temperature (SST; annual mean, max, min for 2013 and the mean for the month of sampling) was obtained from the Australian Bureau of Meteorology (bom.gov.au) and mean sea surface salinity (mean SSS at 5 m depth between 2000 and 2008; resolution = 1/8th degree grid) from the CSIRO Atlas of Regional Seas (Coast8; http://www.marine.csiro.au/atlas).

Draftman's plots were created in PRIMER 6 (Clarke and Gorley 2006) for all environmental variables to examine collinearity. Where pairs of variables had a Pearson's correlation coefficient >0.8, one of the variables was excluded. As a result, latitude, longitude, longshore position, season, grain size, % gravel and chlorophyll (monthly and annual means) were removed, resulting in a final dataset of 28 variables (Table 9.1.1). A number of predictor variables could not be obtained for 25 of the sample sites, so for further analyses we considered a subset of 50 out the 75 sites.

Macrophyte dataset

To determine the influence of predictor variables on species number, biomass and community structure we examined the complete data set and a series of sub-sets as follows: The macrophyte biomass and richness were estimated for species, genus, family, order and phylum. Discrete data sets describing the biomass and species numbers of Rhodophyta, Chlorophyta, Phaeophyceae, Fucales (most abundant Order overall) and Dictyotales (highest number of species overall) at each site were also tested.

Statistical analyses

Sample species richness (α-diversity) and Shannon's diversity index (H') were compared among zones by one-way ANOVAs followed by Tukeys HSD tests in R (R Core Team 2015). Homogeneity of variances and normality of data were confirmed with Bartlett and Shapiro tests respectively. To assess if the sampling reflected the theoretical species diversity of the area, a species accumulation curve was built with random sample order permutated 9999 times in PRIMER 6 (Clarke and Gorley 2006). We fitted the Michaelis Menten model to the curve to estimate the theoretical total number of macroalgal species on shallow reefs in the sample area.

Relationships between macrophytes (assemblages, biomass and richness) and predictor variables were analysed using multivariate routines in the statistical software package PRIMER 6 (Clarke and Gorley 2006) with PERMANOVA+ (Anderson et al. 2008). The macrophyte dataset was fourth root transformed to down-weight the effect of highly abundant species and the high frequency of zero counts in the data. For preliminary exploration of the macrophyte community structure, we used MDS (Multi-Dimensional Scaling) plots based on Bray-Curtis distance measure. Differences in the predictor variables among *a priori* defined groups of sites based on zone and season were tested using permutational multivariate analysis of variance (PERMANOVA) followed by canonical analysis of principal coordinates (CAP) with zone and season as constraining factors (Anderson and Willis 2003). The CAP maximises differences among the *a priori* defined groups and reveals patterns that

can be cryptic in unconstrained ordinations (Anderson and Willis 2003). Pearson correlations of selected environmental and biotic variables were plotted on the CAP.

We analyzed differences in plant communities using distance-based multivariate analysis for a linear model (DistLM) (Anderson 2001). Similarity matrices were constructed using Bray-Curtis distance measure for community structure and Euclidean distance for species richness and biomass. We used stepwise DistLMs to measure the relationships between the macroalgal assemblage structure, biomass and species richness and the physical and biological environment (Anderson 2001; McArdle and Anderson 2001). Marginal tests examined the relationships between individual predictor variables and the macroalgae similarity matrices. Sequential tests were produced by employing 9999 permutations and using the AIC_c (Aikake's Information Criterion corrected for small sample sizes) model selection criterion (Chambers and Hastie 1993) to identify the best models. A distance-based redundancy analysis (dbRDA) was used to visualize the DistLM results (Clarke and Warwick 2001; Clarke and Gorley 2006; Anderson et al. 2008).

9.1.3 RESULTS

Macrophyte abundance and community composition

A total of 187 morphotypes were assigned species level, although 76 of these (40%) were not assigned species names (e.g. reported as Sargassum sp1, sp2). A full list of species is provided in Appendix 1. The species accumulation curve (Appendix 2) estimated the total number of species in the region, Smax = 222 and the number of samples that would capture half of the species present, B = 11.9. This suggested that we had captured > 80% of the total number of species present.

Table 9.1.2 Summary of macrophyte species richness and biomass across the Pilbara region, Western Australia, in November 2013 and May 2014

	NOV-13	MAY-14	OVERALL
Number of sites sampled	34	41	75
Total number of species	153	137	187
Number of species per site ± SE	18 ± 1.7	18 ± 1.9	18 ± 1.3
Median Biomass (g wet weight m^{-2})	643	169	342
Median Biomass (g dry weight m^{-2})	122	49	77
Mean Biomass (g dry weight m^{-2}) ± SE	179 ± 29	94 ± 17	132 ± 17
Max biomass (g dry weight m^{-2})	574	430	574

There was a high degree of overlap in the taxa collected in the two seasons, i.e. many of the same taxa were found in both (Table 9.1.2). Biomass and species richness varied across the region, but no clear spatial pattern was found (Figure 9.1.2). An average of 18 species was collected per site in both seasons (Table 9.1.2), but there were notable hotspots with 52 species at Barrow Island in November and Thevenard Island in May (Figure 9.1.2). Biomass varied seasonally with mean dry biomass in November being almost twice that measured in May and the median biomass around three times higher in November (Table 9.1.2). The average biomass was 132 ± 17 g dry weight m-2 ranging from <1 to 574 g m-2 in November and 430 g m-2 in May. Median biomass was lower at 77 g m-2 (dry weight). The taxonomic composition and contribution to total diversity and abundance is summarized in Table 9.1.3. Rhodophyta accounted for about 60% of the total species richness but only 23% of the biomass while the Phaeophyceae represented 20% of the total species counts but >60% of the average biomass. Within this group, although the Dictyotaceae (Dictyotales) had the

largest number of species (19 species), the Sargassaceae (Fucales) represented the largest biomass (76% of the Phaeophyceae and 51% of total macrophyte biomass). We identified a similar number of species within the Chlorophyta (around 20% of total species count) but they made up only 8% of the biomass. Seagrasses were very sparse and represented by only 5 species making up less than 1% of the total biomass sampled.
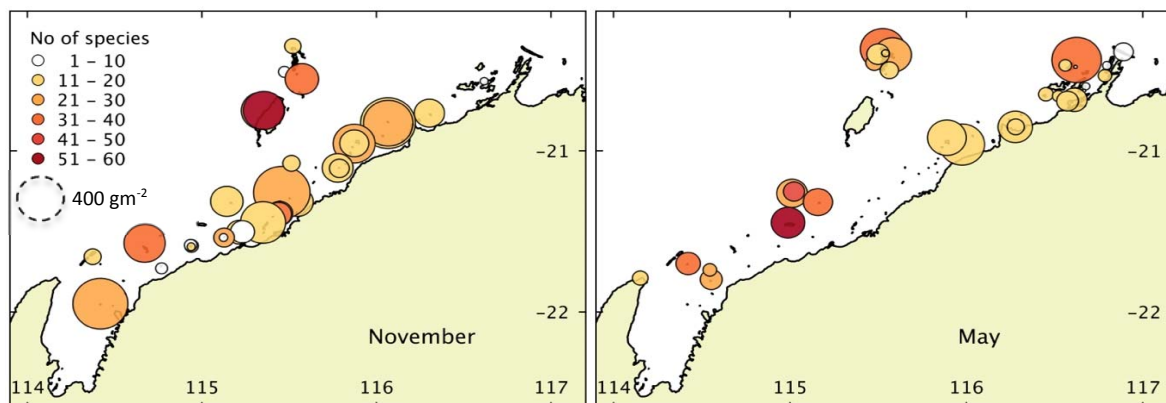
Figure 9.1.2 Species richness and biomass at each site sampled in November 2013 and May 2014. The size of the circles corresponds to the relative abundance of macroalgae.

Table 9.1.3 Summary of the taxonomic composition and contribution to species richness across the study are in the Pilbara, Western Australia. The relative contributions to overall biomass are based on dry weights.

	CHLOROPHYTA	PHAEOPHYCEAE	RHODOPHYTA	TRACHEOPHYTA
Orders	4	4	11	1
Families	12	4	27	2
Genera	18	16	46	4
Species	36	38	108	5
Proportion of Species (%)	19	20	59	2
Proportion of Biomass (%)	8	67	25	<1

Macrophyte regional species richness

There were significant differences in α-diversity among zones (Table 9.1.4; ANOVA: F = 3.72, p = 0.008) with Dampier having a lower α than all zones except Shoals. Onslow and Barrow-Montebellos had the highest numbers of species overall (γ =151 and γ =124 respectively) whereas Dampier had the fewest (γ = 77). Dampier and Onslow had the highest β-diversity suggesting the locations sampled within these zones were diverse and had fewer species in common. Dampier had the lowest mean Shannon's diversity index H' = 1.2, but there was no significant difference in H' among zones (ANOVA, n.s.).

Table 9.1.4 Macroalgal sample species richness (α), large area species richness (γ), turnover species richness (β) and Shannon's diversity index (H') by zone.

ZONE	α (±SE)	n (SITES)	γ	β	H' (±SE)
Barrow and Montebellos	23.7 ± 4.1	12	124	4.2	1.8 ± 0.3
Dampier	10.8 ± 1.9	18	77	6.1	1.2 ± 0.2
Onslow	21.9 ± 2.8	22	151	5.9	1.6 ± 0.2
Shoals	19.4 ± 1.9	14	100	4.1	1.5 ± 0.1

Broad spatial and seasonal patterns

PATTERNS IN PREDICTOR VARIABLES

Predictor variables varied among zones (PERMANOVA; pseudo-F = 3.79, p = 0.0001) and seasons (PERMANOVA; pseudo-F = 3.04, p = 0.001) (Table 9.1.5). The patterns were visualised with a CAP, which maximises differences among the a priori defined groups (Zone × season) (Figure 9.1.3). The CAP was overlaid with vectors of nine predictor variables that illustrate differences among the samples. The two seasons sampled were separated by differences in mean SST. Separation along the first axis (CAP1) divided the sites into two groups: Barrow Montebellos and South versus Onslow, Dampier and Shoals. This pattern was mainly driven by a gradient in mean SSS and diffuse attenuation, but there were also differences in the number of roving herbivores, underwater visibility and rugosity (Figure 9.1.3). Sea surface temperature was the main vector separating sites along the second axis (CAP2) dividing sites by season and, together with hard coral cover and sediment uniformity, by position along the north-south gradient (Figure 9.1.3).

Table 9.1.5 Results from univariate PERMANOVA analysis for differences in environmental variables between seasons (top) and between zones (bottom). Variables were normalised and resemblance among sites calculated using Euclidean distance.

SOURCE	df	SS	MS	PSEUDO-F	*P*(PERM)	UNIQUE PERMS
Season and Zone						
Season	1	62.6	62.6	3.04	0.001	9916
Zone	4	313.2	78.3	3.79	0.0001	9821
Season × Zone	3	97.7	32.6	1.58	0.043	9859
Residual	40	825.4	20.6			
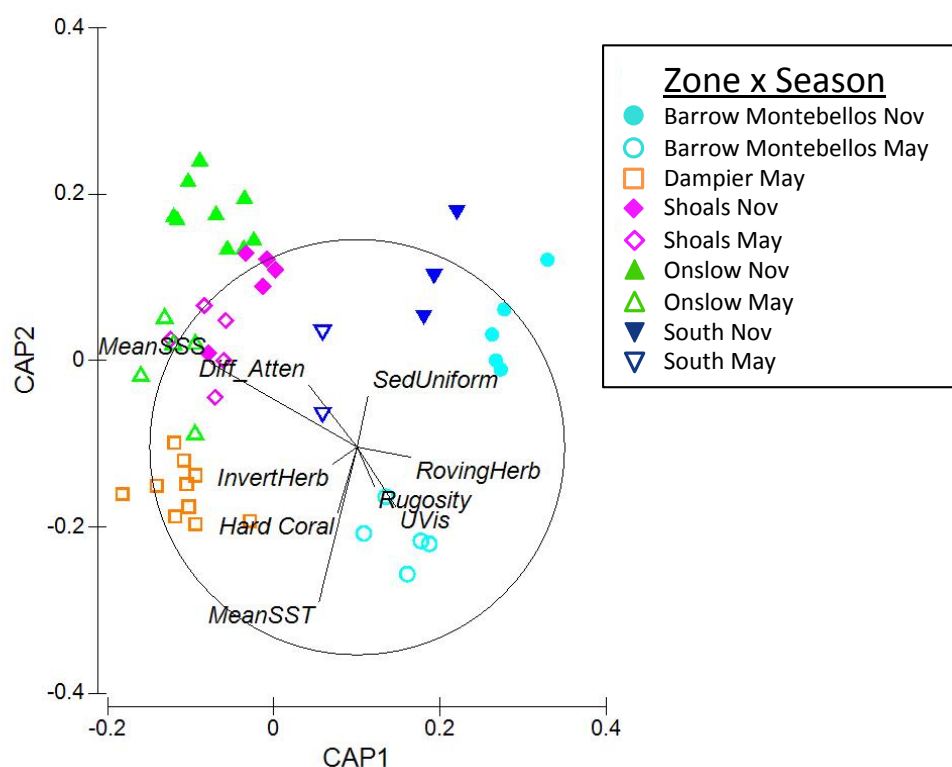
Figure 9.1.3 Constrained ordination (canonical analysis of principal coordinates, CAP) for differences in predictor variables using zone and season as constraining variables.
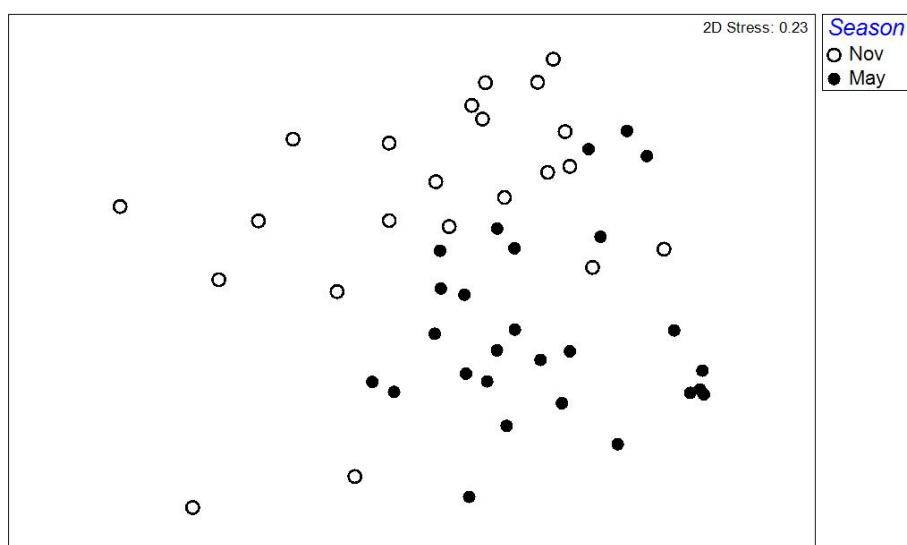
Figure 9.1.4 MDS plotted from the Bray-Curtis similarity matrix of the total macrophyte datatset – fourth-root transformed biomass of each species at each site. Season is plotted as factors.

Table 9.1.6 Results of marginal tests. Variables with significant correlations (*p*<0.05) are shown.

VARIABLE	SS(TRACE)	PSEUDO-*F*	*P*	VARIABILITY EXPLAINED (%)
Total Macroalgal biomass				
Rugosity	14.48	20.33	0.0001	30.2
Hard Coral	13.38	12.03	0.0001	27.9
Bommies	9.78	18.19	0.0013	20.4
Total Rhodophyta biomass				
OffShPos	5.16	8.91	0.005	15.9
MeanSSS	4.56	7.70	0.007	14.1
MaxSST	4.44	7.47	0.012	13.7
Abiotic	4.26	7.12	0.011	13.1
Sand	2.78	4.41	0.040	8.6
SedUniform	2.62	4.13	0.048	8.1
Total Chlorophyta biomass				
MaxSST	9.44	11.12	0.002	19.1
Rugosity	8.13	9.27	0.005	16.5
Pavement	6.21	6.77	0.011	12.6
InvertHerb	5.45	5.83	0.008	11.0
Bommies	5.36	5.72	0.017	10.9
Hard Coral	4.39	4.58	0.030	8.9
Total Phaeophyceae biomass				
Rugosity	21.68	18.46	0.0002	28.2
MeanSSS	15.43	11.79	0.002	20.1
MinSST	12.79	9.37	0.005	16.6
Hard Coral	11.69	8.43	0.003	15.2
Bommies	10.73	7.62	0.005	14.0
%Sand	8.13	5.56	0.023	10.6
RovingHerb	7.73	5.25	0.015	10.05
Depth	7.62	5.17	0.03	9.9

Exploratory analyses of the macrophyte community (biomass of each taxa) through multidimensional scaling (MDS) did not reveal any a priori spatial structure based on zone. The data broadly separated by season, but with some overlap and a very high 2D stress of 0.23, indicating that two dimensions are, in fact, not sufficient to represent the data set (Figure 9.1.4).

Environmental and biotic drivers

DRIVERS OF TOTAL MACROALGAL BIOMASS AND SPECIES RICHNESS

Table 9.1.7 Results of stepwise distance-based multivariate linear models (DistLM) with selection based on AICc.

| VARIABLE | AICC | SS(TRACE) | PSEUDO-F | P | VARIABILITY EXPLAINED (%) | | RES DF |
					PROPORTION	CUMULATIVE	
Total Macroalgal biomass							
Rugosity	-14.41	14.48	20.33	0.0001	30.2	30.2	47
Hard Coral	-27.57	9.04	17.03	0.0002	18.9	49.1	46
MinSST	-34.41	4.19	9.31	0.004	8.7	57.8	45
SedUniform	-35.26	1.33	3.10	0.09	2.9	60.6	43
SST_Inst	-36.81	1.54	3.80	0.06	3.2	63.8	40
Total species richness							
Rugosity	243.68	1133.1	8.21	0.007	14.9	14.9	47
Abiotic	240.36	700.8	5.57	0.02	9.2	24.1	46
MeanSST	238.44	485.8	4.12	0.048	6.4	30.4	45
DiffAtten	234.99	605.0	5.67	0.02	7.9	38.4	44
SST_Inst	233.19	403.7	4.04	0.049	5.3	43.7	43
Hard Coral	231.30	386.9	4.16	0.049	5.1	48.7	42
Macroalgal community (biomass of each species)							
SST_Inst	400.19	15120	4.491	0.0001	8.7	8.7	47
Hard Coral	399.02	10728	3.345	0.0001	6.2	14.9	46
MeanSSS	398.07	9690.2	3.164	0.0001	5.6	20.5	45
Rugosity	398.04	6900.3	2.319	0.0004	4.0	24.5	44
Shannon's diversity index (H')							
Rugosity	-46.78	2.33	6.34	0.014	11.9	11.9	47
RovingHerb	-48.25	1.31	3.76	0.059	6.7	18.6	46
Hard Coral	-50.20	1.32	4.05	0.047	6.7	25.3	45
UVis	-50.95	0.94	3.01	0.086	4.8	30.1	44

Total macroalgal biomass was strongly correlated to three variables; rugosity, hard coral cover and bommies (tested in separate marginal tests; Table 9.1.6). Coral cover (negatively correlated) and rugosity (positively correlated) each explained around 30% of the total variability in macroalgal biomass (Table 9.1.6). The best DistLM attributed 64% of the variability in total macroalgal biomass to five predictor variables; rugosity, hard coral cover, minimum SST, sediment uniformity and SST at the time of sampling (Table 9.1.7, Figure 9.1.5a). Rugosity (positively correlated) explained the highest proportion of variability in biomass (30.2%; Table 9.1.7). Coral cover and macroalgal biomass tended to follow opposite patterns: Where the cover of coral was high, the total biomass of macroalgae was low and vice versa. Minimum SST, and sediment uniformity were also negatively correlated to total macroalgal biomass.

Macrophyte species richness was significantly correlated to six individual predictor variables that each explained 10-15% of the variability in richness; rugosity, % sand, abiotic cover, hard coral cover, sediment uniformity and diffuse attenuation (marginal tests, $p < 0.05$, Appendix 3). The best DistLM explained a total of 49% of the variability in species richness and included six variables; rugosity, abiotic cover, mean SST, diffuse attenuation, SST at the time of sampling and hard coral cover (Table 9.1.7, Figure 9.1.5b). The best DistLM for Shannon's diversity index also included rugosity as the most important variable, but the total model (including four variables; rugosity, abundance of roving herbivores, hard coral cover and underwater visibility) only explained 30% of the variability in the data (Table 9.1.7).
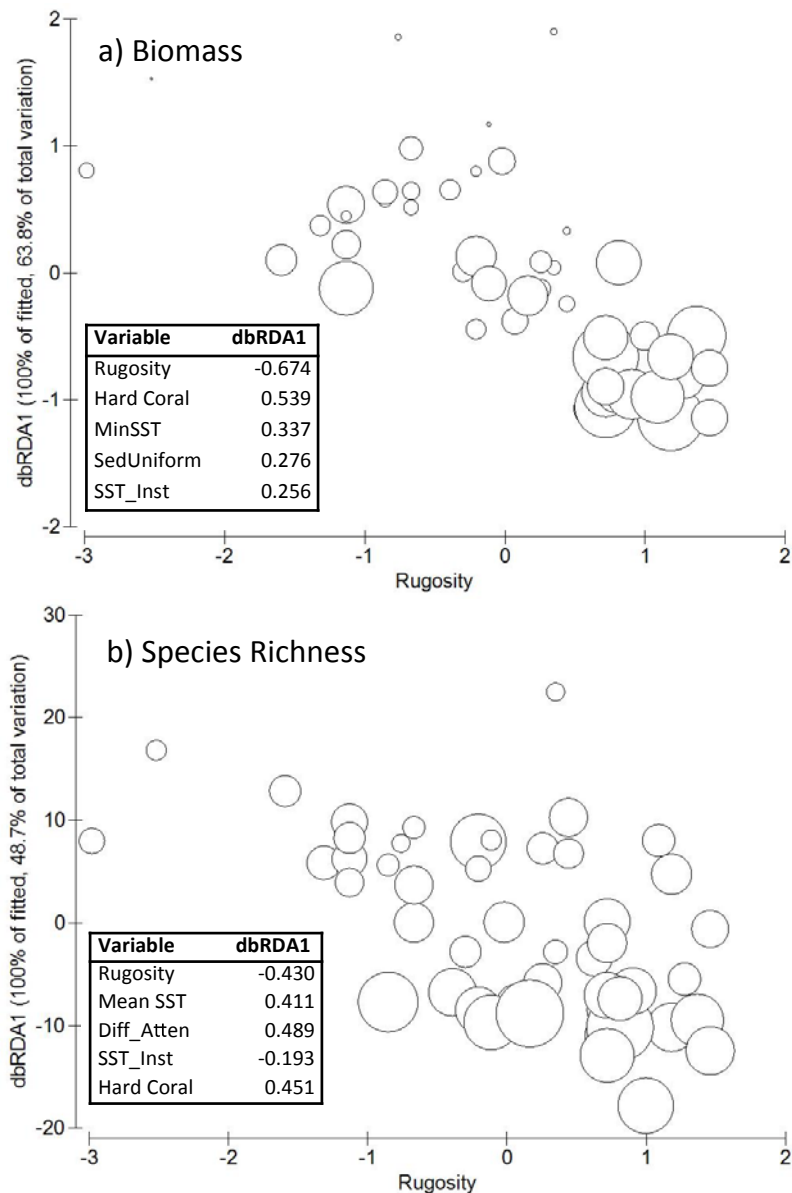
Figure 9.1.5 Distance-based redundancy (dbRDA) plot illustrating the DistLM models based on a) Total macroalgal biomass (g dry weight m^{-2}) and b) Species richness (number of species m^{-2}). Data are plotted against the most important variables. The length and direction of the vectors represent the strength and direction of the effect of each environmental variable in the model. The Y-axis represents 100% of the variation explained by the fitted model and shows the % of total variation explained. The relative biomass or number of species at each site is represented by the size of the circles. The variables included in each model are listed to the right (abbreviations see Table 9.1.1) along with their relationship (multiple partial correlations) with the dbRDA axis.

Drivers of biomass and species richness for red, green and brown macroalgae

Drivers of biomass were taxon-specific (Table 9.1.6). For example, the distance offshore (OffShPos) was correlated to Rhodophyta biomass (p = 0.005, variability explained = 16%), invertebrate herbivore abundance to Chlorophyta biomass (p = 0.008, variability explained = 11%) and abundance of roving herbivores and % sand to Phaeophyceae biomass (p = 0.015, variability explained = 10% and p = 0.02, variability explained = 11% respectively). Similar results were obtained for macrophyte species richness (marginal tests, Appendix 3). The species richness of Chlorophyta was highly correlated to maximum SST, which explained 25% of the variability. Rugosity, sediment uniformity and diffuse attenuation each explained around 17% of Rhodophyta species richness, whereas Phaeophyceae species richness was best explained by hard coral cover (28% of variability).
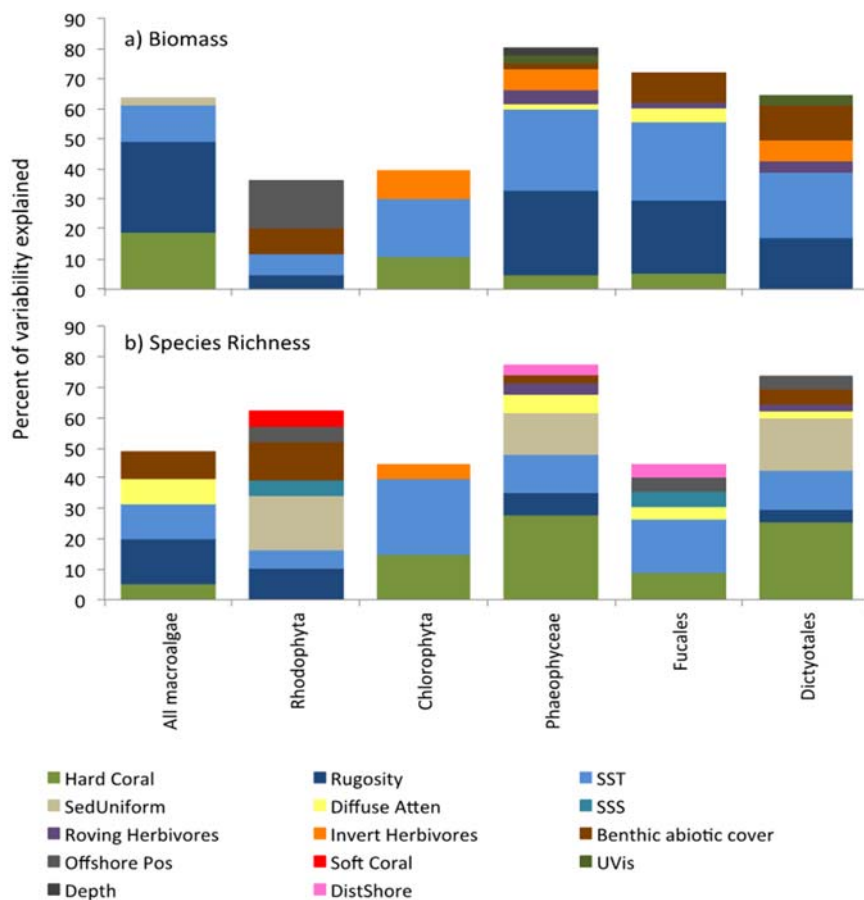
Figure 9.1.6 Summary of step-wise DistLM models for a) Biomass and b) Species richness of the full data set (All macroalgae) and five selected taxonomic groups. The percent variability explained by each variable is shown and the sum of the variability explained (the height of each stack) corresponds to the r^2 of the best model selected by AICc. Variable abbreviations are explained in Table 9.1.1. SST includes any measures of sea surface temperature.

The best DistLMs for total biomass of the Rhodophyta and Chlorophyta explained a limited amount of the variability in the data sets (r^2 < 0.4), whereas the model for biomass of Phaeophyceae explained over 80% (r^2 >0.8) (Figure 9.1.6, Appendix 4). Phaeophyceae biomass was mainly correlated to rugosity and minimum SST. Patterns in species richness were overall better explained by DistLMs with r^2 values of 0.62, 0.44 and 0.78 for Rhodophyta, Chlorophyta and Phaeophyceae respectively (Appendix 4).

A comparison of DistLMs for species richness and biomass revealed some general patterns (Figure 9.1.6). All models included SST, although different taxonomic groupings were more influenced by the SST measured at the time of sampling (the total macrophyte assemblage and Rhodophyta), minimum SST (e.g. Phaeophyta), maximum SST (Chlorophyta) or mean SST (Rhodophyta) (Appendix 4). In general, biomass and species richness were negatively correlated with hard coral cover and positively correlated with rugosity, except for Chlorophyta, (no correlation with rugosity) and Rhodophyta biomass and species richness (no correlation with hard coral). Water clarity, measured as diffuse attenuation and underwater visibility, explained variability in Phaeophyceae biomass and species richness (Figure 9.1.6). Herbivory was not an important driver overall, but may play a role in controlling Chlorophyta and Phaeophyceae, as their biomasses were negatively correlated to the abundance of invertebrate (Chlorophyta and Phaeophyceae) and roving (Phaeophyceae) herbivores. Herbivore abundance was also included in the DistLMs for species richness of Chlorophyta, Phaeophyceae and Dictyotales. Sediment uniformity was negatively correlated with species richness of Rhodophyta and Phaeophyceae (in particular the Dictyotales).

Drivers of community structure and patterns across different taxonomic levels
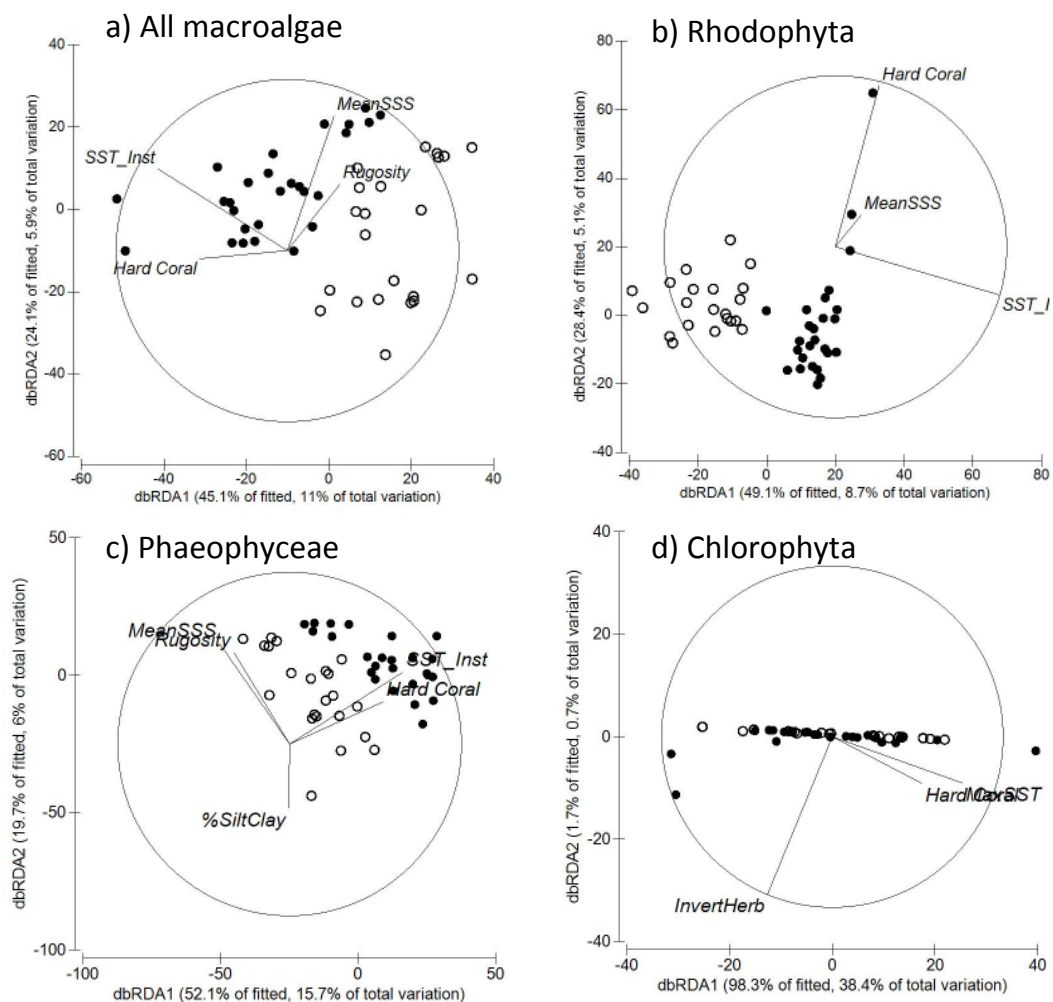
Figure 9.1.7 Distance-based redundancy (dbRDA) plots illustrating the DistLM models for the community structure (biomass of each species at each site) of a) All macroalgae, b) Rhodophyta, c) Phaeophyceae and d) Chlorophyta. Axis legends show the % variation explained by the fitted model and the % of total variation explained by the axis. The length and direction of each vector represents the strength and direction of the relationship. Season is illustrated by closed (November 2013) and open (May 2014) circles. Variable abbreviations are explained in Table 9.1.1.

The ability of individual variables to explain variability in the structure of the macroalgal community (biomass of each species) was poor. We found correlations to 16 individual predictor variables (marginal tests, $p < 0.05$, Appendix 3), but no variable explained more than 8.7%. Similarly, the marginal tests for the structure of the Rhodophyta and Phaeophyceae (as well as Fucales and Dictyotales) were correlated to a large number of variables, typically explaining <10% each (marginal tests, $p < 0.05$, Appendix 3). The structure of the Chlorophyta, in contrast, was only correlated to seven variables (marginal tests, $p < 0.05$, Appendix 3) with maximum SST (21.4%) and rugosity (13.4%) explaining most variability. Similarly, DistLMs were weak in their ability to explain variability in community structure. Only 24.5% of the variability in the total macroalgal community structure was explained by a DistLM, which included SST, hard coral cover, mean SSS and rugosity (Figure 9.1.7a, Table 9.1.7). DistLMs for the community structures of Rhodophyta, Phaeophyceae and Chlorophyta explained only 18-33% of the observed variability in the data (Figure 9.1.7c-d, Figure 9.1.8).
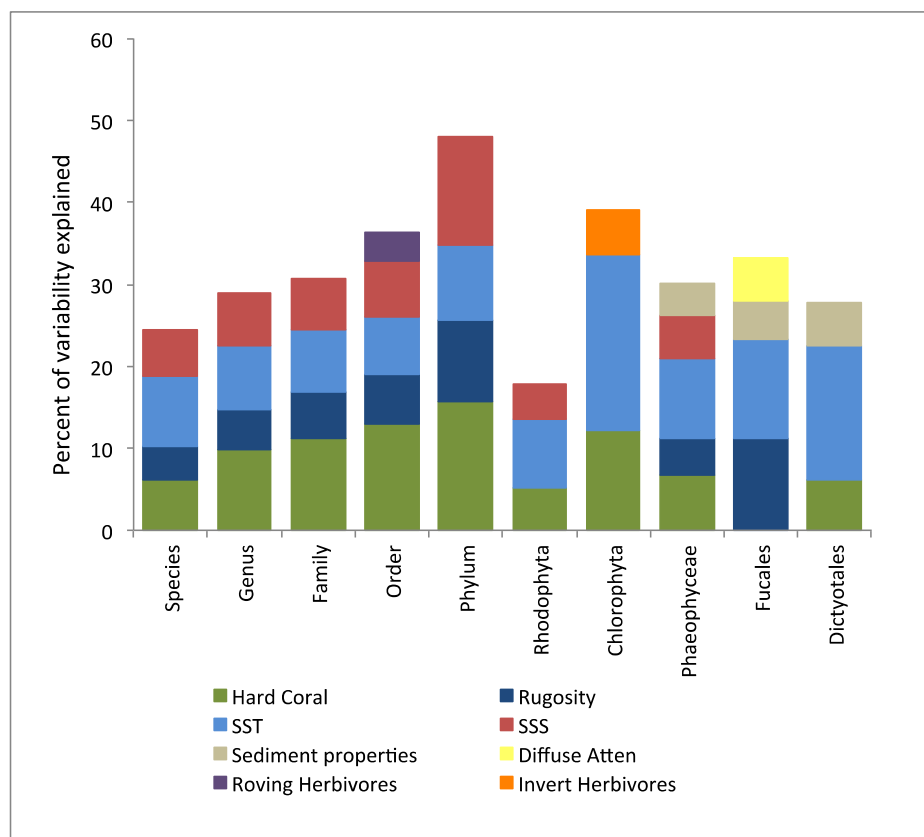
Figure 9.1.8 Summary of step-wise DistLMs for community structure. Data shown are from models explaining the variability in the biomass by species, genus, family, order and phylum of the full data set and for the species of Rhodophyta, Chlorophyta, Phaeophyceae, Fucales and Dictyotales at each site. The percent variability explained by each variable is shown and the sum of the variability explained (the height of each stack) corresponds to the r^2 of the best model selected by AICc. Variable abbreviations are explained in Table 9.1.1. The category "sediment properties" includes %Gravel, %Sand, %Silt/Clay, SedUniform and Sed%OM. SST includes any measures of sea surface temperature.

Separate DistLMs were constructed for macroalgal community structure at different taxonomic levels (Figure 9.1.8). As the level of taxonomic detail decreased from species to genus and so on, the overall percent variation explained by the DistLMs increased from 25 % to 48% (Figure 9.1.8, Appendix 4). All of the selected DistLMs included hard coral cover, rugosity, SSS and SST, with roving herbivore abundance making a small contribution (3.5%) to the models classified to order (Figure 9.1.8). Similar results were seen for the marginal tests (Appendix 3).

The community structures of the Rhodophyta, Chlorophyta, Phaeophyceae, Fucales and Dictyotales were all correlated to SST and hard coral cover (except Fucales) (Figure 9.1.8, Appendix 4). Sediment properties were included in models for the brown algae (Phaeophyceae and Fucales and Dictyotales) whereas diffuse attenuation only featured in the model for Fucales. Herbivory was not significant in these models, except invertebrate herbivore abundance in the DistLM for Chlorophyta structure.

9.1.4 DISCUSSION

We present the first analysis of spatial patterns of diversity, biomass, and community structure of marine macrophyte communities associated with shallow tropical reefs in the Pilbara, Western Australia. We described the distribution of biomass for nearly 190 species from 75 sites surveyed and tested correlations to environmental, geographical and biotic variables. The shallow marine macrophyte communities of the Pilbara region are heterogeneous and vary the most at the site and regional level. Surprisingly, seasonal variation was not very distinct, but this was probably masked by large differences among sites within each sample period. The mechanisms behind the patterns are complex, although a number of key drivers stood out including seabed rugosity, coral cover, sea surface temperature and sea surface salinity. The models for the assemblage at different taxonomic levels, from species to phylum, included the same environmental drivers. This agrees with previous work, which has suggested that spatial patterns in marine benthic community structure are often comparable at genus, family and species levels (Olsgard and Somerfield 2000; Anderson et al. 2005; Goldberg et al. 2006; Smale et al. 2010).

Although the five regions sampled in the present study could be distinguished by the environmental and geographic drivers, there was a lack of clear spatial patterns in macroalgal biomass and diversity. It is possible that, despite the large distances sampled (100 km × 300 km), the high small-scale variability due to habitat heterogeneity, competition for space, canopy-understory interactions and localized hydrodynamic stress and herbivory, may have overwhelmed any differences in assemblage structure across the shelf and along the coastline. Similar patterns of variability in subtidal flora have been observed along the temperate WA coastline with high patchiness at small spatial scales (meters) superimposed on regional variability (on the scale of 1000s of km) (Kendrick et al. 1999; Wernberg et al. 2003; Smale et al. 2011). High variability at small spatial scales (meters) is typical for benthic assemblages and clear patterns may not be evident until comparisons are made across locations or regions (Smale et al. 2010).

Spatial patterns of abundance and species richness

The Phaeophyceae were most abundant (67% of the total biomass) and Rhodophyta the most diverse (108 species = 59% of total) macrophytes. This is in agreement with previous work in the region, e.g. a survey of algae in the Dampier Archipelago found 114 species of Rhodophyta (58% of total), 50 of Chlorophyta and 32 of Phaeophyceae (Huisman and Borowitzka 2003).

The present study found low abundance of seagrass. Meadows in the Pilbara are less speciose and of much lower density than those found in southern parts of WA (Walker and Prince 1987; Carruthers et al. 2007), assemblages are ephemeral and can vary in abundance and distribution over short temporal and spatial scales in response to water quality and physical disturbance.

Influence of environmental and biotic variables on macrophyte assemblages

Understanding the mechanisms that shape and maintain patterns in macroalgal communities on shallow reefs is essential for evaluating and managing future changes. We found that the relative

importance of the drivers tested varied for biomass, species richness and community structure and different drivers emerged for different taxonomic groupings. Despite this, some general patterns emerged. The combination of low coral cover and high rugosity corresponded to high overall diversity and biomass of macrophytes. This pattern was, to some degree, driven by the most abundant group, the Phaeophyceae. In the tropics, algal competition with corals for hard substrate to settle on is an important control on macroalgal diversity and abundance (Keith et al. 2014; Burkepile and Hay 2008) and a negative relationship between live coral cover and biomass of macroalgae have been previously documented (Williams and Polunin 2001; Mora 2008; Graham et al. 2015).

Temperature was important for biomass and species richness of macroalgae and explained a significant portion of the variation in community structure. Macroalgae have unique thermal windows outside which they cannot survive, grow and reproduce and optimal temperatures can enhance growth and offer competitive advantages. Temperature extremes, such as those experienced during a marine heat wave, can result in substantial changes to seaweed assemblages (Wernberg et al. 2013). Temperature also shapes seasonal fluctuations in macroalgal biomass, e.g. the seasonal growth-decay cycle of canopy-forming macroalgae on Ningaloo reefs yielding highest standing crop in the summer, whereas understory algae peak in winter (Fulton et al. 2014). Differences in temperature and heterogeneity at the kilometre scale is also important (Fulton et al. 2014). In the present study, the overall pattern in macroalgal biomass in the Pilbara, which was highest in November compared to May, is therefore similar to that commonly observed for canopy-forming macroalgae.

In the tropics, environmental variables are generally viewed as having reduced explanatory power whereas biotic interactions are thought to be more important in controlling biodiversity (Wiens and Donoghue 2004). Reduced herbivore abundances and/or eutrophication are known to structure benthic reef communities and drive phase shifts from coral to algal dominated states (e.g. Hughes et al. 2003; Mumby et al. 2006). Clear relationships between macroalgal cover and herbivore biomass have been documented for tropical reefs in the Caribbean (Hughes 1994; Williams and Polunin 2001; Mumby et al. 2006) and Hawaii (Friedlander et al. 2007). Inshore reefs of the GBR are characterised by low grazing pressure allowing proliferation of macrophytes (Schaffelke et al. 2005; De'ath and Fabricius 2010). Abundances of herbivorous fish recorded here (mean = 24.4 ± 6.1, median = 7.0 individuals per transect covering 1000 m^2) were in the order of 2-5 times lower compared to similar reefs on the GBR (Russ 1984; Cheal et al. 2012). In Ningaloo reef – located just south of the region sampled in the present study – mean abundances of herbivorous fish were an order of magnitude higher, around 300 individuals per 1000 m^2, which is close to the maximum value recorded in the present study (347 individuals per 1000 m^2) (Vergés et al. 2003). Our results indicated limited influence of roving or invertebrate herbivores on Pilbara shallow reefs. In the present study, we found no relationship between herbivore abundance and total algal biomass and roving herbivore abundance explained just 4.5 % of the overall species richness. A small proportion of variability in Phaeophyceae biomass and species richness (4-5 %) could also be attributed to roving herbivore abundance. The low numbers of herbivorous fish encountered may, in part, explain the lack of a relationship. Sea urchins are important consumers of algae on coral reefs and may mediate the competition for space between corals and algae and even help the recovery of degraded reefs (Edmunds and Carpenter 2001). High densities of herbivorous urchins (>12 individuals m^{-2}) have been encountered on reef slopes of Ningaloo reef, which is considered a relatively intact system (Johansson et al. 2010). Most of the sites sampled here had very low invertebrate herbivore abundances (mean = 0.75 ± 0.34, median = 0.034 individuals m^{-2}), so it is not surprising that there was no correlation to the overall macroalgal biomass or community structure, and that the variability explained in the Chlorophyta was very low (5-8%).

High water clarity had a positive effect on the biomass of Phaeophyceae and on the species richness of all taxonomic groups tested except the Chlorophyta. In the GBR, the opposite pattern has been observed with a strong negative relationship between macroalgal cover and water quality suggesting macroalgal abundance was, in part, enhanced by increased nutrient availability (De'ath and Fabricius 2010). We did not measure nutrient concentrations in the current study, but diffuse attenuation (which was strongly correlated to chlorophyll concentration, a proxy for nutrient concentrations) was never positively correlated to macroalgal biomass, so there is no evidence that the macrophyte biomass on the shallow reefs of the Pilbara coast is regulated by nutrient supply. The positive effect of water clarity on biomass of Phaeophyceae and on the species richness of algae seen here may instead be due to improved light conditions in less turbid water.

Periodic disturbances

The reefs sampled had high alpha diversity, indicating speciose assemblages with high species turnover at the local scale. This suggests that a high level of physical disturbance may be at play in these reefs. In temperate Western Australia, high alpha diversity appears driven by high species turnover associated with winter storm swell driven disturbances (Toohey et al. 2007). Major perturbations like cyclones and tropical storms are thought to be important in shaping Pilbara reef systems, but these were not included in the present analysis. This may, in part, account for the low total predictability of some of our DistLMs. Cyclones have significant localized impacts on macroalgal biomass and species composition. When cyclone Fran passed over Heron Reef in 1992, *Caulerpa cupressoides* was almost completely removed from the reef flat and the cover of *Sargassum* spp. was depressed for several years (Rogers 1996; 1997). In Palau, cyclone disturbance caused catastrophic loss of corals and an ephemeral bloom of the macroalgae *Liagora* sp. reaching up to 40% cover within weeks followed by growth of *Lobophora variegata* (40% cover), which persisted for >18 months (Roff et al. 2015). Similarly, hurricanes can impact algae directly, but algae may also benefit from an increase in substratum resulting from breakage and death of corals (Mumby et al. 2005). Acute disturbance events can therefore be either a mechanism to remove algae from the reef or to trigger phase shifts to algal-dominated states. Although the impact of these storms on macroalgae is variable and not necessarily long-lived (Mumby et al. 2005) this type of disturbance repeated over time may still play a key role in affecting the reef structure.

Conclusion

This study provides the first comprehensive characterisation of macrophytes on shallow coral reefs in the Pilbara region and of the key environmental and biotic factors that influence their distribution. Macrophytes were abundant and diverse, but spatial patterns were weak. The environmental and biotic variables were relatively strongly correlated to biomass and species richness, in particular for the Phaeophyceae. Relationships between the predictor variables and community composition were weak suggesting that other factors not measured in this study, for example, disturbance events, recruitment and nutrient concentrations are important. The explanatory power of the DistLMs and the drivers included in each model differed depending on the taxonomic group and level examined. In general, higher biomass and species richness were found where coral cover was low and rugosity high. Temperature and salinity were also important in explaining variability, whereas herbivores were not found to have a major influence on the overall biomass and species richness and only correlated to biomass, species richness and community composition of the Chlorophyta (invertebrate herbivores). Based on our results, we put forward the hypothesis that coral and macroalgae on Pilbara shallow reefs compete for resources, most likely space, leading to their inverse relationship. We further speculate that herbivory structures the Chlorophyta community, but is not an important control for the overall biomass and species richness of macroalgae. The present study have, thus, allowed us to develop further hypotheses about what influences the distribution of

macroalgae in the region, but, in order to show causation and determine the relative strength of competitive interactions, experimental manipulations would be necessary.

9.1.5 ACKNOWLEDGEMENTS

9.1.6 REFERENCES

Ainsworth CH, Mumby PJ (2015) Coral–algal phase shifts alter fish communities and reduce fisheries production. Global Change Biology 21:165–172.

Anderson MJ, Willis TJ (2003) Canonical analysis of principal coordinates: A useful method of constrained ordination for ecology. Ecology 84:511-525.

Anderson MJ (2001) A new method for non-parametric multivariate analysis of variance. Australian Ecology 26:32-46.

Anderson MJ, Diebel CE, Blom WM, Landers TJ (2005) Consistency and variation in kelp holdfast assemblages: spatial patterns of biodiversity for the major phyla at different taxonomic resolutions. Journal of Experimental Marine Biology and Ecology 320:35–56.

Anderson MJ, Gorley RN, Clarke KR (2008) PERMANOVA+ for PRIMER: guide to software and statistical methods. PRIMER-E Ltd. Plymouth, UK.

Bellwood DR, Hughes TP, Hoey AS (2006) Sleeping functional group drives coral-reef recovery. Current Biology 16:2434-2439.

Burkepile DE, Hay ME (2008) Herbivore species richness and feeding complementarity affect community structure and function on a coral reef. Proceedings of the National Academy of Science 105:16201-16206.

Carruthers TJB, Dennison WC, Kendrick GA, Waycott M, Walker DI, Cambridge ML (2007) Seagrasses of south-west Australia: A conceptual synthesis of the world's most diverse and extensive seagrass meadows Journal of Experimental Marine Biology and Ecology 350:21-45.

Chambers JM, Hastie TJ (1993) Statistical models. S. Chapman and Hall, London.

Cheal A, Emslie M, Miller I, Sweatman H (2012) The distributions of herbivorous fishes on the Great Barrier Reef. Marine Biology 159:1143-1154.

Clarke KR, Gorley RN (2006) PRIMER v6: User Manual/Tutorial. Plymouth UK PRIMER-E.

Clarke KR, Warwick RM (2001) Change in marine communities: an approach to statistical analysis

and interpretation, 2nd edition Plymouth, UK: PRIMER-E.

CSIRO (2015) Pilbara Water Resource Assessment. An overview report to the Government of Western Australia and industry partners from the CSIRO Pilbara Water Resource Assessment. CSIRO Land and Water, Australia.

De'ath G, Fabricius K (2010) Water quality as a regional driver of coral biodiversity and macroalgae on the Great Barrier Reef. Ecological Applications 20:840-850.

Edmunds PJ, Carpenter RC (2001) Recovery of Diadema antillarum reduces macroalgal cover and increases abundance of juvenile corals on a Caribbean reef. Proceedings of the National Academy of Sciences 98:5067-5071.

Evans RD, Wilson SK, Field SN, Moore JAY (2014) Importance of macroalgal fields as coral reef fish nursery habitat in north-west Australia. Marine Biology 161:599-607.

Friedlander AM, Brown E, Monaco ME (2007) Defining reef fish habitat utilization patterns in Hawaii: comparisons between marine protected areas and areas open to fishing. Marine Ecology Progress Series 351:221-233.

Fulton CJ, Depczynski M, Holmes TH, Noble MM, Radford B, Wernberg T, Wilson SK (2014) Sea temperature shapes seasonal fluctuations in seaweed biomass within the Ningaloo coral reef ecosystem. Limnology and Oceanography 59:156-166.

Goldberg NA, Kendrick GA, Walker DI (2006) Do surrogates describe patterns in marine macroalgal diversity in the Recherche Archipelago, temperate Australia? Aquatic Conservation: Marine and Freshwater Ecosystems 16:313–327.

Graham NAJ, Jennings S, MacNeil MA, Mouillot D, Wilson SK (2015) Predicting climate-driven regime shifts versus rebound potential in coral reefs. Nature 518:94–97.

Hughes TP (1994) Catastrophes, phase shifts, and large-scale degradation of a Caribbean coral reef. Science, 265:1547-1551.

Hughes TP, Baird AH, Bellwood DR, Card M, Connolly SR, Folke C, … Roughgarden J (2003) Climate change, human impacts and the resilience of coral reefs. Science 301:929-933.

Hughes TP, Bellwood DR, Folke CS, McCook LJ, Pandolfi JM (2007) No-take areas, herbivory and coral reef resilience. Trends in Ecology and Evolution 22:1–3.

Huisman JM (2004) Marine benthic flora of the Dampier Archipelago, Western Australia Records of the Western Australian Museum, Supplement No. 66:61-68.

Huisman JM (2015) Algae of Australia: marine benthic algae of north-western Australia, 1 green and brown algae. Canberra, Australia: ABRS.

Huisman JM, Borowitzka MA (2003) Marine benthic flora of the Dampier Archipelago, Western Australia. In Wells, FE, Walker, DI and Jones, DS (Eds) The Marine Flora and Fauna of Dampier, Western Australia. Perth, Australia: Western Australian Museum.

Huisman JM, Leliaert F, Verbruggen H, Townsend RA (2009) Marine benthic plants of Western Australia's shelf-edge atolls. Records of the Western Australian Museum Supplement 77. Perth, Australia: Western Australian Museum.

Johansson CL, Bellwood DR, Depczynski M (2010) Sea urchins, macroalgae and coral reef decline: a functional evaluation of an intact reef system, Ningaloo, Western Australia. Marine Ecology Progress Series 414:65-74.

Keith SA, Kerswell AP,Connolly SR (2014) Global diversity of marine macroalgae: environmental conditions explain less variation in the tropics. Global Ecology and Biogeography 23:517-529.

Kendrick GA, Lavery PS, Phillips JC (1999) Influence of Ecklonia radiata kelp canopy on structure of macro-algal assemblages in Marmion Lagoon, Western Australia. Hydrobiologia 398:275–283.

Leathwick JR, Elith J, Hastie T (2006) Comparative performance of generalised additive models and multivariate adaptive regression splines for statistical modelling of species distributions. Ecological Modelling 198:139–153.

Lirman D (2001) Competition between macroalgae and corals: effects of herbivore exclusion and increased algal biomass on coral survivorship and growth. Coral reefs 19:392-399.

McArdle BH and Anderson MJ (2001) Fitting multivariate models to community data: A comment on Distance-Based Redundancy Analysis. Ecology 82:290–297.

McCook LJ (1999) Macroalgae, nutrients and phase shifts on coral reefs: scientific issues and management consequences for the Great Barrier Reef. Coral Reefs 18:357–367.

Mora C (2008) A clear human footprint in the coral reefs of the Caribbean. Proceedings of the Royal Society of London B: Biological Sciences 275:767-773.

Mumby PJ, Foster NL, Fahy EAG (2005) Patch dynamics of coral reef macroalgae under chronic and acute disturbance. Coral Reefs 24:681-692.

Mumby PJ, Dahlgren CP, Harborne AR, Kappel CV, Micheli F, Brumbaugh DR, Buch K (2006) Fishing, trophic cascades, and the process of grazing on coral reefs. Science 311:98-101.

Olsgard F, Somerfield PJ (2000) Surrogates in marine benthic investigations — which taxonomic unit to target? Journal of Aquatic Ecosystem Stress and Recovery 7:25–42.

Phillips JC, Kendrick GA, Lavery PJ (1997) A functional group approach to detecting shifts in macroalgal communities along a disturbance gradient. Marine Ecology Progress Series 153:125-138.

R Core Team (2015) R: A language and environment for statistical computing. R Foundation for Statistical Computing, Vienna, Austria. URL https://www.R-project.org/.

Roff G, Doropoulos C, Zupan M, Rogers A, Steneck RS, Golbuu Y and Mumby PJ (2015) Phase shift facilitation following cyclone disturbance on coral reefs. Oceologia 178:1193-1203.

Rogers RW (1996) Spatial, seasonal and secular patterns in the cover of green algae on Heron reef flat, Great Barrier Reef, Australia. Botanica Marina 39:415-419.

Rogers RW (1997) Brown algae on Heron reef flat, Great Barrier Reef, Australia: spatial, seasonal and secular variation in cover. Botanica Marina 40:113-117.

Russ G (1984) Distribution and abundance of herbivorous grazing fishes in the central Great Barrier Reef I. Levels of variability across the entire continental shelf. Marine Ecology Progress Series 20:23-34.

Schaffelke B, Mellors J, Duke NC (2005) Water quality in the Great Barrier Reef region: responses of mangrove, seagrass and macroalgal communities. Marine Pollution Bulletin 51:279-296.

Smale DA, Kendrick GA, Wernberg T (2010) Assemblage turnover and taxonomic sufficiency of subtidal macroalgae at multiple spatial scales. Journal of Experimental Marine Biology and Ecology 349:405-417.

Smale DA, Kendrick GA, Wernberg T (2011) Subtidal macroalgal richness, diversity and turnover, at multiple spatial scales, along the southwestern Australian coastline. Estuarine Coastal and Shelf Science 91:224-231.

Toohey BD, Kendrick GA, Harvey ES (2007) Disturbance and reef topography maintain high local diversity in Ecklonia radiata kelp forests. Oikos 116:1618-1630.

Walker DI, Prince RIT (1987) Distribution and biogeography of seagrass species on the Northwest coast of Australia. Aquatic Botany 29:19-32.

Vergés A, Bennett S, Bellwood DR (2012) Diversity among Macroalgae-Consuming Fishes on Coral Reefs: A Transcontinental Comparison. PLoS ONE 7(9):e45543.

Wernberg T, Smale DA, Tuya F, Thomsen MS, Langlois TJ, de Bettignies T, Rousseaux CS (2013) An extreme climatic event alters marine ecosystem structure in a global biodiversity hotspot. Nature Climate Change 3:78–82.

Wernberg T, Kendrick GA, Phillips JC (2003) Regional differences in kelp-associated algal assemblages on temperate limestone reefs in south-western Australia. Diversity and Distributions 9:427–441.

Wiens JJ, Donoghue MJ (2004) Historical biogeography, ecology and species richness. Trends in Ecology and Evolution 19:639-44.

Williams I, Polunin N (2001) Large-scale associations between macroalgal cover and grazer biomass on mid-depth reefs in the Caribbean. Coral reefs 19:358-366.

Wilson SK, Depczynski M, Fisher R, Tinkler P (2010) Habitat associations of juvenile fish at Ningaloo Reef, Western Australia: the importance of coral and algae. PLoS ONE 5:e15185.

Wismer S, Hoey AS, Bellwood DR (2009) Cross-shelf benthic community structure on the Great Barrier Reef: relationships between macroalgal cover and herbivore biomass. Marine Ecology Progress Series 376:45-54.

9.1.7 APPENDICES

Appendix 1. Model description

Alphabetic list of macrophyte species collected at 75 sites on shallow reefs (3-9 m) along the Pilbara coastline between Exmouth and Dampier, Western Australia. Collections took place in November 2013 and May 2014.

Acanthophora spicifera
Acrocystis nana (cf)
Amansia rhodantha
Amphiroa foliacea
Amphiroa fragilissima (cf)
Amphiroa sp 1
Amphiroa sp 2
Amphiroa sp 3
Anadyomene plicata
Anotrichium tenue
Asparagopsis taxiformis
Asteromenia sp. (cf)
Avrainvillea obscura (cf)
Betaphycus speciosum
Boodlea composita (cf)
Bornetella oligospora
Bornetella sphaerica
Botryocladia sp 1
Canistrocarpus cervicornis
Caulerpa agardhii (cf)
Caulerpa brachypus
Caulerpa corynephora
Caulerpa cupressoides var. cupressoides
Caulerpa delicatula
Caulerpa lamourouxii
Caulerpa lentillifera
Caulerpa macrodisca
Caulerpa serrulata
Caulerpa taxifolia
Caulerpa sp 1
Caulerpa sp 2
Ceramium galiella (cf)
Ceratodictyon intricatum
Ceratodictyon scoparium
Ceratodictyon sp 1
Ceratodictyon sp 2
Chaetomorpha sp 3

Champia compressa
Champia parvula
Champia stipitata
Champia zostericola (cf)
Champia sp 1
Champia sp 2
Chlorodesmis sp 1
Chondria armata
Chondria dangeardii (cf)
Chondria sp 1
Chondria sp 2
Chondria sp 3
Chondria sp 4
Chondria sp 5
Chondria sp 6
Chondrophycus sp 1
Cladophora catenata
Cladophora sp 1
Codium dwarkense (cf)
Coelarthrum cliftonii
Colpomenia sinuosa
Corynomorpha prismatica (cf)
Cottonelia filamentosa
crustose coralline spp.
Cryptonemia sp 1 (cf)
Cymodocea serrulata
Dasya sp 1
Dasya sp 2
Dichotomaria marginata
Dichotomaria obtusata
Dictyopteris australis
Dictyopteris delicatula
Dictyopteris repens
Dictyopteris serrulata
Dictyopteris woodwardia
Dictyospheria cavernosa
Dictyospheria versluysii
Dictyota ceylanica
Dictyota ciliolate
Dictyota friabilis
Dictyota sp 1
Dictyota sp 2
Digenea simplex
Distromium flabellatum

Erythrymenia sp 1 (cf)
Eucheuma denticulatum
Galaxaura rugose
Gelidiella acerosa
Gelidiella sp 1
Gelidiella sp 2
Gibsmithia hawaiensis
Gracilaria canaliculata
Gracilaria eucheumatoides
Gracilaria Salicornia
Gracilaria sp 1
Gracilaria sp 2
Gracilaria sp 3
Gracilaria sp 4
Halimeda cylindracea
Halimeda discoidea
Halimeda gigus (cf)
Halimeda sp 1
Halimeda sp 2
Halophila decipiens
Halophila ovalis
Heterosiphonia crassipes
Hormophysa cuneiformis
Hydroclathrus clatrathus
Hypnea nidifica
Hypnea pannosa
Hypnea sp 1
Hypnea sp 2
Hypnea sp 3
Hypnea sp 4
Hypnea sp 6
Hypnea sp 7
Hypnea sp 8
Hypoglossum sp 1
Jania adherens
Jania angulate
Jania rosea (cf)
Laurencia brongniartii
Laurencia sp 1
Laurencia sp 2
Laurencia sp 3
Laurencia sp 4
Laurencia sp 5
Laurencia sp 6

Laurencia sp 7
Laurencia sp 8
Laurencia sp 9
Laurencia sp 10
Laurencia sp 11
Laurencioid sp1
Leptofauchea anastomosans (cf)
Leveillea jungermannioides
Lithophyllum sp 1
Lithophyllum sp 2
Lobophora sp 1
Lobophora sp 2
Lomentaria sp 1
Neomeris bilimbata
Osmundaria melvillii
Padina vaughaniella stage
Padina sp 1
Padina sp 2
Padina sp 3
Padina sp 4
Penicillus nodulosus
Peyssonnelia novae-hollandiae
Peyssonnelia sp 1
Peyssonnelia sp 2
Peyssonnelia sp 3
Polysiphonia crassipes
Polysiphonia ferulacea
Polysiphonia sp 1
Polysiphonia sp 2
Portieria sp 1
Pterocladiella caerulescens
Pterocladiella sp 1
Pterocladiella sp 2
Rhodymenia leptophylla (cf)
Rhodymenia sp 1
Sargassopsis decurrens
Sargassum fallax (cf)
Sargassum flavicans
Sargassum ilicifolium
Sargassum ligulatum (cf)
Sargassum linearifolium (cf)
Sargassum polycystum
Sargassum polyphyllum (cf)
Sargassum sp 1

Sargassum sp 2
Sargassum sp 3
Sirophysalis trinodis
Spatoglossum macrodontum
Sporochnus comosus
Spyridia filamentosa
Spyridia sp 1
Struvea plumose
Syringodium isoetifolium
Titanophora sp 1
Tolypiocladia glomerulata
Tricleocarpa cylindracea (cf)
Turbinaria conoides
Turbinaria gracilis
Turbinaria ornate
Udotea argentea
Ulva sp 1
Valonia ventricose

Appendix 2. Model description

Species accumulation curve for macrophytes sampled at 75 sites on shallow reefs (3-9 m) along the Pilbara coastline between Exmouth and Dampier, Western Australia. The observed (Sobs) and estimated (using the Michaelis-Menten equation; MM) number of species in the sampled region are plotted as a function of the sampling effort (number of samples). The total number of species predicted for the shallow reef environment, S_{max} = 222 and the number of samples that would capture half of the species present, B = 11.9.
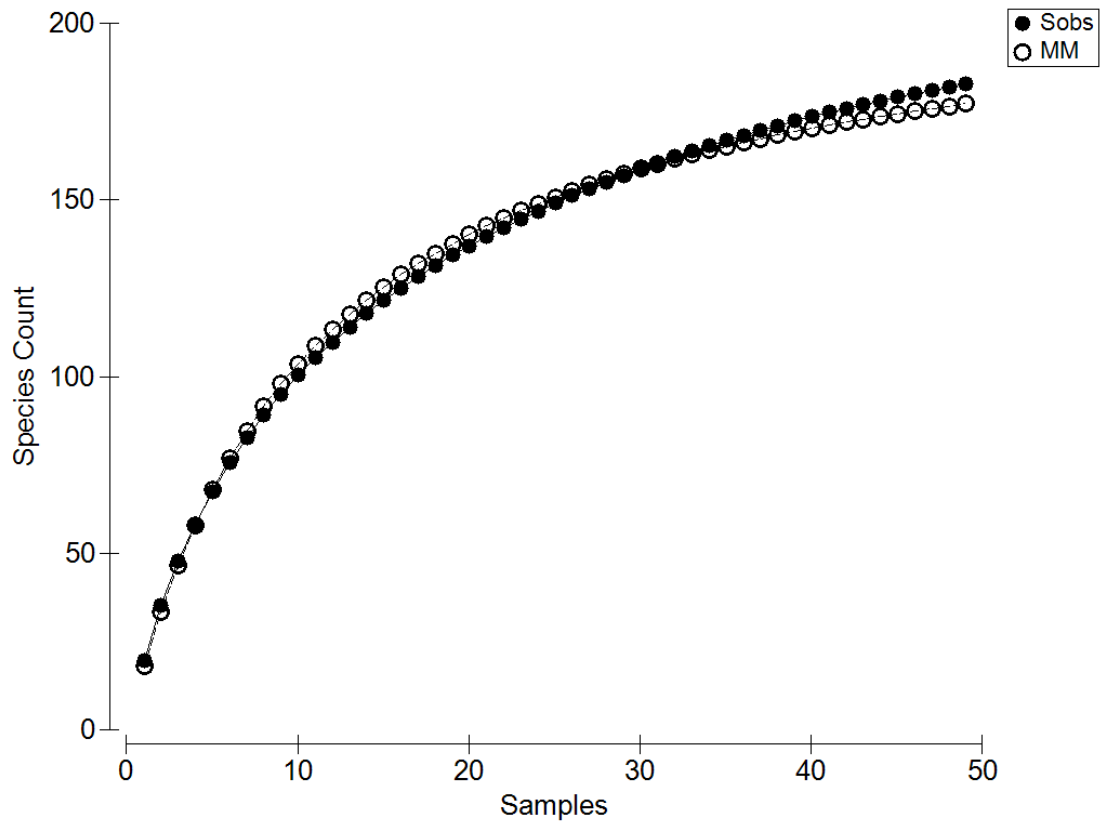
Appendix 3. Model description

Results of marginal tests for predictor variables and macrophyte biomass, species richness and community composition (biomass of each taxa). The abbreviations of the predictor variables at the top of each column are explained in Table 1. Marginal tests were carried out for the total biomass (Bio) and species richness (S) of all macrophytes (Total macrophyte) and for the community composition of the total macrophyte dataset classified into Species, Genus, Family, Order and Phylum. Further tests were carried out for the biomass, species richness and community composition of Rhodophyta, Chlorophyta, Phaeophyta, Fucales and Dictyotales. Finally, marginal tests were carried out for macrophyte diversity calculated as the Shannon diversity index. The numbers shown indicate the percentage of variability explained by each variable and the stars indicate the statistical significance (* <0.05, ** <0.01, *** <0.001).

Marginal tests	OffShPos	DistShore	Depth	Uvis	Rugosity	Sand	Rubble	Boulders	ConRubble	Bommies	Pavement	Abiotic	Hard Coral	Soft Coral	Sponge	Sed%OM	%Sand	%SiltClay	SedUniform	InvertHerb	RovingHerb	DiffAtten_Annual	Diff_Atten	MeanSSS	SST_Inst	MinSST	MaxSST	Mean SST
Total macrophyte Bio					30.2***					20.4**			27.9***															
Total macrophyte S					14.9**	8.5*						10.0*	13.0*						14.2**				12.8*					
Species	4.23**	3.22*			4.1**	3.6*			4.7***	3.5*		4.0**	7.1***						3.4*	3.5*	3.6*			5.8***	8.7***	5.0***	3.9**	3.9**
Genus	4.7**				5.6**				4.2*	4.2*		3.8*	9.8***						3.7*	4.5*	3.7*			6.6***	9.1***	6.3***	4.4*	4.6**
Family					7.2***					5.2*		4.3*	11.3***							4.2*	4.4*			6.4**	9.3***	5.8**	4.3*	
Order					7.5***					5.7**		4.4*	13.0***							4.8*	5.0*			7.1**	9.0***	6.0**	4.6*	
Phylum	6.8*				14.7***					11.4**			15.7**											13.3***		10.3**	9.3**	
Rhodophyta Bio	15.9**					8.6*						13.2**							8.1*					14.1**			13.7**	
Rhodophyta S	9.0*				17.1**							15.4**	8.2*	5.4***				7.4*	17.8**				17.3**	8.4*				
Rhodophyta		3.5*			3.2*	3.4*		3.3*	3.8**	3.3*		4.1**	3.6*					3.0*	3.6*		3.1*			4.1**	8.5***			3.7*
Chlorophyta Bio					16.5**					10.9*	12.6*		8.9*								11.0**						19.1**	
Chlorophyta S	9.6*									8.8*			12.3**											15.7**		8.2*	24.8***	
Chlorophyta					13.4**					11.5**	8.9*		9.9*								6.8*			7.9*			21.4**	
Phaeophyta Bio			9.9*		28.2***					13.9**			15.2**	10.6*							10.1*			20.1**			16.6**	
Phaeophyta S					11.7*								27.6***	8.1*			11.8*	8.8*			9.7*			15.7**		18.2**	8.1*	
Phaeophyta	4.8*				4.5*				4.6*				8.7***		3.8*	4.2**							4.5*	6.0**	9.7**	6.3***		4.9**
Fucales Bio					23.8***				11.0*	8.6*			16.5***	8.1*							7.3*			18.5**			17.0**	
Fucales S																										13.3**		
Fucales					11.3***				6.3*				6.8**		6.0*									9.7**			8.2**	
Dictyotales Bio					17.0**					12.9*			10.4*								11.4*			13.6**			14.5**	
Dictyotales S													25.5***				11.4*	11.0*			8.4*			12.2*		18.2**	8.9*	
Dictyotales	6.4**					4.5*							8.1*					5.4**			4.6*	4.4*		6.8**	9.9***	6.6**		4.8*
Shannon Index					11.9*								9.5*															

Results of DistLMs (distance based linear models) with AICc as selection criterion. The percent variability explained of each predictor variable is shown for all variables included in the best model and for the total model (right hand column). Models were constructed for macrophyte biomass, species richness and community composition (biomass of each taxa). The abbreviations of the predictor variables at the top of each column are explained in Table 1. Models were constructed for the total biomass (Bio) and species richness (S) of all macrophytes (Total macrophyte) and for the community composition of the total macrophyte dataset classified into Species, Genus, Family, Order and Phylum. Further models were constructed for the biomass, species richness and community composition of Rhodophyta, Chlorophyta, Phaeophyta, Fucales and Dictyotales and, finally, for macrophyte diversity calculated as the Shannon diversity index.

% Explained variation	OffShPos	DistShore	Depth	Uvis	Rugosity	Sand	Rubble	Boulders	ConRubble	Bommies	Pavement	Abiotic	Hard Coral	Soft Coral	Sponge	Sed%OM	%Sand	%SiltClay	SedUniform	InvertHerb	RovingHerb	DiffAtten_Annual	Diff_Atten	MeanSSS	SST_Inst	MinSST	MaxSST	Mean SST	Total model
Total macrophyte Bio					30.2								18.9										2.8			3.2	8.7		63.8
Total macrophyte S					14.9							9.2	5.1										7.9			5.3		6.4	48.7
Species					4.0								6.2											5.6	8.7				24.5
Genus					5.0								9.8											6.4	7.8				29.0
Family					5.7								11.3											6.1	7.6				30.7
Order					5.9								13.0								3.5			6.8	7.1				36.4
Phylum					10.0								15.7											13.3			4.7	4.3	48.0
Rhodophyta Bio	15.9				5.0							8.5																6.7	36.2
Rhodophyta S	4.9				10.2						4.2	8.7		5.0					17.8					5.0	3.2			3.1	62.2
Rhodophyta													5.1											4.2	8.5				17.8
Chlorophyta Bio													11.0								9.2							19.1	39.3
Chlorophyta S													15.1								4.5							24.8	44.4
Chlorophyta													12.2								5.4							21.4	39.0
Phaeophyta Bio			2.3	2.7	28.2	2.1							4.7								6.6	4.7	2.2			26.7			80.1
Phaeophyta S		3.3			7.3						2.9		27.6							14.1	3.6		5.7			12.9			77.5
Phaeophyta					4.5								6.7						4.0						5.3	9.7			30.2
Fucales Bio					23.8				1.2	4.7		3.9	5.5								2.1		4.4			26.4			72.0
Fucales S	4.6	4.2											9.0									4.2		5.0	13.3			4.2	44.5
Fucales					11.3														4.6					5.4		12.1			33.3
Dictyotales Bio				3.5	17.0		7.5			4.0										7.1	3.9					21.8			64.7
Dictyotales S	4.0				4.1						4.8	25.5							17.2		2.6		2.2			13.1			73.5
Dictyotales													6.2						5.2							9.8		6.5	27.7
Shannon Index				4.8	11.9								6.7								6.7								30.1

9.2 Temporal and spatial distribution of secondary metabolites in *Sargassum* assemblages and the influence of macroalgal density

Authors: van Hees DH, Olsen YS, Kendrick GA

ABSTRACT

Secondary metabolites produced by macroalgae have a variety of supportive and defensive roles. Phenolic compounds, commonly found in brown macroalgae, mediate abiotic stressors such as UV-B radiation and salinity, as well as deter grazing. Compounds such as these may also be advantageous in areas of high competition for space among macroalgal species. In this study, we aimed to quantify distributions of phenolic compounds in one canopy-forming species of macroalgae, *Sargassum marginatum* in the tropical Dampier Archipelago, Western Australia. To investigate temporal patterns and the effect of abiotic conditions, such as light and turbidity, on phenolic content we sampled inshore and offshore shallow reefs in spring (October) and fall (April). Finally, we examined the relationship between the density of algal fronds – both *S. marginatum* and other macroalgal taxa – and phenolic content by sampling across a range of macroalgal densities. There was a clear seasonal pattern in density with higher densities in the fall. The density of macroalgae was higher at offshore compared to inshore locations in spring, but no spatial pattern was found during the fall. We found significantly higher phenolic concentrations in in the fall, but there was no difference between inshore and offshore locations despite clear in-offshore gradients in turbidity and light. Light, therefore does not appear to be a major driver of phenolic concentrations in *S. marginatum* in the Dampier Archipelago. Concentrations of phenolic compounds were not correlated with *Sargassum* density or with the density of non-*Sargassum* taxa, which indicates that these chemical defences do not play a role in competition for space in shallow reefs. Phenolic concentrations, therefore, appear most strongly linked to season suggesting patterns in temperature as well as growth and reproduction may be the main drivers.

9.2.1 INTRODUCTION

Allelopathy, the production of secondary metabolite compounds mediates interactions between organisms. Allelopathic chemicals are found in many macroalgae on temperate and tropical reefs. Some allelopathic compounds are found in only one or a few species of macroalgae (Paul and Van Alstyne 1988; Van Alstyne et al. 2006; Enge et al. 2012) while others, such as phenolics and dimthelysulphoniopropionate (DMSP) are distributed widely throughout algal taxa (Capon et al. 1983; Steinberg 1994; Van Alstyne et al. 2007). These widely distributed compounds, while produced by a range of taxa, can elicit species-specific outcomes with nearby organisms and mediate competitive interactions with other species, for example as herbivore deterrents (Geiselman and McConnell 1981; Erickson et al. 2006; Lyons et al. 2007; Rasher and Hay 2014), fouling deterrents (Cho et al. 2001) and growth inhibitors of neighboring organisms (Jompa and McCook 2003; Kim et al. 2004; Renjun et al. 2012). Competition for space is often high in marine benthic ecosystems and allelopathic chemicals may be important in mediating interactions for macroalgae like the phaeophyceae that attach to the substrate and compete with other organisms for space.

The amount of allelochemicals produced by marine macroalgae can change in relation to environmental conditions, but the patterns differ among taxa and are compound-specific. The production of DMSP in the northeastern Pacific decreases from northern to southern locations in response to increased water temperature (Van Alstyne et al. 2007). The production of phlorotannins by macroalgae is often variable within a given location (Pavia et al. 1999; Tanniou et al. 2013; van Hees et al. 2017) and has been shown not to correlate to temperature or follow latitudinal trends (Steinberg 1989; Van Alstyne et al. 1999b). Phenolic compounds are generally thought to act as a protective mechanism against UV-B radiation (Pavia et al. 1997; Pavia and Brock 2000; Creis et al. 2015). Light as a resource to the plant may also regulate the amount of energy spent on chemical defences by the plant (Pavia et al. 1997). The light environment is therefore important in regulating phenolic content with higher light levels increasing phenolic content in *Fucus vesiculosus* (Pavia and Toth 2000) and increased UV-B radiation having the same effect on *Ascophyllum nodosum* (Pavia et al. 1997). Phenolic content may therefore vary across gradients in light and turbidity.

Here, we aimed to quantify distributions of phenolic compounds in one canopy-forming species of macroalgae, *Sargassum marginatum* in the tropical Dampier Archipelago, Western Australia. To investigate temporal patterns and the effect of abiotic conditions, such as light and turbidity, on phenolic content, we sampled inshore and offshore shallow reefs in spring (October) and fall (April). Finally, we investigated whether the density of the surrounding macroalgal assemblage regulates concentrations of phenolic compounds in *S. marginatum* by estimating phenolic concentrations in plants collected across a range of macroalgal densities.

9.2.2 METHODS

Site description

The Dampier Archipelago is located on the tropical northern Pilbara coast, Western Australia. It covers an area of 400 km^2 and is comprised of 42 small islands surrounded by shallow reef environments and water depths generally < 35 m. The benthic habitats in the archipelago include both lush macroalgal meadows and coral reefs. Sampling was conducted in October 2015 (spring) and April 2016 (fall) at two inshore sites at West Intercourse Island near the Port of Dampier and two offshore sites at Goodwyn and Rosemary Islands (Figure 9.2.1). Depth at the study sites was 3-5 m and the substrate was a mixture of sand and limestone. The benthic habitats in the archipelago

included both lush macroalgal meadows and coral reef. The macroalgal assemblage was dominated by *Sargassum* spp*.* and *S. marginatum* made up the majority of the biomass and was distributed throughout the archipelago.
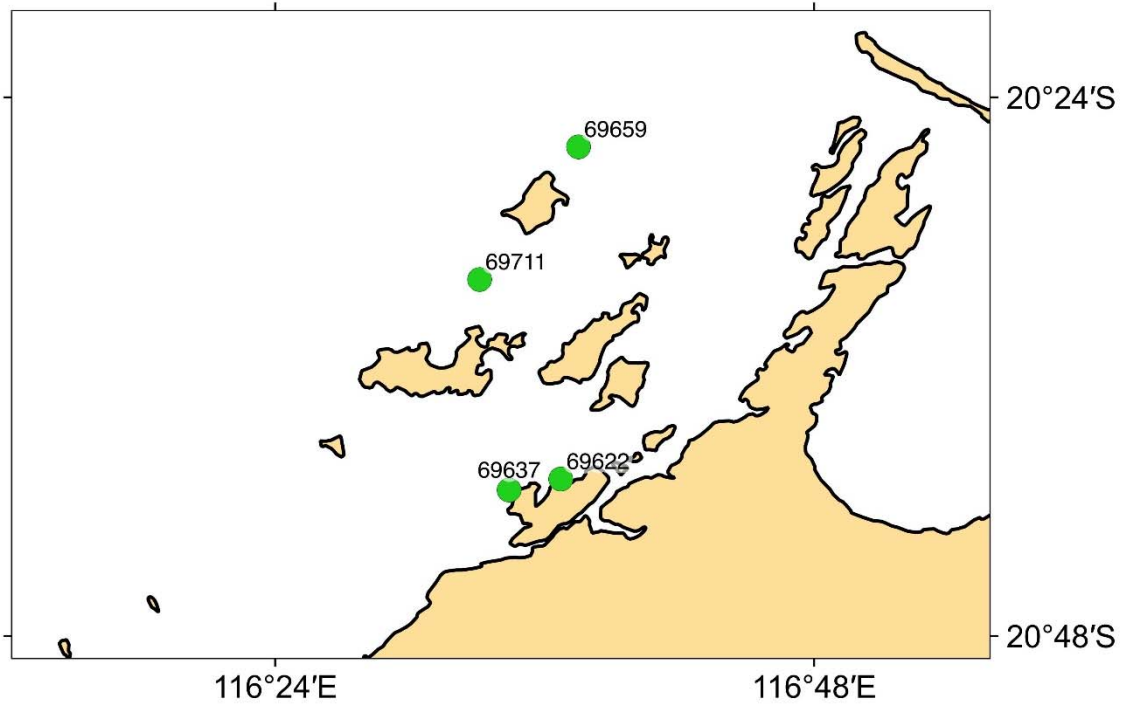

Figure 9.2.1 Map of the Dampier Archipelago showing the location of the four study sites; Goodwyn Island (69711), Rosemary Island (69659), West Intercourse Island (69622 and 69637).

Table 9.2.1. Abiotic conditions at inshore and offshore locations of the Dampier Archipelago in October 2015 and April 2016. Values shown are maximums, minimums and means ± SE. Means for irradiance are based on measurements between sunrise and sunset only.

PARAMETER		OCTOBER 2016 (SPRING)			APRIL 2017 (FALL)		
		INSHORE	OFFSHORE	SURFACE	INSHORE	OFFSHORE	SURFACE
Light - PAR (uE)							
	Mean			841.4 ± 25.0	148.6 ± 2.86	175.1 ± 2.72	781.3 ± 7.87
	Max			2003.8	1803.8	1631.3	1748.8
Temperature (°C)							
	Mean	27.1 ± 0.007	25.6 ± 0.002		28.6 ± 0.005	28.8 ± 0.004	
	Min	26.6	25.5		27.5	27.6	
	Max	27.5	25.8		29.8	29.5	
Secchi Depth (m)							
	Mean	3 ± 0.76	4.8 ± 0.16		3.33 ± 0.88	4.67 ± 0.73	
	Min	1.5	3.5		2	4.5	
	Max	4	5		5	5	

Abiotic conditions

Abiotic conditions were measured inshore and offshore in both field trips (Table 9.2.1). Water temperature of bottom waters was measured at one inshore (69622) and one offshore (69712) site. Surface irradiance was measured as photosynthetically active radiation (PAR) in both seasons by attaching an onset Hobo light logger to the roof of the diving vessel for five days. In addition, benthic PAR was also measured inshore and offshore in the fall. As a proxy for turbidity, the secchi depth was measured twice at all sites at midday in both seasons.

Macroalgal density

To determine the relationship between macroalgal density and concentrations of phenolic compounds in *Sargassum marginatum*, we carried out *in situ* assessments of the macroalgal assemblage at the four study sites on SCUBA. At each site, ten 0.25 m² quadrats were placed haphazardly within the macroalgal bed by dropping the quadrat from a height of ~1 m while swimming. Within each quadrat, we counted the number of individual thalli of each taxa classified to the lowest taxonomic level possible. The density of *S. marginatum* within each quadrat included mature plants, recruits as well as rosettes. The total density, *Sargassum* density and non-*Sargassum* density were calculated for each quadrat.

Phenolic concentrations

In each quadrat (n=10 per site), we collected a tissue sample from the apical meristem region of three haphazardly selected *S. marginatum* plants for phenolic compound analysis. Tissue samples were cleaned of all epiphytes and frozen at -20 °C within two hours of collection. Frozen samples were transferred to the University of Western Australia and stored at -80 °C until further processing.

The total soluble phenolic compound concentrations of tissues were measured using a micro Folin-Ciocalteu method (Van Alstyne 1995), a variation on the Folin-Ciocalteu method that was optimized for a microplate reader. Approximately 10 mg of lyophilized *Sargassum* tissue was placed in a microcentrifuge tube with 1.0 mL 80% methanol. Each tube was vortexed, stored in darkness overnight and then centrifuged at 5000 rpm for 2 min. We diluted 50 μL of this extract with 950 μL of Type 1 Reagent-Grade water. We then took three replicate 100 μL aliquots from each diluted extract and plated them on 96-well Grainer clear microplates. Phloroglucinol dihydrate standards (Sigma) were included in each plate to create a standard curve. To each well, 40μL of Folin Ciocalteu reagent was added using a FLUO-Star Omega microplate reader. The plate was agitated for 30 s before incubating for five minutes at 50 °C. Extracts were made alkaline by the addition of 100μL of 2N sodium carbonate. The plate incubated an additional 30 minutes before reading absorbance in a FLUOStar spectrophotometer at 765 nm. The phenolic concentrations of the three plants were averaged to produce a mean value for each quadrat.

Statistical analyses

Data were analysed in R (R Core Team 2016). To evaluate the effect of macroalgal density, season and location (in- or offshore) on phenolic content, we used the 'lme' function with the 'nlme' package (Pinheiro et al. 2014). Three models were constructed; one each for total density, *Sargassum* density and non-*Sargassum* density. The 'lme' function was also used to examine spatial and temporal patterns in phenolic composition and total macroalgal density. In all models, Site was included as a random effect nested within location (in-offshore). Where the residual plots indicated heteroscedasticity (non-constant variance), the variance structure of the data was modelled using the 'weights' option in the 'lme' function. The best variance structure was then determined by comparing AIC and standardised residual plots (Zuur et al. 2009). Once the best variance structure

and transformations had been determined, each model was simplified by step-wise dropping terms from the model until a minimum AIC was achieved. Terms in the final models were evaluated by marginal t-tests and p-values using the model 'summary' function.

We then compared phenolic concentrations to total, *Sargassum* and non-*Sargassum* macroalgal densities with single linear regressions. Regressions were split by season due to highly significant differences in both density and phenolic content with season.

9.2.3   RESULTS

The abiotic measurements highlighted differences between inshore and offshore locations (Table 9.2.1). Water clarity was higher offshore and sites were characterised by deeper secchi depths (>1.3 m deeper) and higher light levels (>25 µE higher in April). The mean temperature was similar between inshore and offshore in April, but slightly higher (~1.5°C) inshore than offshore in October.

The densities of the macroalgal assemblage varied with season. We found significantly higher macroalgal densities ($p < 0.001$, Table S9.2.1) during April (Figure 9.2.2). There was a significant interaction between location and season ($p < 0.05$, Table S9.2.1) indicating that location did not matter in April, but that macroalgal density was higher offshore than inshore in October.

A seasonal pattern was also found for phenolic concentrations of *Sargassum marginatum*. Average concentrations were 0.78 % DM ± 0.07 in October and 1.63 % DM ± 0.08 – around twice as high - in April ($p < 0.001$, Figure 9.2.3, Table S9.2.2). The highest phenolic concentration we found in an individual plant was 4.19 %DM and the lowest concentration was 0.22 %DM (Figure 9.2.3). There was no significant effect of location.
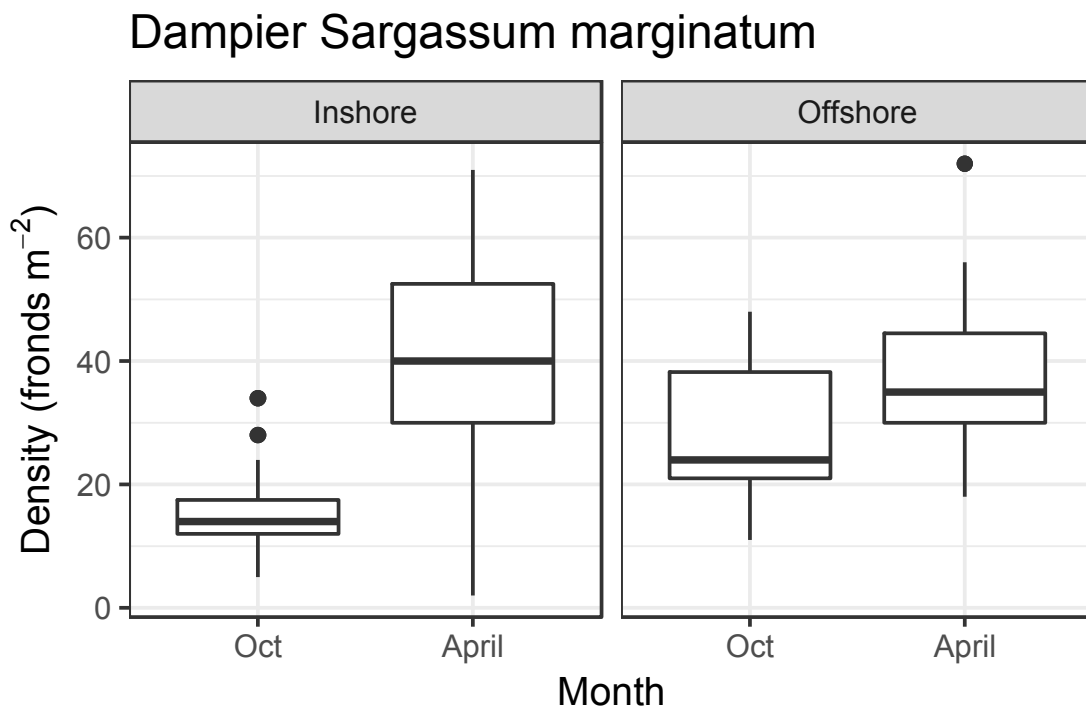

Figure 9.2.2 Density of macroalgae in haphazardly placed 0.25 m² quadrats at inshore and offshore sites of the Dampier archipelago in October 2015 and April 2016.
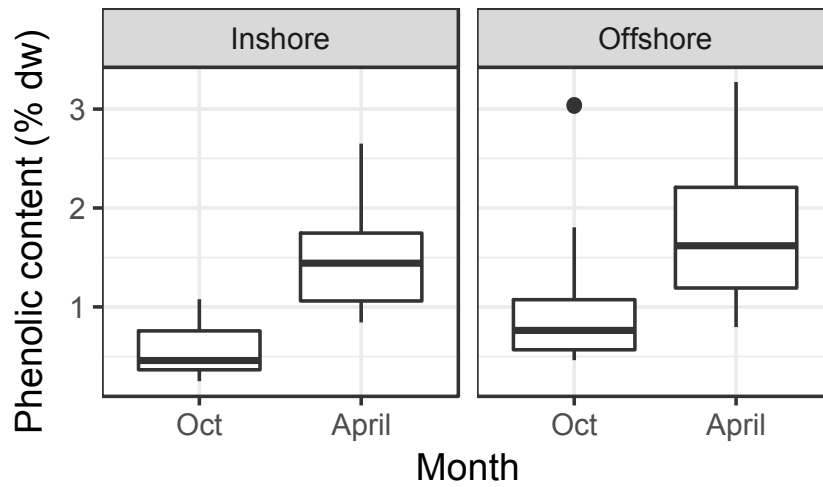
Figure 9.2.3 Phenolic content of *Sargassum marginatum* (as percent dry weight) collected at inshore and offshore sites of the Dampier archipelago in October 2015 and April 2016.
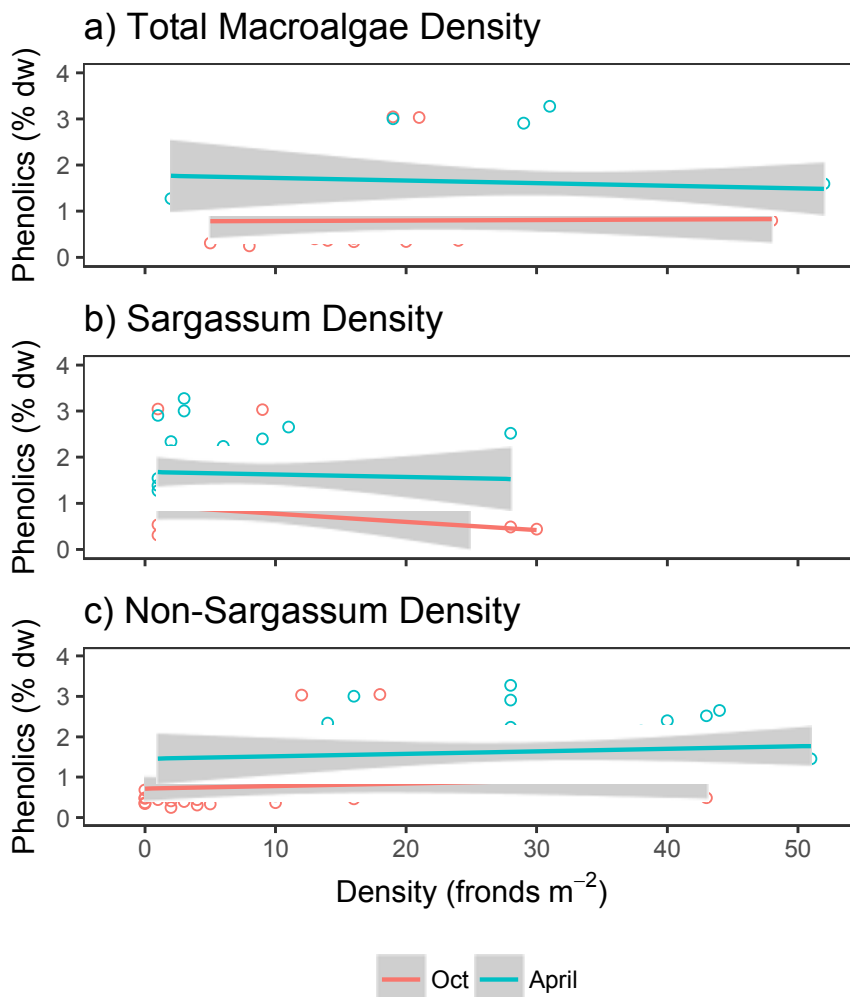

Figure 9.2.4 Mean phenolic content (as percent dry mass) of *Sargassum marginatum* in the Dampier Archipelago compared to the frond density of macroalgae of a) all macroalgae present b) algae in the family Sargassaceae c) non-*Sargassum* macroalgae.

Full models containing macroalgal density, season and location with a random factor of site nested in location best explained the mean phenolic content of *Sargassum marginatum* (Table S9.2.3). Season was significant in two out of the three models (*Sargassum* density and non-*Sargassum* density) ($p<0.05$, Table S9.2.3), but there was no effect of location or of macroalgal density (total, *Sargassum* density or non-*Sargassum* density) in any of the three models.

In accordance with these results, phenolic concentrations were not related to densities of total (Figure 9.2.4a) conspecific *Sargassum* (Figure 9.2.4b) or non-*Sargassum* (Figure 9.2.4c) macroalgae when considered for each season separately (Table S9.2.4).

9.2.4 DISCUSSION

The average phenolic concentrations of *Sargassum marginatum* in the Dampier Archipelago were similar to those of other *Sargassum* species from Western Australia (Steinberg and Paul 1990; van Hees et al. 2017). Phenolic compounds are known to vary in their distribution spatially (Steinberg 1989; Van Alstyne et al. 1999a; Stiger et al. 2004) and temporally (Hammerstrom et al. 1998; Mannino et al. 2014). We found strong seasonal patterns in macroalgal densities and phenolic concentrations of *Sargassum marginatum* in the Dampier Archipelago, but little spatial variation. This indicates that differences in abiotic conditions, e.g. water clarity, light levels and temperature, between offshore and inshore sites were not strong enough or were simply not involved in regulating phenolic content in the plants. Seasonal differences in light and temperature as well as seasonal cycles in plant growth and reproduction may instead be more important at this location.

We expected light to be an important regulator of phenolic concentrations, but despite the in-offshore differences in secchi depth and light levels, no spatial patterns were observed. We also found lower phenolic concentrations during October. This is the opposite to what we would expect, as light levels (surface irradiance) were highest in October. While effective, phenolic compounds are energetically costly to produce (Hammerstrom et al. 1998; Arnold and Targett 2003) and their protective benefit may be outweighed by the energetic cost of production. *S. marginatum* may allocate less energy to the production of phenolic compounds in April conditions in order to focus resources on other processes such as growth (Pavia et al. 2003).

Phenolic concentrations are known to vary temporally (Steinberg 1989; Pavia et al. 2003) and patterns in the Dampier Archipelago were no exception. We found higher phenolic concentrations in *S. marginatum* at the end of the growing season. This seasonal difference may be a result of phenotypic plasticity of phenolic concentrations. Additionally, the age of the plants at the end of the growing season may affect growing tissue phenolic concentrations. Peckol et al. (2003) suggested production of phenolic compounds may be up regulated in mature fronds rather than juveniles as more importance is placed on survival rather than early-stage growth. While we only measured meristem phenolic concentrations from mature plants, the age of those plants was greater in the fall. The algae we measured in April may therefore have shifted resources away from growth towards the production of phenolic compounds as has been observed in other brown seaweed species (Pavia 2003).

We hypothesised that phenolic content in *Sargassum marginatum* would increase in response to increasing densities of non-*Sargassum* algae, but not to an increase in conspecific density. Phenolic compounds may competitive advantages over other species, whereas there may be facilitative benefits of higher conspecific densities, e.g. macroalgae are known to be taller and more reproductive in stands of high-density conspecific assemblages (Schiel and Choat 1980; Schiel 1985). In the present study, concentrations in *S. marginatum* did not display a relationship to macroalgal

density. This is in agreement with the only known previous study on density, which found no relationship between phenolic concentration and conspecific density in the seaweed *Ascophyllum nodosum* (Svensson et al. 2007)*.* It is possible that phenolic content does, in fact, not confer any competitive advantage over other taxa as had previously been hypothesised.

Season was the main source of variation of phenolic content in *Sargassum marginatum* in the Dampier Archipelago. Spatial patterns in light and turbidity were not reflected in phenolic content. Light, therefore does not appear to be a major driver of phenolic concentrations in *S. marginatum* at this location. Density of macroalgae also did not have any effect on phenolic concentrations and it is possible that phenolics do not confer competitive advantages in interactions with non-conspecific algae. We therefore suggest that in this shallow tropical reef environment, phenolic content is most strongly linked to patterns in growth and reproductive status of the algae.

9.2.5 ACKNOWLEDGEMENTS

9.2.6 REFERENCES

Arnold TM, Targett NM (2003) To grow and defend: lack of tradeoffs for brown algal phlorotannins. Oikos 100:406–408.

Capon RJ, Ghisalberti EL, Jefferies PR (1983) Metabolites of the green algae, *Caulerpa* species. Phytochemistry 22:1465–1467.

Cho JY, Kwon E, Choi J, et al (2001) Antifouling activity of seaweed extracts on the green alga *Enteromorpha prolifera* and the mussel *Mytilus edulis*. J Appl Phycol 13:117–125.

Creis E, Delage L, Charton S, et al (2015) Constitutive or inducible protective mechanisms against UV-B radiation in the brown alga *Fucus vesiculosus*? A study of gene expression and phlorotannin content responses. PLoS One 10:1–15.

Enge S, Nylund GM, Harder T, Pavia H (2012) An exotic chemical weapon explains low herbivore damage in an invasive alga. Ecology 93:2736–2745.

Erickson AA, Paul VJ, Van Alstyne KL, Kwiatkowski LM (2006) Palatability of macroalgae that use different types of chemical defenses. J Chem Ecol 32:1883–1895.

Geiselman JA, McConnell OJ (1981) Polyphenols in brown algae *Fucus vesiculosus* and *Ascophyllum nodosum*: Chemical defenses against the marine herbivorous snail,Littorina littorea. J Chem Ecol 7:1115–1133.

Hammerstrom K, Dethier MN, Duggins DO (1998) Rapid phlorotannin induction and relaxation in five Washington kelps. Mar Ecol 165:293–305.

Jompa J, McCook LJ (2003) Coral – algal competition: macroalgae with different properties have different effects on corals. Mar Ecol Prog Ser 258:87–95.

Kim MJ, Choi JS, Kang SE, et al (2004) Multiple allelopathic activity of the crustose coralline alga *Lithophyllum yessoense* against settlement and germination of seaweed spores. J Appl Phycol 16:175–179.

Lyons DA, Van Alstyne KL, Scheibling RE (2007) Anti-grazing activity and seasonal variation of dimethylsulfoniopropionate- associated compounds in the invasive alga *Codium fragile* ssp. tomentosoides. Mar Biol 153:179–188.

Mannino AM, Vaglica V, Oddo E (2014) Seasonal variation in total phenolic content of *Dictyopteris polypodioides* (Dictyotaceae) and *Cystoseira amentacea* (Sargassaceae) from the Sicilian coast. Flora Mediterr 24:39–50.

Paul VJ, Van Alstyne KL (1988) Chemical defense and chemical variation in some tropical Pacific species of *Halimeda*. Coral Reefs 6:263–269.

Pavia H, Brock E (2000) Extrinsic factors influencing phlorotannin production in the brown alga *Ascophyllum nodosum*. Mar Ecol Prog Ser 193:285–294.

Pavia H, Cervin G, Lindgren A, Åberg P (1997) Effects of UV-B radiation and simulated herbivory on phlorotannins in the brown alga *Ascophylum nodosum*. Mar Ecol Prog Ser 157:139–146.

Pavia H, Toth GB (2000) Influence of light and nitrogen on the phlorotannin content on the brown seaweeds *Ascophyllum nodosum* and *Fucus vesiculosus*. Hydrobiol 440:299–305.

Pavia H, Toth GB, Aberg P (1999) Trade-offs between phlorotannin production and annual growth in natural populations of the brown seaweed *Ascophyllum nodosum*. J Ecol 87:761–771.

Pavia H, Toth GB, Lindgren A, Aberg P (2003) Intraspecific variation in the phlorotannin content of the brown alga *Ascophyllum nodosum*. Phycologia 42:378–383.

Pinheiro J, Bates D, DebRoy S, Sarkar D and R Core Team (2017) nlme: Linear and Nonlinear Mixed Effects Models. R package version 3.1-131, URL: https://CRAN.R-project.org/package=nlme.

R Core Team (2016) R: A language and environment for statistical computing. R Foundation for Statistical Computing, Vienna, Austria. URL https://www.R-project.org/.

Rasher DB, Hay ME (2014) Competition induces allelopathy but suppresses growth and anti-herbivore defence in a chemically rich seaweed. Proc Biol Sci 281:20132615.

Renjun W, You W, Xuexi T (2012) Identification of the toxic compounds produced by *Sargassum thunbergii* to red tide microalgae. Chinese J Oceanol Limnol 30:778–785.

Schiel DR (1985) Growth, survival and reproduction of two species of marine algae at different densities in natural stands. J Ecol 73:199–217.

Schiel DR, Choat J (1980) Effects of density on monospecific stands of marine algae. Nature 285:324–326.

Steinberg PD (1994) Lack of short-term induction of phlorotannins in the Australasian brown algae *Ecklonia radiata* and *Sargassum vestitum*. Mar Ecol Prog Ser 112:129–133.

Steinberg PD (1989) Biogeographical variation in brown algal polyphenolics and other secondary metabolites: comparison between temperate Australasia and North America. Oceologia 78:373–382.

Steinberg PD, Paul VJ (1990) Fish feeding and chemical defenses of tropical brown algae in Western Australia. Mar Ecol Prog Ser 58:253–259.

Stiger V, Deslandes E, Payri CE (2004) Phenolic contents of two brown algae, *Turbinaria ornata* and *Sargassum mangarevense* on Tahiti (French Polynesia): Interspecific, ontogenic and spatio-temporal variations. Bot Mar 47:402–409.

Svensson CJ, Pavia H, Toth GB (2007) Do plant density, nutrient availability, and herbivore grazing interact to affect phlorotannin plasticity in the brown seaweed *Ascophyllum nodosum*. Mar Biol 151:2177–2181.

Tanniou A, Vandanjon L, Incera M, et al (2013) Assessment of the spatial variability of phenolic contents and associated bioactivities in the invasive alga *Sargassum muticum* sampled along its European range from Norway to Portugal. J Appl Phycol 26:1–16.

Van Alstyne KL (1995) Comparison of three methods for quantifying brown algal polyphenolic compounds. J Chem Ecol 21:45–58.

Van Alstyne KL, Koellermeier L, Nelson TA (2007) Spatial variation in dimethylsulfoniopropionate (DMSP) production in *Ulva lactuca* (Chlorophyta) from the Northeast Pacific. Mar Biol 150:1127–1135.

Van Alstyne KL, McCarthy III JJ, Hustead CL, Kearns LJ (1999a) Phlorotannin allocation among tissues of northeastern pacific kelps and rockweeds. J Phycol 35:483–492.

Van Alstyne KL, McCarthy JJ, Hustead CL, Duggins DO (1999b) Geographic variation in polyphenolic levels of northeastern Pacific kelps and rockweeds. Mar Biol 133:371–379.

Van Alstyne KL, Nelson A V, Vyvyan JR, Cancilla DA (2006) Dopamine functions as an antiherbivore defense in the temperate green alga *Ulvaria obscura*. Oceologia 148:304–311.

van Hees DH, Olsen YS, Wernberg T, et al (2017) Phenolic concentrations of brown seaweeds and relationships to nearshore environmental gradients in Western Australia. Mar Biol 164:1–13.

Zuur, A., Ieno, E.N., Walker, N., Saveliev, A.A., Smith, G.M., 2009. Mixed EffectsModels and Extensions in Ecology. R. Springer Science & Business Media.

9.2.7 SUPPLEMENTARY TABLES

Table S9.2.1 The final mixed model to describe seasonal and spatial patterns in macroalgal density was lme(density ~ season*location, random = ~1|location:site).The fixed terms retained in the best model (lowest AIC) are shown along with their estimated coefficient values (Value, standard errors for these values (SE), degrees of freedom (DF), t-values and p-values.

	Value	SE	DF	t-value	p
Season	22.969	3.628	72	6.331	<0.001***
Location	12.493	5.072	72	2.463	0.1328
Season:Location	-13.553	5.563	2	-2.436	0.0173*

Table S9.2.2 The final mixed model to describe seasonal and spatial patterns in macroalgal phenolic concentration was lme(phenolic concentration ~ season*location, random = ~1|location:site, weights = varPower()).The fixed terms retained in the best model (lowest AIC) are shown along with their estimated coefficient values (Value, standard errors for these values (SE), degrees of freedom (DF), t-values and p-values.

	Value	SE	DF	t-value	p
Season	0.939	0.179	72	5.228	<0.001***
Location	0.459	0.143	72	3.199	0.085
Season:Location	-0.188	0.291	2	-0.646	0.520

Table S9.2.3 The final mixed models to describe the effect of season, location and macroalgal density on phenolic concentration. The fixed terms retained in the best model (lowest AIC) are shown along with their estimated coefficient values (Value, standard errors for these values (SE), degrees of freedom (DF), t-values and p-values.

	Value	SE	DF	t-value	p
Model for total density:					
lme(phenolic concentration ~ total algal density * season * location, random = ~1|location:site, weights = varPower())					
Density	-0.005	0.008	68	-0.563	0.576
Season	0.623	0.404	68	1.542	0.128
Location	1.049	0.362	2	2.899	0.101
Density:Season	0.011	0.012	68	0.873	0.386
Density:Location	-0.019	0.012	68	-1.511	0.135
Season:Location	-0.277	0.777	68	-0.357	0.723
Density:Season:Location	0.005	0.021	68	0.253	0.801
Model for *Sargassum* density:					
lme(phenolic concentration ~ Sargassum density * season * location, random = ~1|location:site, weights = varIdent(form = ~1|location))					
Density	-0.008	0.012	68	-0.650	0.518
Season	0.666	0.235	68	2.838	0.006**
Location	0.239	0.352	2	0.678	0.568
Density:Season	0.027	0.018	68	1.481	0.143
Density:Location	0.031	0.048	68	0.642	0.523
Season:Location	0.400	0.464	68	0.862	0.392
Density:Season:Location	-0.079	0.058	68	-1.378	0.173
Model for non-*Sargassum* density:					
lme(phenolic concentration ~ non-Sargassum density * season * location, random = ~1|location:site, weights = varPower())					
Density	0.036	0.019	68	1.874	0.065
Season	0.823	0.401	68	2.049	0.044*
Location	1.196	0.287	2	4.175	0.053
Density:Season	-0.028	0.023	68	-1.195	0.236
Density:Location	-0.063	0.021	68	-2.993	0.004**
Season:Location	-0.658	0.842	68	-0.781	0.437
Density:Season:Location	0.054	0.033	68	1.637	0.106

Table S9.2.4 Results from one-way ANOVAs testing phenolic concentration as a function of algal density.

	DF	Sum Sq	Mean Sq	F-value	p
April: phenolics ~ total algal density					
Density	1	0.0378	0.0378	0.0846	0.773
Residuals	36	16.085	0.4468		
April: phenolics ~ Sargassum density					
Density	1	0.0561	0.0561	0.1258	0.725
Residuals	36	16.067	0.4463		
April: phenolics ~ non-Sargassum density					
Density	1	0.1776	0.1776	0.4009	0.531
Residuals	36	15.945	0.4429		
October: phenolics ~ total algal density					
Density	1	0.0056	0.0056	0.0146	0.904
Residuals	38	14.454			
October: phenolics ~ Sargassum density					
Density	1	0.5811		1.591	0.215
Residuals	38	13.879			
October: phenolics ~ non-Sargassum density					
Density	1	0.2443		0.6529	0.424
Residuals	38	14.216			